Net Lifecycle Greenhouse Gas Emissions from Hydroelectric Development on the Lower Nelson River: Implications for Energy Policy

by

Robert Emil Gill

A Thesis submitted to the

Faculty of Graduate and Postdoctoral Studies

of the University of Manitoba

in partial fulfilment of the requirements of the degree of

Doctor of Philosophy

Department of Environment & Geography

Clayton H. Riddell Faculty of Environment, Earth, and Resources

University of Manitoba

Winnipeg, Manitoba, Canada

Copyright © 2026, Robert Gill

Supervised by

Dr. Tim Papakyriakou
Professor
Centre for Earth Observation Science
Department of Environment and Geography
University of Manitoba
Winnipeg, Manitoba, Canada

Advisory Committee

Dr. Greg McCullough
Centre for Earth Observation Science
Department of Environment and Geography
University of Manitoba
Winnipeg, Manitoba, Canada

Mr. Bill Hamlin, P.Eng.
Electricity GHG Implications Specialist
Winnipeg, Manitoba, Canada

Dr. Tricia Stadnyk
Professor
Schulich School of Engineering
Department of Civil Engineering
University of Calgary
Calgary, Alberta, Canada

The late Dr. David G Barber
Centre for Earth Observation Science
Department of Environment and Geography
University of Manitoba
Winnipeg, Manitoba, Canada

External Examiner

Dr. Annie Levasseur
Professeure
Département de génie de la construction
École de Technologie Supérieure – ETS
Montréal, Québec, Canada

Abstract

Creating reservoirs through flooding land for the purpose of hydroelectric power generation may impact carbon cycling and alter greenhouse gas (GHG) emissions. To examine the impacts of flooding in northern peatland environments for hydroelectric production, the pre-impoundment and post-impoundment net 100-year lifecycle GHG emissions were modelled for the recently created Keeyask hydroelectric reservoir located on the Nelson River in northern Manitoba, Canada. Net 100-year lifecycle GHG emissions were also modelled for all hydroelectric reservoirs on the lower Nelson River, including the Churchill River Diversion (CRD) and possible future hydroelectric development. The UNESCO/IHA GHG Reservoir (G-res) Tool, version 3.31 was selected to model lifecycle GHG emissions from both the Keeyask and lower Nelson River reservoirs.

Annual Net Keeyask reservoir GHG emissions are modelled to be 86 $gCO_2e/m^2/yr$ (95% Confidence Interval 75 – 98). Total Net GHG emissions for the 100-year life of the Keeyask reservoir are estimated to be 861,990 tonnes CO_2e (95% CI 749,988 – 987,936). The modelled reservoir GHG 100-year average lifecycle emission intensity is estimated to be 2.2 gCO_2e/kWh. Total Net GHG emissions for the hydroelectric reservoirs located on the lower Nelson River, including the CRD, Keeyask, Kettle, Long Spruce, and Limestone reservoirs are modelled to be 24,339,968 t CO_2e (95% CI 21,349,582 - 27,729,138) over the 100-year lifecycle of the reservoirs. Approximately 95% of the Net emissions are modelled to occur from the CRD (80%) and the Kettle reservoir (15%). From 2025 to 2075, the remaining lifecycle GHG emission intensity for the lower Nelson River reservoirs, including the CRD, is modelled to be 7.9 g CO_2e/kWh, similar to median values (that range from 8 to

52 g CO_2e/kWh) for electricity generated from ocean waves, nuclear, wind, solar, and biomass technologies. The largest source of modelling uncertainty lies with the CO_2 and CH_4 emission factors selected for the pre-flood reservoir footprint, and with how well the G-res Tool was calibrated for northern, peatland reservoirs. Modelled lifecycle reservoir GHG emissions and emission intensity associated with the lower Nelson River are low and declining. Electricity generated from lower Nelson River hydropower can help Manitoba and Canada achieve net-zero GHG emission goals.

Acknowledgements

This thesis has been a journey of discovery and friendship, with support, encouragement and wisdom given so generously by so many along the way, whom I wish to thank.

To the Thesis Advisory Committee:
Dr. Tim Papakyriakou, thank you for giving me an opportunity to learn, for patiently guiding me for so many years, and for not giving up on me. Thank you for your scientific insight, for your never-ending cheerfulness, and for treating me so well. Studying under you has been an academic and workplace highlight. Dr. Tricia Stadnyk, thank you for bringing a rigorous, disciplined approach to this research project, for inciting me to learn about modelling – you opened a whole new world for me, and thank for training me to critically evaluate research results. Dr. Greg McCullough, your firsthand knowledge of Manitoba reservoirs and waterways has improved this research effort and document. Your thoughtful discussions and questions have expanded the scope and value of this thesis. Thank You. Mr. Bill Hamlin, thank you for your gentle guidance and thoughtful, challenging questions. You have helped this study align scientific discovery with the needs of industry and society as we navigate the implications of energy use and climate change. And thank you to the late Dr. Barber, who, with his positive outlook and boundless enthusiasm, encouraged me to continue learning, motivated me to expand the boundaries of this project, and energized me to continue with the endeavour.

Thank you Dr. Levasseur for your thorough review, insightful comments and inspiration.

Thank you Celia at the Faculty of Graduate and Postdoctoral Studies for your extraordinary patience. You joyfully guided me for so long and endured my many missteps and questions.

To my fieldwork companions, Emma Ausen, Bailey Baldwin, Nick Decker, Daniel Gedig, Keilan Ledger, Rachel Mandryk, Jarod Morrison, Jessy Ritchot, Ashley Soloway, and Kate Yezhova, thank you for your youthful enthusiasm, ingenuity and good humour.

Thank you to Manitoba Hydro and the Keeyask Limited Hydropower Partnership for allowing me to work on this project, granting access to information, and for cheering me throughout this adventure. Thank you Wil DeWit, Nick Gomes, Richard Goulet, Gavin LeBeau, Chris Magura, Shelley Matkowski, Danielle McLeod, Jarod Morrison, Scott Powell, Mark Reed, Russ Schmidt, Efrem Teklemariam, Jason Westmacot, Leo Wong, and Allison Zacharias, I am very appreciative. I am very thankful for the G-res Tool modelling support provided by Sara Mercier-Blais, Alice Parkes, and Dr. Yves Prairie at Université du Québec à Montréal.

To my good friends Penny and Allan, Robyn and David, Connie and Larry, Daisanne and Kurtis, you never stopped encouraging me, asking about the project and wishing me well.

To my family Hillary and Scott, Nathalia and Christopher, Elizabeth, Wendy and Ron, Carrie and Don. You cheered me on and gave up much too much so I could succeed.

And to my loving wife Heidi, with your everlasting faith. I never would have completed this without you. You selflessly sacrificed so much and gave me the strength to continue. You truly are an angel.

Contents

1 Introduction and Rationale 1
1.1 Introduction 1
1.2 Rationale 3
1.3 Land Acknowledgement 4
1.4 Thesis Overview 4
1.5 Objectives 5
1.6 Thesis Structure 6
2 Literature Review: Reservoir GHG Science and Implications for GHG Modelling 7
2.1 Hydroelectric Reservoirs and Potential GHG Impacts 8
2.1.1 Reservoir Processes and GHG Emission Pathways 9
2.2 Overview of Reservoir GHG Modelling 20
2.2.1 Reservoir GHG Lifecycle Modelling 21
2.2.2 Review of Reservoir GHG Models 22
2.2.3 UNESCO/IHA GHG Reservoir (G-res) Tool 33
2.3 Overview of the Keeyask Reservoir: Attributes that Affect GHG Emissions and Lifecycle Modelling 39
2.4 Lower Nelson River Landscape 56
2.4.1 Water Regime and Physiography 58
2.4.2 Lower Nelson River Reservoirs 63
2.5 Churchill River Diversion 69
2.5.1 CRD Overview 69
2.5.2 CRD Flooding 71
2.5.3 Preflood Landcover and Relevance for GHG Modelling 72
3 Methods 75
3.1 Application of the G-res Tool to the Keeyask Reservoir 75
3.1.1 Reservoir Information 75
3.1.2 Modelled Pre-Flood GHG Emissions 76
3.1.3 Pre-flood Terrestrial and Aquatic GHG Emission Factors 91
3.1.4 Modelling Inputs 104
3.2 Application of the G-res Tool to the Remainder of Lower Nelson River Reservoirs and CRD 105
3.2.1 Kettle Reservoir 106
3.2.2 Long Spruce Reservoir 106

3.2.3 Limestone Reservoir 107
3.2.4 Potential Conawapa Reservoir (Modelling Scenario) 107
3.2.5 CRD 107
4 Net Lifecycle GHG Emissions for the Keeyask Hydroelectric Reservoir 108
4.1 Annual and Lifetime GHG Emissions 108
4.2 Gross Emissions by Gas Type and Pathway 109
4.3 Pre-Impoundment Emissions 110
4.4 Keeyask Reservoir Net Lifecycle GHG Emissions 110
4.4.1 Net 100-Year Lifecycle Emissions 110
4.4.2 GHG Emission Rates: 2025 onwards; 2035 onwards; and 2050 onwards 115
4.4.3 Keeyask Reservoir GHG Lifecycle Emission Intensity 117
4.5 Discussion 118
4.5.1 Modelling Pre-Flood Emissions 118
4.5.2 G-res Predictions of Gross Post-flood Emissions 119
4.5.3 Gas Type 120
4.5.4 Net GHG Emissions 122
4.5.5 G-res Estimate of GHG Emission Intensity 124
4.5.6 Comparison of G-res Estimated Emission Intensity to Other Forms of Electricity Generation 128
4.6 Limitations of the G-res Tool 129
5 Net Lifecycle GHG Emissions for Hydroelectric Reservoirs on the Lower Nelson River 133
5.1 Results for Lower Nelson River Reservoirs 133
5.1.1 Total Lifecycle GHG Emissions 133
5.1.2 Gas Composition and Emission Pathway 134
5.1.3 Comparison to Manitoba Hydro Direct GHG Emissions 139
5.1.4 Cumulative Net Reservoir GHG Emissions 141
5.1.5 Modelled GHG Emission Intensity 142
5.2 Results of Lower Nelson River Reservoirs Including the Flooded Lands of the Churchill River Diversion 145
5.2.1 Net Lifecycle GHG Emissions 145
5.2.2 Comparison of Lower Nelson River Reservoirs and CRD to Manitoba Hydro Direct GHG Emissions 151
5.3 Modelled Full Lifecycle GHG Emissions for the Lower Nelson River Including Construction, Landuse Change, Operation, and Decommissioning 152

6 Uncertainty Analysis 155
6.1 Data Uncertainty 155
6.1.1 Pre-flood Landcover Classification 156
6.2 Structural Uncertainty 184
6.2.1 Pre-Flood Landcover: Peatlands and Re-surfacing Peat 185
6.2.2 Assessment of Reservoirs in the G-res Database 185
6.2.3 Littoral Zone 188
6.3 Uncertainty Analysis: Conclusions 191
6.3.1 Data Uncertainty Analysis 191
6.3.2 Structural Uncertainty 192
7 GHG Implications of Hydroelectric Reservoirs on the Lower Nelson River in Terms of Climate Change and Energy Policy 194
7.1 The Evolving Energy Landscape: Background for Hydroelectric Reservoir GHG Quantification 194
7.1.1 Climate Change Science 195
7.1.2 The Paris Agreement 196
7.1.3 Conference of the Parties (COP) 30 – Belém, Brazil, November 2025 197
7.1.4 Canada's Commitment 197
7.1.5 Manitoba 203
7.1.6 GHG Accounting and Reporting 203
7.1.7 Market Place 212
7.1.8 Synthesis of Evolving Energy Landscape 214
7.2 Implications of Hydroelectric Reservoirs on the Lower Nelson River 214
8 Conclusions 216
8.1 Canada-wide Collaboration 216
8.2 Emission Intensity 216
8.3 Reservoir Lifecycle Assessment and Going Forward 217
8.4 Living Baseline and On-Going Lifecycle GHG Model 217
8.5 Pre-Flood Emissions 217
8.6 Conclusions About Keeyask G-res Reservoir GHG Modelling Results 218
8.7 Conclusions About Lower Nelson River G-res Reservoir Modelling Results 219
8.8 Conclusions About the G-res Model 222
9 Recommendations 225
9.1 Canada-wide Reservoir GHG Lifecycle Initiatives 225

9.2 Keeyask Reservoir GHG Lifecycle Modelling 225
9.3 Lower Nelson River Reservoir GHG Lifecycle Modelling 226
9.4 Manitoba Hydro Hydraulic System 227
9.5 Recommendations for Reducing Limitations and Uncertainty with the G-res Tool 227
9.6 Recommended Future Research to Reduce Limitations and Uncertainty with the G-res Tool 227
9.6.1 Cascading Reservoirs 227
9.6.2 CO_2 Degassing Emissions 228
9.6.3 CH_4 Degassing Emissions 228
10 References 229

Appendix 1: Application of the G-res Tool to the Keeyask Reservoir
Appendix 2: Keeyask Reservoir Lifecycle GHG Model Uncertainty Analysis
Appendix 3: Application of the G-res Tool to the Kettle Generating Station Reservoir (Stephens Lake)
Appendix 4: Application of the G-res Tool to the Long Spruce Generating Station Reservoir
Appendix 5: Application of the G-res Tool to the Limestone Generating Station Reservoir
Appendix 6: Application of the G-res Tool to a Possible Scenario for the Potential Conawapa Generating Station Reservoir
Appendix 7: Application of the G-res Tool to the Churchill River Diversion

Tables

Table 2-1 Reservoir GHG Model Review 23
Table 2-2 Lower Nelson River Reservoirs 58
Table 3-1 Keeyask Reservoir G-res Tool Inputs 76
Table 3-2 Keeyask Pre-Flood Landcover: Vegetation Structure 81
Table 3-3 Vegetation Structure Classes 81
Table 3-4 Summary of Evaluation of Classification Schemes to Describe the Keeyask Pre-Flood Landcover for Applying the G-res Tool 86
Table 3-5 Ecological Land Classification Aligned for G-res Tool Pre-Flood Landcover Categories 87
Table 3-6 Ecological Land Classification: Re-Align Bogs for G-res Tool 90
Table 3-7 Pre-Impoundment Landcover: G-res Tool Input 91
Table 3-8 Assessment of CO_2 Terrestrial Emission Factors 92
Table 3-9 Evaluation Results: CO_2 Emission Factor Studies 93
Table 3-10 Assessment of CH_4 Emission Factors 95
Table 3-11 Evaluation Results: CH_4 Emission Factor Studies 96
Table 3-12 CO_2 Emission Factors for Keeyask G-res Lifecycle Model 98
Table 3-13 Calculation of Keeyask Pre-Flood Wetland Composite CH_4 Emission Factor 102
Table 3-14 Composite Methane Emission Factors for Keeyask G-res Model 103
Table 4-1 Modelled Post-Impoundment, Pre-Impoundment and Net 100-Year Lifecycle GHG Emissions for the Keeyask Hydroelectric Reservoir 111
Table 4-2 Modelled Keeyask Reservoir Pre-Impoundment and 100-Year Annual Average Post-Impoundment Emissions by Gas Type per m^2 112
Table 4-3 Modelled Pre-Impoundment and 100-Year Annual Average Post-Impoundment Emissions by Gas Type for the Entire Keeyask Reservoir 112
Table 4-4 Total Annual Gross Lifecycle Emissions by Gas Type and Emission Pathway 115
Table 5-1 Lower Nelson River Reservoirs: Net Lifecycle GHG Emissions 135
Table 5-2 Lower Nelson River Reservoirs Including the Potential Conawapa Reservoir: Net Lifecycle GHG Emissions 136
Table 5-3 Gross Annual Average Lifecycle GHG Emissions by Gas Type and Pathway 137
Table 5-4 Gross Annual Average Lifecycle GHG Emissions by Gas Type and Pathway (Percent) 137
Table 5-5 Gross Annual Average GHG Emissions by Gas Type and Pathway including Potential Conawapa Reservoir 138
Table 5-6 Gross Annual Average GHG Emissions by Gas Type and Pathway (Percentage), including Potential Conawapa Reservoir 139
Table 5-7 Modelled Lower Nelson River Reservoir 143
Table 5-8 Modelled Net Reservoir 100-Year Lifecycle GHG Emissions: Lower Nelson River Reservoirs Including CRD 146
Table 5-9 Modelled Net Reservoir Annual Average Lifecycle GHG Emissions: Lower Nelson River Reservoirs Including CRD 148
Table 6-1 Sensitivity Analysis: Landcover and Emission Factor Scenarios 160
Table 6-2 Summary of Modelling Scenarios: Predicted Keeyask Reservoir 162
Table 6-3 Keeyask Reservoir GHG Uncertainty Assessment: Littoral Zone Scenarios 178
Table 6-4 Keeyask Reservoir GHG Uncertainty Assessment Total Phosphorous Scenarios 181

Table 6-5 Keeyask Reservoir GHG Uncertainty Assessment: Water Residence Time Scenarios 183
Table 6-6 Keeyask Reservoir GHG Uncertainty Assessment: Water Residence Time Scenarios ... 184
Table 6-7 Keeyask Reservoir GHG Uncertainty Assessment: Risk Analysis 193

Figures

Figure 2-1 Reservoir GHG Processes and Pathways 20
Figure 2-2 Location of Keeyask Generating Station 40
Figure 2-3 Keeyask Reservoir Modelled Water Depth 46
Figure 2-4 Keeyask Reservoir Modelled Water Velocity 47
Figure 2-5 Heterogeneous Peatlands in the Keeyask Reservoir Area 48
Figure 2-6 Pre-Flood Keeyask Area Peatlands, 2019 49
Figure 2-7 Images of Floating and Resurfacing Peat in Keeyask Reservoir Flooded Backbay 2023 ... 55
Figure 2-8 Images of Floating and Semi-Submerged Vegetation in Flooded Shallow Shoreline Along the Keeyask Reservoir South Dike Road 2023 55
Figure 2-9 Nelson-Churchill River Watershed 56
Figure 2-10 Lower Nelson River Reservoirs/Generating Stations 58
Figure 2-11 Lower Nelson River 59
Figure 2-12 Lake Winnipeg Regulation 60
Figure 2-13 Stephens Lake: Lentic and Lotic Environments 65
Figure 2-14 Churchill River Diversion 71
Figure 3-1 Methodology for Adapting Keeyask Landcover Classifications to G-res Tool Land Class 79
Figure 3-2 Keeyask Pre-Flood Landcover: Terrestrial Habitat (Course and Fine Ecosite)Classification 83
Figure 3-3 Keeyask Pre-Flood Landcover: Ecological Land Classification 85
Figure 3-4 Methodology for Selecting and Developing Pre-flood CO_2 & CH_4 Emissions Factors for G-res Tool 92
Figure 3-5 G-res Tool Default Pre-Flood GHG Emission Factors 104
Figure 3-6 Pre-flood GHG Emission Factors Developed for the Keeyask G-res Model 105
Figure 4-1 Modelled Keeyask Reservoir Pre-Impoundment GHG Emissions 113
Figure 4-2 Annual Total Gross Lifecycle Emissions by Emission Pathway 113
Figure 4-3 Keeyask Reservoir Modelled Net Lifecycle GHG Emissions 114
Figure 4-4 Keeyask Reservoir 100-Year Annual Average Gross GHG Emissions by GasType 114
Figure 4-5 Keeyask Reservoir Modelled Net Lifecycle Emissions 117
Figure 4-6 Modelled Keeyask Reservoir Net GHG Emission Intensity 118
Figure 4-7 Proportion of CO_2 and CH_4 Emissions Modelled for the First 5 Years Following Reservoir Impoundment 122
Figure 4-8 Comparison of 100-Year Annual Net Lifecycle Reservoir GHG Emissions per m^2 Modelled by G-res 124
Figure 4-9 Modelled Total Keeyask GHG Emissions by Lifecycle Stage (%) 125
Figure 4-10 Modelled Total Keeyask GHG Emissions by Lifecycle Source Including G-res Results 126
Figure 4-11 Comparison of Modelled Keeyask Lifecycle Reservoir GHG Emission Intensity to Modelled Lifecycle GHG Emission Intensity of Other Northern Reservoirs 128
Figure 5-1 Lower Nelson River Reservoirs: Lifecycle GHG Emissions (Percent of Total) 135
Figure 5-2 Lower Nelson River Reservoirs Including Potential Conawapa: Net Lifecycle Emissions (Percent of Total) 136
Figure 5-3 Gross Annual Average GHG Emissions: Gas Type and Pathway 138

Figure 5-4 Gross Annual Average GHG Emissions: Gas Type and Pathway, including Potential Conawapa 139
Figure 5-5 Modelled Current (2023-2027 Average) Lower Nelson River Reservoir GHG Emissions Compared to Manitoba Hydro 2023 Direct Emissions 141
Figure 5-6 Lower Nelson River Reservoir Cumulative Net GHG Lifecycle Emissions (including the Potential Conawapa reservoir as hypothetically being flooded in 2050) 142
Figure 5-7 Modelled Lower Nelson River Reservoirs Lifecycle GHG Emission Intensity: Comparison to Other Forms of Electricity Generation 144
Figure 5-8 Modelled Net Reservoir 100-Year Lifecycle GHG Emissions: Lower Nelson River Reservoirs Including CRD 147
Figure 5-9 Modelled Net Reservoir 100-Year Lifecycle GHG Emissions: Lower Nelson River Reservoirs Including CRD (%) 147
Figure 5-10 Modelled Net Reservoir 100-Year Lifecycle GHG Emissions: Lower Nelson River Reservoirs Including CRD and Potential Conawapa (%) 148
Figure 5-11 Modelled Net Reservoir Annual Average Lifecycle GHG Emissions: Lower Nelson River Reservoirs Including 149
Figure 5-12 Lower Nelson River Reservoirs (Including CRD): Cumulative Net Lifecycle GHG Emissions 150
Figure 5-13 Modelled Current Annual Average (2023 – 2027 average) Lower Nelson River Reservoir and CRD GHG Emissions Compared to Manitoba Hydro 2023 Direct Emissions 151
Figure 5-14 Modelled Annual 100-Year Average Full Lifecycle Emission Intensity for the Lower Nelson River Generating Stations Including CRD and Potential Conawapa 153
Figure 5-15 Modelled Lifecycle GHG Emissions for the Lower Nelson River Including Construction, Reservoirs, Other Landuse Change, and Operations 154
Figure 6-1 Modelling Scenarios: Keeyask Reservoir Net Annual Average Lifecycle GHG Emissions (with 95% Confidence Intervals) 163
Figure 6-2 Modelling Scenarios: Keeyask Reservoir Net Annual Average Lifecycle 163
Figure 6-3 Keeyask Reservoir Modelling Scenarios: Net Average Annual Lifecycle GHG Emissions (95% Confidence Intervals) 166
Figure 6-4 Keeyask Reservoir Modelling Scenarios: Lifecycle GHG Emission Intensity (95% Confidence Intervals) 166
Figure 6-5 Ecological Land Classification: Re-class Forest (sub-class bogs) to Wetlands (sub-class bogs) 167
Figure 6-6 Keeyask G-res Pre-Impoundment Landcover Classification: Re-class Bogs from Forest to Wetlands 168
Figure 6-7 Keeyask G-res Model: Comparison of 100-year Annual Average Net GHG Emissions with Bogs Classified as Wetlands or as Forest 169
Figure 6-8 Modelled Keeyask Net Reservoir GHG Intensity: Uncertainty Assessment Comparing Pre-Flood Bogs Classified as Wetlands or Forests 169
Figure 6-9 Comparison of Modelled Net Reservoir GHG Intensity: Accounting for Keeyask Pre-Flood Bogs as Wetlands or Forests 170
Figure 6-10 Kettle G-res Pre-Impoundment Landcover Classification: Re-class Bogs from Forest to Wetlands 171
Figure 6-11 CRD G-res Pre-Impoundment Landcover: Re-class Bogs from Forest to Wetlands 171

Figure 6-12 Lower Nelson River G-res Model: Comparison of Total Lifecycle Net GHG Emissions with Bogs Classified as Wetlands or as Forest 172
Figure 6-13 Total Lifetime GHG Emissions Comparing Keeyask Model to Mean, Upper and Lower Emission Factor Limits (with 95% CI) 174
Figure 6-14 Total Lifecycle Emission Intensity Comparing Keeyask Model to Mean, Upper and Lower Limits of GHG Emission Factors (with 95% CI) 175
Figure 6-15 Comparison of Modelled Keeyask Reservoir Lifecycle GHG Emission Intensity to Other Northern Reservoirs 176

Copyrighted Material

Figure 2 1 Reservoir GHG Processes and Pathways 20
Source: Hertwich, 2013

Net Lifecycle Greenhouse Gas Emissions from Hydroelectric Development on the Lower Nelson River: Implications for Energy Policy

1 Introduction and Rationale

1.1 Introduction

It is imperative for industry, government and society to understand the impact that hydropower development and operation have on carbon cycling and the release of greenhouse gases (GHG) to the atmosphere.

The hydropower industry is operating in a global landscape where climate is changing, temperatures are increasing, extreme weather events are becoming more frequent, energy demand is growing, and energy policy is shifting amongst jurisdictions towards and away from incentivizing investment in low carbon sources of energy generation (IEA, 2025; WMO, 2025; H.ConRes.14-119th Congress, 2025; US Department of the Interior, 2025; IPCC, 2023; Canadian Net-Zero Emissions Accountability Act S.C. 2021, c. 22).

The Intergovernmental Panel on Climate Change (IPCC, 2023) concluded that human activities are responsible for the 1.1^{o}C rise in global surface temperatures during 2011-2020 as compared to pre-industrial times (1850-1900), primarily through the release of GHGs. Energy use, land-use and land-use change are amongst the human activities cited as contributing to global climate change. There is an estimated 70% chance that the average annual global temperature increase will exceed 1.5^{o}C during 2025-2029 over pre-industrial levels (WMO, 2025). The IPCC urges that the increase in global warming be

limited to 1.5°C above pre-industrial times to minimize the risk that climate change may have on natural and human systems (IPCC, 2018). Constraining the average annual global temperature increase to 1.5°C above pre-industrial times is also a goal established by the 195 Parties who signed the United Nations Framework Convention on Climate Change (UNFCCC) 2015 Paris Agreement, which includes Canada (UNFCCC, 2026a).

Low carbon energy sources will be integral to meet future energy demands and combat the effects of climate change. The Government of Canada has committed to achieve a national target of net-zero GHG emissions by 2050 through the passing of the Canadian Net-Zero Emissions Accountability Act (S.C. 2021, c. 22). The Province of Manitoba endeavours to achieve a net-zero electricity grid by 2035 and a carbon neutral economy by 2050 (Government of Manitoba, 2025).

Many jurisdictions (including Canada and Manitoba), industries and research institutions are looking towards increased electrification as one of the pathways towards decarbonizing the economy and minimizing GHG emissions (Zhou and Mai, 2021; Electrifying Canada, 2022a, 2022b; Hamlin and Zhang, 2024; Canadian Energy Regulator, 2025; Dunsky Energy + Climate Advisors, 2025; IEA, 2025; Natural Resources Canada, 2026). Electricity producers will have to demonstrate that their carbon footprint qualifies as being part of the climate change solution. Industry must have scientifically defensible techniques to measure carbon cycling and greenhouse gas emissions, to develop current emission inventories and to predict future emissions. GHG quantification methods and reported results must be transparent. Global corporate GHG accounting and reporting standards are being revised (World Resources Institute & World Business Council for

Sustainable Development, 2025a, 2025b), corporate GHG reporting is under public scrutiny for uncertainty, incompleteness, inaccuracy and corporate accountability (Salo et al., 2024; Jiang et al., 2025; Richer, 2025), and governments are starting to regulate the disclosure of environmental and climate change information, such as through amendments to the Canadian Competition Act (R.S.C., 1985 c. C-34).

1.2 Rationale

Reservoir GHG emissions are not well constrained globally (Deemer & Holgerson, 2019; Harrison et al., 2021; Rosentreter et al., 2021). Worldwide reservoir GHG emissions have been modelled to be significant at 1,076 $TgCO_2e\ km^{-2}\ yr^{-1}$ with the highest emissions coming from the tropics and sub-tropics (Harrison et al., 2021). Earlier global estimates have ranged from 741 – 3,380 $TgCO_2e\ km^{-2}\ yr^{-1}$ (St. Louis et al., 2000; Deemer et al., 2016). DelSontro et al. (2018) concluded that global GHG emissions from lakes and reservoirs combined could equal nearly 20% of the CO_2 emissions generated annually from fossil fuel combustion.

In Canada, there has been extensive research in Québec to understand reservoir GHG processes, emission pathways and to model provincial GHG emissions from hydroelectric reservoirs (Demarty and Tremblay, 2019; Levasseur et al., 2021; Prairie et al., 2023; Barbosa et al., 2023, 2025; del Giorgio et al., 2023, 2025; Demarty et al., 2026). Published studies of hydroelectric reservoir GHG research is more limited from other locations in Canada (Tremblay et al., 2005a; Demarty et al., 2009; Gedig et al., 2025). GHG measurements are currently being conducted at the newly created Keeyask reservoir on the Nelson River in northern Manitoba (Manitoba Hydro, 2023), at the Nááchę Mege

reservoir (formerly referred to as Site C reservoir) on the Peace River in northeastern B.C. (BC Environmental Assessment Office, 2026) and through a Canada-wide study of hydroelectric and non-hydro reservoirs (Prairie et al., 2025).

Although the scientific community and industry have been working diligently to quantify GHG emissions resulting from hydropower reservoirs, including over two decades of studies conducted within Canada, uncertainties remain in terms of emission processes and trajectory and modelling approaches (Goldenfum, 2010, 2012; Deemer et al., 2016; Levasseur et al., 2021; Soued et al., 2022; Barbosa et al., 2023; Bastviken and Johnson, 2025).

1.3 Land Acknowledgement

Although this thesis discusses reservoirs in terms of km^2 and ranks reservoirs as being small, intermediate and large, we must never forget the impact that flooding and land use change has on northern Manitoba Indigenous communities. The landscape has been changed forever. What took generations to learn, experience and understand has now been lost (Pawlowska-Mainville and Massen, 2022).

1.4 Thesis Overview

This thesis models pre-impoundment, post-impoundment and net 100-year lifecycle GHG emissions for the recently created Keeyask hydroelectric reservoir located on the Nelson River in northern Manitoba, Canada. The thesis also modelled both net 100-year lifecycle GHG emissions and net GHG emissions for the remaining life of all hydroelectric reservoirs on the lower Nelson River, including a hypothetical future hydroelectric reservoir.

To this author's knowledge, this is the first time net lifecycle GHG emissions have been modelled for the lower Nelson River reservoirs. The methods used to develop GHG lifecycle emissions could serve as a template for modelling current and future reservoir GHG emissions for the remainder of Manitoba Hydro's hydraulic system. The results of this thesis could become a key component for calculating the GHG emission intensity (e.g., tCO_2e/GWh) of the Manitoba electricity grid. GHG emission intensity is a metric used by energy and climate change policymakers, the energy industry and by the public for comparing the carbon footprint of electricity generating sources and electrical grids worldwide.

Modelling limitations and uncertainties are identified when applying the model to northern peatland reservoirs. Recommendations are made regarding further in-situ reservoir GHG measurements to improve model calibration and model design.

1.5 Objectives

The objectives of this research are to:

1) Estimate baseline, pre-impoundment GHG emissions within the footprint of the Keeyask reservoir.
2) Estimate, using models, net lifecycle GHG emissions for the Keeyask reservoir.
3) Estimate, using models, net lifecycle reservoir GHG emissions for hydroelectric development on the lower Nelson River, including current and potential hydroelectric development.
4) Assess the net carbon footprint of hydroelectric reservoirs on the lower Nelson River in terms of climate change and energy policy.

1.6 Thesis Structure

Chapter 1: Introduction and Rationale

Chapter 2: Literature Review: Reservoir GHG Science and Implications for Reservoir GHG Modelling

Chapter 3: Methods

Chapter 4: Net Lifecycle GHG Emissions for the Keeyask Hydroelectric Reservoir

Chapter 5: Net Lifecycle GHG Emissions for Hydroelectric Reservoirs on the Lower Nelson River

Chapter 6: Uncertainty Analysis

Chapter 7: GHG Implications of Hydroelectric reservoirs on the Lower Nelson River in Terms of Climate Change and Energy Policy

Chapter 8: Conclusions

Chapter 9: Recommendations

References

Appendices

2 Literature Review: Reservoir GHG Science and Implications for GHG Modelling

GHGs are produced and exchanged naturally within and amongst terrestrial and freshwater ecosystems and with the atmosphere (Cole et al., 2007; Prairie and Cole, 2009; Bastviken et al., 2015; Hessen et al., 2017).

Flooding land and waterways to create hydroelectric reservoirs has the potential to generate a GHG emission footprint that differs from the pre-flood landscape (Prairie et al., 2021). Impounding land transforms a terrestrial ecosystem into an aquatic or semi-aquatic system, which impacts carbon cycling processes and GHG emission profiles (Hendzel et al., 2005; Tremblay et al., 2005a; Prairie et al., 2018; Wang et al., 2023). Similarly, flooding aquatic systems can potentially alter carbon and nitrogen cycling and GHG emissions in the post-flood aquatic system (Hertwich, 2013); Wang et al., 2023). The resultant reservoir GHG footprint may differ in terms of the magnitude and type of GHGs emitted, the location of GHG emissions within the watercourse, the timing of emissions, and the dominant GHG emission pathways (Barros et al., 2011; Teodoru et al., 2011; Wang et al., 2018; Demarty & Tremblay, 2019; Rust et al., 2022).

It is essential that a lifecycle model be able to simulate the GHG emissions profile of both the pre-flood and post-flood landscape to predict net GHG emissions. This requires an understanding of the main processes that are cycling carbon on land and in the aquatic environment and the pathways that are releasing GHG emissions to the atmosphere before and after flooding. This knowledge is necessary to evaluate a lifecycle model's

applicability for the reservoir(s) in question, and to assess the uncertainty of the modelling results.

The sections below review reservoir GHG science as it relates to lifecycle GHG modelling with a focus on northern reservoirs.

2.1 Hydroelectric Reservoirs and Potential GHG Impacts

Early research (approximately 1993 – 2003) of Canadian boreal reservoirs indicated there can be a temporary pulse of CO_2 and CH_4 emissions following reservoir flooding, but after about 10 years reservoir GHG emissions are similar to those of the surrounding natural aquatic systems (Tremblay et al., 2005a, 2005b). It was noted by Tremblay et al. (2005a, 2005b) that these conclusions were based on small-scale and short-term studies. Similarly, early studies indicated that CO_2 diffusive emissions were the dominant GHG pathway for northern reservoirs and CH_4 emissions were less significant (Bastien et al., 2011; Demarty et al., 2011; Teodoru et al., 2012).

Contemporary research refines those early conclusions, as illustrated by the following examples. Paix des Braves (formerly Eastmain-1) reservoir, Québec, is one of the most extensively studied northern reservoirs in the world (Teodoru et al., 2012, Demarty and Tremblay, 2019; Demarty et al., 2026). The Paix des Braves reservoir was a large but declining net source of CO_2 emissions during the first three years following impoundment (Teodoru et al., 2012). Based on 17 years of post-flood monitoring (2005 – 2022), CO_2 emissions continued to decline and they may take longer than 20 years to reach background/natural levels (Demarty et al., 2019; 2026). In contrast, CO_2 surface concentrations from the deep reservoirs RO2 and RO3 of La Romaine complex, Québec,

remained relatively stable during the first 4 and 2 post-flood years, respectively (Rust et al., 2022).

There is less certainty regarding the magnitude and duration of CH_4 emissions, especially if flooding involves permafrost landscapes (Barros et al., 2011; Teodoru et al., 2012; Deemer et al., 2016). Post-flood CH_4 emissions have demonstrated different emission trajectories than CO_2 in some of Canada's northern reservoirs. CH_4 diffusive emissions were very low at the Paix des Braves reservoir and did not demonstrate a pattern during the seventeen-year post-flood measurement period (Demarty & Tremblay, 2019; 2026). This may be due to limited anoxic zones and methane oxidation in the well mixed, well oxygenated, cold northern reservoirs (Teodoru et al., 2012; Demarty & Tremblay, 2019). Methane concentrations in the La Romaine reservoirs were low in the first post-flood year and were stable afterwards (Rust et al., 2022).

Boreal reservoirs have been observed to have lower GHG emissions than reservoirs located in the lower latitudes of the sub-tropics and tropics because of their colder climate and winter ice cover (Harrison et al., 2021; Soued et al., 2022). The lower temperatures tend to slow down the microbial decomposition of flooded biomass and the production of GHGs (St. Louis et al., 2000; Gudasz et al., 2010; DelSontro, et al., 2016b)

2.1.1 Reservoir Processes and GHG Emission Pathways

Impounding land and flooding waterways to create reservoirs can affect GHG processes in many ways (Tremblay et al., 2005b; Goldenfum, 2010; Barros et al., 2011; Hertwich et al., 2013; Deemer et al., 2016; Prairie et al., 2018, 2021; Kumar et al., 2019; Li et al., 2019; Rust et al., 2022; Zhu et al., 2025):

- Replacing the pre-flood terrestrial GHG processes with aquatic GHG processes.
- Flooding land and wetlands, which drown plants and soils. A portion of the readily available (labile) organic carbon stored in the plants and primarily in the flooded soils, decomposes through microbial degradation and photooxidation, releasing CO_2 and/or CH_4 to the atmosphere. CO_2 is primarily produced in oxic environments, and CH_4 and CO_2 is produced in anoxic environments.
- A large, but poorly defined, proportion of CH_4 produced in reservoir sediments can be oxidized to CO_2 before evading to the atmosphere (and emitted to the atmosphere as CO_2 rather than CH_4).
- The type of flooded land (e.g., wetlands, shrubs, etc.) can lead to varying rates of GHG production.
- Flooding can change hydrology, which can affect water depth, temperatures in the water column and sediments, which can increase microbial decomposition rates and production of GHGs.
- Decreasing water velocity and increasing water residence time in a reservoir can provide more time for microbial decomposition and primary production within the reservoir and increase GHG production and emissions to the atmosphere. This affects i) the decomposition of flooded organic matter and ii) the decomposition of organic matter transported into the reservoir from upstream, laterally and through ground water.
- Altering water chemistry by introducing nutrients from flooded land can change GHG production and emission characteristics.

- Changing the ice regime could lead to more open water and a change in water temperature.
- Creating anoxic aquatic zones, either through impacting thermal stratification in the water column, or by creating shallow littoral zones.
- Introducing a new emission pathway, degassing, as water exits the powerhouse and spillway.

2.1.1.1 GHG Pathways

Reservoirs can emit GHGs through diffusive flux, methane sediment ebullition, degassing, downstream transport, and flux through aquatic/emergent/floating vegetation (Figure 2-1) (Scott et al., 1999; St. Louis et al., 2003; Hertwich, 2013; Wang et al., 2018).

2.1.1.1.1 Diffusive Fluxes

Diffusive fluxes are the two-way exchange of gases at the reservoir water/air boundary and have been observed to be a principal emission pathway for some boreal reservoirs (Tremblay et al., 2010; Bastien et al., 2011; Demarty et al., 2011). Diffusion is the movement of gas from a high concentration to a lower concentration and the gas exchange is a function of the gas concentration gradient, wind (speed, fetch and shear), thermal convection and heat loss, and waterbody morphology (slope, discharge, velocity, roughness, etc.), all of which are influenced by site-specific reservoir conditions (Bade, 2009; Cole et al., 2010; Huotari et al., 2013; Vachon & Prairie, 2013).

2.1.1.1.2 Methane Ebullition

Methane ebullition refers to the release of methane bubbles from reservoir sediments into the water column (DelSontro et al., 2015). Methane concentrations build-up in sediment pore water as microbes decompose organic material in anoxic sediments (Joyce & Jewell, 2003; McClure et al., 2020). Methane ebullition is temperature dependent, that is, warmer temperatures can increase methane production and bubble growth (Maeck et al., 2014; Männistö et al., 2019). Ebullition occurs intermittently, varying in location and time, making it challenging to measure (Ostrovsky et al., 2008; DelSontro et al., 2015). Bubble release can be triggered by a decrease in hydrostatic pressure, decrease in water levels, low water levels, decrease in atmospheric pressure, a change in temperature which can change CH_4 solubility, turbulent energy applied to sediments, and shear stress (Maeck et al., 2014; DelSontro et al., 2016a; Männistö et al., 2019).

Ebullition can be associated with the shallow zones of the reservoir (approximately less than 3 m deep) where bubble partial pressure exceeds the pressure of the overlying water column and atmosphere, allowing bubbles to rise (DelSontro et al., 2010; 2015; 2016a; Prairie et al., 2021).

Methane ebullition has been observed to be a dominant GHG emission pathway in some temperate and tropical reservoirs (DeSontro et al., 2010, 2011), is of growing interest in northern waters (DelSontro et al., 2016; Wik et al., 2018; Engram et al., 2020), and is actively being measured in Canadian reservoirs (Prairie et al., 2023, 2024).

2.1.1.1.3 Aquatic/Emergent/Floating Vegetation

2.1.1.1.3.1 Macrophytes

Many wetland plants have adapted a strategy to transport oxygen from the atmosphere through their internal tissues into their root zone (Villa et al., 2020). This same mechanism can transport CH_4 from anoxic sediment porewater, through the rhizosphere and through plant internal tissues to the atmosphere (Villa et al., 2020). This "chimney effect" can account for over half of the methane emitted from some wetlands (Bhular et al., 2013). Through this process, CH_4 can avoid oxidation by bypassing oxic zones in the upper sediment layers and in the water column. 30% to 40% of the oxygen that is transported from the atmosphere through the plant "chimney" can diffuse into the rhizosphere, creating a substrate for methanotrophic bacteria and methane oxidizing conditions (Stepniewska et al., 2014).

2.1.1.1.3.2 Floating / Semi-Submerged Peat

Floating peat islands occur naturally around the world and have been observed for millennia (Zaccone et al., 2017). They resulted after building the Churchill River Diversion (CRD) and impounding Stephens Lake in northern Manitoba (Keeyask Hydropower Limited Partnership, 2012a), when creating the Keeyask reservoir (Manitoba Hydro, 2024), and when flooding other northern peatlands for hydroelectric development (Rönkä & Uusinoka,1976; St. Louis et al., 2003; Momcilovic-Petronijevic et al., 2009).

Studies at the Experimental Lakes Area (ELA) in northwestern Ontario have helped to gauge the range of potential emissions and understand the processes that generate and emit GHGs from floating peat (St. Louis et al., 2003). The ELA studies measured CH_4

emissions from floating peat islands to be higher than: 1) the flooded, submerged peat, 2) open reservoir water, and 3) the pre-flood peatlands (Scott et al., 1999; Saquet, 2003). CH_4 emission rates from the main peat islands and eroded island pieces were similar, which helps to simplify estimating GHG emissions (St. Louis et al., 2003). The cause of the buoyant peat and elevated CH_4 emissions involved a rise of water level within the peat substrate (St. Louis et al., 2003). The rise in water level increases the size of the anoxic zone, which in turn fosters methanogenesis and methane production (Kelly et al., 1997). Methane bubbles generated in the peat substrate lift the peat to the water surface (Scott et al., 1999). Reservoir water circulated under the floating peat and warmed the peat substrate which promoted methane production (Scott et al., 1999). The water level within the islands was close to the surface of the peat. This minimized the size of the aerobic zone above the water table resulting in less oxidation of CH_4 as CH_4 travels through the peat layers to the atmosphere (Scott et al., 1999). This led to a higher portion of emissions being released as CH_4 as opposed to CO_2 (Scott et al., 1999; St. Louis et al., 2000).

In spite of the early research conducted at ELA, emissions from floating peat are not well constrained and remain a current gap in reservoir GHG science and emission accounting.

A GHG lifecycle model should be evaluated in terms of how well it can simulate the impacts of floating/semi-submerged peat and aquatic vegetation on GHG emissions, and other complex shallow water biological processes.

2.1.1.1.4 Degassing and Downstream Emissions

2.1.1.1.4.1 Degassing Emissions

Degassing refers to dissolved gases that are released during the turbulent process of water passing through the hydroelectric generating station turbines and spillway (Goldenfum, 2010). The concept underpinning this emission pathway is that gases that are supersaturated within the reservoir water will be released due to pressure differences between the water and atmospheric concentrations when passing through the turbines or being spilled downstream. Degassing can potentially be an important source of emissions if a generating station draws water from an anoxic layer of the reservoir water column and releases CH_4 directly to the atmosphere when these gases may have otherwise been subject to aquatic methane oxidation and released as CO_2 (IPCC, 2019; Prairie et al., 2021).

Methods have been developed for calculating degassing emissions, where the difference between GHG concentrations in water upstream and downstream of the powerhouse/spillway are multiplied by the reservoir outflow (Goldenfum, 2010). Some lifecycle GHG models include CH_4 degassing emissions but have not yet incorporated CO_2 degassing emissions (Prairie et al., 2021). Degassing emission estimation methods continue to be reviewed by the by the scientific community (Prairie, 2025).

2.1.1.1.4.2 Downstream Emissions

Emissions may occur downstream of degassing that result from the reservoir discharging dissolved and particulate organic carbon that are attributable to the reservoir (Goldenfum, 2010). This may result in downstream diffusive and ebullition emissions, or

eventual flow into a receiving waterbody, in the case of Keeyask that would ultimately be Hudson Bay, but more locally Stephens Lake.

This pathway should be considered when modelling peatland reservoirs, such as the Keeyask reservoir, as floating peat mats occur in the reservoir (Manitoba Hydro, 2025a) and peat particulates could be transported downstream.

2.1.1.2 Nitrous Oxide (N_2O) Emissions

The G-res Tool does not model net reservoir lifecycle nitrous oxide N_2O emissions (Prairie et al., 2017).

Nitrous oxide (N_2O) is produced from the microbial decomposition of organic matter through nitrification (ammonia oxidation and denitrifier denitrification) and nitrate dissimilation (denitrification and nitrite ammonification), and chemo-denitrification (Baggs, 2008; Wrage-Mönnig et al., 2018). Microbial decomposition is conducted by archaea, bacteria and fungi whose diversity appears to vary with latitude (increased archaea diversity towards low latitudes and increased bacteria diversity in mid-latitudes), and temperature (fungi diversity peaks when mean annual temperatures range between 10°C – 15°C) (Bahram et al., 2022). N_2O production occurs in soils, sediments, freshwater lakes, rivers and reservoirs, and oceans (Bernhard et al., 2010; Deemer et al., 2016; DelSontro et al., 2018); in aerobic and anaerobic environments (Khalil et al., 2004; Seitzinger et al., 2006). N_2O is a potent GHG with a 100-year global warming potential of 273 CO_2e (Smith et al., 2021).

A recent study has modelled N_2O to comprise more than 80% of total emissions from 79 reservoirs in China (Chen et al., 2025). The source of nitrogen was attributed to

agriculture and industry inputs to the watersheds. Reservoirs older than 50 years were the highest emitters, as sediments accumulated over time and underwent nitrification and denitrification and N_2O production (Chen et al., 2025). Shi et al. (2020) observed increased N_2O production in reservoir littoral zones where water level fluctuations caused wetting and drying cycles. Wu et al. (2020) observed elevated N_2O emissions where reservoirs were discharging water from the bottom of the reservoirs where dissolved concentrations of N_2O were high. Factors contributing to elevated N_2O concentrations included reservoir age, where reservoirs older than 10 years had large stores of organic matter, discharges of domestic sewage into the watershed near the reservoir, and aquaculture operations in the reservoir (Wu et al., 2020).

Wang et al. (2023) modelled a global increase in N_2O emissions from inland freshwaters from 1900 to 2010. The highest N_2O contribution was modelled to come from within and downstream of reservoirs and in southern Asia, southeast North America and Europe where the population density is high and there is intense agricultural activity. Elevated N_2O emissions were associated with nitrification in the water column and denitrification in the reservoir sediments. Organic material that accumulated in the reservoirs is decaying, the decay processes use oxygen and create low-oxygen and hypoxic conditions. This is facilitating incomplete nitrification and denitrification, resulting in N_2O production. The study associates these conditions with increased human populations, intensifying agriculture and increased wastewater discharges that are loading nitrogen into freshwaters (Wang et al., 2023). The model also indicated that northern latitudes, including the Nelson River, had low N_2O emissions and some of these waters were

modelled to be N_2O sinks. In these northern waters, the low water temperatures limit N_2O production and increases N_2O solubility, and nitrogen inputs from the surface waters were modelled to be low (Wang et al., 2023).

A study involving 773 N_2O fluxes from 122 lakes, 24 rivers, 4 estuaries and 55 anthropogenic reservoirs from 1993 to 2003 in the boreal region of Canada concluded that gross N_2O emissions from reservoirs were within the same range as natural lakes and rivers (Trembley et al., 2005).

The Flooded Upland Dynamics Experiment (FLUDEX) at ELA yielded similar results as those discussed above for boreal Canada. Three experimentally flooded reservoirs acted as slight N_2O sinks (Hendzel et al., 2005). The suggested reasons for the N_2O sink were that the flooded landscape contained low amounts of nitrates (NO_3^-) to decompose and release N_2O; and there were low O_2 concentrations in the flooded soils and therefore N_2O was consumed as an electron acceptor in the decomposition (denitrification) processes (Hendzel et al., 2005).

Three years of post-flood measurements at the Eastmain-1 hydroelectric reservoir in Quebec concluded there was no significant difference in N_2O emissions after flooding (Tremblay et al., 2009).

Reservoir N_2O emissions have not been well-constrained (Goldenfum, 2012; Wu et al., 2020; Li et al., 2023). Although it appears that reservoir N_2O emissions may be low unless there are significant influxes of nitrogen from the watershed (Tremblay et al., 2010), it would be beneficial to measure in-situ N_2O emissions from the young Keeyask reservoir and the mature Kettle reservoir, the largest of the lower Nelson River reservoirs, to confirm

their N_2O emissions. Goldenfum (2010) identifies methods to measure the three forms of nitrogen (ammonium NH_4^+, nitrites NO_2^-, nitrates NO_3^-) that can be transformed into N_2O, and techniques to measure reservoir N_2O fluxes. N_2O emissions can vary significantly amongst wetland types and soils (Crestey-Chury et al., 2025) and by season (Kortelainen et al., 2019).

2.1.1.3 Synthesis of Hydroelectric Reservoirs and GHG Impacts

All of the emission pathways described above (i.e., diffusion, ebullition, emissions from vegetation, degassing and downstream) and gas species (CO_2, CH_4 and N_2O) should be considered when evaluating and selecting a GHG lifecycle model for the reservoirs of the lower Nelson River. How well does the model represent each of these pathways and gas types over time, especially the complex littoral zones where there are semi-submerged vegetation and re-surfaced peat mats? Similarly, how well does the model represent emissions from the complex pre-flood landscape, largely dominated by soil carbon-rich peatland systems?

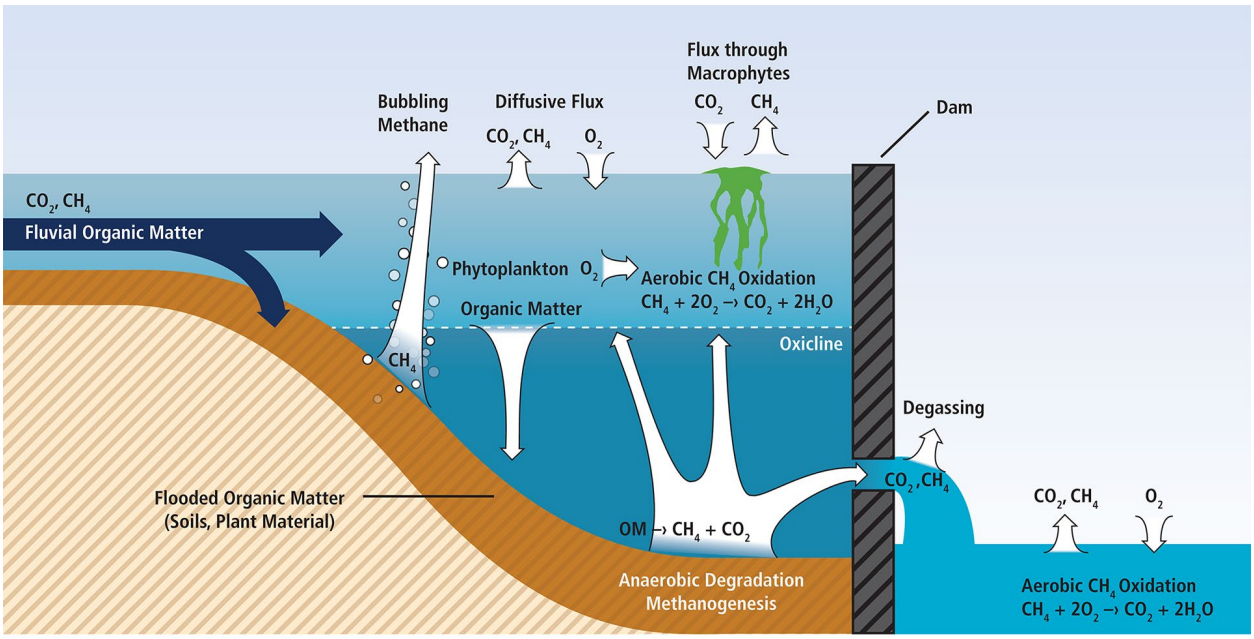


Figure 2-1 Reservoir GHG Processes and Pathways
Source: Hertwich, 2013

2.2 Overview of Reservoir GHG Modelling

Models have been used to estimate reservoir GHG emissions globally, regionally, for provincial electricity-grids, and for individual reservoirs. They have been used to estimate current emissions and to forecast future emissions. Model types vary and continue to evolve. Reservoir GHG models include those that: apply GHG emission factors to estimate reservoir-wide emissions (Briones Hildrovo et al., 2017; IPCC, 2019), use year-to-year reservoir GHG measurements to extrapolate future emissions, such as developing an exponential decay model (Teodoru et al., 2012); assess the change in carbon stock within the reservoir system over time (Bernardo et al., 2017); assess the biogeochemical processes that produce GHG emissions (e.g. physical models/process models) (Wang et al., 2018); develop statistical relationships amongst reservoir attributes and GHG

emissions (e.g. semi-empirical models, regression tress, etc.) (Beaulieu et al., 2020; Prairie et al., 2021) to estimate current and project future GHG emissions.

These models have advanced our collective understanding of the spatial and temporal impact that creating reservoirs has on carbon cycling, the biogeochemical processes that produce reservoir GHG gases, the pathways that release GHG emissions to the atmosphere, the mechanisms that store carbon in reservoirs, and the methods that transport carbon downstream.

2.2.1 Reservoir GHG Lifecycle Modelling

Not all of the model types mentioned above are capable of estimating GHG emissions over the lifecycle of the reservoir, and not all are capable of estimating net lifecycle emissions. Net reservoir GHG emissions refer to the incremental change in post-flood GHG emissions as compared to pre-flood GHG emissions. Net emissions are defined as Gross GHG emissions (post-flood) minus Baseline (pre-flood) GHG emissions. It is essential that a reservoir GHG lifecycle model be able to represent the GHG emissions profile of the pre-flood landscape, predict post-flood emissions and forecast the incremental change.

Estimating reservoir GHG lifecycle emissions requires an understanding of the main processes that are cycling carbon on land and in the aquatic environment, and the pathways that are releasing GHG emissions to the atmosphere before and after flooding. It is important to understand if a model is capable of representing the reservoir(s) to be modelled and to assess the uncertainty of the modelling results. That is, how well has the

model been calibrated for the reservoir(s) to be examined and how accurate are the results.

Reservoir GHG lifecycle emissions are typically modelled over a 100-year lifespan of the reservoir (Levasseur et al., 2021). Emissions may be calculated by individual emission pathways (e.g. diffusion, ebullition, degassing, etc.) and by gas type (e.g., CO_2, CH_4, N_2O) for the entire 100-year period and for groups of years or individual years (Prairie et al., 2021). Lifecycle models may produce metrics, such as emission intensity, which compares the amount of net GHG emissions per unit of energy output (e.g. tCO_2e/GWh) and power density (e.g. W/m^2) which is the ratio of the installed capacity of the generating station (e.g. MW) to the total reservoir surface area (Prairie et al., 2017). Lifecycle GHG emission estimates and metrics enable GHG comparisons amongst hydroelectric reservoirs and amongst other forms of electricity production (NREL, 2021).

The section below reviews the state of reservoir GHG models and projections.

2.2.2 Review of Reservoir GHG Models

Each of the studies referenced below has helped to advance the understanding of reservoir GHG science and reservoir GHG modelling (Table 2-1). In terms of lifecycle assessment, the models were reviewed for their ability to predict net lifecycle GHG emissions over the 100-year engineered lifetime of the generating station/reservoir, completeness of GHG types projected by the model (i.e. CO_2, CH_4, N_2O), completeness of GHG emission pathways projected by the model (i.e. diffusion, ebullition, exchange by submerged or floating vegetation, degassing, downstream), and ability to model pre-flood GHG emissions for the reservoir footprint.

Table 2-1 Reservoir GHG Model Review

GHG Model Review
Global Models / Global Studies
Barros et al., 2011 Global estimates of reservoir GHG emissions were estimated by gas type (CO_2 and CH_4) by developing GHG emission rates by climate zones (mg Cm^{-2} d^{-1}) and multiplying emission rates by reservoir area. Regression analysis was used to correlate reservoir parameters (e.g. age and latitude) to GHG emissions. 🔴 Ability to Forecast Net Reservoir GHG Lifecycle Emissions 🟡 Completeness of Gas Types (e.g. CO_2, CH_4, N_2O) 🟡 Completeness of GHG Pathways 🔴 Ability to Model Pre-flood Emissions
Hertwich, 2013 Developed a multiple linear regression (MLR) equation to estimate global GHG emissions from hydropower. Correlated CH_4 fluxes per reservoir area with Net Primary Production and reservoir age. Estimated global CO_2 and CH_4 intensity per unit of electricity output (g kWh). 🔴 Ability to Forecast Net Reservoir GHG Lifecycle Emissions 🟡 Completeness of Gas Types (e.g. CO_2, CH_4, N_2O) 🟡 Completeness of GHG Pathways 🔴 Ability to Model Pre-flood Emissions
Li and Zhang, 2014 Estimated global CO_2 and CH_4 emissions with the addition of emissions from the drawdown zone (based on a regression equation) and degassing (based on a formula comparing upstream and downstream emissions and water flow). 🔴 Ability to Forecast Net Reservoir GHG Lifecycle Emissions 🟡 Completeness of Gas Types (e.g. CO_2, CH_4, N_2O) 🟡 Completeness of GHG Pathways 🔴 Ability to Model Pre-flood Emissions
Deemer et al., 2016 Estimated global CO_2, CH_4 and N_2O reservoir emissions based on a regression model. Reservoir productivity was found to be a strong predictor of emissions. 🔴 Ability to Forecast Net Reservoir GHG Lifecycle Emissions 🟡 Completeness of Gas Types (e.g. CO_2, CH_4, N_2O) 🟡 Completeness of GHG Pathways 🔴 Ability to Model Pre-flood Emissions

Scherer and Pfister, 2016

Estimated global average GHG emission intensity for CO_2 and CH_4 by latitude using linear models and predictor variables (generalized linear modeling – GLM).

- 🔴 Ability to Forecast Net Reservoir GHG Lifecycle Emissions
- 🟡 Completeness of Gas Types (e.g. CO_2, CH_4, N_2O)
- 🟡 Completeness of GHG Pathways
- 🔴 Ability to Model Pre-flood Emissions

DelSontro et al., 2018

Estimated global lake and reservoir CO_2, CH_4 and N_2O emissions. Multivariate models (Size-Productivity Model - SPM) were developed for each GHG type based on predictor variables (lake/reservoir size, CHl *a*, TP and TN) from a lake/database developed by the authors, and upscaled the models to the global population of lakes and reservoirs.

- 🔴 Ability to Forecast Net Reservoir GHG Lifecycle Emissions
- 🟢 Completeness of Gas Types (e.g. CO_2, CH_4, N_2O)
- 🟡 Completeness of GHG Pathways
- 🔴 Ability to Model Pre-flood Emissions

Harrison et al., 2021

Used the G-res Tool to estimate global reservoir CO_2 and CH_4 emissions by emission pathway and latitude.

- 🟢 Ability to Forecast Net Reservoir GHG Lifecycle Emissions
- 🟡 Completeness of Gas Types (e.g. CO_2, CH_4, N_2O)
- 🟡 Completeness of GHG Pathways
- 🟢 Ability to Model Pre-flood Emissions

Li and He, 2022

Modelled global reservoir GHG emissions (CO_2, CH_4, and N_2O) by biome (tundra, boreal, temperate and tropics) and by reservoir size using a global lake and reservoir database developed by DelSontro et al., (2018) and empirical models based on Chl *a* and TP concentrations.

- 🔴 Ability to Forecast Net Reservoir GHG Lifecycle Emissions
- 🟢 Completeness of Gas Types (e.g. CO_2, CH_4, N_2O)
- 🟢 Completeness of GHG Pathways
- 🔴 Ability to Model Pre-flood Emissions

Soued et al., 2022

The G-res Tool was used to model global CO_2 and CH_4 reservoir lifecycle GHG from 1900 – 2060.

- 🟢 Ability to Forecast Net Reservoir GHG Lifecycle Emissions
- 🟡 Completeness of Gas Types (e.g. CO_2, CH_4, N_2O)
- 🟡 Completeness of GHG Pathways
- 🟢 Ability to Model Pre-flood Emissions

Regional Analysis
Räsänen et al., 2018 Applied the linear regression model of Scherer and Pfister, (2016) to estimate gross CO_2 and CH_4 emissions from 141 existing and planned reservoirs on the Mekong River Basin in Southeast Asia over 100 years. Applied the Hertwich, (2013) model to estimate CO_2 emission intensity, and applied the Scherer and Pfister, (2016) model to estimate the CH_4 emission intensity of the reservoirs. 🔴 Ability to Forecast Net Reservoir GHG Lifecycle Emissions 🟡 Completeness of Gas Types (e.g. CO_2, CH_4, N_2O) 🟡 Completeness of GHG Pathways 🔴 Ability to Model Pre-flood Emissions
Li et al., 2019 Modelled net reservoir GHG lifecycle emissions for the 5 largest hydroelectric projects in China using the G-res tool. 🟢 Ability to Forecast Net Reservoir GHG Lifecycle Emissions 🟡 Completeness of Gas Types (e.g. CO_2, CH_4, N_2O) 🟡 Completeness of GHG Pathways 🟢 Ability to Model Pre-flood Emissions
Beaulieu et al., 2020 Measured CO_2 and CH_4 diffusive and ebullition rates from 32 reservoirs located along an agriculture-forest gradient in the USA. Boosted regression trees (machine-learning algorithms) were used to identify variables to predict emission rates (e.g. reservoir morphology, CHl *a* and TP). Models could be trained to upscale results to other US reservoirs. The study did not estimate lifecycle emissions. 🔴 Ability to Forecast Net Reservoir GHG Lifecycle Emissions 🟡 Completeness of Gas Types (e.g. CO_2, CH_4, N_2O) 🟡 Completeness of GHG Pathways 🔴 Ability to Model Pre-flood Emissions
Levasseur et al., 2021 The G-res Tool was used to model net lifecycle GHG emissions for all Québec reservoirs, and the GHG intensity of the Québec electricity grid. G-res results were compared lifecycle modelling results using generic gross literature values of (Hertwich, 2013; Deemer et al., 2016; Scherer and Pfister, 2016), a generic net Product Category Rules approach, net extrapolation of an Eastmain-1 decay model (Teodoru et al., 2012), gross emission factor approach for <10 years and & 10-100 years (IPCC, 2006 inspired approach), and gross emission factors developed from Québec reservoirs. 🟢 Ability to Forecast Net Reservoir GHG Lifecycle Emissions 🟡 Completeness of Gas Types (e.g. CO_2, CH_4, N_2O)

🟡 Completeness of GHG Pathways 🟢 Ability to Model Pre-flood Emissions
Hansen et al., 2022 The G-res Tool was used to estimate net lifecycle GHG emissions from 28 reservoirs within the USA, covering all ecoregions. 🟢 Ability to Forecast Net Reservoir GHG Lifecycle Emissions 🟡 Completeness of Gas Types (e.g. CO_2, CH_4, N_2O) 🟡 Completeness of GHG Pathways 🟢 Ability to Model Pre-flood Emissions
Reservoir-Specific
Teodoru et al., 2012 Applied a 1st order decay model based on the first 4 years of post-flood CO_2 and CH_4 measured emissions from the Eastmain-1 reservoir, Québec, to estimate net 100-year lifecycle emissions for the reservoir. 🟢 Ability to Forecast Net Reservoir GHG Lifecycle Emissions 🟡 Completeness of Gas Types (e.g. CO_2, CH_4, N_2O) 🟡 Completeness of GHG Pathways 🟢 Ability to Model Pre-flood Emissions
Bernardo et al., 2017 Applied a change in carbon stock method to the Capivari Reservoir, Brazil. 🔴 Ability to Forecast Net Reservoir GHG Lifecycle Emissions 🟡 Completeness of Gas Types (e.g. CO_2, CH_4, N_2O) 🟡 Completeness of GHG Pathways 🟢 Ability to Model Pre-flood Emissions
Briones Hildrovo et al., 2017 Calculated net lifecycle emissions for the Mazar-Dudas (run-of-river) and Baba Hydropower Schemes, Ecuador by: applying literature values to estimate reservoir GHG emissions and the loss of primary production from the flooded land; allocated a percentage of reservoir emissions to estimate degassing and downstream emissions. 🟢 Ability to Forecast Net Reservoir GHG Lifecycle Emissions 🔴 Completeness of Gas Types (e.g. CO_2, CH_4, N_2O) 🟡 Completeness of GHG Pathways 🟢 Ability to Model Pre-flood Emissions
Wang et al., 2018 Developed a biogeochemical model (FAQ-DNDC), lifecycle to estimate lifecycle CO_2 emissions for the Eastmain-1 Reservoir. 🟢 Ability to Forecast Net Reservoir GHG Lifecycle Emissions

🟡 Completeness of Gas Types (e.g. CO_2, CH_4, N_2O) 🟡 Completeness of GHG Pathways 🟢 Ability to Model Pre-flood Emissions
Li et al., 2020a, 2020b Estimated net reservoir emissions 13 years after flooding the Three Gorges Dam, China. Pre-flood landcover emissions were estimated following IPCC methodology. CO_2 pre-flood aquatic emissions were estimated using a biogeochemical model. CH_4 pre-flood emissions were estimated using an empirical regression model. Post-flood emissions: a semi-empirical and semi-mechanistic model was developed, using in-situ measurements. Net emissions were calculated by comparing post-flood (first 13 post-flood years) and pre-flood emissions. The study did not develop reservoir GHG lifecycle emissions. 🔴 Ability to Forecast Net Reservoir GHG Lifecycle Emissions 🟡 Completeness of Gas Types (e.g. CO_2, CH_4, N_2O) 🟢 Completeness of GHG Pathways 🟢 Ability to Model Pre-flood Emissions
Waldo et al., 2021 Used the G-res Tool (Prairie et al., 2021), Size-Productivity Model (DelSontro et al., 2018), Multiple Linear Regressions (Hertwich, 2013), and generalized linear modeling (Scherer and Pfister, 2016) to model lifecycle GHG emissions from Lake Mead and Lake Powell, USA. 🟢 Ability to Forecast Net Reservoir GHG Lifecycle Emissions 🟡 Completeness of Gas Types (e.g. CO_2, CH_4, N_2O) 🟡 Completeness of GHG Pathways 🟢 Ability to Model Pre-flood Emissions

Assessment Criteria:

Ability to Forecast Net Reservoir GHG Lifecycle Emissions
- The model cannot forecast net reservoir GHG lifecycle emissions
- The model forecasts net reservoir GHG lifecycle emissions

Completeness of Gas Types (i.e. CO_2, CH_4, N_2O)
- The model cannot estimate reservoir GHG emissions by gas type
- The model estimates some but not all reservoir GHG types (e.g. CO_2, CH_4, N_2O)
- The model estimates all reservoir GHG types (e.g. CO_2, CH_4, N_2O)

Completeness of GHG Pathways
- The model cannot estimate reservoir GHG emissions by gas type
- The model estimates some but not all reservoir GHG emission pathways
- The model estimates all reservoir GHG emission pathways

Ability to Model Pre-flood Emissions
- The model cannot estimate pre-flood GHG emissions from the reservoir footprint
- The model estimates pre-flood GHG emissions from the reservoir footprint

2.2.2.1 Review: Global Models/Global Studies

Several models have been developed to assess reservoir GHG emissions at a global scale (Barros et al., 2011; Hertwich et al., 2013; Li and Zhang, 2014; Deemer et al., 2016; Scherer and Pfister, 2016; DelSontro et al., 2018., Harrison et al., 2022; Li and He, 2022; Soued et al., 2022). They identified parameters that influence reservoir GHG emissions such as reservoir age, reservoir size and depth, temperature, latitude, nutrients and trophic status, watershed inputs, etc. However, these global models, except for those using the G-res Tool (Harrison et al., 2021; Soued et al., 2022) estimated gross GHG emissions and at a point-in-time to provide an understanding of the magnitude of reservoir GHG emissions worldwide and the contribution of gas species (e.g., CO_2, CH_4 and N_2O). They were not designed to estimate net lifecycle GHG emissions on a global scale nor for

individual reservoirs. Also, these models varied in terms of the GHG emission pathways included in the studies.

Most of the models were developed from published measurements of reservoir GHG emissions that were available at that time. Since reservoirs vary in size, shape, age, location, pre-flood landcover, etc., and since reservoir GHG studies are on-going and measurements continue to be published, and measurement techniques continue to evolve, these previously used databases and global models may not represent all types of hydroelectric reservoirs worldwide. The global models should not be expected to represent characteristics of all reservoirs. To illustrate, the measurements from Manitoba hydroelectric northern reservoirs that were included in many of these global models included only point-in-time measurements from mature reservoirs located on the Winnipeg River (e.g., McArthur Falls, Slave Falls, Pointe du Bois, etc.) (Hertwich et al., 2011). It is understood that the main reservoir GHG pulse from these older reservoirs has subsided and their emission rates are similar to those of natural water bodies in the region (Hesslein and Cooley, 2016; 2017). It would be unlikely that emissions from these reservoirs could be used to model emissions of a newly flooded reservoir, especially with different landscape and landcover characteristics.

Harrison et al. (2021) estimated global reservoir CO_2 and CH_4 emissions by pathway and latitude using the G-res Tool. Soued et al. (2022) modelled global reservoir lifecycle CO_2 and CH_4 emissions from 1900 – 2060 using the G-res Tool. The G-res Tool will be discussed in further detail in Section 2.2.3.

2.2.2.2 Review: Regional Modelling/Assessments

The reservoir GHG models cited in Table 2-1 that assessed regional reservoirs modeled either point-in-time GHG emissions or partial components of lifecycle GHG emissions, with the exception of Li et al. (2019), Levasseur et al. (2021) and Hansen et al. (2022) who used the G-res Tool for their modelling studies.

The approach used by Räsänen et al. (2018) was an initial attempt to assess gross lifecycle emissions for existing and planned reservoirs in the Mekong River Basin in Southeast Asia. They estimated GHG emissions per unit of energy produced by the generating stations ($kgCO_2e/MWh$) using linear regression formulas that included the reservoir area-to-electricity ratio for estimating CO_2 emissions following the approach used by Hertwich (2013) and added maximum temperature to the model for estimating CH_4 emissions per unit of energy, adopting the approach used by Scherer and Pfister (2016). Räsänen et al. (2018) estimated GHG emissions per reservoir area (tCO_2e/yr) using linear regression formulas that included reservoir age and erosion rates for estimating CO_2 emissions and added reservoir age and temperature to the model for estimating CH_4 emissions, following Scherer and Pfister (2016).

Li et al. (2019) modelled net reservoir GHG lifecycle emissions for the five largest hydroelectric projects in China using the G-res Tool. The G-res Tool will be discussed in further detail in Section 2.2.3.

Beaulieu et al. (2020) measured CO_2 and CH_4 diffusive and ebullition rates from 32 US reservoirs located along an agriculture-forest gradient. They used boosted regression trees (machine-learning algorithms) to identify variables (e.g. reservoir morphology, CHl *a*

and TP) to explain their CO_2 and CH_4 measurements of diffusive and ebullition emissions. They concluded the algorithms they developed could be used to estimate GHG emissions for other US reservoirs. These models do not estimate reservoir GHG lifecycle emissions.

Levasseur et al. (2021) modelled net lifecycle GHG emissions for all Québec reservoirs and modelled the GHG intensity of the Québec electricity grid using the G-res Tool. Hansen et al. (2022) estimated net lifecycle GHG emissions from 28 reservoirs within the USA, covering all ecoregions using the G-res Tool. The G-res Tool will be discussed in further detail in Section 2.2.3.

2.2.2.3 Review: Reservoir-Specific Models

The reservoir GHG models cited in Table 2-1 that assessed individual reservoirs were either: site-specific models that are not applicable to be transferred to other reservoirs; were not lifecycle assessments; where partial lifecycle assessment models, missing elements such as gas type (e.g. CH_4 not included) or emission pathways and not ready to be applied to other reservoirs. The exception was Waldo et al. (2021) who modelled lifecycle GHG emissions Lake Mead and Lake Powell, the two largest reservoirs in the USA, using the G-res Tool. The G-res Tool will be discussed in further detail in Section 2.2.3.

Teodoru et al. (2012) described the extensive pre-flood and post-flood measurements of the Eastmain-1 Reservoir, developed a first order decay model to describe the first four years of observed post-flood CO_2 and CH_4 emissions (2006-2009) and extrapolated these results over the 100-year engineered lifespan of the reservoir. They noted that this approach is specific to this flooded river basin.

Bernardo et al. (2017) applied a change in carbon stock method to the Capivari Reservoir, Brazil. The method examines the amount of carbon that has changed in vegetation, soils, sediments, and the water column from pre-flood to post-flood. The method cannot determine or quantify the GHG species (e.g. CO_2, CH_4, N_2O) that are released to the atmosphere, which is a shortcoming for GHG lifecycle assessment.

Briones Hildrovo et al. (2017) modelled net lifecycle emissions for the Mazar-Dudas (run-of-river) and Baba Hydropower Schemes, Ecuador by applying reservoir GHG emission rates from other tropical reservoirs (literature values) to estimate GHG emissions from the reservoirs, applied literature values to estimate the loss of primary production from the land flooded to create the reservoirs; and estimated post-flood degassing and downstream emissions as a percentage of post-flood reservoir emissions. They assumed post-flood emissions from years 19-100 were constant. Pre-flood aquatic emissions were assumed to be zero and were excluded from the model. Although this is a helpful model, it was not based on site-specific GHG measurements nor validated with in-situ GHG measurements.

Wang et al. (2018) developed a processed-based, biogeochemical model to estimate 100-year lifecycle CO_2 emissions for the Eastmain Reservoir in Québec. The model helped to identify key processes that influence GHG production and emissions, such as increasing temperature (Wang et al., 2018). However, the model did not estimate CH_4 lifecycle emissions.

Li et al. (2020a, 2020b) assessed net GHG emissions of the Three Gorges Dam in China by comparing GHG pre-flood estimates and post-flood measurements that were collected 13 years after impoundment. The study did not assess lifecycle GHG emissions.

2.2.2.4 Outcome of Review of GHG Models

The UNESCO/IHA GHG Reservoir (G-res) Tool, version 3.31 (Prairie et al., 2017) is commercially available, ready to use, and the UNESCO/IHA G-res Tool team provides technical support and validation of results. The other models cited above are either under development, estimate only a component of lifecycle modelling such as estimating point-in-time/annual GHG budgets, focused on only one gas species of interest (e.g., CO_2 only), estimate change in carbon stock but not able to estimate the species of GHG emissions, did not include all GHG emission pathways, or their emphasis was on determining the main variables that influence GHG emissions for those reservoirs studied.

2.2.3 UNESCO/IHA GHG Reservoir (G-res) Tool

The UNESCO Chair for Global Environmental Change and the International Hydropower Association (IHA) led a decade-long multi-stakeholder research project to develop the G-res Tool (IHA, 2020). The G-res Tool is based on the conceptual framework built by researchers from the Université du Québec à Montréal (UQAM), the Norwegian Foundation for Scientific and Industrial Research (SINTEF), and the Natural Resources Institute of Finland (LUKE) (IHA, 2020). Manitoba Hydro and other Canadian hydropower companies provided input and tested preliminary versions of G-res as it was being developed.

The G-res Tool estimates GHG emissions that can be attributed to the impoundment and operation of a reservoir over a 100-year timeframe (Prairie et al., 2017, 2021). The tool is intended to estimate net life cycle emissions, which are the incremental change in GHG emissions resulting from flooding land and the pre-existing aquatic systems to create a reservoir. G-res was designed as a screening model to identify if the GHG emissions resulting from a reservoir have the potential to be high (Prairie et al., 2017). The G-res Tool is based on empirical relationships from reservoir research world-wide.

The G-res Tool is recognized by the Intergovernmental Panel on Climate Change (IPCC) 2019 Guidelines for National Greenhouse Gas Inventories as an accepted GHG quantification method (IPCC, 2019). It has been used by researchers and industry to estimate the net life cycle GHG emissions and emissions per electricity produced from the hydroelectric reservoirs in Quebec (Levasseur et al., 2021); to estimate net GHG emissions and emissions per electricity produced from China's largest hydroelectric reservoirs, which are amongst the largest hydroelectric projects in the world (Li et al., 2019); to estimate annual GHG emission rates and emissions per electricity produced from the two largest reservoirs in the USA (Waldo et al., 2021); to assess emissions and dominant emission pathways from multiple US reservoirs and to compare them to global reservoir emission estimates (Hansen et al., 2022); to assess the magnitude of reservoir GHG emission pathways at a global scale (Harrison et al., 2021); and to model future reservoir GHG emissions at a global scale (Soued et al., 2022). The G-res Tool is accepted by financial organizations such as the Climate Bond Initiative as an approved methodology for assessing compliance with "Green Bond" and "Climate Bond" criteria (Climate Bond

Initiative, 2021) and by the World Bank for assessing GHG emissions from new hydroelectric projects (World Bank Group, 2023). There are more than 2,100 registered G-res users from 129 countries (Prairie et al., 2023).

It is important to understand the limitations of G-res and the uncertainty associated with using G-res to model Keeyask reservoir lifecycle GHG emissions. Model limitations and uncertainty are discussed in Chapter 6 Uncertainty Analysis.

2.2.3.1 G-res Tool Calculation Method

G-res estimates net GHG emissions over the 100-year lifetime of the reservoir. Net reservoir GHG emissions refer to the incremental change in post-flood GHG emissions as compared to pre-flood GHG emissions. Net emissions are defined as Gross GHG emissions minus Baseline (pre-flood) GHG emissions.

The G-res Tool calculates Net emissions as:

= [Post-impoundment GHG balance from the catchment after introduction of a reservoir] - [Pre-impoundment GHG balance of the catchment before introduction of a reservoir] - [Emissions from the reservoir due to unrelated anthropogenic sources] (2.1)

Post-flood GHG emissions are estimated using semi-empirical models embedded in G-res. These models were developed by assessing reservoir GHG studies worldwide and establishing statistical relationships between CO_2 and CH_4 emissions and reservoir characteristic (Prairie et al., 2018, 2021). The general format of the statistical models is (Prairie et al., 2017).

Post-Flood GHG Emissions =

log (GHG emissions) = *f* (Temperature, Age, other drivers of GHG ...) (2.2)

G-res calculates the pre-flood emissions by multiplying the surface area of each land cover class by an emission factor for CO_2 and CH_4. G-res land cover classes are based upon the European Space Agency and Climate Change Initiative categories. Default CO_2 and CH_4 emission factors are based primarily on IPCC 2006 and IPCC 2014 values, plus sources from scientific literature (Prairie et al., 2024).

The user enters the areal extent (km^2 or %) of each applicable landcover type, and G-res assigns default GHG emission factors. The user can override the default model-derived GHG Emission Factors and enter country-specific or site-specific GHG Emission Factors, such as those developed from direct measurements of the pre-flood landscape. This aligns with IPCC good practice (IPCC, 2019).

Pre-Flood GHG Emissions =

(GHG Emission Factors) x (Pre-Flood Land Cover Type) (2.3)

The goal of G-res is to estimate total net GHG emissions over the 100-year lifetime of the reservoir. It is not designed to compare annual field measurements with year-to-year model estimates. Although G-res has recently added a function to estimate GHG emission on an annual basis, there is more confidence in the model results when predicting lifecycle emissions over the 100-year reservoir lifetime.

Emissions are calculated by each emission pathway (e.g., diffusion, ebullition, degassing, etc.), and by gas type (e.g., CO_2 and CH_4).

Emission intensity is calculated as the amount of net GHG emissions unit of energy output, for example, tCO_2e/GWh.

Lifecycle GHG emission estimates are a GHG metric that enables GHG comparisons amongst hydroelectric reservoirs, and amongst other forms of electricity production.

2.2.3.2 Overview of Data Inputs

The G-res Tool inputs include biophysical, biogeochemical, and meteorological information about the upstream catchment area and reservoir characteristics, plus technical information about the generating station to be modelled.

Data inputs include entry sheets (or Tabs) to describe the Pre-Flood Landscape, Reservoir Characteristics, and Reservoir Services (to allocate GHG emissions to other uses of the reservoir). G-res also includes options to enter site-specific CO_2 and CH_4 emission factors for the pre-flood landscape based on landcover and soil type.
G-res is explained in detail by Prairie et al. (2021), by the G-res Technical Documentation and G-res User Guide (updated version 3.31) (Prairie et al., 2017a, 2017b).

Section 3.1 summarizes the inputs used for modelling the Keeyask reservoir and the reservoirs on the lower Nelson River. The details of the input selection and rationale are described in Appendix 1.

2.2.3.3 G-res Tool Assumptions

A key assumption of the G-res Tool is that the field measurements used to develop each of the G-res semi-empirical models are representative of reservoirs to which the G-res Tool will be applied. The database that underpins the G-res Tool is comprised of

published CO_2 and CH_4 emissions data from 233 reservoirs worldwide prior to 2016 (Prairie et al., 2017). Sixty-one reservoirs are from the boreal region, and of these, 13 are "young" reservoirs (20 years of age, or less). It is important to understand the data that underpins the G-res Tool represents reservoirs that have been studied up until the time that G-res was developed. Thus, reservoirs that have unique characteristics (such as the Keeyask reservoir with flooded peatlands) that were not well-studied prior to the development of G-res, may be underrepresented in the G-res dataset. The extent to which G-res formulas adequately represent these reservoirs and the ability of G-res to model these reservoirs remains uncertain.

Although the G-res database includes an exhaustive review of published studies, the reservoir studies were conducted by multiple researchers where there is variation in: reservoir type (size, configuration, amount and composition of flooded material, etc.); reservoir age (young, mature); and research methods (sampling design, sampling techniques, measurement instruments, sampling time periods, etc.). Since reservoir characteristics influence the quantity, composition, and timing of reservoir GHGs, it is important to understand if G-res has been calibrated to model the Keeyask reservoir. In other words, how well can G-res be expected to represent the Keeyask reservoir GHG processes and be able to model Keeyask GHG emissions if the model was not calibrated with measurements from a similar reservoir?

None of the young reservoirs in the G-res database closely match the Keeyask reservoir in terms of size, age, type of pre-flood landcover (peatlands), and extent of littoral zone. It is uncertain how well G-res is able to model flooded peatlands, on-going shoreline

erosion and peatland disintegration, and re-surfacing peat. Of the mature boreal reservoirs in the G-res database, Stephens Lake is the closest surrogate to the Keeyask reservoir. Data from Stephens Lake was collected 30 years after the impoundment and missed the initial pulse of GHG emissions. The Stephens Lake data included in the G-res database is limited to 2004 – 2007. These data represent dissolved gas concentrations in the Kettle Generating Station forebay, and do not necessarily represent emissions occurring in the more distant reaches of Stephens Lake and backbays.

2.3 Overview of the Keeyask Reservoir: Attributes that Affect GHG Emissions and Lifecycle Modelling

The Keeyask Generating Station (Keeyask GS) is a 695-megawatt hydroelectric power plant located on the lower Nelson River in northern Manitoba (Figure 2-2). The Keeyask GS was developed by the Keeyask Hydropower Limited Partnership, comprising the Tataskweyak Cree Nation, War Lake Cree Nation, Fox Lake Cree Nation, York Factory Cree Nation and Manitoba Hydro (Keeyask Hydropower Limited Partnership, 2012a). Construction commenced in 2014 and concluded when all seven of the generating units were put into service on March 9, 2022 (Manitoba Hydro, 2025b).

As per the Keeyask Interim Water Power Act licence, the reservoir operates within a range of 1.0 m from a Minimum Licence Forebay Elevation of 158 m ASL to a Maximum Licence Forebay Elevation of 159 m ASL (Manitoba Conservation and Water Stewardship, 2014).

The key attributes that influence Keeyask reservoir GHG emissions and lifecycle modelling are the reservoir's northern location, size and configuration, and the nature of the pre-flooded landcover. In particular, the reservoir configuration and the type of flooded land cover render this a challenging reservoir for modelling lifecycle GHG emissions. These attributes and their relationship with GHG emissions and modelling are summarized below.

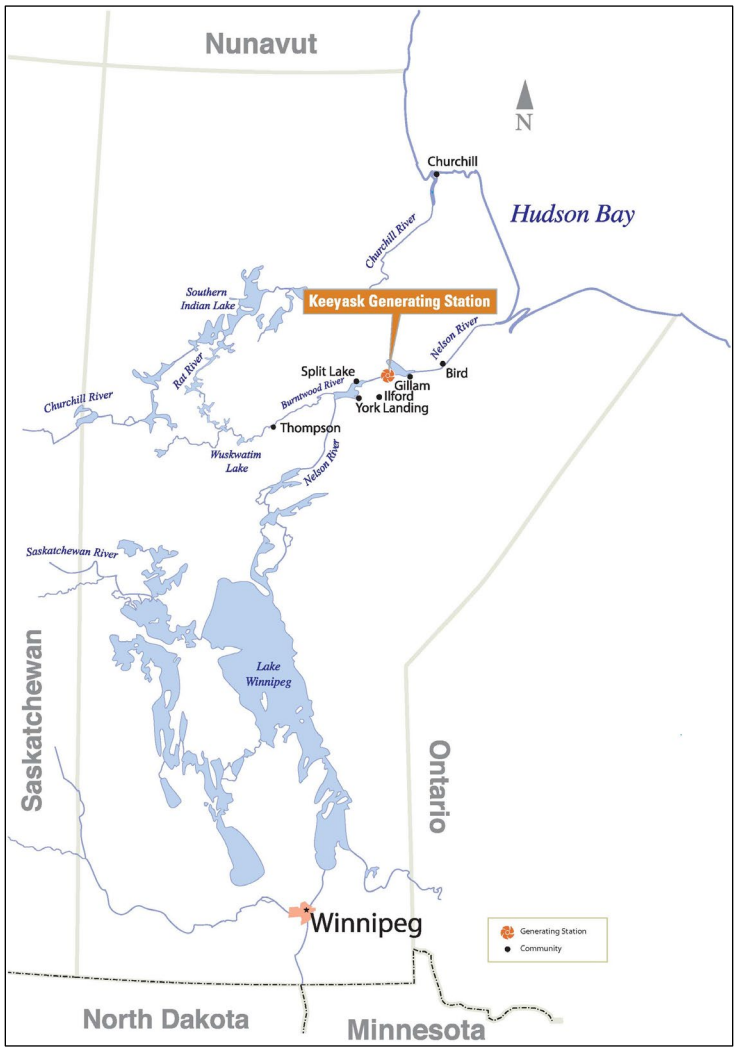


Figure 2-2 Location of Keeyask Generating Station
Source: Keeyask Hydropower Limited Partnership https://keeyask.com/the-project/

2.3.1.1 Geographic Location

The Keeyask reservoir is located within the Boreal Shield Ecozone (Government of Canada, 2013). Boreal reservoirs have been observed to have lower GHG emissions than those located in the lower latitudes of the sub-tropics and tropics because of their colder climate and winter ice cover (Tremblay et al., 2010; Harrison et al., 2021; Soued et al., 2022). The lower temperatures tend to slow down the microbial decomposition of flooded biomass and the production of GHGs (St. Louis et al., 2000; Gudasz et al., 2010; DelSontro, et al., 2016b). Factors related to Keeyask's northern geography, such as mean monthly temperatures and solar radiation (kWh/m^2/day), are important modelling variables that can affect the production of CO_2 and CH_4 diffusive emissions and CH_4 ebullition (bubble emissions).

2.3.1.2 Reservoir Size

The Keeyask reservoir was flooded between August 31 to September 5, 2020 (Manitoba Hydro, 2021). The initial impoundment was approximately 93.1 km^2 (Keeyask Hydropower Limited Partnership, 2012a). This comprised approximately 45.1 km^2 of flooded land and approximately 48.0 km^2 of flooded aquatic systems. The reservoir is predicted to increase to 100.4 km^2 thirty years after the initial flooding (Keeyask Hydropower Limited Partnership, 2012a). This is the result of the flooded land base (forest and peatlands) expanding from 45.1 km^2 at the time of the original flooding to 52.4 km^2 through peatland disintegration and shoreline erosion.

To avoid underestimating GHGs, the values of 100.4 km^2, 52.4 km^2 and 48.0 km^2 were used to represent the size of the total reservoir, flooded land base, and flooded aquatic systems respectively, when modelling Keeyask reservoir life cycle GHG emissions over a 100-year timeframe.

The Keeyask reservoir is the fifth largest flooded area of the Manitoba Hydro hydraulic system, being outranked by the Churchill River Diversion, Grand Rapids G.S./Cedar Lake, Kettle G.S./Stephens Lake, and the Kelsey Generating Station reservoir (Manitoba Hydro, 2015a). In comparison with reservoirs around the world (including those not associated with hydropower production), the Keeyask reservoir would fall into the intermediate size category (10 km^2 - 100 km^2) according to some cataloguing schemes (Soued et al., 2022). The Keeyask reservoir is less than the average size (488 km^2) of high latitude (30°N – 68°N) hydroelectric reservoirs (Barros et al., 2011).

Reservoir size can influence the potential to generate and emit GHGs. The size of the reservoir surface area determines the space available to emit GHGs, affects the total quantity or flux of GHGs released to the atmosphere, and the amount of flooded biomass potentially available to decompose and produce GHGs (Goldenfum, 2012; Rosentreter et al., 2021; Hansen et al., 2023). Studies have identified reservoir size as a predictor of CO_2 and CH_4 emissions (Scherer & Pfister, 2016; DelSontro et al., 2018), and reservoir size is a parameter used to estimate national reservoir GHG inventories (IPCC, 2019), and for modelling reservoir lifecycle GHG emissions (Prairie et al., 2021).

2.3.1.3 Keeyask Reservoir Configuration

The Keeyask reservoir comprises 1) a mainstem or main river channel and 2) a shallow littoral zone that includes shoreline waters, and flooded backbays (e.g., tributaries and wetlands).

2.3.1.3.1 Main Channel

The main channel of the Keeyask Reservoir/Nelson River is deeper, faster flowing with water residence times of approximately 15 – 30 hours, and well-oxygenated as compared to the littoral zones (Keeyask Hydropower Limited Partnership, 2012a; Manitoba Hydro, 2023). Water residence times refer to the average length of time a parcel of water stays within a defined water system (Goldenfum, 2010).

Post-flood monitoring by Manitoba Hydro confirms that dissolved oxygen in the main channel upstream, within, and downstream of the reservoir is typically between 95%-100% saturation during the summer and winter (Manitoba Hydro, 2024). These results are based on discrete monitoring (11 sites in summer and 4 sites in winter) and continuous monitoring (5 sites in summer and 4 sites in winter) (Manitoba Hydro, 2023). Dissolved oxygen concentrations are high and typically range from 8.5-10.0 mg/l in the summer to 14-15 mg/l in the winter (Manitoba Hydro, 2024).

2.3.1.3.2 Littoral Zone

For modelling purposes, the littoral zone is defined as the area of the reservoir where water depths are 3 m or less (Prairie et al., 2021). The littoral zone is estimated to comprise approximately 26% of the total Keeyask reservoir area, 30 years after flooding (W. DeWit, personal communication, July 5, 2023).

Keeyask littoral zone water residence times are longer than those of the main channel and may be 30 days or more in backbay settings depending on water flow conditions (Keeyask Hydropower Limited Partnership, 2012a; W. DeWit, personal communication, May 1, 2020). Longer water residence times can provide more time for: photosynthesis (carbon fixation/carbon production); microbial and photo degradation of carbon resulting in GHG production; accumulation of nutrients, which can facilitate microbial degradation, and which can facilitate primary production; and carbon burial within reservoir sediments (Prairie et al., 2018; Wang et al., 2018).

Dissolved oxygen concentrations in the littoral zone can potentially be lower and more varied than those of the main channel. This can be due to: less mixing of water with the well-oxygenated main channel, temperatures being higher in the shallower waters and thus being physically less able to retain higher levels of dissolved oxygen, lower wind speeds in sheltered areas which inhibit oxygen exchange (aeration) at the water surface, and there may be a higher oxygen demand from the decomposition of flooded organic material (Keeyask Hydropower Limited Partnership, 2012a; Manitoba Hydro, 2023).

The Keeyask Physical Environmental Monitoring Program results illustrate that dissolved oxygen concentrations vary within the reservoir from site to site, within the water column, and from season to season (Manitoba Hydro, 2023). These results are based on discrete monitoring (12 sites in summer and 12 sites in winter) and continuous monitoring (6 sites in summer) (Manitoba Hydro, 2023). Many of the discrete backbay monitoring sites (e.g., 72% in 2022) indicated high levels of dissolved oxygen concentrations during the summer which varied between 6-10 mg/l and 80%-100% saturation (Manitoba Hydro,

2023). Some of the backbay sampling locations exhibited high dissolved oxygen concentrations at the surface and lower concentrations near the bottom of the water column during the summer. For example, at the backbay site where an eddy covariance GHG monitoring tower is located, surface water concentrations of dissolved oxygen were generally high during the summer of 2023 exceeding 7 mg/l (Manitoba Hydro, 2023). There were periods during mid-July and mid-August where concentrations at the bottom of the water column dipped to 6 mg/l and 4 mg/l, respectively (Manitoba Hydro, 2023). This site also had the most events during the summer of 2023 where concentrations of dissolved oxygen were below 6 mg/l (Manitoba Hydro, 2024). During the winter of 2022, dissolved oxygen concentrations were high throughout the water column at most (71%) of the backbay monitoring locations. At 25% of the backbay locations, concentrations were high at the surface and moderate at the bottom of the water column, and at 4% of the backbay monitoring sites, concentrations were moderate at the surface and lower at the bottom (Manitoba Hydro, 2023).

Figures 2-3 to 2-4 illustrate the concept of a Keeyask reservoir main channel and littoral zones based on water depth and water flow, respectively (Keeyask Hydropower Limited Partnership, 2012a).

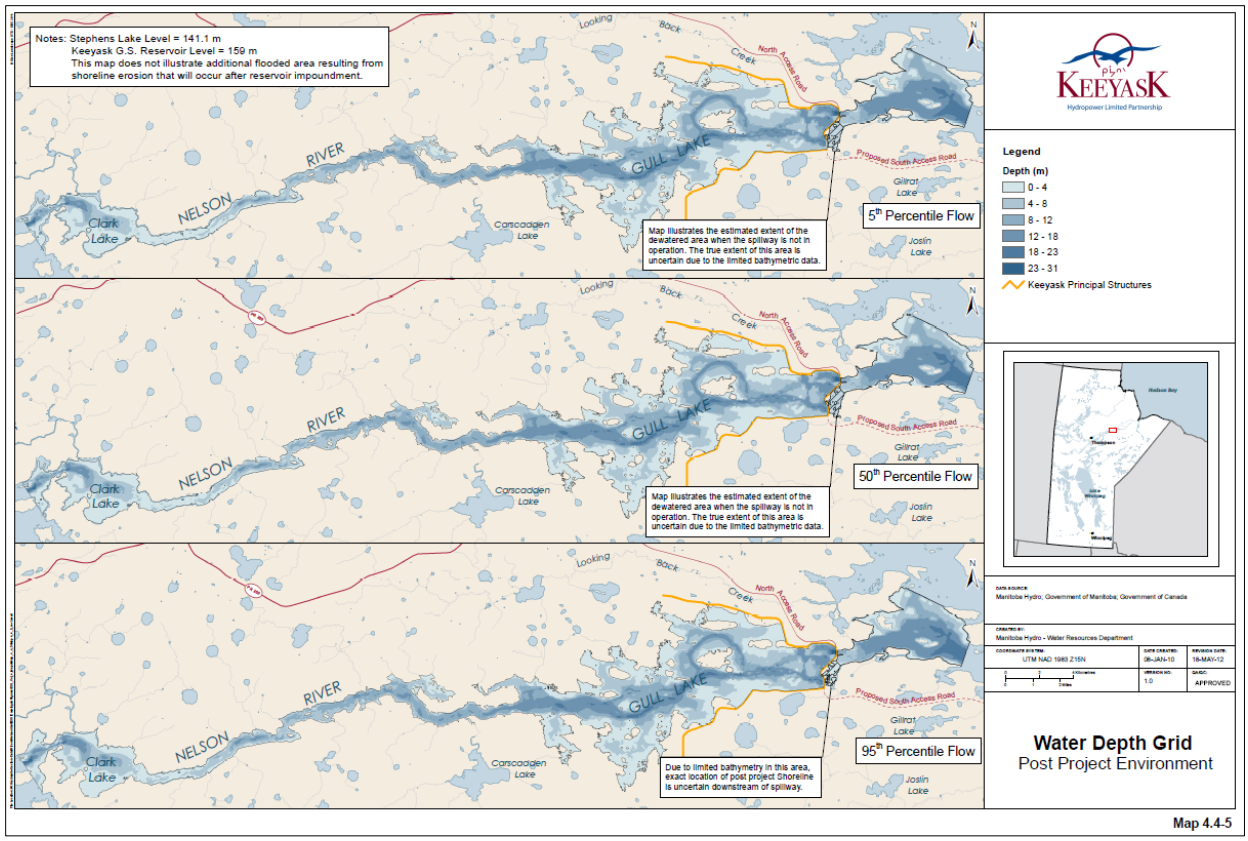


Figure 2-3 Keeyask Reservoir Modelled Water Depth
Source: Keeyask Hydropower Limited Partnership, 2012a

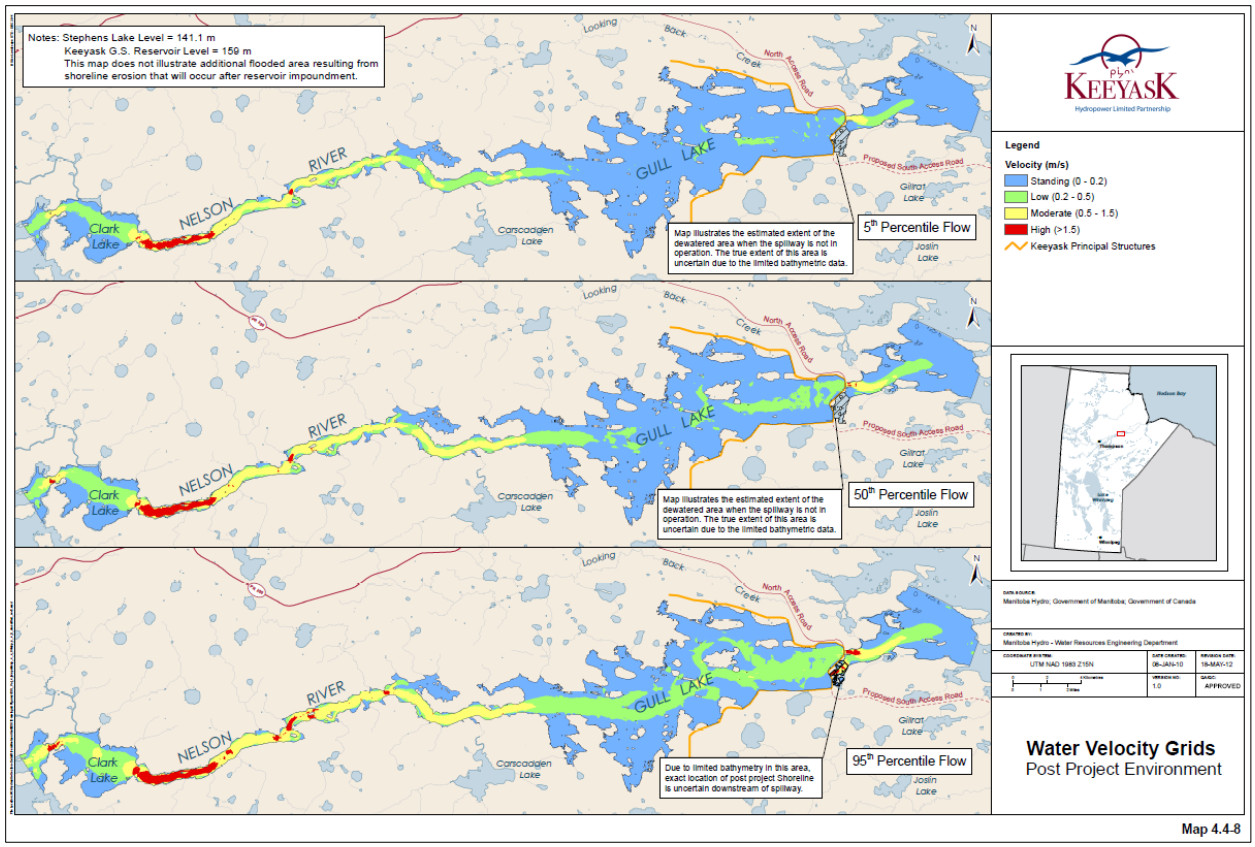


Figure 2-4 Keeyask Reservoir Modelled Water Velocity
Source: Keeyask Hydropower Limited Partnership, 2012a

2.3.1.4 Relevance of Reservoir Attributes for Keeyask Reservoir GHG Emissions Modelling

The relevance of the above discussion is to explain there is a difference in water characteristics between the main channel and littoral zones. These differences have the potential to affect GHG production. Collecting post-flood measurements of the Keeyask reservoir will be valuable for validating and calibrating models such as the G-res Tool and PB-res model that is under development (Prairie et al., 2024) so they will more accurately predict GHG emissions from the Keeyask reservoir and from other northern Canadian reservoirs.

Defining the areal extent of the littoral zone is a key input for the G-res lifecycle modelling scenarios for the Keeyask reservoir.

2.3.1.5 Flooded Land Base

Approximately 90% of the flooded land was comprised of heterogeneous peatland, underlain by discontinuous and sporadic discontinuous permafrost in about 78% of the flooded area (Figures 2-5 and 2-6) (Keeyask Hydropower Limited Partnership, 2012a).

This landscape mosaic presents a significant challenge for establishing a pre-flood GHG emission baseline as carbon cycling and GHG emissions differ amongst the various peatland and forest types (Webster et al., 2018; Delwiche et al., 2021; Kuhn et al., 2021; Virkkala et al., 2021).

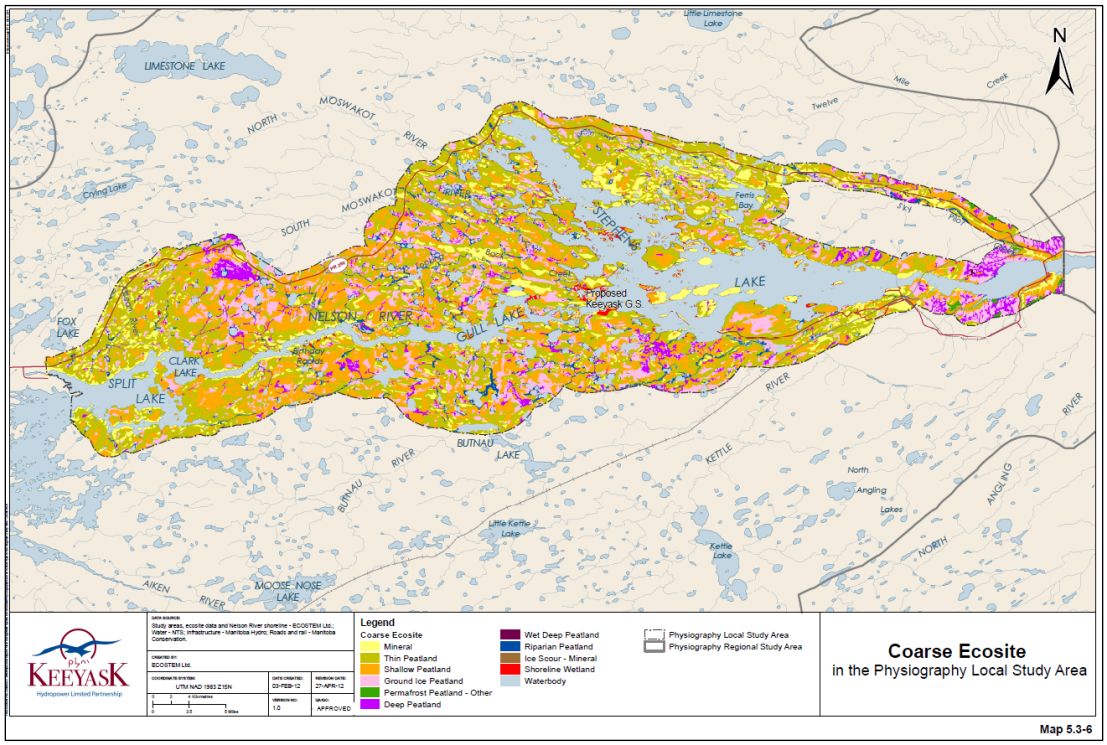


Figure 2-5 Heterogeneous Peatlands in the Keeyask Reservoir Area
Source: Keeyask Hydropower Limited Partnership 2012a



Figure 2-6 Pre-Flood Keeyask Area Peatlands, 2019

2.3.1.6 Peatlands

Peatlands are complex wetland systems where organic material accumulates in waterlogged conditions (Baird et al., 2009; Strack et al., 2017; Amesbury et al., 2019; Nichols and Petreet, 2019; Hugelius et al., 2020; Yu et al., 2021). They are comprised of a variety of landform types, they cycle carbon and emit GHGs through intricate and interrelated systems (Belyea, 2009; Frokling et al., 2009).

Peatland carbon cycling and GHG emissions vary in time (e.g., diurnally, seasonally, and annually) and in space (e.g., from within the same peatland, amongst peatlands in the same physiographic region, and amongst peatlands in different physiographic regions, such as northern, temperate and tropical regions) (Pelletier et al., 2007, Pelletier et al.,

2011, 2015; Turetsky et al., 2014; Griffiths et al., 2017; Leifeld et al., 2019; Loisel et al., 2021).

Each peatland is unique in some respects, and there must be careful consideration when applying GHG flux rates from one peatland to another. Peatland GHG emissions are impacted by many complex and interrelated variables such as peat landform type, hydrological controls, regional climate, vegetation type, soil respiration, trophic level, and microbial populations (Baird et al., 2009; Griffiths et al., 2017; Loisel et al., 2021; Strack et al., 2022).

Northern peatlands have been considered as a "worst-case" scenario for flooding to create reservoirs (St. Louis et al., 2000) as they store thousands of years of net carbon accumulation (Nichols and Petreet, 2019). Once impounded, the flooded carbon can potentially become available for decomposition and the release of CO_2 and CH_4 emissions, plus, flooding will eliminate an important, pre-flood carbon sink (St. Louis et al., 2000; St. Louis et al., 2003).

The pre-flood Keeyask reservoir footprint is comprised of a variety of peatland types (e.g., bog, rich-intermediate fen, poor fen, and marsh) and micro landforms within these peatland types (e.g., hummock, lawn, hollow, and pools) (Keeyask Hydropower Limited Partnership, 2012a, 2012b). Each of these peatland types and microforms have the potential to store, generate, and release GHGs at varying rates (Pelletier et al., 2007, 2011, 2015; Turetsky et al., 2014; Treat et al., 2021). Peatland GHG emissions vary in space and in time and are impacted by variables such as peat landform type, hydrological controls, regional climate, vegetation type, soil respiration, trophic level, and composition and

abundance of microbial populations (Strack, 2008; Trudeau et al., 2013; Webster et al., 2018; Kuhn et al., 2021; Graham et al., 2022).

A challenge for modelling net Keeyask reservoir GHG emissions involves assigning or developing appropriate GHG emission factors to adequately represent GHG emissions from the pre-flood diverse peat landscape. This challenge is further complicated when trying to model post-flood GHG emissions as peatlands respond to environmental change in a non-linear manner (Baird et al., 2009; Mahdiyasa et al., 2023). That is, a small change to the peatland environment can lead to a disproportionate change in GHG emissions (Belyea, 2009; Mozafari et al., 2023).

Although peatlands have been classified in many ways depending on the intended purpose of the classification (Lindsay, 2018), there is no globally recognized system that classifies peatlands according to their potential to store carbon or release GHG emissions (Lourenco et al., 2023). Similarly, the pre-flood landscape for Keeyask was classified in several ways in the Keeyask EIS for conducting various types of ecological assessments (Keeyask Hydropower Limited Partnership, 2012a, 2012b) but it was not classified specifically for assessing carbon cycling. The ultimate question for determining net reservoir GHG emissions is how much of the flooded carbon will decompose and of this, what proportion of the GHG emissions will be released as CO_2 and CH_4.

2.3.1.7 Discontinuous Permafrost

There are two issues related to GHG emissions when creating a reservoir in an environment that is underlain with discontinuous and sporadic discontinuous permafrost.

The first issue relates to the permafrost that is flooded. To what degree will the flooded permafrost thaw, expose previously frozen organic material to microbial degradation, and release GHGs (CO_2 and CH_4) from within the reservoir? These emissions could be regarded as being directly related to the creation of the reservoir and should be included in the net reservoir GHG footprint.

The second issue is related to the impact of climate change and migration of organic material into the reservoir. As global temperatures increase, there is the potential for northern permafrost peatlands to thaw, release organic material that may decompose and emit GHGs (Schuur et al., 2015; Mann et al., 2022). Northern peatlands could shift from being a net carbon sink to becoming a carbon source (Hugelius et al., 2020). The Hudson Bay Lowlands, the world's second largest peatland carbon store, has been identified as being particularly vulnerable to permafrost thaw (Spence et al., 2020). As permafrost thaws, liberated organic material may migrate into waterways, such as the Keeyask reservoir, through groundwater and surface water, decompose, and emit GHGs (Bridgham, 2017; Elder et al., 2018). In this scenario, the impact of climate change would be adding carbon to the reservoir in a manner that is analogous to upstream or watershed inputs (allochthonous carbon inputs). Once these carbon inputs have entered the reservoir, they may be stored in the reservoir sediments, mineralized within the reservoir and released to the atmosphere as CO_2 and CH_4, or transported downstream (Casas-Ruiz et al., 2023). It can be argued that the reservoir did not cause these emissions, and these emissions should not be included in the net carbon footprint of the reservoir. Although these carbon flows should be properly accounted for, it is very challenging. Quantification

methods such as net watershed exchange and net ecosystem carbon balance, which involves estimating carbon mass balances, coupled with field measurements (Chapin et al., 2006; Bogard & Butman, 2018; D'Acunha et al., 2019; Casas-Ruiz et al., 2023) may assist with accounting for carbon inputs received from thawing permafrost, but have not yet been included in reservoir GHG lifecycle models.

2.3.1.8 Floating Peat Islands

The Keeyask Environmental Impact Statement predicted that approximately 15 – 16 km^2 (35% - 36%) of the flooded peat would re-surface and float (Keeyask Hydropower Limited Partnership, 2012a). Re-surfacing peat was predicted to occur along shorelines and in backbays, with over 80% of the floating peat to occur in water less than 2 meters deep (Keeyask Hydropower Limited Partnership, 2012a). The Keeyask EIS forecasted about two thirds of peat re-surfacing would occur in the first year after flooding, with the maximum total mobile peat mass occurring in the fifth year after flooding, and no new re-surfacing would occur after 10 years post-impoundment (Keeyask Hydropower Limited Partnership, 2012a).

A challenge for modelling GHG emissions arising from floating peat is that their impact on reservoir emissions is poorly understood and constrained (Kelly et al., 1997; Scott et al., 1999; St. Louis et al., 2003). Currently, reservoir GHG models such as the G-res Tool, have not been designed to predict: how much of the floating peat will decompose and release GHGs; what proportion of the emissions will be released as CO_2 and CH_4; the impact on emissions from changing water column concentrations of particulate and dissolved organic material associated with the disintegration of the peat; and the

timeframe for releasing GHG emissions from floating peat or from surrounding waters affected by floating peat. It is important for semi-empirical models such as the G-res Tool to be calibrated and validated with reservoir studies where emissions from floating peat have been measured. Similarly, it is also important for process-based models such as the PB-res model under development by Prairie et al. (2023) to incorporate the underlying processes that generate peat islands, and cycle carbon and release GHG emissions from floating peat (e.g., water table position, position of oxic and anoxic zones, temperature, etc.) (Kelly et al., 1997; Scott et al., 1999; St. Louis et al., 2003).

The Keeyask EIS predicted areas within the reservoir where floating peat was likely to occur, such as in water less than 2 m deep, including flooded "backbays" (Keeyask Hydropower Limited Partnership, 2012a). The Keeyask reservoir GHG monitoring program was designed to include GHG measures from flooded backbays and shallow shorelines (Keeyask Hydropower Limited Partnership, 2015). Measurements from the reservoir monitoring program could be used to help with on-going calibration of the G-res Tool and with the development of a new process-based reservoir GHG model through Manitoba Hydro's and the University of Manitoba's participation in the national study "Constraining the GHG Footprint of Canada's Flooded Land (GHG-CaRe)" led by Université du Québec à Montréal and the University of Waterloo (Prairie et al., 2023). Figures 2-7 and 2-8 illustrate floating peat in the flooded Rabbit Creek backbay and along the shoreline of the South Dike Road, respectively.



Figure 2-7 Images of Floating and Resurfacing Peat in Keeyask Reservoir Flooded Backbay 2023



Figure 2-8 Images of Floating and Semi-Submerged Vegetation in Flooded Shallow Shoreline Along the Keeyask Reservoir South Dike Road 2023

2.4 Lower Nelson River Landscape

It is essential for a reservoir GHG lifecycle model to have the capacity to effectively estimate pre-flood emissions, as the magnitude of baseline emissions can determine whether the modelled reservoir will be a net GHG source or sink.

The lower Nelson River reservoirs present noteworthy circumstances for GHG modelling. They are located in the Nelson-Churchill River Basin (NCRB), which is the third largest river basin in North America, draining over 1 million km^2 (Ahmed et al., 2023; Phillips et al., 2023). The NCRB covers parts of Alberta, Saskatchewan, Manitoba and Ontario in Canada, and portions of Montana, North Dakota, South Dakota and Minnesota in the USA (Figure 2-9).

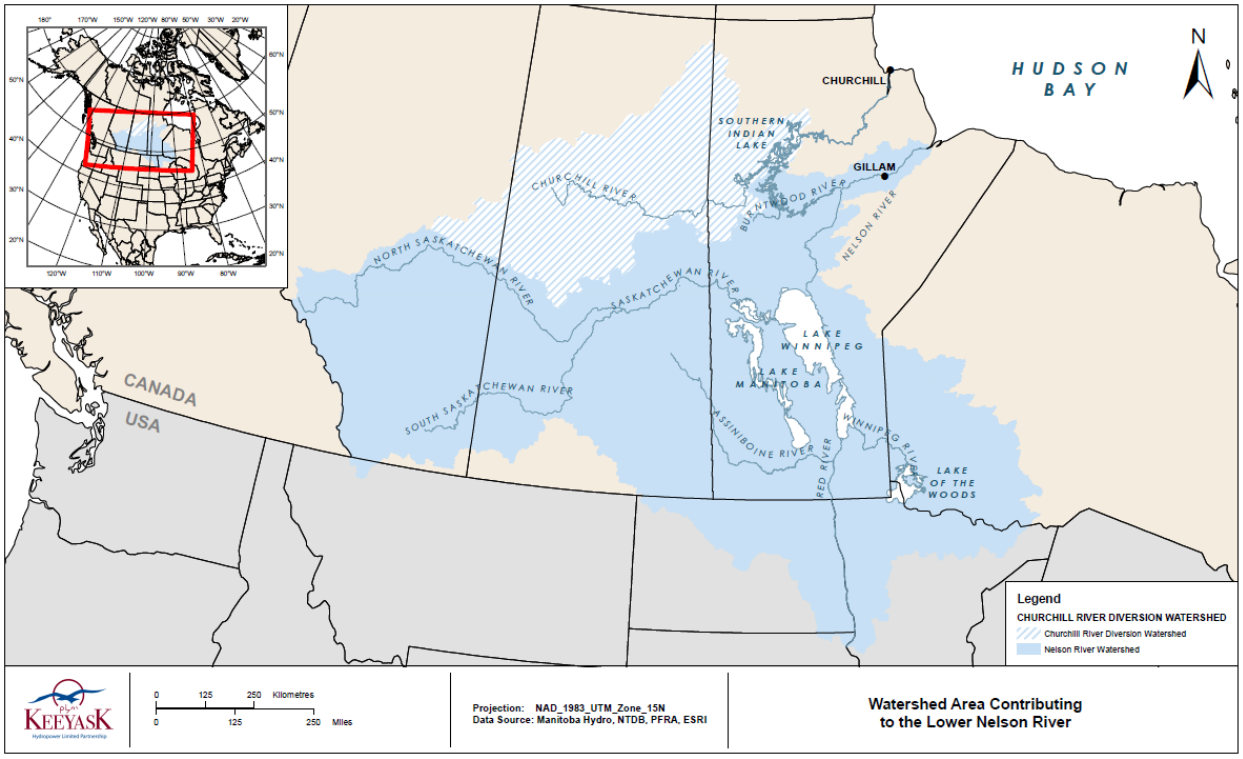


Figure 2-9 Nelson-Churchill River Watershed
Source: Keeyask Hydropower Limited Partnership, 2012a (Map 4.3-1)

Four, cascading hydroelectric generating stations are located on the lower Nelson River (Figure 2-10). The reservoirs range in size from 27 to 319 km^2, range in age from newly flooded (5 years) to mature (50+ years), and they vary in their type of operation which includes both water storage and modified run-of-river (Table 2-2). The two up-stream reservoirs, Keeyask and Kettle (Stephens Lake) flooded a mosaic of heterogeneous peatlands, while the two downstream reservoirs are mostly contained within the natural banks of the Nelson River (Keeyask Hydropower Limited Partnership, 2012a; Manitoba Hydro, 2014).

Over 70% of the hydroelectricity generated in Manitoba is produced by the stations on the lower Nelson River, and over 99% of the hydroelectricity generated in Manitoba is produced on waterways that eventually flow through the lower Nelson River (Manitoba Hydro, 2025b).

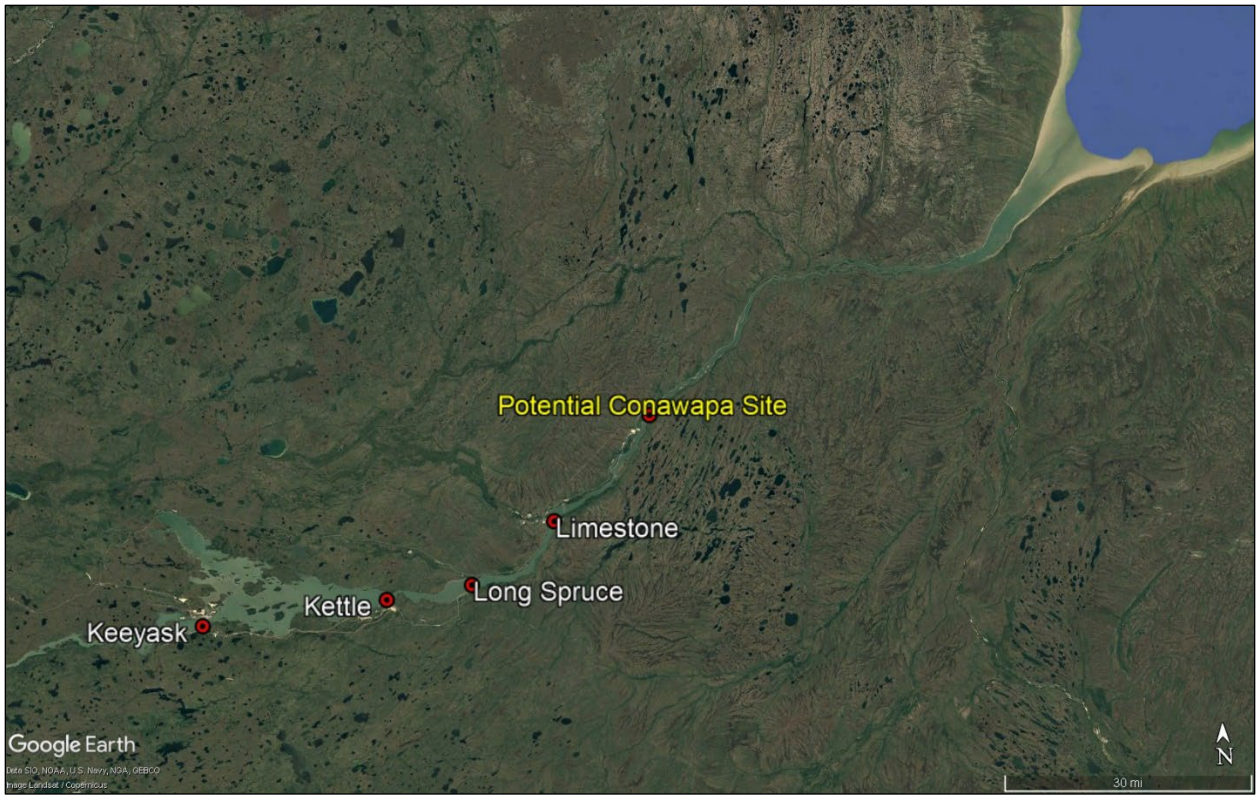


Figure 2-10 Lower Nelson River Reservoirs/Generating Stations

Table 2-2 Lower Nelson River Reservoirs

Lower Nelson River Hydroelectric Reservoirs

	Generating Capacity (MW)	Total Reservoir km^2	Flooded Area km^2	Year of Impoundment	Age Years
Keeyask	695	100	45	2020	5
Kettle	1220	319	221	1971	54
Long Spruce	980	30	15	1979	46
Limestone	1350	27	2	1992	33
Potential Conawapa (modelling scenario)	1485	39	11	n/a	n/a

Source: Adapted from Manitoba Hydro, 2015; KHLP, 2012a

2.4.1 Water Regime and Physiography

The lower Nelson River is defined as the segment of the river that flows downstream of Split Lake to Hudson Bay (Figure 2-11). Split Lake is the location where the waters from

the upper Nelson River/Lake Winnipeg Regulation and waters from the Burntwood River/Churchill River Diversion meet. This definition of the lower Nelson River is consistent with that which is presented by Manitoba Hydro in the Regional Cumulative Effects Assessment for Hydroelectric Developments on the Churchill, Burntwood and Nelson River Systems (Manitoba Hydro, 2015b).

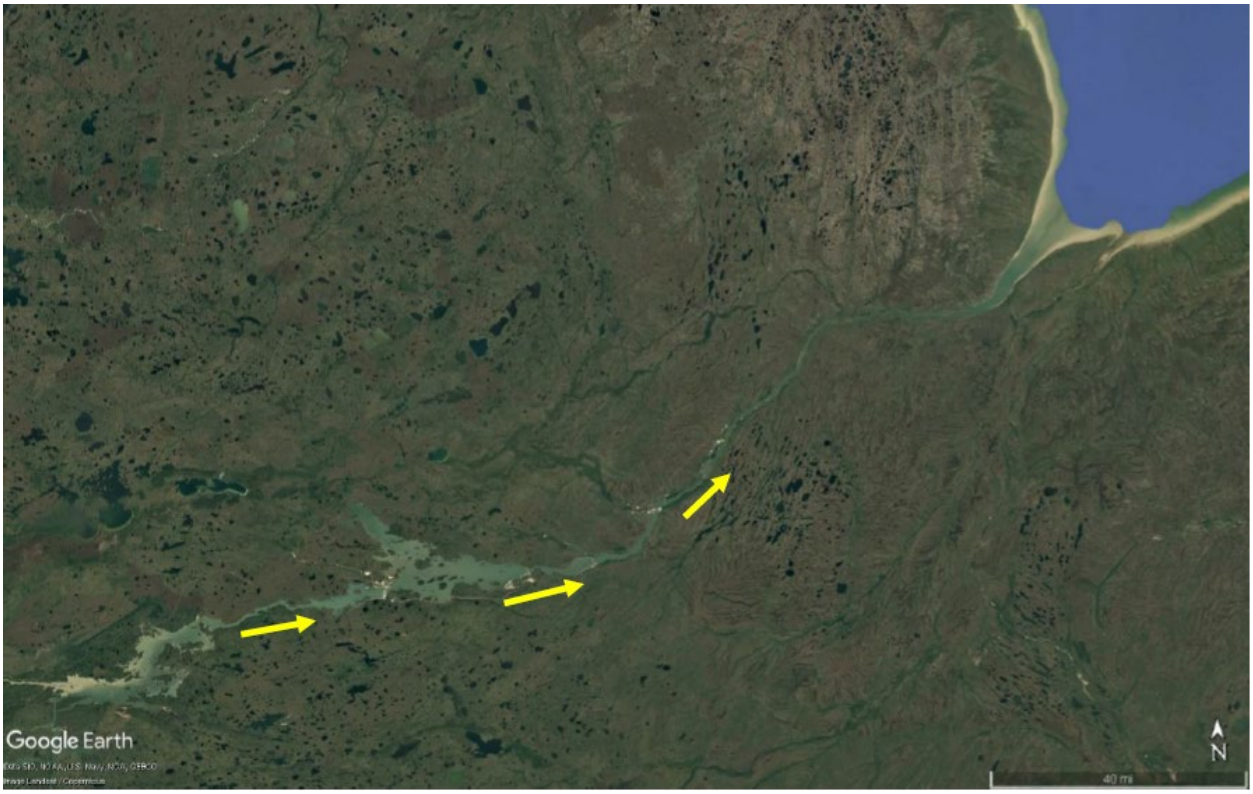


Figure 2-11 Lower Nelson River

Lake Winnipeg Regulation (LWR) regulates the outflow of Lake Winnipeg into the upper Nelson River (Figure 2-12). It was designed to help minimize overland flooding in the vicinity of Lake Winnipeg and to optimize flows for hydroelectric generation on the Nelson River (Manitoba and Manitoba Hydro, 2015). LWR was constructed between 1970-1976. It comprises a series of channels (e.g., Two-Mile Channel, Eight-Mile Channel, Ominawin Bypass, and Kisipachewuk Channel Improvement), outlet structures (e.g., Kiskitto Lake

Inlet Control Structure, Black Duck Control Structure) and the Jenpeg Generating Station downstream of Lake Winnipeg. LWR increases the outflows of Lake Winnipeg by approximately 50% during flood conditions (Manitoba and Manitoba Hydro, 2015).

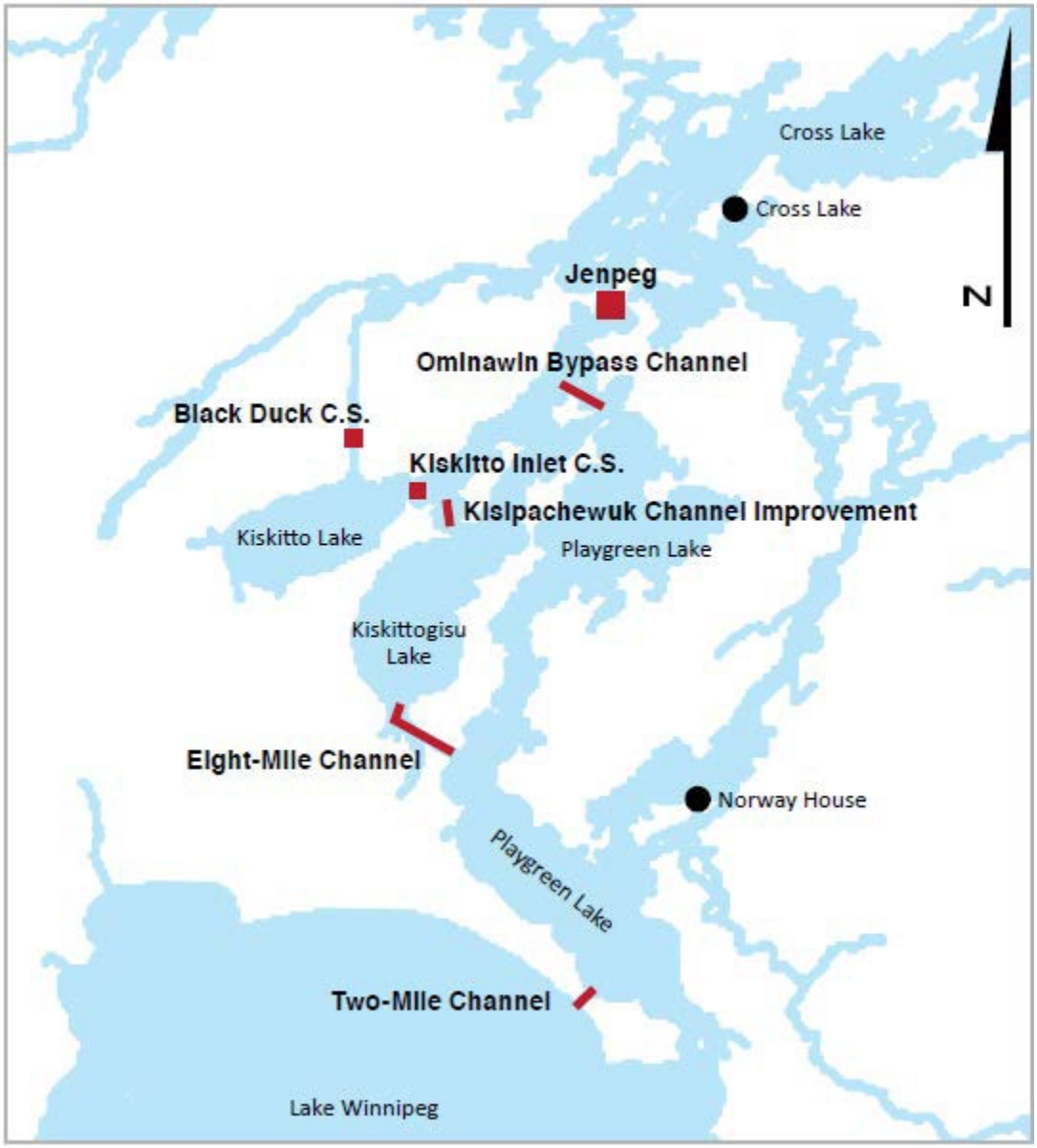


Figure 2-12 Lake Winnipeg Regulation
Source: Manitoba and Manitoba Hydro, 2015

The lower Nelson River lies within two physiographic regions, the Precambrian Shield and the Hudson Bay Lowlands. The boundary between these two regions is located

roughly midway through the Long Spruce reservoir, which runs diagonally from approximately 56°23'19" N -94°28'14" W in the northwest to approximately 56°22'13" N - 94°26'34" W in the southeast (Natural Resources Canada, 2019).

The segment of the lower Nelson River located within the Precambrian Shield Physiographic Region includes the Keeyask reservoir, Stephens Lake (Kettle Generating Station reservoir), and the upstream portion of the Long Spruce reservoir (Natural Resources Canada, 2019). This region is also located within the Boreal Shield Ecozone (Government of Canada, 2013). The landscape is dominated by sporadic discontinuous permafrost and extensive discontinuous permafrost (Keeyask Hydropower Limited Partnership, 2012a; Government of Canada, 2021). Peatlands cover over 80% of the area, occurring on gentle slopes, glacial fluvial deposits, and heterogeneous till (Keeyask Hydropower Limited Partnership, 2012a).

The boreal biome is one of the largest bioclimatic zones in the world, comprising a diverse assemblage of cold-tolerant forests, other wooded lands, peatlands, wetlands, aquatic systems, and soils (Brandt et al., 2013; Hugelius et al., 2020). Over the past millennium, the boreal biome has had a significant influence on carbon cycling (carbon storage, CO_2 and CH_4 emissions, carbon transport) and hence atmospheric radiative forcing. CO_2 has been absorbed and released by terrestrial and aquatic vegetation through photosynthesis and respiration, CO_2 and CH_4 have been emitted through the decomposition of organic material, large amounts of CO_2 have been released to the atmosphere from forest fires (Byrne et al., 2024; Virkkala et al., 2025), carbon has been stored in soil layers and transported laterally by surface water and ground water (Vonk et

al., 2019), thereby impacting carbon cycling of downstream systems (Regnier et al., 2022), and releases of boreal forest organic vapour may have deflected incoming solar radiation by modifying cloud albedo (Spracklen et al., 2008; Kurz et al., 2013; Zhao et al., 2016; Walker et al., 2019; Sothe et al., 2022; Casas-Ruiz et al., 2023; Grosbois et al., 2023). The boreal biome is estimated to store more carbon than contained in the atmosphere several times over, and a large portion of this boreal carbon is stored in peatlands (Kou et al., 2022).

The segment of the lower Nelson River that is located within the Hudson Bay Lowlands Physiographic Region and which is also located within the Hudson Plains Ecozone (Government of Canada, 2013), includes a portion of the Long Spruce reservoir, the entire Limestone reservoir, and the site of the potential, future Conawapa reservoir (Natural Resources Canada, 2019). The Hudson Bay Lowlands are the world's second largest continuous peatland (Packalen et al., 2014) and this landscape is dominated by extensive discontinuous permafrost (Government of Canada, 2021).

The peatland mosaic landscapes of the Boreal Shield Ecozone and the Hudson Plains Ecozone present a significant challenge for establishing a pre-flood GHG emission baseline as carbon cycling and GHG emissions differ amongst the various peatland and forest types (Webster et al., 2018; Delwiche et al., 2021; Kuhn et al., 2021; Virkkala et al., 2021).

2.4.2 Lower Nelson River Reservoirs

2.4.2.1 Kettle Reservoir (Stephens Lake)

The Kettle Generating Station is a 1220 MW hydroelectric facility located at the former Kettle Rapids on the lower Nelson River, approximately 3 kilometers upstream of the Canadian National Railway crossing near the Town of Gillam (Manitoba Hydro, 2013). Construction of the generating station began in 1966 and was completed in 1974. The Kettle Generating Station is Manitoba Hydro's second largest hydroelectric generating station, next to the Limestone Generating Station whose electricity generating capacity is 1350 MW.

The operating head, or waterfall created by the station, is approximately 30m. The discharge capacities of the generating station and spillway are 4,333 m^3/s and 8,349 m^3/s of water, respectively (Manitoba Hydro, 2013).

The reservoir, Stephens Lake, was created in 1971 by flooding the Nelson River and Moose Lake to the north. Flooding involved approximately 221 km^2 of land and 98 km^2 of water, for a total reservoir size of approximately 331 km^2 (Manitoba and Manitoba Hydro, 2015). The reservoir is located almost immediately downstream of the Keeyask Generating Station/reservoir. The reservoir water level is controlled by the Kettle Generating Station and operates between 139.2 m ASL and 141.1 m ASL at the 5^{th} and 95^{th} percentile, respectively (Keeyask Hydropower Limited Partnership, 2012a).

Stephens Lake can be roughly described as having a lotic environment in the south and a lentic environment in the north (Manitoba Hydro, 2012) Figure 2-13. The Nelson River thalweg is located in the south where the water quality is similar to that of the upstream

and downstream portions of the Nelson River, prior to creating the Keeyask reservoir (Keeyask Hydropower Limited Partnership, 2012c). The southern portion of Stephens Lake has higher concentrations of nutrients and oxygen (over winter) than the northern portion, and it does not stratify (Keeyask Hydropower Limited Partnership, 2012c). The northern portion can have low oxygen levels, become anoxic and may stratify near some shorelines and in some backbays over winter (Keeyask Hydropower Limited Partnership, 2012c). Some backbays may stratify during the open water season during hot and very low wind conditions (Keeyask Hydropower Limited Partnership, 2012c). The western and northern portions of the reservoir comprise a large amount of flooded land.

Approximately 85% of the landcover is comprised of heterogeneous peatlands and approximately 78% of the landscape is underlain by extensive discontinuous and sporadic discontinuous permafrost (Keeyask Hydropower Limited Partnership, 2012a).

Further information about the Kettle Generating Station and Stephens Lake reservoir is available in Appendix 3.

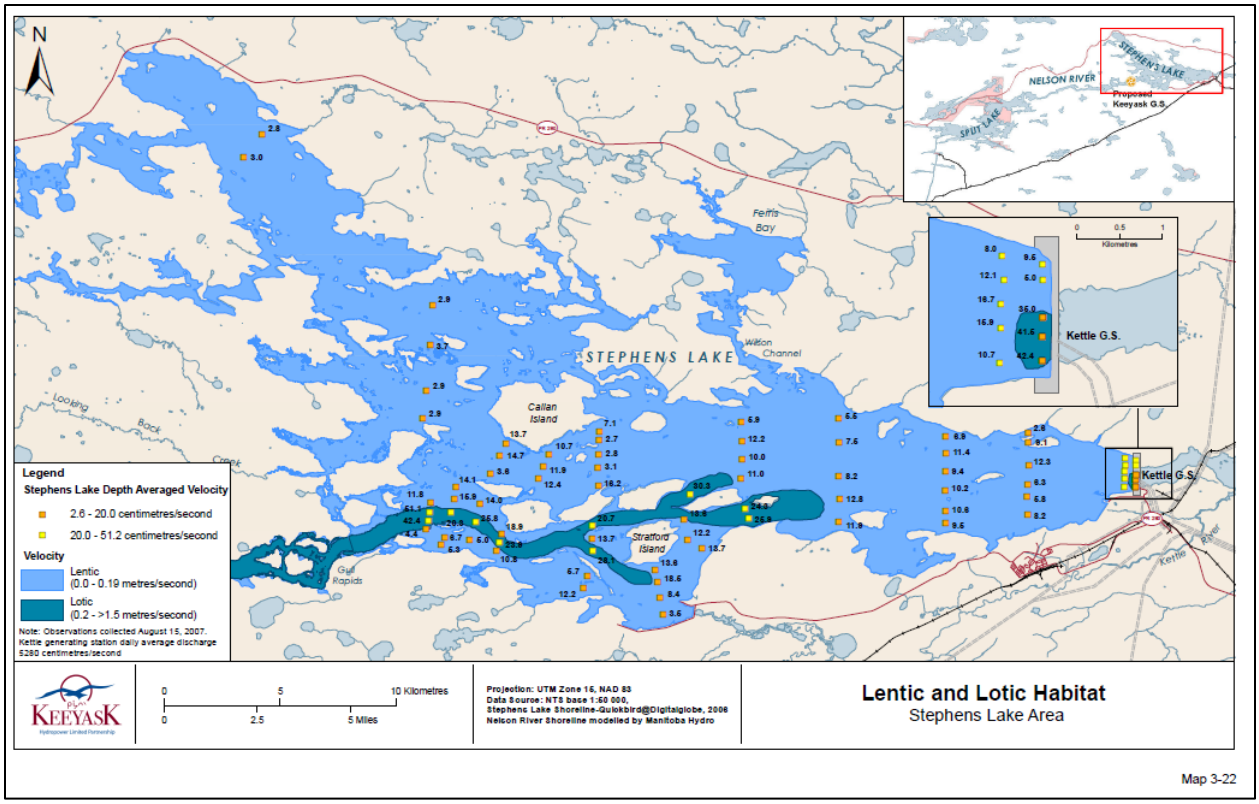


Figure 2-13 Stephens Lake: Lentic and Lotic Environments
Source: Keeyask Hydropower Limited Partnership, 2012c

2.4.2.2 Long Spruce Reservoir

The Long Spruce Generating Station is a 980 MW hydroelectric facility located at the former Long Spruce Rapids on the lower Nelson River (Manitoba Hydro, 2025b). The station is located approximately 16 km downstream of the Kettle Generating Station and 23 km upstream of the Limestone Generating Station (Manitoba Hydro, 2018). Provincial Road 280 crosses the Nelson River at the generation station. Construction of the generating station began in 1971 and was completed in 1979.

The operating head, or waterfall created by the station, is approximately 24.4 m (Manitoba and Manitoba Hydro, 2015). The discharge capacities of the generating station

and spillway are 4,528 m^3/s and 9,700 m^3/s of water, respectively (Manitoba and Manitoba Hydro, 2015).

The Long Spruce reservoir flooded approximately 14.5 km^2 of land and 15.9 km^2 of water, for a total reservoir size of approximately 30.4 km^2 (Manitoba and Manitoba Hydro, 2015). The reservoir is located downstream of the Kettle Generating Station and is contained almost entirely within the natural banks of the Nelson River (Manitoba and Manitoba Hydro, 2014) with the assistance of approximately 13 km of dykes (Manitoba and Manitoba Hydro, 2015). The reservoir is operated as a run of the river reservoir where the water levels are controlled by the discharges of the Kettle Generating Station (Manitoba Hydro, 2014). The water level on the reservoir generally operates just below 110.0 m ASL in the open water period and just below 110.3 m ASL during the winter, and is positioned above 109.4 ASL in the forebay approximately 95% of the time (Manitoba and Manitoba Hydro, 2014).

Further information about the Long Spruce Generating Station and reservoir is available in Appendix 4.

2.4.2.3 Limestone Generating Station

The Limestone Generating Station is a 1350 MW hydroelectric facility located at the former Limestone Rapids on the lower Nelson River and it is Manitoba Hydro's largest hydroelectric generating station (; Manitoba and Manitoba Hydro, 2015; Manitoba Hydro 2025b). The station is located approximately 23 km downstream of the Long Spruce Generating Station and approximately 55 km downstream from the Town of Gillam (Manitoba and Manitoba Hydro, 2015).

The operating head, or waterfall created by the station, is approximately 27.6 m (Manitoba Hydro, 2021). The discharge capacities of the generating station and spillway are 5,000 m^3/s and 9,600 m^3/s of water, respectively (Manitoba and Manitoba Hydro, 2015).

The Limestone reservoir flooded approximately 2.2 km^2 of land and 25.0 km^2 of water, for a total reservoir size of approximately 27.2 km^2 (Manitoba and Manitoba Hydro, 2015). The reservoir is contained almost entirely within the natural banks of the Nelson River (Manitoba Hydro, 1990). The banks of the pre-flood Limestone reservoir footprint are ice-scoured and typically, seasonal vegetation does not occur below the well-defined high-ice trim line, and little organic material is present in the overburden (Maclaren Plansearch Inc. & InterGroup Consultants Ltd., 1986). The reservoir water level is maintained below the winter trimline except near the Limestone Generating Station (Maclaren Plansearch Inc. & InterGroup Consultants Ltd., 1986). Flooding was predicted at the mouths of Brook Creek and Clements Creek (Maclaren Plansearch Inc. & InterGroup Consultants Ltd., 1986).

The reservoir is operated as a run of the river reservoir where the water levels are controlled by the discharges of the Kettle Generating Station (Manitoba and Manitoba Hydro, 2014). The water level on the reservoir generally operates at 85.3 m ASL (Manitoba Hydro, 2021). The maximum operating forebay elevation during open water is 85.313 m ASL and the normal minimum operating forebay elevation is 82.296 m ASL (Manitoba and Manitoba Hydro, 2014).

Further information about the Limestone Generating Station and reservoir is available in Appendix 5.

2.4.2.4 Potential Conawapa Reservoir

Developing a hydroelectric generating station at the Conawapa site on the lower Nelson River was an option conceived in the early 1970s, and Manitoba Hydro commissioned studies for a potential Conawapa Generation Project in the 2000s (Manitoba and Manitoba Hydro, 2015).

The Conawapa G-res Model described in this thesis represents a hypothetical scenario for possible future hydroelectric development at the Conawapa site. It does not represent a development plan being proposed by Manitoba Hydro. This author is not aware of any current plans to build the Conawapa Generating Station. Such a project is not included as a potential option in the Manitoba Hydro 2025 Integrated Resource Plan, which recommends the type and quantity of energy investments needed in Manitoba by 2035 (Manitoba Hydro, 2025c) and which is currently under review by the Manitoba Public Utilities Boad.

The Conawapa modelling scenario is roughly based on design concepts presented in the Needs For and Alternatives To (NFAT) review by the Public Utilities Board (PUB) of Manitoba Hydro's preferred development plan (Manitoba Hydro, 2013a, 2013b) and the Manitoba/Manitoba Hydro Regional Cumulative Effects Assessment (Manitoba and Manitoba Hydro, 2015). Under this modelling scenario, the Conawapa Generating Station would be a 1,485 MW hydroelectric facility located on the lower Nelson River and it would become Manitoba Hydro's largest hydroelectric generating station. The station would be

located approximately 28.5 km downstream of the Limestone Generating Station and approximately 90 km northeast of the Town of Gillam.

The Conawapa reservoir would flood approximately 11 km^2 of land and 27.8 km^2 of water, for a total reservoir size of approximately 38.8 km^2. The reservoir would be contained almost entirely within the natural banks of the Nelson River. To be conservative, the areal extent of flooded land employed in this model is double that which was cited in the NFAT documents (Manitoba Hydro, 2013a) so as not to understate potential lifecycle GHG emissions. The reservoir would be operated as a modified run of the river reservoir where the reservoir has limited storage capability. The Full Supply Level of the reservoir is estimated to be at 57.2 m ASL. Further information about the potential Conawapa Generating Station and reservoir is available in Appendix 6.

2.5 Churchill River Diversion

2.5.1 CRD Overview

The Churchill River Diversion (CRD) was constructed between 1973-1976 (Manitoba Hydro, 2014) (Figure 2-14). It diverts approximately 80% of the flow from the Churchill River into the lower Nelson River to increase water flows for hydroelectric power generation (Manitoba and Manitoba Hydro, 2015). The CRD comprises three main components: 1) Missi Falls Control Structure; 2) South Bay Diversion Channel; and 3) Notigi Control Structure.

The Missi Falls Control Structure is a dam that was built at Missi Falls, which is the natural outlet of Southern Indian Lake (Manitoba and Manitoba Hydro, 2014; Manitoba and Manitoba Hydro, 2015). Southern Indian Lake is a natural swelling or enlargement of the

Churchill River. The control structure regulates the amount of water that discharges downstream through the Churchill River and amount of water impounded in Southern Indian Lake and subsequently diverted into the Nelson River basin. In accordance with the final Manitoba Water Power Act Licence for the CRD, minimum releases from the control structure shall not be less than 14 m^3/s during the open water period and 42 m^3/s during the ice cover period (Manitoba Conservation and Climate, 2021).

The South Bay Diversion Channel is a passageway that was excavated to connect the South Bay of Southern Indian Lake to Issett Lake of the Rat River-Burntwood River-Nelson River system (Manitoba and Manitoba Hydro, 2015). The channel is approximately 61 m wide at its base and approximately 9.3 km long (Manitoba and Manitoba Hydro, 2015).

The Notigi Control Structure is located on the Rat River at the outlet of Notigi Lake. The structure controls the flow of the diverted Churchill River/Southern Indian Lake and the Rat River into the Burntwood River-Nelson River system (Manitoba and Manitoba Hydro, 2015). In accordance with the final Manitoba Water Power Act Licence for the CRD, average weekly flows released from the Notigi Control Structure shall not exceed 991 m^3/s from May 16th and October 31st, and shall not exceed 963 m^3/s from November 1st and May 15th (Manitoba Conservation and Climate, 2021). Mean monthly water levels in the Notigi forebay range from approximately 254.4 m to 258.3 m ASL (Manitoba and Manitoba Hydro, 2014).

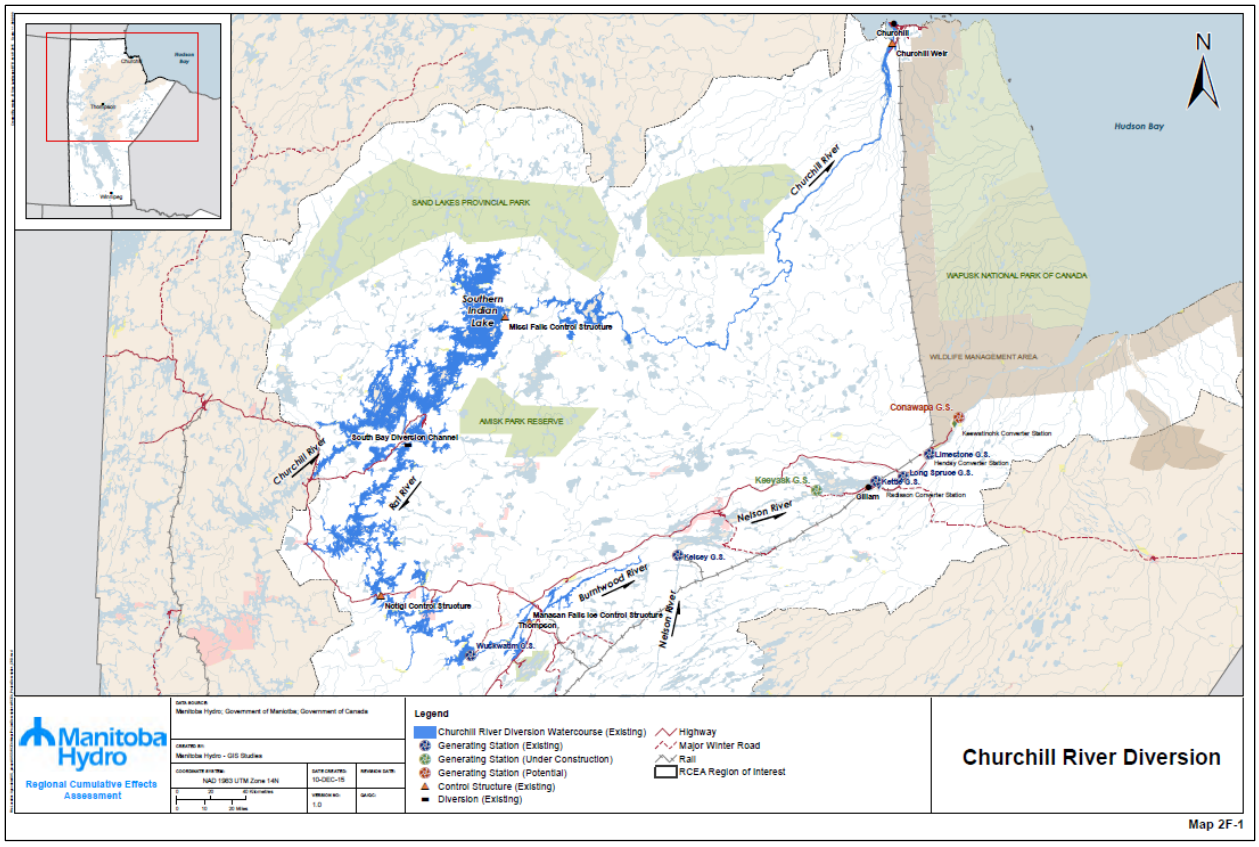


Figure 2-14 Churchill River Diversion
Source: Manitoba and Manitoba Hydro, 2015

2.5.2 CRD Flooding

The Missi Falls and Notigi Control Structures are operated so the mean daily water level (without the effect of wind and waves) on Southern Indian Lake is not greater than 258.32 m above sea level (Manitoba Conservation and Climate, 2021; Manitoba Hydro, 2022). Water levels on Southern Indian Lake are approximately 2.7 m higher than pre-CRD levels and approximately 15.2 m higher upstream of the Notigi Control Structure (Manitoba and Manitoba Hydro, 2014).

The surface area of the flooded aquatic system in the Regional Cumulative Effects Assessment (RCEA) Zone 4 (e.g. Southern Indian Lake) and RCEA Zone 6 (e.g. Rat River, Issett Lake, Karsakawigimak Lake, Pemichigamau Lake, Central and West Mynarski Lakes,

Rat Lake, and Notigi Lake) are estimated to be 2,914 km^2 (Newbury et al., 1984; Manitoba and Manitoba Hydro, 2014). This includes approximately 759 km^2 of flooded land (Manitoba and Manitoba Hydro, 2014), which is more than 2.5 times the amount of land flooded for all of the lower Nelson River reservoirs (Table 2-2).

As discussed by McCullough (1981) the impact of flooding on water retention times varied amongst the flooded areas. Overall, estimated water retention times increased from 0.51-year pre-flood to 0.72-year after flooding (McCullough, 1981).

2.5.3 Preflood Landcover and Relevance for GHG Modelling

The CRD is located within the Precambrian Shield Physiographic Region (Natural Resources Canada, 2019). The northern portion of the CRD, which includes the portion of Southern Indian Lake north of Long Point, is located in the Taiga Shield Ecozone, Selwyn Lake Upland, Northern Indian Lake Ecodistrict (Smith et al., 1998). The southern portion of the CRD is located within the Boreal Shield Ecozone, Churchill River Upland Ecoregion, Southern Indian Lake Ecodistrict (Smith et al., 1998). Similarly, the northern portion of the CRD, which includes the northern part of Southern Indian Lake, is in the Low Subarctic Wetland Region and the southern portion of the CRD is located within the High Boreal Wetland Region (Tarnocai, 2006).

2.5.3.1 Geology

The surficial geology is primarily comprised of Quaternary glaciolacustrine sediments that were deposited in glacial Lake Agassiz (Matile and Keller, 2006). The layered Quaternary deposits are composed of clay, silt, and to a lesser amount sand, that range approximately 1 to 20 m thick (Matile and Keller, 2006). These clayey glaciolacustrine deposits

extensively cover the area and have smoothed the underlying bedrock into a landscape that ranges from undulating to hummocky, with episodes of steeps slopes, irregular bedrock ridges and outcrops (Smith et al., 1998). Below these deposits are Paleozoic carbonates, and beneath these are Precambian granitoid and greenstone (Gauthier et al., 2022).

2.5.3.1.1 Modelling Carbonate Watersheds

It is necessary to understand how carbon is cycled amongst terrestrial and aquatic systems before and after flooding in order to determine the impact that hydroeletric reservoirs have on GHG emissions. An aspect of carbon cycling that is challenging and not well studied is the lateral transfer of all organic and inorganic species of carbon from land to surface waters (Tank et al., 2018; Wang et al., 2019), including the transport of dissolved inorganic carbon (DIC) (Jarvie et al., 2017). In areas with carbonate strata (such as the Paleozoic carbonates that are beneath the CRD), chemical weathering of carbonate rock can produce significant quantities of DIC in the form of bicarbonate HCO_3^- (Jarvie et al., 2017; Tank et al., 2018). Impounding rivers for hydroelectric development can alter the dominant biogeochemical processes that influence carbon cycling in the waterway (Han et al., 2018).

A challenge for modelling CRD GHG emissions is applying a model such as G-res, whose formulas were developed from reservoir datasets that may not represent the carbonate deposits that lay beneath the CRD. For example, data collected from Quebec reservoirs (and which underpin in part, G-res formulas) may be more representative of Precambian bedrock (Vincent, 1985) than the carbonate strata underlying the CRD. It is

challenging to model GHG emissions from flooding and land use change if the models have not been calibrated with data that is site-specific to the area of interest. Calibrating the G-res Tool for Canadian reservoirs is an active area of research (Prairie et al., 2025).

2.5.3.2 Peatlands

Peatlands cover much of the poorly drained clayey deposits, with deeper accumulations occuring in the topographic depressions (Smith et al., 1998b; Tarnocai et al., 2011). Peat types include shallow peat, peat veneer, peat plateau bogs, and less frequently, fens and palsa bogs (Smith et al., 1998). Each of these peatland types have the potential to store, generate, and release GHGs at varying rates (Pelletier et al., 2007, 2011, 2015; Turetsky et al., 2014; Treat et al., 2021). Discontinuous permafrost occurs widely throughout the area and is associated with peat deposits (Smith et al., 1998). A challenge for modelling net CRD GHG emissions involves assigning or developing appropriate GHG emission factors to adequately represent GHG emissions from the pre-flood diverse peat landscape.

3 Methods

3.1 Application of the G-res Tool to the Keeyask Reservoir

The following sections summarize the data inputs that were used to model GHG emissions for the Keeyask reservoir. A more comprehensive explanation of the data inputs is included in Appendix 1

3.1.1 Reservoir Information

Table 3-1 illustrates the inputs that are used to model pre and post Keeyask GHG emissions.

Table 3-1 Keeyask Reservoir G-res Tool Inputs

Reservoir Information			
Country	Canada	River Length before Impoundment (m)	
Longitude of Dam (DD)	-95.23	Phosphorus Concentration (ug/L)	58.5
Latitude of Dam (DD)	56.34	Trophic Level	Eutrophic
Climate Zone (Reservoir Area)	Boreal	Mean Global Horizontal Radiance (kWh/m^2/d)	4.8
Impoundment Year	2020	Mean Temperature per Month (°C)	
Reservoir Area (km^2)	100.4	January	-25.6
Reservoir Volume (km^3)	0.3587	February	-22.16
Water Level (m above sea level)	159	March	-15.37
Maximum Depth (m)	31	April	-4.37
Mean Depth (m)	3.6	May	4.58
Littoral Area (%)	26	June	11.13
Thermocline Depth (m)	0	July	15.23
Water Intake Depth (m)	28	August	13.61
Secondary Water Intake Depth (m)		September	6.8
Soil Carbon Content (kgC/m^2)	11.94	October	-0.1
Annual Wind Speed at 10 m (m/s)	4.0	November	-11.84
Water Residence Time (WRT, yrs)	0.0034	December	-22.62
Annual Discharge Main Intake (m^3/s)	3300		
Annual Discharge Secondary Intake (m^3/s)		Mean Annual Air Temperature (C°)	-4.2

3.1.2 Modelled Pre-Flood GHG Emissions

G-res estimates pre-flood GHG emissions by classifying the pre-flood landscape into landcover types and applying GHG emission factors to each landcover category, as illustrated below.

Landcover Classification (ha)
- Class 1
- Class 2
- Class 3
- ...

X

GHG Emission Factors
- Class 1 EF
- Class 2 EF
- Class 3 EF
- ...

(3.1)

The G-res landcover classifications are listed below. The categories are general, as the model is intended to address reservoirs and pre-flood landscapes worldwide, and include:

- Bare Areas,
- Croplands,
- Forest,
- Grasslands/Shrubland,
- Settlements,
- River Area Before Impoundment,
- Wetlands,
- Drained Peatlands.

Default GHG emission factors are built into G-res for each of the pre-flood landcover types listed above. They are provided for each terrestrial landcover class (i.e., all of the above except for categories: River Area Before Impoundment and Drained Peatlands) for mineral and organic soils. The source of G-res default emission factors for forests on mineral soils is Pan et al. (2011). All remaining G-res default emission factors for the other terrestrial landcover types were derived from IPCC 2006 and IPCC 2014 Tier 1 default values (Prairie et al., 2024). G-res advises model users to replace the G-res default emission factors with site-specific/user-defined values if such information is available (Prairie et al., 2024). Similarly, the IPCC (2019) recognizes there is high uncertainty in using their Tier 1 default emission factors which were developed at a global level. It is IPCC Good Practice to choose a method that results in higher accuracy and to develop country-specific emission factors to reduce uncertainty, if sufficient data exists (IPCC, 2019).

There is a twofold challenge with using the preset G-res method for estimating pre-flood GHG emissions from the Keeyask reservoir footprint. First, the G-res pre-flood landcover classification is very general. A more detailed classification system may align more appropriately with the Keeyask pre-flood reservoir landcover which is an assemblage of heterogeneous peatlands, that are underlain with discontinuous permafrost, and contain various types of freshwater systems such as streams, ponds, pools, shorelines, etc. (Keeyask Hydropower Limited Partnership, 2012a). This spatially diverse landscape presents a challenge for establishing a pre-flood baseline for GHG emissions. The general G-res classification of "wetlands" and the single generic G-res wetland emission factor may not adequately represent the majority of the Keeyask pre-flood landscape. The Keeyask environmental impact assessment developed several landscape classification schemes for various types of environmental and ecological analyses (Keeyask Hydropower Limited Partnership, 2012a, 2012b). These more detailed landcover classifications have been helpful for assessing Keeyask pre-flood GHG emissions and are discussed further in Section 3.1.2.1.

Second, the generic G-res GHG landcover emission factors are general in nature. The GHG emission factors are derived from Pan et al. (2011) for forests on mineral soils, and from the IPCC Tier 1 2006 and IPCC Tier 1 2014 GHG inventory guidance documents for all other northern terrestrial landcover types (Prairie et al., 2017). Peatland GHG emissions can be highly variable within a peatland and amongst peatlands, and over time (Roulet et al., 2007; Pelletier et al., 2011; Trudeau et al., 2013; Turetsky et al., 2014; Griffiths et al., 2017; McLaughlin & Packalen, 2021). This presents a challenge for developing peatland

GHG emission factors (Kazmere et al., 2024; Treat et al., 2024). In recent years GHG studies of northern peatlands have been conducted, synthesis of northern peatland GHG research has been assembled, and databases of northern peatland GHG emissions have been developed (Webster et al., 2018; Delwiche et al., 2021; Kuhn et al., 2021; Virkkala et al., 2021; Nelson et al., 2024; Treat et al., 2024).

This study explored the suitability of using this recent research to develop peatland GHG emission rates for use in the Keeyask G-res model.

The following sections explain the methods used to assess 1) Keeyask EIS landcover classifications and 2) northern peatland GHG emission factors derived from recent research, for use in the Keeyask G-res model. The approach is summarized in Figure 3-1.

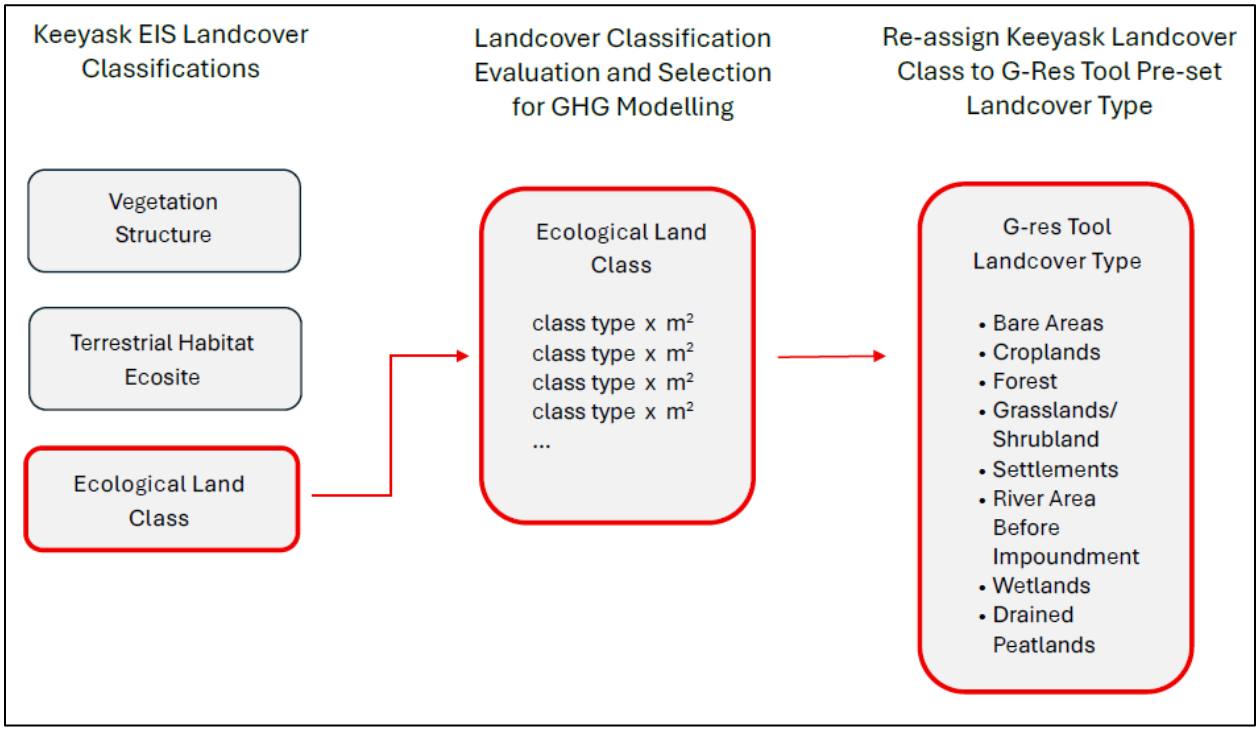


Figure 3-1 Methodology for Adapting Keeyask Landcover Classifications to G-res Tool Land Class

3.1.2.1 Pre-flood Landcover Classification

As discussed in Section 2.3.1.6 Peatlands, there is no globally recognized system that classifies peatlands according to their potential to store carbon or release GHG emissions (Lourenco et al., 2023). The Keeyask EIS classified the pre-flood Keeyask landscape, including the Keeyask pre-flood reservoir footprint, into three land cover schemes (Keeyask Hydropower Limited Partnership, 2012a, 2012b). They included: 1) Vegetation Structure Classification; 2) Terrestrial Habitat (Course and Fine Ecosite Type) Classification; and 3) Ecological Land Classification. Each of these classification schemes are described below.

3.1.2.1.1 Pre-Flood Landcover Classification: Vegetation Structure Classification

The Keeyask EIS terrestrial habitat studies categorized the Keeyask reservoir pre-flood landscape by Vegetation Structure (Keeyask Hydropower Limited Partnership, 2012b). Vegetation Structure was defined as the tallest vegetation layer having at least 25% total cover. Landcover and soil type (mineral or organic) were assessed as of 2003. Landcover categories included: Forest; Woodland; Mixture of Woodland and Sparsely Treed; Sparsely Treed; Tall Shrub; and Low Vegetation for Broadleaf, Needle and un-treed land, for both organic and mineral soils (Table 3.2). These categories are defined in Table (3-3).

Table 3-2 Keeyask Pre-Flood Landcover: Vegetation Structure

Terrestrial Habitat In Proposed Keeyask Project Footprint: Vegetation and Soil Type Areas as of 2003 (hectares)

Recent Burn *	Tree Type	Vegetation Structure		Land Type		All
				Mineral	Peatland	
No	Broadleaf	Forest	Initial flooding & reservoir expansion	41	5	46
		Woodland	Initial flooding & reservoir expansion	1	2	3
		Mixture of woodland and sparsely treed	Initial flooding & reservoir expansion		2	2
		Sparsely treed	Initial flooding & reservoir expansion	1	0	1
	Needle	Forest	Initial flooding & reservoir expansion	209	357	567
		Woodland	Initial flooding & reservoir expansion	33	748	781
		Mixture of woodland and sparsely treed	Initial flooding & reservoir expansion	2	424	426
		Sparsely treed	Initial flooding & reservoir expansion	21	441	462
	Untreed	Tall shrub	Initial flooding & reservoir expansion	25	192	217
		Low vegetation	Initial flooding & reservoir expansion	41	413	454
		Burned between 1993 to 2003	Initial flooding & reservoir expansion	13	356	369
2005	Broadleaf	Forest	Initial flooding & reservoir expansion	9	3	12
	Needle	Forest	Initial flooding & reservoir expansion	79	272	350
		Woodland	Initial flooding & reservoir expansion	23	675	698
		Mixture of woodland and sparsely treed	Initial flooding & reservoir expansion	2	255	257
		Sparsely treed	Initial flooding & reservoir expansion	4	140	144
	Untreed	Tall shrub	Initial flooding & reservoir expansion	0	6	6
		Low vegetation	Initial flooding & reservoir expansion	1	32	34
All				504.9	4,324	4,829
Percent of Total				10.5%	89.5%	100.0%

* Burned since 2003. Tree type shown is what was present in 2003.

Source: Adapted from ECOSTEM 2009.

Table 3-3 Vegetation Structure Classes

Vegetation Structure Type	**Percent Cover**
Forest	61% - 100% trees
Forest/ Tall Shrub	61% - 100% trees in upper canopy/ > 25% tall shrubs in lower canopy
Woodland	26% - 60% trees
Woodland/ Tall Shrub	26% - 60% trees in upper canopy / > 25% tall shrubs in lower canopy
Sparsely Treed	10% - 25% trees
Sparsely Treed/ Tall Shrub	10% - 25% trees in upper canopy / > 25% tall shrubs in lower canopy
Heterogeneous mixture of woodland and sparsely treed	Mixture of woodland and sparsely treed
Heterogeneous mixture of woodland and sparsely treed/ Tall Shrub	Mixture of woodland and sparsely treed with TS lower canopy
Tall Shrub	<10% tree cover and > 25% tall shrub cover
Low Shrub and/or Graminoid and/ or Bryoid	<10% trees and < 25% tall shrub and > 10% ground cover
Emergent	> 25% emergent vegetation cover
Barren	< 10% vegetation cover
Unclassified Young Regeneration	Burned after 1992, insufficient information to classify into vegetation structure type

Source: (Keeyask Hydropower Limited Partnership, 2012b; Table 2b-2)

3.1.2.1.2 Pre-Flood Landcover Classification: Terrestrial Habitat (Course and Fine Ecosite Type)

Terrestrial Habitat (Course and Fine Ecosite Type) Classification System of the Keeyask EIS is based upon vegetation type, vegetation age class, ecosite type, topographic position and either recent disturbance type (e.g., large fires, ice scouring) or water depth duration zone (Keeyask Hydropower Limited Partnership, 2012b Page 2-9). This classification scheme was used to categorize the area of land that would be flooded when the water level in the reservoir is 159 m above sea level. This is the maximum reservoir level allowed by the Keeyask Environment Act Licence under normal operating conditions (Manitoba Conservation and Water Stewardship, 2014). The classification system is illustrated in Figure 3-2.

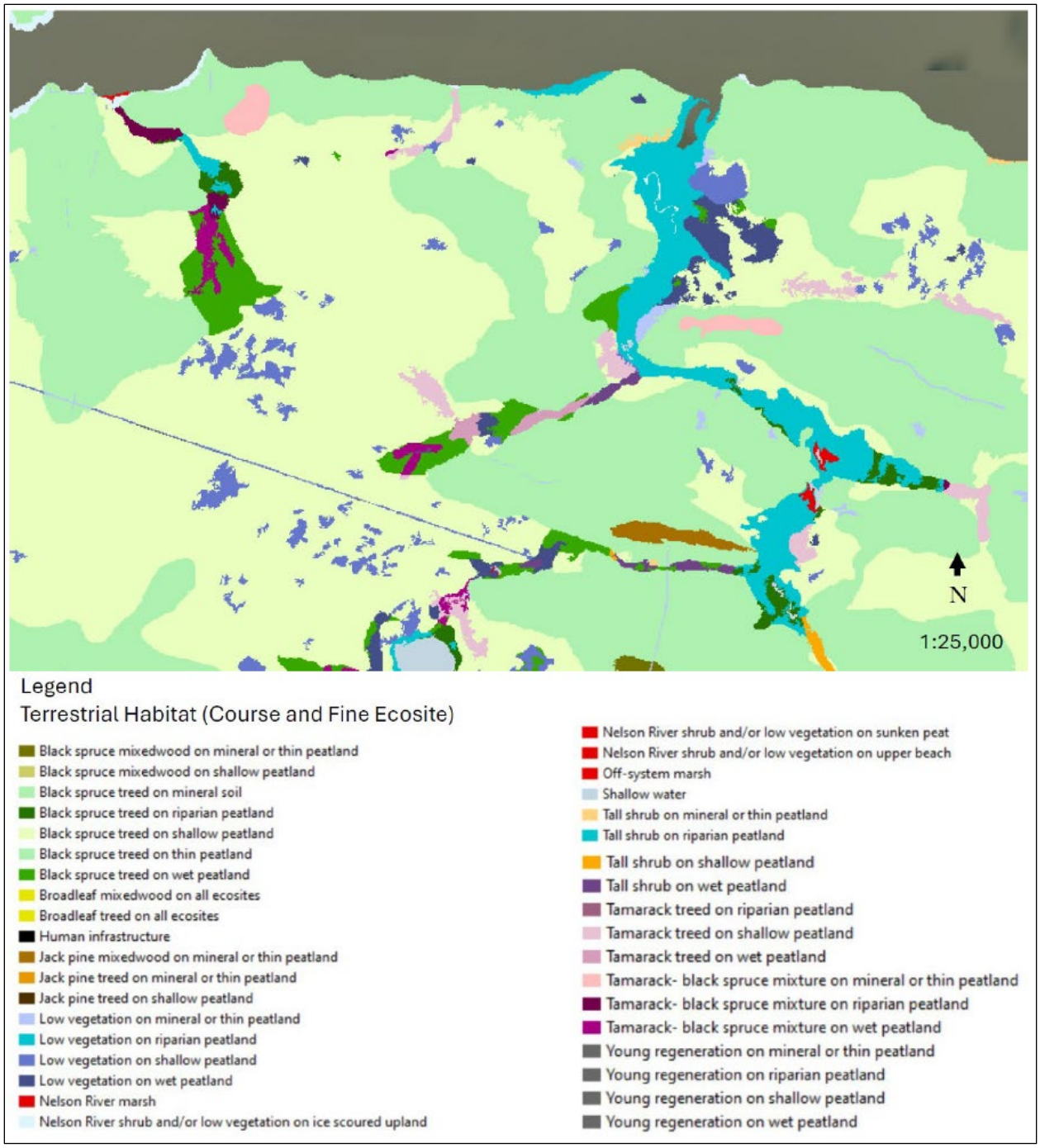


Figure 3-2 Keeyask Pre-Flood Landcover: Terrestrial Habitat (Course and Fine Ecosite)Classification
Source: Keeyask Geographical Information System Web Map

The above Terrestrial Habitat (Course and Fine Ecosite Type) Classification categories can be aligned with the G-res Tool input classes for pre-flood land cover.

3.1.2.1.3 Pre-Flood Landcover Classification: Ecological Land Classification

The Ecological Land Classification System of the Keeyask EIS categorized the Keeyask landscape according to ecologically distinct areas, considering surface geology, landforms, soils, vegetation, climate, wildlife, surface water, natural disturbances, human features, etc. (Keeyask Hydropower Limited Partnership, 2012b). The purpose of the classification scheme was to assess the potential impacts of the Keeyask Project on ecosystem composition, structure, and dynamics (Keeyask Hydropower Limited Partnership, 2012b). The Ecological Land Classification System is illustrated in Figure 3-3.

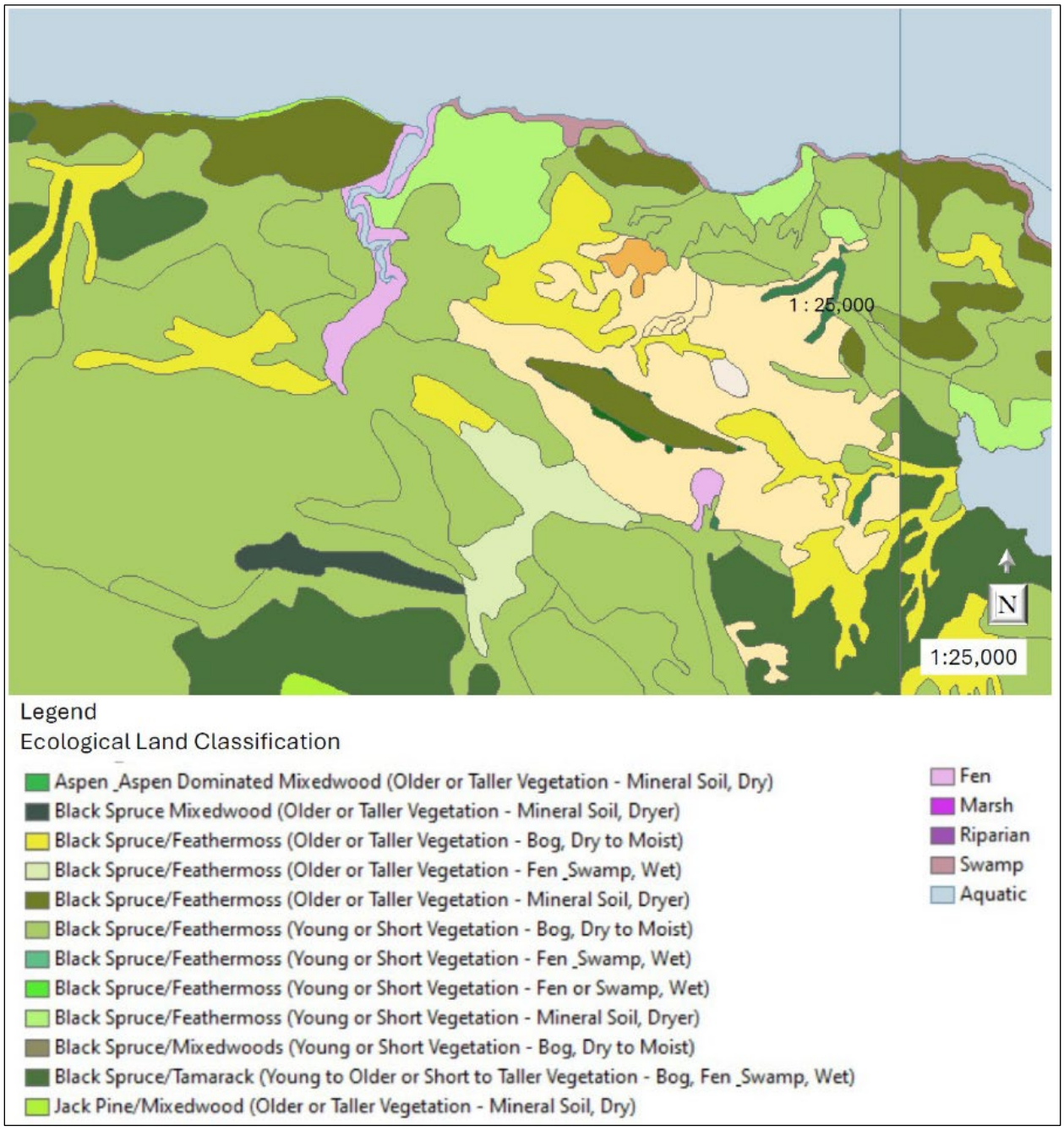


Figure 3-3 Keeyask Pre-Flood Landcover: Ecological Land Classification
Source: Keeyask Geographical Information System Web Map

The Ecological Land Classification System categories can be aligned with the G-res Tool input classes for pre-flood land cover.

3.1.2.2 Evaluation of Pre-Flood Landcover Classification Schemes:

Although none of the above classifications were designed for carbon accounting, each has potential to be used for defining the pre-flood Keeyask reservoir GHG emissions. Each of these classifications were assessed for suitability for use in G-res for modelling Keeyask lifecycle GHG emissions. The assessment is summarized in Table 3-4.

Table 3-4 Summary of Evaluation of Classification Schemes to Describe the Keeyask Pre-Flood Landcover for Applying the G-res Tool

Summary of Evaluation of Classifications to Describe the Keeyask Pre-Flood Land Cover for Applying the G-res Tool

Weight out of 100%	Evaluation Criteria	Vegetation Structure Score	Vegetation Structure Weighted Score	Terrestrial Habitat Score	Terrestrial Habitat Weighted Score	Ecological Land Score	Ecological Land Weighted Score
40%	Ability of landform classifiaction system to represent carbon cycling and GHG emissions for a heterogeneous boreal peatland environment . Includes ability to apply landform classification to the Keeyask reservoir pre-flood environment	50	20	70	28	85	34
35%	Availability of GHG emission factors for the landcover classification . Includes emission factors for CO2 and CH4 . Includes GHG emission factors for growing season/non-growing season; ice-free and ice-cover seasons	80	28	80	28	80	28
25%	Ability to transform landcover classes into G-res input categories	80	20	60	15	80	20
100%		**Score**	**68**	**Score**	**71**	**Score**	**82**

The Ecological Land Classification was evaluated to be the most suitable land classification for use in the G-res Tool. It was assessed to be a "Good" category for quantifying GHG emissions from the pre-flood Keeyask reservoir footprint.

3.1.2.2.1 Preparation of The Ecological Land Classification for Use in G-res Modelling

The Ecological Land Classification categorizes the boreal forest into the following sub-categories (Table 3-5), which provides adequate detail for the G-res LCA.

Table 3-5 Ecological Land Classification Aligned for G-res Tool Pre-Flood Landcover Categories

ECOLOGICAL LAND CLASSIFACTION
ALIGNED FOR G-RES TOOL PRE-IMPOUNDMENT LAND COVER CATEGORIES

BARE AREAS (MINERAL SOILS)
None

WETLANDS (ORGANIC SOILS)
Fen
Marsh
Swamp
Riparian

FOREST (MINERAL SOILS)
Aspen & Aspen Dominated Mixedwood (Older or Taller Vegetation - Mineral Soil, Dry)
Black Spruce Mixedwood (Older or Taller Vegetation - Mineral Soil, Dryer)
Black Spruce/Feathermoss (Older or Taller Vegetation - Mineral Soil, Dryer)
Black Spruce/Feathermoss (Young or Short Vegetation - Mineral Soil, Dryer)
Jack Pine/Mixedwood (Older or Taller Vegetation - Mineral Soil, Dry)

FOREST (ORGANIC SOILS)
Black Spruce/Feathermoss (Older or Taller Vegetation - **Bog**, Dry to Moist)
Black Spruce/Feathermoss (Young or Short Vegetation - **Bog**, Dry to Moist)
Black Spruce/Mixedwoods (Young or Short Vegetation - **Bog**, Dry to Moist)
Black Spruce/Feathermoss (Older or Taller Vegetation - Fen & Swamp, Wet)
Black Spruce/Feathermoss (Young or Short Vegetation - Fen & Swamp, Wet)
Black Spruce/Tamarack (Young to Older or Short to Taller Vegetation - **Bog**, Fen & Swamp, Wet)

AQUATIC
Aquatic (Included as "Pre-Flood Waterbodies")

The categories identify forest type (underlain by either mineral soils or organic soils). Wetlands are categorized by fen, marsh, riparian, and swamp. The Ecological Land Classification also identifies inland waters (e.g., aquatic areas), and bare areas (e.g., none).

A challenge with the Keeyask Ecological Land Classification is that forests located on bogs were classified as “Forests”. This is illustrated in Table 3-5 where the following categories are classified as Forest.

- Black Spruce/Feathermoss (Older or Taller Vegetation - **Bog**, Dry to Moist),
- Black Spruce/Feathermoss (Young or Short Vegetation - **Bog**, Dry to Moist),
- Black Spruce/Mixedwoods (Young or Short Vegetation - **Bog**, Dry to Moist),
- and the “Bog-dominated” sections of the Black Spruce/Tamarack (Young to Older or Short to Taller Vegetation - **Bog**, Fen & Swamp, Wet)

3.1.2.2.1.1 Modification of Pre-Flood Forest Land and Wetlands

Bogs are the largest land cover type in the Keeyask reservoir pre-flood footprint, amounting to over 90% of the pre-flood forest land cover (Keeyask Hydropower Limited Partnership 2012a). It is therefore important to couple land cover type with the appropriate GHG emission factors for estimating pre-flood GHG emissions. According to with *The Canadian Wetland Classification System* (National Wetlands Working Group, 1987) bogs are considered to be wetlands. The four bog classes highlighted above were redefined as “Wetlands” (Table 3-6).

The reclassification involved realigning the following forest categories to Wetlands (Bogs):

- Black Spruce/Feathermoss (Older or Taller Vegetation - **Bog**, Dry to Moist),
- Black Spruce/Feathermoss (Young or Short Vegetation - **Bog**, Dry to Moist),
- Black Spruce/Mixedwoods (Young or Short Vegetation - **Bog**, Dry to Moist),
- and the “Bog-dominated” sections of the Black Spruce/Tamarack (Young to Older or Short to Taller Vegetation - **Bog**, Fen & Swamp, Wet)

The forest classifications that remained as Forest (Organic Soils) included:

- Black Spruce/Feathermoss (Older or Taller Vegetation - Fen & Swamp, Wet),
- Black Spruce/Feathermoss (Young or Short Vegetation - Fen & Swamp, Wet), and
- "Fen & Swamp-dominated" sections of the Black Spruce/Tamarack (Young to Older or Short to Taller Vegetation - Bog, **Fen & Swamp**, Wet)

This realignment not only aligns with *The Canadian Wetland Classification System* (National Wetlands Working Group, 1987), but it also harmonizes with the classification of CO_2 and CH_4 emission factors developed by Virkkala et al., (2021) and Kuhn et al., (2021), respectively. The GHG emission factors developed by these studies were used in the G-res Keeyask model and are discussed in the section below. The re-organization of bogs from the forest to wetland category is based on the author's interpretation of the Keeyask Ecological Land Classification. This may introduce error or bias when computing the areal extent of each pre-flood land class since it is a deviation from the Ecological Land Classification as produced for the Keeyask Environmental Impact Assessment and Statement. The impact is discussed in Section 6.1.1 Uncertainty Analysis Pre-flood Landcover Classification.

Table 3-6 Ecological Land Classification: Re-Align Bogs for G-res Tool

ECOLOGICAL LAND CLASSIFACTION
ALIGNED FOR G-RES TOOL PRE-IMPOUNDMENT LAND COVER CATEGORIES
RE-ASSIGN BOGS TO WETLAND LAND COVER CATEGORY

BARE AREAS (MINERAL SOILS)
None

WETLANDS (ORGANIC SOILS)
Fen
Marsh
Swamp
Riparian
Bog
- Black Spruce/Feathermoss (Older or Taller Vegetation - Bog, Dry to Moist)
- Black Spruce/Feathermoss (Young or Short Vegetation - Bog, Dry to Moist)
- Black Spruce/Mixedwoods (Young or Short Vegetation - Bog, Dry to Moist)
- Black Spruce/Tamarack (Young to Older or Short to Taller Vegetation - **Bog**, Fen & Swamp, Wet)

FOREST (MINERAL SOILS)
Aspen & Aspen Dominated Mixedwood (Older or Taller Vegetation - Mineral Soil, Dry)
Black Spruce Mixedwood (Older or Taller Vegetation - Mineral Soil, Dryer)
Black Spruce/Feathermoss (Older or Taller Vegetation - Mineral Soil, Dryer)
Black Spruce/Feathermoss (Young or Short Vegetation - Mineral Soil, Dryer)
Jack Pine/Mixedwood (Older or Taller Vegetation - Mineral Soil, Dry)

FOREST (ORGANIC SOILS)
Black Spruce/Feathermoss (Older or Taller Vegetation - Fen & Swamp, Wet)
Black Spruce/Feathermoss (Young or Short Vegetation - Fen & Swamp, Wet)
Black Spruce/Tamarack (Young to Older or Short to Taller Vegetation - Bog, **Fen & Swamp,** Wet)

AQUATIC
Aquatic (Included as "Pre-Flood Waterbodies")

The pre-impoundment land cover in the reservoir area entered as inputs in the G-res Tool are as follows (Table 3-7):

Table 3-7 Pre-Impoundment Landcover: G-res Tool Input

Pre-Impoundment Land Cover in the Reservoir Area
Ecological Land Classification
Re-Assign Bog Landcover

	% Mineral Soil	% Organic Soil	% Total
Croplands			
Bare Areas	2.3%		2.3%
Wetlands		35.1%	35.1%
Forest	6.0%	3.4%	9.4%
Grassland/Shrubland			
Permanent Snow/Ice			
Settlements			
Total Terrestrial			**46.8%**
Water Bodies			53.2%
Total			**100.0%**

3.1.3 Pre-flood Terrestrial and Aquatic GHG Emission Factors

The scientific literature was examined to identify CO_2 and CH_4 emission rates from the northern and boreal peatlands. The search identified studies that focused on specific research sites, synthesis reports that assessed the results of multiple studies involving many research locations over several years, and newly created databases of CO_2 and CH_4 emissions at the Canadian, northern (arctic, boreal, permafrost regions), and global scales.

The approach followed the procedure illustrated in Figure 3-4 and explained in further detail in the sections below.

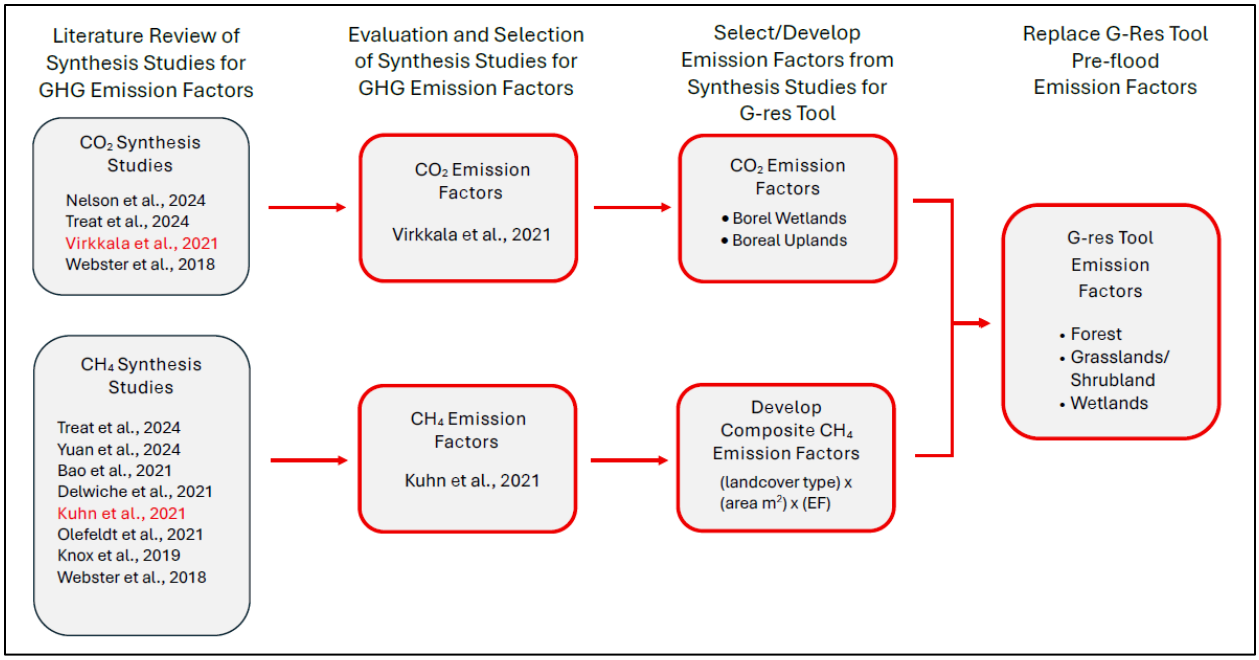


Figure 3-4 Methodology for Selecting and Developing Pre-flood CO_2 & CH_4 Emissions Factors for G-res Tool

3.1.3.1 CO_2 Terrestrial Emission Factor Studies

Based on a literature review, four studies containing a synthesis of CO_2 emission databases were selected for further evaluation for suitability for use in the G-res modelling of Keeyask lifecycle emissions. They are listed in Table 3-8. A summary of the assessment results is illustrated in Table 3-9.

Table 3-8 Assessment of CO_2 Terrestrial Emission Factors

Northern Peatland/Forest Synthesis Studies and Databases of Carbon Dioxide Emissions Evaluated for G-res Modelling of Keeyask Lifecycle Emissions	
Nelson et al., 2024	X-BASE: the first terrestrial carbon and water flux products from an extended data-driven scaling framework, FLUXCOM-X
Treat et al., 2024	Permafrost Carbon: Progress on Understanding Stocks and Fluxes Across Northern Terrestrial Ecosystems
Virkkala et al., 2021	Statistical upscaling of ecosystem CO_2 fluxes across the terrestrial tundra and boreal domain: Regional patterns and uncertainties
Webster et al., 2018	Spatially-integrated estimates of net ecosystem exchange and methane fluxes from Canadian peatlands

Table 3-9 Evaluation Results: CO_2 Emission Factor Studies

Evaluation Criteria to Assess Northern Peatland/Forest CO_2 Synthesis and Upscaling Studies for Applying the G-res Tool

Weight out of 100%	Evaluation Criteria	Virkkala et al., 2021 Score	Virkkala et al., 2021 Weighted Score	Treat et al., 2024 Score	Treat et al., 2024 Weighted Score	Nelson et al., 2024 Score	Nelson et al., 2024 Weighted Score	Webster et al., 2018 Score	Webster et al., 2018 Weighted Score
40%	Ability of the GHG emission factors derived from synthesis study to represent GHG emissions from the heterogeneous Keeyask pre-flood landscape . Does the study generate emission factors that represent the heterogeniuos peatlands by peatland type (e.g. bog, fen, marsh, swamp), boreal forest/upland, and grassland/shrub? or . Does the study generate composite GHG emission factors that represent boreal wetlands and the boreal forest?	80	32	80	32	60	24	75	30
30%	Does the study present emission factors that represent the entire year? . Annual emission factors, and/or . Emission factors for the growing season/non-growing season; and ice-free and ice-cover seasons?	90	27	75	22.5	40	12	75	22.5
30%	Breadth of sysnthesis study . Does the synthesis study/database include multiple site-specific studies (multiple representative sample sites) and/or other synthesis studies? . Does the synthesis study cover multiple years of site investigations/data collection? (i.e. assess a lengthy time series?)	85	25.5	85	25.5	80	24	80	24
100%		**Score**	**84.5**	**Score**	**80.0**	**Score**	**60.0**	**Score**	**76.5**

3.1.3.1.1 CO_2 Terrestrial Emission Factor Assessment Results

The database compiled by Virkkala et al. (2021) was selected as the source of pre-flood CO_2 emission factors for describing the Keeyask reservoir pre-flood terrestrial footprint based on the criteria described above.

Virkkala et al. (2021) examined ecosystem CO_2 fluxes from the high latitude tundra and boreal biomes, for latitudes greater than 45°N throughout the northern hemisphere. They compiled measurements of gross primary productivity, ecosystem respiration and net ecosystem exchange (CO_2 emissions to the atmosphere). The study reviewed a lengthy time series (1990 – 2015) of CO_2 emissions that were collected from eddy covariance networks, FLUXNET2015 (Pastorello et al., 2020) plus chamber studies. Incorporating both eddy covariance and chamber studies is complimentary and beneficial. Eddy covariance networks measure GHG exchange between the land and atmosphere at a larger measurement footprint than chamber studies and these studies have provided a long-term, continuous record of CO_2 and CH_4 emissions (Margolis et al., 2006; Lund et al., 2010; Strachan et al., 2015; Knox et al., 2021). Chamber studies have a smaller measurement footprint (m^2) which allows for a focused investigation such as on a specific vegetation type (Strack et al., 2017; Järveoja et al., 2018; Thalasso et al., 2023; Boonman et al., 2024). Chamber studies have been used widely in the boreal biome, providing widespread coverage of the heterogeneous landscape (Bao et al., 2021; Zhao & Zhuang, 2023). Virkkala et al. (2021) assessed data from 148 field locations, and for 1448 annual and growing season CO_2 fluxes.

Virkkala et al. (2021) presents CO_2 emissions for boreal uplands and boreal wetlands for the growing season and on an annual basis. These emission factor categories are well suited to be used as inputs for the G-res pre-flood landcover classes of forest, grasslands/shrub, and wetlands.

Although the Virkkala et al. (2021) boreal sites do not include measurements directly from the Keeyask area, they do include measurements from the boreal forest and boreal peatlands near Thompson, Manitoba (BOREAS site), which is approximately 200 kms to the southwest of Keeyask, and other boreal forest sites in Quebec and Alberta. Boreal CO_2 emission measurements were also incorporated from the Hudson Bay Lowlands on the western side of southern James Bay in the Attawapiskat River, Kinoje Lake, Moosonee region and other northern hemisphere boreal locations.

3.1.3.2 CH_4 Emission Factor Selection

Based on an extensive literature review, seven studies that included a synthesis of CH_4 emission databases were selected for further evaluation for suitability for use in the G-res modelling of Keeyask lifecycle emissions, and these are listed in Table 3-10. The databases were further assessed for suitability for the G-res modelling of Keeyask lifecycle emissions. A summary of the assessment results is illustrated in Table 3-11.

Table 3-10 Assessment of CH_4 Emission Factors

Northern Peatland/Forest Synthesis Studies and Databases of Methane Emissions Evaluated for G-res Modelling of Keeyask Lifecycle Emissions	
Treat et al., 2024	Permafrost Carbon: Progress on Understanding Stocks and Fluxes Across Northern Terrestrial Ecosystems
Yuan et al., 2024	Boreal–Arctic wetland methane emissions modulated by warming and vegetation activity
Bao et al., 2021	Wetland Heterogeneity Determines Methane Emissions: A Pan-Arctic Synthesis
Delwiche et al., 2021	FLUXNET-CH4: a global, multi-ecosystem dataset and analysis of methane seasonality from freshwater wetlands
Kuhn et al., 2021 Olefeldt et al., 2021	BAWLD-CH4: a comprehensive dataset of methane fluxes from boreal and arctic ecosystems
Knox et al., 2019	FLUXNET-CH4 SYNTHESIS ACTIVITY Objectives, Observations, and Future Directions
Webster et al., 2018	Spatially-integrated estimates of net ecosystem exchange and methane fluxes from Canadian peatlands

Table 3-11 Evaluation Results: CH_4 Emission Factor Studies

Evaluation Criteria to Assess Northern Peatland/Forest CH_4 Synthesis and Upscaling Studies for Applying the G-res Tool

Weight out of 100%	Evaluation Criteria	Yuan et al., 2024 Score	Yuan et al., 2024 Weighted Score	Treat et al., 2024 Score	Treat et al., 2024 Weighted Score	Kuhn et al., 2021 Score	Kuhn et al., 2021 Weighted Score	Webster et al., 2018 Score	Webster et al., 2018 Weighted Score
40%	Ability of the GHG emission factors derived from synthesis study to represent GHG emissions from the heterogeneous Keeyask pre-flood landscape . Does the study generate emission factors that represent the heterogeniuos peatlands by peatland type (e.g. bog, fen, marsh, swamp), boreal forest/upland, and grassland/shrub? or . Does the study generate composite GHG emission factors that represent boreal wetlands and the boreal forest?	50	20	80	32	85	34	75	30
30%	Does the study present emission factors that represent the entire year? . Annual emission factors, and/or . Emission factors for the growing season/non-growing season; and ice-free and ice-cover seasons?	70	21	75	22.5	85	25.5	75	22.5
30%	Breadth of sysnthesis study . Does the synthesis study/database include multiple site-specific studies (multiple representative sample sites) and/or other synthesis studies? . Does the synthesis study cover multiple years of site investigations/data collection? (i.e. assess a lengthy time series?)	80	24	85	25.5	80	24	80	24
100%		**Score**	**65.0**	**Score**	**80.0**	**Score**	**83.5**	**Score**	**76.5**

Weight out of 100%	Evaluation Criteria	Delwiche et al., 2021 Score	Delwiche et al., 2021 Weighted Score	Knox et al., 2019 Score	Knox et al., 2019 Weighted Score	Bao et al., 2021 Score	Bao et al., 2021 Weighted Score
40%	Ability of the GHG emission factors derived from synthesis study to represent GHG emissions from the heterogeneous Keeyask pre-flood landscape . Does the study generate emission factors that represent the heterogeniuos peatlands by peatland type (e.g. bog, fen, marsh, swamp), boreal forest/upland, and grassland/shrub? or . Does the study generate composite GHG emission factors that represent boreal wetlands and the boreal forest?	65	26	70	28	65	26
30%	Does the study present emission factors that represent the entire year? . Annual emission factors, and/or . Emission factors for the growing season/non-growing season; and ice-free and ice-cover seasons?	75	22.5	75	22.5	60	18
30%	Breadth of sysnthesis study . Does the synthesis study/database include multiple site-specific studies (multiple representative sample sites) and/or other synthesis studies? . Does the synthesis study cover multiple years of site investigations/data collection? (i.e. assess a lengthy time series?)	80	24	80	24	80	24
100%		**Score**	**72.5**	**Score**	**74.5**	**Score**	**68.0**

3.1.3.2.1 CH_4 Terrestrial Emission Factor Selection

The Boreal–Arctic Wetland and Lake Methane Dataset (BAWLD-CH4) database, as described by Kuhn et al. (2021) and Olefeldt et al. (2021), was selected as the primary source of CH_4 emission factors for this GHG LCA. BAWLD-CH4 is an extensive database of methane fluxes collected at the site-level from the northern hemisphere boreal and arctic ecosystems at latitudes greater than 50°N. At the time of publishing the Kuhn et al. (2021) and Olefeldt et al. (2021) studies, BAWLD-CH4 included data up to 2020.

BAWLD-CH4 includes terrestrial CH_4 emission factors for Boreal Forest, Dry Tundra, Permafrost Bog, Bog, Fen, Tundra Wetland and Marsh landcover types. The Boreal Forest, Permafrost Bog, Bog, Fen and Marsh landcover categories and emission factors align well with the Keeyask Ecological Land Classification of Fen, Marsh, Swamp, Riparian and Forest. They also align well with the G-res pre-flood landcover classes of Forest, Grassland/Shrubland and Wetland.

The database includes aquatic CH_4 emission factors for Large Lakes, Midsize Lakes, Small Glacial, Midsize Yedoma, Midsized Peatland, Small Peatland and Small Yedoma lake classes. The Midsized Peatland Lake and Small Peatland Lake categories align with the Keeyask “Shallow Water” Ecological Land Class. The classifications also aligned well with the G-res pre-flood “Aquatic” land class.

BAWLD-CH4 includes data collected using both the eddy covariance and chamber methods. Most of the data are from chamber-based studies, which have provided extensive coverage in the northern regions.

BAWLD-CH4 does not include winter CH_4 terrestrial emissions for boreal forests and wetlands. Terrestrial winter CH_4 fluxes for these classifications were estimated following the approach by Treat et al. (2018) where non-growing season terrestrial CH_4 emissions amounted on average to 16% of annual CH_4 terrestrial emissions. BAWLD-CH4 does include aquatic winter CH_4 fluxes for Midsized and Small Peatland Lakes.

3.1.3.3 Preparation of Terrestrial Emission Factors for Use in G-res Modelling

3.1.3.3.1 CO_2 Terrestrial Emission Factors

Annual CO_2 emission factors (Net Ecosystem Exchange) for the Boreal Upland and Boreal Wetland were selected from Virkkala et al. (2021) (Table 3-12). They were based on a study period of 1990-2015. Virkkala et al. (2021) did not develop separate emission factors for mineral and organic soils. These emission factors were used as composite emission factors for both mineral and organic soils in the Keeyask G-res model. The Virkkala et al. (2021) Boreal Upland CO_2 emission factors were used for the G-res categories of Forest and Grassland/Shrubland, and the Boreal Wetland CO_2 emission factors were used for the G-res Wetland category.

Table 3-12 CO_2 Emission Factors for Keeyask G-res Lifecycle Model

CO_2 Emission Factors for Ecological Land Classification		
Land Class	**Annual NEE g CO_2-C/m^{-2}/yr**	**Annual NEE t CO_2-C/ha/yr (Converted for G-res)**
Boreal Uplands (Forest, and Grassland/Shrubland)	-47	-0.47
Boreal Wetlands	-38	-0.38
Source: Virkakkala et al., 2021 (Table 1)		

3.1.3.3.1 CH_4 Terrestrial Emission Factors

CH_4 emission factors were adapted from the Boreal–Arctic Wetland and Lake Methane Dataset (BAWLD-CH4) (Kuhn et al., 2021).

3.1.3.3.1.1 Terrestrial Emissions

Growing season CH_4 terrestrial emission factors were adopted from Kuhn et al. (2021) Table 3 median values for Boreal Forest, Permafrost Bog, Bog, Fen and Marsh land classes. Non-growing season emission factors were not included in the BAWLD-CH4 database/Kuhn et al. (2021) study. They were therefore estimated as being 16% of total annual emissions according to Treat et al. (2018). The Keeyask Ecological Land Classifications of "Swamps" and "Riparian" were assigned the same emissions factors as the BAWLD-CH4 emission factors for bogs and fens, respectively, following descriptions by Kuhn et al. (2021).

A composite wetland emission factor was developed by calculating a weighted average for the land classifications of Permafrost Bog, Bog, Fen, Marsh and Peatland Lakes (small and medium). This involved multiplying each [wetland class] by their [CH_4 emission factor], by their [areal extent (km^2) as defined by the Keeyask ECO Land Class], and by summing these calculations. The results are displayed in Table 3-13.

Length of Growing Season/Non-Growing Season and Ice Free/Ice Cover

For the G-res modelling exercise, the length of the growing season in the Keeyask area was defined as 135 days and non-growing season as 230 days. The ice-free period was defined as being 185 days and ice cover period as 180 days. The calculation methodology is as follows.

3.1.3.3.1.2 Growing Season

Growing season was calculated according to the methods adopted by Lund et al. (2010) who assessed CO_2 exchange amongst northern and tundra peatlands, Strachan et al. (2016) who assessed CO_2 exchange in a boreal bog; and Webster et al. (2018) who assessed CO_2 and CH_4 fluxes from Canadian peatlands.

Lund et al. (2010) and Strachan et al. (2016) defined the start of growing season as the first day where the mean daily air temperature remains above 5°C for seven consecutive days. Growing season ends on the first day of seven consecutive days when the air temperature is below 5°C. Webster et al. (2018) defined the growing season as starting on first day where the mean daily air temperature is above 5°C for five consecutive days beginning on March 1. Growing season ends on the day when the minimum air temperature is less than − 2°C occurring after August 1st.

Hourly and daily average temperatures collected at the Manitoba Hydro Keeyask Meteorological Station (05UF597) and by the Government of Canada Historical Climate Data at Gillam, Manitoba were used to establish the growing season at Keeyask. The average growing season for the 10-year period from 2014–2023 using the Lund et al. (2010) and Strachan et al. (2016) approach was 134 days. The average growing season for the same period using the Webster et al. (2018) approach was 136 days. The mean/median value of 135 derived from these two approaches was used for modelling pre-flood Keeyask reservoir GHG emissions.

3.1.3.3.1.3 Length of Ice Cover

Determining the number of days when the Keeyask Reservoir and surrounding inland waterbodies are free of ice for the purpose of estimating pre and post flood GHG emissions is challenging. The timing, extent and location of spring melting and winter freeze-up varies within the reservoir and surrounding inland waters within any given year and varies from year to year. The transition between open water and ice cover is best described as a process and not as a precise measurement in time.

The method used for assessing ice thaw and ice formation for this modelling exercise involved examining Sentinel-2 L2A false colour satellite images from April–June and October–December for 2017 to 2024. Based on satellite data, May 15 to November 15 (185 days) would be a reasonable and conservative estimate to use for the length of the ice-free period Keeyask reservoir GHG modelling.

Table 3-13 Calculation of Keeyask Pre-Flood Wetland Composite CH_4 Emission Factor

CALCULATION OF KEEYASK PRE-FLOOD WETLAND COMPOSITE CH_4 EMISSION FACTOR FOR ECOLOGICAL LAND CLASSIFICATION

	% of Total Wetland Area	GROWING SEASON/ OPEN WATER FLUXES mg CH_4 m^2 d	GROWING SEASON/ OPEN WATER FLUXES Weighted Average mg CH_4 m^2 d	GROWING SEASON/ OPEN WATER FLUXES Weighted Average g CH_4 m^2 season Growing Season Days 135 Days	WINTER FLUXES PER SEASON g CH_4 m^2 season 230 Days	Annual Flux kg CH_4 / ha / Year
BOG	77.2%					
Permafrost	8.0%	2.3	0.2	0.02	0.00	0.3
Bog	69.2%	24.6	17.0	2.29	0.44	27.3
FEN	2.6%	54.0	1.4	0.19	0.04	2.2
MARSH	0.7%	106.0	0.7	0.10	0.02	1.1
SWAMP	5.9%	24.6	1.4	0.19	0.04	2.3
RIPARIAN	0.4%	54.0	0.2	0.03	0.00	0.3
Wetland (Sub-Total)	**86.7%**			**2.82**	**0.5**	**33.6**
INLAND AQUATIC						
	% of Total Wetland Area	OPEN WATER FLUXES mg CH_4 m^2 d	OPEN WATER FLUXES Weighted Average mg CH_4 m^2 d	OPEN WATER FLUXES Weighted Average g CH_4 m^2 season 185 Ice Free Days	WINTER SEASONAL FLUXES Weighted Average g CH_4 m^2 / season 180 Ice Cover Days	Annual Flux kg CH_4 / ha / Year
SMALL PEATLAND LAKE	1.7%					
Growing Season Diffusive		16.4	0.3	0.1		0.5
Ebullitive		22.5	0.4	0.1		0.7
Winter Storage					0.02	0.2
Ice Bubble Storage					0.02	0.2
MID-PEATLAND LAKE	11.7%					
Diffusive		18.4	2.1	0.4		4.0
Ebullitive		45.1	5.3	1.0		9.7
Winter Storage					0.10	1.0
Ice Bubble Storage					0.10	1.0
Sub-Total Inland Water Ice Free Days Weighted Average Flux				**1.5**	**0.3**	**17.5**
ANNUAL COMPOSITE WETLAND (WETLAND + INLAND AQUATIC) EMISSION FACTOR						**51.13**

Notes:

Percentage of Wetland based on Keeyask GIS ECO Land Class within 159m Shoreline

Wetland CH_4 Growing Season Fluxes: CH_4 Based on "Warm Season" (~May - October) median values from Kuhn et al 2021 Table 3

Length of Growing Season: Calculated as 135 days for the period 2014-2023. Based on methods of Lund et al (2010), Strachan et al (2016), and Webster et al (2018).

Wetland CH_4 Non-Growing Season Fluxes: Estimated as per Treat et al 2018. Non-growing season CH4 emissions average 16% of annual emissions.

Aquatic (Peatland Lake) CH_4 Ice Free Fluxes (e.g. small and medium sized lakes): from Kuhn et al 2021 Table 4 (Diffusive and Ebullition Emissions)

Aquatic (Peatland Lake) CH_4 Winter Fluxes (e.g. small and medium sized lakes): from Kuhn et al 2021 Table 5 (Storage and Ice Bubble Storage Emissions)

Length of Ice Free Season: Based on Papakyriakou et al (2024), interpretation of satellite imagery (2017 - 2024) and field photography (2017 - 2021).

Table 3-14 illustrates the final CH_4 emission factors used in the Keeyask G-res model. Values are displayed in the G-res Tool emission factor metrics ($kgCH_4/ha/yr$).

Table 3-14 Composite Methane Emission Factors for Keeyask G-res Model

Land Class	**Annual Emissions kg CH_4/ha/yr (G-res Emission Factor Metrics)**
Boreal Uplands (Forest, and Grassland/Shrubland)	-0.64
Boreal Wetlands	51.13

3.1.3.1 Pre-flood Aquatic GHG Emission Factors

3.1.3.1.1 Pre-Flood Aquatic CH_4 Emission Factors

The G-res default pre-flood CH_4 emission factor for "Water Bodies", for the Keeyask model, is 4.4 kg CH_4/ha/yr, which is applied to the river/lake to be flooded. This emission factor would not be applied to the peatland pools or other water bodies within the terrestrial landscape (uplands) to be flooded. Alternatively, for Keeyask modelling, the G-res default emission factor was replaced by the pre-flood flux of 5 mg CH_4/m^2/yr which translates into 9.25 kg CH_4/ha/yr. This emission factor was derived by Environnement Illimité inc. from their in-situ measurements of CH_4 diffusive emissions from Gull Lake and associated backbays during 2009 – 2013 (Marchand et al., 2015).

3.1.3.1.2 Pre-Flood Aquatic CO_2 Emission Factors

G-res does not include pre-flood CO_2 emission factors for water bodies, and G-res does not estimate net CO_2 diffusive emissions by subtracting post-flood CO_2 emissions from pre-flood CO_2 emissions (Prairie et al., 2017). G-res recognizes that a portion of CO_2 emissions that occur within the reservoir result from organic material being brought into the reservoir from upstream sources. These emissions are considered to be "displaced" emissions, and they would have occurred within the reservoir footprint or downstream

regardless of whether the reservoir existed or not. These emissions were not caused by the reservoir and are removed from G-res estimates of net reservoir lifecycle GHG emissions. G-res applies a regression model to the gross post-flood CO_2 emissions to estimate net CO_2 reservoir emissions (Prairie et al., 2018). The results of the regression calculation are that over the 100-year life of the reservoir, an average of 31 (±6) % of CO_2 emissions are allocated to the reservoir (Prairie et al., 2021).

3.1.4 Modelling Inputs

Figure 3-5 illustrates the G-res default pre-flood emission factors. Figure 3-6 illustrates the emission factors replaced for the Keeyask G-res model. The remainder of the Keeyask reservoir G-res inputs are described in Appendix 1.

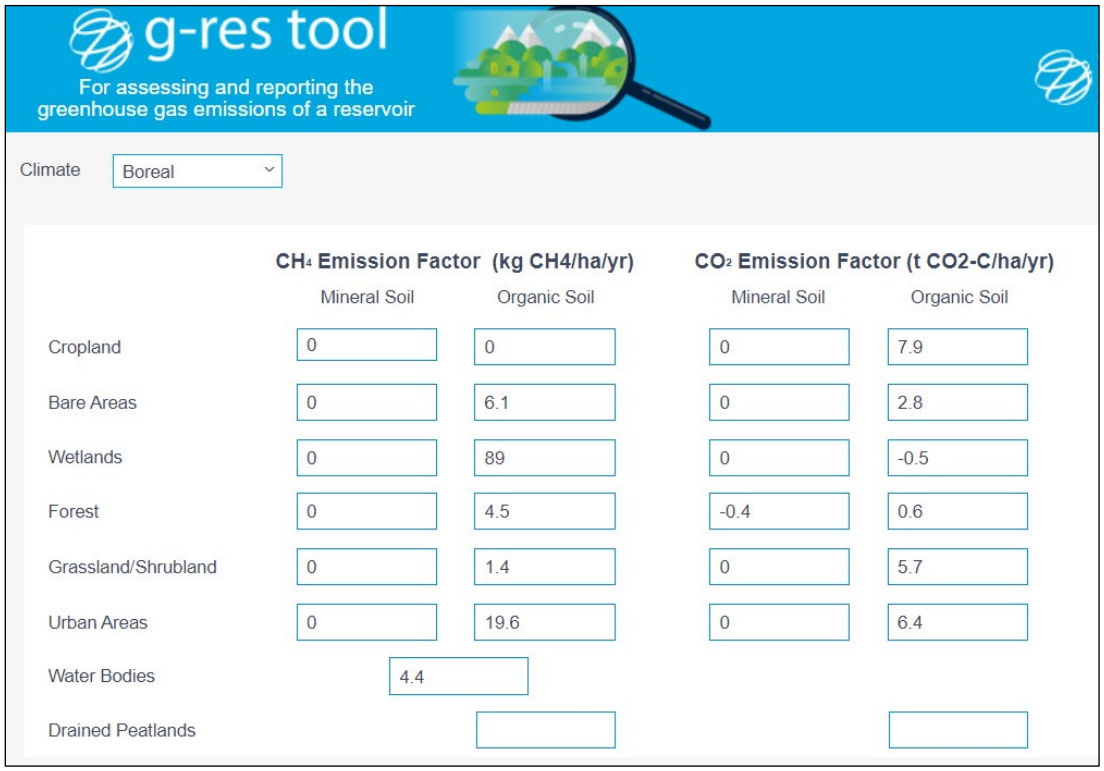


Figure 3-5 G-res Tool Default Pre-Flood GHG Emission Factors

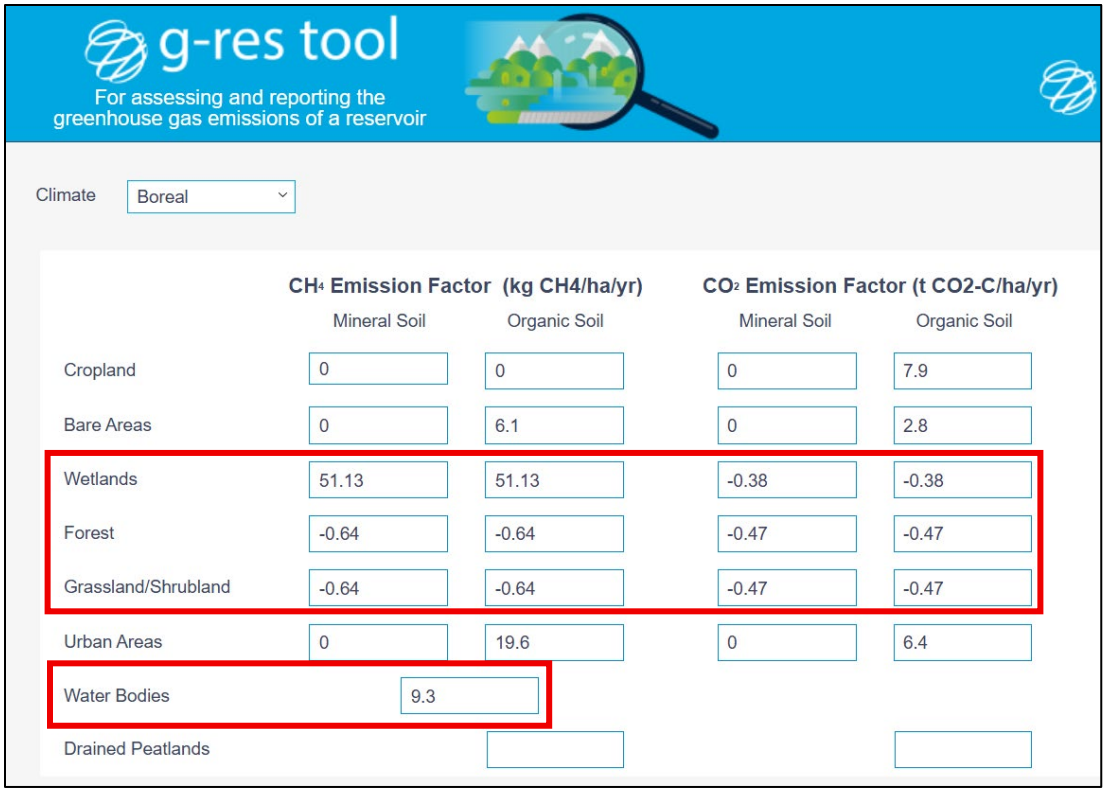


Figure 3-6 Pre-flood GHG Emission Factors Developed for the Keeyask G-res Model

3.2 Application of the G-res Tool to the Remainder of Lower Nelson River Reservoirs and CRD

The G-res Tool was used to model lifecycle GHG emissions for the Kettle, Long Spruce, Limestone and hypothetical Conawapa reservoirs, and for the CRD. Key inputs are summarized below and the details are described in Appendices 3-7, respectively.

The site-specific pre-flood CO_2 and CH_4 emission factors developed for the Keeyask model were also used for each of the G-res reservoir/flooded lands models. This included the emission factors for the G-res categories for forest, grassland/shrubland, wetlands and water bodies.

3.2.1 Kettle Reservoir

In the absence of detailed pre-flood land cover data for the Kettle reservoir and given the similar terrain (Keeyask Hydropower Limited Partnership, 2012a), the Keeyask Ecological Land Classification was apportioned to the Kettle reservoir footprint to estimate pre-flood land cover type and area.

3.2.2 Long Spruce Reservoir

The Long Spruce reservoir is located almost entirely within the natural banks of the Nelson River (Manitoba and Manitoba Hydro, 2014). The Regional Cumulative Effects Study (Manitoba and Manitoba Hydro, 2014) describes the Nelson River reach between the Kettle and Limestone Generating Stations as:

- Having the highest banks of the Nelson River
- Approximately 80% of this river reach is comprised of ice-scoured till banks
    - Vegetation below the winter trim line is comprised of grasses and stunted willows
    - Vegetation above the winter trim line includes closed forest of white and black spruce
    - Bedrock is often observed at the open water shoreline
- The remaining 20% is composed of slumping overburden.
    - The bottom half is often steep and bare

In the absence of detailed pre-flood landcover data for the Long Spruce reservoir, the above information was used to estimate the pre-flood land cover categories for the Long Spruce G-res model. Approximately one third of the pre-flood landscape was allocated to

each of the following: forest, grasslands/shrublands and wetlands (to address the riparian edges of the Nelson River and tributaries).

3.2.3 Limestone Reservoir

The banks in the pre-flood Limestone reservoir footprint are ice-scoured and typically, seasonal vegetation does not occur below the well-defined high-ice trim line and little organic material is present in the overburden (Maclaren Plansearch Inc. & InterGroup Consultants Ltd., 1986). The reservoir water level is maintained below the winter trimline except near the Limestone Generating Station (Maclaren Plansearch Inc. & InterGroup Consultants Ltd., 1986). Flooding was predicted at the mouths of Brook Creek and Clements Creek (Maclaren Plansearch Inc. & InterGroup Consultants Ltd., 1986).

In the absence of detailed pre-flood landcover data for the Limestone reservoir, the above information was used to estimate the pre-flood land cover categories for the Limestone G-res model. For the G-res model, one half of the flooded land was allocated to forest and one half to grassland/shrubland on mineral soils.

3.2.4 Potential Conawapa Reservoir (Modelling Scenario)

Under this modelling scenario, the reservoir would be contained almost entirely within the natural banks of the Nelson River. The pre-flood land cover was estimated to comprise forest (22%), grassland/shrubland (77%) and bare areas (1%).

3.2.5 CRD

In the absence of detailed pre-flood land cover data for the CRD, the Keeyask Ecological Land Classification was apportioned to the CRD flooded footprint to estimate the pre-flood land cover type and area.

4 Net Lifecycle GHG Emissions for the Keeyask Hydroelectric Reservoir

G-res modelling results for the Keeyask reservoir are described below and illustrated in Tables 4-1 to 4-4, and Figures 4-1 to 4-6. Post-flood emissions are estimated from G-res empirical formulas. Pre-flood emissions are calculated by applying GHG emission factors (user-defined or G-res default) to the pre-flood landcover type (user-defined or G-res derived). The Keeyask reservoir is modelled to be a net source of GHG emissions over the modelled 100-year lifetime.

4.1 Annual and Lifetime GHG Emissions

Post-Impoundment Keeyask reservoir lifecycle GHG emissions were modelled as follows:

Total for 100 Years: 972,198 tCO_2e

Annual Average for 100 Years: 9,722 tCO_2e/yr

Annual Average for 100 Years per square meter: 97 $gCO_2e/m^2/yr$

Pre-Impoundment Keeyask reservoir lifecycle GHG emissions were modelled as follows:

Total for 100 Years: 110,208 tCO_2e

Annual Average for 100 Years: 1,102 tCO_2e/yr

Annual Average for 100 Years per square meter: 11 $gCO_2e/m^2/yr$

NET Keeyask reservoir lifecycle GHG emissions were modelled as follows:

Total for 100 Years: 861,990 tCO_2e (95% Confidence Interval 749,988 – 987,936)

Annual Average for 100 Years: 8,620 tCO_2e/yr (95% CI 7,500 – 9,879)

Annual Average for 100 Years per square meter: 86 $gCO_2e/m^2/yr$ (95% CI 75 – 98)

G-res calculates the 95% confidence interval as follows (Prairie et al., 2017a, 2021). The 95% confidence interval is calculated for each of the G-res GHG pathways (i.e. CO_2 diffusion, CH_4 diffusion, CH_4 ebullition and CH_4 degassing) using the Root Mean Square Error. This involves comparing the G-res predicted values against the observed values for each of the GHG pathway models. The normal Gaussian distributions of the four models are randomly selected 1000 times using the Box-Muller algorithm. A distribution is created from the 1000 randomly selected GHG predictions, and this distribution is used to determine the 95% confidence intervals for the 100-year GHG lifecycle estimates.

4.2 Gross Emissions by Gas Type and Pathway

On a carbon dioxide equivalency basis, the amount of Post Impoundment CO_2 and CH_4 emissions are estimated to be 4,435 tCO_2e/yr, (45.6%) and 5,287 tCO_2e/yr (54.4%), respectively, over the 100-year life of the reservoir (Table 4-3). G-res uses a methane global warming potential over 100 years (GWP 100) of 34 for conversion to CO_2 equivalency (Prairie et al., 2024).

CO_2 emissions are estimated to be entirely from diffusion. They are estimated to be 345.2 $gCO_2/m^2/yr$ in Year 1, decline to 110.0 $gCO_2/m^2/yr$ in Year 10, to 67.8 $gCO_2/m^2/yr$ in Year 20, and reach 0 $gCO_2/m^2/yr$ in Year 100 (Table 4-4 and Figure 4-2).

CH_4 emissions are estimated to be 75% from diffusion, 16% from degassing (emissions as water passes through the generating station turbines and spillway), and 9% from ebullition (sediment generated bubbling) (Figure 4-4). CH_4 diffusive emissions are estimated to be 129.6 $gCO_2e/m^2/yr$ in Year 1, decline to 96.6 in Year 10, to 69.7 $gCO_2e/m^2/yr$ in Year 20, and reach 5.1 $gCO_2e/m^2/yr$ in Year 100 (Table 4-4). CH_4 degassing

emissions and CH_4 bubble emissions are estimated at a constant rate of 8.7 and 4.5 $gCO_2e/m^2/yr$, respectively, over the 100-year life of the reservoir.

Annual Post-Impoundment CO_2 and CH_4 emissions combined from all pathways are estimated to be 488.1 $gCO_2e/m^2/yr$ in Year 1 (2021), 290.1 $gCO_2e/m^2/yr$ in Year 5 (2025), 219.8 $gCO_2e/m^2/yr$ in Year 10 (a year often referenced with boreal reservoirs), and 150.7 $gCO_2e/m^2/yr$ in Year 20 (a year referenced by the IPCC), and 18.3 $gCO_2e/m^2/yr$ in Year 100 (Table 4-4).

4.3 Pre-Impoundment Emissions

The pre-impounded reservoir footprint is modelled to be an overall net source of GHG emissions, releasing an estimated 1,102 tCO_2e/yr (Table 4-1 and Figure 4-1). This comprises a CO_2 sink of -6,560 tCO_2/yr related to CO_2 absorption from the forest, grassland/shrubland, and wetland land cover types (Table 4-3). The pre-impounded reservoir is modelled to be a source of CH_4 at an estimated rate of 7,662 tCO_2e/yr (Table 4-3). These emissions are a result of the areal extent of the wetlands and the wetland emission factors used in the G-res model.

4.4 Keeyask Reservoir Net Lifecycle GHG Emissions

4.4.1 Net 100-Year Lifecycle Emissions

Annual Net GHG emissions are modelled to be 86 $gCO_2e/m^2/yr$ (95% CI 75 – 98), and 8,620 tCO_2e/yr (95% CI 7,500 – 9,897) for the entire reservoir, on average over the 100-year life of the reservoir (Table 4-1). Total Net emissions for the 100-year life of the reservoir are estimated to be 861,990 tCO_2e (95% Confidence Interval 749,988 – 987,936) (Table 4-1).

Post-Impoundment Net emissions for the entire reservoir are estimated to be 477 $gCO_2e/m^2/yr$ in Year 1 (2021), 279 $gCO_2e/m^2/yr$ in Year 5 (2025), 209 $gCO_2e/m^2/yr$ in Year 10 (2030) (a year often referenced with boreal reservoirs), and 140 $gCO_2e/m^2/yr$ in Year 20 (2040) (a year referenced by the IPCC), and 7 $gCO_2e/m^2/yr$ in Year 100 (Figure 4-3).

Table 4-1 Modelled Post-Impoundment, Pre-Impoundment and Net 100-Year Lifecycle GHG Emissions for the Keeyask Hydroelectric Reservoir

Emissions per m^2 of Reservoir $gCO_2e/m^2/yr$				
Post-Impoundment	Pre-Impoundment	Net GHG Footprint	95% Confidence Intervals	
97	11	86	75	98
Total Reservoir Emissions per Year tCO_2e/yr				
Post-Impoundment	Pre-Impoundment	Net GHG Footprint	95% Confidence Intervals	
9,722	1,102	8,620	7,500	9,897
Total Lifetime Reservoir Emissions tCO_2e				
Post-Impoundment	Pre-Impoundment	Net GHG Footprint	95% Confidence Intervals	
972,198	110,208	861,990	749,988	987,936

Table 4-2 Modelled Keeyask Reservoir Pre-Impoundment and 100-Year Annual Average Post-Impoundment Emissions by Gas Type per m^2

Emissions per m^2 of Reservoir $gCO_2e/m^2/yr$				
Post-Impoundment				
Total	of which CO_2	of which CH_4		
97	44	53		
Pre-Impoundment				
Total	of which CO_2	of which CH_4		
11	-65	76		
Net GHG Footprint			**95% Confidence Intervals (for Total Net Only)**	
Total	of which CO_2	of which CH_4		
86	110	-24	75	98

Table 4-3 Modelled Pre-Impoundment and 100-Year Annual Average Post-Impoundment Emissions by Gas Type for the Entire Keeyask Reservoir

Emissions Rate for Entire Reservoir tCO_2e/yr				
Post-Impoundment				
Total	of which CO_2	of which CH_4		
9,722	4,435	5,287		
Pre-Impoundment				
Total	of which CO_2	of which CH_4		
1,102	(6,560)	7,662		
Net GHG Footprint			95% Confidence Intervals (for Total Only)	
Total	of which CO_2	of which CH_4		
8,620	10,995	(2,375)	7,500	9,897

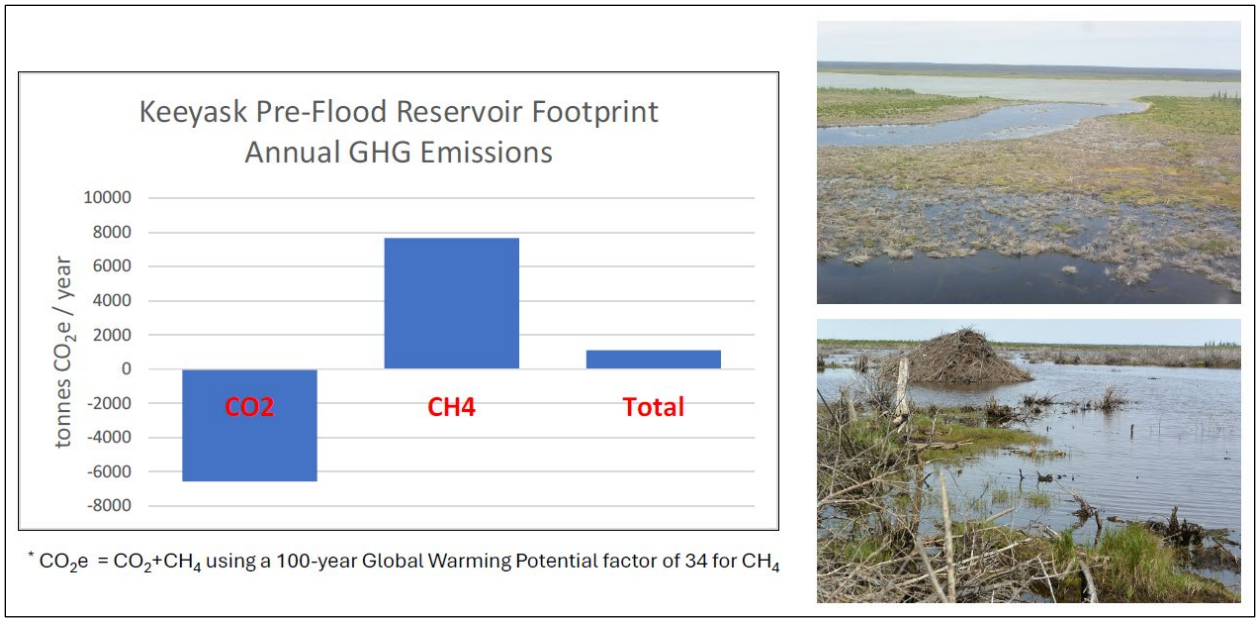


Figure 4-1 Modelled Keeyask Reservoir Pre-Impoundment GHG Emissions

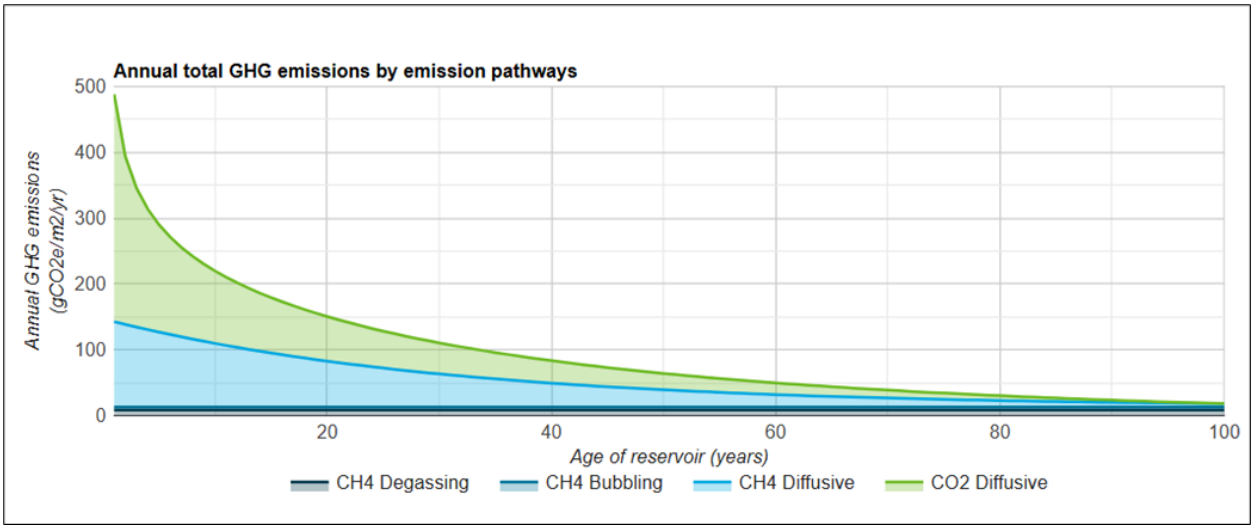


Figure 4-2 Annual Total Gross Lifecycle Emissions by Emission Pathway

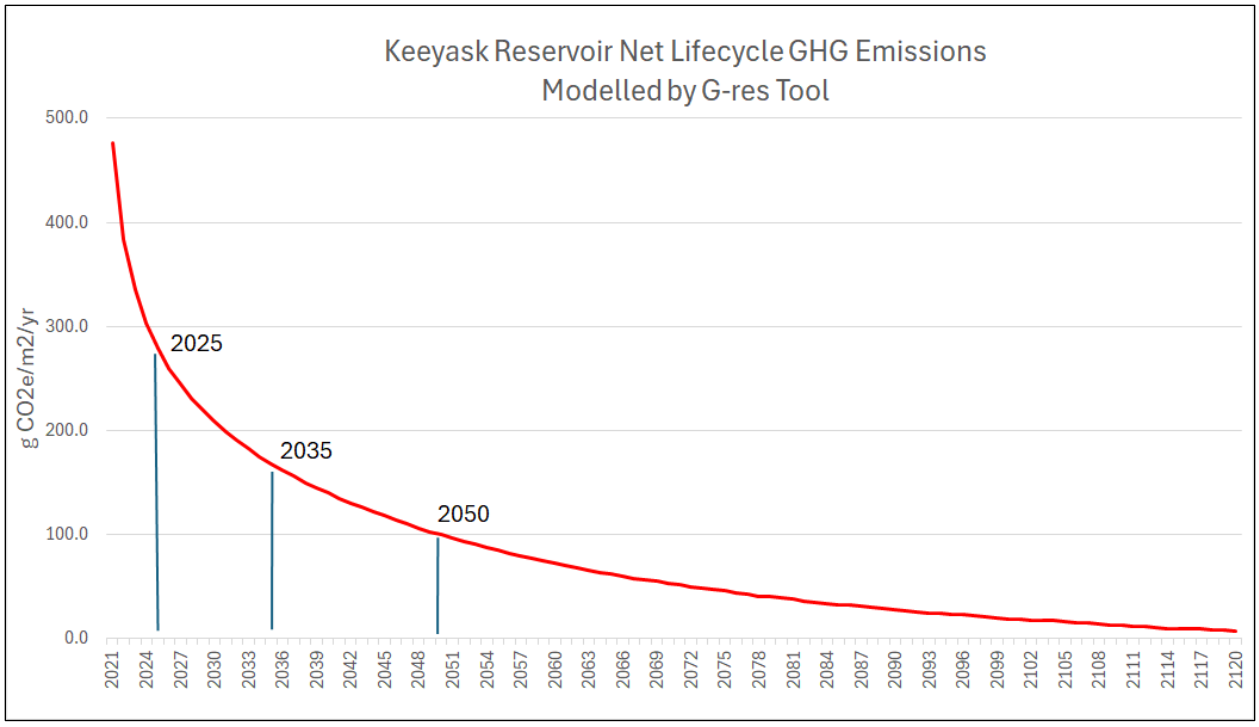


Figure 4-3 Keeyask Reservoir Modelled Net Lifecycle GHG Emissions

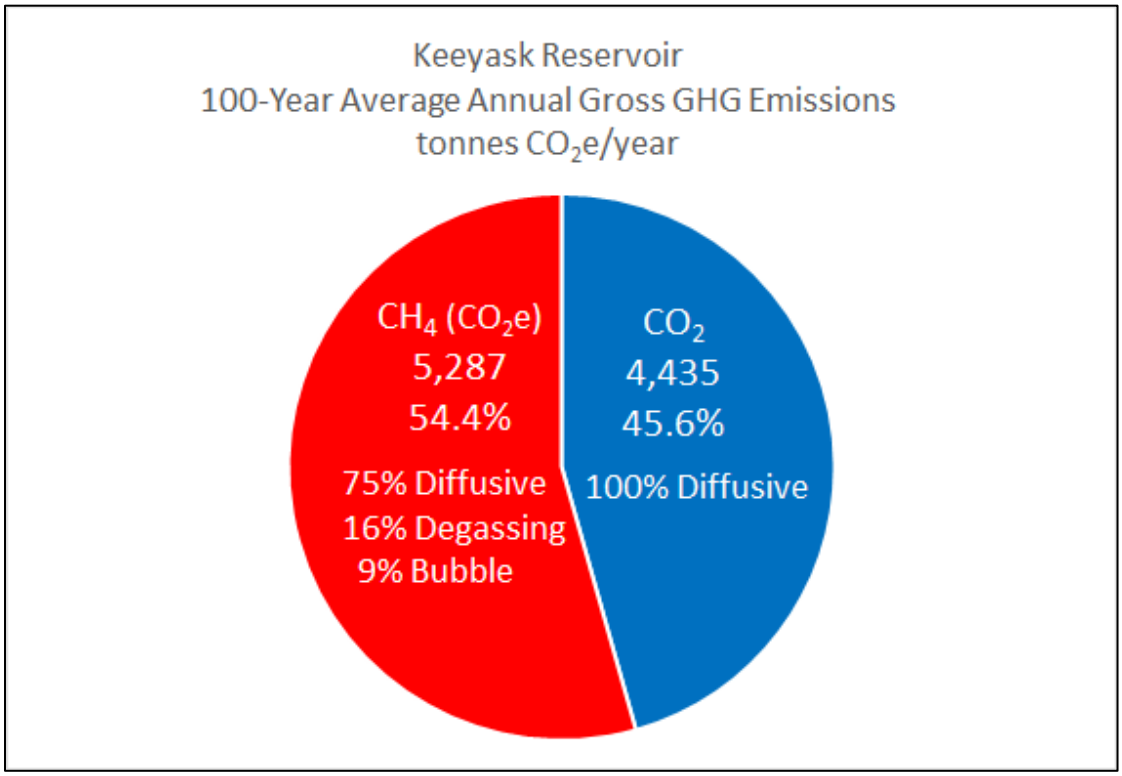


Figure 4-4 Keeyask Reservoir 100-Year Annual Average Gross GHG Emissions by GasType

Table 4-4 Total Annual Gross Lifecycle Emissions by Gas Type and Emission Pathway

G-res Tool Estimated Emissions for the Keeyask Reservoir
Using Ecological Land Classification and
User-Defined Preflood GHG Emission Factors

Total Annual Gross GHG Emissions by Emission Pathway
Excluding "Displaced" Diffusive CO_2 Fluxes
g $CO_2e/m^2/yr$

Year	CO_2	CH_4			Total
	Diffusive	Diffusive	Bubble	Degassing	
1	345.194	129.641	4.545	8.675	488.1
2	254.855	125.473	4.545	8.675	393.5
3	210.833	121.440	4.545	8.675	345.5
4	182.985	117.536	4.545	8.675	313.7
5	163.132	113.758	4.545	8.675	290.1
6	147.963	110.101	4.545	8.675	271.3
7	135.830	106.562	4.545	8.675	255.6
8	125.807	103.136	4.545	8.675	242.2
9	117.326	99.821	4.545	8.675	230.4
10	110.014	96.612	4.545	8.675	219.8
20	67.754	69.684	4.545	8.675	150.7
100	0.000	5.100	4.545	8.675	18.3

4.4.2 GHG Emission Rates: 2025 onwards; 2035 onwards; and 2050 onwards

Net Keeyask reservoir lifecycle GHG emissions were modelled for 2025 onwards (2025 to 2120), 2035 onwards (2035 to 2120), and 2050 onwards (2050 to 2120) to coincide with (Figure 4-5):

- Manitoba Hydro's 2025 Integrated Resource Plan

  The Manitoba Hydro 2025 Integrated Resource Plan (IRP) is a road map to meet Manitoba's growing energy needs to 2035 through energy efficiency, by adding more electricity capacity and by setting a pathway to achieving a net-zero electricity grid (Manitoba Hydro, 2025c).

- Manitoba's 2035 net-zero electricity grid target

  Manitoba's goal is to achieve a net-zero electricity grid by 2035 (Manitoba, 2025).

- Manitoba's and Canada's 2050 carbon neutral economy goals

  Manitoba plans to work towards a carbon-neutral economy by 2050 (Manitoba, 2025).

  The Government of Canada has committed to achieve a national target of net-zero GHG emissions by 2050 through the passing of the Canadian Net-Zero Emissions Accountability Act (S.C. 2021, c. 22) on June 29, 2021.

Total net Keeyask reservoir emissions are modelled to be:

- 2025 onwards: 701,696 tonnes CO_2e (95% Confidence Interval 610,475 – 804,143)
- 2035 onwards: 481,719 tonnes CO_2e (95% Confidence Interval 419,096 – 552,050)
- 2050 onwards: 282,425 tonnes CO_2e (95% Confidence Interval 245,710 – 323,659)

G-res calculates the 95% CI for total 100-year lifecycle emissions. It does not calculate confidence intervals for individual years or ranges of years. The G-res generated 100-year 95% CI (-13% and +15%) for the Keeyask reservoir was applied as the uncertainty for the net Keeyask reservoir emissions for 2025 onwards, 2035 onwards, and 2050 onwards. This approach may introduce bias to the uncertainty values.

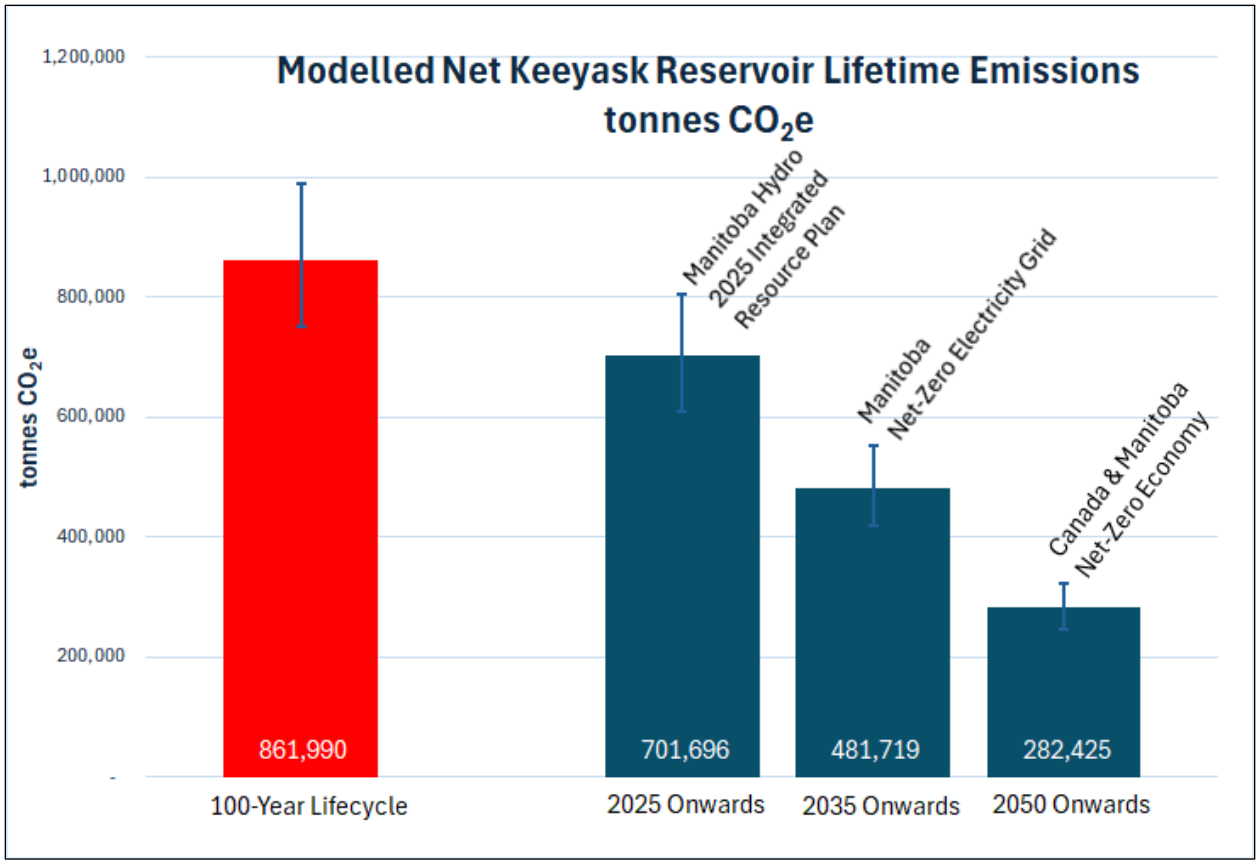


Figure 4-5 Keeyask Reservoir Modelled Net Lifecycle Emissions

4.4.3 Keeyask Reservoir GHG Lifecycle Emission Intensity

The modelled reservoir GHG 100-year average lifecycle emissions intensity is estimated to be 2.2 gCO_2e/kWh (95% Confidence Interval 2.0 – 3.0). Emission intensity was calculated using the net annual average power produced by the Keeyask Generating Station (3,886 GWh/year) from 2022 – 2025 (Manitoba Hydro, 2026). Net power refers to the power available to the electricity grid. GHG emission intensity has been modelled for 2025 onwards (2025 to 2120), 2035 onwards (2035 to 2120), and 2050 onwards (2050 to 2120) as follows (Figure 4-6):

- 2025 onwards: 1.9 gCO_2e/kWh

- 2035 onwards: 1.4 gCO_2e/kWh
- 2050 onwards: 1.0 gCO_2e/kWh

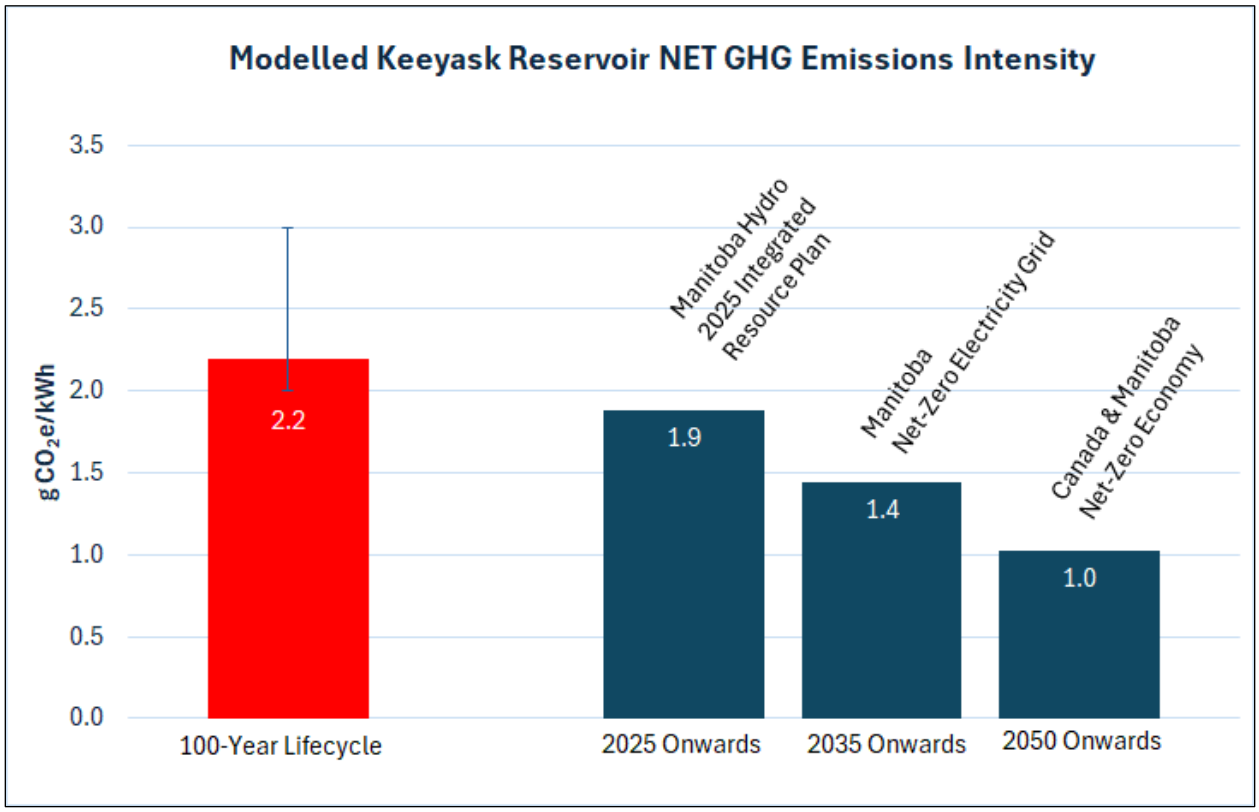


Figure 4-6 Modelled Keeyask Reservoir Net GHG Emission Intensity

4.5 Discussion

4.5.1 Modelling Pre-Flood Emissions

Accurately modelling pre-flood GHG emissions is especially important for the Keeyask and Kettle reservoirs where most of the pre-flood land was a heterogeneous peatland (Keeyask Hydropower Limited Partnership, 2012a). Carbon cycling within peatlands can be complex and challenging to quantify GHG emissions (Pelletier et al., 2007, 2009, 2011, 2014; Trudeau et al., 2013, 2014; Turetsky et al., 2014; Lourenco et al., 2023; Treat et al., 2021, 2024). Furthermore, there is natural variability in terrestrial carbon

cycling (e.g., forest fires and forest succession, pest infestations, etc.), coupled with the impact of climate change (e.g., warming, drought, permafrost melt, increased nutrient loading, longer ice-free season, etc.) (Baldocchi et al., 2016; Keenan & Williams, 2018; Bastviken and Johnson, 2025; Virkkala et al., 2025) that complicates developing an emissions baseline. It would be worthwhile to develop a "living" baseline, that would reflect ongoing emissions as if the reservoir did not exist.

4.5.2 G-res Predictions of Gross Post-flood Emissions

4.5.2.1 Comparison of Predicted Post-flood Emissions to In-situ Measurements

This section discusses a methodology for comparing the gross, post-flood emissions estimated by G-res to the gross post-flood emissions measured in-situ at the Keeyask reservoir. Gross emissions refer to emissions leaving the reservoir and entering the atmosphere. Gross emissions do not deduct baseline emissions, which are the emissions that would have occurred if the reservoir was not in place. The comparison could be conducted as a rudimentary attempt to assess the G-res predictions to actual measurements.

A direct comparison between annual gross G-res GHG predictions and actual in-situ gross GHG measurements at Keeyask is challenging to make. This is because G-res modelling results exclude "displaced CO_2 emissions" (Prairie et al., 2021). These are CO_2 emissions that occur from the decomposition of organic material that is brought into the reservoir from upstream sources. These emissions would have occurred within the reservoir footprint or downstream regardless of whether the reservoir existed or not.

G-res is designed to predict 100-year lifecycle emissions and therefore, there is more confidence in the G-res total 100-year estimates as opposed to G-res predictions for any single year (G-res Modelling Team, February 27, 2025). A comparison between G-res modelling results and in-situ measurements should involve 5-year averages at a minimum (G-res Modelling Team, February 27, 2025).

The assessment should examine if G-res over-predicted or under-predicted total gross emissions. It will also be important to assess whether measured reservoir gross emissions steadily decline after impoundment or if they remain elevated for a period, or if they increase in some years after flooding. This will be an important assessment for understanding and modelling northern reservoir GHG emissions. Measurements from other boreal reservoirs, such as Eastmain-1 in Quebec, have observed net CO_2 emissions to decline during the first three years after flooding and continue to decline 17 years after flooding (Demarty & Tremblay, 2019; Demarty et al., 2026). G-res is designed to predict post-flood CO_2 and CH_4 diffusive emissions to steadily decline after flooding. The model is not capable of predicting emission increase in any given year. The results of this type of study would aid in assessing lifecycle GHG predictions and help to calibrate reservoir GHG lifecycle models such as G-res.

4.5.3 Gas Type

G-res estimated that CO_2 and CH_4 (on a CO_2 equivalent basis) would comprise 71% and 29%, respectively, of annual emissions during 2021, the first year of impoundment (Figure 4-7). After 5 years of impoundment (2025) the proportions of CO_2 and CH_4 (CO_2e) emissions are modelled to be 56% and 44%, respectively. The reason for the change in

relative contribution of CO_2 and CH_4 is that G-res is modelling CO_2 emissions to decline at a faster rate than CH_4 emissions.

It would be valuable to compare in-situ GHG emission measurements at the Keeyask reservoir to the G-res modelling results. The Keeyask reservoir is comprised of a main channel, that is generally well-mixed in terms of dissolved oxygen and has a short water residence time (approximately 15 to 30 hours) (Keeyask Hydropower Limited Partnership 2012a; Manitoba Hydro 2023). In addition, approximately 20% of the reservoir (in the initial post-flood years) has shallow shorelines and backbays with longer water residence times (approximately up to 30 days) than the main channel (Keeyask Hydropower Limited Partnership 2012a; Manitoba Hydro 2023; W. DeWit, personnel communication, May 1, 2020). To further illustrate the complexities of the Keeyask reservoir, portions of the shallow littoral zone consist of flooded peatlands, semi-submerged peat and other vegetation, and floating islands that have migrated into the main channel and forebay. Decomposition of flooded and floating peat can elevate GHG emissions (Scott et al 1999; St. Louis et al 2000; Saquet, 2003).

G-res calculates CH_4 diffusive and bubble emissions based on the areal extent of the littoral zone (water depth less than 3 meters). These functions of G-res could be explored further by assessing in-situ measurements of GHG emissions collected from reservoir littoral zones (such as from the Keeyask reservoir). The objective could be to determine if the effects of submerged and semi-submerged peatlands on GHG emissions are adequately modelled or if the formulas for estimating CH_4 diffusive and bubble emissions could be enhanced.

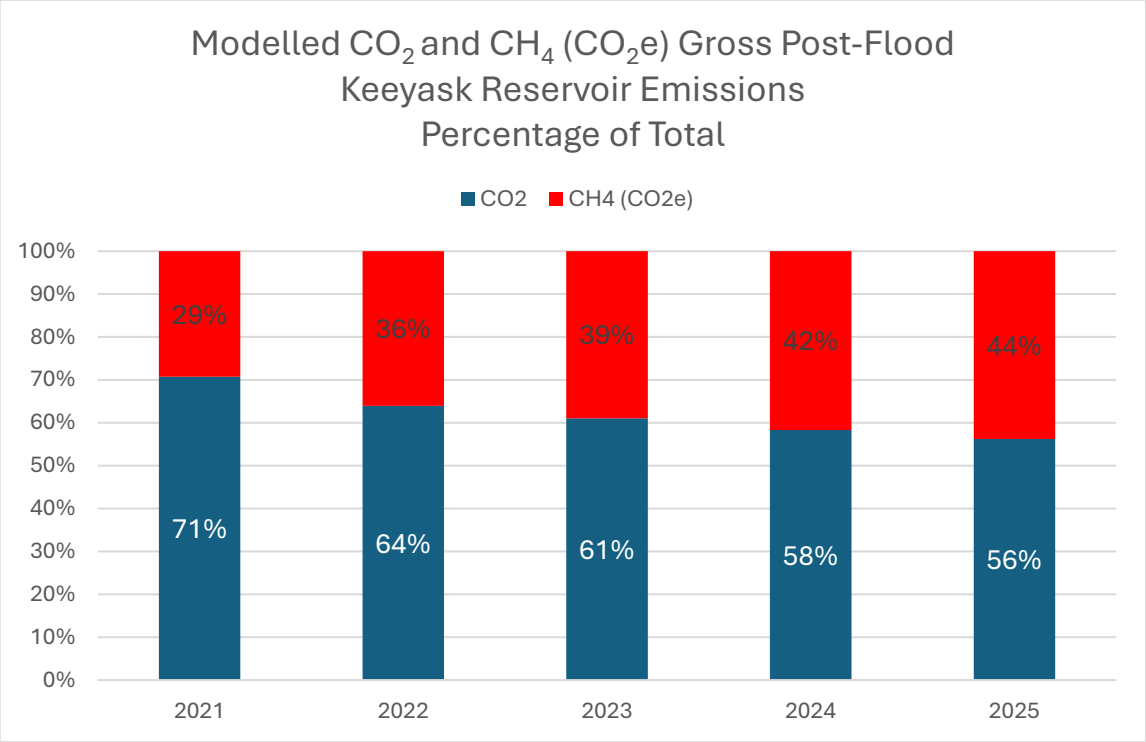


Figure 4-7 Proportion of CO_2 and CH_4 Emissions Modelled for the First 5 Years Following Reservoir Impoundment

4.5.4 Net GHG Emissions

The net emissions over the 100-year lifetime of the Keeyask reservoir are modelled to be 861,990 t/CO_2e (95% Confidence Interval 749,988 – 987,936). These are similar to the maximum net lifecycle emissions estimated for the Keeyask reservoir (975,426 t/CO_2e) in the Keeyask Environmental Impact Assessment (Keeyask Hydropower Limited Partnership 2012a). The Keeyask Environmental Impact Assessment reservoir GHG lifecycle assessment adapted the IPCC 2006 guidelines where CO_2 and CH_4 emission factors were used to estimate 100-year reservoir lifecycle emissions.

The annual 100-year average net emissions for Keeyask are modelled to be 86g $CO_2e/m^2/yr$ (95% Confidence Interval 75 – 98) using the G-res Tool. This emission rate is similar to other Canadian boreal reservoirs (Figure 4-8). For illustration, annual 100-year average net emissions of the Eastmain-1 & 1A (Paix-des-Braves) reservoir (Québec) and the Romaine-2 reservoir (Québec) have been modelled using the G-res Tool to be 84.1 (2.5% & 97.5% CI 62.3 – 104.0) and 148.5 $gCO_2e/m^2/yr$ (2.5% & 97.5% CI 133.3 – 167.2), respectively, as adapted from Levasseur et al. (2021 Table A.4). The Eastmain-1 & 1A (Paix-des-Braves) and Romaine-2 reservoirs were selected for comparison because these reservoirs are amongst the most extensively studied northern reservoirs in the world. Eastmain-1 & 1A pre-flood and post-flood emissions have been measured using similar techniques as those used at the Keeyask reservoir (eddy covariance, floating chambers, surface water partial pressure, and continuous measurements of forebay water running through the powerhouse). The Romaine-2 reservoir is of a similar size (85.8 km^2) as the Keeyask reservoir (100.4 km^2) and was flooded in a comparable timeframe as the Keeyask reservoir, 2014 and 2020, respectively (Keeyask Hydropower Limited Partnership, 2012a; Barbosa et al., 2023).

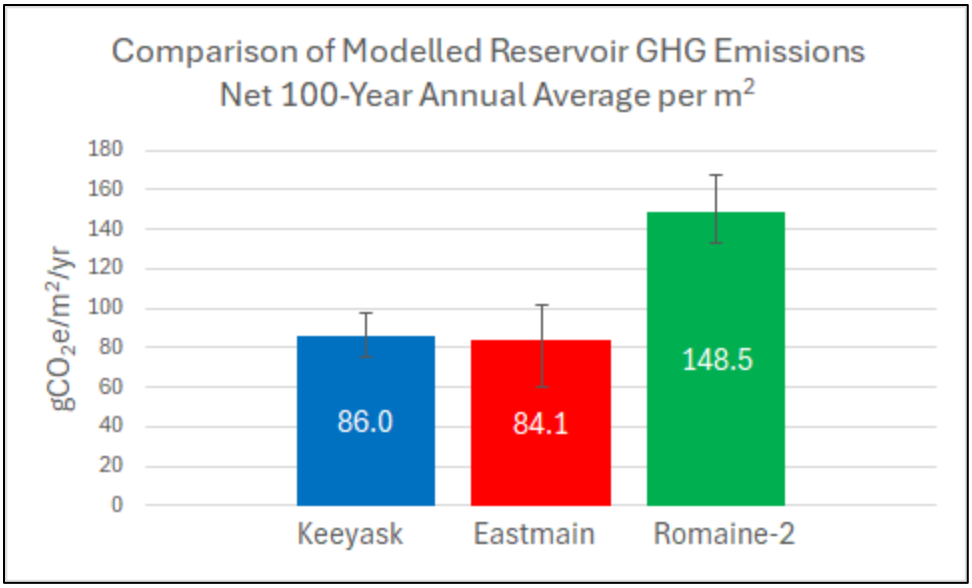


Figure 4-8 Comparison of 100-Year Annual Net Lifecycle Reservoir GHG Emissions per m^2 Modelled by G-res
Source: Eastmain and Romain-2 emissions adapted from Levasseur et al., 2021 Table A.4

4.5.5 G-res Estimate of GHG Emission Intensity

4.5.5.1 Comparison of G-res Predictions to Keeyask EIS Lifecycle GHG Predictions

The G-res modelled the Keeyask reservoir lifecycle GHG emissions intensity of 2.2 gCO_2e/kWh (95% Confidence Interval 2.0 – 3.0) compares to the Keeyask EIS GHG LCA value of 1.18 gCO_2e/kWh for reservoir lifecycle emissions (95% of 1.24 gCO_2e/kWh for total land use change) (The Pembina Institute, 2012).

The entire Keeyask Generating Station lifecycle GHG emissions, as modelled by The Pembina Institute (2012) are illustrated in Figure 4-9 by percentage of total emissions. Reservoir emissions comprise approximately 48% of total lifecycle emissions.

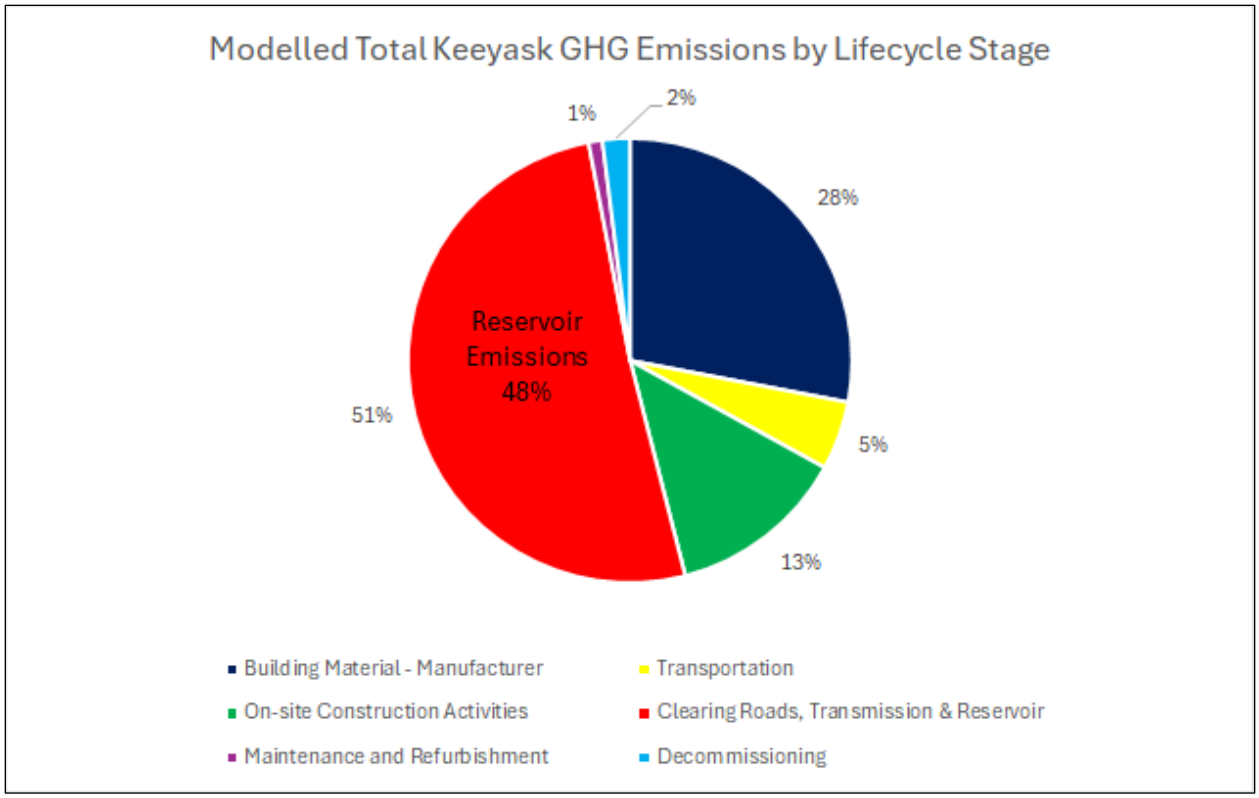


Figure 4-9 Modelled Total Keeyask GHG Emissions by Lifecycle Stage (%)
Source: The Pembina Institute, 2012

If the Keeyask reservoir GHG lifecycle emissions modelled by G-res are substituted into The Pembina Institute lifecycle model, reservoir GHG emissions amount to approximately 56% of the total Keeyask Generating Station lifecycle emissions (Figure 4-10). Total 100-year lifecycle GHG emissions for all stages would increase by 58% from an estimated 979,019 tonnes CO_2e (The Pembina Institute, 2012) to an estimated 1,544,373 tonnes CO_2e when incorporating the G-res reservoir GHG modelled lifecycle emissions.

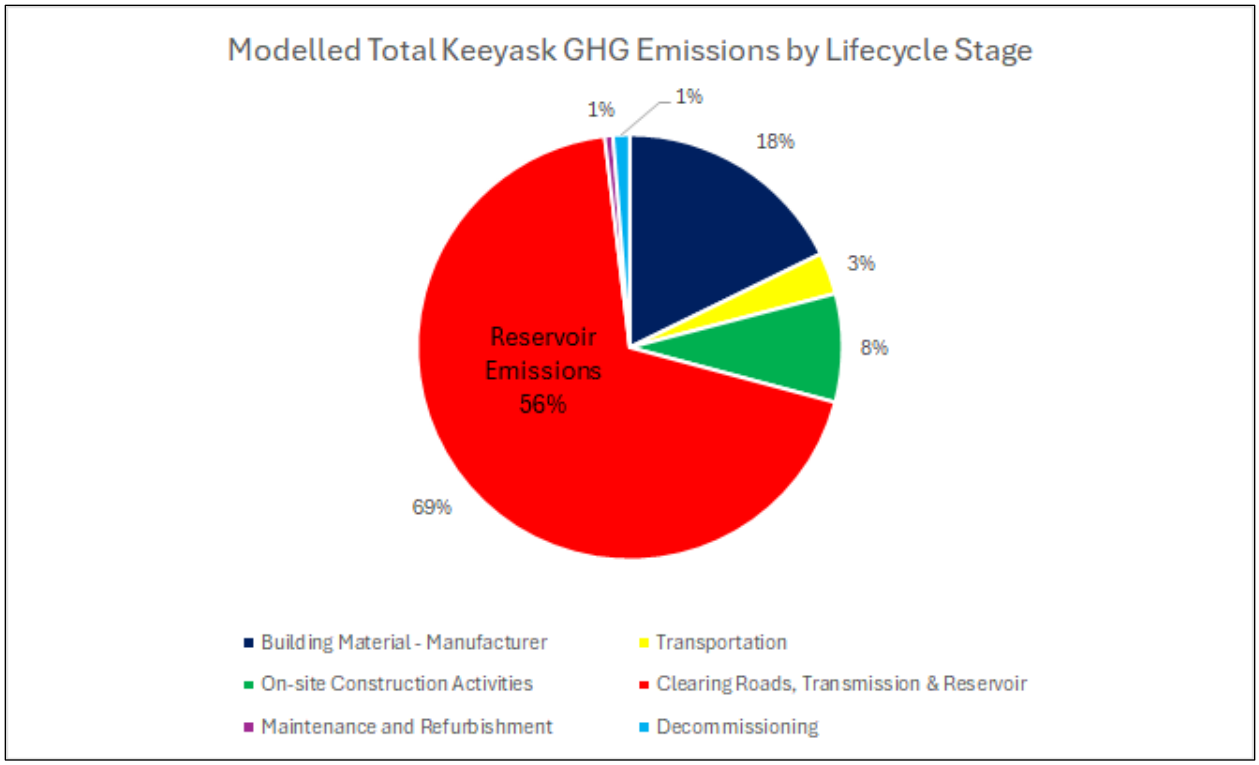


Figure 4-10 Modelled Total Keeyask GHG Emissions by Lifecycle Source Including G-res Results
Source: Adapted from The Pembina Institute, 2012

4.5.5.2 Comparison of G-res Predictions to Other Reservoirs

The modelled G-res lifecycle GHG emissions intensity factor (2.2 gCO_2e/kWh 95% Confidence Interval 2.0 – 3.0) for the Keeyask reservoir was compared to modelled lifecycle GHG emissions intensities for Québec reservoirs (Figure 4-11). The purpose of the comparison was to evaluate whether the G-res result from this study seemed reasonable. It was not to contest one reservoir against another. The Keeyask emission intensity was compared to Québec reservoirs because GHG emission intensities have been assessed for every hydroelectric reservoir in Québec using the G-res Tool (Levasseur et al., 2021) which makes for a very good comparison. Plus, Québec reservoirs are the most extensively studied hydroelectric reservoirs in Canada for assessing GHG emissions.

The Keeyask lifecycle GHG emission intensity factor was modelled to be lower than many of the hydroelectric reservoirs in Québec and similarly for the overall GHG emission intensity value for Québec hydroelectric reservoirs. Québec GHG emission intensities ranged from 0, for watersheds where there was no flooding, to 73.2 gCO_2e/kWh (Levasseur et al., 2021). A key reason why the Keeyask emission intensity is low compared to many of those modelled in Québec, is that the Keeyask reservoir is smaller than several of the Québec reservoirs whose sizes range from 10.9 km^2 to 4,378.4 km^2 (Levasseur et al., 2021). The Keeyask reservoir is estimated to be 100.4 km^2 after 30 years of post-flood shoreline erosion and disintegration. Keeyask is also modelled to have relatively lower emissions in total, plus, Keeyask has a relatively high electrical generating capacity (4400 GWh/yr, 695 MW). However, on a per square meter basis, 100-year average Keeyask GHG emissions are modelled to be similar, larger or smaller than reservoirs in Québec, depending on the reservoir. For example, 100-year average Net CO_2 emissions for Keeyask are modelled to be 110 g $CO_2/m^2/yr$ (by this study) compared to the Eastmain-1 reservoir (Québec) of 46.7 g $CO_2/m^2/yr$ (2.5% & 97.5% CI 35.1 – 59.8) (Levasseur et al., 2021). The Eastmain reservoir is 588.5 km^2 (Levasseur et al., 2021), which is nearly 6 times larger than the Keeyask reservoir, and its installed generating capacity is 480 MW (Hydro-Québec, 2014) compared to that of Keeyask (695 MW). Therefore, total lifecycle emissions emanating from the entire Eastmain-1 reservoir are modelled to be larger than those of the Keeyask reservoir. Comparing these emissions to the electrical generating capacity of Eastmain-1, which is smaller than Keeyask, the resulting emission intensity factor is greater than that of Keeyask.

For the sake of comparison, the emission intensity of gross GHG emissions (CO_2 + CH_4) as modelled by G-res for Keeyask for the first year after impoundment, is calculated to be 12.6 gCO_2e/kWh = (488.1 g $CO_2e/m^2/yr$ x 100.4 km^2 ÷ 3886 GWh/yr).

The modelled Keeyask lifecycle GHG emission intensity value estimated by G-res (2.2 g CO_2e/kWh) appears to be lower than the average emission intensity factor for reservoirs in boreal Québec, and similar in magnitude to the Romaine reservoir.

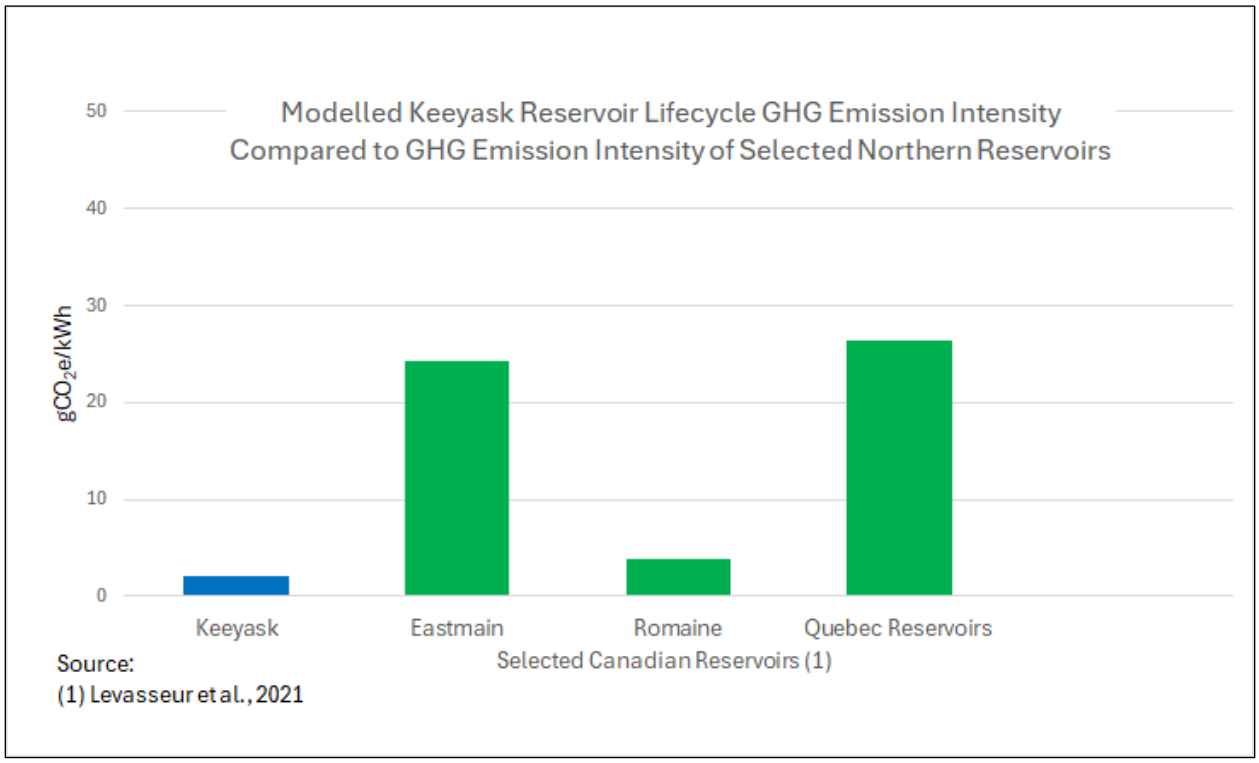


Figure 4-11 Comparison of Modelled Keeyask Lifecycle Reservoir GHG Emission Intensity to Modelled Lifecycle GHG Emission Intensity of Other Northern Reservoirs

4.5.6 Comparison of G-res Estimated Emission Intensity to Other Forms of Electricity Generation

The modelled Keeyask reservoir lifecycle GHG emissions intensity factor (2.2 gCO_2e/kWh 95% Confidence Interval 2 – 3) is much lower than lifecycle assessment (LCA)

results reported for electricity produced from fossil fuels and is lower than or comparable to electricity production from nuclear, wind, solar and other technologies. For example, Whitaker et al. (2012) reported a median value of 1,001 t CO_2e/GWh for coal-fired electricity generation, and O'Donoughue et al. (2014) reported median values of 450 and 670 t CO_2e/GWh for electricity generated by natural gas-fired combined cycle combustion turbines and natural gas-fired combustion turbines, respectively. A study conducted by the U.S. National Renewable Energy Laboratory (2021) reported median lifecycle GHG emission intensity values ranging from 8 to 52 g CO_2/kWh for electricity generated from ocean waves, nuclear, wind, solar, and biomass technologies. For the Keeyask reservoir GHG emissions intensity to approach the upper limit of 52 g CO_2e/kWh, actual in-situ fluxes would have to measure approximately 2013 g CO_2e/m^2/yr. For comparison, and as discussed in Section 4.2 and displayed in Table 4-4, the highest modeled gross emission rate for the Keeyask reservoir is 488.1 g CO_2e/m^2/yr in post-flood year 1.

4.6 Limitations of the G-res Tool

G-res was designed as a screening tool to identify if a reservoir's GHG emissions have the potential to be high (Prairie et al., 2018). Although G-res predicts reservoir GHG lifecycle emissions and reservoir GHG emission intensity, it may not be able to predict emissions from an individual reservoir at the level of precision and accuracy required for a corporation's GHG accounting requirements or to inform climate change public policy.

G-res is based on empirical relationships amongst GHG emissions and reservoir attributes that were developed from reservoir studies conducted around the world prior to 2016 (Prairie et al., 2021). G-res may not be capable of predicting GHG emissions from a

given reservoir if the characteristics of that reservoir are different from those which were used to build G-res. As discussed in Section 6.3.2, Structural Uncertainty, G-res has not been calibrated with a reservoir similar to Keeyask. The Canada-wide research study, GHG-CaRe (Prairie et al., 2025), that is currently underway and being led by L'Université du Québec à Montréal and the University of Waterloo, and which is sponsored by WaterPower Canada and member companies, including Manitoba Hydro, Environment and Climate Change Canada, Grand River Conservation Authority, and supported by the University of Manitoba, will help to calibrate G-res to Canadian reservoirs, including the Keeyask reservoir.

G-res is an empirical model where statistical formulas describe the relationship between reservoir characteristics and observed GHG emissions (Prairie et al., 2021). The model predicts future emissions based on what has been observed from past reservoir studies. A potential limitation of this approach is that there has not been a GHG measurement study conducted over the entire lifecycle of a reservoir to serve as a benchmark to compare modelled lifecycle GHG emissions to actual measurements. Also, as mentioned above, the reservoirs that have been studied may not necessarily represent all reservoirs to be modelled, such as the Keeyask reservoir. G-res does not model the processes that produce and release GHG emissions. A more advanced, “process-based” model is being developed by the GHG-CaRe Project mentioned above. A processed-based model simulates the biogeochemical interactions that impact carbon cycling, GHG emissions, organic carbon transport and sequestration (Sharifi et al., 2013; Dorgeist et al., 2024; Li et al., 2024).

Other considerations include:

- G-res does not predict downstream GHG emissions that occur beyond degassing at the generating station and spillway, and which are directly attributable to the reservoir.
- Currently, G-res does not predict CO_2 degassing emissions due to a lack of measurement data to develop predictive models (Prairie et al., 2021).
- G-res predicts a constant value for CH_4 degassing emissions for the entire 100-year lifetime of the reservoir. This may not be representative of actual long-term emissions, which could be confirmed by comparing is-situ measurements to modelled results.
- G-res predicts a constant value for CH_4 bubble emissions for the entire 100-year lifetime of the reservoir. Since CH_4 bubble emissions are sporadic in space and time (DelSontro et al., 2015), this may not be representative of actual lifetime reservoir emissions. Longer-term monitoring of sediment ebullition at the Keeyask reservoir could help to refine Keeyask lifecycle CH_4 bubble emissions and help to calibrate G-res for northern Canadian peatland reservoirs.
- G-res does not model carbon sequestration through sedimentation and burial.
- Currently, G-res predicts lifecycle emissions for a single reservoir. It does not predict emissions for a series of cascading reservoirs such as those of the lower Nelson River. This is an area of on-going research by the G-res team.
- G-res is designed to estimate emissions over the 100-year lifecycle of a reservoir. Although G-res can estimate emissions for a single year, these estimates have a

higher uncertainty than the full lifecycle estimate (G-res Validation Team, personal communication, February 27, 2025).

5 Net Lifecycle GHG Emissions for Hydroelectric Reservoirs on the Lower Nelson River

5.1 Results for Lower Nelson River Reservoirs

5.1.1 Total Lifecycle GHG Emissions

Total Net GHG emissions for the hydroelectric reservoirs located on the lower Nelson River are modelled to be 4,921,109 t CO_2e (95% CI 4,331,822 - 5,582,738) over the 100-year lifecycle of the reservoirs (Table 5-1). (The 95% CI was generated by G-res for individual reservoirs and summed for the 95% CI for total lower Nelson River reservoirs).

Over 90% of the Net emissions are modelled to occur from the Kettle reservoir (74%) and the Keeyask reservoir (18%) (Figure 5-1). Long Spruce and Limestone reservoirs accounted for 7% and 2%, respectively.

If the potential Conawapa reservoir is included in the modelling exercise, the total Net GHG emissions are 5,250,086 t CO_2e (95% CI 4,635,626 - 5,940,086) (Table 5-2). (As with modelling total Net lifecycle emissions without the Conawapa reservoir, the 95% CI was generated by G-res for individual reservoirs and summed for the 95% CI for total lower Nelson River reservoirs). Under this modelling scenario, approximately 86% of total Net GHG emissions would occur from the Kettle (70%) and Keeyask (16%) reservoirs, with the remaining lifecycle emissions from Long Spruce (6%), Limestone (1%) and Conawapa (6%) (Table 5-2, Figure 5-2).

5.1.2 Gas Composition and Emission Pathway

The proportion of modelled total Gross lifecycle emissions for the lower Nelson River reservoirs are nearly evenly split between CO_2 and CH_4, at 51% and 49%, respectively (Table 5-4, Figure 5-3). Gross emissions are those that are generated by the reservoir, prior to subtracting pre-flood baseline emissions. On an individual reservoir basis, the percentage of CO_2 emissions ranged from 46%-54% for the Keeyask, Kettle and Long Spruce reservoirs. The modelled results for the Limestone reservoir are an anomaly at 16% for CO_2 and 84% for CH_4 (CO_2e). The Limestone reservoir is not modelled as a high emitter of CH_4. On the contrary, both CH_4 and CO_2 emission rates are modelled to be low at 36 g $CO_2(e)/m^2/yr$ and 7 g $CO_2(e)/m^2/yr$, respectively. The formula for estimating gross, post-flood diffusive CO_2 emissions is partially based on the amount of flooded land, which is especially small for the Limestone reservoir (2.2 km^2). Hence, modelled CO_2 emission rates are low. The formulae for estimating diffusive and bubble CH_4 emissions are based on the size of the post-flood littoral zone and temperature. Although the size of the littoral zone is estimated to be small (10%), the impact is larger on estimated CH_4 emission rates than on than that of CO_2 emissions.

CO_2 and CH_4 (CO_2e) diffusive emissions are modelled to be the dominant Gross emission pathways, at 51% and 35%, respectively for the lower Nelson River reservoirs, excluding the proposed Conawapa reservoir (Table 5-4). CH_4 degassing and bubble emissions accounted for respectively, 10% and 4%.

The proportion of CO_2 and CH_4 (CO_2e) emissions remain the same at 51% and 49%, respectively when including the potential Conawapa reservoir to the total lower Nelson River reservoir model (Table 5-5, Table 5-6, Figure 5-4).

Table 5-1 Lower Nelson River Reservoirs: Net Lifecycle GHG Emissions

Lower Nelson River Reservoirs
Modelled Total Net Lifecycle Reservoir GHG Emissions
tonnes CO_2e

		95%			95%			95%	
	m^2	CI		**Annual**	CI		**Lifetime**	CI	
Keeyask	86	75	98	8,620	7,500	9,879	861,990	749,988	987,936
Kettle	114	101	130	36,513	32,123	41,438	3,651,272	3,212,330	4,143,810
Long Spruce	109	101	118	3,313	3,061	3,593	331,276	306,128	359,328
Limestone	28	23	34	766	634	917	76,571	63,376	91,664
Total				**49,212**	43,318	55,827	**4,921,109**	4,331,822	5,582,738

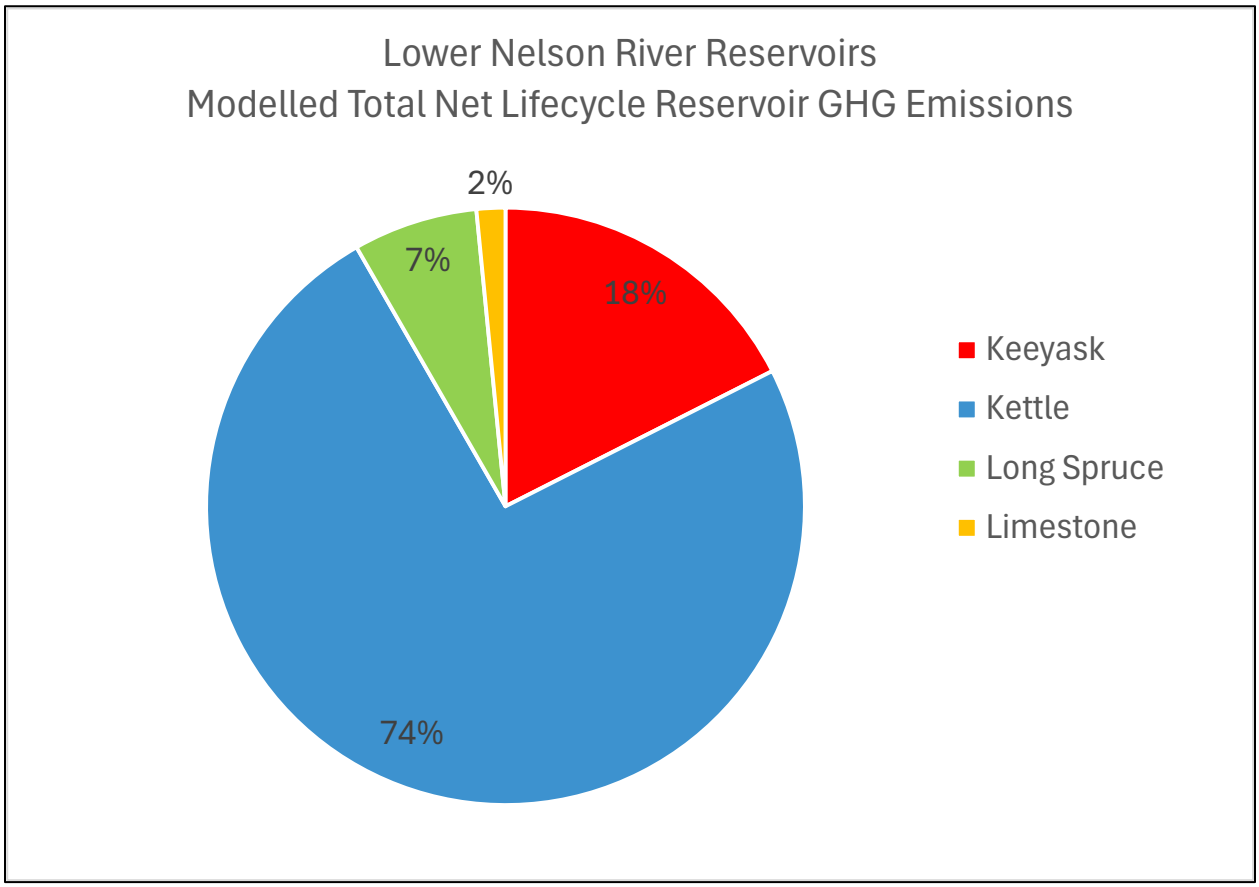


Figure 5-1 Lower Nelson River Reservoirs: Lifecycle GHG Emissions (Percent of Total)

Table 5-2 Lower Nelson River Reservoirs Including the Potential Conawapa Reservoir: Net Lifecycle GHG Emissions

Lower Nelson River Reservoirs
Modelled Total Net Lifecycle Reservoir GHG Emissions
tonnes CO_2e

	m^2	95% CI		Annual	95% CI		Lifetime	95% CI	
Keeyask	86	75	98	8,620	7,500	9,879	861,990	749,988	987,936
Kettle	114	101	130	36,513	32,123	41,438	3,651,272	3,212,330	4,143,810
Long Spruce	109	101	118	3,313	3,061	3,593	331,276	306,128	359,328
Limestone	28	23	34	766	634	917	76,571	63,376	91,664
Conawapa (Potential)	85	78	92	3,290	3,038	3,573	328,977	303,804	357,348
Total				**52,502**	46,356	59,400	**5,250,086**	4,635,626	5,940,086

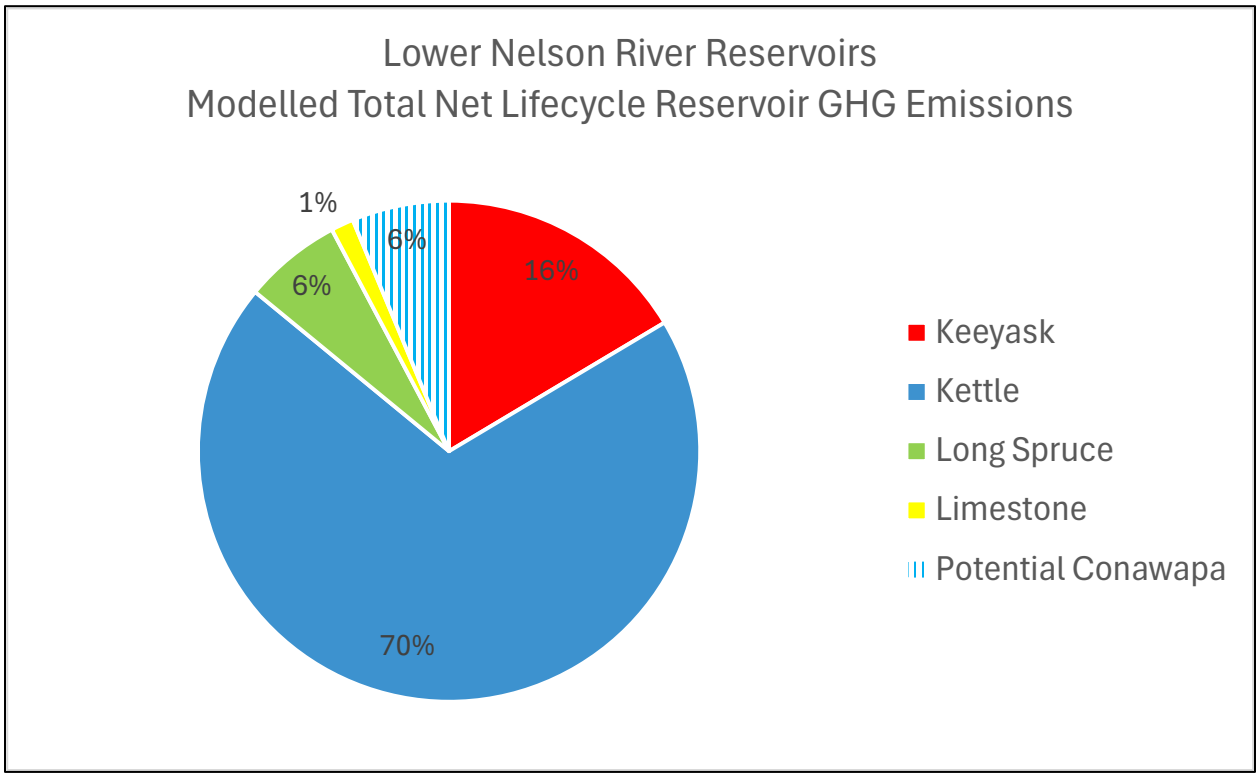


Figure 5-2 Lower Nelson River Reservoirs Including Potential Conawapa: Net Lifecycle Emissions (Percent of Total)

Table 5-3 Gross Annual Average Lifecycle GHG Emissions by Gas Type and Pathway

Modelled Post-Flood Gross Annual 100-Year Average Reservoir GHG Emissions
tonnes CO_2e/year

	CO_2	CH_4				TOTAL
	Diffusive	Diffusive	Bubble	Degassing	Total CH_4	
Keeyask	4,435	3,965	476	846	5,287	9,722
Kettle	20,509	12,585	1,438	3,955	17,978	38,487
Long Spruce	1,244	770	64	235	1,069	2,313
Limestone	187	687	59	235	981	1,168
Total	**26,375**	**18,006**	**2,037**	**5,272**	**25,315**	**51,690**

Table 5-4 Gross Annual Average Lifecycle GHG Emissions by Gas Type and Pathway (Percent)

Modelled Post-Flood Gross Annual 100-Year Average Reservoir GHG Emissions
Percentage by Emission Pathway and Gas Type per Reservoir

	CO_2	CH_4				TOTAL
	Diffusive	Diffusive	Bubble	Degassing	Total CH_4	
Keeyask	45.6%	40.8%	4.9%	8.7%	54.4%	100.0%
Kettle	53.3%	32.7%	3.7%	10.3%	46.7%	100.0%
Long Spruce	53.8%	33.3%	2.8%	10.2%	46.2%	100.0%
Limestone	16.0%	58.8%	5.0%	20.2%	84.0%	100.0%
Total	**51.0%**	**34.8%**	**3.9%**	**10.2%**	**49.0%**	**100.0%**

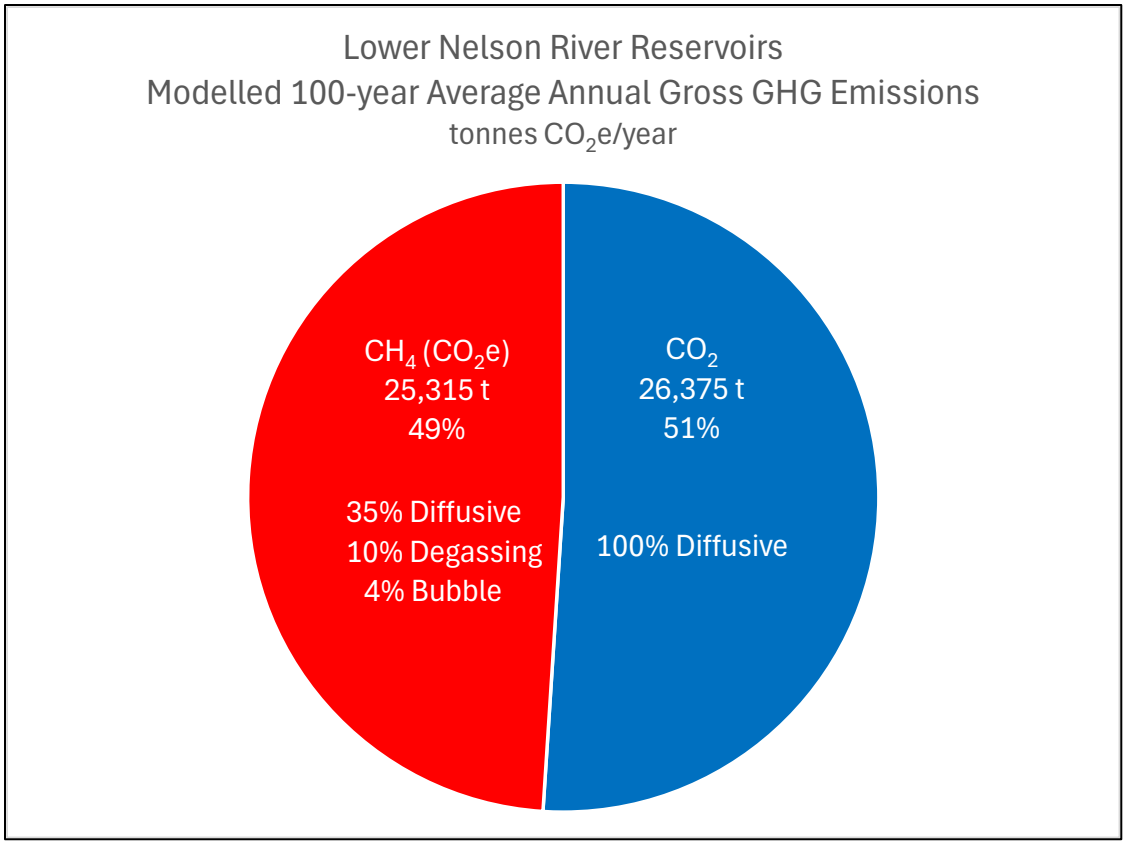


Figure 5-3 Gross Annual Average GHG Emissions: Gas Type and Pathway

Table 5-5 Gross Annual Average GHG Emissions by Gas Type and Pathway including Potential Conawapa Reservoir

Modelled Post-Flood Gross Annual 100-Year Average Reservoir GHG Emissions
tonnes CO_2e/year

	CO_2	CH_4				TOTAL
	Diffusive	Diffusive	Bubble	Degassing	Total CH_4	
Keeyask	4,435	3,965	476	846	5,287	9,722
Kettle	20,509	12,585	1,438	3,955	17,978	38,487
Long Spruce	1,244	770	64	235	1,069	2,313
Limestone	187	687	59	235	981	1,168
Conawapa (Potential)	957	987	78	234	1,299	2,256
Total	**27,332**	**18,993**	**2,115**	**5,506**	**26,614**	**53,946**

Table 5-6 Gross Annual Average GHG Emissions by Gas Type and Pathway (Percentage), including Potential Conawapa Reservoir

Modelled Post-Flood Gross Annual 100-Year Average Reservoir GHG Emissions
Percentage by Emission Pathway and Gas Type per Reservoir

	CO_2	CH_4				TOTAL
	Diffusive	Diffusive	Bubble	Degassing	Total CH_4	
Keeyask	45.6%	40.8%	4.9%	8.7%	54.4%	100.0%
Kettle	53.3%	32.7%	3.7%	10.3%	46.7%	100.0%
Long Spruce	53.8%	33.3%	2.8%	10.2%	46.2%	100.0%
Limestone	16.0%	58.8%	5.0%	20.2%	84.0%	100.0%
Conawapa (Potential)	42.4%	43.8%	3.5%	10.4%	57.6%	100.0%
Total	**50.7%**	**35.2%**	**3.9%**	**10.2%**	**49.3%**	**100.0%**

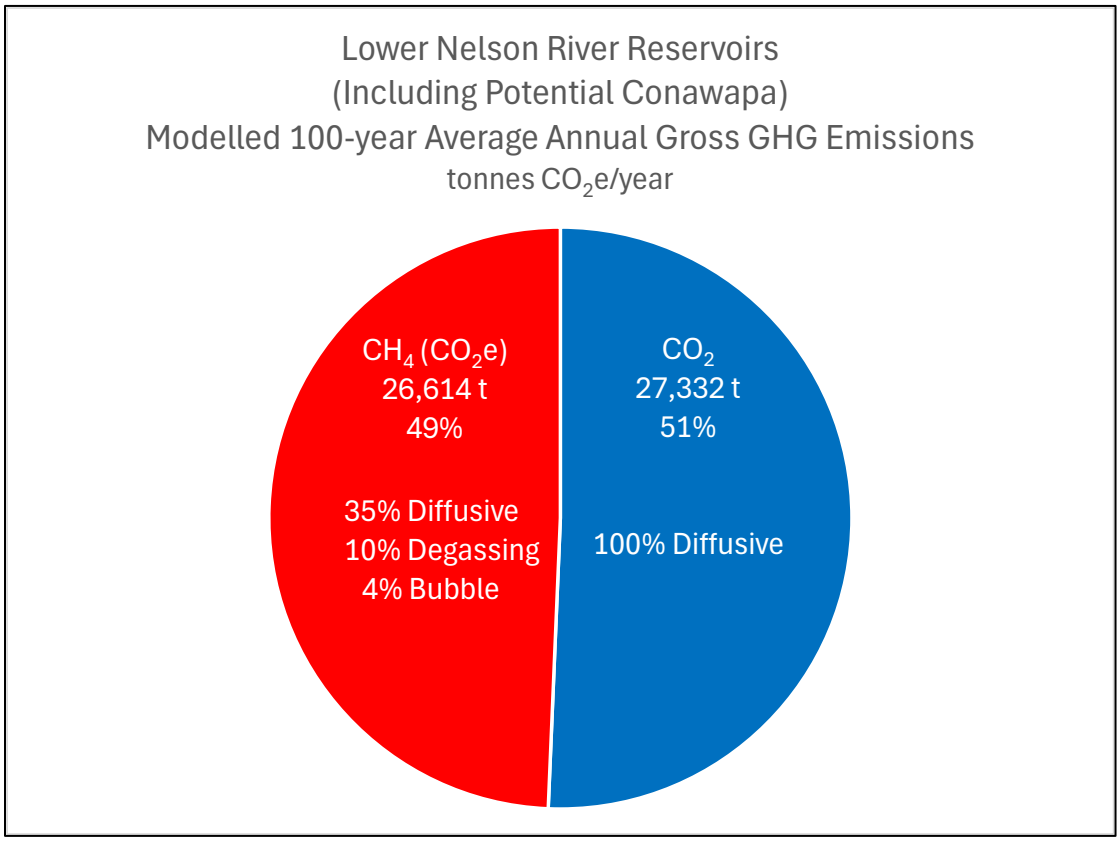


Figure 5-4 Gross Annual Average GHG Emissions: Gas Type and Pathway, including Potential Conawapa

5.1.3 Comparison to Manitoba Hydro Direct GHG Emissions

The size of modelled 2025 lower Nelson River net reservoir GHG emissions were compared to Manitoba Hydro's 2023 Direct GHG emissions, which are emissions from

Manitoba Hydro's operations (e.g. electricity generation from natural gas-fired combustion turbines and off-grid diesel generators, natural gas operations, fleet vehicles and buildings). The purpose of the comparison is to provide a rough indication of the size of Lower Nelson River Reservoir emissions in relation to Manitoba Hydro's GHG emissions from company-wide operations.

The 2025 GHG reservoir emissions were calculated as the average of annual emissions modelled from 2023 – 2027. There is more confidence in comparing a minimum of 5-year modelled averages as opposed to a single year. G-res is designed to predict 100-year lifecycle emissions and not annual fluctuations.

Present day annual (2025) lower Nelson River reservoir net GHG emissions are modelled to be 52,962 (±3563) tCO_2e (Figure 5-5). This compares to approximately 41% of Manitoba Hydro's 2023 Direct, Scope 1 emissions (128,000 t CO_2e) (Manitoba Hydro, 2025). Scope 1 GHG emissions refer to emissions that occur from sources that are owned or controlled by the company (World Resources Institute, 2004). Reservoir GHG emissions are not included in Scope 1 reporting. The majority of the modelled lower Nelson River reservoir GHGs are attributed to the Kettle and Keeyask reservoirs (Figure 5-5).

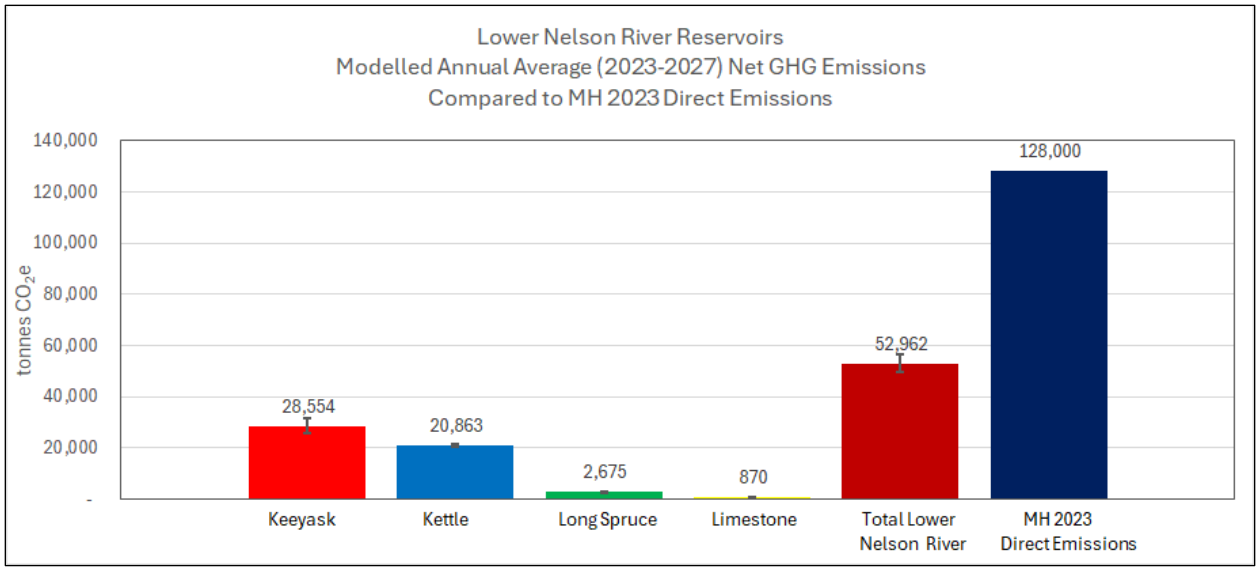


Figure 5-5 Modelled Current (2023-2027 Average) Lower Nelson River Reservoir GHG Emissions Compared to Manitoba Hydro 2023 Direct Emissions

5.1.4 Cumulative Net Reservoir GHG Emissions

Net reservoir GHG emissions were the highest in the early 1970s, associated with the impoundment of the Kettle reservoir (Stephens Lake) (Figure 5-6). Afterwards, Net GHG emissions declined steadily until the impoundment of the Long Spruce reservoir in 1980 and Limestone reservoir in 1993 where there were modelled 9% and 3% rises in annual emissions, respectively. Emissions rose again in 2021 with the flooding of the Keeyask reservoir, where annual Net emissions were modelled to increase by 169% for the lower Nelson River reservoirs.

The potential Conawapa Reservoir was included in the analysis as hypothetically being flooded in 2050 to illustrate the potential emissions profile of the reservoir relative to the other Lower Nelson River reservoirs.

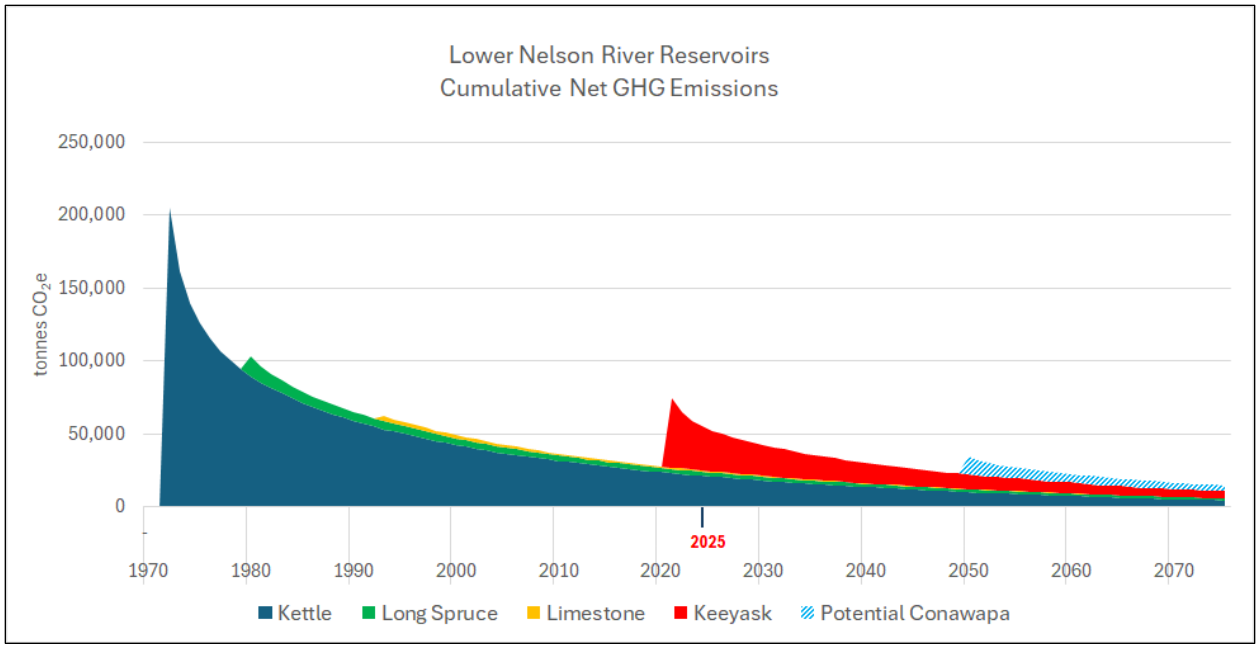


Figure 5-6 Lower Nelson River Reservoir Cumulative Net GHG Lifecycle Emissions (including the Potential Conawapa reservoir as hypothetically being flooded in 2050)

5.1.5 Modelled GHG Emission Intensity

Modelled net 100-year lifecycle GHG emission intensity of the lower Nelson River reservoirs ranged from 5.5 g CO_2e/kWh for the Kettle reservoir (Stephens Lake) to 0.1 g CO_2e/kWh for the Limestone reservoir (Table 5-7).

Table 5-7 Modelled Lower Nelson River Reservoir
Net 100-Year Lifecycle GHG Emission Intensity

Modelled Lower Nelson River Reservoirs
Net 100-Year Lifecycle GHG Emission Intensity

Reservoir	Lifecycle GHG Intensity gCO_2e/kWh	(95% CI)	
Keeyask	2.2	2	3
Kettle	5.5	5	6
Long Spruce	0.6	1	1
Limestone	0.1	0	0
Potential Conawapa	0.5	0	1

5.1.5.1 Comparison to Other forms of Electricity Generation

The modelled lifecycle GHG emissions intensity for the reservoirs on the lower Nelson River, which range from (0.1 to 5.5 g CO_2e/kWh) are lower than or comparable to electricity production from nuclear, wind, solar and other technologies (Figure 5-7). Some studies have reported median values to range from 8 to 52 t CO_2e/GWh for electricity generated from ocean waves, nuclear, wind, solar, and biomass technologies (National Renewable Energy Laboratory, 2021).

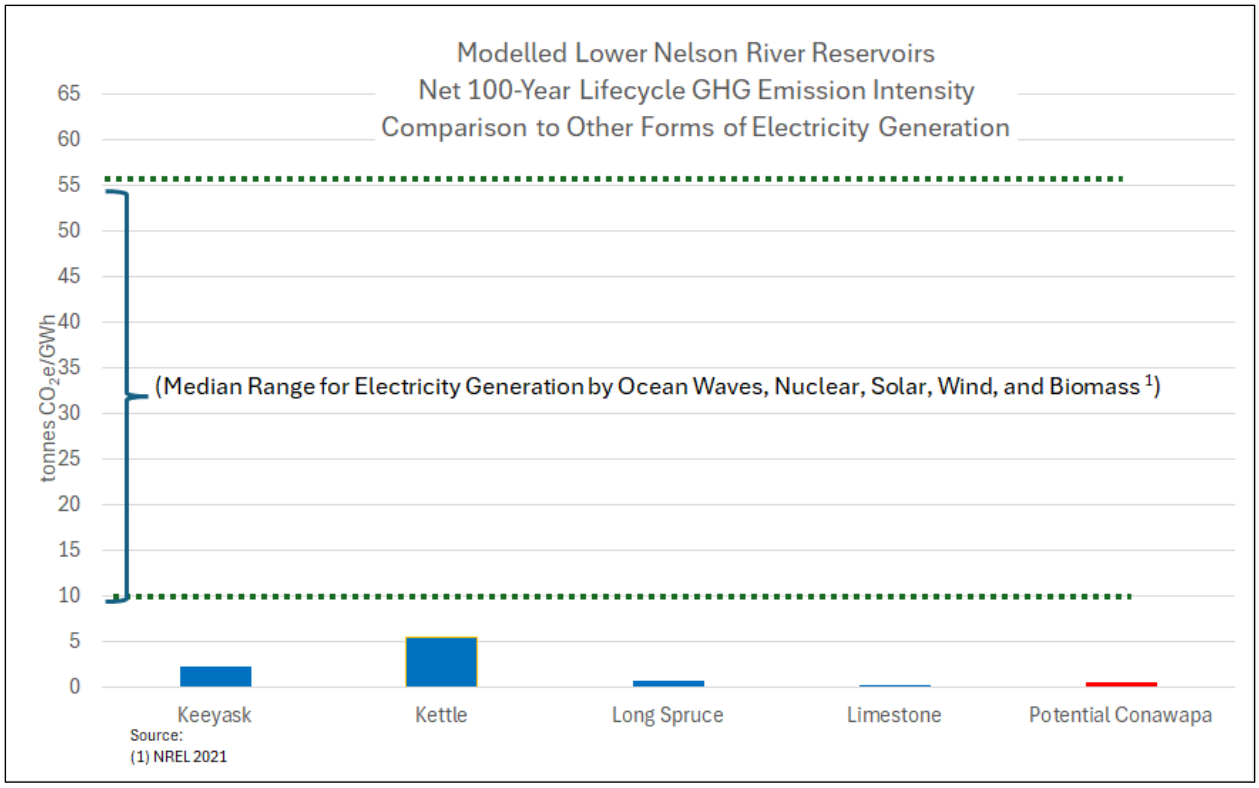


Figure 5-7 Modelled Lower Nelson River Reservoirs Lifecycle GHG Emission Intensity: Comparison to Other Forms of Electricity Generation

5.2 Results of Lower Nelson River Reservoirs Including the Flooded Lands of the Churchill River Diversion

This section presents an assessment of the lower Nelson River reservoir GHG lifecycle emissions, which includes the GHG emissions associated with lands flooded by the CRD. Appendix 7 describes the CRD and G-res CRD model inputs in further detail.

5.2.1 Net Lifecycle GHG Emissions

Total Net CRD 100-year lifecycle GHG emissions were modelled to be 19,418,859 t CO_2e (95% CI 17,017,760 - 22,146,400) (Table 5-8, Figure 5-8).

Total Net GHG emissions for the hydroelectric reservoirs located on the lower Nelson River, including the CRD, Keeyask, Kettle, Long Spruce, and Limestone reservoirs are modelled to be 24,339,968 t CO_2e (95% CI 21,349,582 - 27,729,138) over the 100-year lifecycle of the reservoirs (Table 5-8). (The 95% CI was generated by G-res for individual reservoirs, and summed for the 95% CI for total lower Nelson River reservoirs).

Approximately 95% of the Net emissions are modelled to occur from the CRD (80%) and the Kettle reservoir (15%) (Figure 5-9). Keeyask, Long Spruce and Limestone reservoirs account for the remaining 5% of the GHG emissions.

If the potential Conawapa reservoir is included in the modelling exercise, the total Net GHG emissions are modelled to be 24,668,945 t CO_2e (95% CI 21,653,386 – 28,086,486) (Table 5-8). (As with modelling total Net lifecycle emissions without the Conawapa reservoir, the 95% CI was generated by G-res for individual reservoirs, and summed for the 95% CI for total lower Nelson River reservoirs). Under this modelling scenario, approximately 94% of total Net GHG emissions would occur from the CRD (79%)

and Kettle (15%) reservoirs, with the remaining 6% of lifecycle GHG emissions associated with the Keeyask, Kettle, Long Spruce, Limestone, and Conawapa reservoirs (Figure 5-10).

The CRD net annual 100-year average GHG emissions were modelled to be 67 g CO_2e/m^2/year (95% CI 58 - 76) (Table 5-9; Figure 5-11). This was the second lowest GHG emission rate per m^2 for the lower Nelson River reservoirs. The reason why CRD net emissions were modelled to be low in comparison to the other lower Nelson River reservoirs is that the pre-flood reservoir footprint was modelled to be a net source of emissions. Approximately 74% of the total reservoir footprint (approximately 759 km^2 flooded land / approximately 2914 km^2 total reservoir, as described in Section 2.5.2 CRD Flooding) was a pre-existing aquatic environment. The pre-existing aquatic environment is modelled to be a net source of GHG (CH_4) emissions.

Table 5-8 Modelled Net Reservoir 100-Year Lifecycle GHG Emissions: Lower Nelson River Reservoirs Including CRD

Modelled Net Reservoir 100-year Lifecycle GHG Emissions tonnes CO_2e

		95% CI	
CRD [(1)]	19,418,859	17,017,760	22,146,400
Kettle	3,651,272	3,212,330	4,143,810
Keeyask	861,990	749,988	987,936
Long Spruce	331,276	306,128	359,328
Limestone	76,571	63,376	91,664
Sub-Total	**24,339,968**	21,349,582	27,729,138
Potential Conawapa	328,977	303,804	357,348
Total	**24,668,945**	21,653,386	28,086,486

(1) Churchill River Diversion

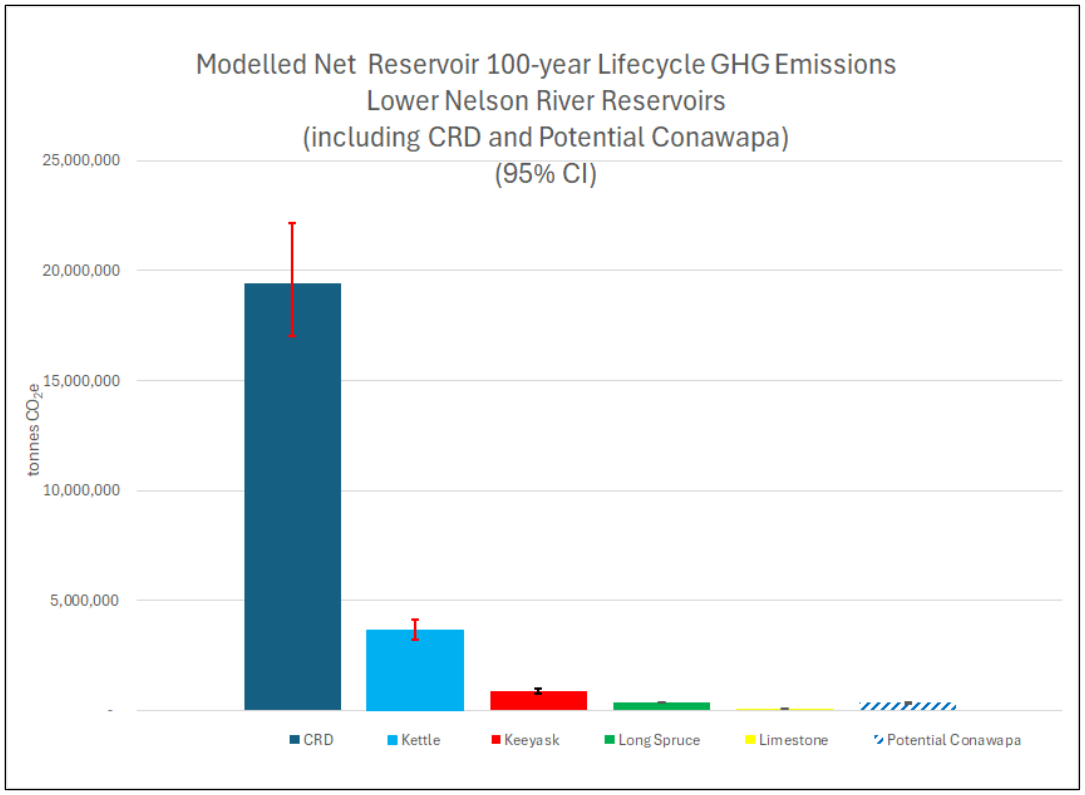


Figure 5-8 Modelled Net Reservoir 100-Year Lifecycle GHG Emissions: Lower Nelson River Reservoirs Including CRD

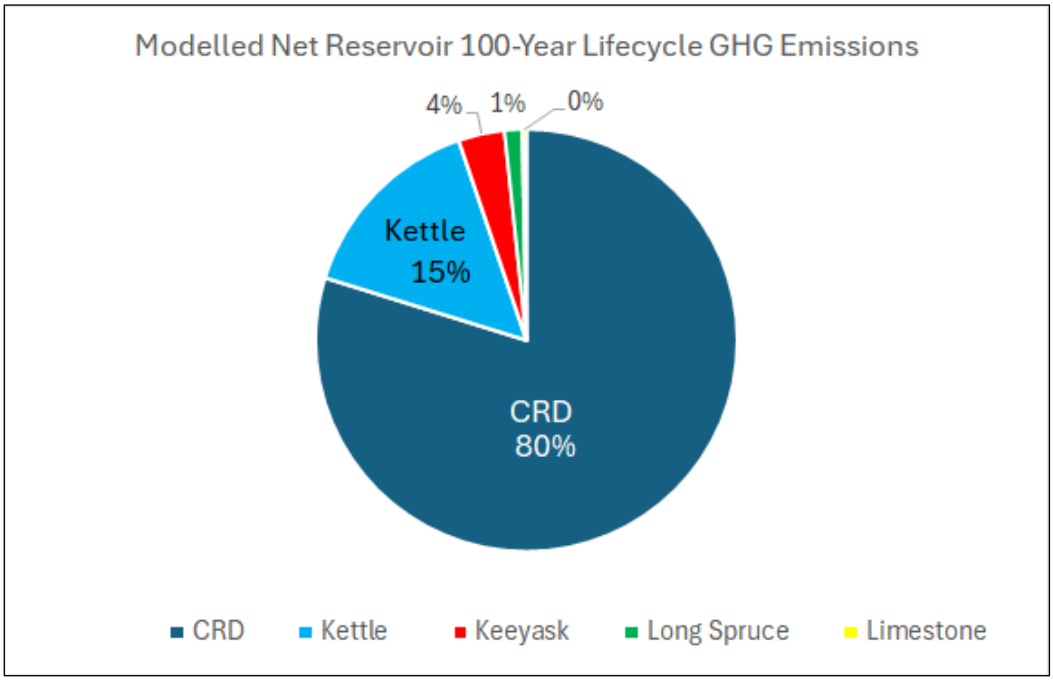


Figure 5-9 Modelled Net Reservoir 100-Year Lifecycle GHG Emissions: Lower Nelson River Reservoirs Including CRD (%)

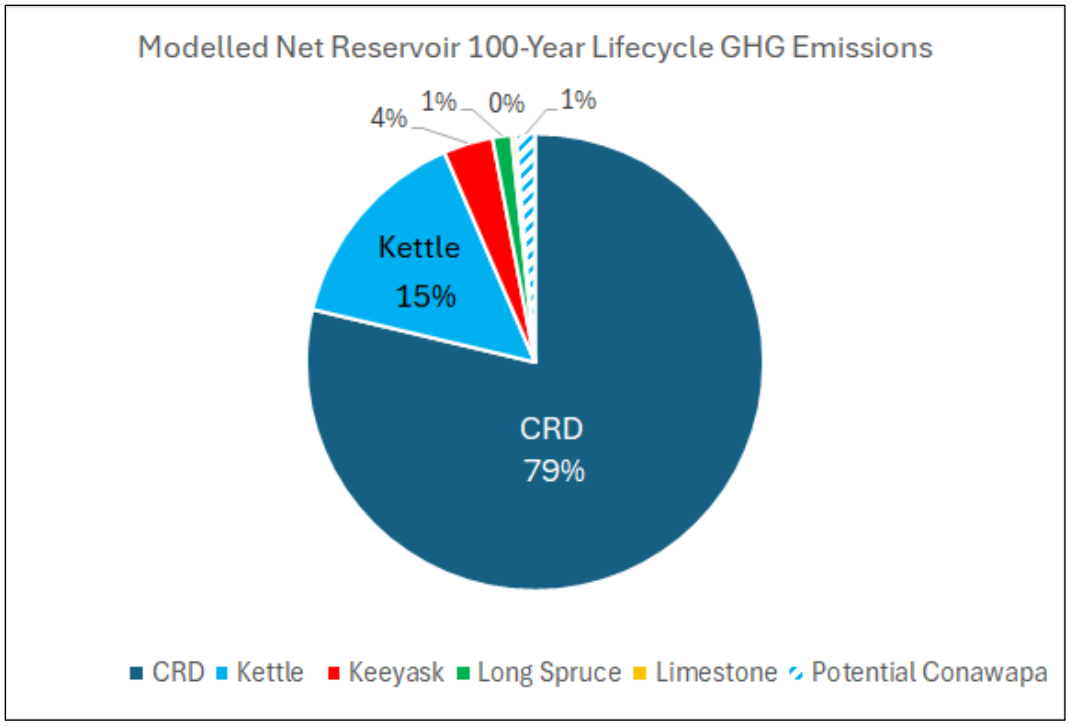


Figure 5-10 Modelled Net Reservoir 100-Year Lifecycle GHG Emissions: Lower Nelson River Reservoirs Including CRD and Potential Conawapa (%)

Table 5-9 Modelled Net Reservoir Annual Average Lifecycle GHG Emissions: Lower Nelson River Reservoirs Including CRD

Modelled Net Reservoir 100-year Lifecycle GHG Emissions
Annual Average
g $CO_2e/m^2/yr$

		95% CI	
CRD [1]	67	58	76
Kettle	114	101	130
Keeyask	86	75	98
Long Spruce	109	101	118
Limestone	28	23	34
Potential Conawapa	85	78	92

(1) Churchill River Diversion

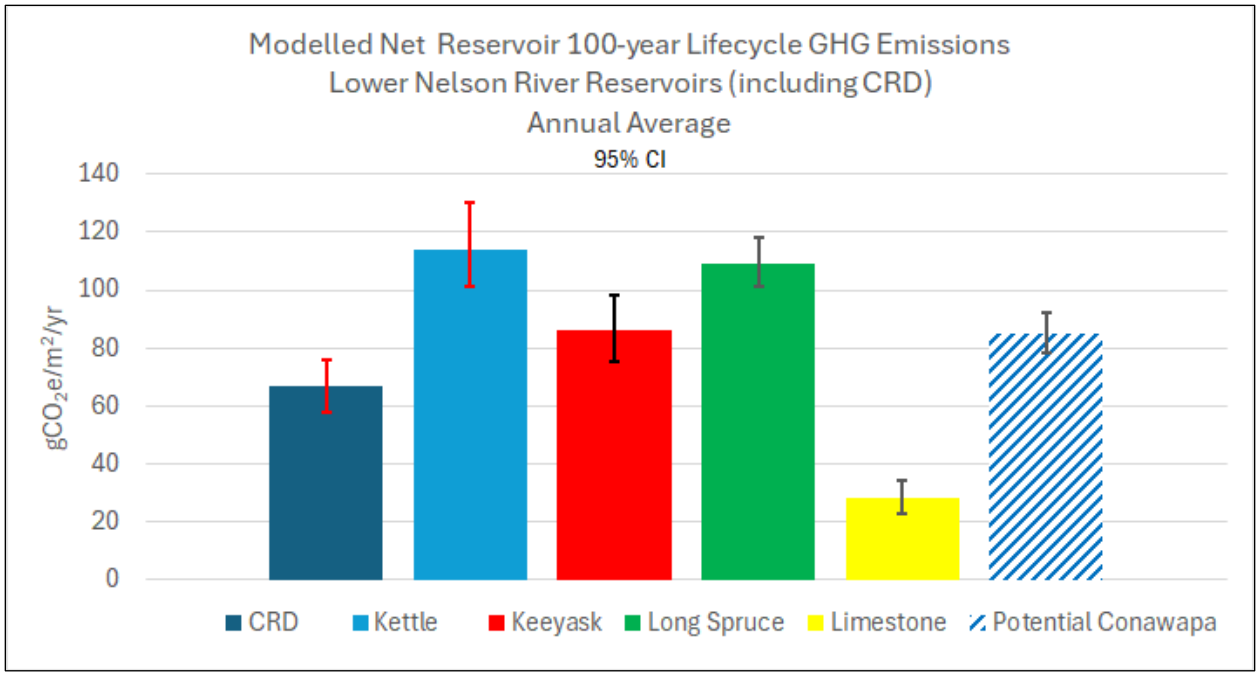


Figure 5-11 Modelled Net Reservoir Annual Average Lifecycle GHG Emissions: Lower Nelson River Reservoirs Including

5.2.1.1 Cumulative Net Reservoir Lifecycle GHG Emissions

Modelled cumulative Net reservoir (and flooded land) lifecycle GHG emissions are illustrated for the lower Nelson River from 1970 to 2075 (Figure 5-12). Net emissions were modelled to be 205,100 t CO_2e (95% CI 180,503 – 231,782) in 1972 following the impoundment of the Kettle reservoir. They are modelled to rise in 1977 after the impoundment of CRD to an estimated 1,030,900 t CO_2e (95% CI 907,211 – 1,175,251), comprising an estimated 923,700 t CO_2e (95% CI 812,889 – 1,053,061) from the CRD and 107,200 t CO_2e (95% CI 94,322 – 121,118) from the Kettle reservoir.

Lower Nelson River reservoir net GHG emissions are modelled to be approximately 182,344 tCO_2e (95% CI 160,462 – 207,872) in 2025. The majority of these emissions are modelled to arise from the CRD (71%) (Figure 5-12). Roughly 16% of the emissions are associated with the Keeyask reservoir, 11% from the Kettle reservoir, and the remaining 2%

from the Long Spruce and Limestone reservoirs. These modelled emissions are in the same order of magnitude as Manitoba Hydro's direct emissions reported for 2023 (Manitoba Hydro, 2025), as discussed in Section 5.1.3.

G-res calculates the 95% CI for total 100-year lifecycle emissions. It does not calculate confidence intervals for individual years. The G-res generated 100-year 95% CI (-12% and +13%) for the Kettle reservoir was applied as the uncertainty for the net Kettle reservoir emissions in 1972. This same value, 100-year 95% CI (-12% and +13%) was also applied as the uncertainty for the net Kettle reservoir emissions in 1977. The G-res generated 100-year 95% CI (-12% and +14%) for the CRD reservoir was applied as the uncertainty for the CRD net emissions in 1977. The G-res generated 100-year 95% CI (-12% and +14%) for the CRD reservoir was applied as the uncertainty for the total net GHG emissions for the Lower Nelson River reservoirs in 2025, as the CRD was the dominate GHG emission source.

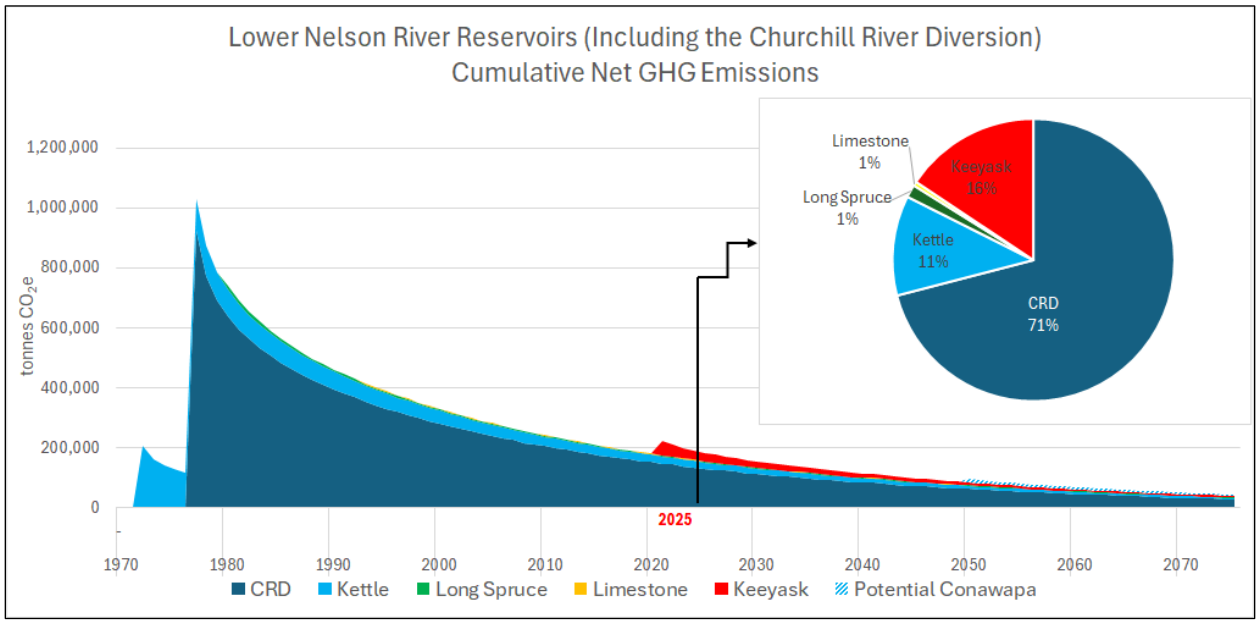


Figure 5-12 Lower Nelson River Reservoirs (Including CRD): Cumulative Net Lifecycle GHG Emissions

5.2.2 Comparison of Lower Nelson River Reservoirs and CRD to Manitoba Hydro Direct GHG Emissions

The size of modelled 2025 net GHG emissions from the lower Nelson River reservoirs and CRD flooded lands were compared to Manitoba Hydro's 2023 Direct GHG emissions from Manitoba Hydro's operations. The 2025 GHG reservoir/flooded land emissions were calculated as the average of annual emissions modelled from 2023 – 2027.

Present day annual (2025) lower Nelson River reservoir and CRD net GHG emissions are modelled to be 182,344 (160,463 – 207,872) tCO_2e (Figure 5-13). This is approximately 42% greater than Manitoba Hydro's 2023 Direct, Scope 1 emissions (128,000 tCO_2e) (Manitoba Hydro, 2025).

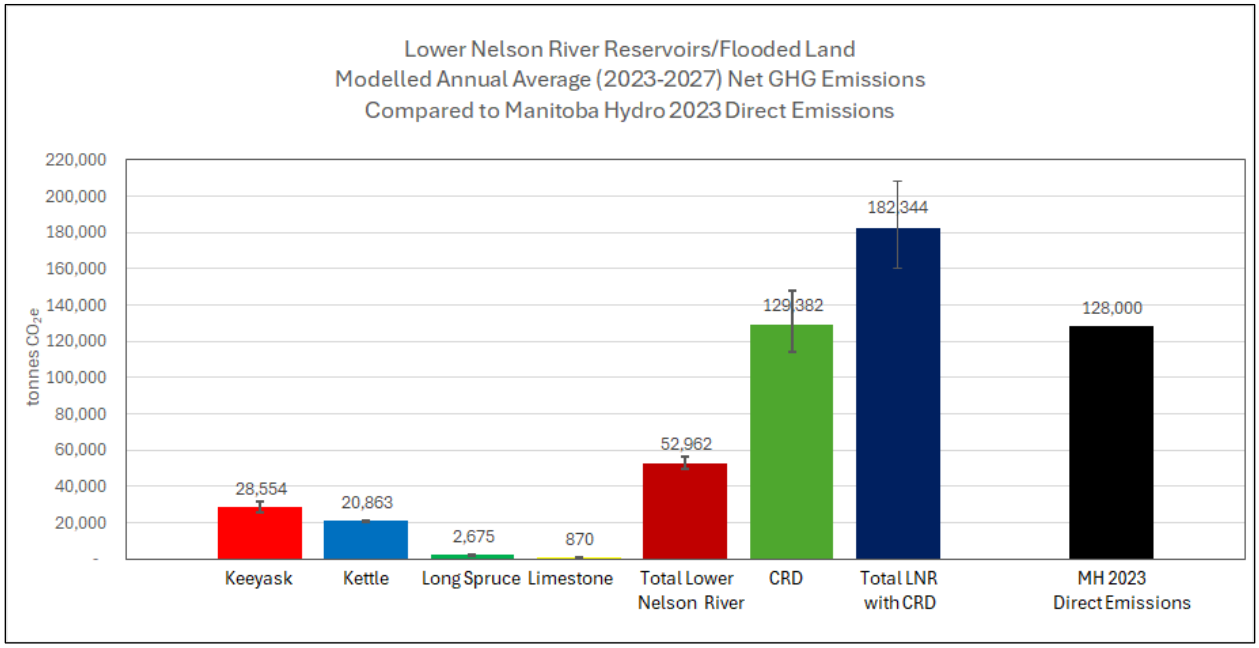


Figure 5-13 Modelled Current Annual Average (2023 – 2027 average) Lower Nelson River Reservoir and CRD GHG Emissions Compared to Manitoba Hydro 2023 Direct Emissions

5.3 Modelled Full Lifecycle GHG Emissions for the Lower Nelson River Including Construction, Landuse Change, Operation, and Decommissioning

As a high-level, order of magnitude assessment, full net lifecycle GHG emissions, including construction, land use change, operation and decommissioning are modelled for the lower Nelson River reservoirs (Keeyask, Kettle, Long Spruce, Limestone, and the potential Conawapa reservoirs) and the CRD. Lifecycle GHG emissions from construction, land use change (other than reservoirs), operation and decommissioning for Keeyask and the Conawapa scenario were adapted from 2013 NFAT Table 1 Appendix 7.3 *Summary of Life Cycle GHG Emissions for the Proposed Keeyask and Conawapa Generation Projects* (Manitoba Hydro, 2013b). The Conawapa lifecycle GHG emissions for construction, land use change (excluding reservoirs), operation and decommissioning were used as a proxy for lifecycle emissions for Kettle, Long Spruce, and Limestone Generating Stations. Similarly, the Keeyask lifecycle emissions (excluding reservoirs) were used as a proxy for the lifecycle emissions of the CRD control structures (Missi Falls and Notigi Control Structures). Reservoir GHG modelling results from this study were used in place of the reservoir GHG values cited in the NFAT document. This approach introduces uncertainty to the lifecycle models. It may overestimate lifecycle emissions for Kettle, Long Spruce, and Limestone as these generating stations are smaller than the proposed Conawapa Station. Similarly, the CRD control structures are smaller than the Keeyask Generating Station.

As noted in Figure 5-14, modelled emissions from reservoirs and flooded land comprise the majority of lifecycle GHG emissions for the Keeyask and Kettle Generating

Stations at 63% and 82%, respectively and comprise approximately 85% of full lifecycle GHG emissions for the Lower Nelson River reservoirs including the CRD.

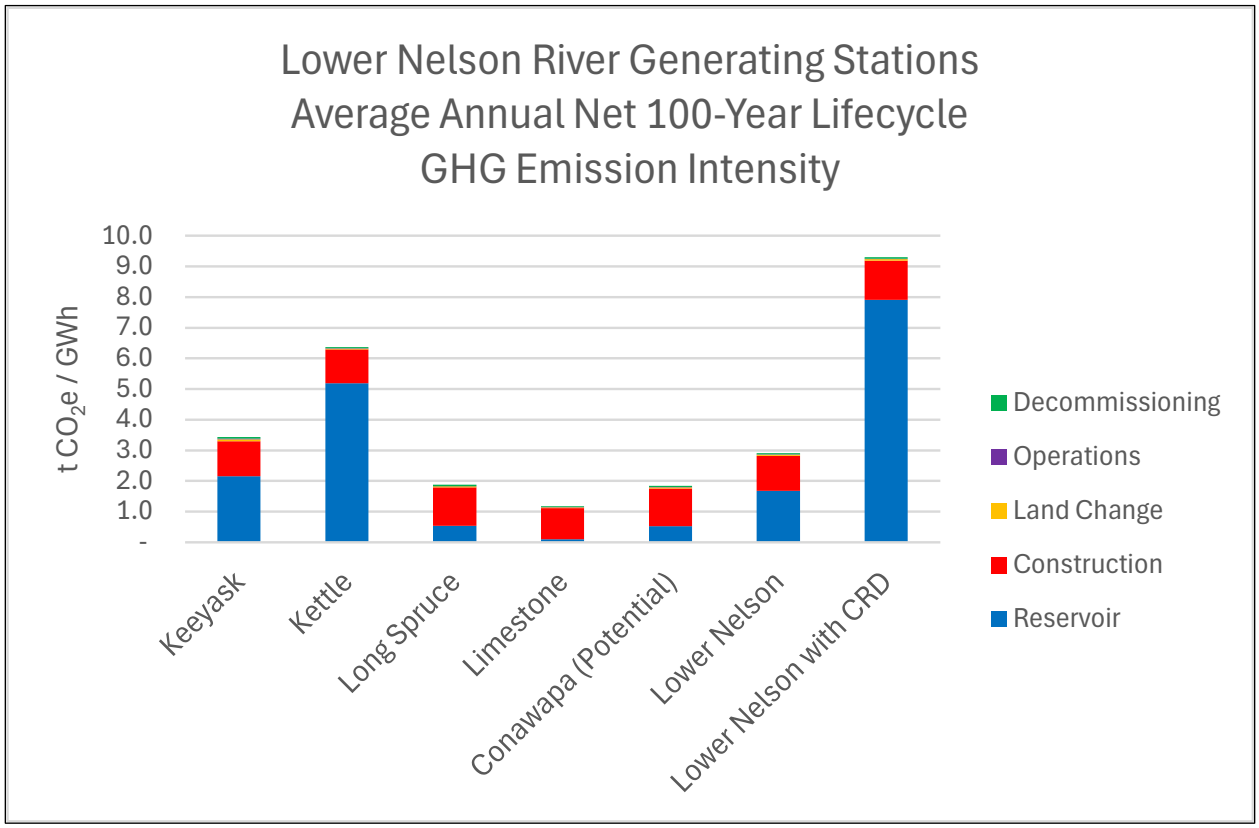


Figure 5-14 Modelled Annual 100-Year Average Full Lifecycle Emission Intensity for the Lower Nelson River Generating Stations Including CRD and Potential Conawapa

Annual GHG emission intensity was modelled to be the highest in the early 1970s with the construction and impoundment of the Kettle reservoir (Stephens Lake), CRD, and Long Spruce reservoir (Figure 5-15). Afterwards, GHG emission intensity declined. On a going forward basis, the remaining lifecycle GHG emission intensity over the next 50 years for the lower Nelson River reservoirs is modelled to be as follows. In this modelling exercise, the hypothetical Conawapa reservoir is assumed to be impounded in 2050.

- 7.9 g CO_2e/kWh in 2026 (5 year average from 2024 to 2028, including CRD)
- 3.7 g CO_2e/kWh from 2025 to 2075 (including CRD)

- 3.0 g CO_2e/kWh from 2035 to 2075 (including CRD)
- 2.0 g CO_2e/kWh from 2050 to 2075 (including CRD and potential Conawapa)

These modelled net GHG emission intensity rates from 2025 to 2075 are similar to median values (that range from 8 to 52 g CO_2e/kWh) for electricity generated from ocean waves, nuclear, wind, solar, and biomass technologies (National Renewable Energy Laboratory, 2021).

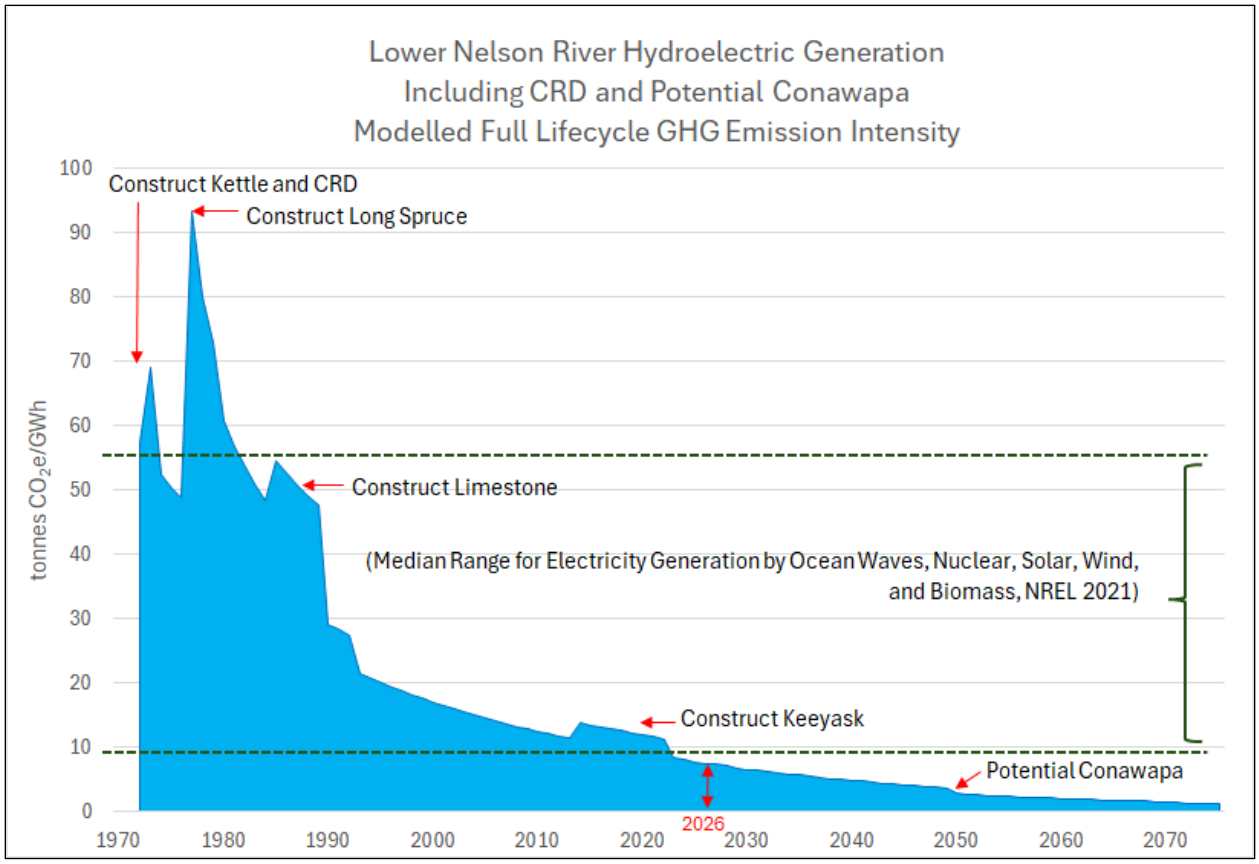


Figure 5-15 Modelled Lifecycle GHG Emissions for the Lower Nelson River Including Construction, Reservoirs, Other Landuse Change, and Operations

6 Uncertainty Analysis

The Keeyask Reservoir Lifecycle GHG Model was assessed in terms of Data Uncertainty and Structural Uncertainty. The details of the assessment are described in Appendix 2.

For this study, Data Uncertainty refers to the uncertainty associated with the data inputs that were used to run the Keeyask G-res model. Structural Uncertainty refers to the uncertainty associated with the database of reservoir GHG studies that underpin the G-res Tool equations. The approach to this assessment was generally guided by the uncertainty assessment methods conducted by Pokorny et al. (2021) on streamflow modelling of the Lower Nelson River.

6.1 Data Uncertainty

The Data Uncertainty assessment focused on those data inputs that had the largest impact on the Keeyask Reservoir Lifecycle GHG Model results. These included the following data related to the Keeyask Reservoir:

1) Pre-flood Landcover Classification;

2) Pre-flood GHG Emission Factors;

3) Size of Littoral Zone;

4) Concentration of Total Phosphorous; and

5) Length of Water Residence Time.

6.1.1 Pre-flood Landcover Classification

The G-res Tool estimates pre-flood GHG emissions by classifying the pre-flood landscape into landcover types and by applying GHG emission factors to each landcover category. This is the largest source of uncertainty related to data entered in the Keeyask G-res model.

The default G-res pre-flood landcover classification and the default G-res GHG landcover emission factors are general in nature, which is understandable as G-res was designed to be applicable for reservoirs worldwide. As described in Section 3.1.2.1 Pre-Flood Landcover Classification, three pre-flood landcover classification schemes were assessed. They involved the Keeyask EIS Vegetation Structure Land Class; the Keeyask EIS Terrestrial Habitat Land Class; and the Keeyask EIS Ecological Land Class. The Keeyask EIS Ecological Land Class was selected to represent the Keeyask pre-flood landcover and replace the G-res default landcover classes.

Pre-flood aquatic CO_2 and CH_4 emissions factors were developed from the Keeyask reservoir GHG baseline studies ("Pre-Project" 2009 – 2013) and replaced G-res default values. Pre-flood terrestrial CO_2 and CH_4 emissions factors were derived from recently published, extensive databases of GHG emissions from boreal and northern landscapes and replaced default G-res terrestrial GHG emission factors.

A sensitivity assessment was conducted to explore the potential range of Keeyask net lifecycle GHG emissions by modelling with alternative pre-flood landcover classification schemes and pre-flood GHG emission factors. Seventeen scenarios were compared against the Keeyask G-res Model (Keeyask EIS Ecological Land Classification) to

assess the possible uncertainty associated with coupling various landcover classification schemes and GHG emission factors (Table 6 -1). Each scenario is not considered to be equally plausible.

6.1.1.1 Pre-Flood Landcover Scenarios

The scenarios included the following:

- Scenarios 1-5: (Keeyask EIS Vegetation Structure Land Class) x (alternative GHG emission factors)
- Scenarios 6-10: (Keeyask EIS Terrestrial Habitat Land Class) x (alternative GHG emission factors)
- Scenarios 11-16: (Keeyask EIS Ecological Land Class) x (alternative GHG emission factors)
- Scenario 17: "Conservative" scenario, pre-flood landscape fixed as "Boreal Forest", a net GHG sink

6.1.1.2 Pre-flood GHG Emission Factors

Below is a description of the 5 Groups of CO_2 and CH_4 emission factors used in Scenarios 1 – 16.

Emission Factors (Group a)

G-res default values, as described by the GHG Reservoir Tool (G-res) Technical Documentation v3.31 (Prairie et al., 2017).

Emission Factors (Group b)

CO_2 emission factors were adapted from Treat et al. (2024); CH_4 emission factors were adapted from the Boreal–Arctic Wetland and Lake Methane Dataset (BAWLD-CH4)

(Kuhn et al., 2021) and Treat et al. (2018, 2024). Individual CH_4 and CO_2 emission factors were developed for the G-res input categories Wetlands, and for Forests and Grassland/Shrubland combined. The length of the Growing Season/"Warm Period" was defined by the Kuhn et al. (2021) study as approximately May through October, 188 days.

Emission Factors (Group c)

Developing CO_2 and CH_4 pre-flood emission factors for Wetlands, Forests and Grassland/Shrubland, followed the same approach as that used for Emission Factor Group (b) above. That is, CO_2 emission factors were adapted from Treat et al. (2024); CH_4 emission factors were adapted from the Boreal–Arctic Wetland and Lake Methane Dataset (BAWLD-CH4) (Kuhn et al., 2021) and Treat et al. (2018, 2024). Individual CH_4 and CO_2 emission factors were developed for the G-res input categories Wetlands, and Forests and Grassland/Shrubland combined. The difference between Group b and c emission factors is that Group c used a Keeyask-specific growing period of 135 days and an ice-free period of 199 days when calculating annual emissions. The methodology for determining the length of the growing period and ice-free period is described in Appendix 1 of this thesis.

Emission Factors (Group d)

CO_2 and CH_4 emission factors were adapted from Treat et al (2018, 2024). Treat reviewed CH_4 and CO_2 fluxes from nearly 20 synthesis studies, including the Boreal–Arctic Wetland and Lake Methane Dataset (BAWLD-CH4) dataset and the FLUXNET-CH4. The review covered synthesis studies conducted from 2002 – 2024 of the Circum-Arctic Permafrost Region, including Alaska, Canadian tundra, boreal Western Canada, Eastern Canada, and Eurasia. Landscape types included marsh, fen, bog, permafrost wetland,

permafrost bog, boreal forest, and upland tundra. Study methods included both eddy covariance and chamber measurement techniques.

Individual CH_4 emission factors were developed for Wetlands, and for Forests and Grassland/Shrubland combined. A composite CO_2 emission factor was developed for the Keeyask uplands, which includes Wetlands, Forests and Grassland/Shrubland combined. The length of the growing season and ice-free season were kept consistent with Scenarios b, and e, at 184 days.

Emission Factors (Group e)

Emission factors were derived from a review of published studies of GHG emissions from northern peatlands, with an emphasis on Canadian research where available. Literature sources included: a synthesis of CO_2 (net ecosystem exchange) and CH_4 emissions from Canadian peatlands (Webster et al 2018); the Boreal–Arctic Wetland and Lake Methane Dataset (BAWLD-CH4) which is a comprehensive dataset of CH_4 fluxes from circumpolar boreal and arctic ecosystems (Kuhn et al., 2021; Olefeldt et al., 2021); a synthesis of CH_4 emissions from northern high latitude wetlands, including bog, poor fen, rich fen, and swamp (Turetsky et al., 2014); CO_2 and CH_4 emissions at a cool-temperate Canadian freshwater marsh (Strachan et al., 2015), and boreal forest CO_2 emissions (net ecosystem exchange) from the BOReal Ecosystem–Atmosphere Study (BOREAS) Northern Study Area near Thompson, Manitoba (Goulden et al., 2011). The length of the growing season and ice-free season were kept consistent with Scenarios b, and d, at 184 days.

Emission Factors (Scenario 17) (reclassified the pre-flood terrestrial land as boreal forest)

G-res Tool default emission factors were used for modelling.

Table 6-1 Sensitivity Analysis: Landcover and Emission Factor Scenarios

Net Lifecycle Greenhouse Gas Emissions from the Keeyask Hydroelectric Reservoir Sensitivity Analyses

Landcover and Emission Factor Scenarios Using the G-res Tool

	Scenarios
1	Vegetation Structure: G-res Tool Default EF (a)
2	Vegetation Structure: User-Defined EF (b)
3	Vegetation Structure: User-Defined EF (c)
4	Vegetation Structure: User-Defined EF (d)
5	Vegetation Structure: User-Defined EF (e)
6	Terrestrial Habitat (Course and Fine Ecosite Type): G-res Default EF (a)
7	Terrestrial Habitat (Course and Fine Ecosite Type): User-Defined EF (b)
8	Terrestrial Habitat (Course and Fine Ecosite Type): User-Defined EF (c)
9	Terrestrial Habitat (Course and Fine Ecosite Type): User-Defined EF (d)
10	Terrestrial Habitat (Course and Fine Ecosite Type): User-Defined EF (e)
11	Ecological Land Classification: G-res Tool Default EF (a)
12	Ecological Land Classification: User-Defined EF (e)
13	Ecological Land Classification (incl. BOG as Wetland): User-Defined EF (b)
14	Ecological Land Classification (incl. BOG as Wetland): User-Defined EF (c)
15	Ecological Land Classification (incl. BOG as Wetland): User-Defined EF (d)
16	Ecological Land Classification (incl. BOG as Wetland): User-Defined EF (e)
17	Test - Re-Class Pre-Flood Land to Forest

Emission Factor Descriptions

a) G-res Tool Default Preflood CO_2 and CH_4 Emission Factors

b) User-Defined Preflood CO2 and CH4 Emission Factors for Wetlands and Uplands. CO_2 EF adapted from Treat et al (2024); CH_4 adapted from Kuhn et al (2021) and Treat et al (2018; 2024). Growing Season/"Warm Period" as defined by Kuhn et al (2021).

c) User-Defined Preflood CO_2 and CH_4 Emission Factors for Wetlands and Uplands. CO_2 EF adapted from Treat et al (2024); CH_4 adapted from Kuhn et al (2021) and Treat et al (2018; 2024). Growing Season and Ice Free Period user-defined for Keeyask region.

d) User-Defined Preflood CO2 and CH4 Emission Factors for Wetlands and Uplands. CO_2 and CH_4 EF adapted from Treat et al (2018; 2024)

e) User-Defined Preflood CO_2 and CH_4 Emission Factors for Wetlands and Uplands. CO_2 and CH_4 EF adapted from Canadian Studies and International Studies.

6.1.1.3 Pre-Flood Landcover Class Sensitivity Analysis Results

Results of the sensitivity analysis are summarized in Table 6-2 and Figures 6-1 and 6-2.

Detailed results are included in Appendix 2.

Table 6-2 Summary of Modelling Scenarios: Predicted Keeyask Reservoir Net Annual Emissions and Emission Intensity

Net 100-Year Lifecycle Greenhouse Gas Emissions from the Keeyask Hydroelectric Reservoir
Modelling Scenarios using the G-res Tool

Predicted Net Annual Emissions per m^2

Scenarios	Emissions per m^2 of Reservoir $gCO_2e/m^2/yr$					Emission Intensity gCO_2e/kWh		
	Post-Impoundment	Pre-Impoundment	Net GHG Footprint	95% Confidence Intervals			95% Confidence Intervals	
1 Vegetation Structure: G-res Tool Default EF (a)	93	69	24	13	36	0.5	0	1
2 Vegetation Structure: User-Defined EF (b)	93	5	88	78	100	2.0	2	2
3 Vegetation Structure: User-Defined EF (c)	93	-18	112	101	123	2.5	2	3
4 Vegetation Structure: User-Defined EF (d)	93	47	46	36	58	1.1	1	1
5 Vegetation Structure: User-Defined EF (e)	93	(66)	159	148	171	3.6	3	4
6 Terrestrial Habitat (Course and Fine Ecosite Type): G-res Default EF (a)	93	195	(101)	(112)	(90)	-2.3	-3	-2
7 Terrestrial Habitat (Course and Fine Ecosite Type): User-Defined EF (b)	93	(56)	150	139	161	3.4	3	4
8 Terrestrial Habitat (Course and Fine Ecosite Type): User-Defined EF (c)	93	(63)	156	146	168	3.6	3	4
9 Terrestrial Habitat (Course and Fine Ecosite Type): User-Defined EF (d)	93	(40)	133	123	145	3.0	3	3
10 Terrestrial Habitat (Course and Fine Ecosite Type): User-Defined EF (e)	93	(35)	128	8	179	2.9	3	3
11 Ecological Land Classification: G-res Tool Default EF (a)	88	85	3	(7)	14	0.1	0	0
12 Ecological Land Classification: User-Defined EF (e)	88	(51)	139	129	150	3.2	3	3
13 Ecological Land Classification (incl. BOG as Wetland): User-Defined EF (b)	88	(5)	93	83	104	2.1	2	2
14 Ecological Land Classification (incl. BOG as Wetland): User-Defined EF (c)	88	(18)	106	96	117	2.4	2	3
15 Ecological Land Classification (incl. BOG as Wetland): User-Defined EF (d)	88	2	86	76	97	2.0	2	2
16 Ecological Land Classification (incl. BOG as Wetland): User-Defined EF (e)	88	(54)	142	132	153	3.2	3	3
17 Test - Re-Class Pre-Flood Land to Forest	88	(61)	149	139	160	3.4	3	4
All Scenarios								
Min	88.0	(66.0)	(101.0)	(112.0)	(90.0)	(2.3)	-3	-2
Max	93.0	195.0	159.0	148.0	178.8	3.6	3	
Avg	90.9	(3.8)	94.9	63.2	126.5	2.2	1	3
All Scenarios except (All Forest)								
Min	88.0	(66.0)	(101.0)	(112.0)	(90.0)	(2.3)	-3	-2
Max	93.0	195.0	159.0	148.0	178.8	3.6	3	4
Avg	91.1	(0.2)	91.5	58.6	124.4	2.1	1	3
Vegetation Structure:								
Min	93.0	(66.0)	24.0	13.0	36.0	0.5	0	1
Max	93.0	69.0	159.0	148.0	171.0	3.6	3	4
Avg	93.0	7.4	85.8	43.8	127.8	1.9	1	3
Terrestrial Habitat (Course and Fine Ecosite Type):								
Min	93.0	(63.0)	(101.0)	(112.0)	(90.0)	(2.3)	-3	-2
Max	93.0	195.0	156.0	146.0	178.8	3.6	3	4
Avg	93.0	0.2	93.2	7.6	178.8	2.1	0	4
Ecological Land Classification:								
Min	88.0	(54.0)	3.0	(7.0)	14.0	0.1	0	0
Max	88.0	85.0	142.0	132.0	153.0	3.2	3	3
Avg	88.0	(6.8)	94.8	57.9	131.8	2.2	1	3
Test - Re-Class Pre-Flood Land to Forest	88.0	(61.0)	149.0	139.0	160.0	3.4	3	4

Explanatory Notes:

a) G-res Tool Default Preflood CO_2 and CH_4 Emission Factors

b) User-Defined Preflood CO_2 and CH_4 Emission Factors for Wetlands and Uplands.
CO_2 EF adapted from Treat et al (2024); CH_4 adapted from Kuhn et al (2021) and Treat et al (2018; 2024). Growing Season/"Warm Period" as defined by Kuhn et al (2021).

c) User-Defined Preflood CO_2 and CH_4 Emission Factors for Wetlands and Uplands.
CO_2 EF adapted from Treat et al (2024); CH_4 adapted from Kuhn et al (2021) and Treat et al (2018; 2024). Growing Season and Ice Free Period user-defined for Keeyask region.

d) User-Defined Preflood CO_2 and CH_4 Emission Factors for Wetlands and Uplands.
CO_2 and CH_4 EF adapted from Treat et al (2018; 2024)

e) User-Defined Preflood CO_2 and CH_4 Emission Factors for Wetlands and Uplands.
CO_2 and CH_4 EF adapted from Canadian Studies and International Studies.

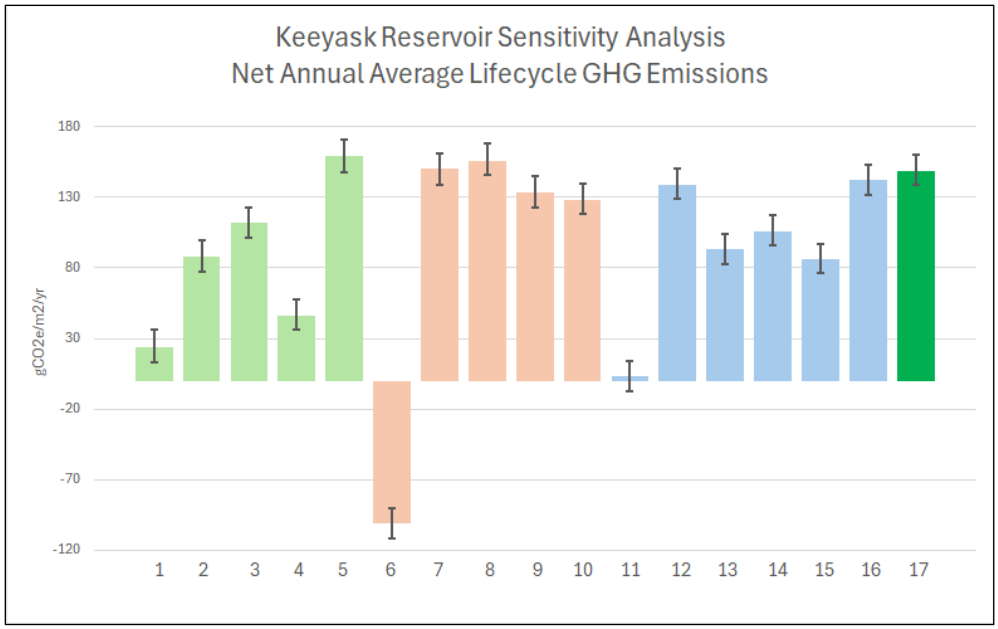


Figure 6-1 Modelling Scenarios: Keeyask Reservoir Net Annual Average Lifecycle GHG Emissions (with 95% Confidence Intervals)

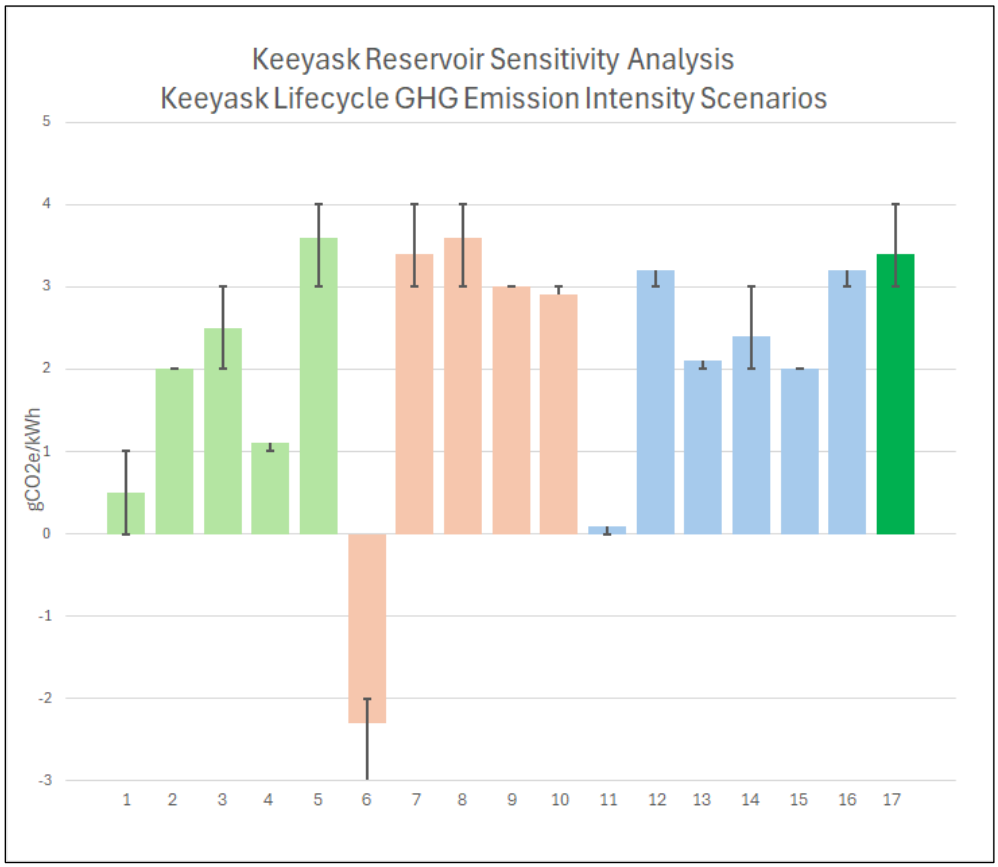


Figure 6-2 Modelling Scenarios: Keeyask Reservoir Net Annual Average Lifecycle GHG Emission Intensity (with 95% Confidence Intervals)

6.1.1.4 Pre-Flood Landcover Class Sensitivity Analysis: Discussion

Scenarios 1-5 are variations of the Vegetation Structure land class and emissions factors; Scenarios 6-10 are variations of the Terrestrial Habitat Ecosite land class; and Scenarios 11-16 are variations of the Ecological Land Classification and emission factors. Scenario 17 is a conservative benchmark, where all pre-flood terrestrial land was set to be as boreal forest (net GHG sink).

Annual Net lifecycle emissions for individual scenarios range from -101 $gCO_2e/m^2/yr$ to 159 $gCO_2e/m^2/yr$, with an average of 95 $gCO_2e/m^2/yr$ (Table 6-2). This represents a decrease of -217% to an increase of 85% as compared to the Keeyask G-res Model. GHG Emission Intensity ranged from -2.3 gCO_2e/kWh to 3.6 gCO_2e/kWh, with an average of 2.2 gCO_2e/kWh for Scenarios 1–17.

Annual Net lifecycle emissions are modelled to be on average 85.8 $gCO_2e/m^2/yr$ (95% CI 43.8 – 127.8) for Scenarios 1-5 (Vegetation Structure); 93.2 $gCO_2e/m^2/yr$ (95% CI 7.6 – 178.8) for Scenarios 6-10 (Terrestrial Habitat Ecosite); and 94.8 $gCO_2e/m^2/yr$ (95% CI 57.9 – 131.8) for Scenarios 11-16 (Ecological Land Classification) (Table 6-2) Figure (6-3). This compares to 86.0 $gCO_2e/m^2/yr$ (95% CI 75 - 98) for the Keeyask G-res model, representing a decrease of -0.1% to an increase of 10%. Scenario 17 was modelled to be 149.0 $gCO_2e/m^2/yr$ (95% CI 139 - 160).

GHG Emission Intensity is modelled to be on average 1.9 gCO_2e/kWh (95% CI 1 - 3) for Scenarios 1-5 (Vegetation Structure); 2.1 gCO_2e/kWh (95% CI 0 - 4) for Scenarios 6-10 (Terrestrial Habitat Ecosite); and 2.2 gCO_2e/kWh (95% CI 1 - 3) for Scenarios 11-16 (Ecological Land Classification) (Table 6-2, Figure 6-4). This compares to 2.2 gCO_2e/kWh

(95% CI 2 - 3) for the Keeyask G-res model. Scenario 17 was modelled to be 3.4 gCO_2e/kWh (95% CI 3 - 4).

In conclusion, when comparing individual scenarios, the impact on estimated net lifecycle emissions is high, with annual net emission per m^2 ranging from a decrease of -217% to an increase of 85% compared to the Keeyask G-res Model results. The lowest net emissions overall, and the lowest within each scenario group (e.g., Scenarios Vegetation Structure 1(a), Terrestrial Habitat 6(a) and Ecological Land 11(a) resulted from using the G-res default emission factors. The G-res default emission factors characterize the pre-flood landcover as being an emission source. In these scenarios, flooding an emission source reduced net lifecycle emissions. The scenarios that resulted in the largest net lifecycle emissions resulted from using emission factors that characterized the preflood landcover as emission sinks. When comparing the average for each scenario class (e.g., Vegetation Structure; Terrestrial Habitat; and Ecological Land Class) the results of the Sensitivity Analyses for scenarios 1-16 compared well with the Keeyask G-res model for both annual GHG emissions on a CO_2 equivalency basis per m^2, and for GHG emissions intensity. These scenarios are not a validation of the Keeyask G-res Model. Rather, the Sensitivity Analysis indicates that on average, the scenario results are similar to the Keeyask G-res Model. Scenario 17, which is a conservative benchmark, results in an estimate of GHG emissions intensity that is also similar to the Keeyask G-res Model.

The Keeyask G-res Model could be improved by developing site-specific terrestrial pre-flood GHG emission factors. These could be developed by measuring emissions from

the unflooded land adjacent to the reservoir. This is similar to the "buffer method" described by G-res (Prairie et al., 2017).

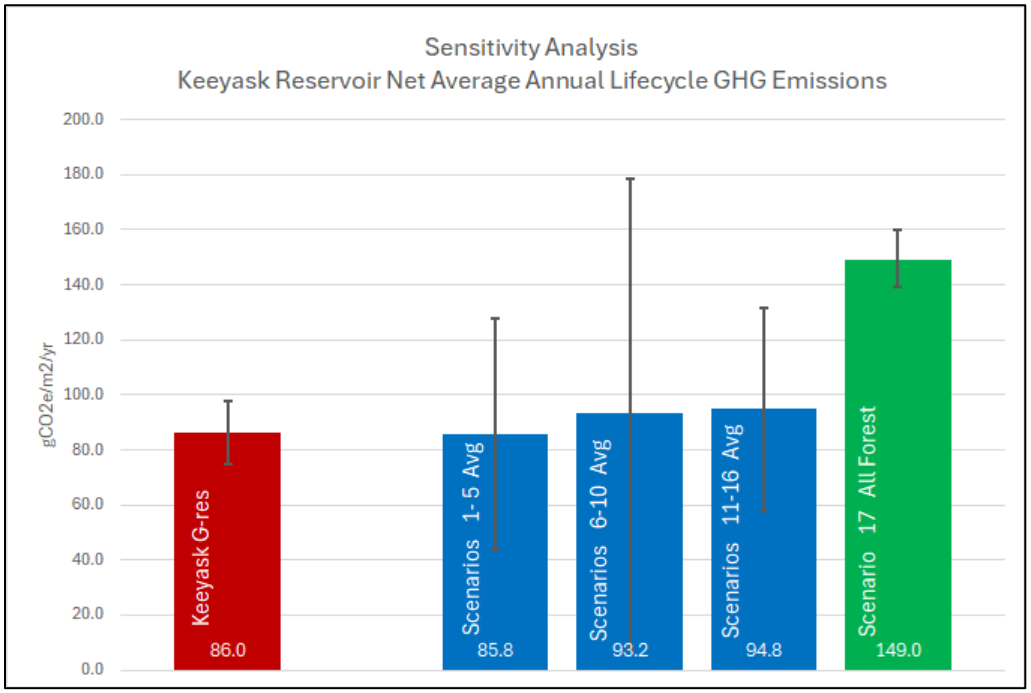


Figure 6-3 Keeyask Reservoir Modelling Scenarios: Net Average Annual Lifecycle GHG Emissions (95% Confidence Intervals)

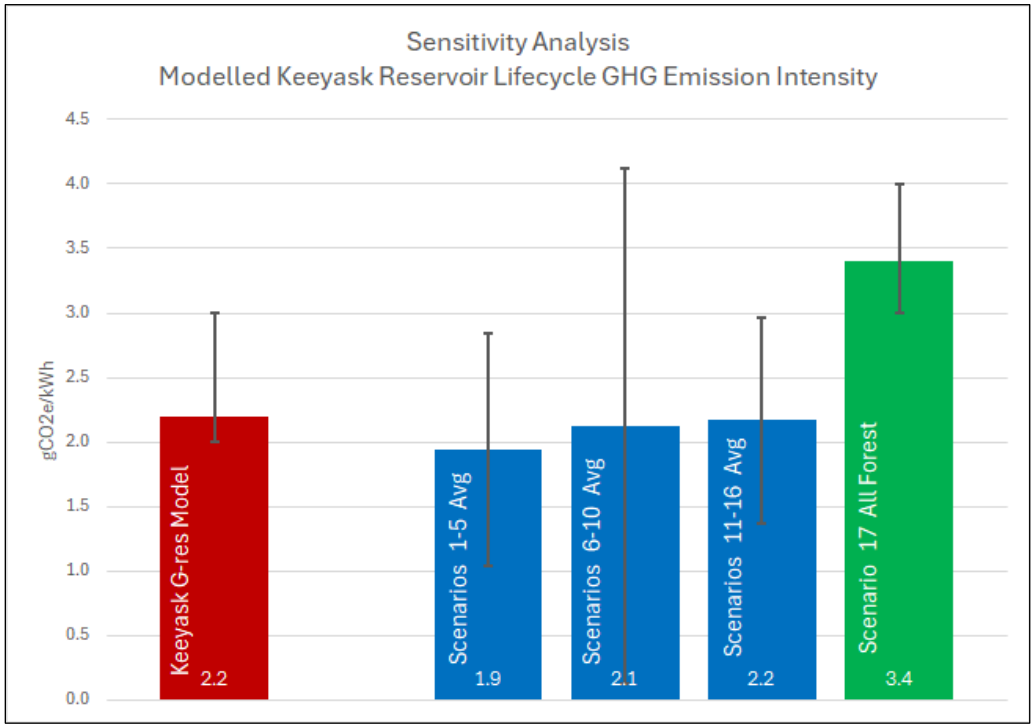


Figure 6-4 Keeyask Reservoir Modelling Scenarios: Lifecycle GHG Emission Intensity (95% Confidence Intervals)

6.1.1.5 Uncertainty Within Ecological Land Classification

6.1.1.5.1 Keeyask Reservoir

As described in Section 3.1.2.2.1 Preparation of The Ecological Land Classification for Use in G-res Modelling, the following categories of the Ecological Land Classification (which were used to categorize the pre-flood Keeyask landcover) were re-classified from forest to wetlands (bogs) (Figure 6-5):

- Black Spruce/Feathermoss (Older or Taller Vegetation - **Bog**, Dry to Moist),
- Black Spruce/Feathermoss (Young or Short Vegetation - **Bog**, Dry to Moist),
- Black Spruce/Mixedwoods (Young or Short Vegetation - **Bog**, Dry to Moist),
- and the "Bog-dominated" sections of the Black Spruce/Tamarack (Young to Older or Short to Taller Vegetation - **Bog**, Fen & Swamp, Wet)

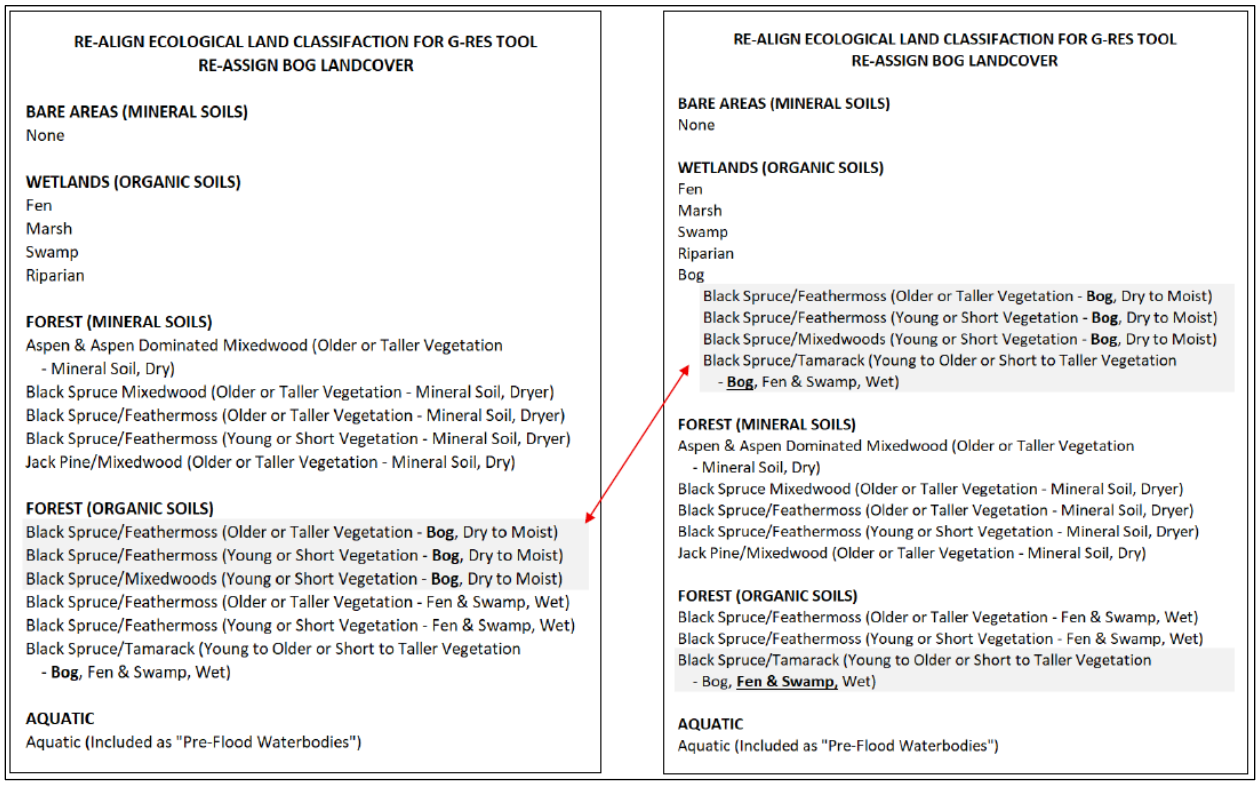


Figure 6-5 Ecological Land Classification: Re-class Forest (sub-class bogs) to Wetlands (sub-class bogs)

The re-organization is based on the author's interpretation of the Keeyask Ecological Land Classification which may introduce bias when computing the areal extent of each pre-flood land class. The re-class of bogs from forest to wetlands decreases the amount of pre-flood forest in the reservoir footprint from 40.7% to 9.4%. The extent of wetlands increases from 3.8% to 35.1% (Figure 6-6).

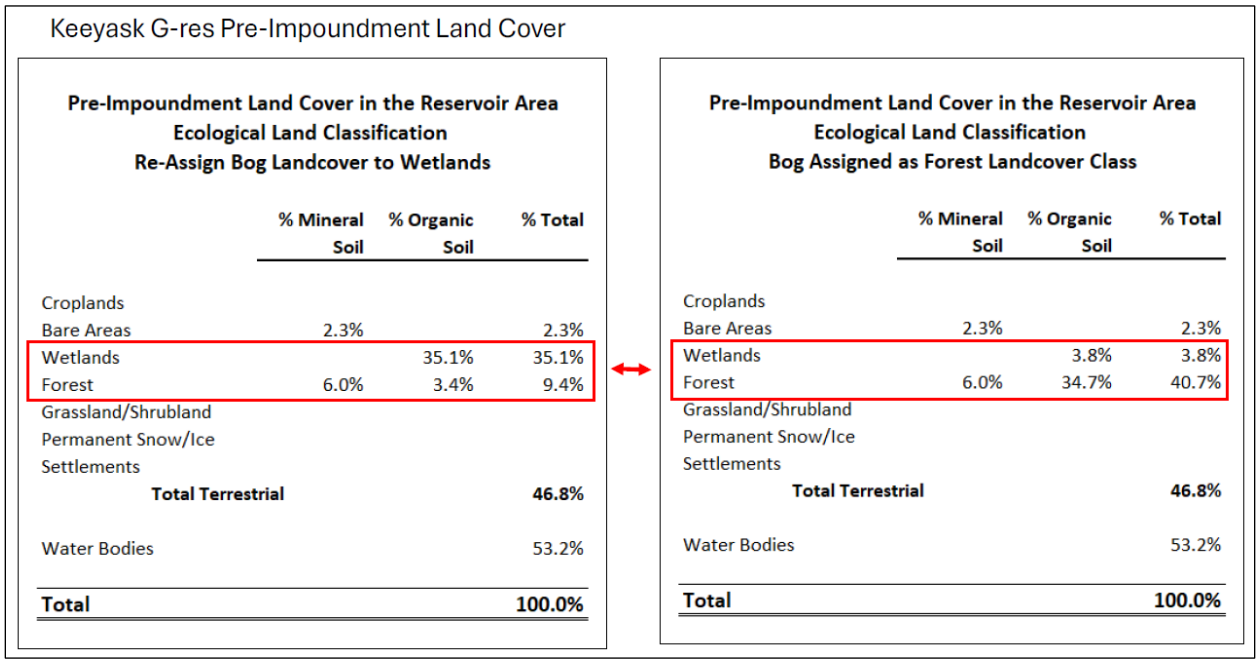


Figure 6-6 Keeyask G-res Pre-Impoundment Landcover Classification: Re-class Bogs from Forest to Wetlands

The implications of bias are examined below. Keeyask reservoir 100-year annual average net GHG emissions per m^2 were modelled to increase from 86.0 to 143.0 gCO_2e, a rise of 66.3% if bogs are classified as forests rather than wetlands (Figure 6-7). 100-year annual average emission intensity rises from 2.2 to 3.7 gCO_2e/kWh, a 68.2% increase (Figure 6-8). Keeyask reservoir lifecycle emission intensity remains comparable to or low as compared to other Canadian reservoirs when pre-flood bogs are classified as forests (Figure 6-9).

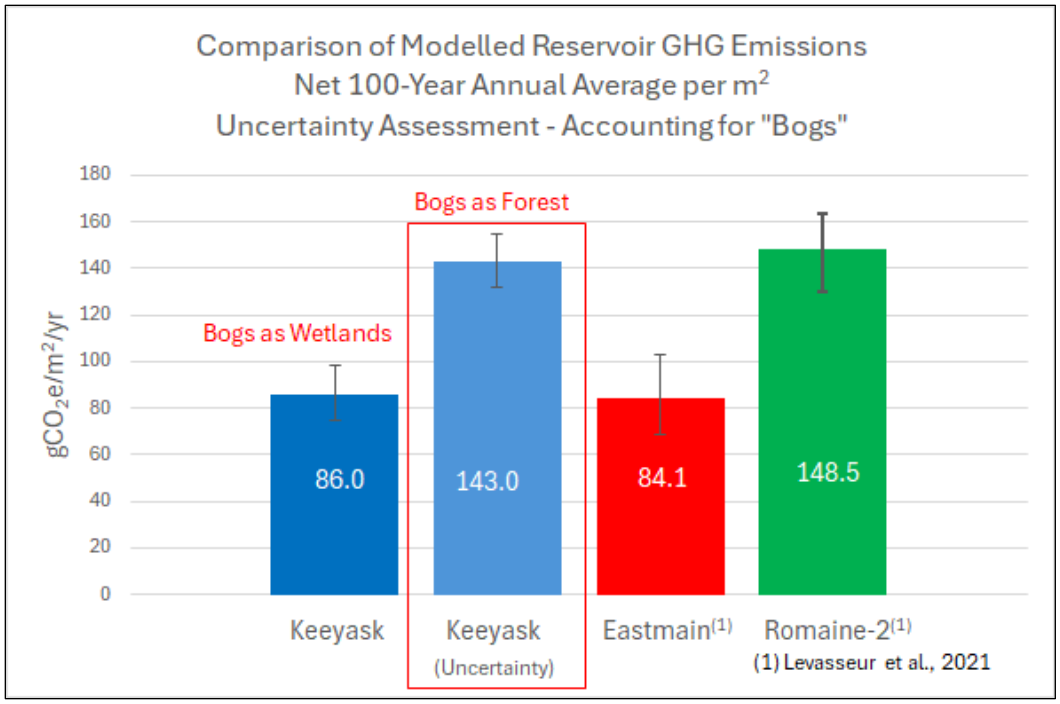


Figure 6-7 Keeyask G-res Model: Comparison of 100-year Annual Average Net GHG Emissions with Bogs Classified as Wetlands or as Forest

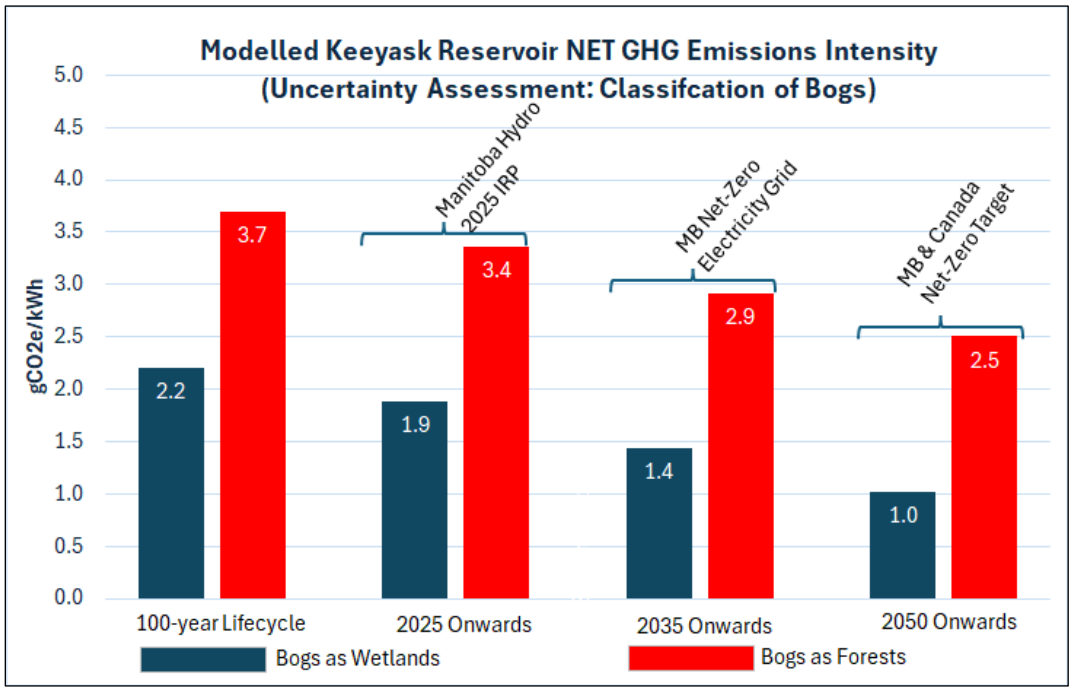


Figure 6-8 Modelled Keeyask Net Reservoir GHG Intensity: Uncertainty Assessment Comparing Pre-Flood Bogs Classified as Wetlands or Forests

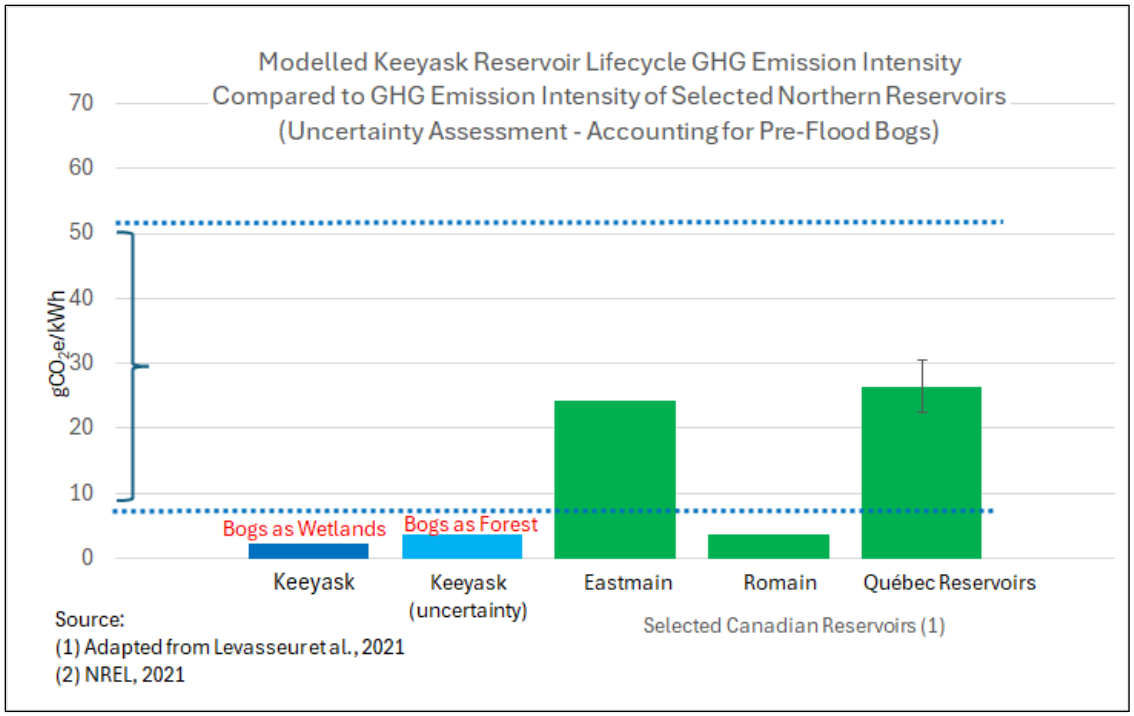


Figure 6-9 Comparison of Modelled Net Reservoir GHG Intensity: Accounting for Keeyask Pre-Flood Bogs as Wetlands or Forests

6.1.1.5.2 Lower Nelson River

The impact of re-classifying pre-flood landcover that included bogs from wetlands to forest was examined collectively for the largest flooded areas of the lower Nelson River which included the Keeyask and Kettle and reservoirs, and the CRD (Figures 6-10 to 6-12). Total lifecycle emissions rose 15.4% for the CRD, by 67.9% and 66.7% for the Kettle and Keeyask reservoirs, respectively, and by 24.5% overall for the lower Nelson River reservoirs and flooded land (Figure 6-12).

Kettle G-res Pre-Impoundment Land Cover

Pre-Impoundment Land Cover in the Kettle Reservoir Area
Adaptation of Keeyask Ecological Land Classification
Bogs Classified as Wetlands

	% Mineral Soil	% Organic Soil	% Total
Croplands			
Bare Areas	3.0%		3.0%
Wetlands		46.6%	46.6%
Forest	8.0%	4.5%	12.5%
Grassland/Shrubland			
Permanent Snow/Ice			
Settlements			
Total Terrestrial			**62.1%**
Water Bodies on Land			7.2%
Total			**69.3%**

Pre-Impoundment Land Cover in the Kettle Reservoir Area
Adaptation of Keeyask Ecological Land Classification
Bogs Classified as Forest

	% Mineral Soil	% Organic Soil	% Total
Croplands			
Bare Areas	3.0%		3.0%
Wetlands		5.1%	5.1%
Forest	8.0%	46.0%	54.0%
Grassland/Shrubland			
Permanent Snow/Ice			
Settlements			
Total Terrestrial			**62.1%**
Water Bodies on Land			7.2%
Total			**69.3%**

Figure 6-10 Kettle G-res Pre-Impoundment Landcover Classification: Re-class Bogs from Forest to Wetlands

CRD G-res Pre-Impoundment Land Cover

Pre-Impoundment Land Cover in the CRD Area
Adaptation of Keeyask Ecological Land Classification
Bogs Classified as Wetlands

	% Mineral Soil	% Organic Soil	% Total
Croplands			
Bare Areas	1.1%		1.1%
Wetlands		17.5%	17.5%
Forest	3.0%	1.7%	4.7%
Grassland/Shrubland			
Permanent Snow/Ice			
Settlements			
Total Terrestrial			**23.4%**
Water Bodies on Land			2.7%
Total			**26.0%**

Pre-Impoundment Land Cover in the CRD Area
Adaptation of Keeyask Ecological Land Classification
Bogs Classified as Forests

	% Mineral Soil	% Organic Soil	% Total
Croplands			
Bare Areas	1.1%		1.1%
Wetlands		1.9%	1.9%
Forest	3.0%	17.3%	20.3%
Grassland/Shrubland			
Permanent Snow/Ice			
Settlements			
Total Terrestrial			**23.4%**
Water Bodies on Land			2.7%
Total			**26.0%**

Figure 6-11 CRD G-res Pre-Impoundment Landcover: Re-class Bogs from Forest to Wetlands

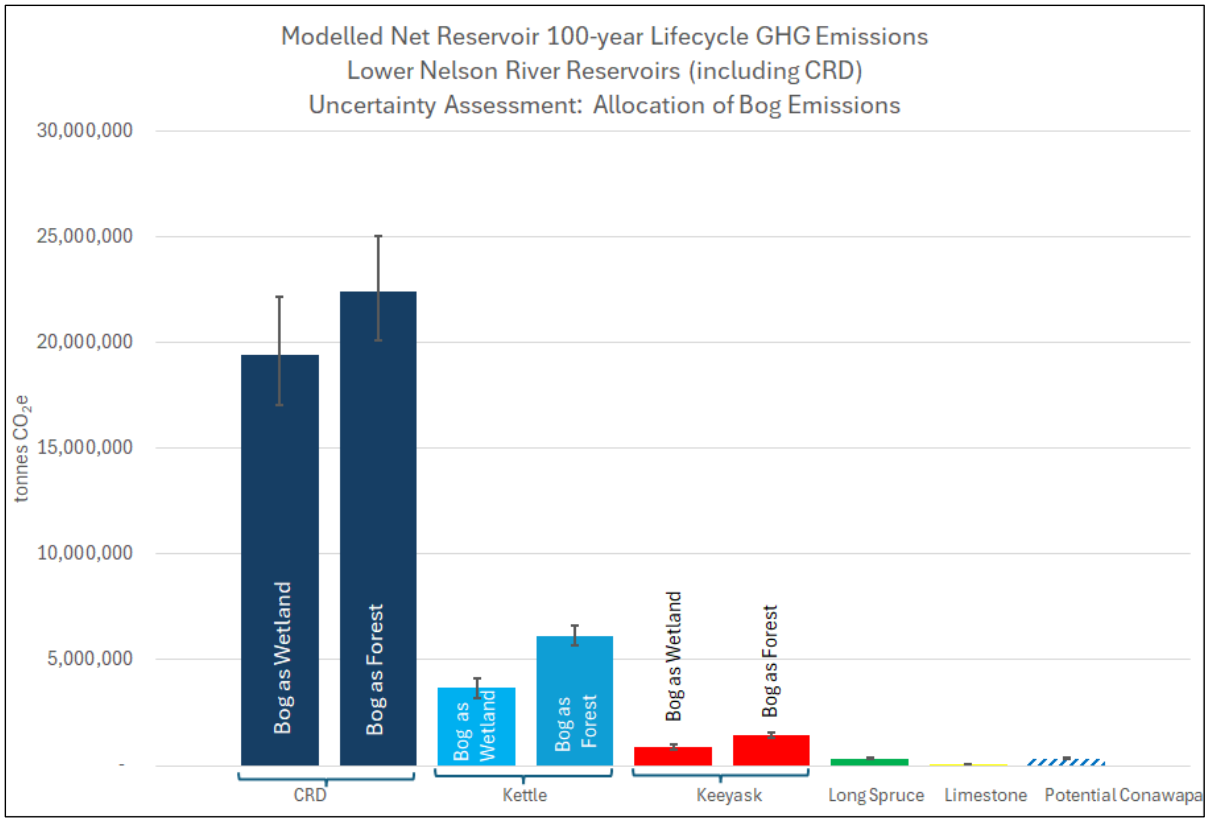


Figure 6-12 Lower Nelson River G-res Model: Comparison of Total Lifecycle Net GHG Emissions with Bogs Classified as Wetlands or as Forest

6.1.1.6 Pre-Flood CH_4 and CO_2 Emission Factors

The Keeyask Reservoir Lifecycle GHG Model used pre-flood CH_4 emission factors derived from Kuhn et al. (2021) and CO_2 emission factors derived from Virkkala et al. (2021). To be conservative, median emission factors were adopted where available, so as not to overstate pre-flood emissions and therefore understate net emissions. Median emission factors were available for CH_4 as published by Kuhn et al. (2021). Median emission factors were not available for CO_2 from the Virkkala et al. (2021) dataset, so CO_2 mean were used in the Keeyask G-res model.

To evaluate the uncertainty of GHG pre-flood emission factors, the G-res Keeyask model was also run using the following GHG emission factor scenarios (Figures 6-13 and 6-14):

1) Mean CH_4 and CO_2 emission factors: as published by Kuhn et al. (2021), and Virkkala et al., (2021), respectively.
2) Lower Limits: 25th percentile for CH_4, as published by Kuhn et al. (2021) and the lower limit 90% confidence interval as published by Virkkala et al., (2021) . (Low pre-flood emission factors, which will result in higher **net** emissions).
3) Upper Limits: 75th percentile for CH_4, as published Kuhn et al. (2021) and the upper 90% confidence interval as published by Virkkala et al., (2021). (High pre-flood emission factors, which will result in lower **net** emissions).

Using **mean** pre-flood emission factors, modelled total net lifetime reservoir emissions declined by 47.3% from 861,990 tCO_2e (95% CI 749,988 – 987,936) to 454,301 tCO_2e (95% CI 345,376 – 577,300). Emission intensity drops by 40% from 2.2 (95% CI 2 - 3) to 1.2 (95% CI 1 - 1) gCO_2e/kWh. Although it could be defensible to adopt mean pre-flood emission factors, Median values were used in the Keeyask G-res Model when available so as not to understate lifecycle emissions and not to overstate lifecycle emission intensity.

Using the **lower and upper limits** of the pre-flood GHG emission factors, modelled total net lifetime reservoir emissions ranged from 1,864,915 tCO_2e (95% CI 1,753,988 – 1,989,928) to -400,410 tCO_2e (95% CI -512,040 & -274,092), respectively. This represents a percentage change of 116.3% and -146.5%, respectively as compared to the Keeyask model. Emission intensity ranged from 4.8 (95% CI 5 - 5) to -1.0 (95% CI -1 & - 1)

gCO_2e/kWh, respectively, which are very low values. Figure 6-15 compares the range of modelled Keeyask reservoir emissions intensities to other northern reservoirs. The lower and upper limits of the pre-flood GHG emission factors illustrate the potential range of GHG emissions and emission intensity.

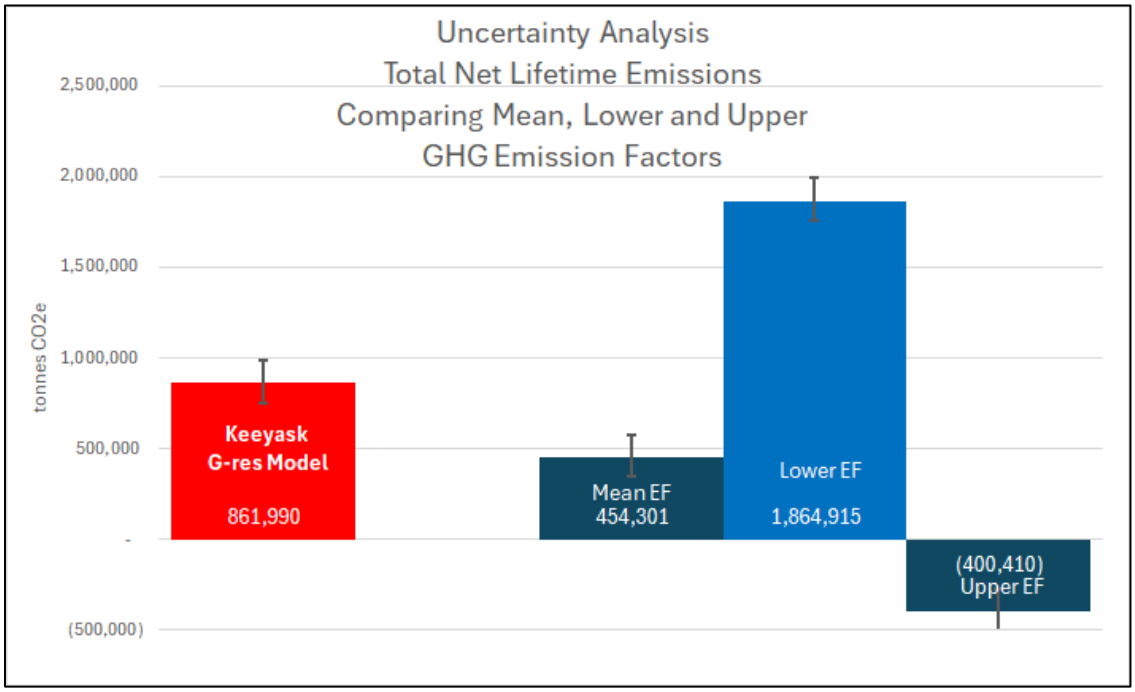


Figure 6-13 Total Lifetime GHG Emissions Comparing Keeyask Model to Mean, Upper and Lower Emission Factor Limits (with 95% CI)

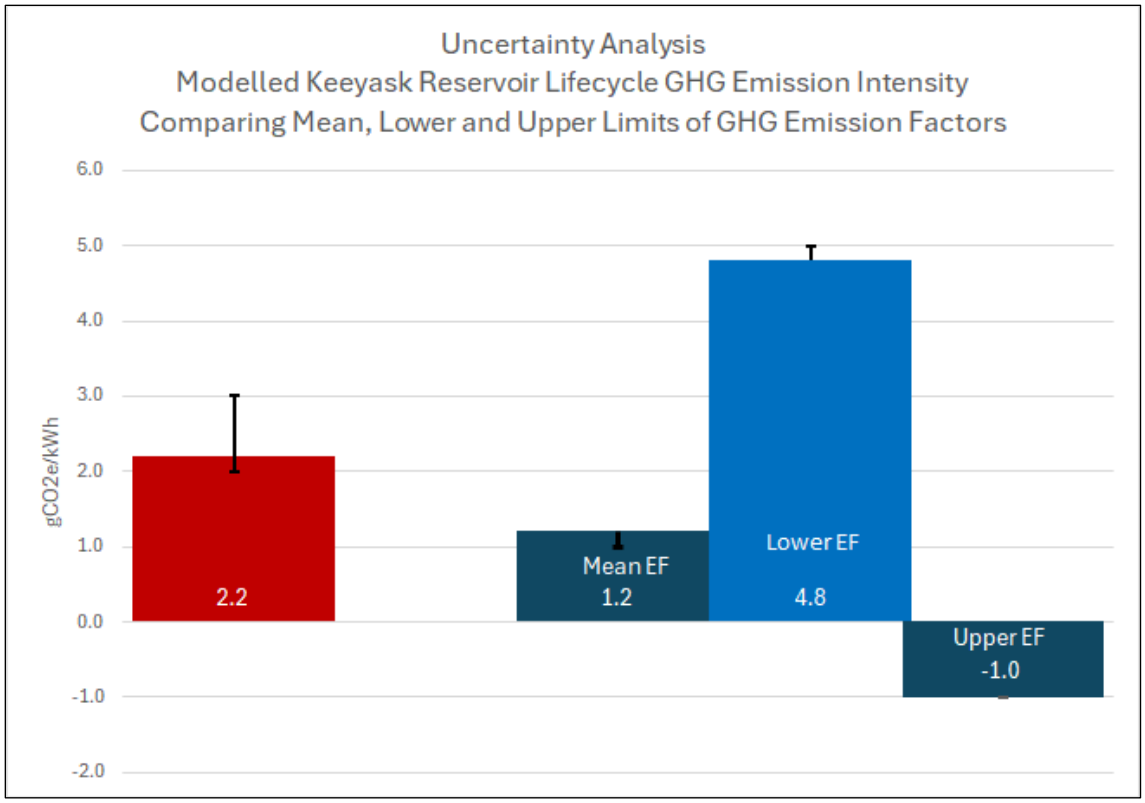


Figure 6-14 Total Lifecycle Emission Intensity Comparing Keeyask Model to Mean, Upper and Lower Limits of GHG Emission Factors (with 95% CI)

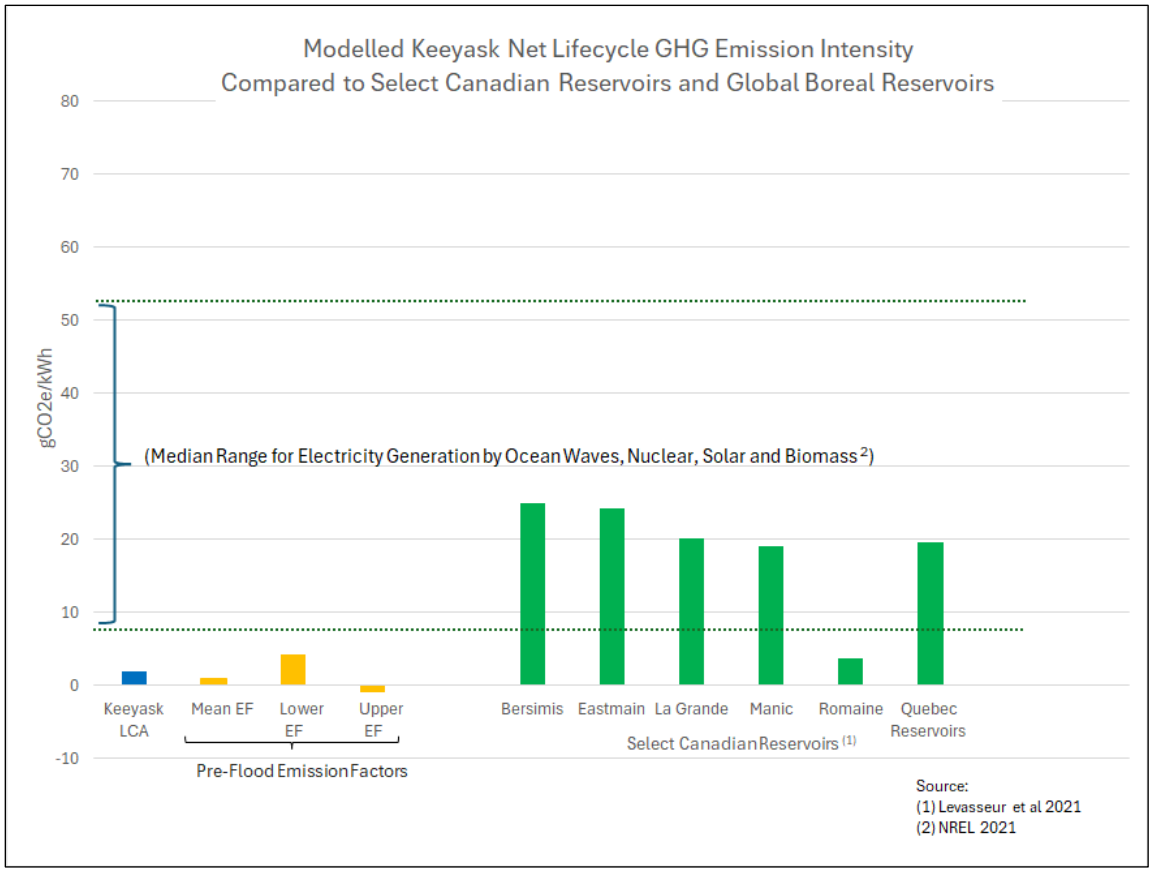


Figure 6-15 Comparison of Modelled Keeyask Reservoir Lifecycle GHG Emission Intensity to Other Northern Reservoirs

Another source of uncertainty with the selected pre-flood emission factors is they are not site-specific to the Keeyask reservoir footprint. There is uncertainty related to how well do these factors represent the site-specific conditions at Keeyask. The CH_4 emission factors were derived from the Boreal–Arctic Wetland and Lake Methane Dataset (Kuhn et al., 2021) for the pre-flood peatlands and forests. This dataset did not include winter fluxes. Winter fluxes were estimated as being 16% of the total annual emissions according to the findings of a synthesis of non-growing season methane emissions from boreal and tundra wetlands and uplands (Treat et al., 2018). Although this approach for estimating winter CH_4 emissions has been used by other researchers studying Canadian peatlands

(Webster et al., 2018), it introduces a source of uncertainty for describing pre-flood emissions within the Keeyask reservoir footprint. CO_2 emission factors were selected from an extensive international study of the boreal and tundra landscape (Virkkala et al., 2021). CO_2 emissions were compiled into broad categories of Boreal Upland and Boreal Wetland. Although these categories aligned well with the G-res pre-flood landcover classes of Forest, Grassland/Shrubland, and Wetland, the G-res pre-flood emission estimates may have benefitted from a more detailed classification.

6.1.1.7 Size of Littoral Zone

The littoral zone comprises approximately 20% of the Keeyask reservoir following the impoundment and is predicted to expand to approximately 26% thirty years after flooding due to shoreline erosion (W. DeWit personal communication, July 5, 2023). To be conservative, the value of 26% was used to model Keeyask lifecycle GHG emissions.

A sensitivity analysis was conducted by running the G-res model for littoral zone values of 20% (initial flooding); 26% (reservoir expansion after 30 years), and 30%. When the extent of the littoral zone was reduced from 26% to 20%, total net lifecycle emissions were reduced by 9.3% (Table 6-3). A 4% increase in the extent of the littoral zone from 26% to 30% resulted in a 6% increase in net lifecycle GHG emissions.

A decrease in the size of the littoral zone from 26% to 20% resulted in Emission Intensity dropping 9.1% from 2.2 to 2.0 gCO_2e/kWh (Table 6-3). An increase in the size of the littoral zone from 26% to 30% increased Emission Intensity by 9.1% from 2.2 to 2.4 gCO_2e/kWh. This is rated as a low impact, given that median GHG life cycle emission factors for what some studies have considered as renewable electricity generation

technologies range from 8 to 52 gCO_2e/kWh (National Renewable Energy Laboratory, 2021).

The probability of over or underestimating the extent of the Keeyask littoral zone is rated as being low, because the size of the Keeyask littoral zone is based on site-specific measurements and modelling (Hydropower Limited Partnership, 2012a; W. DeWit personal communication, July 5, 2023).

The uncertainty associated with estimating the extent of the littoral zone for the post-flood Keeyask reservoir is rated as having a low impact.

Table 6-3 Keeyask Reservoir GHG Uncertainty Assessment: Littoral Zone Scenarios

Estimated Net Lifecycle GHG Emissions from the Keeyask Hydroelectric Reservoir Modelling Using the G-res Tool Littoral Zone Scenarios

	Keeyask Model			Littoral Zone Scenarios					
		95%			95%			95%	
	Model	Confidence Interval		Scenario	Confidence Interval		Scenario	Confidence Interval	
Extent of Littoral Zone	**26%**			**20%**			**30%**		
Net Emissions per m^2 of Reservoir									
$gCO_2e/m^2/yr$	86	75	98	78	68	89	91	79	104
Percent Change Compared to Keeyask Model				-9.3%			5.8%		
Total Lifetime Net Reservoir Emissions									
tCO_2e	861,990	749,988	987,936	781,827	680,712	895,568	913,452	7,972	10,452
Percent Change Compared to Keeyask Model				-9.3%			6.0%		
Emission Intensity									
gCO_2e/kWh	2.2	2	3	2.0	2	2	2.4	2	3
Percent Change Compared to Keeyask Model				-9.1%			9.1%		

6.1.1.8 Concentration of Total Phosphorous

G-res uses the mean concentration of Total Phosphorous as one of the model inputs to estimate post-flood reservoir CO_2 diffusive emissions (Prairie et al., 2017).

The Total Phosphorus concentration of 58.0 µg/L was used in the Keeyask G-res Model, as this was the benchmark value established by the Keeyask Generation Project Aquatic Environmental Monitoring Plan (Dowd and Hrenchuck, 2024). Measured post-flood Total Phosphorus concentrations ranged from 28.5 to 158 µg/L during the seasonal sampling events conducted from 2021 to 2023 (Hrenchuk 2021, 2022; Dowd and Hrenchuck, 2023, 2024).

A sensitivity analysis was conducted by running the G-res model for Total Phosphorus concentrations of 28.5 µg/L (minimum monitored value), 58 µg/L (benchmark), and 158 µg/L (maximum monitored value). A reduction in the concentration of Total Phosphorous from 58 µg/L (benchmark) to 28.5 µg/L (minimum) resulted in a 7.7% decrease in total net reservoir lifecycle emissions (t/CO_2e) (Table 6-4). An increase in phosphorous concentrations from 58 µg/L (benchmark) to 158 µg/L (maximum) resulted in a 13.0% increase in total net lifecycle GHG emissions (Table 6-4).

A decrease in phosphorous concentrations from 58 to 28.5 µg/L resulted in Emission Intensity dropping 9.1% from 2.2 to 2.0 gCO_2e/kWh. An increase in phosphorous concentrations from 58 to 158 µg/L resulted in Emission Intensity increasing 13.6% from 2.2 to 2.5 gCO_2e/kWh.

The G-res formula for calculating CO_2 diffusive emissions uses a positive correlation between Total Phosphorous concentrations and CO_2 diffusive emissions (Prairie et al., 2017), as phosphorous is a nutrient that can stimulate microbial decomposition of organic material (Smith and Prairie, 2004) and generate GHG emissions. The relationship between phosphorus concentrations and microbial decomposition is

complex and can be influenced by many water quality parameters (such as pH, nitrogen, ammonium, etc.), the quality and quantity of organic material, and the abundance and composition of the microbial community (Rantakari and Kortelainen, 2008; Straková et al., 2011; Räsänen et al., 2014; Bottino et al., 2015). Since Total Phosphorous concentrations were relatively high in the lower Nelson River/Keeyask reservoir prior to and after flooding (Keeyask Hydropower Limited Partnership, 2012c; Manitoba Hydro, 2024), Total Phosphorous may not impact CO_2 emissions to the same degree as in reservoirs where phosphorous availability is a limiting factor. The Keeyask reservoir appears to be limited more so by light availability than by phosphorus (Gedig et al., 2025). G-res would benefit from reviewing how well the CO_2 diffuse emission formula applies to the water quality and environmental characteristics of the Keeyask reservoir.

The uncertainty associated with Total Phosphorous concentrations is rated as being **Low**. This is due to two factors. One, the annual average concentrations measured from 2021-2023, which ranged from 51.8 to 56.8 µg/L (Hrenchuk 2021, 2022; Dowd and Hrenchuck 2024, 2023) are similar to the Benchmark value of 58 µg/L that was used in the G-res model. Second, the impact of substituting the minimum measured Total Phosphorous concentration of 28.5 µg/L or the maximum measured concentration of 158 µg/L impacted the modelled Keeyask GHG Emission Intensity by only 0.5 gCO_2e/kWh (i.e. range of 2.0 to 2.5 gCO_2e/kWh).

Table 6-4 Keeyask Reservoir GHG Uncertainty Assessment Total Phosphorous Scenarios

Estimated Net Lifecycle GHG Emissions from the Keeyask Hydroelectric Reservoir
Modelling Using the G-res Tool
Total Phosphorous Scenarios

	Keeyask Model			Total Phosphorous					
		95%			95%			95%	
	Model	Confidence Interval		Scenario	Confidence Interval		Scenario	Confidence Interval	
Concentration of Total Phosphorous (µg/L)	**58**			**28.5**			**158**		
Net Emissions per m^2 of Reservoir									
$gCO_2e/m^2/yr$	86	75	98	79	69	90	97	85	110
Percent Change Compared to Keeyask Model				-8.1%			12.8%		
Total Lifetime Net Reservoir Emissions									
tCO_2e	861,990	749,988	987,936	795,369	695,772	907,616	973,833	854,404	1,108,416
Percent Change Compared to Keeyask Model				-7.7%			13.0%		
Emission Intensity									
gCO_2e/kWh	2.2	2	3	2.0	2	2	2.5	2	3
Percent Change Compared to Keeyask Model				-9.1%			13.6%		

6.1.1.9 Length of Water Residence Time

The Water Residence Time refers to the amount of time a molecule of water spends in the reservoir. Longer water residence times allows more time for dissolved organic material to decompose within the reservoir (Vachon et al., 2017). G-res uses Water Residence Time to calculate CH_4 degassing emissions (Prairie et al., 2017).

Water Residence Time is a user-defined input. The Water Residence Time for the main channel of the Keeyask Reservoir is estimated to vary from 15 to 30 hours; 0.0017 to 0.0034 years (Keeyask Hydropower Limited Partnership, 2012b). The Water Residence Time for backbays may be up to 30 days; 0.082 years (Keeyask Hydropower Limited Partnership, 2012b) or possibly longer (personal communication W. DeWit, P.Eng. Manitoba Hydro May 1, 2020). Water residence time in backbay environments can be very challenging to estimate as it is influenced by water inflows from creeks, wind driven currents and other factors. The upper boundary of 0.0034 for the main channel was used

for the Keeyask reservoir G-res Model. For comparison, the G-res Tool was also run using the Water Residence Time value of 0.082 years (the estimated water residence time for backbays). Total Net Lifecycle GHG emissions were estimated to increase by 58.5% from 861,990 to 1,366,083 tCO_2e (Table 6-5) by increasing Water Residence Time. The driving force for this was a 212.3% increase in CH_4 emissions, resulting from a modelled rise in Degassing Emissions. Lifecycle Emission Intensity rose from 2.2 to 3.5 gCO_2e/kWh.

This scenario has demonstrated that Water Residence Time has a significant impact on G-res CH_4 degassing emission results and is a source of uncertainty for the Keeyask G-res model. The Keeyask G-res model would benefit from conducting sampling in the Keeyask forebay and nearby littoral zones to confirm how much influence the forebay littoral zones are having on GHG concentrations in water flowing through the Powerhouse and on degassing emissions.

For comparison, the G-res Tool was also run using the Water Residence Time value of 0.0017 years (the lower boundary of estimated water residence time for the main channel). Total Net Lifecycle GHG Emission estimates declined by 3.4% and Lifecycle GHG Emission Intensity declined from 2.2 to 2.1 gCO_2e/kWh (Table 6-6).

The uncertainty associated with Water Residence Time is rated as being **Moderate.** This is since the contribution of dissolved CH_4 and CO_2 from the littoral zones, where water residence times may be higher, is unknown.

Table 6-5 Keeyask Reservoir GHG Uncertainty Assessment:
Water Residence Time Scenarios

Estimated Net Lifecycle GHG Emissions from the Keeyask Hydroelectric Reservoir
Modelling Using the G-res Tool
Water Residence Time

	Keeyask Model			Water Residence Time		
	Model	95% Confidence Intervals		Scenario	95% Confidence Intervals	
Water Residence Time (Years)	**0.0034**			**0.082**		
Net Emissions per m^2 of Reservoir						
$gCO_2e/m^2/yr$	86	75	98	136	119	155
Percent Change Compared to Keeyask Model				58.1%		
Total Lifetime Net Reservoir Emissions						
tCO_2e	861,990	749,988	987,936	1,366,083	1,197,772	1,556,200
Percent Change Compared to Keeyask Model				58.5%		
Emission Intensity						
gCO_2e/kWh	2.2	2.0	3.0	3.5	3	4
Percent Change Compared to Keeyask Model				59.1%		

Table 6-6 Keeyask Reservoir GHG Uncertainty Assessment:
Water Residence Time Scenarios

Estimated Net Lifecycle GHG Emissions from the Keeyask Hydroelectric Reservoir
Modelling Using the G-res Tool
Water Residence Time

	Keeyask Model			Water Residence Time		
	Model	95% Confidence Intervals		Scenario	95% Confidence Intervals	
Water Residence Time (Years)	**0.0034**			**0.0017**		
Net Emissions per m^2 of Reservoir						
$gCO_2e/m^2/yr$	86	75	98	83	73	95
Percent Change Compared to Keeyask Model				-3.5%		
Total Lifetime Net Reservoir Emissions						
tCO_2e	861,990	749,988	987,936	832,289	727,900	949,784
Percent Change Compared to Keeyask Model				-3.4%		
Emission Intensity						
gCO_2e/kWh	2.2	2.0	3.0	2.1	2	2
Percent Change Compared to Keeyask Model				-4.5%		

6.2 Structural Uncertainty

Structural uncertainty is defined in this assessment as the uncertainty associated with the data that was used to develop the semi-empirical models that are the foundation of the G-res Tool.

There is a degree of uncertainty in applying G-res, or applying any model, to the Keeyask reservoir that was built from data derived from other reservoirs. The uncertainty lies in how well the measurements from other reservoirs represent the Keeyask reservoir? In other words, how well is G-res able to model Keeyask reservoir GHG lifecycle emissions if G-res has been calibrated with GHG measurements from reservoirs that may not be similar to Keeyask?

6.2.1 Pre-Flood Landcover: Peatlands and Re-surfacing Peat

A distinguishing characteristic of the Keeyask reservoir is that approximately 90% of the pre-flooded landscape was comprised of heterogeneous peatlands (ECOSTEM, 2011). This is an important attribute that should be considered when modelling Keeyask lifecycle emissions. Peatlands are complex wetland systems (Baird et al., 2009) and northern peatlands store a large amount of carbon (Amesbury et al., 2019; Gong et al., 2020; Hugelius et al., 2020). Peatland GHG emissions vary in time (i.e. diurnally, seasonally, and annually) and in space (i.e. from within the same peatland, amongst peatlands in the same physiographic region, and amongst peatlands in different physiographic regions (Strack 2008; Pelletier et al., 2007; 2011, 2014, 2015; Trudeau et al., 2013; Turetsky et al., 2014; Treat et al., 2021).

A potential source of uncertainty is that G-res may not have been calibrated with GHG emissions data that represents a similar pre-flood land cover as the Keeyask reservoir. The uncertainty with applying data from other reservoirs involves: 1) the areal extent of peatlands flooded; 2) the age of flooded peatland reservoirs when GHG measurements were conducted; 3) and presence of floating peat mats.

6.2.2 Assessment of Reservoirs in the G-res Database

The characteristics of the reservoirs in the G-res database were examined to assess how representative their pre-flood landcover is of the Keeyask reservoir. Data from 61 boreal reservoirs were used to calibrate G-res for modelling lifecycle GHG emissions from boreal reservoirs (Prairie et al., 2021b). Of these, 13 reservoirs were sampled within 20 years after their impoundment. The 20-year timeframe is of interest for this peatland

assessment as 20 years is the timeframe the IPCC (2019) considers the bulk of CO_2 emissions to occur from reservoir flooding. None of these 13 reservoirs flooded peatlands to the extent of the Keeyask reservoir. That is, none of these reservoirs had a pre-flood land cover of 90% peatlands. Amongst these reservoirs, the La Grande 3 and 4 reservoirs, Québec, and L. Skinnmuddselet reservoir in Sweden had the highest pre-flood peatland cover.

La Grande 3 and 4 reservoirs are located within the La Grande Rivière watershed where peatland distribution is close to 25% (Appendix 2). These reservoirs were sampled at 19 and 20 years after the impoundment (Prairie et al., 2021) and may not represent the early stages of the newly flooded Keeyask reservoir and its extensive peatlands. Approximately 29% of the landscape in the vicinity of the L. Skinnmuddselet reservoir in Sweden are peatlands, and the reservoir was sampled 12 years after flooding (Åberg et al., 2004b). There was little post-flood microbiological activity in the littoral zone of the L. Skinnmuddselet reservoir due to fluctuations in reservoir water levels and ice erosion (Åberg et al., 2004b). This is quite different than the Keeyask reservoir where the littoral zone includes flooded peatlands (Keeyask Hydropower Limited Partnership, 2012a) which have been shown to generate elevated CH_4 emissions (Kelly et al., 1997; Scott et al., 1999; St. Louis et al., 2000). For this reason, the L. Skinnmuddselet reservoir may not be fully representative of the young, peatland Keeyask reservoir.

Other young reservoirs that are included in the G-res database, such as Eastmain-1 and Romaine-2, Québec, have been studied extensively but their pre-flood landcover

comprised smaller portions of peatlands, approximately 14% and 3%, respectively (Hydro-Québec 2008; Pelletier et al., 2009).

Of the mature boreal reservoirs (sampled later than 20 years after flooding) included in the G-res database, Stephens Lake is the closest surrogate to the Keeyask reservoir for assessing flooded and re-surfaced peatlands. Stephens Lake is located immediately downstream of the Keeyask reservoir and is the reservoir for Manitoba Hydro's Kettle Generating Station. The landcover is similar to that of the Keeyask reservoir where approximately 90% is classified as wetlands (Keeyask Hydropower Limited Partnership, 2012b). However, the Stephens Lake data that is included in the G-res database pertains to dissolved concentrations of CO_2 and CH_4 in the forebay waters passing through the generating station and flowing downstream. The data is relevant for calculating diffusive fluxes from the reservoir forebay and degassing emissions as reservoir water passes through the generating station turbines and spillway. These data may not be representative of GHG emissions occurring upstream in Stephens Lake, nor in backbays, or from floating peat mats. Furthermore, the Stephens Lake data represents GHG concentrations associated with a mature reservoir, and not necessarily of a newly flooded reservoir such as Keeyask where peak emissions may occur in the initial years (first 7 to 10 years) following impoundment (Tremblay et al., 2005; Demarty and Tremblay, 2019).

From 2009 to 2014 spatial, point-in-time partial pressure measurements and direct diffusive flux measurements of CO_2 and CH_4 were collected within the Stephens Lake main channel and shallow backbays (Bastien et al., 2010; Marchand et al., 2015a). These data

are not included in the G-res database but could help to calibrate G-res for future modelling of the Keeyask reservoir.

The Lokka and Porttipahta reservoirs, located in Finland, are amongst the two largest reservoirs in Western Europe (Huttunen et al., 2002). The Lokka reservoir is approximately 417 km^2, and about 76% of the flooded land was comprised of peatlands (Huttunen et al., 2002; Maljanen et al., 2009). The Porttipahta reservoir is approximately 214 km^2 and about 45% of the footprint comprises peatlands (Huttunen et al., 2002; Maljanen et al., 2009). Sampling was conducted in the Lokka reservoir 26 and 27 years after impoundment and sampling occurred 25 years after Porttipahta was impounded (Huttunen et al., 2002). The water residence times are approximately 218 – 901 days for Lokka, and 62 - 559 days for Porttipahta (Huttunen et al., 2002). This would not seem to be a close match for the Keeyask reservoir, whose water residence times are approximately 15 – 30 hours for the main channel.

6.2.3 Littoral Zone

G-res defines the littoral zone as the area along the reservoir shoreline where water is less than 3 m deep (Prairie et al., 2017). The size of the littoral zone is used by G-res to estimate post-flood CH_4 diffusive emissions, and post-flood CH_4 bubble emissions (Prairie et al., 2017).

The littoral zone can be an important area of a reservoir for generating GHGs. Water flow can be slower through the shallow shorelines and backbays, providing more time for photosynthesis (carbon fixation/carbon production); microbial and photo degradation of carbon resulting in GHG production; accumulation of nutrients, which can facilitate

microbial degradation and primary production; and carbon burial within reservoir sediments (Wang et al., 2018; Prairie et al., 2018).

There are two aspects to how the uncertainty related to the littoral zone may affect the Keeyask G-res modelling results. One is the uncertainty associated with estimating the extent of the littoral zone for the post-flood Keeyask reservoir. This was discussed in Section 5.7.2.6 above. The second aspect relates to how well the reservoirs in the G-res database represent the Keeyask littoral zone.

6.2.3.1 Keeyask Reservoir Littoral Zone

The Keeyask reservoir littoral zone is predicted to expand from approximately 20% at impoundment to about 26% 30 years after flooding due to shoreline erosion (Keeyask Hydropower Limited Partnership, 2012a; W. DeWit personal communication July 5, 2023). The Keeyask reservoir littoral zones comprises floating peat mats, and emergent and submerged vegetation (Appendix 2).

6.2.3.2 Assessment of Reservoirs in the G-res Database

Similar to the assessment of the pre-flooded landcover, the characteristics of the reservoirs in the G-res database were examined to assess how representative their littoral zones are of the Keeyask reservoir.

The closest surrogate to the Keeyask reservoir for assessing the littoral zone is Stephens Lake. The size of the Stephens Lake littoral zone is estimated to be 27% of the reservoir (Prairie et al., 2021b) and the pre-flood peatland landscape is similar to that of the pre-flooded Keeyask reservoir (Keeyask Hydropower Limited Partnership, 2012b). As discussed in Section 2.2.3.3, G-res includes GHG monitoring data from Stephens Lake for

2004 to 2007 that was derived from continuous GHG monitors installed within the Kettle Generating Station (Demarty et al., 2009; Prairie et al., 2021a). These data may not be representative of emissions from the shallow Stephens Lake zones (Marchand et al., 2015a) nor the Keeyask littoral zones.

None of the other reservoirs in the G-res database closely resemble the Keeyask reservoir littoral zone in terms of areal extent, pre-flood landcover composition, reservoir configuration, and reservoir age. The following discussion highlights the reservoirs that compared the closest to the Keeyask reservoir. Appendix 2 describes the assessment in further detail.

The littoral zones of Laforge 1 and 2, Québec comprise approximately 26% and 27% respectively (Prairie et al., 2021b). Since peatlands cover a relatively smaller portion of the Laforge region (15%) than Keeyask (90%), GHG emissions occurring in the littoral zones of the Laforge and Keeyask reservoirs may not be directly comparable.

The littoral zone of the Eastmain-1 reservoir is estimated to be 16% of the total reservoir (Prairie et al., 2021). This is close to the extent of the Keeyask reservoir littoral zone at the time of initial flooding (20%), but less than the predicted 26% after 30 years of shoreline erosion. Brothers et al., (2012) studied respiration (CO_2 emissions) within the Eastmain-1 water column and sediments. Although they suspected respiration rates may be higher in the littoral zone, this was not quantified. Since the extent of peatlands underlying the Eastmain reservoir is less than that of Keeyask, and since the percentage of the reservoir that is littoral zone is smaller than that of Keeyask, it is uncertain as to how well the Eastmain-1 data represents the Keeyask reservoir.

Although nearly one third (29%) of the pre-flood footprint of the L. Skinnmuddselet reservoir, Sweden, was comprised of peatlands, there was little post-flood microbiological activity in the littoral zone due to fluctuations in reservoir water levels and ice erosion (Åberg et al., 2004b). This is quite different than Keeyask reservoir where reservoir levels are kept within one meter (Manitoba Conservation and Water Stewardship, 2014). GHG measurements from the L. Skinnmuddselet reservoir, which were collected 12 years after the reservoir was impounded, do not appear to be an ideal surrogate for modelling GHG emissions from the Keeyask littoral zone.

6.3 Uncertainty Analysis: Conclusions

The conclusions of the Uncertainty Analysis and the potential risks to Manitoba Hydro are summarized in Table 6-7 below.

6.3.1 Data Uncertainty Analysis

The largest uncertainty regarding data inputs to the G-res Model involves quantifying the pre-flood GHG emissions. The uncertainty lies with classifying the pre-flood landcover and selecting appropriate published GHG emission factors. As highlighted in Table 6-7, uncertainty can amount to over 200% for the Keeyask G-res Model.

Modelling pre-flood emissions can be difficult, such as for the Keeyask reservoir where most of the pre-flood land was a heterogeneous peatland (Keeyask Hydropower Limited Partnership, 2012a). Carbon cycling within peatlands can be complex and challenging to quantify GHG emissions (Pelletier et al., 2007, 2009, 2011, 2014; Trudeau et al., 2013, 2014; Turetsky et al., 2014; Lourenco et al., 2023; Treat et al., 2021, 2024). Furthermore, there is natural variability in terrestrial carbon cycling (e.g., forest fires and

forest succession, pest infestations, etc.), coupled with the impact of climate change (e.g., warming, drought, permafrost melt, increased nutrient loading, longer ice-free season, etc.) (Baldocchi et al., 2016; Keenan & Williams, 2018; Bastviken and Johnson, 2025; Virkkala et al., 2025) that complicates developing an emissions baseline.

Modelling uncertainty can be reduced by conducting in-situ measurements of the unflooded land adjacent to the Keeyask reservoir and using this information to develop site-specific pre-flood emission factors. This is similar to the "buffer method" described by G-res (Prairie et al., 2017).

It would be worthwhile to develop a "living" GHG baseline for these complex landscapes, that would reflect ongoing emissions as if the reservoir did not exist.

6.3.2 Structural Uncertainty

None of the reservoirs in the G-res database closely represent the Keeyask reservoir in terms of type of flooded landcover, re-surfacing peat, size of littoral zone, reservoir configuration, and age. The uncertainty is associated with how well are the G-res formulas able to model Keeyask reservoir emissions if G-res has not been calibrated with reservoirs like Keeyask.

Table 6-7 Keeyask Reservoir GHG Uncertainty Assessment: Risk Analysis

Keeyask Reservoir Lifecycle GHG Model Uncertainty Analysis

Assessment Parameters	Impact on G-Res Keeyask Model	Recommendations / Mitigation
Pre-Flood Landcover Classification	**High** Selection of pre-flood landcover class and GHG emission factors can result in the Keeyask reservoir being modelled as a Net source or sink. Individual scenarios range from a decrease of 218% to an increase of 85% in Net lifecycle emissions. The average for each Scenario category ranges from a decrease of 0.1% to 10% in Net lifecycle emissions.	**Recommendation** Measure unflooded reservoir buffer to develop site-specific pre-flood GHG emission factors
Pre-Flood Emission Factor Selection	**High** Pre-flood emission factors are highly variable. Selection of median, mean, high or low can impact results by 150% or more	**Recommendation** Measure unflooded reservoir buffer to develop site-specific pre-flood GHG emission factors to minimize uncertainty
Littoral Zone Size	**Low** The impact to Net lifecycle GHG emissions is 10% or less when the size of the littoral zone varies from 20% to 26% to 30%	**Recommendation** Confirm with MH if the estimated size of the Keeyask reservoir littoral zone has changed, and revise the G-res model input if appropriate
Phosphorous Concentration	**Low** The impact to Net lifecycle GHG emissions is 15% or less when phosphorous concentrations range from measured high, to Keeyask Target, to measured low	**Recommendation** Review Keeyask monitoring results and update the phosphorous value used in the Keeyask G-res model if appropriate
Water Residence Time	**Moderate** The impact to Net lifecycle GHG emissions reaches approximately 60% when water residence time range from the main channel to backbay values	**Recommendation** Conduct additional water sampling/GHG monitoring in the forebay and nearby littoral zones.
Representation of G-res Database	**Unknown** It appears that none of the reservoir data currently in the G-res database closely represents the Keeyask reservoir in terms of type of pre-flood landcover, re-surfacing peat mats, extent and composition of littoral zone, reservoir configuration, and age	**Recommendation** Continue to measure Keeyask reservoir GHG post-flood emissions Share Keeyask / MH reservoir data with the GHG-CaRe Project to calibrate G-res with Keeyask, Manitoba and Canadian reservoir data

Rating	
High	Variable impacts G-res results by more than 100%
Moderate	Variable impacts G-res results by 25% to 100%
Low	Variable impacts G-res results by less than 25%

7 GHG Implications of Hydroelectric Reservoirs on the Lower Nelson River in Terms of Climate Change and Energy Policy

7.1 The Evolving Energy Landscape: Background for Hydroelectric Reservoir GHG Quantification

The hydroelectric industry is facing a rapidly evolving "energy landscape". In broad terms, the energy landscape refers to an energy transition away from use of carbon-emitting fuels to non-carbon-emitting fuels (National Energy Board, 2019). It involves changes to how energy is generated, stored, used and traded (United Nations Development Programme, 2025). Four drivers are underpinning the energy transition (Asif, 2022). *Decarbonization*, shifting to low carbon forms of energy generation (Asif, 2022), *Digitization*, using digital technologies to connect energy systems to make them more intelligent, efficient, reliable and sustainable (IEA, 2017), *Decentralization*, decentralizing ownership and distribution of energy sources, such as using roof top solar voltaics, battery storage, etc. (Scott, 2022), and *Decreasing Energy Use*, through energy efficiency (Asif, 2022).

This section discusses emerging climate change science, climate change and energy policy, industry initiatives, investor requirements, and customer/market needs. These are the impetus for measuring, quantifying and projecting reservoir GHG emissions for informing the energy transition.

7.1.1 Climate Change Science

Intergovernmental Panel on Climate Change (IPCC) Fifth Assessment Report on Mitigation of Climate Change (IPCC, 2014b) was used as a scientific basis for the 2015 United Nations Framework Convention on Climate Change in Paris. This IPCC report concluded that the global average temperature increase should be limited to 2°C above pre-industrial levels and that a target of 1.5°C should be considered (IPCC, 2014b).

Subsequently, a revised outlook by the IPCC urged that the increase in global warming be limited to 1.5°C above pre-industrial times to limit climate change risk to natural and human systems (IPCC, 2018). The IPCC Synthesis of the Sixth Assessment Report (AR6) report estimates the anthropogenic induced rise in global surface temperatures from (1850 – 1900) to (2011 – 2020) is 1.1°C (IPCC, 2023). The IPCC concludes that if GHG emissions continue to increase or if GHG reductions are delayed or our ability to limit global warming to 1.5°C above pre-industrial times may be unachievable (IPCC, 2018). As announced by the UN Secretary-General António Guterres, the 1.5°C is still achievable but emission reductions are required from all countries, from all sectors of the economy, and on all timeframes (United Nations, 2023). This includes emissions reductions from land use change (IPCC, 2018). G20 members are called upon to reach carbon neutrality by 2050, and for developed countries to reach net zero electricity by 2035 (United Nations, 2023).

Global atmospheric concentrations in 2019 were reported as: CO_2 (410 ppm), CH_4 (1866 ppb) and N_2O (332 ppb) (IPCC, 2023). These concentrations represent an increase of CO_2 (47%), CH_4 (156%) and N_2O (23%) since 1750 (IPCC, 2023). The IPCC (2023)

concludes with high confidence that atmospheric CO_2 concentrations in 2019 were the highest they have been in the last 2 million years, and they conclude with very high confidence that CH_4 and N_2O 2091 concentrations were the highest they have been in the last 800,000 years.

The IPCC (2023) concluded that human activities are responsible for the 1.1°C rise in global surface temperatures during 2011-2020 as compared to pre-industrial times (1850-1900), primarily through the release of GHGs. Energy use, land use and land-use change are amongst the human activities cited as contributing to global climate change. There is an estimated 70% chance that the average annual global temperature will exceed 1.5°C during 2025-2029 (WMO, 2025).

Constraining the average annual global temperature increase to 1.5°C above pre-industrial times is a goal established by the 195 countries who signed the United Nations Framework Convention on Climate Change (UNFCCC) 2015 Paris Agreement, which includes Canada (UNFCCC, 2026b).

7.1.2 The Paris Agreement

The Paris Agreement was signed on December 12, 2015, in Paris at the United Nations Framework Convention on Climate Change (UNFCCC) Conference of the Parties (COP) 21 by 195 Parties, including Canada (UNFCCC, 2026b). The UNFCCC is an international treaty that was established in 1992 and came into force in 1994. Its goal is to stabilize atmospheric concentrations of GHGs to prevent harmful changes to the global climate system (UNFCCC, 1992). The Paris Agreement came into effect on November 4, 2016 (UNFCCC, 2026b). Article 2 of the Agreement commits the Parties to "*Holding the*

increase in the global average temperature to well below 2°C above pre-industrial levels and pursuing efforts to limit the temperature increase to 1.5°C above pre-industrial levels, …" (UNFCCC, 2015, Article 2.1 (a) page 3). In addition, each Party to the Paris Agreement is required to submit a nationally determined contribution (NDC), which is the country's climate action plan (UNFCCC, 2015).

7.1.3 Conference of the Parties (COP) 30 – Belém, Brazil, November 2025

Data Integrity was prioritized for the first time at a United Nations Climate Conference, during COP 30, Belém, Brazil (United Nations, 2025). The Declaration on Data Information Integrity on Climate Change was launched by The Global Initiative for Information Integrity on Climate Change. The declaration promotes consistent, accurate, evidence-based information on climate change to enable accountability and foster public trust. Canada is a signatory to the Declaration (Environment and Climate Change Canada, 2025a).

7.1.4 Canada's Commitment

As a Party to the United Nations Framework Convention on Climate Change, Canada is required to prepare and submit a national inventory on its anthropogenic GHG sources and removals by April 15 of each year (Government of Canada, 2025a). The IPCC has been publishing guidance to assist countries develop their national inventories since the early 1990s. The IPCC 2019 Refinement to the 2006 IPCC Guidelines for National Greenhouse Gas Inventories provides methodologies to estimate GHG emissions from reservoirs used for hydroelectric energy production (IPCC, 2019). Environment and Climate Change Canada (2025b) is endeavouring to refine their quantification

methodology and annual inventory of hydroelectric reservoir GHG emissions and is collaborating with research scientists and the Canadian hydropower industry. This is an opportunity to advance and apply reservoir GHG science and inform Canadian GHG inventories and possibly inform emerging climate change and energy policy.

Canada ratified the Paris Agreement by a vote in Parliament on October 5th 2016 and submitted their first NDC to the UNFCCC that same year (Government of Canada, 2016). The NDC required Canada to reduce GHG emissions to 30% below 2005 levels by 2030 (Government of Canada, 2017). In accordance with the Paris Agreement to upgrade the NDC every 5 years with a more ambitious GHG reduction target, Canada enhanced its NDC in February 2025, compelling the nation to reduce its GHG emissions up to half below 2005 levels by 2035 (Government of Canada, 2025b).

The Government of Canada has committed to achieve a national target of net-zero GHG emissions by 2050 through the passing of the Canadian Net-Zero Emissions Accountability Act (S.C. 2021, c. 22) on June 29, 2021. The GHG reduction target for 2030 has been set as described above, to reduce GHG emissions by 40% below 2005 levels by 2030. The Act also requires milestone targets to be set as follows, using the best available science and Indigenous knowledge:

- Target year 2035, by December 1, 2024
- Target year 2040, by December 1, 2029
- Target year 2045, by December 1, 2034

Credible, science-based emission reduction plans must also be prepared for each of these targets, within 5 years of the target start date. The emission reduction plans are to include GHG inventories and projections of annual GHG reductions for the economic sectors that Canada reports to the United Nations Framework Convention on Climate Change (Minister of Justice, 2021). It would be a very progressive milestone if the Canadian hydropower industry helped develop a sound scientifically defensible framework for preparing annual reservoir GHG emission inventories and reservoir GHG projections to inform Canada's 5-year emission reduction targets and emission reduction plans.

On December 12, 2024, the Government of Canada released its 2035 Emissions Reduction Plan pursuant to the Canadian Net-Zero Emissions Accountability Act (S.C. 2021, c. 22). The Plan outlines how Canada intends to achieve its target to reduce GHG emissions by 45-50% below 2005 levels by 2035 and net-zero emissions by 2050.

In May 2026 Canada released its National Strategy for an Electrified Canadian Economy Clean Electricity Strategy (Natural Resources Canada, 2026). The strategy states that Canada has one of the "cleanest" electricity grids in the world. Canada's electricity supply will have to double by 2050 to foster Canada's economic competitiveness and address climate change. This will require an investment of more than $1 trillion over the next 25 years (Natural Resources Canada, 2026).

Canada finalized the Clean Electricity Regulations (SOR/2024-263) in December 2024 as part of their strategy to achieve a net-zero emissions economy by 2050 and to provide affordable and reliable electricity (Minister of Justice, 2025). The CER limits CO_2 emissions from "units" (e.g. power plants) that use fossil fuels to generate electricity, starting in

2035. From 2035 to 2050, such generating units will be limited to an emission intensity cap of 65 tCO_2/GWh per calendar year. They may be allowed to emit up to an additional 35 tCO_2/GWh per calendar year provided these emissions are offset though Canadian credits. After 2050, these units must emit 0 tCO_2/GWh in a calendar year, but they may be allowed to emit up to 42 tCO_2/GWh per calendar year through Canadian offset credits.

In July 2022, Canada finalized the Clean Fuel Regulations (CFR) (SOR/2022-140). The CFR requires primary producers and importers of liquid fossil fuels to reduce the carbon intensity (CI) of those fuels to approximately 15% below 2016 levels by 2030, according to annual reduction targets. In 2023, the first year of implementation, the reduction requirement was 3.5 gCO_2e/MJ. In each subsequent year the reduction requirement is 1.5 gCO_2e/MJ until achieving a liquid fossil fuel intensity of 14 gCO_2e/MJ in 2030. The CFR adopts a lifecycle approach where CI reductions apply to fossil fuel extraction through processing, distribution and end use. CI reductions may be achieved through actions such as implementing carbon capture and storage or switching to low carbon forms of electricity in the liquid fuel lifecycle, blend/supply low CI fuels such as biofuels, or supply energy or fuel to electric vehicles or hydrogen powered vehicles.

Of direct relevance to this thesis and to the hydropower industry is how the CFR calculates CI. The CFR uses a Fuel Life Cycle Assessment (LCA) Model developed by the Government of Canada to calculate the CI for fuel and energy produced and used in Canada (ECCC, 2024). The LCA Model assigns a CI for each provincial electricity grid, which includes emissions from hydroelectric reservoirs (ECCC, 2024). Lifecycle reservoir GHG were adopted from a study of Quebec reservoirs conducted by Levasseur et al. (2021)

and do not consider reservoir GHG measurements or modelling from Manitoba reservoirs (ECCC, 2024). The CI assigned by the LCA Model to the Manitoba electricity grid is 7 gCO_2e/MJ (1.94 gCO_2e/KWh) (ECCC, 2025c).

It would be advantageous to the LCA Model, plus for those entities affected by the CFR, and to Manitoba Hydro if the LCA Model incorporated provincial data on hydroelectric reservoir GHG emissions and their CI, as opposed to relying on a study pertaining to a single jurisdiction. ECCC adopted the Levassuer et al, (2021) study as a proxy for the CI of all Canadian hydroelectric reservoirs. This is because hydroelectric reservoir CI information at a provincial level was not available at the time of developing the LCA Model. In Manitoba, a lifecycle CI had been modelled for proposed/new projects, such as the Keeyask Generation Project (Keeyask Hydropower Limited Partnership, 2012a) but the lifecycle CI has not been modelled for all hydroelectric reservoirs in Manitoba.

The LCA Model incorporates lifecycle reservoir GHG emissions into its CI calculation for the electricity grid. This approach blends reservoir GHG emissions from the past with emissions from the present and future. Since observations from northern reservoirs have shown that GHG emissions tend to be highest in the first few years after flooding and then decline or stabilize (Tremblay et al., 2005; Demarty & Tremblay, 2019; IPCC, 2019), an estimate of lifecycle emissions may not be appropriate to reflect the CI of the current and future electricity grid. The modelled grid CI may be inappropriately biased towards past emissions. This could disadvantage a company that is fuel switching to electricity by not realizing full credit for the GHG emission savings. Plus, overestimating the CI of the electricity grid could lead to inappropriate investment and energy policy decisions.

The Impact Assessment Act (IAA) came into force in August 2019 (S.C. 2019, c. 28, s. 1). The Strategic Assessment of Climate Change component of the IAA was added in July 2020 and revised in October 2020 (Environment and Climate Change Canada, 2020). This component requires an assessment to determine if a designated project hinders or supports Canada's ability to meet its Paris Agreement commitments and Canada's goal to achieve net-zero emissions by 2050. Project proponents are required to provide a credible plan that describes how the project will achieve net-zero emissions by 2050. They must describe methodologies, models, data, emission factors and assumptions used to estimate net GHG emissions. The development, operation and decommissioning of a new hydroelectric generating facility (including reservoir) whose production capacity is 200 MW or greater would be classified as a "Designated Project" under the Physical Activities Regulations (SOR/2019-285) of the IAA. Possible future hydroelectric development on the lower Nelson River, such as the potential Conawapa Generating Station, whose generating capacity could be 1,485 MW, would be subject to the IAA and would require a climate change/GHG assessment.

7.1.4.1 Canadian Competition Act R.S.C., 1985 c. C-34.

Amendments were made to the Canadian Competition Act R.S.C., 1985, c. C-34 on June 20, 2024 when Bill C-59, the Fall Economic Statement Implementation Act, 2023 received Royal Assent (Statutes of Canada, 2024). Revisions to the Canadian Competition Act intend to safeguard against businesses making environmental claims that are false, misleading or not adequately tested or substantiated. Subsequently, Bill C-15 Budget

2025 Implementation Act, No.1 was introduced in the House of Commons on November 18, 2025 and received Royal Assent on March 26, 2026 (House of Commons of Canada, 2025; Statutes of Canada, 2026). Division 43 of Part 5 of the Bill amends the Competition Act to remove the requirement that environmental claims made by a business must be substantiated according to internationally recognized methods, since "internationally recognized methods" are not defined in the Canadian Competition Act. The implications for the Canadian hydropower industry are that their statements about their GHG emissions and carbon footprint must be based on adequate and proper substantiation. The burden of proof lies with those making the environmental statements.

7.1.5 Manitoba

In September 2024, Manitoba's Affordable Energy Plan was released (Manitoba, 2024). Although the plan did not proclaim any GHG emission reduction targets, it presented a "vision" to build the next generation of clean energy to achieve net-zero targets by 2050. It portrayed Manitoba as having a "clean", low-carbon electricity system. The Province of Manitoba endeavours to achieve a net-zero electricity grid by 2035 and a carbon neutral economy by 2050 (Government of Manitoba, 2025).

7.1.6 GHG Accounting and Reporting

7.1.6.1 GHG Protocol

The Greenhouse Gas (GHG) Protocol is an endevour to develop internationally accepted GHG accounting and reporting standards for the public and private sectors (https://ghgprotocol.org).

The initiative was launched in 1998 through a partnership between the World Resources Institute and the World Business Council for Sustainable Development, and in collaboration with multiple stakeholders involving businesses, nongovernmental organizations, governments, and others (World Resources Institute & World Business Council for Sustainable Development, 2014).

The GHG Protocol initiative has developed a Corporate Standard (GHG Protocol Corporate Standard) to guide businesses, government and non-government organizations on how to account for and report GHG emissions (World Resources Institute & World Business Council for Sustainable Development, 2014). The standard is intended to ensure that GHG reporting represents "a faithful, true, and fair account of a company's GHG emissions" (page 6, World Resources Institute & World Business Council for Sustainable Development, 2014). The Corporate Standard is written from the perspective of a corporation preparing their GHG inventory and it is designed to be compatible with other GHG quantification and reporting initiatives such as those produced by Intergovernmental Panel on Climate Change (IPCC), national GHG reporting, and industry sector-specific reporting protocols (World Resources Institute & World Business Council for Sustainable Development, 2014).

The GHG Protocol continues to evolve and expand, developing GHG accounting guidance for specific industries and for the public sector (https://ghgprotocol.org/guidance-0).

Of relevance to this thesis is that the GHG Protocol provides guidance on how to account for GHG emissions from the production, transmission, purchase, and consumption of electricity (World Resources Institute & World Business Council for Sustainable Development , 2014, 2015, 2023). Furthermore, the GHG Protocol has developed guidance for companies on how to account for and report GHG emissions related to land use change, including GHG emissions from hydroelectric reservoirs (World Resources Institute & World Business Council for Sustainable Development, 2022a,2022b; 2024; 2025c; 2026). Draft guidance was released for review and pilot testing in September 2022, and the standard was released in January 2026.

The GHG Protocol Corporate Standard describes three categories of GHG emissions a company is to report (World Resources Institute & World Business Council for Sustainable Development, 2014, 2015, 2023, 2026). They include Scope 1, 2 and 3 emission categories.

7.1.6.1.1 Scope 1 Direct Emissions

Direct Emissions are emissions the company owns or controls and is a direct result of the company's activities. The Corporate Standard explicitly explains that companies that produce electricity from fossil fuels using stationary sources such as boilers and turbines, are to quantify and report these GHG emissions. As of June 30, 2026, hydroelectric companies are to report reservoir GHG emissions as Scope 1.

7.1.6.1.2 Scope 2 Indirect Emissions

Scope 2 emissions are defined as being the consequence of the reporting company, but the emissions occur at a source that is owned or controlled by another company. To illustrate, a company that consumes electricity that is purchased from another entity must report the GHG emissions associated with the electricity generation and transmission. In other words, to be in compliance with this Standard, an industrial or commercial customer of Manitoba Hydro would have to report the GHG emissions associated with the electricity purchased from Manitoba Hydro.

The Standard explains how to calculate the GHG emissions associated with the electricity purchased and used, as follows:

Activity Factor (Amount of Energy Used) e.g. MWhrs of Electricity	X	**Emission Factor** (GHG emissions per unit of energy) e.g. $gCO_2eq \cdot kWh$	(7.1)

The "Emission Factor" is to be derived from the energy/electricity supplier (e.g. Manitoba Hydro) or adopted from regional or national values. It is incumbent upon and advantageous for the energy supplier to know and provide their company-specific Emission Factors to accurately represent the GHG footprint of their product. This is especially important if a company such as Manitoba Hydro is trying to present their electricity as a low carbon source of energy and part of the climate change solution. Presently, Manitoba Hydro does not have emission factors for the Manitoba electricity grid. As discussed above, the Government of Canada LCA Model has developed a carbon

intensity factor for the Manitoba grid, but this value has not considered measurements nor models of Manitoba reservoirs. There is an opportunity to use site-specific information to improve the estimates of the Manitoba grid GHG intensity values.

The GHG Protocol has launched a public consultation, ending January 31, 2026, to review and update the Scope 2 Standard (World Resources Institute & World Business Council for Sustainable Development, 2025a). The goal is to ensure Scope 2 GHG inventories provide useful information for decision-making, and to deliver comparable reporting data that can be used for setting GHG targets and be used by regulatory authorities and investors.

7.1.6.1.3 Scope 3 Corporate Value Chain

Scope 3 emissions include all other indirect emissions that occur in a company's value chain (World Resources Institute & World Business Council for Sustainable Development , 2013).

7.1.6.1.4 Land Sector and Removals

Since 2020 the WRI and WBCSD have been developing guidance under the GHG Protocol on how to account for Corporate GHG emissions and removals from the land sector (World Resources Institute & World Business Council for Sustainable Development, 2024). The Land Sector and Removals (LSR) Standard was released on January 30, 2026 and will go into effect on January 1, 2027 (World Resources Institute & World Business Council for Sustainable Development, 2026).

Underpinning this initiative are results from a World Resources Institute & World Business Council for Sustainable Development survey conducted in 2019 where over 400 responses were received from businesses, governments, NGOs, and consultants representing more than 50 countries (World Resources Institute & World Business Council for Sustainable Development, 2024). Eighty-eight percent of respondents identified that accounting for GHGs related to land use change (which includes hydroelectric reservoirs) was important but only 16% of the respondents were accounting for these emissions (World Resources Institute & World Business Council for Sustainable Development, 2024). Lack of guidance and lack of data were the two predominant reasons, respectively, for not accounting for GHGs from land use change (World Resources Institute & World Business Council for Sustainable Development, 2024).

In September 2022 the World Resources Institute & World Business Council for Sustainable Development released the draft Greenhouse Gas Protocol Land Sector and Removals Guidance, which was open for review and pilot testing until Q1 2023 (World Resources Institute & World Business Council for Sustainable Development, 2022b and c; 2024). The Standard was released on Januray 30, 2026 (World Resources Institute & World Business Council for Sustainable Development, 2026).

The Standard recognizes that approximately 22% of global anthropogenic GHG emissions result from the agriculture, forestry, and other land use change (land sector sector) and that GHG reduction targets and GHG management strategies must be underpinned by sound GHG accounting and reporting methods (World Resources Institute & World Business Council for Sustainable Development, 2022a,2022b, 2024, 2026).

To be compliant under the Standard, the land sector would be required to account for GHG emissions and GHG removals from the atmosphere. This would compel hydroelectric companies that adhere to the GHG Protocol to account for GHG emissions resulting from creating and operating their reservoirs.

The Standard requires companies that own or control hydroelectric reservoirs to report reservoir CO_2 and CH_4 emissions as Scope 1 (World Resources Institute & World Business Council for Sustainable Development, 2026). Companies that purchase electricity generated by hydropower are required to report reservoir CO_2 and CH_4 emissions as Scope 3 Category 3 (World Resources Institute & World Business Council for Sustainable Development, 2026). CO_2 emissions should be accounted for the first 20 years after flooding and CH_4 emissions should be accounted for the first 100 years after flooding. The hierarchy of accounting methods are: 1) Conducting on-site emission measurements, using 5-10 years averages; 2) GHG modelling, such as using the G-res Tool; and 3) using IPCC GHG emission factors.

The Standard requires companies that purchase electricity from hydroelectric sources (e.g. land use change through use of reservoirs) report emissions as Scope 3 Category 3. The GHG Protocol plans to issue a Guidance document in the second quarter of 2026 to provide further information about implementing the Standard. A key issue is that international GHG accounting authorities are including reservoir emissions in GHG reporting standards. It is important for the hydropower industry to study their reservoir GHG emissions, to understand their current emission profile, participate in developing

GHG quantification methods, and to provide reliable GHG emission information to their customers.

7.1.6.1.5 Electricity-Sector Consequential Methods Public Consultation

The GHG Protocol has launched a public consultation on updated corporate standards and guidance (World Resources Institute & World Business Council for Sustainable Development, 2025a). The consultation includes an update to the Electricity-Sector Consequential Methods. These are accounting methods to estimate GHG emissions avoided because of changes to the electricity grid. For example, a new hydroelectric project, such as Conawapa may displace GHG emissions that would have occurred from the use of electricity generated by fossil fuels elsewhere on the electrical grid. Consultation closed on January 31, 2026.

7.1.6.1.6 GHG Protocol and ISO Harmonization

The International Organization for Standardization (ISO) and the GHG Protocol have collaborated to deliver harmonized, science-based international standards for GHG accounting by 2028 (World Resources Institute & World Business Council for Sustainable Development, 2025b). The framework is intended to foster credible GHG emission reporting, support carbon markets, and inform GHG regulations. It will apply to corporations, products and projects.

7.1.6.2 Science Based Targets initiative (SBTi)

The Science Based Targets initiative (SBTi) released the Corporate Net-Zero Standard in October 2021, with revisions in 2023 and 2024, and is currently undergoing a major revision (SBTi, 2024, 2025). The Net-Zero Standard is the world's first science-based

guidance for companies to set net-zero GHG emission reduction targets. The Net-Zero Standard is aligned with the IPCC goal of limiting the rise in global temperatures to 1.5°C above pre-industrial levels (Rogelj et al., 2018), and it complements the GHG Protocol Corporate Standard for accounting and reporting GHG emissions (World Resources Institute and World Business Council for Sustainable Development, 2014). The Science Based Targets initiative is a collaboration amongst CDP, the United Nations Global Compact, World Resources Institute, the World Wide Fund for Nature, and the We Mean Business Coalition (SBTi, 2025).

The Net-Zero Standard has four parts. They include setting near-term (5 – 10 year) and long-term (no later than 2050) science-based GHG emission reduction targets, neutralizing residual emissions after achieving long term targets, and take action in or invest in activities beyond the company's value chain (SBTi 2024). Net-Zero Science-Based Targets are defined as lowering Scope 1, 2 and 3 emissions to zero or to a residual amount that aligns with accomplishing net-zero emissions for the sector or at a global scale (SBTi 2024). Plus, neutralizing any residual emissions at the target year and beyond (SBTi 2024).

The draft revision is proposing enhanced target setting for Scope 3 emissions. This includes incentivizing companies to act on the most relevant sources of emissions in their value chain. This includes procuring from entities whose goods and services align with global net-zero goals. This could have implications for the hydropower industry. Customers could align their electricity purchases with those companies that have low GHG emissions or are perceived as working towards lowering their GHG emission profile.

The power sector is to reach long-term emission targets by 2040. Overall, the sector is to reduce GHG emissions by at least 90% compared to 2020 levels (SBTi 2024). Companies purchasing electricity are required to procure 80% from renewable electricity sources by 2025 and to procure 100% of their electricity from renewable electricity sources by 2030 and thereafter (SBTi 2024).

7.1.7 Market Place

7.1.7.1 Manitoba Electricity Demand Forecast

The Manitoba Hydro 2025 Integrated Resource Plan (IRP) is a development plan that recommends how to meet Manitoba's growing energy needs to 2035 (Manitoba Hydro, 2025c). The IRP is designed to enable Manitoba to meet its net-zero electricity goals by 2035, support the net-zero economy by 2050, and to align with Manitoba's Affordable Energy Plan.

The IRP recommends how an additional 1760 MW of energy capacity can be acquired over the next 10 years. The recommendation involves implementing Customer Solutions, such as reducing energy demand through energy efficiency initiatives, altering the timing of energy consumption to lessen peak demands, etc. (860 MW), installing additional natural gas/biomethane Combustion Turbines (750 MW), employing Wind Power (120 MW), upgrading existing Manitoba Hydro hydropower (25 MW), and commissioning short-term utility-scale battery storage (5 MW). The IRP is not proposing to develop new hydropower generating stations to meet the 2035 electricity demand.

The IRP proposes three scenarios for electricity demand in Manitoba to 2050. The Baseline scenario projects electricity demand will increase by about 1.5 times higher than

the current peak demand of approximately 5,000 MW (Manitoba Hydro, 2025d). The Medium scenario projects electricity demand will approximately double by 2050, and the High scenario projects electricity demand will nearly triple by 2050. For comparison, an independent study projects that Manitoba's electrical capacity would need to approximately double by 2050 (Hamlin & Zhang 2024). The 2025 IRP does not propose how electricity demand will be met beyond 2035.

7.1.7.2 MISO Market

Manitoba Hydro trades electricity with the USA through the Midcontinent Independent System Operator (MISO). MISO is an independent, not-for-profit, member-based organization (MISO, 2025). It manages the flow of high voltage electricity through 15 USA states and Manitoba, and is one of the world's largest energy markets.

7.1.7.2.1 Minnesota Clean Energy Bill

Minnesota passed a Bill on February 7, 2023 establishing a carbon-free electricity standard (Minnesota Commerce Department, 2023). The carbon-free standard requires all Minnesota electrical utilities to generate or procure 90% of their electricity from a carbon-free technology by 2035, and to reach 100% carbon-free electricity by 2040 (Minnesota Legislature, 2023).

The Bill defines "carbon-free" as electricity generated from a technology that does not emit carbon dioxide. Eligible energy technologies include hydroelectricity, with the following provisions. Hydro generating capacity is less than 100 megawatts, or capacity is 100 megawatts or greater provided the facility was in operation on the day the Bill came into force (Minnesota Legislature, 2023 Chapter 7--H.F.No. 7).

In February 2025, Bill HF75 was introduced to the Minnesota House Energy, Finance & Policy Committee, proposing to remove the 100-megawatt cap from the Minnesota Clean Energy law (Minnesota Legislature, 2025). The Bill remains under consideration. In March 2025, Bill HF787 was introduced to the Minnesota House Energy Committee, which proposes to remove the requirement for out-of-state energy to be carbon-free. The Bill was returned to the Committee in May 2025.

7.1.8 Synthesis of Evolving Energy Landscape

The above discussion provides a snapshot of the energy landscape. Global concentrations of GHGs and temperatures have reached record levels. The international science community is urging that global temperature increases be held to 1.5°C above pre-industrial times to limit climate change risk to natural and human systems. Canada and Manitoba have committed to achieving a net-zero economy by 2050, and that electrification is vital to attain this goal. Scholarly institutions are providing guidance on setting science-based GHG reduction targets and on GHG quantification and reporting standards for private and public entities. And electricity markets are setting carbon limits on the electricity generated, procured and distributed in their jurisdictions.

7.2 Implications of Hydroelectric Reservoirs on the Lower Nelson River

The energy landscape described above has implications for hydroelectric power generated from the lower Nelson River and for possible future hydropower development on the lower Nelson River. Modelling results indicate the current reservoir GHG emissions and carbon intensity associated with hydropower generated from the lower Nelson River are low and declining. The modelled carbon intensity of the lower Nelson River reservoirs

(including the CRD) is similar to that of electricity generated by solar, wind and other forms of electricity generation that is referred to as renewable energy. This applies to the current reservoir GHG emission rate and on a going forward basis (until the end of their modelled 100-year lifespan). GHG emissions and carbon intensity of potential future hydropower development on the lower Nelson River, such as the possible Conawapa Generating Station/Reservoir, are modelled to be low and align with emission intensity of renewable electricity generation. Manitoba hydropower, as of today and going forward, can help Manitoba and Canada achieve net-zero emission goals.

8 Conclusions

8.1 Canada-wide Collaboration

As demand for electricity in Manitoba and Canada is projected to increase over the next decade, Manitoba, Canada and the Canadian hydropower industry would benefit from a country-wide initiative to quantify Canadian hydroelectric reservoir GHG lifecycle emissions and emissions going forward. This could be accomplished through a collaboration amongst the Canadian scientific community, the Canadian hydropower industry, and government policymakers who are responsible for developing energy and climate change mitigation strategies and regulations.

Under this initiative, measurement and modelling methods should not be prescriptive but rather be designed to best suit the reservoirs and hydraulic systems under study, as each waterway is unique to some extent. Reservoir studies could be prioritized provincially and nationally, such as addressing the potentially largest GHG emitters first. Selection criteria could include parameters which can impact GHG emissions, such as reservoir size, amount and type of flooded land, reservoir age, reservoir configuration, cascading reservoirs, etc.

8.2 Emission Intensity

Emission intensity (e.g. tonnes CO_2e/Gwh) is a metric of paramount importance for assessing the GHG footprint of current and future hydroelectricity and for comparing hydroelectricity with other forms of energy generation. Estimates of reservoir GHG emission intensity must be clearly defined and their uncertainty explained so the

limitations of the estimate are understood. A statement of completeness could explain the method used to estimate net GHG emissions (e.g. modelling, measurements, etc.) and declare the GHG emission pathways (e.g. diffusion, ebullition, degassing, etc.) and GHG types (e.g. CO_2, CH_4, N_2O) included in the estimate. The statement could explain how power production was determined (e.g. power production over the last 5 years, 10 years, etc.) and how representative this value may be of future electricity production.

8.3 Reservoir Lifecycle Assessment and Going Forward

Reservoir 100-year lifecycle assessments are fundamental for understanding the lifetime magnitude, timing and composition of reservoir GHG emissions. For assessing current and going forward emissions and emission intensity of existing reservoirs, assessing the remaining life of the reservoir GHG emission profile is a valuable metric.

8.4 Living Baseline and On-Going Lifecycle GHG Model

A reservoir GHG lifecycle model would benefit from incorporating a “living” baseline to reflect ongoing emissions from the reservoir footprint as if the reservoir did not exist. The living baseline would simulate the impact of climate change (e.g., warming, drought, permafrost melt, increased nutrient loading, longer ice-free season, etc.) plus natural variability in what would have existed in the pre-flood terrestrial landcover and aquatic systems.

8.5 Pre-Flood Emissions

As demonstrated in the uncertainty assessment, the selection of GHG emission factors when modelling emissions from the pre-flood reservoir footprint can result in the reservoir being a net source or sink of GHG emissions. A lifecycle GHG model would

benefit from having pre-flood GHG emission factors developed from in-situ GHG measurements from within the reservoir footprint or from measurements of representative pre-flood landcover.

8.6 Conclusions About Keeyask G-res Reservoir GHG Modelling Results

- Keeyask reservoir lifecycle GHG emissions are modeled to be low on a square meter basis, and within an order of magnitude agreement with other northern Canadian hydroelectric reservoirs.
- Keeyask reservoir lifecycle GHG emission intensity (2.2 gCO_2e/kWh) is very low compared to other Canadian hydroelectric reservoirs modelled by G-res.
- Keeyask reservoir lifecycle GHG emission intensity (2.2 gCO_2e/kWh) is low compared to published lifecycle GHG intensities for other forms of electricity generation technology such as wind power, solar power, photovoltaic, hydrogen fuel cell, and others.
- The Keeyask G-res reservoir modelling results, including net GHG emissions and GHG emission intensity, align with the results of the Keeyask reservoir lifecycle GHG emissions presented in the Keeyask Environmental Impact Statement.
- Uncertainties with the Keeyask G-res Reservoir Lifecycle Model:
    - Representation of the pre-flood landscape GHG emission factors. There is uncertainty with the Keeyask pre-flood terrestrial GHG baseline as these estimates were derived from published literature sources. Expanding the reservoir GHG monitoring program to include a larger portion of the unflooded peatlands would better constrain pre-flood GHG emission factors. These results could be used as a surrogate for pre-flood GHG emissions.

- Representation of CH_4 production and shallow water emission pathway processes. There is uncertainty with the constant CH_4 bubble emission estimate of 4.5 $gCO_2e/m^2/yr$ for each year over the 100-year lifecycle of the reservoir. Researching CH_4 dynamics in the shallow water sediments of the Keeyask reservoir would help to refine the G-res statistical model for estimating CH_4 bubble emissions.
- Representation of degassing emission estimates in unstratified reservoirs. There is uncertainty with the constant CH_4 degassing emission estimate of 8.7 $gCO_2e/m^2/yr$ for each year over the 100-year lifecycle of the reservoir. Researching CH_4 and CO_2 degassing emissions in unstratified reservoirs would help to calibrate G-res.

8.7 Conclusions About Lower Nelson River G-res Reservoir Modelling Results

- Lower Nelson River lifecycle reservoir GHG emissions are modeled to be low on a square meter basis, and they are within an order of magnitude agreement with other northern Canadian hydroelectric reservoirs.
- The majority (95%) of total Net 100-year lifecycle reservoir emissions are modelled to occur from the CRD (80%) and the Kettle reservoir (15%), with the remaining 5% of emissions resulting from the Keeyask, Long Spruce and Limestone reservoirs. In 2025, approximately 98% of Net GHG emissions were modelled to be from the CRD (71%), the young Keeyask reservoir (16%) and the mature Kettle reservoir (11%). Even though the CRD is 50 years old, it is modelled to be the current dominant source of lower Nelson River reservoir net lifecycle GHG emissions.

- Modelled lifecycle reservoir GHG emissions and emission intensity associated with the lower Nelson River are low and declining. Electricity generated from lower Nelson River hydropower can help Manitoba and Canada achieve net-zero GHG emission goals.
- From today going forward, the remaining lifecycle GHG emission intensity for the lower Nelson River reservoirs, including the CRD, is modelled to be similar or lower than median values for electricity generated from ocean waves, nuclear, wind, solar, and biomass technologies.
- Modelled total lifecycle reservoir GHG emissions for the potential Conawapa reservoir are low (less than 400,000 tCO_2e), and modelled lifecycle GHG emission intensity is very low (less than 1 gCO_2e/kWh). These values are similar to those modelled for the Long Spruce reservoir. Under the modelled parameters, the Conawapa reservoir would be a low GHG emitting source of electricity generation and would help Manitoba and Canada achieve their net-zero emissions goals.
- Although the full lifecycle GHG assessment (which included emissions from construction, reservoirs and other land use change, operations and decommissioning) was conducted at a very high level with considerable uncertainty, GHG emissions from hydropower on the lower Nelson River (including the CRD) are modelled to be low today and going forward. They are modelled to be near the low range of what could be referred to as renewable sources of electricity generation (e.g. wind power, solar power, nuclear, biomass, etc.)
- It is beyond the capability of the G-res Tool to model the lower Nelson River reservoirs as a cascading hydraulic system and to determine the impact that one reservoir has on

another downstream. For this study, the reservoirs were modelled individually and the results were totaled. It would be helpful to conduct GHG emission/water quality measurements downstream of each of the lower Nelson River reservoirs to assess the influence on carbon cycling that these reservoirs may have on one another. This would help to advance reservoir GHG modelling on a system-wide basis and to refine reservoir GHG emission estimates for the Manitoba Hydro hydraulic system.

- This study was a first attempt to model lifecycle GHG emissions for the lower Nelson River reservoirs and for potential future hydroelectric development on the Nelson River. This model could be refined by conducting additional GHG measurements at the reservoirs and surrounding areas to improve the pre-flood emission estimates used in the model, and to compare modelling results to actual emissions. The largest sources of modelling uncertainty were with assigning GHG emission factors to the pre-flood landscape, and whether the G-res Tool was adequately calibrated for modelling peatland reservoirs such as those in northern Manitoba. This exercise would be especially helpful for improving the lifecycle models for the CRD, Keeyask and Kettle reservoirs. These flooded lands represent the largest current and future source of GHG emissions from the lower Nelson River reservoirs.
- The lower Nelson River reservoir GHG model could be used as a template for modelling the remaining reservoirs and flooded lands associated with Manitoba Hydro's hydraulic system to assess GHG emissions and GHG emission intensity for the entire Manitoba electrical grid.

8.8 Conclusions About the G-res Model

- The UNESCO/IHA GHG Reservoir (G-res) Tool, despite limitations, is currently the best available model for estimating 100-year lifecycle GHG emissions from the Keeyask and lower Nelson River reservoirs, and provides a common metric, against which to compare lifecycle emissions from these reservoirs against other reservoirs worldwide.
- G-res was designed as a screening tool. This should be considered when using the model, such as for GHG accounting or informing energy policy.
- G-res has limitations and uncertainty that must be understood when interpreting and presenting results.
    - G-res has not been calibrated with young boreal reservoirs that are similar to the Keeyask reservoir that have extensive peatland flooding, on-going peatland disintegration and re-surfacing peat. This leads to uncertainty when estimating Keeyask reservoir lifecycle GHG emissions.
    - G-res results have not been validated against actual GHG measurements from peatland reservoirs like the Keeyask reservoir.
    - G-res does not estimate downstream emissions beyond degassing at the generating station and spillway. This potential source of emissions results from dissolved and particulate organic matter being transported downstream. These emissions are challenging to model without sufficient monitoring data.
    - Degassing emissions are estimated for CH_4 only, and at a constant lifetime rate.

  - G-res estimates a constant lifetime rate for CH_4 bubble emissions. Since CH_4 bubble emissions are highly variable in space and time and can be significant, G-res would benefit from refining how this emission pathway is estimated.
  - G-res estimates CO_2 and CH_4 diffusive emissions according to functions that decline over the lifecycle of the reservoir. G-res cannot predict emission fluctuations over time nor increases in emissions in any year.
  - G-res modelling does not accommodate upstream changes in water/watershed carbon cycling that could impact reservoir GHG emissions.
  - G-res modelling does not accommodate changing GHG emission characteristics resulting from regional global warming associated with climate change.
- The G-res pre-flood landcover categories are general in nature, which is understandable for a model that is built to address reservoirs worldwide. G-res could benefit from including options to customize the landcover categories to describe site-specific conditions for individual reservoirs.
- The calibration of G-res for northern peatland reservoirs such as the Keeyask reservoir, could be improved by continuing to measure Keeyask reservoir GHG emissions and by sharing Keeyask reservoir GHG data with the G-res Expert Committee.
- G-res Mechanics
  - The G-res Tool is easy to access from the IHA website.
  - The G-res Tool user interface screens are straightforward.
  - The G-res Tool provides thorough documentation, including a User Guide, a Technical Document, and other reference materials.

- The G-res Expert Committee provides helpful and timely technical support.
- G-res would benefit if site-specific pre-flood landcover and aquatic classifications and associated GHG emission factors could be directly incorporated into G-res.

9 Recommendations

9.1 Canada-wide Reservoir GHG Lifecycle Initiatives

- Quantify Canadian hydroelectric reservoir GHG lifecycle emissions and emissions going forward through a collaboration amongst the Canadian scientific community, the Canadian hydropower industry, and government policymakers.
- Establish a protocol for estimating hydroelectric reservoir GHG emission intensity to facilitate comparison within and external to the electricity sector, and to measure progress towards net zero policy goals. Develop guidance for calculating emission intensity, for preparing a statement of completeness to explain how GHG emissions and power production were calculated, for declaring omissions and estimating uncertainty.

9.2 Keeyask Reservoir GHG Lifecycle Modelling

- The Keeyask G-res lifecycle GHG model would benefit from:
  - Measuring Keeyask reservoir GHG emissions and related environmental parameters to:
    - Validate G-res Tool modelling results through a comparison with actual in-situ GHG emission measurements.
    - Provide Keeyask in-situ measurement data to the G-res Tool developers to help refine the G-res Tool calibration for northern peatland reservoirs underlain by a carbonate substrate.

- Measure GHG emissions from the unflooded peatlands adjacent to the Keeyask reservoir as a proxy for developing site-specific pre-flood GHG emission factors to improve the Keeyask pre-flood GHG emissions baseline.
- Develop a “living baseline” to reflect ongoing emissions from the reservoir footprint as if the reservoir did not exist.
- Measure GHG emissions from floating peat/peat particulates and semi-submerged vegetation within the reservoir to improve the accuracy of modelling post-flood lifecycle emissions.
- Research CH_4 dynamics in the Keeyask reservoir littoral zones to understand the drivers of CH_4 bubble emissions and to assess potential improvements for modelling this emission pathway.
- Assess dissolved concentrations of CH_4 and CO_2 upstream and immediately downstream of the Keeyask reservoir to evaluate the G-res methodology for calculating CH_4 and CO_2 degassing emissions.

9.3 Lower Nelson River Reservoir GHG Lifecycle Modelling

- The lower Nelson River reservoir G-res lifecycle GHG model would benefit from:
  - Measuring GHG and related environmental parameters within the CRD, and within the Keeyask and Kettle reservoir to develop a record of in-situ GHG emission measurements to compare against modelled results.
  - Conducting GHG emission/water quality measurements within and downstream of each of the lower Nelson River reservoirs to assess the influence on carbon cycling that these reservoir discharges may have on one another.

9.4 Manitoba Hydro Hydraulic System

- Extend the lower Nelson River G-res model to include the remainder of the reservoirs/flooded lands associated with the Manitoba Hydro hydraulic system.

9.5 Recommendations for Reducing Limitations and Uncertainty with the G-res Tool

- Calibrate G-res with GHG measurements from young boreal reservoirs, such as the Keeyask reservoir, that have extensive peatland flooding, on-going peatland disintegration, and re-surfacing peat.
- Validate G-res modelling results against in-situ GHG measurements from peatland reservoirs like the young Keeyask reservoir.
- Incorporate the ability for G-res users to add site-specific pre-flood landcover and aquatic classifications and related GHG emission factors to G-res.

9.6 Recommended Future Research to Reduce Limitations and Uncertainty with the G-res Tool

9.6.1 Cascading Reservoirs

- Measure concentrations of dissolved and particulate CO_2 and CH_4, and carbon sedimentation/sequestration in the Lower Nelson River Reservoirs (e.g. Keeyask, Kettle, Long Spruce, and Limestone), and CO_2 and CH_4 discharges into Hudson Bay. Attempt to model 1) GHG emissions downstream of degassing at the generating station and spillway, and 2) cascading GHG emissions (the effect of upstream reservoir carbon discharges on downstream reservoir GHG emissions).

9.6.2 CO_2 Degassing Emissions

- Measure dissolved concentrations of CO_2 at varying depths of the water column along the Keeyask and Kettle forebay shorelines to mid-reservoir (main Nelson River channel), plus, measure concentrations of dissolved CO_2 upstream and downstream of the reservoirs. Attempt to develop a CO_2 degassing model to include CO_2 degassing emissions in the G-res Tool with possibly an emission rate that varies over the lifetime of the reservoir.

9.6.3 CH_4 Degassing Emissions

- Measure concentrations of dissolved CH_4 at varying depths of the water column along the Keeyask and Kettle forebay shorelines to mid-reservoir (main Nelson River channel), plus measure dissolved concentrations of CH_4 upstream and downstream of the reservoirs. Attempt to refine CH_4 degassing emission model in the G-res Tool with possibly an emission rate that varies over the lifetime of the reservoir.

  <u>CH_4 Bubble Emissions</u>

- Conduct CH_4 bubble measurements in the littoral zones of the Keeyask and Kettle reservoirs. Attempt to refine the CH_4 bubble emission model in the G-res Tool and with possibly an emission estimation rate that varies over the lifetime of the reservoir.

10 References

Åberg, J., Bergström, A. K., Algesten, G., Söderback, K., & Jansson, M. (2004). A comparison of the carbon balances of a natural lake (L. Örträsket) and a hydroelectric reservoir (L. Skinnmuddselet) in northern Sweden. *Water Research*, *38*(3), 531–538. https://doi.org/10.1016/j.watres.2003.10.035

Ahmed, M. I., Stadnyk, T., Pietroniro, A., Awoye, H., Bajracharya, A., Mai, J., Tolson, B. A., Shen, H., Craig, J. R., Gervais, M., Sagan, K., Wruth, S., Koenig, K., Lilhare, R., Déry, S. J., Pokorny, S., Venema, H., Muhammad, A., & Taheri, M. (2023). Learning from hydrological models' challenges: A case study from the Nelson basin model intercomparison project. *Journal of Hydrology*, *623*. https://doi.org/10.1016/j.jhydrol.2023.129820

Amesbury, M. J., Gallego-Sala, A., & Loisel, J. (2019). Peatlands as prolific carbon sinks. In *Nature Geoscience* (Vol. 12, Issue 11, pp. 880–881). Nature Publishing Group. https://doi.org/10.1038/s41561-019-0455-y

Asif, M. (ed). (2022). The 4Ds of Energy Transition: Decarbonization, Decentralization, Decreasing Use
and Digitalization. WILEY-VCH. 414 pages. ePDF ISBN: 978-3-527-83144-9. https://onlinelibrary.wiley.com/doi/book/10.1002/9783527831425

Bade, D. L. (2009). *Gas Exchange at the Air-Water Interface*. Encyclopedia of Inland Waters. Likens G E, ed (Oxford: Academic Press) 70-78.

Baggs, E. M. (2008). A review of stable isotope techniques for N2O source partitioning in soils: Recent progress, remaining challenges and future considerations. *Rapid Communications in Mass Spectrometry*, *22*(11), 1664–1672. https://doi.org/10.1002/rcm.3456

Bahram, M., Espenberg, M., Pärn, J., Lehtovirta-Morley, L., Anslan, S., Kasak, K., Kõljalg, U., Liira, J., Maddison, M., Moora, M., Niinemets, Ü., Öpik, M., Pärtel, M., Soosaar, K., Zobel, M., Hildebrand, F., Tedersoo, L., & Mander, Ü. (2022). Structure and function of the soil microbiome underlying N2O emissions from global wetlands. *Nature Communications*, *13*(1). https://doi.org/10.1038/s41467-022-29161-3

Baldocchi, D., Ryu, Y., & Keenan, T. (2016). Terrestrial Carbon Cycle Variability. In *F1000Research* (Vol. 5). F1000 Research Ltd. https://doi.org/10.12688/f1000research.8962.1

Baird, A., Belyea, L., Comas, X., Reeve, A.S., Slater, L. (2009). Understanding Carbon Cycling in Northern Peatlands: Recent Developments and Future Prospects. DOI 10.1029/2008GM000875. In book: Carbon Cycling in Northern Peatlands. Geophysical Monograph Series 184 (pp.1-3) Chapter: Understanding Carbon Cycling in Northern Peatlands: Recent Developments and Future Prospects. Publisher: American Geophysical Union Editors: Andrew J. Baird, Lisa R. Belyea, Xavier Comas, A.S. Reeve, Lee D. Slater

Bao, T., Jia, G., & Xu, X. (2021). Wetland Heterogeneity Determines Methane Emissions: A Pan-Arctic Synthesis. *Environmental Science and Technology*, *55*(14), 10152–10163. https://doi.org/10.1021/acs.est.1c01616

Barbosa, P. M., Bodmer, P., Stadler, M., Rust, F., Tremblay, A., & del Giorgio, P. A. (2023). Ecosystem Metabolism Is the Dominant Source of Carbon Dioxide in Three Young Boreal Cascade-Reservoirs (La Romaine Complex, Québec). *Journal of Geophysical Research: Biogeosciences*, *128*(4). https://doi.org/10.1029/2022JG007253

Barros, N., Cole, J. J., Tranvik, L. J., Prairie, Y. T., Bastviken, D., Huszar, V. L. M., Del Giorgio, P., & Roland, F. (2011). Carbon emission from hydroelectric reservoirs linked to reservoir age and latitude. *Nature Geoscience*, *4*(9), 593–596. https://doi.org/10.1038/ngeo1211

Bastien, J., Gravel, R., Demarty, M., Smith, M., and Gill, R. (2010). Reservoir Greenhouse Gas Monitoring Report – 2008-2009. Report prepared by Environnement Illimité inc. for Manitoba Hydro, 111 p. and 1 appendix.

Bastien, J., M. Demarty, M. Smith and R. Gill. (2011). Reservoir Greenhouse Gas Monitoring Report – 2010. Report prepared by Environnement Illimité inc. for Manitoba Hydro, Tier 1: 40 p. and 2 appendices; Tier 2: 55 p

Bastien, J., Demarty, M., & Tremblay, A. (2011). *CO 2 and CH 4 diffusive and degassing emissions from 2003 to 2009 at Eastmain 1 hydroelectric reservoir, Québec, Canada*. *1*, 113–123. https://doi.org/10.5268/IW-1.2.349

Bastviken, D., Sundgren, I., Natchimuthu, S., Reyier, H., & Gälfalk, M. (2015). Technical Note: Cost-efficient approaches to measure carbon dioxide (CO2) fluxes and concentrations in terrestrial and aquatic environments using mini loggers. *Biogeosciences*, *12*(12), 3849–3859. https://doi.org/10.5194/bg-12-3849-2015

Bastviken, D., Johnson, M.S. (2025). Future methane emissions from lakes and reservoirs. Nature Water 3, 1397–1410. https://doi-org.uml.idm.oclc.org/10.1038/s44221-025-00532-6

Beaulieu, J. J., Waldo, S., Balz, D. A., Barnett, W., Hall, A., Platz, M. C., & White, K. M. (2020). Methane and Carbon Dioxide Emissions From Reservoirs: Controls and Upscaling. *Journal of Geophysical Research: Biogeosciences*, *125*(12). https://doi.org/10.1029/2019JG005474

Belyea, L.R., 2009. Nonlinear dynamics of peatlands and potential feedbacks on the climate system. Carbon Cycling in Northern Peatlands, pp. 5–18.

Bergström, A. K., Algesten, G., Sobek, S., Tranvik, L., & Jansson, M. (2004). Emission of CO2 from hydroelectric reservoirs in northern Sweden. *Archiv Fur Hydrobiologie*, *159*(1), 25–42. https://doi.org/10.1127/0003-9136/2004/0159-0025

Bernhard, A. (2010). The Nitrogen Cycle: Processes, Players, and Human Impact. Nature Education Knowledge 3(10):25.

Bernardo, J. W. Y., Mannich, M., Hilgert, S., Fernandes, C. V. S., & Bleninger, T. (2017). A method for the assessment of long-term changes in carbon stock by construction of a hydropower reservoir. *Ambio*, *46*(5), 566–577. https://doi.org/10.1007/s13280-016-0874-6

Bhullar, G. S., Iravani, M., Edwards, P. J., & Olde Venterink, H. (2013). Methane transport and emissions from soil as affected by water table and vascular plants. *BMC Ecology*, *13*. https://doi.org/10.1186/1472-6785-13-32

Bird, J. B. (1980). The Natural Landscapes of Canada. A Study in Regional Earth Science. Second Edition. Toronto, John Wiley & Sons Canada Limited. 260 pages.

Bogard, M. J., & Butman, D. E. (2018). No blast from the past. In *Nature Climate Change* (Vol. 8, Issue 2, pp. 99–100). Nature Publishing Group. https://doi.org/10.1038/s41558-018-0070-8

Bona, K. A., Shaw, C., Thompson, D. K., Hararuk, O., Webster, K., Zhang, G., Voicu, M., & Kurz, W. A. (2020). The Canadian model for peatlands (CaMP): A peatland carbon model for national greenhouse gas reporting. *Ecological Modelling*, *431*. https://doi.org/10.1016/j.ecolmodel.2020.109164

Bottino, F., M. B. Cunha-Santino, I. Bianchini Jr. (2015). Decomposition of Particulate Organic Carbon from Aquatic Macrophytes Under Different Nutrient Conditions, Aquatic Geochemistry, 22, pages 17–33, DOI 10.1007/s10498-015-9275-x.

Boonman, J., Buzacott, A. J. V., van den Berg, M., van Huissteden, C., & van der Velde, Y. (2024). Transparent automated CO2 flux chambers reveal spatial and temporal patterns of net carbon fluxes from managed peatlands. *Ecological Indicators*, *164*. https://doi.org/10.1016/j.ecolind.2024.112121

Bowen, J. C., Ward, C. P., Kling, G. W., & Cory, R. M. (2020). Arctic amplification of global warming strengthened by sunlight oxidation of permafrost carbon to CO_2. Geophysical Research Letters, 47, e2020GL087085. https://doi.org/10.1029/2020GL087085

Brandt, J. P., Flannigan, M. D., Maynard, D. G., Thompson, I. D., & Volney, W. J. A. (2013). An introduction to Canada's boreal zone: Ecosystem processes, health, sustainability, and environmental issues1. *Environmental Reviews*, *21*(4), 207–226. https://doi.org/10.1139/er-2013-0040

Bridgham, S.D. (2017). Methane origins. Nature Climate Change, Nature, vol. 7(7), pages 477-478, July.

Briones Hidrovo, A., Uche, J., & Martínez-Gracia, A. (2017). Accounting for GHG net reservoir emissions of hydropower in Ecuador. *Renewable Energy*, *112*, 209–221. https://doi.org/10.1016/j.renene.2017.05.047

Brothers, S. M., Prairie, Y. T., & Del Giorgio, P. A. (2012). Benthic and pelagic sources of carbon dioxide in boreal lakes and a young reservoir (Eastmain-1) in eastern Canada. *Global Biogeochemical Cycles*, *26*(1). https://doi.org/10.1029/2011GB004074

Byrne, B., Liu, J., Bowman, K.W. Pascolini-Campbell, M., Chatterjee, A., Pandey, S., Miyazaki, K., van der Werf, G.R., Wunch, D., Wennberg, P.O., Roehl, C.M., Sinha, S. (2024). Carbon emissions from the 2023 Canadian wildfires. Nature 633, 835–839. https://doi.org/10.1038/s41586-024-07878-z

Canadian Competition Act, RSC c. C-34 (1985). https://laws-lois.justice.gc.ca/eng/acts/c-34/fulltext.html

Canada Energy Regulator. (2025). Renewable Energy in Canada: Current Status and Near-Term Developments. Canada Energy Regulator Website. /en/data-analysis/energy-commodities/electricity/report/canadas-renewable-power/

Canadian Net-Zero Emissions Accountability Act, SC c. 22 (2021). https://laws-lois.justice.gc.ca/eng/acts/c-19.3/fulltext.html

Casas-Ruiz, J. P., Bodmer, P., Bona, K. A., Butman, D., Couturier, M., Emilson, E. J. S., Finlay, K., Genet, H., Hayes, D., Karlsson, J., Paré, D., Peng, C., Striegl, R., Webb, J., Wei, X., Ziegler, S. E., & del Giorgio, P. A. (2023). Integrating terrestrial and aquatic ecosystems to constrain estimates of land-atmosphere carbon exchange. *Nature Communications*, *14*(1). https://doi.org/10.1038/s41467-023-37232-2

Chapin, F. S., Woodwell, G. M., Randerson, J. T., Rastetter, E. B., Lovett, G. M., Baldocchi, D. D., Clark, D. A., Harmon, M. E., Schimel, D. S., Valentini, R., Wirth, C., Aber, J. D., Cole, J. J., Goulden, M. L., Harden, J. W., Heimann, M., Howarth, R. W., Matson, P. A., McGuire, A. D., … Schulze, E. D. (2006). Reconciling carbon-cycle concepts, terminology, and methods. In *Ecosystems* (Vol. 9, Issue 7, pp. 1041–1050). https://doi.org/10.1007/s10021-005-0105-7

Chen, H., Pan, H., Xiao, S., & Deng, S. (2025). Nitrous oxide dominates greenhouse gas emissions from hydropower's reservoirs in China from 2020 to 2060. *Water Research*, *279*. https://doi.org/10.1016/j.watres.2025.123420

Clean Electricity Regulations, SOR/2024-263. (2024). https://laws-lois.justice.gc.ca/PDF/SOR-2024-263.pdf

Clean Fuel Regulations, SOR/2022-140. (2024). https://laws-lois.justice.gc.ca/PDF/SOR-2022-140.pdf

Cliche Trudeau, N., Garneau, M. & Pelletier, L. (2014). Interannual variability in the CO2 balance of a boreal patterned fen, James Bay, Canada. Biogeochemistry 118, 371–387 (2014). https://doi.org/10.1007/s10533-013-9939-9

Climate Bonds Initiative Hydropower Criteria. (2021). Hydropower Criteria: The Hydropower Criteria for the Climate Bonds Standard & Certification Scheme. Version 1. 12 pages.

Cole, J. J., Prairie, Y. T., Caraco, N. F., McDowell, W. H., Tranvik, L. J., Striegl, R. G., Duarte, C. M., Kortelainen, P., Downing, J. A., Middelburg, J. J., & Melack, J. (2007). Plumbing the global carbon cycle: Integrating inland waters into the terrestrial carbon budget. *Ecosystems*, *10*(1), 171–184. https://doi.org/10.1007/s10021-006-9013-8

Cole, J. J., Bade, D. L., Bastviken, D., Pace, M. L., & Van de Bogert, M. (2010). Multiple approaches to estimating air-water gas exchange in small lakes. *Limnology and Oceanography: Methods*, *8*(JUNE), 285–293. https://doi.org/10.4319/lom.2010.8.285

Corkery, M.T., 1996. Geology and landforms of Manitoba, p. 11-30. In J. Welsted, J. Everitt, and C. Stadel, eds., The Geography of Manitoba: Its Land and Its People. The University of Manitoba Press, Winnipeg, 328 p. https://www.gov.mb.ca/iem/min-ed/teensrock/history/files/corkery_article.pdf

Crestey-Chury, T., Darnajoux, R. Kanaan, R. Aurela, M., Butlers, A., De Dobbelaer, T., Escarmena, L., Gandois, L., Jauhiainen, J., Juutinen, S., Larmola, T., Mander, 0., Poblador, S., Raman, M., Sabater, F., Schindler, T., Soosaar, K., Ukonmaanaho, L., Sanchez-Perez, J-M. (2025). N2O Wetland Emissions Europe. European Geosciences Union General Assembly 2025 (EGU25), held 27 April-2 May, 2025 in Vienna, Austria. Online at https://www.egu25.eu/, id. EGU25-20384

Cuerrier, S., del Giorgio, P., Prairie, Y. (2024). Constraining Hydrological and Biochemical Processes that Simultaneously Control the Dissolved Gases Concentrations in the Water Column of Canadian Reservoirs Using a Process-based Modeling Approach. GHG-CaRe All Partners Meeting. [Unpublished presentation]. L'Université du Québec à Montréal. Montréal, Québec.

D'Acunha, B., Morillas, L., Black, T. A., Christen, A., & Johnson, M. S. (2019). Net Ecosystem Carbon Balance of a Peat Bog Undergoing Restoration: Integrating CO2 and CH4 Fluxes From Eddy Covariance and Aquatic Evasion With DOC Drainage Fluxes. *Journal of Geophysical Research: Biogeosciences*, *124*(4), 884–901. https://doi.org/10.1029/2019JG005123

Deblois, C. P., Demarty, M., Bilodeau, F., & Tremblay, A. (2023). Automated CO2 and CH4 monitoring system for continuous estimation of degassing related to hydropower. *Frontiers in Environmental Science*, *11*. https://doi.org/10.3389/fenvs.2023.1194994

Deemer, B. R., Harrison, J. A., Li, S., Beaulieu, J. J., Delsontro, T., Barros, N., Bezerra-Neto, J. F., Powers, S. M., Dos Santos, M. A., & Vonk, J. A. (2016). Greenhouse gas emissions from reservoir water surfaces: A new global synthesis. In *BioScience* (Vol. 66, Issue 11, pp. 949–964). Oxford University Press. https://doi.org/10.1093/biosci/biw117

del Giorgio, P. (2023). La Romaine Project: Looking ahead. [Unpublished Presentation]. Mini-Symposium Hydro-Québec sur les émissions biogéniques de GES / Mini-Symposium Hydro-Québec on biogenic GHG emissions. November 8-9, 2023. Montréal, Québec.

DelSontro, T., Mcginnis, D. F., Sobek, S., Ostrovsky, I., & Wehrli, B. (2010). Extreme methane emissions from a swiss hydropower Reservoir: Contribution from bubbling sediments. *Environmental Science and Technology*, *44*(7), 2419–2425. https://doi.org/10.1021/es9031369

DelSontro, T., Kunz, M. J., Kempter, T., Wüest, A., Wehrli, B., & Senn, D. B. (2011). Spatial heterogeneity of methane ebullition in a large tropical reservoir. *Environmental Science and Technology*, *45*(23), 9866–9873. https://doi.org/10.1021/es2005545

DelSontro, T., McGinnis, D. F., Wehrli, B., & Ostrovsky, I. (2015). Size does matter: Importance of large bubbles and small-scale hot spots for methane transport. *Environmental Science and Technology*, *49*(3), 1268–1276. https://doi.org/10.1021/es5054286

DelSontro, T., Boutet, L., St-Pierre, A., del Giorgio, P. A., & Prairie, Y. T. (2016a). Methane ebullition and diffusion from northern ponds and lakes regulated by the interaction between temperature and system productivity. *Limnology and Oceanography*, *61*, S62–S77. https://doi.org/10.1002/lno.10335

DelSontro, T., Perez, K. K., Sollberger, S., & Wehrli, B. (2016b). Methane dynamics downstream of a temperate run-of-the-river reservoir. *Limnology and Oceanography*, *61*, S188–S203. https://doi.org/10.1002/lno.10387

DelSontro, T., del Giorgio, P. A., & Prairie, Y. T. (2018). No Longer a Paradox: The Interaction Between Physical Transport and Biological Processes Explains the Spatial Distribution of Surface Water Methane Within and Across Lakes. *Ecosystems*, *21*(6), 1073–1087. https://doi.org/10.1007/s10021-017-0205-1

DelSontro, T., Beaulieu, J. J., Downing, J. A., Stanley, E., & Del Giorgio, P. (2018). *SPECIAL ISSUE-CURRENT EVIDENCE Greenhouse gas emissions from lakes and impoundments: Upscaling in the face of global change*. https://doi.org/10.6084/m9.figshare.5220001

Delwiche, K. B., Knox, S. H., Malhotra, A., Fluet-Chouinard, E., McNicol, G., Feron, S., Ouyang, Z., Papale, D., Trotta, C., Canfora, E., Cheah, Y. W., Christianson, D., Alberto, M. C. R., Alekseychik, P., Aurela, M., Baldocchi, D., Bansal, S., Billesbach, D. P., Bohrer, G., … Jackson, R. B. (2021). FLUXNET-CH4: A global, multi-ecosystem dataset and analysis of methane seasonality from freshwater wetlands. *Earth System Science Data*, *13*(7), 3607–3689. https://doi.org/10.5194/essd-13-3607-2021

Demarty, M., Bastien, J., Tremblay, A., Hesslein, R. H., & Gill, R. (2009). Greenhouse gas emissions from boreal reservoirs in Manitoba and Québec, Canada, measured with automated systems. *Environmental Science and Technology*, *43*(23), 8908–8915. https://doi.org/10.1021/es8035658

Demarty, M., Bastien, J., & Tremblay, A. (2011). Annual follow-up of gross diffusive carbon dioxide and methane emissions from a boreal reservoir and two nearby lakes in Québec, Canada. *Biogeosciences*, *8*(1), 41–53. https://doi.org/10.5194/bg-8-41-2011

Demarty, M., & Tremblay, A. (2019). Long term follow-up of pCO2, pCH4 and emissions from Eastmain 1 boreal reservoir, and the Rupert diversion bays, Canada. *Ecohydrology and Hydrobiology*, *19*(4), 529–540. https://doi.org/10.1016/j.ecohyd.2017.09.001

Demarty, M., del Giorgio, P. A., Deblois, C., Bilodeau, F., & Tremblay, A. (2026). The Long-Term C Footprint Trajectory and Emissions Attribution of a Large Boreal Reservoir (Paix Des Braves (Eastmain 1), Quebec). Borealis. https://doi.org/10.5683/SP3/XHMY5E

Dorgeist, L., Schwingshackl, C., Bultan, S., Pongratz, J. (2024). A consistent budgeting of terrestrial carbon fluxes. Nat Commun 15, 7426 (2024). https://doi.org/10.1038/s41467-024-51126-x

Dowd, M.B and C.L. Hrenchuck. (2023). Results of water quality monitoring in the Nelson River, 2022: Year 1 Operation. Keeyask Generation Project Aquatic Effects Monitoring Plan Report. #AEMP-2023-13. A report prepared for Manitoba Hydro by North/South Consultants Inc,. June 2023. xv +295 pages. https://keeyask.com/wp-content/uploads/2023/06/AEMP-2023-13-Water-Quality-Monitoring.pdf

Dowd, M.B and C.L. Hrenchuck. (2024). Results of water quality monitoring in the Nelson River, 2023: Year 2 Operation. Keeyask Generation Project Aquatic Effects Monitoring Plan Report. #AEMP-2024-11. A report prepared for Manitoba Hydro by North/South Consultants Inc,. June 2024. xvi +301 pages. https://keeyask.com/wp-content/uploads/2024/06/AEMP-2024-11-Water-Quality-Monitoring.pdf

Duchemin, E., Lucotte, M., Canuel, R., Queiroz, A. G., Almeida, D. C., Pereira, H. C., & Dezincourt, J. (2000). Comparison of greenhouse gas emissions from an old tropical reservoir with those from other reservoirs worldwide. *SIL Proceedings, 1922-2010*, *27*(3), 1391–1395. https://doi.org/10.1080/03680770.1998.11901464

Dunsky Energy + Climate Advisors. (2025). Forecasting Canada's electricity future. The Transition Accelerator. https://transitionaccelerator.ca/reports/forecasting-canadas-electricity-future/

ECOSTEM Inc. 2011. Keeyask Generation Project, Stage IV Studies – Physical Environment: Composition and Distribution of Shoreline and Inland Peatlands in the Keeyask Reservoir Area and Historical Trends in Peatland Disintegration (GN 9.2.1). Prepared for Manitoba Hydro. September 2011.

Elder, C. D., Xu, X., Walker, J., Schnell, J. L., Hinkel, K. M., Townsend-Small, A., Arp, C. D., Pohlman, J. W., Gaglioti, B. V., & Czimczik, C. I. (2018). Greenhouse gas emissions from diverse Arctic Alaskan lakes are dominated by young carbon. *Nature Climate Change*, *8*(2), 166–171. https://doi.org/10.1038/s41558-017-0066-9

Electrifying Canada. (2022a). Scaling up clean electricity. International Institute for Sustainable Development. https://www.iisd.org/system/files/2022-05/scaling-up-clean-electricity-en.pdf

Electrifying Canada. (2022b). Canada’s electrification advantage in the race to net-zero: Five catalysts to accelerate business electrification. International Institute for Sustainable Development. https://www.iisd.org/system/files/2022-05/canada-elecrification-advantage-net-zero-en.pdf

Energy Institute Statistical Review of World Energy. (2026). 2026|75th edition Statistical Review of World Energy. ISSN 2976-7857
https://www.energyinst.org/__data/assets/file/0004/1827616/Statistical-Review-of-World-Energy-PDF-Report.pdf

Engram, M., Walter Anthony, K. M., Sachs, T., Kohnert, K., Serafimovich, A., Grosse, G., & Meyer, F. J. (2020). Remote sensing northern lake methane ebullition. *Nature Climate Change*, *10*(6), 511–517. https://doi.org/10.1038/s41558-020-0762-8

Environment and Climate Change Canada (ECCC). (2020). Strategic Assessment of Climate Change Revised October 2020. Cat. No.: En14-417/2021E-PDF ISBN: 978-0-660-39128-1 EC: 21011 https://www.strategicassessmentclimatechange.ca/home11

Environment and Climate Change Canada (ECCC 2023). Fuel Life Cycle Assessment Model Methodology. Environment and Climate Change Canada. Cat. No.: En4-418/1-2023E-PDF ISBN: 978-0-660-43852-8 EC22081 file:///C:/Users/donation/Downloads/Fuel-LCA-Model-Methodology_January2023%20(2).pdf

Environment and Climate Change Canada (ECCC 2024). Fuel Life Cycle Assessment Model User Manual, June 2024. Cat. No.: En4-418/3-2024E-PDF ISBN: 978-0-660-71928-3 EC24065 https://www.canada.ca/en/environment-climate-change/services/managing-pollution/fuel-life-cycle-assessment-model/user-manual.html

Environment and Climate Change Canada (ECCC 2025a). Canada affirms Indigenous leadership and global climate action at the 30th United Nations Climate Change Conference (COP30). News release November 13, 2025 – Belém, Brazil. https://www.canada.ca/en/environment-climate-change/news/2025/11/canada-affirms-indigenous-leadership-and-global-climate-action-at-the-30th-united-nations-climate-change-conference-cop30.html

Environment and Climate Change Canada (ECCC 2025b). Emissions and absorptions from hydroelectricity production and transmission: The perspective of Canada's national GHG inventory. Symposium on GHG biogenic emissions and hydroclimatic impacts. Kruger Pavillon – Université Laval. September 22-24, 2025.

Environment and Climate Change Canada (ECCC 2025c). Clean Fuel Regulations: Specifications for Fuel LCA Model CI Calculations. Version 4.0 January 2025. file:///G:/Policy/Canada/CFR-Specifications-for-Fuel-LCA-Model-CI-Calculations-v4.0%20(1)%20(1).pdf

Environnement Illimité Inc., 2012. Keeyask Environmental Impact Statement – Reservoir Greenhouse Gases Technical Memo. GN-9.5.6. Keeyask Project Environmental Studies Program Report prepared for Manitoba Hydro. 26 pp.

Frolking, S., Roulet, R., Lawrence, D. (2009). Issues Related to Incorporating Northern Peatlands into Global Climate Models. DOI 10.1029/2008GM000875. In book: Carbon Cycling in Northern Peatlands. Geophysical Monograph Series 184 (pp. 19-36) Chapter: Issues Related to Incorporating Northern Peatlands into Global Climate Models. Publisher:

American Geophysical Union Editors: Andrew J. Baird, Lisa R. Belyea, Xavier Comas, A.S. Reeve, Lee D. Slater

Gauthier, M. S., Breckenridge, A.&Hodder,T. J. 2022 (April): Patterns of ice recession and ice streamactivity for the MIS 2 Laurentide Ice Sheet in Manitoba, Canada. Boreas, Vol. 51, pp. 274–298. https://doi.org/10.1111/bor.12571, ISSN 0300-9483.

Gedig, D. P., Soloway, A. D., Gill, R., & Papakyriakou, T. N. (2025). Aquatic metabolism after impoundment of a low productivity boreal reservoir using free water oxygen. Inland Waters, 15(1). https://doi.org/10.1080/20442041.2025.2489254

Goldenfum, J.A. [Ed.] (2010). GHG Measurement Guidelines for Freshwater Reservoirs – Derived from: the UNESCO/IHA GHG Emissions from Freshwater Reservoirs Research Project. London, UK: The International Hydropower Association (IHA). 138 p. https://cdn.prod.website-files.com/64f9d0036cb97160cc26feba/64f9d0036cb97160cc270fe8_GHG%20Measurement%20Guidelines%20for%20Freshwater%20Reservoirs.pdf

Goldenfum, J. A. (2012). Challenges and solutions for assessing the impact of freshwater reservoirs on natural GHG emissions. *Ecohydrology and Hydrobiology*, *12*(2), 115–122. https://doi.org/10.2478/v10104-012-0011-5

Gong, Y., Wu, J., Vogt, J., & Ma, W. (2020). Greenhouse gas emissions from peatlands under manipulated warming, nitrogen addition, and vegetation composition change: A review and data synthesis. In *Environmental Reviews* (Vol. 28, Issue 4, pp. 428–437). Canadian Science Publishing. https://doi.org/10.1139/er-2019-0064

Goulden, M. L., Mcmillan, A. M. S., Winston, G. C., Rocha, A. V., Manies, K. L., Harden, J. W., & Bond-Lamberty, B. P. (2011). Patterns of NPP, GPP, respiration, and NEP during boreal forest succession. *Global Change Biology*, *17*(2), 855–871. https://doi.org/10.1111/j.1365-2486.2010.02274.x

Government of Canada. (2013). National Ecological Framework for Canada. Ecozones, Ecoregions, and Ecodistricts. https://sis.agr.gc.ca/cansis/publications/maps/eco/all/districts/eco_all_districts_1m_manitoba.jpg

Government of Canada. (2016). The Paris Agreement. https://www.canada.ca/en/environment-climate-change/services/climate-change/paris-agreement.html

Government of Canada. (2017). Canada's 2017 Nationally Determined Contribution Submission to the United Nations Framework. https://unfccc.int/sites/default/files/NDC/2022-06/Canada%20First%20NDC-Revised%20submission%202017-05-11.pdf#:~:text=To%20contribute%20to%20the%20achievement%20of%20the,by%202.2%20degrees%20between%201948%20and%202013.

Government of Canada, Natural Resources Canada, Geological Survey of Canada. (2021, August 31). Permafrost, Atlas of Canada, 5th Edition. Natural Resources Canada, Federal

Geospatial Platform. https://osdp-psdo.canada.ca/dp/en/search/metadata/NRCAN-FGP-1-d1e2048b-ccff-5852-aaa5-b861bd55c367

Government of Canada. (2025a). Canada's official greenhouse gas inventory – Main page. https://www.canada.ca/en/environment-climate-change/services/climate-change/greenhouse-gas-emissions/inventory.html

Government of Canada. (2025b). Cutting pollution and building a strong economy for the future: Canada's 2035 commitment under the Paris Agreement. News release February 12, 2025 – Ottawa, Ontario. https://www.canada.ca/en/environment-climate-change/news/2025/02/cutting-pollution-and-building-a-strong-economy-for-the-future-canadas-2035-commitment-under-the-paris-agreement.html

Government of Canada. (2025c). Powering Canada's Future: A Clean Electricity Strategy. https://natural-resources.canada.ca/sites/admin/files/documents/2025-08/Clean-Electricity-Strategy.pdf

Government of Manitoba. (2023). Manitoba Hydro Mandate Letter. Minister Responsible for Manitoba Hydro. https://manitoba.ca/asset_library/en/executivecouncil/mandate/hydro_mandate_letter_2023.pdf

Government of Manitoba. (2024). Manitoba's Affordable Energy Plan: Building the Next Generation of Affordable Energy. Minister of Finance, Minister of Environment and Climate Change. https://www.gov.mb.ca/asset_library/en/energyplan/mb-affordable-energy-plan.pdf

Government of Manitoba. (2025). Manitoba's Path to Net Zero: guided by the Spirit of Manoomin. https://www.manitoba.ca/asset_library/en/netzero/mb-path-to-net-zero.pdf

Graham, J. D., Ricciuto, D. M., Glenn, N. F., & Hanson, P. J. (2022). Incorporating Microtopography in a Land Surface Model and Quantifying the Effect on the Carbon Cycle. *Journal of Advances in Modeling Earth Systems*, *14*(2). https://doi.org/10.1029/2021MS002721

Griffiths, N. A., Hanson, P. J., Ricciuto, D. M., Iversen, C. M., Jensen, A. M., Malhotra, A., McFarlane, K. J., Norby, R. J., Sargsyan, K., Sebestyen, S. D., Shi, X., Walker, A. P., Ward, E. J., Warren, J. M., & Weston, D. J. (2017). Temporal and Spatial Variation in Peatland Carbon Cycling and Implications for Interpreting Responses of an Ecosystem-Scale Warming Experiment. *Soil Science Society of America Journal*, *81*(6), 1668–1688. https://doi.org/10.2136/sssaj2016.12.0422

Grosbois, G., Lau, D. C. P., Berggren, M., Girona, M. M., Goedkoop, W., Messier, C., Hjältén, J., & del Giorgio, P. (2023). Land and Freshwater Complex Interactions in Boreal Forests: A Neglected Topic in Forest Management. In *Advances in Global Change Research* (Vol. 74, pp. 719–745). Springer Science and Business Media B.V. https://doi.org/10.1007/978-3-031-15988-6_29

Gudasz, C., Bastviken, D., Steger, K., Premke, K., Sobek, S., & Tranvik, L. J. (2010). Temperature-controlled organic carbon mineralization in lake sediments. *Nature*, *466*(7305), 478–481. https://doi.org/10.1038/nature09186

Hamlin, B., and Zhang, A. (2024). Net zero future for Manitoba through bigger, cleaner, smarter electricity. Canadian Climate Institute. 17 pages. https://climateinstitute.ca/wp-content/uploads/2024/07/A-Net-Zero-Future-for-Manitoba.pdf

Hansen, C., Pilla, R., Matson, P., Skinner, B., Griffiths, N., & Jager, H. (2022). Variability in modelled reservoir greenhouse gas emissions: comparison of select US hydropower reservoirs against global estimates. *Environmental Research Communications*, *4*(12). https://doi.org/10.1088/2515-7620/acae24

Hansen, C. H., Matson, P. G., & Griffiths, N. A. (2023). Diversity in reservoir surface morphology and climate limits ability to compare and upscale estimates of greenhouse gas emissions. *Science of the Total Environment*, *893*. https://doi.org/10.1016/j.scitotenv.2023.164851

Harrison, J. A., Prairie, Y. T., Mercier-Blais, S., & Soued, C. (2021). Year-2020 Global Distribution and Pathways of Reservoir Methane and Carbon Dioxide Emissions According to the Greenhouse Gas From Reservoirs (G-res) Model. *Global Biogeochemical Cycles*, *35*(6). https://doi.org/10.1029/2020GB006888

Hendzel, L. L., Matthews, C. J. D., Venkiteswaran, J. J., St. Louis, V. L., Burton, D., Joyce, E. M., & Bodaly, R. A. (2005). Nitrous oxide fluxes in three experimental boreal forest reservoirs. *Environmental Science and Technology*, *39*(12), 4353–4360. https://doi.org/10.1021/es049443j

Hertwich, E. G. (2013). Addressing biogenic greenhouse gas emissions from hydropower in LCA. *Environmental Science and Technology*, *47*(17), 9604–9611. https://doi.org/10.1021/es401820p

Hessen, D. O., Håll, J. P., Thrane, J. E., & Andersen, T. (2017). Coupling dissolved organic carbon, CO2 and productivity in boreal lakes. *Freshwater Biology*, *62*(5), 945–953. https://doi.org/10.1111/fwb.12914

Hesslein, R., and Cooley, M. (2016). Status of Greenhouse Gas Emissions at Manitoba Hydro's Mature Reservoirs. Prepared for Manitoba Hydro by North/South Consultants Inc. Winnipeg, Manitoba. 68 pages.

Hesslein, R., and Cooley, M. (2017). Manitoba Hydro's Greenhouse Gas Monitoring Program: Summary of Current Issues and Recommendations for Future Monitoring. Prepared for Manitoba Hydro by North/South Consultants Inc. Winnipeg, Manitoba. 16 pages.

House of Commons of Canada. (2025). BILL C-15 An Act to implement certain provisions of the budget tabled in Parliament on November 4, 2025. First Session, Forty-fifth Parliament, 3-4 Charles III, 2025. First Reading, November 18, 2025. https://www.parl.ca/Content/Bills/451/Government/C-15/C-15_1/C-15_1.PDF

H.ConRes.14-119th Congress. (2025). Establishing the congressional budget for the United States Government for fiscal year 2025 and setting forth the appropriate budgetary levels for fiscal years 2026 through 2034. https://www.congress.gov/bill/119th-congress/house-concurrent-resolution/14

Hrenchuk, C. (2021). Results of water quality monitoring in the Nelson River, 2020: Year 7 Construction. Keeyask Generation Project Aquatic Effects Monitoring Plan Report #AEMP-2021-06. A report prepared for Manitoba Hydro by North/South Consultants Inc., June 2021. xxv + 124 pp. https://keeyask.com/wp-content/uploads/2021/06/AEMP-2021-06-Water-Quality-Monitoring.pdf

Hrenchuk, C. (2022). Results of water quality monitoring in the Nelson River, 2021: Year 8 Construction. Keeyask Generation Project Aquatic Effects Monitoring Plan Report #AEMP-2022-14. A report prepared for Manitoba Hydro by North/South Consultants Inc., June 2022. xxviii + 301 pp. https://keeyask.com/wp-content/uploads/2022/06/AEMP-2022-14-Water-Quality.pdf

Hugelius, G., Loisel, J., Chadburn, S., Jackson, R. B., Jones, M., MacDonald, G., Marushchak, M., Olefeldt, D., Packalen, M., Siewert, M. B., Treat, C., Turetsky, M., Voigt, C., & Yu, Z. (2020). Large stocks of peatland carbon and nitrogen are vulnerable to permafrost thaw. *Proceedings of the National Academy of Sciences of the United States of America*, *117*(34), 20438–20446. https://doi.org/10.1073/pnas.1916387117

Huotari, J., Haapanala, S., Pumpanen, J., Vesala, T., & Ojala, A. (2013). Efficient gas exchange between a boreal river and the atmosphere. *Geophysical Research Letters*, *40*(21), 5683–5686. https://doi.org/10.1002/2013GL057705

Huttunen, J. T., Väisänen, T. S., Hellsten, S. K., Heikkinen, M., Nykänen, H., Jungner, H., Niskanen, A., Virtanen, M. O., Lindqvist, O. V., Nenonen, O. S., & Martikainen, P. J. (2002). Fluxes of CH4, CO2, and N2O in hydroelectric reservoirs Lokka and Porttipahta in the northern boreal zone in Finland. *Global Biogeochemical Cycles*, *16*(1). https://doi.org/10.1029/2000gb001316

Hydro-Québec (2008). Romaine Complex: Environmental Impact Statement Summary. Hydro-Québec Production.

Hydro-Québec (2014). Eastmain-1 Hydroelectric Development: Environmental Activities, 2002-2013-Highlights. Hydro-Québec Production.

Hydropower Limited Partnership, K. (2012a). *Supporting Volume Physical Environment Keeyask Generation Project Environmental Impact Statement*. Keeyask Hydropower Limited Partnership, Winnipeg, Manitoba. Canadian Environmental Assessment Registry Reference Number 11-03-64144. Manitoba Conservation and Water Stewardship Client File Number: 5550.00

Hydropower Limited Partnership, K. (2012b). *Supporting Volume Terrestrial Environment Keeyask Generation Project Environmental Impact Statement*. Keeyask Hydropower Limited Partnership, Winnipeg, Manitoba. Canadian Environmental Assessment Registry Reference

Number 11-03-64144. Manitoba Conservation and Water Stewardship Client File Number: 5550.00

Hydropower Limited Partnership, K. (2012c). *Supporting Volume Aquatic Environment Keeyask Generation Project Environmental Impact Statement*. Keeyask Hydropower Limited Partnership, Winnipeg, Manitoba. Canadian Environmental Assessment Registry Reference Number: 11-03-64144

Impact Assessment Act S.C. c. 28, s. 1. (2019). https://laws.justice.gc.ca/PDF/I-2.75.pdf

International Energy Agency (IEA). (2017).Digitization and Energy. https://iea.blob.core.windows.net/assets/b1e6600c-4e40-4d9c-809d-1d1724c763d5/DigitalizationandEnergy3.pdf

International Energy Agency (IEA). (2025). Global Energy Review 2025. https://iea.blob.core.windows.net/assets/5b169aa1-bc88-4c96-b828-aaa50406ba80/GlobalEnergyReview2025.pdf

Intergovernmental Panel on Climate Change (IPCC). (2006). 2006 IPCC Guidelines for National Greenhouse Gas Inventories. Prepared by the National Greenhouse Gas Inventories Programme, Eggleston H.S., Buendia L., Miwa K., Ngara T. and Tanabe K. (eds). Published: IGES, Japan.

Intergovernmental Panel on Climate Change (IPCC). (2014a), 2013 Supplement to the 2006 IPCC Guidelines for National Greenhouse Gas Inventories: Wetlands, Hiraishi, T., Krug, T., Tanabe, K., Srivastava, N., Baasansuren, J., Fukuda, M. and Troxler, T.G. (eds). Published: IPCC, Switzerland.

Intergovernmental Panel on Climate Change (IPCC). (2014b): Climate Change 2014: Mitigation of Climate Change. Contribution of Working Group III to the Fifth Assessment Report of the Intergovernmental Panel on Climate Change [Edenhofer, O., R. Pichs-Madruga, Y. Sokona, E. Farahani, S. Kadner, K. Seyboth, A. Adler, I. Baum, S. Brunner, P. Eickemeier, B. Kriemann, J. Savolainen, S. Schlömer, C. von Stechow, T. Zwickel and J.C. Minx (eds.)]. Cambridge University Press, Cambridge, United Kingdom and New York, NY, USA.

Intergovernmental Panel on Climate Change (IPCC). (2018). Summary for Policymakers. In: Global Warming of 1.5°C. An IPCC Special Report on the impacts of global warming of 1.5°C above pre-industrial levels and related global greenhouse gas emission pathways, in the context of strengthening the global response to the threat of climate change, sustainable development, and efforts to eradicate poverty [Masson-Delmotte, V., P. Zhai, H.-O. Pörtner, D. Roberts, J. Skea, P.R. Shukla, A. Pirani, W. Moufouma-Okia, C. Péan, R. Pidcock, S. Connors, J.B.R. Matthews, Y. Chen, X. Zhou, M.I. Gomis, E. Lonnoy, T. Maycock, M. Tignor, and T. Waterfield (eds.)]. Cambridge University Press, Cambridge, UK and New York, NY, USA, pp. 3-24. https://doi.org/10.1017/9781009157940.001.

Intergovernmental Panel on Climate Change (IPCC). (2019). Wetlands. Chapter 7_Volume 4 (Agriculture, Forestry and Other Land Use), 2019 Refinement to the 2006 IPCC Guidelines for National Greenhouse Gas Inventories.

Intergovernmental Panel on Climate Change (IPCC). (2023). Summary for Policymakers. In: Climate Change 2023: Synthesis Report. Contribution of Working Groups I, II and III to the Sixth Assessment Report of the Intergovernmental Panel on Climate Change [Core Writing Team, H. Lee and J. Romero (eds.)]. IPCC, Geneva, Switzerland, pp. 1-34, doi: 10.59327/IPCC/AR6-9789291691647.001

International Hydropower Association (IHA). (2020). 2020 Hydropower Status Report: Sector Trends and Insights. 2020 International Hydropower Association Limited. London, United Kingdom. 54 pages.

Järveoja, J., Nilsson, M. B., Gažovič, M., Crill, P. M., & Peichl, M. (2018). Partitioning of the net CO2 exchange using an automated chamber system reveals plant phenology as key control of production and respiration fluxes in a boreal peatland. *Global Change Biology*, *24*(8), 3436–3451. https://doi.org/10.1111/gcb.14292

Jarvie, H. P., King, S. M., & Neal, C. (2017). Inorganic carbon dominates total dissolved carbon concentrations and fluxes in British rivers: Application of the THINCARB model – Thermodynamic modelling of inorganic carbon in freshwaters. Science of the Total Environment, 575, 496–512. https://doi.org/10.1016/j.scitotenv.2016.08.201

Jiang, X., Kim, S., & Lu, S. (2025). Limited accountability and awareness of corporate emissions target outcomes. *Nature Climate Change*, *15*(3), 279–286. https://doi.org/10.1038/s41558-024-02236-3

Joyce, J., & Jewell, P. W. (2003). *Physical Controls on Methane Ebullition from Reservoirs and Lakes*. Environmental & Engineering Geoscience, Vol. IX, No. 2, pp. 167–178

Khalil, K., Mary, B., & Renault, P. (2004). Nitrous oxide production by nitrification and denitrification in soil aggregates as affected by O2 concentration. *Soil Biology and Biochemistry*, *36*(4), 687–699. https://doi.org/10.1016/j.soilbio.2004.01.004

Kazmere, D., Feofilovs, M., & Romagnoli, F. (2024). Comparative Analysis of Peatland Emission Factors: Unravelling the Need for Standardized Measurement and Reporting. *Environmental and Climate Technologies*, *28*(1), 437–452. https://doi.org/10.2478/rtuect-2024-0034

Keenan, T. F., & Williams, C. A. (2018). *Annual Review of Environment and Resources The Terrestrial Carbon Sink*. https://doi.org/10.1146/annurev-environ

Keeyask Hydropower Limited Partnership. (2012a). Keeyask Generation Project: Environmental Impact Statement; Physical Environment Response to EIS Guidelines, Supporting Volume. 1018 pages.

Keeyask Hydropower Limited Partnership. (2012b). Keeyask Generation Project: Environmental Impact Statement; Terrestrial Environment Response to EIS Guidelines, Supporting Volume. 1346 pages.

Keeyask Hydropower Limited Partnership. (2012c). Keeyask Generation Project: Environmental Impact Statement; Aquatic Environment Response to EIS Guidelines, Supporting Volume. 1745 pages.

Keeyask Hydropower Limited Partnership. (2015). Keeyask Generation Project: Physical Environment Monitoring Plan. Prepared by Keeyask Hydropower Limited Partnership. Winnipeg, Manitoba. 97 pages. https://keeyask.com/wp-content/uploads/2014/08/KGP-Physical-Environment-Monitoring-Plan-Final.pdf

Keeyask Hydropower Limited Partnership. (2015). Keeyask Generation Project: Reservoir Clearing Plan. Prepared by Keeyask Hydropower Limited Partnership. Winnipeg, Manitoba. 78 pages. Manitoba Hydro SCI File No.: 00195-13100-0005_02

Kelly, C.A, Rudd, J.W,M, Bodaly, R,A, Roulet, N.P., St LOUIS, V.L., Heyes, A., Moore, T.R., Schiff, S., Aravena, R., Scott, K.J., Dyck, B., Harris, R., Warner, B., Edwards, G. (1997). Increases in fluxes of greenhouse gases and methyl mercury following flooding of an experimental reservoir. Environmental Science & Technology, 31(5), 1334-1344. ISSN: 0013-936X. EISSN: 1520-5851.

Klaus, M., & Vachon, D. (2020). Challenges of predicting gas transfer velocity from wind measurements over global lakes. *Aquatic Sciences*, *82*(3). https://doi.org/10.1007/s00027-020-00729-9

Knox, S. H., Jackson, R. B., Poulter, B., McNicol, G., Fluet-Chouinard, E., Zhang, Z., Hugelius, G., Bousquet, P., Canadell, J. G., Saunois, M., Papale, D., Chu, H., Keenan, T. F., Baldocchi, D., Torn, M. S., Mammarella, I., Trotta, C., Aurela, M., Bohrer, G., … Zona, D. (2019). FluXNET-CH4 synthesis activity objectives, observations, and future directions. Bulletin of the American Meteorological Society, 100(12), 2607–2632. https://doi.org/10.1175/BAMS-D-18-0268.1

Knox, S. H., Bansal, S., McNicol, G., Schafer, K., Sturtevant, C., Ueyama, M., Valach, A. C., Baldocchi, D., Delwiche, K., Desai, A. R., Euskirchen, E., Liu, J., Lohila, A., Malhotra, A., Melling, L., Riley, W., Runkle, B. R. K., Turner, J., Vargas, R., … Jackson, R. B. (2021). Identifying dominant environmental predictors of freshwater wetland methane fluxes across diurnal to seasonal time scales. *Global Change Biology*, *27*(15), 3582–3604. https://doi.org/10.1111/gcb.15661

Kou, D., Virtanen, T., Treat, C. C., Tuovinen, J. P., Räsänen, A., Juutinen, S., Mikola, J., Aurela, M., Heiskanen, L., Heikkilä, M., Weckström, J., Juselius, T., Piilo, S. R., Deng, J., Zhang, Y., Chaudhary, N., Huang, C., Väliranta, M., Biasi, C., … Shurpali, N. J. (2022). Peatland Heterogeneity Impacts on Regional Carbon Flux and Its Radiative Effect Within a Boreal Landscape. *Journal of Geophysical Research: Biogeosciences*, *127*(9). https://doi.org/10.1029/2021JG006774

Kortelainen, P., Larmola, T., Rantakari, M., Juutinen, S., Alm, J., & Martikainen, P. J. (2020). Lakes as nitrous oxide sources in the boreal landscape. *Global Change Biology*, *26*(3), 1432–1445. https://doi.org/10.1111/gcb.14928

Kuhn, M. A., Varner, R. K., Bastviken, D., Crill, P., Macintyre, S., Turetsky, M., Walter Anthony, K., McGuire, A. D., & Olefeldt, D. (2021). BAWLD-CH4: A comprehensive dataset of methane fluxes from boreal and arctic ecosystems. In *Earth System Science Data* (Vol. 13, Issue 11, pp. 5151–5189). Copernicus Publications. https://doi.org/10.5194/essd-13-5151-2021

Kumar, A., Yang, T., & Sharma, M. P. (2019). Long-term prediction of greenhouse gas risk to the Chinese hydropower reservoirs. *Science of the Total Environment*, *646*, 300–308. https://doi.org/10.1016/j.scitotenv.2018.07.314

Kurz, W. A., Shaw, C. H., Boisvenue, C., Stinson, G., Metsaranta, J., Leckie, D., Dyk, A., Smyth, C., & Neilson, E. T. (2013). Carbon in Canada's boreal forest — A synthesis. *Reviews*, *21*(4), 260–292. https://doi.org/10.2307/envirevi.21.4.260

Leifeld, J., Wüst-Galley, C., & Page, S. (2019). Intact and managed peatland soils as a source and sink of GHGs from 1850 to 2100. In *Nature Climate Change* (Vol. 9, Issue 12, pp. 945–947). Nature Research. https://doi.org/10.1038/s41558-019-0615-5

Levasseur, A., Mercier-Blais, S., Prairie, Y. T., Tremblay, A., & Turpin, C. (2021). Improving the accuracy of electricity carbon footprint: Estimation of hydroelectric reservoir greenhouse gas emissions. *Renewable and Sustainable Energy Reviews*, *136*. https://doi.org/10.1016/j.rser.2020.110433

Li, S., & Zhang, Q. (2014). Carbon emission from global hydroelectric reservoirs revisited. *Environmental Science and Pollution Research*, *21*(23), 13636–13641. https://doi.org/10.1007/s11356-014-3165-4

Li, Z., Du, H., Xu, H., Xiao, Y., Lu, L., Guo, J., Prairie, Y., & Mercier-Blais, S. (2019). The carbon footprint of large- and mid-scale hydropower in China: Synthesis from five China's largest hydro-project. *Journal of Environmental Management*, *250*. https://doi.org/10.1016/j.jenvman.2019.109363

Li, Z., Sun, Z., Chen, Y., Li, C., Pan, Z., Harby, A., Lv, P., Chen, D., & Guo, J. (2020a). The net GHG emissions of the China Three Gorges Reservoir: I. Pre-impoundment GHG inventories and carbon balance. *Journal of Cleaner Production*, *256*. https://doi.org/10.1016/j.jclepro.2020.120635

Li, Z., Sun, Z., Chen, Y., Li, C., Pan, Z., Harby, A., Lv, P., Chen, D., & Guo, J. (2020b). The net GHG emissions of the Three Gorges Reservoir in China: II. Post-impoundment GHG inventories and full-scale synthesis. *Journal of Cleaner Production*, *277*. https://doi.org/10.1016/j.jclepro.2020.123961

Li, M., & He, N. (2022). Carbon intensity of global existing and future hydropower reservoirs. *Renewable and Sustainable Energy Reviews*, *162*. https://doi.org/10.1016/j.rser.2022.112433

Li, C., Wang, Y., Yi, Y., Wang, X., Augusto Guimarães Santos, C., & Liu, Q. (2024). A review of reservoir carbon Cycling: Key Processes, influencing factors and research methods. In

Ecological Indicators (Vol. 166). Elsevier B.V. https://doi.org/10.1016/j.ecolind.2024.112511

Lindsay, R. (2018). Peatland classification. In *The Wetland Book: I: Structure and Function, Management, and Methods* (pp. 1515–1528). Springer Netherlands. https://doi.org/10.1007/978-90-481-9659-3_341

Loisel, J., Gallego-Sala, A. V., Amesbury, M. J., Magnan, G., Anshari, G., Beilman, D. W., Benavides, J. C., Blewett, J., Camill, P., Charman, D. J., Chawchai, S., Hedgpeth, A., Kleinen, T., Korhola, A., Large, D., Mansilla, C. A., Müller, J., van Bellen, S., West, J. B., … Wu, J. (2021). Expert assessment of future vulnerability of the global peatland carbon sink. *Nature Climate Change*, *11*(1), 70–77. https://doi.org/10.1038/s41558-020-00944-0

Loisel, J., Gallego-Sala, A. (2022). Ecological resilience of restored peatlands to climate change. Commun Earth Environ 3, 208. https://doi.org/10.1038/s43247-022-00547-x

Louis, V. L. S., Partridge, A. D., Kelly, C. A., & Rudd, J. W. M. (2003). *Mineralization rates of peat from eroding peat islands in reservoirs*.

Lourenco, M., Fitchett, J. M., & Woodborne, S. (2023). Peat definitions: A critical review. *Progress in Physical Geography*, *47*(4), 506–520. https://doi.org/10.1177/03091333221118353

Lund, M., Lafleur, P. M., Roulet, N. T., Lindroth, A., Christensen, T. R., Aurela, M., Chojnicki, B. H., Flanagan, L. B., Humphreys, E. R., Laurila, T., Oechel, W. C., Olejnik, J., Rinne, J., Schubert, P., & Nilsson, M. B. (2010). Variability in exchange of CO2 across 12 northern peatland and tundra sites. *Global Change Biology*, *16*(9), 2436–2448. https://doi.org/10.1111/j.1365-2486.2009.02104.x

Maavara, T., Lauerwald, R., Regnier, P., & Van Cappellen, P. (2017). Global perturbation of organic carbon cycling by river damming. *Nature Communications*, *8*. https://doi.org/10.1038/ncomms15347

Maeck, A., Hofmann, H., & Lorke, A. (2014). Pumping methane out of aquatic sediments – Ebullition forcing mechanisms in an impounded river. *Biogeosciences*, *11*(11), 2925–2938. https://doi.org/10.5194/bg-11-2925-2014

MacLaren Plansearch Inc. InterGroup Consultants Ltd. (1986). Limestone Generating Station Environmental Impact Study: Final Report. 189 pages.

Mahdiyasa, A. W., Large, D. J., Muljadi, B. P., & Icardi, M. (2023). Modelling the influence of mechanical-ecohydrological feedback on the nonlinear dynamics of peatlands. *Ecological Modelling*, *478*. https://doi.org/10.1016/j.ecolmodel.2023.110299

Maljanen, M., Sigurdsson, B. D., Guðmundsson, J., Oskarsson, H. ´, Huttunen, J. T., & Martikainen, P. J. (2009). Land-use and greenhouse gas balances of peatlands Land-use and greenhouse gas balances of peatlands in the Nordic countries-present knowledge and gaps Land-use and greenhouse gas balances of peatlands. In *Biogeosciences Discuss* (Vol. 6). www.biogeosciences-discuss.net/6/6271/2009/

Manitoba and Manitoba Hydro. (2014). Regional Cumulative Effects Assessment for Hydroelectric Developments on the Churchill, Burntwood and Nelson River Systems. Phase I Report. May 2014. https://www.hydro.mb.ca/docs/regulatory_affairs/pdf/rcea/part123_rcea_phase1.pdf

Manitoba and Manitoba Hydro. (2015). Regional Cumulative Effects Assessment for Hydroelectric Developments on the Churchill, Burntwood and Nelson River Systems. Phase II Report: Hydroelectric Development Project Description in the Region of Interest. Part II. December 2015. https://www.hydro.mb.ca/docs/regulatory_affairs/pdf/rcea/rcea_phase2_part_ii_hydroelectric_development_project_description.pdf

Manitoba. (2024). Manitoba's Affordable Energy Plan: Building the Next Generation of Clean Energy. September 2024. https://www.gov.mb.ca/asset_library/en/energyplan/mb-affordable-energy-plan.pdf

Manitoba. (2025). Manitoba's Path to Net Zero: Guided by the Spirit of Manoomin. October 2025. https://www.gov.mb.ca/asset_library/en/netzero/mb-path-to-net-zero.pdf

Manitoba Conservation and Climate. (2021). Final Licence for the Diversion of Water from The Churchill River to the Nelson River, and the Impoundment of Water on the Rat River and Southern Indian Lake. https://www.gov.mb.ca/sd/water/water-power/churchill/cover_letter_licence_churchill_river_diversion.pdf

Manitoba Conservation and Water Stewardship. (2014). Interim Licence for the Development of Water Power, Keeyask Site, Nelson River. Issued in accordance with The Water Power Act (C.C.S.M., c.W60), and the Water Power Regulation (MR. 25/88R). Manitoba Conservation and Water Stewardship, The Province of Manitoba.

Manitoba Geological Survey. (2004). Geological Map of Manitoba, Scale 1:1 000 000, Map 79-2. https://home.cc.umanitoba.ca/~mlast/rpublications/assets/mapManitoba.pdf

Manitoba Hydro. (2012). Keeyask Transmission Project Environmental Assessment Report. Chapter 4 Environmental Setting. November 2012. 49 pages.

Manitoba Hydro. (2013). Kettle Generating Station. Manitoba Hydro. Public Affairs. Winnipeg, Manitoba.

Manitoba Hydro. (2013b). Needs For and Alternatives To Appendix 7.3 – Life Cycle Greenhouse Gas Assessment Overview. 15 pages. https://www.pubmanitoba.ca/nfat/pdf/hydro_application/appendix_07_3_life_cycle_greenhouse_gas_assessment_overview.pdf

Manitoba Hydro. (2015). Flooded Areas for Manitoba Hydro System. [Unpublished manuscript]. Manitoba Hydro, Winnipeg, Manitoba.

Manitoba Hydro. (2018). Manitoba Hydro Long Spruce Generating Station Licence Implementation Guide for Water Levels. Report No. PS&O 18/07. https://www.gov.mb.ca/sd/pubs/water/licensing/long_spruce/long_spruce_lig.pdf

Manitoba Hydro 2020. Manitoba Hydro's Climate Change Report. March 2020. 34 pages. www.hydro.mb.ca/docs/corporate/climate_change_report_2020.pdf

Manitoba Hydro 2021. 2020-2021 Physical Environment Monitoring Report. Year 7 Construction. Keeyask Generation Project Physical Environment Monitoring Plan Report #PEMP-2021-01. June 2021. https://keeyask.com/wp-content/uploads/2021/06/PEMP-2021-01-Physical-Environment-Monitoring.pdf

Manitoba Hydro 2023. 2022-2023 Physical Environment Monitoring Report. Year 2 Operation. Keeyask Generation Project Physical Environment Monitoring Plan Report #PEMP-2023-01. June 2023. https://keeyask.com/wp-content/uploads/2023/06/PEMP-2023-01-Physical-Environment-Monitoring.pdf

Manitoba Hydro 2024. 2023-2024 Physical Environment Monitoring Report. Year 3 Operation. Keeyask Generation Project Physical Environment Monitoring Plan Report #PEMP-2024-01. June 2024. https://keeyask.com/wp-content/uploads/2024/06/PEMP-2024-01-Physical-Environment-Monitoring.pdf

Manitoba Hydro 2025a. 2024-2025 Physical Environment Monitoring Report. Year 4 Operation. Keeyask Generation Project Physical Environment Monitoring Plan Report #PEMP-2025-01. June 2025. https://keeyask.com/wp-content/uploads/2025/06/PEMP-2025-01-Physical-Environment-Monitoring.pdf

Manitoba Hydro. (2025b). Manitoba Hydro Generation. https://www.hydro.mb.ca/corporate/operations/generation

Manitoba Hydro. (2025c). 2025 Integrated Resource Plan: Road Map. https://www.hydro.mb.ca/docs/corporate/irp/2025-irp-roadmap.pdf

Manitoba Hydro. (2025d). 2023 Integrated Resource Plan Document Library: Appendix 1 – Existing System & Load https://www.hydro.mb.ca/docs/corporate/irp/irp-2023-a1-existing-system-and-load.pdf

Manitoba Hydro. (2026). Manitoba Hydro Station Generation. [Unpublished report]. Manitoba Hydro, Winnipeg, Manitoba.

Mann, P. J., Strauss, J., Palmtag, J., Dowdy, K., Ogneva, O., Fuchs, M., Bedington, M., Torres, R., Polimene, L., Overduin, P., Mollenhauer, G., Grosse, G., Rachold, V., Sobczak, W. V, Spencer, R. G. M., & Juhls, B. (2022). *Degrading permafrost river catchments and their impact on Arctic Ocean nearshore processes*. Ambio 2022, 51:439–455. https://doi.org/10.1007/s13280-021-01666-z

Männistö, E., Korrensalo, A., Alekseychik, P., Mammarella, I., Peltola, O., Vesala, T., & Tuittila, E. S. (2019). Multi-year methane ebullition measurements from water and bare peat surfaces of

a patterned boreal bog. *Biogeosciences*, *16*(11), 2409–2421. https://doi.org/10.5194/bg-16-2409-2019

Marchand D., M. Demarty and R. Gill. (2012). Reservoir Greenhouse Gas Monitoring Report –2012. Report prepared by Environnement Illimité inc. for Manitoba Hydro, Tier 1: 34 p. and 1 appendix and Tier 2: 51 p.

Marchand D., M. Demarty, and R. Gill. 2015. Keeyask Technical Summay – 2014. Summary prepared by Environnement Illimité for Manitoba Hydro, 11 p.

Margolis, H. A., Flanagan, L. B., & Amiro, B. D. (2006). The Fluxnet-Canada Research Network: Influence of climate and disturbance on carbon cycling in forests and peatlands. In *Agricultural and Forest Meteorology* (Vol. 140, Issues 1–4, pp. 1–5). https://doi.org/10.1016/j.agrformet.2006.08.013

Matile, G.L.D. and Keller, G.R. (2206). Surficial geology of the Uhlman Lake map sheet (NTS 64B), Manitoba; Manitoba Science, Technology, Energy and Mines, Manitoba Geological Survey, Surficial Geology Compilation Map Series, SG-64B, scale 1:250,000. https://www.manitoba.ca/iem/geo/gis/surfgeomap.html

McClure, R. P., Lofton, M. E., Chen, S., Krueger, K. M., Little, J. C., & Carey, C. C. (2020). The Magnitude and Drivers of Methane Ebullition and Diffusion Vary on a Longitudinal Gradient in a Small Freshwater Reservoir. *Journal of Geophysical Research: Biogeosciences*, *125*(3). https://doi.org/10.1029/2019JG005205

McCullough, G.K. 1981. Water budgets for Southern Indian Lake, before and after impoundment and Churchill River diversion, 1972-79. Can. MS Rep. Fish. Aquat. Sci. 1620: iv + 22 p. https://waves-vagues.dfo-mpo.gc.ca/Library/74117.pdf

McLaughlin, J. W., & Packalen, M. S. (2021). Peat Carbon Vulnerability to Projected Climate Warming in the Hudson Bay Lowlands, Canada: A Decision Support Tool for Land Use Planning in Peatland Dominated Landscapes. *Frontiers in Earth Science*, *9*. https://doi.org/10.3389/feart.2021.650662

Minister Responsible for Manitoba Hydro. (2023). Manitoba Hydro-Electric Board Mandate Letter. https://manitoba.ca/asset_library/en/executivecouncil/mandate/hydro_mandate_letter_2023.pdf

Minnesota Department of Commerce. (2023). Governor Walz Signs Bill Moving Minnesota to 100 Percent Clean Energy by 2040. February 7, 2023. https://mn.gov/commerce/news/?id=17-563384

Minnesota Legislature Chapter 7--H.F.No. 7. (2023). Laws of Minnesota 2023. https://www.revisor.mn.gov/laws/2023/0/Session+Law/Chapter/7/2023-08-07%2011:36:24+00:00/pdf

Minnesota Legislature H. F. No. 75. (2025). Hydroelectric capacity that qualifies as an eligible energy technology under the renewable energy standard modified. https://www.revisor.mn.gov/bills/94/2025/0/HF/75/

MISO. (2025). Midcontinent Independent System Operator (MISO). https://www.misoenergy.org/meet-miso/about-miso/

Momcilovic-Petronijevic, A., Trajkovic, S., & Randjelovic, V. (2009). Anthropogenic effects on environment: Case study: Peat islands of lake Vlasina. *Facta Universitatis - Series: Architecture and Civil Engineering*, *7*(1), 95–105. https://doi.org/10.2298/fuace0901095m

Mozafari, B., Bruen, M., Donohue, S., Renou-Wilson, F., & O'Loughlin, F. (2023). Peatland dynamics: A review of process-based models and approaches. In *Science of the Total Environment* (Vol. 877). Elsevier B.V. https://doi.org/10.1016/j.scitotenv.2023.162890

National Energy Boad. (2019). Canada's Energy Transition: An Energy Market Assessment. NE2-23E-PDF ISSN 2562-5314. 52 pages. https://www.cer-rec.gc.ca/en/data-analysis/energy-markets/canadas-energy-transition/cndsnrgtrnstn-eng.pdf

National Renewable Energy Laboratory (2021). Life Cycle Greenhouse Gas Emissions from Electricity Generation. NREL/FS-6A50-80580

National Wetlands Working Group. (1987). The Canadian wetland classification system / National Wetlands Working Group, Canada Committee on Ecological Land Classification. Ecological land classification series ; No. 21. [Ottawa] : Lands Conservation Branch, Canadian Wildlife Service, Environment Canada, 1987. https://publications.gc.ca/site/eng/9.867506/publication.html

Natural Resources Canada. (2019). The Atlas of Canada - Physiographic Regions. Government of Canada. https://atlas.gc.ca/phys/en/index.html

Natural Resources Canada. (2026). Powering Canada Strong: A National Strategy for an Electrified Canadian Economy. ISBN: 978-0-660-98304-2 Cat. No.: M4-287/2026E-PDF
https://natural-resources.canada.ca/energy-sources/electricity-infrastructure/powering-canada-strong-national-strategy-electrified-canadian-economy

Neal, J. W., & Lloyd, M. C. (2018). Response of Fish Populations to Floating Streambed Wetlands. In *JSAFWA Journal of the Southeast. Association of Fish and Wildlife Agencies* (Vol. 5).

Nelson, J. A., Walther, S., Gans, F., Kraft, B., Weber, U., Novick, K., Buchmann, N., Migliavacca, M., Wohlfahrt, G., Šigut, L., Ibrom, A., Papale, D., Göckede, M., Duveiller, G., Knohl, A., Hörtnagl, L., Scott, R. L., Zhang, W., Hamdi, Z. M., … Jung, M. (2024). *X-BASE: the first terrestrial carbon and water flux products from an extended data-driven scaling framework, FLUXCOM-X*. https://doi.org/10.5194/egusphere-2024-165

Nichols, J. E., & Peteet, D. M. (2019). Rapid expansion of northern peatlands and doubled estimate of carbon storage. *Nature Geoscience*, *12*(11), 917–921. https://doi.org/10.1038/s41561-019-0454-z

Nicholson, S., & Heath, G. (2012). *Life Cycle Greenhouse Gas Emissions from Electricity Generation: Update Life Cycle Assessment of Energy Systems*. https://data.nrel.gov/submissions/171

O'Donoughue, P. R., Heath, G. A., Dolan, S. L., & Vorum, M. (2014). Life Cycle Greenhouse Gas Emissions of Electricity Generated from Conventionally Produced Natural Gas: Systematic Review and Harmonization. *Journal of Industrial Ecology*, *18*(1), 125–144. https://doi.org/10.1111/jiec.12084

Olefeldt, D., Hovemyr, M., Kuhn, M. A., Bastviken, D., Bohn, T. J., Connolly, J., Crill, P., Euskirchen, E. S., Finkelstein, S. A., Genet, H., Grosse, G., Harris, L. I., Heffernan, L., Helbig, M., Hugelius, G., Hutchins, R., Juutinen, S., Lara, M. J., Malhotra, A., … Watts, J. D. (2021). The boreal-arctic wetland and lake dataset (BAWLD). *Earth System Science Data*, *13*(11), 5127–5149. https://doi.org/10.5194/essd-13-5127-2021

Ostrovsky, I., McGinnis, D.F., Lapidus, L., Eckert, W. (2008). Quantifying gas ebullition with echosounder: the role of methane transport by bubbles in a medium-sized lake. Limnol. Oceanogr.: Methods 6, 2008, 105–118.

Packalen, M. S., Finkelstein, S. A., & McLaughlin, J. W. (2014). Carbon storage and potential methane production in the Hudson Bay Lowlands since mid-Holocene peat initiation. *Nature Communications*, *5*. https://doi.org/10.1038/ncomms5078

Pan Y, Birdsey RA, Fang J, et al. 2011. A Large and Persistent Carbon Sink in the World's Forests. Science 333 (6045): 988-993. DOI: 10.1126/science.1201609.

Pastorello, G., Trotta, C., Canfora, E. et al. (2020). The FLUXNET2015 dataset and the ONEFlux processing pipeline for eddy covariance data. Sci Data 7, 225. https://doi.org/10.1038/s41597-020-0534-3

Pawlowska-Mainville & Massan. (2022). "The Flooders" and "the Cree": Challenging the Hydro Metanarrative Using Achimowinak "Stories". In A. Craft & J. Blakley (Eds.), *In Our Backyard: Keeyask and the Legacy of Hydroelectric Development* (pp. 147-172). University of Manitoba Press.

Pelletier, Luc. (2007). *Carbon dioxide and methane fluxes of three peatlands in the La Grande Rivière watershed, James Bay lowland, Canada*. Library and Archives Canada = Bibliothèque et Archives Canada.

Pelletier, L., Garneau, M., & Tremblay, A. (2009). CO2 and CH4 ecosystem exchange from peatlands: Eastmain-1 hydroelectric project, Quebec, Canada. In *Verh. Internat. Verein. Limnol* (Vol. 30).

Pelletier, L., Garneau, M., & Moore, T. R. (2011). Variation in CO2 exchange over three summers at microform scale in a boreal bog, Eastmain region, Québec, Canada. *Journal of Geophysical Research: Biogeosciences*, *116*(3). https://doi.org/10.1029/2011JG001657

Pelletier, L., Strachan, I. B., Garneau, M., & Roulet, N. T. (2014). Carbon release from boreal peatland open water pools: Implication for the contemporary C exchange. *Journal of Geophysical Research: Biogeosciences*, *119*(3), 207–222. https://doi.org/10.1002/2013JG002423

Pelletier, L., Strachan, I. B., Roulet, N. T., Garneau, M., & Wischnewski, K. (2015). Effect of open water pools on ecosystem scale surface-atmosphere carbon dioxide exchange in a boreal peatland. *Biogeochemistry*, *124*(1–3), 291–304. https://doi.org/10.1007/s10533-015-0098-z

Phillips I., Jardine T.D., Lindenschmidt K.E., Westbrook C., Pomeroy J. (2023). Nelson and Churchill River Basins. In Rivers of North America. 2nd ed. Edited by Delong M.D., Jardine T.D., Benke A.C., Cushing C.E. Academic Press. pp. 794–834.

Physical Activities Regulations, SOR/2019-285. (2019). https://laws.justice.gc.ca/PDF/SOR-2019-285.pdf

Pokorny, S., Stadnyk, T. A., Ali, G., Lilhare, R., Déry, S. J., & Koenig, K. (2021). Cumulative effects of uncertainty on simulated streamflow in a hydrologic modeling environment. *Elementa*, *9*(1). https://doi.org/10.1525/elementa.431

Prairie, Y. & Cole, J. (2009). Carbon, Unifying Currency. Encyclopedia of Inland Waters. 2. 743-746. 10.1016/B978-012370626-3.00107-1.

Prairie YT, Alm J, Harby A, Mercier-Blais S, Nahas R. (2017a). The GHG Reservoir Tool (Gres) Technical documentation. Updated version 3.31 (03-07-2025). UNESCO/IHA research project on the GHG status of freshwater reservoirs. Joint publication of the UNESCO Chair in Global Environmental Change and the International Hydropower Association. 72 pages.

Prairie YT, Alm J, Harby A, Mercier-Blais S, Nahas R. (2017b). The GHG Reservoir Tool (G-res) User guide, UNESCO/IHA research project on the GHG status of freshwater reservoirs. Updated version 3.31 (03-07-2025). Joint publication of the UNESCO Chair in Global Environmental Change and the International Hydropower Association. 44 pages.

Prairie, Y. T., Alm, J., Beaulieu, J., Barros, N., Battin, T., Cole, J., del Giorgio, P., DelSontro, T., Guérin, F., Harby, A., Harrison, J., Mercier-Blais, S., Serça, D., Sobek, S., & Vachon, D. (2018). Greenhouse Gas Emissions from Freshwater Reservoirs: What Does the Atmosphere See? *Ecosystems*, *21*(5), 1058–1071. https://doi.org/10.1007/s10021-017-0198-9

Prairie, Y. T., Mercier-Blais, S., Harrison, J. A., Soued, C., Giorgio, P. del, Harby, A., Alm, J., Chanudet, V., & Nahas, R. (2021). A new modelling framework to assess biogenic GHG emissions from reservoirs: The G-res tool. *Environmental Modelling and Software*, *143*. https://doi.org/10.1016/j.envsoft.2021.105117

Prairie, Y.T., DelSontro, T., del Giorgio, P., Mercier-Blais, S., Albert, E., Cuerrier, S., Islam, R. (2023). GHG-CaRe: an update Constraining the GHG footprint of Canada's flooded land. [Unpublished presentation] Mini-Symposium Hydro-Québec sur les émissions biogéniques

de GES / Mini-Symposium Hydro-Québec on biogenic GHG emissions. November 8-9, 2024. Montréal, Québec.

Prairie, Y.T. (2024). GHG-CaRe All Partners Meeting: Introduction. [Unpublished presentation]. L'Université du Québec à Montréal. February 12-14, 2024. Montreal, Québec.

Prairie, Y.T. (2025). GHG-CaRe All Partners Meeting: Introduction. [Unpublished presentation]. L'Université du Québec à Montréal. February 26-28, 2025. Montreal, Québec.

Rantakari, M. and P. Kortelainen. (2008). Controls of organic and inorganic carbon in randomly selected Boreal lakes in varied catchments, Biogeochemistry, 91, pages 151–162, DOI 10.1007/s10533-008-9266-8

Räsänen, N., P. Kankaala, T. Tahvanainen, J. Akkanen, S. Saarnio. (2014). Short-term effects of phosphorus addition and pH rise on bacterial utilization and biodegradation of dissolved organic carbon (DOC) from boreal mires, Aquatic Ecology, 48, pages 435–446, DOI 10.1007/s10452-014-9496-x

Rasanen, T. A., Varis, O., Scherer, L., & Kummu, M. (2018). Greenhouse gas emissions of hydropower in the Mekong River Basin. *Environmental Research Letters*, *13*(3). https://doi.org/10.1088/1748-9326/aaa817

Regnier, P., Resplandy, L., Najjar, R.G., Ciais, P. (2022). The land-to-ocean loops of the global carbon cycle. Nature 603, 401–410. https://doi.org/10.1038/s41586-021-04339-9

Reinsel, M. (2014). Floating islands for stormwater and other applications. Water Online. https://www.wateronline.com/doc/floating-islands-for-stormwater-and-other-applications-0001

Richer, M. (2025). All about uncertainty in carbon footprint measurement. Tennaxia. https://www.tennaxia.com/en/blog/tout-savoir-sur-lincertitude-dans-la-mesure-de-lempreinte-carbone

Rogelj, J., D. Shindell, K. Jiang, S. Fifita, P. Forster, V. Ginzburg, C. Handa, H. Kheshgi, S. Kobayashi, E. Kriegler, L. Mundaca, R. Séférian, and M.V.Vilariño. (2018). Mitigation Pathways Compatible with 1.5°C in the Context of Sustainable Development. In: Global Warming of 1.5°C. An IPCC Special Report on the impacts of global warming of 1.5°C above pre-industrial levels and related global greenhouse gas emission pathways, in the context of strengthening the global response to the threat of climate change, sustainable development, and efforts to eradicate poverty [Masson-Delmotte, V., P. Zhai, H.-O. Pörtner, D. Roberts, J. Skea, P.R. Shukla, A. Pirani, W. Moufouma-Okia, C. Péan, R. Pidcock, S. Connors, J.B.R. Matthews, Y. Chen, X. Zhou, M.I. Gomis, E. Lonnoy, T. Maycock, M. Tignor, and T. Waterfield (eds.)]. Cambridge University Press, Cambridge, UK and New York, NY, USA, pp. 93-174. https://doi.org/10.1017/9781009157940.004.

Rönkä, E., Uusinoka, R. (1976). The problem of peat upheaval in Finnish artificial reservoirs. *Bulletin of The International Association of Engineering Geology* (Vol. 14), 71-74. https://doi.org/10.1007/BF02634763

Rosenberg, D., Chambers, P., Culp, J., & Franzin, W. (2005). Nelson and Churchill river basins. In A. Benke & C. Cushing (Eds.), Rivers of North America (pp. 853–892). Massachusetts: Elsevier Academic Press Burlington.

Rosentreter, J. A., Borges, A. V., Deemer, B. R., Holgerson, M. A., Liu, S., Song, C., Melack, J., Raymond, P. A., Duarte, C. M., Allen, G. H., Olefeldt, D., Poulter, B., Battin, T. I., & Eyre, B. D. (2021). Half of global methane emissions come from highly variable aquatic ecosystem sources. *Nature Geoscience*, *14*(4), 225–230. https://doi.org/10.1038/s41561-021-00715-2

Roulet, N. T., Lafleur, P. M., Richard, P. J. H., Moore, T. R., Humphreys, E. R., & Bubier, J. (2007). Contemporary carbon balance and late Holocene carbon accumulation in a northern peatland. *Global Change Biology*, *13*(2), 397–411. https://doi.org/10.1111/j.1365-2486.2006.01292.x

Rust, F., Bodmer, P., & del Giorgio, P. (2022). Modeling the spatial and temporal variability in surface water CO2 and CH4 concentrations in a newly created complex of boreal hydroelectric reservoirs. *Science of the Total Environment*, *815*. https://doi.org/10.1016/j.scitotenv.2021.152459

Salo, J., Venkatesh, P., Patel, C. (2024). The complexities of data quality and company-reported emissions. https://www.spglobal.com/esg/insights/blog/the-complexities-of-data-quality-and-company-reported-emissions

Saquet, M. (2003). Greenhouse gas flux and budget from an experimentally flooded wetland using stable isotopes and geochemistry. UWSpace. http://hdl.handle.net/10012/1249

Scherer, L., & Pfister, S. (2016). Hydropower's biogenic carbon footprint. *PLoS ONE*, *11*(9). https://doi.org/10.1371/journal.pone.0161947

Schuur, E. A. G., McGuire, A. D., Schädel, C., Grosse, G., Harden, J. W., Hayes, D. J., Hugelius, G., Koven, C. D., Kuhry, P., Lawrence, D. M., Natali, S. M., Olefeldt, D., Romanovsky, V. E., Schaefer, K., Turetsky, M. R., Treat, C. C., & Vonk, J. E. (2015). Climate change and the permafrost carbon feedback. In *Nature* (Vol. 520, Issue 7546, pp. 171–179). Nature Publishing Group. https://doi.org/10.1038/nature14338

Science Based Targets initiative (SBTi). (2024). SBTi Corporate Net-Zero Standard. Version 1.2. March 2024. https://sciencebasedtargets.org/net-zero

Science Based Targets initiative (SBTi). (2025). SBTi Corporate Net-Zero Standard. Version 2.0 - Initial Consultation Draft with Narrative. March 2025. https://files.sciencebasedtargets.org/production/files/Net-Zero-Standard-v2-Consultation-Draft.pdf

Scott, K. J., Kelly, C. A., & Rudd, J. W. M. (1999). The importance of floating peat to methane fluxes from flooded peatlands. In *Biogeochemistry* (Vol. 47, Issue 9). KluwerAcademic Publishers.

Scott, C. (2022). Energy in Transition: Achieving Decentralisation with Distributed Technology. Tony Blair Institute for Global Change. https://institute.global/insights/climate-and-energy/energy-transition-achieving-decentralisation-distributed-technology

Seitzinger, S., Harrison, J. A., Böhlke, J. K., Bouwman, A. F., Lowrance, R., Peterson, B., Tobias, C., & Van Drecht, G. (2006). Denitrification across landscapes and waterscapes: A synthesis. In *Ecological Applications* (Vol. 16, Number 6, pp. 2064–2090). https://doi.org/10.1890/1051-0761(2006)016[2064:DALAWA]2.0.CO;2

Sharif, S., Mann, J.D., Smith, J.B., Cook, G.N. (2012). Techniques for 3D Geological and Hydrogeological Modeling. A Case Study of Conawapa Generating Station. Canadian Geotechnical Society Annual Conference, Winnipeg, Manitoba. September 30 – October 3, 2012.

Sharifi, A., Kalin, L., Hantush, M. M., Isik, S., & Jordan, T. E. (2013). Carbon dynamics and export from flooded wetlands: A modeling approach. *Ecological Modelling*, *263*, 196–210. https://doi.org/10.1016/j.ecolmodel.2013.04.023

Shi, W., Chen, Q., Zhang, J., Zheng, F., Liu, D., Yi, Q., & Chen, Y. (2020). Enhanced riparian denitrification in reservoirs following hydropower production. *Journal of Hydrology*, *583*. https://doi.org/10.1016/j.jhydrol.2019.124305

Smith, R.E., Veldhuis, H., Mills, G.F., Eilers, R.G., Fraser, W.R., Lelyk, G.W. (1998). Terrestrial Ecozones, Ecoregions, and Ecodistricts of Manitoba, An Ecological Stratification of Manitoba's Natural Landscapes. Technical Bulletin 1998-9E. Land Resource Unit, Brandon Research Centre, Research Branch, Agriculture and Agri-Food Canada, Winnipeg, Manitoba. Report and map at 1:1 500 000 scale

Smith, E. Prairie, Y. (2004). Bacterial metabolism and growth efficiency in lakes: the importance of phosphorous availability. Limnol Oceangr 49(1):137-147

Smith, C., Z.R.J. Nicholls, K. Armour, W. Collins, P. Forster, M. Meinshausen, M.D. Palmer, and M. Watanabe. (2021). The Earth's Energy Budget, Climate Feedbacks, and Climate Sensitivity Supplementary Material. In Climate Change 2021: The Physical Science Basis. Contribution of Working Group I to the Sixth Assessment Report of the Intergovernmental Panel on Climate Change [Masson-Delmotte, V., P. Zhai, A. Pirani, S.L. Connors, C. Péan, S. Berger, N. Caud, Y. Chen, L. Goldfarb, M.I. Gomis, M. Huang, K. Leitzell, E. Lonnoy, J.B.R. Matthews, T.K. Maycock, T. Waterfield, O. Yelekçi, R. Yu, and B. Zhou (eds.)]. Available from https://www.ipcc.ch/

Sothe, C., Gonsamo, A., Arabian, J., & Snider, J. (2022). Large scale mapping of soil organic carbon concentration with 3D machine learning and satellite observations. *Geoderma*, *405*. https://doi.org/10.1016/j.geoderma.2021.115402

Soued, C., & Prairie, Y. T. (2020). The carbon footprint of a Malaysian tropical reservoir: measured versus modelled estimates highlight the underestimated key role of downstream processes. *Biogeosciences*, *17*(2), 515–527. https://doi.org/10.5194/bg-17-515-2020

Soued, C., Harrison, J. A., Mercier-Blais, S., & Prairie, Y. T. (2022). Reservoir CO2 and CH4 emissions and their climate impact over the period 1900–2060. *Nature Geoscience*, *15*(9), 700–705. https://doi.org/10.1038/s41561-022-01004-2

Spence, C., Norris, M., Bickerton, G., Bonsal, B. R., Brua, R., Culp, J. M., Dibike, Y., Gruber, S., Morse, P. D., Peters, D. L., Shrestha, R., & Wolfe, S. A. (2020). The Canadian water resource vulnerability index to permafrost thaw (Cwrvipt). *Arctic Science*, *6*(4), 437–462. https://doi.org/10.1139/as-2019-0028

Spracklen, D. V., Bonn, B., & Carslaw, K. S. (2008). Boreal forests, aerosols and the impacts on clouds and climate. *Philosophical Transactions of the Royal Society A: Mathematical, Physical and Engineering Sciences*, *366*(1885), 4613–4626. https://doi.org/10.1098/rsta.2008.0201

St. Louis, V. L., Kelly, C. A., Duchemin, É., Rudd, J. W. M., & Rosenberg, D. M. (2000). Reservoir surfaces as sources of greenhouse gases to the atmosphere: A global estimate. In *BioScience* (Vol. 50, Issue 9, pp. 766–775). Oxford University Press. https://doi.org/10.1641/0006-3568(2000)050[0766:RSASOG]2.0.CO;2

St. Louis, V.L., Partridge, A.D., Kelly, C.A., Rudd, J. (2003). Mineralization rates of peat from eroding peat islands in reservoirs. Biogeochemistry 64, 97–110. https://doi.org/10.1023/A:1024982915493

Stępniewska, Z., & Goraj, W. (2014). Transformation of methane in peatland environments. *Forest Research Papers*, *75*(1), 101–110. https://doi.org/10.2478/frp-2014-0010

Strachan, I. B., Nugent, K. A., Crombie, S., & Bonneville, M. C. (2015). Carbon dioxide and methane exchange at a cool-temperate freshwater marsh. *Environmental Research Letters*, *10*(6). https://doi.org/10.1088/1748-9326/10/6/065006

Strachan, I. B., Pelletier, L., & Bonneville, M. C. (2016). Inter-annual variability in water table depth controls net ecosystem carbon dioxide exchange in a boreal bog. *Biogeochemistry*, *127*(1), 99–111. https://doi.org/10.1007/s10533-015-0170-8

Strack, M (ed). (2008). Peatlands and Climate Change. International Peat Society, ISBN 9529940114, 9789529940110, 223 pages

Strack, M., Mwakanyamale, K., Hassanpour Fard, G., Bird, M., Bérubé, V., & Rochefort, L. (2017). Effect of plant functional type on methane dynamics in a restored minerotrophic peatland. *Plant and Soil*, *410*(1–2), 231–246. https://doi.org/10.1007/s11104-016-2999-6

Strack, M., Davidson, S. J., Hirano, T., & Dunn, C. (2022). The Potential of Peatlands as Nature-Based Climate Solutions. In *Current Climate Change Reports* (Vol. 8, Issue 3, pp. 71–82). Springer Science and Business Media Deutschland GmbH. https://doi.org/10.1007/s40641-022-00183-9

Statutes of Canada 2024 Chapter 15 Bill C-59. (2024). An Act to implement certain provisions of the fall economic statement tabled in Parliament on November 21, 2023 and certain provisions

of the budget tabled in Parliament on March 28, 2023. Assented to June 20, 2024. https://laws-lois.justice.gc.ca/PDF/2024_15.pdf

Statutes of Canada. (2026). An Act to implement certain provisions of the budget tabled in Parliament on November 4, 2025. Assented to March 26, 2026. https://www.parl.ca/Content/Bills/451/Government/C-15/C-15_4/C-15_4.PDF

Straková, P., R. M. Niemi, C. Freeman, K. Peltoniemi, H. Toberman, I. Heiskanen, H. Fritze, R. Laiho. (2011). Litter type affects the activity of aerobic decomposers in a boreal peatland more than site nutrient and water table regimes, Biogeosciences, 8, pages 2741–2755, www.biogeosciences.net/8/2741/2011/doi:10.5194/bg-8-2741-2011.

Tank, S. E., Fellman, J. B., Hood, E., & Kritzberg, E. S. (2018). Beyond respiration: Controls on lateral carbon fluxes across the terrestrial-aquatic interface. Limnology And Oceanography Letters, 3(3), 76–88. https://doi.org/10.1002/lol2.10065

Tarnocai, C. (2006). The effect of climate change on carbon in Canadian peatlands. Global and Planetary Change, 53(4), 222–232. https://doi.org/10.1016/j.gloplacha.2006.03.012

Teodoru, C. R., Prairie, Y. T., & del Giorgio, P. A. (2011). Spatial Heterogeneity of Surface CO2 Fluxes in a Newly Created Eastmain-1 Reservoir in Northern Quebec, Canada. *Ecosystems*, *14*(1), 28–46. https://doi.org/10.1007/s10021-010-9393-7

Teodoru, C. R., Bastien, J., Bonneville, M. C., Del Giorgio, P. A., Demarty, M., Garneau, M., Hélie, J. F., Pelletier, L., Prairie, Y. T., Roulet, N. T., Strachan, I. B., & Tremblay, A. (2012). The net carbon footprint of a newly created boreal hydroelectric reservoir. *Global Biogeochemical Cycles*, *26*(2). https://doi.org/10.1029/2011GB004187

Thalasso, F., Riquelme, B., Gómez, A., MacKenzie, R., Aguirre, F. J., Hoyos-Santillan, J., Rozzi, R., & Sepulveda-Jauregui, A. (2023). Technical note: Skirt chamber - an open dynamic method for the rapid and minimally intrusive measurement of greenhouse gas emissions from peatlands. *Biogeosciences*, *20*(18), 3737–3749. https://doi.org/10.5194/bg-20-3737-2023

The Pembina Institute, 2012. A Life Cycle Assessment of Greenhouse Gases and Select Criteria Air Contaminants. GN-9.5.5. Keeyask Project Environmental Studies Program Report prepared for Manitoba Hydro. 89 pp

Treat, C. C., Bloom, A. A., & Marushchak, M. E. (2018). Nongrowing season methane emissions–a significant component of annual emissions across northern ecosystems. *Global Change Biology*, *24*(8), 3331–3343. https://doi.org/10.1111/gcb.14137

Treat, C. C., Jones, M. C., Brosius, L., Grosse, G., Walter Anthony, K., & Frolking, S. (2021). The role of wetland expansion and successional processes in methane emissions from northern wetlands during the Holocene. *Quaternary Science Reviews*, *257*. https://doi.org/10.1016/j.quascirev.2021.106864

Treat, C. C., Virkkala, A. M., Burke, E., Bruhwiler, L., Chatterjee, A., Fisher, J. B., Hashemi, J., Parmentier, F. J. W., Rogers, B. M., Westermann, S., Watts, J. D., Blanc-Betes, E., Fuchs, M.,

Kruse, S., Malhotra, A., Miner, K., Strauss, J., Armstrong, A., Epstein, H. E., ... Hugelius, G. (2024). Permafrost Carbon: Progress on Understanding Stocks and Fluxes Across Northern Terrestrial Ecosystems. *Journal of Geophysical Research: Biogeosciences*, *129*(3). https://doi.org/10.1029/2023JG007638

Tremblay, A., Therrien, J., Hamelin, B., Wichmann, E., LeDrew, L.J. (2005). GHG emissions from boreal reservoirs and natural aquatic ecosystems. In: Tremblay, A., Varfalvy, L., Roehm, C., Garneau, M. (Eds.), Greenhouse Gas Emissions: Fluxes and Processes, Hydroelectric Reservoirs and Natural Environments. Springer-Verlag, Berlin, Heidelberg/
New York, pp. 209–231.

Tremblay, A., Demers, C., Bastien, J. Demarty, M. (2009). GHG fluxes (CO2, CH4, N2O) before and during the first 3 years after flooding at the Eastmain 1 reservoir, Quebec, Canada. In: Abstracts and electronic proceedings of the Canadian Dam Association's 2009 annual conference: protecting people, property and the environment. 214 pages. OSTI ID: 21245490. TRN: CA0905286.

Tremblay, A., Bastien, J., Bonneville, MC., del Giorgio, P., Demarty, M., Garneau, M., Helie, JF., Pelletier, L., Prairie, Y., Roulet, N., Strachan, I., & Teodoru, C. (2010). Net greenhouse gas emissions at Eastmain-1 reservoir, Quebec, Canada. World Energy Congress.

Tremblay, A. (2011). Greenhouse Gases: Measuring Net Emissions from Eastmain 1 Reservoir. Renewable Energy World. Issue 5, Volume 30. https://www.renewableenergyworld.com/energy-business/greenhouse-gases-measuring-net-emissions-from-eastmain-1-reservoir/

Trudeau, N. C., Garneau, M., & Pelletier, L. (2013). Methane fluxes from a patterned fen of the northeastern part of the La Grande river watershed, James Bay, Canada. *Biogeochemistry*, *113*(1–3), 409–422. https://doi.org/10.1007/s10533-012-9767-3

Trudeau, N., Garneau, M., & Pelletier, L. (2014). Interannual variability in the CO2 balance of a boreal patterned fen, James Bay, Canada. *Biogeochemistry*, *118*(1–3), 371–387. https://doi.org/10.1007/s10533-013-9939-9

Turetsky, M. R., Kotowska, A., Bubier, J., Dise, N. B., Crill, P., Hornibrook, E. R. C., Minkkinen, K., Moore, T. R., Myers-Smith, I. H., Nykänen, H., Olefeldt, D., Rinne, J., Saarnio, S., Shurpali, N., Tuittila, E. S., Waddington, J. M., White, J. R., Wickland, K. P., & Wilmking, M. (2014). A synthesis of methane emissions from 71 northern, temperate, and subtropical wetlands. *Global Change Biology*, *20*(7), 2183–2197. https://doi.org/10.1111/gcb.12580

Turetsky, M. R., Abbott, B. W., Jones, M. C., Anthony, K. W., Olefeldt, D., Schuur, E. A. G., Grosse, G., Kuhry, P., Hugelius, G., Koven, C., Lawrence, D. M., Gibson, C., Sannel, A. B. K., & McGuire, A. D. (2020). Carbon release through abrupt permafrost thaw. *Nature Geoscience*, *13*(2), 138–143. https://doi.org/10.1038/s41561-019-0526-0

Ubierna, M., Diez Santos, C. & Mercier-Blais, S. (2021). Water Security and Climate Change: Hydropower Reservoir Greenhouse Gas Emissions, in Water Security Under Climate Change (eds Biswas, A. & Tortajada, C.) 69–94 (Springer, 2021); https://doi.org/10.1007/978-981-16-5493-0

United Nations. (2023). Secretary-General's video message for press conference to launch the Synthesis Report of the Intergovernmental Panel on Climate Change. Statements | António Guterres, Secretary-General Interlaken, Switzerland 20 March 2023. https://www.un.org/sg/en/content/sg/statements/2023-03-20/secretary-generals-video-message-for-press-conference-launch-the-synthesis-report-of-the-intergovernmental-panel-climate-change#:~:text=Today%2C%20I%20am%20presenting%20a,Specifically:

United Nations. (2025). Countries seal landmark declaration at COP30—marking first time information integrity is prioritized at UN Climate Conference. Press Release. November 12, 2025. https://unfccc.int/news/countries-seal-landmark-declaration-at-cop30-marking-first-time-information-integrity-is-prioritized#:~:text=The%20Declaration%20commits%20signatories%20to,action%20and%20threaten%20societal%20stability.

United Nations Development Programme. (2025). What is the sustainable energy transition and why is it key to tackling climate change? February 3, 2025. https://climatepromise.undp.org/news-and-stories/what-sustainable-energy-transition-and-why-it-key-tackling-climate-change#:~:text=sustainable%20energy%20transition?-,The%20sustainable%20energy%20transition%20is%20a%20transformative%20shift%20in%20how,equity%2C%20inclusion%20and%20human%20development

United Nations Framework Convention on Climate Change (UNFCCC). (1992). United Nations Framework Convention on Climate Change. https://unfccc.int/files/essential_background/background_publications_htmlpdf/application/pdf/conveng.pdf

United Nations Framework Convention on Climate Change (UNFCCC). (2015). Paris Agreement. https://unfccc.int/sites/default/files/english_paris_agreement.pdf

United Nations Framework Convention on Climate Change (UNFCCC). (2026a). 7. d Paris Agreement. Status. https://treaties.un.org/Pages/ViewDetails.aspx?src=TREATY&mtdsg_no=XXVII-7-d&chapter=27&clang=_en

United Nations Framework Convention on Climate Change (UNFCCC). (2026b). The Paris Agreement. Process and meetings. https://unfccc.int/process-and-meetings/the-paris-agreement

U.S. Department of the Interior. (2025). Interior Ends Preferential Treatment for Unreliable, Subsidy-Dependent Wind and Solar Energy. https://www.doi.gov/pressreleases/interior-ends-preferential-treatment-unreliable-subsidy-dependent-wind-and-solar

Vachon, D., & Prairie, Y. T. (2013). The ecosystem size and shape dependence of gas transfer velocity versus wind speed relationships in lakes. *Canadian Journal of Fisheries and Aquatic Sciences*, *70*(12), 1757–1764. https://doi.org/10.1139/cjfas-2013-0241

Vachon, D., Prairie, Y. T., Guillemette, F., & del Giorgio, P. A. (2017). Modeling Allochthonous Dissolved Organic Carbon Mineralization Under Variable Hydrologic Regimes in Boreal Lakes. *Ecosystems*, *20*(4), 781–795. https://doi.org/10.1007/s10021-016-0057-0

Vachon, D., Sponseller, R. A., & Karlsson, J. (2021). Integrating carbon emission, accumulation and transport in inland waters to understand their role in the global carbon cycle. *Global Change Biology*, *27*(4), 719–727. https://doi.org/10.1111/gcb.15448

Vincent, J.-S. (1985). Géologie des formations en surface. Réservoir La Grande 2, Québec; Commission géologique du Canada, Carte 1590A, échelle 1/100 000

Vonk, J. E., Tank, S. E., & Walvoord, M. A. (2019). Integrating hydrology and biogeochemistry across frozen landscapes. In *Nature Communications* (Vol. 10, Issue 1). Nature Research. https://doi.org/10.1038/s41467-019-13361-5

Villa, J. A., Ju, Y., Stephen, T., Rey-Sanchez, C., Wrighton, K. C., & Bohrer, G. (2020). Plant-mediated methane transport in emergent and floating-leaved species of a temperate freshwater mineral-soil wetland. *Limnology and Oceanography*, *65*(7), 1635–1650. https://doi.org/10.1002/lno.11467

Virkkala, A. M., Aalto, J., Rogers, B. M., Tagesson, T., Treat, C. C., Natali, S. M., Watts, J. D., Potter, S., Lehtonen, A., Mauritz, M., Schuur, E. A. G., Kochendorfer, J., Zona, D., Oechel, W., Kobayashi, H., Humphreys, E., Goeckede, M., Iwata, H., Lafleur, P. M., … Luoto, M. (2021). Statistical upscaling of ecosystem CO2 fluxes across the terrestrial tundra and boreal domain: Regional patterns and uncertainties. *Global Change Biology*, *27*(17), 4040–4059. https://doi.org/10.1111/gcb.15659

Virkkala, A. M., Rogers, B. M., Watts, J. D., Arndt, K. A., Potter, S., Wargowsky, I., Schuur, E. A. G., See, C. R., Mauritz, M., Boike, J., Bret-Harte, M. S., Burke, E. J., Burrell, A., Chae, N., Chatterjee, A., Chevallier, F., Christensen, T. R., Commane, R., Dolman, H., … Natali, S. M. (2025). Wildfires offset the increasing but spatially heterogeneous Arctic–boreal CO2 uptake. *Nature Climate Change*. https://doi.org/10.1038/s41558-024-02234-5

Waldo, S., Deemer, B. R., Bair, L. S., & Beaulieu, J. J. (2021). Greenhouse gas emissions from an arid-zone reservoir and their environmental policy significance: Results from existing global models and an exploratory dataset. *Environmental Science and Policy*, *120*, 53–62. https://doi.org/10.1016/j.envsci.2021.02.006

Walker, X. J., Baltzer, J. L., Cumming, S. G., Day, N. J., Ebert, C., Goetz, S., Johnstone, J. F., Potter, S., Rogers, B. M., Schuur, E. A. G., Turetsky, M. R., & Mack, M. C. (2019). Increasing wildfires threaten historic carbon sink of boreal forest soils. *Nature*, *572*(7770), 520–523. https://doi.org/10.1038/s41586-019-1474-y

Wang, F., Maberly, S. C., Wang, B., & Liang, X. (2018). Effects of dams on riverine biogeochemical cycling and ecology. *Inland Waters*, *8*(2), 130–140. https://doi.org/10.1080/20442041.2018.1469335

Wang, W., Roulet, N. T., Kim, Y., Strachan, I. B., del Giorgio, P., Prairie, Y. T., & Tremblay, A. (2018). Modelling CO2 emissions from water surface of a boreal hydroelectric reservoir. *Science of the Total Environment*, *612*, 392–404. https://doi.org/10.1016/j.scitotenv.2017.08.203

Wang, J., Vilmin, L., Mogollón, J. M., Beusen, A. H. W., van Hoek, W. J., Liu, X., Pika, P. A., Middelburg, J. J., & Bouwman, A. F. (2023). Inland Waters Increasingly Produce and Emit Nitrous Oxide. *Environmental Science and Technology*, *57*(36), 13506–13519. https://doi.org/10.1021/acs.est.3c04230

Webster, K. L., Bhatti, J. S., Thompson, D. K., Nelson, S. A., Shaw, C. H., Bona, K. A., Hayne, S. L., & Kurz, W. A. (2018). Spatially-integrated estimates of net ecosystem exchange and methane fluxes from Canadian peatlands. *Carbon Balance and Management*, *13*(1). https://doi.org/10.1186/s13021-018-0105-5

Whitaker, M., Heath, G. A., O'Donoughue, P., & Vorum, M. (2012). Life Cycle Greenhouse Gas Emissions of Coal-Fired Electricity Generation: Systematic Review and Harmonization. *Journal of Industrial Ecology*, *16*(SUPPL.1). https://doi.org/10.1111/j.1530-9290.2012.00465.x

Wik, M., Johnson, J. E., Crill, P. M., DeStasio, J. P., Erickson, L., Halloran, M. J., Fahnestock, M. F., Crawford, M. K., Phillips, S. C., & Varner, R. K. (2018). Sediment Characteristics and Methane Ebullition in Three Subarctic Lakes. *Journal of Geophysical Research: Biogeosciences*, *123*(8), 2399–2411. https://doi.org/10.1029/2017JG004298

World Bank. (2023). Climate Toolkits: For Infrastructure PPPs, Hydropower Sector. The World Bank. Washington D.C. 86 pages.

World Meteorological Organization (WMO). (2025). Global climate predictions show temperatures expected to remain at or near record levels in coming 5 years. Press Release. 28 May 2025. https://wmo.int/news/media-centre/global-climate-predictions-show-temperatures-expected-remain-or-near-record-levels-coming-5-years

World Resources Institute & World Business Council for Sustainable Development (WRI & WBCSD). (2014). The Greenhouse Gas Protocol: Corporate Accounting and Reporting Standard (Revised Edition). [Link: https://ghgprotocol.org/sites/default/files/standards/ghg-protocol-revised.pdf].

World Resources Institute & World Business Council for Sustainable Development (WRI & WBCSD). (2015). The Greenhouse Gas Protocol: Scope 2 Guidance An amendment to the GHG Protocol Corporate Standard https://ghgprotocol.org/sites/default/files/2023-03/Scope%202%20Guidance.pdf

World Resources Institute & World Business Council for Sustainable Development (WRI & WBCSD). (2022a). Greenhouse Gas Protocol Land Sector and Removals Guidance: Part 1: Accounting and Reporting Requirements and Guidance (Draft for Pilot Testing and Review, September 2022). https://ghgprotocol.org/sites/default/files/2022-12/Land-Sector-and-Removals-Guidance-Pilot-Testing-and-Review-Draft-Part-1.pdf

World Resources Institute & World Business Council for Sustainable Development (WRI & WBCSD). (2022b). Greenhouse Gas Protocol Land Sector and Removals Guidance: Part 2: Calculation Guidance (Draft for Pilot Testing and Review, September 2022). https://ghgprotocol.org/sites/default/files/2022-12/Land-Sector-and-Removals-Guidance-Pilot-Testing-and-Review-Draft-Part-2.pdf

World Resources Institute & World Business Council for Sustainable Development (WRI & WBCSD). (2024). Greenhouse Gas Protocol Land Sector and Removals Initiative: Project Overview. https://ghgprotocol.org/sites/default/files/2024-07/Project%20Overview_25%20July%202024.pdf

World Resources Institute & World Business Council for Sustainable Development (WRI & WBCSD). (2023). The Greenhouse Gas Protocol: Corporate Value Chain (Scope 3) Standard. https://ghgprotocol.org/corporate-value-chain-scope-3-standard.

World Resources Institute & World Business Council for Sustainable Development (WRI & WBCSD). (2025a). The Greenhouse Gas Protocol: Public Consultation – Consequential Electricity-Sector Emissions Impacts. https://ghgprotocol.org/sites/default/files/2025-10/GHG-Protocol-Consequential-Electricity-Sector-Emissions-Impacts-Public-Consultation.pdf

World Resources Institute & World Business Council for Sustainable Development (WRI & WBCSD). (2025b). RELEASE: ISO and GHG Protocol Announce Strategic Partnership to Deliver Unified Global Standards for Greenhouse Gas Emissions Accounting. https://ghgprotocol.org/blog/release-iso-and-ghg-protocol-announce-strategic-partnership-deliver-unified-global-standards

World Resources Institute & World Business Council for Sustainable Development (WRI & WBCSD). (2025c). Land Sector and Removals Standard. https://ghgprotocol.org/land-sector-and-removals-standard

World Resources Institute & World Business Council for Sustainable Development (WRI & WBCSD). (2026). Land Sector and Removals Standard: Version 1.0: Agriculture and CO_2 removal technologies. Supplement to the GHG Protocol Corporate Standard and Scope 3 Standard. https://ghgprotocol.org/land-sector-and-removals-standard

Wrage-Mönnig, N., Horn, M. A., Well, R., Müller, C., Velthof, G., & Oenema, O. (2018). The role of nitrifier denitrification in the production of nitrous oxide revisited. In *Soil Biology and Biochemistry* (Vol. 123, pp. A3–A16). Elsevier Ltd. https://doi.org/10.1016/j.soilbio.2018.03.020

Wu, W., Wang, J., Zhou, X., Yuan, B., Guo, M., & Ren, L. (2021). Spatiotemporal distribution of nitrous oxide (N2O) emissions from cascade reservoirs in Lancang-Mekong River Yunnan section, Southwestern China. *River Research and Applications*, *37*(8), 1055–1069. https://doi.org/10.1002/rra.3726

Yuan, K., Li, F., McNicol, G., Chen, M., Hoyt, A., Knox, S., Riley, W. J., Jackson, R., & Zhu, Q. (2024). Boreal–Arctic wetland methane emissions modulated by warming and vegetation activity. Nature Climate Change, 14(3), 282–288. https://doi.org/10.1038/s41558-024-01933-3

Yu, Z., Joos, F., Bauska, T. K., Stocker, B. D., Fischer, H., Loisel, J., Brovkin, V., Hugelius, G., Nehrbass-Ahles, C., Kleinen, T., & Schmitt, J. (2021). No support for carbon storage of >1,000 GtC in northern peatlands. *Nature Geoscience*, *14*(7), 465–467. https://doi.org/10.1038/s41561-021-00769-2

Zaccone, C., Lobianco, D., Shotyk, W., Ciavatta, C., Appleby, P. G., Brugiapaglia, E., Casella, L., Miano, T. M., & D'Orazio, V. (2017). Highly anomalous accumulation rates of C and N recorded by a relic, free-floating peatland in Central Italy. *Scientific Reports*, *7*. https://doi.org/10.1038/srep43040

Zhao, J., Peichl, M., Öquist, M., & Nilsson, M. B. (2016). Gross primary production controls the subsequent winter CO2 exchange in a boreal peatland. In *Global Change Biology* (Vol. 22, Issue 12, pp. 4028–4037). Blackwell Publishing Ltd. https://doi.org/10.1111/gcb.13308

Zhao, B., & Zhuang, Q. (2023). Peatlands and their carbon dynamics in northern high latitudes from 1990 to 2300: a process-based biogeochemistry model analysis. *Biogeosciences*, *20*(1), 251–270. https://doi.org/10.5194/bg-20-251-2023

Zhou, E., & Mai, T. (2021). Electrification Futures Study: Operational Analysis of U.S. Power Systems with Increased Electrification and Demand-Side Flexibility. https://doi.org/10.2172/1785329

Zhu, D., Liu, X., Liu, X., Wu, L., & Huang, W. (2025). Strategies for phosphorus management and greenhouse gas reduction via plant harvesting in the water-level fluctuation zone of the Three Gorges Reservoir. *Environmental Research*, *268*. https://doi.org/10.1016/j.envres.2025.120804

Appendix 1

Application of the G-res Tool to the Keeyask Reservoir

Report on Data Inputs

This document describes the data inputs used to apply the G-res Tool to the Keeyask Reservoir located on the lower Nelson River in northern Manitoba.

1 Keeyask Generation Project Overview:

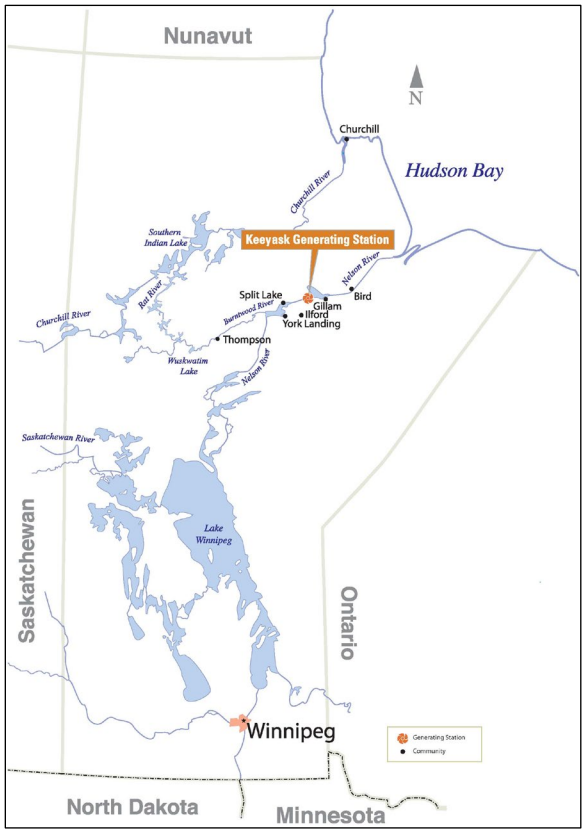
The Keeyask Generating Station (Keeyask GS) is a 695-megawatt hydroelectric power plant located on the lower Nelson River in northern Manitoba (Figure 1-1). The Keeyask GS was developed by the Keeyask Hydropower Limited Partnership, comprising the Tataskweyak Cree Nation, War Lake Cree Nation, Fox Lake Cree Nation, York Factory Cree Nation and Manitoba Hydro (Keeyask Hydropower Limited Partnership, 2012a).

Keeyask is Manitoba's fourth largest hydroelectric generating station. Construction started on July 16, 2014 (Keeyask Hydropower Limited Partnership, 2014). The last of the seven generating units was brought into service as part of the Manitoba Hydro power grid on March 9, 2022 (Manitoba Hydro, 2024).

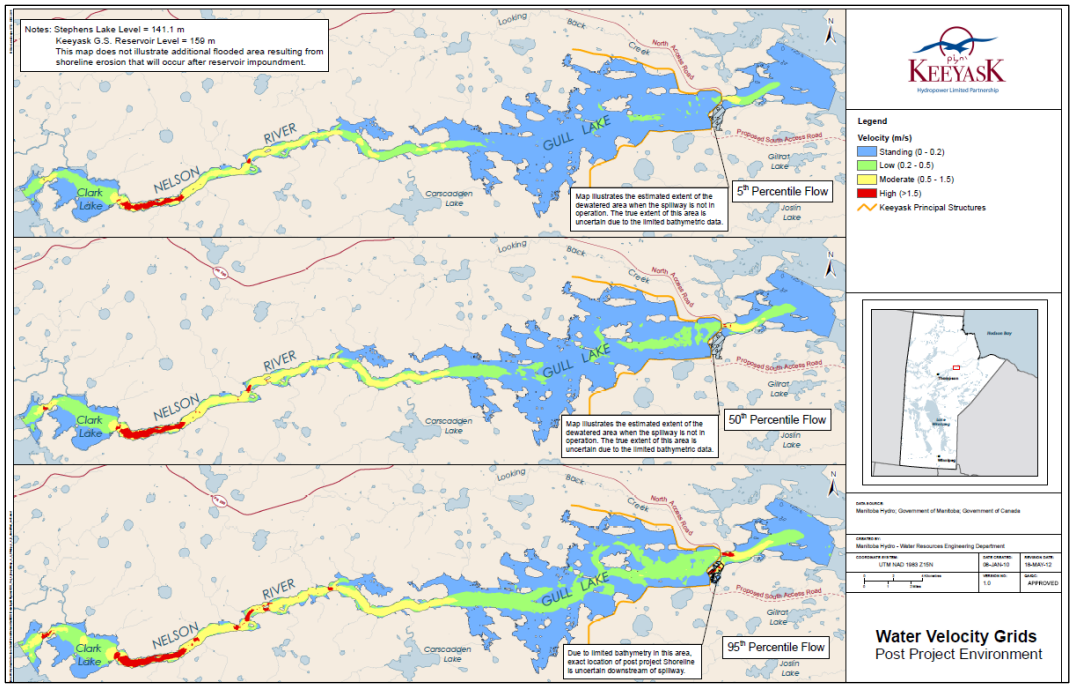
Reservoir impoundment (flooding) occurred from August 31 to September 5, 2020 (Keeyask Hydropower Limited Partnership, 2020). The Keeyask Reservoir is estimated to comprise

approximately 52.4 km^2 of flooded land and 48.0 km^2 of existing aquatic systems for a total reservoir area of 100.4 km^2 (Keeyask Hydropower Limited Partnership, 2012b). These values represent the estimated size of the reservoir thirty years after flooding commences. The size of the flooded land is predicted to increase from 45.1 km^2 at initial flooding to 52.4 km^2 thirty years afterwards due to peatland disintegration and shoreline erosion.

The reservoir will comprise 1) a fast flowing, well-oxygenated main channel and 2) backbays with slower water flows, longer water residence time, and potentially less oxygenated waters (Keeyask Hydropower Limited Partnership, 2012b). Figure 1-2 illustrates modelled post-impoundment Keeyask reservoir water velocity.



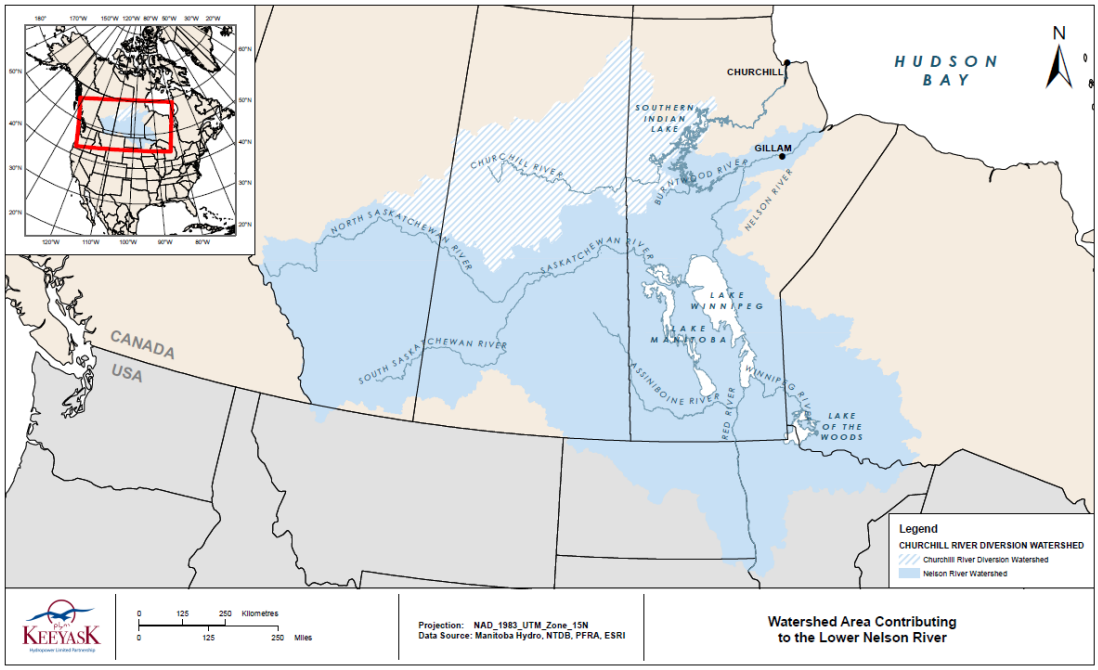
Source: Keeyask Hydropower Limited Partnership https://keeyask.com/the-project/
Figure 1-1 Location of Keeyask Generating Station



Source: Keeyask Hydropower Limited Partnership, 2012a (Map 4.4-8)
Figure 1-2 Modelled Post-Impoundment Keeyask Reservoir Water Velocity

2 G-res Tool "Catchment Data"

The Keeyask Project/Reservoir watershed area is illustrated below in Figure 2-1.



Source: Keeyask Hydropower Limited Partnership, 2012a (Map 4.3-1)
Figure 2-1 Lower Nelson River Watershed

Model inputs pertaining to: Catchment Area, Population in the Catchment, and Catchment Annual Runoff were derived from the G-res Tool Earth Engine (Figure 2-2).

Community Wastewater Treatment was selected as being biological, upstream of the Keeyask generating station. So as not to understate net reservoir GHG emissions, the release of phosphorus from community sewage and the release of phosphorus from industrial sewage were set to zero. This will result in all net reservoir GHG emissions being assigned to the Keeyask reservoir. None of the reservoir emissions will be assigned to another anthropogenic source.

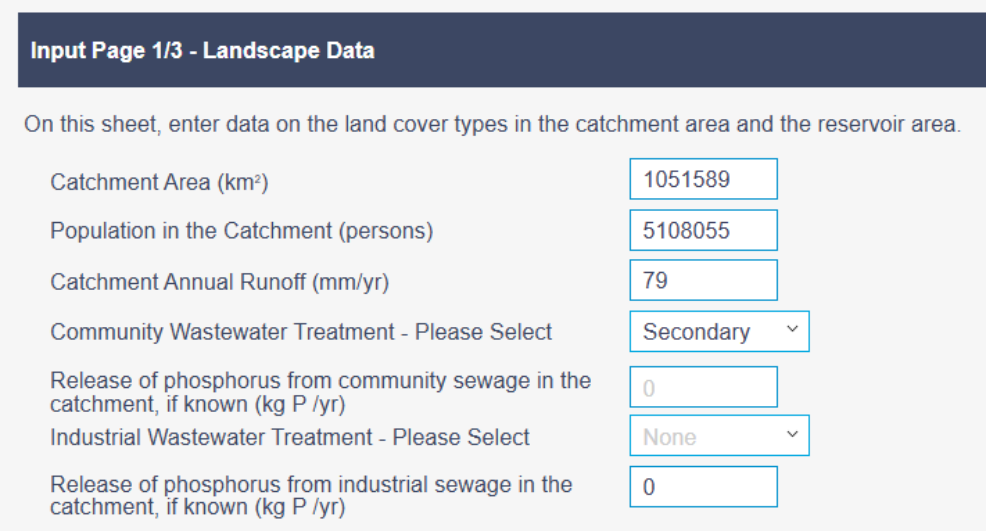


Figure 2-2 G-res Landscape Data Generated by G-res Earth Engine

2.1 Land Cover in the Catchment Area

Land Cover in the Catchment Area inputs were derived from the G-res Tool Earth Engine (Figure 2-3). It is understood that these inputs will not be used in the G-res Tool calculations of pre-flood GHG emissions. Pre-flood GHG remissions will be calculated using Pre-Impoundment Land Cover in the Reservoir Area, which were derived from Keeyask reservoir site-specific information, as described in Section 2.2 below.

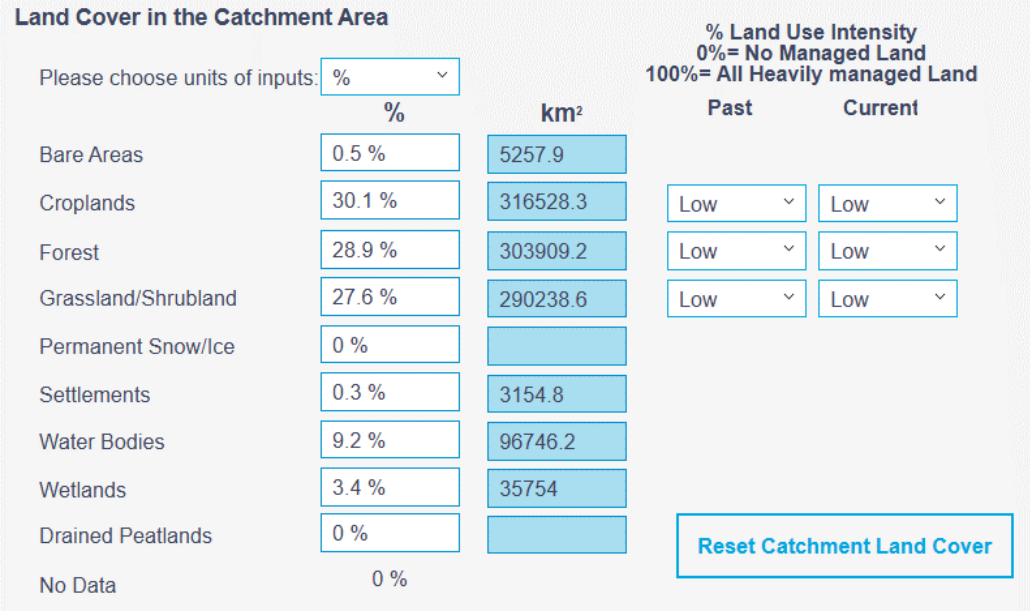


Figure 2-3 Landcover Data Generated by the Keeyask G-res Earth Engine

2.2 Pre-Impoundment Land Cover in the Reservoir Area

Pre-Impoundment Land Cover in the Reservoir Area inputs were derived from extensive, site-specific studies that were conducted as part of the Keeyask Generation Project Environmental Impact Statement, as described below.

2.2.1 Reservoir Area (km2)

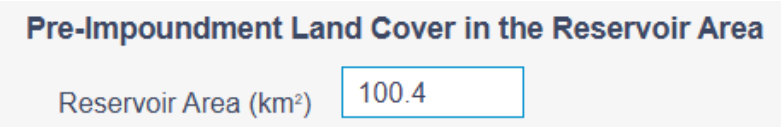


Figure 2-4 Total Keeyask Reservoir Area (km^2)

The Keeyask Reservoir will comprise approximately 52.4 km^2 of flooded land and 48.0 km^2 of existing aquatic systems for a total area of 100.4 km^2 (Keeyask Hydropower Limited Partnership, 2012b). These values represent the size of the reservoir thirty years after flooding commences. The size of the flooded land is predicted to increase from 45.1 km^2 at initial

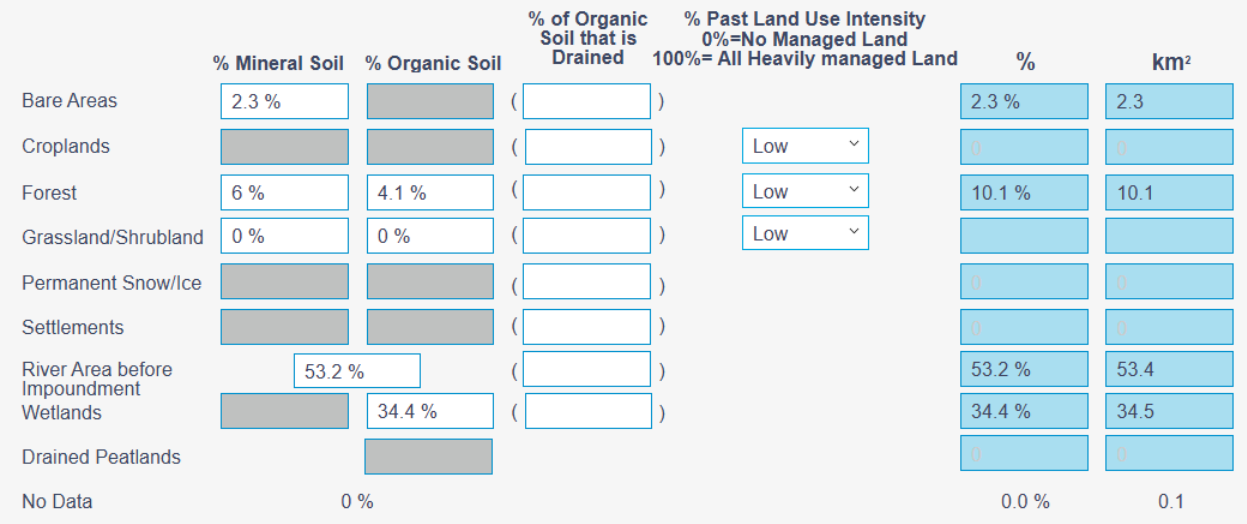
flooding to 52.4 km^2 thirty years afterwards due to peatland disintegration and shoreline erosion.

The expanded reservoir size of **100.4 km^2** was used so as not to underestimate life cycle GHG emissions.

2.2.2 Pre-Impoundment Land Cover in the Reservoir Area

2.2.2.1 Input Values

The pre-impoundment land cover input values used are as follows (Figure 2-5):



	% Mineral Soil	% Organic Soil	% of Organic Soil that is Drained	% Past Land Use Intensity 0%=No Managed Land 100%= All Heavily managed Land	%	km²
Bare Areas	2.3 %				2.3 %	2.3
Croplands				Low	0	0
Forest	6 %	4.1 %		Low	10.1 %	10.1
Grassland/Shrubland	0 %	0 %		Low		
Permanent Snow/Ice					0	0
Settlements					0	0
River Area before Impoundment	53.2 %				53.2 %	53.4
Wetlands		34.4 %			34.4 %	34.5
Drained Peatlands					0	0
No Data	0 %				0.0 %	0.1

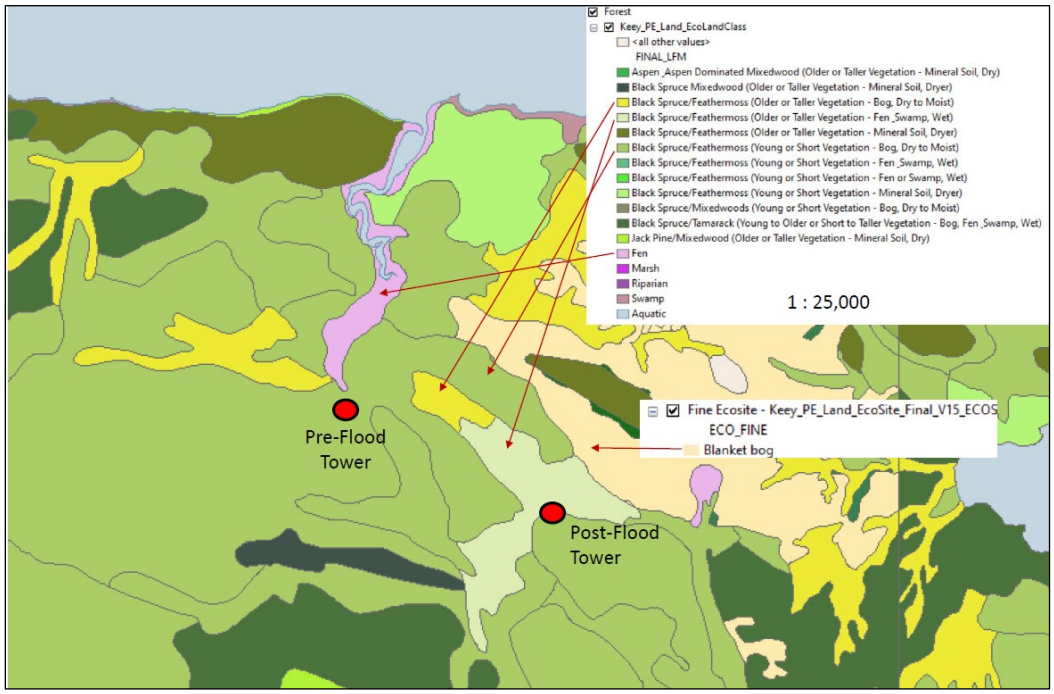
Figure 2-5 Keeyask Reservoir Pre-Impoundment Landcover Data

2.2.2.2 Overview of Pre-Impoundment Land Cover in the Reservoir Area

Approximately 90% of the Keeyask Reservoir and adjacent lands are peatlands (Keeyask Hydropower Limited Partnership, 2012b).

Soil profiles were sampled in the lower Nelson River area and at sites in the Keeyask region from 2002 to 2012 as part of the Keeyask Generation Project Environmental Impact Statement studies (Keeyask Hydropower Limited Partnership, 2012b).

The Ecological Land Classification System of the Keeyask EIS categorized the Keeyask landscape according to ecologically distinct areas, considering surface geology, landforms, soils, vegetation, climate, wildlife, surface water, natural disturbances, human features, etc. (Keeyask Hydropower Limited Partnership, 2012b). The purpose of the classification scheme was to assess the potential impacts of the Keeyask Project on ecosystem composition, structure, and dynamics (Keeyask Hydropower Limited Partnership, 2012b). The Ecological Land Classification System is illustrated in Figure 2-6.



Source: Keeyask Hydropower Limited Partnership 2012b
Figure 2-6 Keeyask EIS Ecological Land Classification

The Ecological Land Classification System categories can be aligned with the G-res Tool input classes for pre-flood land cover.

2.2.2.3 Preparation of The Ecological Land Classification for Use in G-res Modelling

The Ecological Land Classification categorizes the boreal forest into the following sub-categories (Figure 2-7).

The categories identify forest type (underlain by either mineral soils or organic soils). Wetlands are categorized by fen, marsh, riparian, and swamp. The Ecological Land Classification also identifies inland waters (e.g. aquatic areas), and bare areas (e.g. none).

ECOLOGICAL LAND CLASSIFACTION
ALIGNED FOR G-RES TOOL PRE-IMPOUNDMENT LAND COVER CATEGORIES
RE-ASSIGN BOGS TO WETLAND LAND COVER CATEGORY

BARE AREAS (MINERAL SOILS)
None

WETLANDS (ORGANIC SOILS)
Fen
Marsh
Swamp
Riparian
Bog
- Black Spruce/Feathermoss (Older or Taller Vegetation - Bog, Dry to Moist)
- Black Spruce/Feathermoss (Young or Short Vegetation - Bog, Dry to Moist)
- Black Spruce/Mixedwoods (Young or Short Vegetation - Bog, Dry to Moist)
- Black Spruce/Tamarack (Young to Older or Short to Taller Vegetation - **Bog**, Fen & Swamp, Wet)

FOREST (MINERAL SOILS)
Aspen & Aspen Dominated Mixedwood (Older or Taller Vegetation - Mineral Soil, Dry)
Black Spruce Mixedwood (Older or Taller Vegetation - Mineral Soil, Dryer)
Black Spruce/Feathermoss (Older or Taller Vegetation - Mineral Soil, Dryer)
Black Spruce/Feathermoss (Young or Short Vegetation - Mineral Soil, Dryer)
Jack Pine/Mixedwood (Older or Taller Vegetation - Mineral Soil, Dry)

FOREST (ORGANIC SOILS)
Black Spruce/Feathermoss (Older or Taller Vegetation - Fen & Swamp, Wet)
Black Spruce/Feathermoss (Young or Short Vegetation - Fen & Swamp, Wet)
Black Spruce/Tamarack (Young to Older or Short to Taller Vegetation - Bog, **Fen & Swamp,** Wet)

AQUATIC
Aquatic (Included as "Pre-Flood Waterbodies")

Figure 2-7 Ecological Land Classification Aligned for G-res Tool Pre-Flood Landcover Categories

The pre-impoundment land cover in the reservoir area entered as inputs in the G-res Tool are as follows (Table 2-1):

Table 2-1 Pre-Impoundment Landcover: G-res Input

Pre-Impoundment Land Cover in the Reservoir Area
Ecological Land Classification
Re-Assign Bog Landcover

	% Mineral Soil	% Organic Soil	% Total
Croplands			
Bare Areas	2.3%		2.3%
Wetlands		35.1%	35.1%
Forest	6.0%	3.4%	9.4%
Grassland/Shrubland			
Permanent Snow/Ice			
Settlements			
Total Terrestrial			**46.8%**
Water Bodies			53.2%
Total			**100.0%**

2.2.3 Replacement of G-res Tool Generic Emission Factors

G-res calculates pre-flood emissions by applying CO_2 and CH_4 emission factors by landcover type for mineral and organic soils. The majority of default emission factors are from the IPCC (IPCC, 2014). Default emission factors for forests with mineral soils were from Pan (2011), and default methane emission factors for waterbodies were developed by the model developers (Prairie et al., 2021) using a method described in Rasilo et al. (2014).

Since approximately 90% of the flooded land are heterogeneous peatlands, it was important to review the pre-flood emission factors, especially for wetlands as this will heavily influence **Net** Keeyask reservoir GHG emissions.

2.2.3.1 Pre-flood Terrestrial and Aquatic GHG Emission Factors

The scientific literature was examined to identify CO_2 and CH_4 emission rates from the northern and boreal peatlands. The search identified studies that focused on specific research sites,

synthesis reports that assessed the results of multiple studies involving many research locations over several years, and newly created databases of CO_2 and CH_4 emissions at the Canadian, northern (arctic, boreal, permafrost regions), and global scales.

2.2.3.1.1 CO_2 Terrestrial Emission Factor Studies

Based on an extensive literature review, four studies containing a synthesis of CO_2 emission databases were selected for further evaluation for suitability for use in the G-res modelling of Keeyask lifecycle emissions. They are listed in Table 2-2. A summary of the assessment results is illustrated in Table 2-3.

Table 2-2 Description of CO_2 Terrestrial Emission Factor Studies

Northern Peatland/Forest Synthesis Studies and Databases of Carbon Dioxide Emissions Evaluated for G-res Modelling of Keeyask Lifecycle Emissions	
Nelson et al., 2024	X-BASE: the first terrestrial carbon and water flux products from an extended data-driven scaling framework, FLUXCOM-X
Treat et al., 2024	Permafrost Carbon: Progress on Understanding Stocks and Fluxes Across Northern Terrestrial Ecosystems
Virkkala et al., 2021	Statistical upscaling of ecosystem CO_2 fluxes across the terrestrial tundra and boreal domain: Regional patterns and uncertainties
Webster et al., 2018	Spatially-integrated estimates of net ecosystem exchange and methane fluxes from Canadian peatlands

Table 2-3 Evaluation Results: CO_2 Emission Factor Studies

Evaluation Criteria to Assess Northern Peatland/Forest CO_2 Synthesis and Upscaling Studies for Applying the G-res Tool

Weight out of 100%	Evaluation Criteria	Virkkala et al., 2021 Score	Virkkala et al., 2021 Weighted Score	Treat et al., 2024 Score	Treat et al., 2024 Weighted Score	Nelson et al., 2024 Score	Nelson et al., 2024 Weighted Score	Webster et al., 2018 Score	Webster et al., 2018 Weighted Score
40%	Ability of the GHG emission factors derived from synthesis study to represent GHG emissions from the heterogeneous Keeyask pre-flood landscape . Does the study generate emission factors that represent the heterogeniuos peatlands by peatland type (e.g. bog, fen, marsh, swamp), boreal forest/upland, and grassland/shrub? or . Does the study generate composite GHG emission factors that represent boreal wetlands and the boreal forest?	80	32	80	32	60	24	75	30
30%	Does the study present emission factors that represent the entire year? . Annual emission factors, and/or . Emission factors for the growing season/non-growing season; and ice-free and ice-cover seasons?	90	27	75	22.5	40	12	75	22.5
30%	Breadth of sysnthesis study . Does the synthesis study/database include multiple site-specific studies (multiple representative sample sites) and/or other synthesis studies? . Does the synthesis study cover multiple years of site investigations/data collection? (i.e. assess a lengthy time series?)	85	25.5	85	25.5	80	24	80	24
100%		**Score**	**84.5**	**Score**	**80.0**	**Score**	**60.0**	**Score**	**76.5**

2.2.3.1.2 CO_2 Terrestrial Emission Factor Assessment Results

The database compiled by Virkkala et al. (2021) was selected as the source of pre-flood CO_2 emission factors for describing the Keeyask reservoir pre-flood terrestrial footprint based on the criteria described above.

Virkkala et al. (2021) examined ecosystem CO_2 fluxes from the high latitude tundra and boreal biomes, for latitudes greater than 45°N throughout the northern hemisphere. They compiled measurements of gross primary productivity, ecosystem respiration, and net ecosystem exchange (CO_2 emissions to the atmosphere). The study reviewed a lengthy time series (1990 – 2015) of CO_2 emissions that were collected from eddy covariance networks, FLUXNET2015 (Pastorello et al., 2020), plus chamber studies. Incorporating both eddy covariance and chamber studies is complimentary and beneficial. Eddy covariance networks measure GHG exchange between the land and atmosphere at a larger measurement footprint than chamber studies, and these studies have provided a long-term, continuous record of CO_2 and CH_4 emissions (Margolis et al., 2006; Lund et al., 2010; Strachan et al., 2015; Knox et al., 2021). Chamber studies have a smaller measurement footprint (m^2) which allows for a focused investigation such as on a specific vegetation type (Strack et al., 2017; Järveoja et al., 2018; Thalasso et al., 2023; Boonman et al., 2024). Chamber studies have been used widely in the boreal biome, providing widespread coverage of the heterogeneous landscape (Bao et al., 2021; Zhao & Zhuang, 2023). Virkkala et al. (2021) assessed data from 148 field locations, and for 1448 annual and growing season CO_2 fluxes.

Virkkala et al. (2021) presents CO_2 emissions for boreal uplands and boreal wetlands for the growing season and on an annual basis. These emission factor categories are well suited to be used as inputs for the G-res pre-flood landcover classes of forest, grasslands/shrub, and wetlands.

Although the Virkkala et al. (2021) boreal sites do not include measurements directly from the Keeyask area, they do include measurements from the boreal forest and boreal peatlands near Thompson, Manitoba (BOREAS site), which is approximately 200 kms to the southwest of Keeyask, and other boreal forest sites in Quebec and Alberta. Boreal CO_2 emission measurements were also incorporated from the Hudson Bay Lowlands on the western side of southern James Bay in the Attawapiskat River, Kinoje Lake, and Moosonee region, and other northern hemisphere boreal locations.

2.2.3.1.3 CH_4 Emission Factor Selection

Based on an extensive literature review, seven studies containing a synthesis of CH_4 emission databases were selected for further evaluation for suitability for use in the G-res modelling of Keeyask lifecycle emissions, and these are listed in Table 2-4. The databases were further assessed for suitability for the G-res modelling of Keeyask lifecycle emissions. A summary of the assessment results is illustrated in Table 2-5.

Table 2-4 Description of CH_4 Emission Factor Studies

Northern Peatland/Forest Synthesis Studies and Databases of Methane Emissions Evaluated for G-res Modelling of Keeyask Lifecycle Emissions	
Treat et al., 2024	Permafrost Carbon: Progress on Understanding Stocks and Fluxes Across Northern Terrestrial Ecosystems
Yuan et al., 2024	Boreal–Arctic wetland methane emissions modulated by warming and vegetation activity
Bao et al., 2021	Wetland Heterogeneity Determines Methane Emissions: A Pan-Arctic Synthesis
Delwiche et al., 2021	FLUXNET-CH4: a global, multi-ecosystem dataset and analysis of methane seasonality from freshwater wetlands
Kuhn et al., 2021 Olefeldt et al., 2021	BAWLD-CH4: a comprehensive dataset of methane fluxes from boreal and arctic ecosystems
Knox et al., 2019	FLUXNET-CH4 SYNTHESIS ACTIVITY Objectives, Observations, and Future Directions
Webster et al., 2018	Spatially-integrated estimates of net ecosystem exchange and methane fluxes from Canadian peatlands

Table 2-5 Evaluation Results: CH_4 Emission Factor Studies

Evaluation Criteria to Assess Northern Peatland/Forest CH_4 Synthesis and Upscaling Studies for Applying the G-res Tool

Weight out of 100%	Evaluation Criteria	Yuan et al., 2024 Score	Yuan et al., 2024 Weighted Score	Treat et al., 2024 Score	Treat et al., 2024 Weighted Score	Kuhn et al., 2021 Score	Kuhn et al., 2021 Weighted Score	Webster et al., 2018 Score	Webster et al., 2018 Weighted Score
40%	Ability of the GHG emission factors derived from synthesis study to represent GHG emissions from the heterogeneous Keeyask pre-flood landscape . Does the study generate emission factors that represent the heterogeniuos peatlands by peatland type (e.g. bog, fen, marsh, swamp), boreal forest/upland, and grassland/shrub? or . Does the study generate composite GHG emission factors that represent boreal wetlands and the boreal forest?	50	20	80	32	85	34	75	30
30%	Does the study present emission factors that represent the entire year? . Annual emission factors, and/or . Emission factors for the growing season/non-growing season; and ice-free and ice-cover seasons?	70	21	75	22.5	85	25.5	75	22.5
30%	Breadth of sysnthesis study . Does the synthesis study/database include multiple site-specific studies (multiple representative sample sites) and/or other synthesis studies? . Does the synthesis study cover multiple years of site investigations/data collection? (i.e. assess a lengthy time series?)	80	24	85	25.5	80	24	80	24
100%		**Score**	**65.0**	**Score**	**80.0**	**Score**	**83.5**	**Score**	**76.5**

Weight out of 100%	Evaluation Criteria	Delwiche et al., 2021 Score	Delwiche et al., 2021 Weighted Score	Knox et al., 2019 Score	Knox et al., 2019 Weighted Score	Bao et al., 2021 Score	Bao et al., 2021 Weighted Score
40%	Ability of the GHG emission factors derived from synthesis study to represent GHG emissions from the heterogeneous Keeyask pre-flood landscape . Does the study generate emission factors that represent the heterogeniuos peatlands by peatland type (e.g. bog, fen, marsh, swamp), boreal forest/upland, and grassland/shrub? or . Does the study generate composite GHG emission factors that represent boreal wetlands and the boreal forest?	65	26	70	28	65	26
30%	Does the study present emission factors that represent the entire year? . Annual emission factors, and/or . Emission factors for the growing season/non-growing season; and ice-free and ice-cover seasons?	75	22.5	75	22.5	60	18
30%	Breadth of sysnthesis study . Does the synthesis study/database include multiple site-specific studies (multiple representative sample sites) and/or other synthesis studies? . Does the synthesis study cover multiple years of site investigations/data collection? (i.e. assess a lengthy time series?)	80	24	80	24	80	24
100%		**Score**	**72.5**	**Score**	**74.5**	**Score**	**68.0**

2.2.3.1.4 CH_4 Terrestrial Emission Factor Selection

The Boreal–Arctic Wetland and Lake Methane Dataset (BAWLD-CH4) database, as described by Kuhn et al. (2021) and Olefeldt et al. (2021), was selected as the primary source of CH_4 emission factors for this GHG LCA. BAWLD-CH4 is an extensive database of methane fluxes collected at the site-level from the northern hemisphere boreal and arctic ecosystems at latitudes greater than 50°N. At the time of publishing the Kuhn et al. (2021) and Olefeldt et al. (2021) studies, BAWLD-CH4 included data up to 2020.

BAWLD-CH4 includes terrestrial CH_4 emission factors for Boreal Forest, Dry Tundra, Permafrost Bog, Bog, Fen, Tundra Wetland, and Marsh landcover types. The Boreal Forest, Permafrost Bog, Bog, Fen, and Marsh landcover categories and emission factors align well with the Keeyask Ecological Land Classification of Fen, Marsh, Swamp, Riparian and Forest. They also align well with the G-res pre-flood landcover classes of Forest, Grassland/Shrubland, and Wetland.

The database includes aquatic CH_4 emission factors for Large Lakes, Midsize Lakes, Small Glacial, Midsize Yedoma, Midsized Peatland, Small Peatland, and Small Yedoma lake classes. The Midsized Peatland Lake and Small Peatland Lake categories align with the Keeyask "Shallow Water" Ecological Land Class. The classifications also aligned well with the G-res pre-flood "Aquatic" land class.

BAWLD-CH4 includes data collected using both the eddy covariance and chamber methods. Most of the data are from chamber-based studies, which has provided extensive coverage in the northern regions.

BAWLD-CH4 does not include winter CH_4 terrestrial emissions for boreal forests and wetlands. Terrestrial winter CH_4 fluxes for these classifications were estimated following the approach by Treat et al. (2018) where non-growing season terrestrial CH_4 emissions amounted on average to 16% of annual CH_4 terrestrial emissions. BAWLD-CH4 does include aquatic winter CH_4 fluxes for Midsized and Small Peatland Lakes.

2.2.3.1.5 Preparation of Terrestrial Emission Factors for Use in G-res Modelling

CO_2 Terrestrial Emission Factors

Annual CO_2 emission factors (Net Ecosystem Exchange) for the Boreal Upland and Boreal Wetland were selected from Virkkala et al. (2021) (Table 2-6). They were based on a study period of 1990-2015. Virkkala et al. (2021) did not develop separate emission factors for mineral and organic soils. These emission factors were used as composite emission factors for both mineral and organic soils in the Keeyask G-res model. The Virkkala et al. (2021) Boreal Upland CO_2 emission factors were used for the G-res categories of Forest and Grassland/Shrubland, and the Boreal Wetland CO_2 emission factors were used for the G-res Wetland category.

Table 2-6 CO_2 Emission Factors for Keeyask G-res Lifecycle Model

CO_2 Emission Factors for Ecological Land Classification		
Land Class	**Annual NEE** **g CO_2-C/m^{-2}/yr**	**Annual NEE** **t CO_2-C/ha/yr** **(Converted for G-res)**
Boreal Uplands (Forest, and Grassland/Shrubland)	-47	-0.47
Boreal Wetlands	-38	-0.38
Source: Virkakkala et al., 2021 (Table 1)		

2.2.3.1.6 CH_4 Terrestrial Emission Factors

CH_4 emission factors were adapted from the Boreal–Arctic Wetland and Lake Methane Dataset (BAWLD-CH4) (Kuhn et al., 2021).

Terrestrial Emissions

Growing season CH_4 terrestrial emission factors were adopted from Kuhn et al. (2021) Table 3 median values for Boreal Forest, Permafrost Bog, Bog, Fen, and Marsh land classes. Non-growing season emission factors were not included in the BAWLD-CH4 database/Kuhn et al. (2021) study. They were therefore estimated as being 16% of total annual emissions according to Treat et al. (2018). The Keeyask Ecological Land Classifications of “Swamps” and “Riparian” were assigned the same emissions factors as the BAWLD-CH4 emission factors for bogs and fens, respectively, following descriptions by Kuhn et al. (2021).

A composite wetland emission factor was developed by developing a weighted average for the land classifications of Permafrost Bog, Bog, Fen, Marsh, and Peatland Lakes (small and medium). This involved multiplying each [wetland class] by their [CH_4 emission factor], by their [areal extent (km^2) as defined by the Keeyask ECO Land Class], and by summing these calculations. The results are displayed in Table 2-7.

Length of Growing Season/Non-Growing Season and Ice Free/Ice Cover

For the G-res modelling exercise, the length of the growing season in the Keeyask area was defined as 135 days and non-growing season as 230 days. The ice-free period was defined as being 185 days and ice cover period as 180 days. The calculation methodology is as follows.

2.2.3.1.7 Growing Season

Growing season was calculated according to the methods adopted by Lund et al. (2010) who assessed CO_2 exchange amongst northern and tundra peatlands, Strachan et al. (2016) who assessed CO_2 exchange in a boreal bog; and Webster et al. (2018) who assessed CO_2 and CH_4 fluxes from Canadian peatlands.

Lund et al. (2010) and Strachan et al. (2016) defined the start of growing season as the first day where the mean daily air temperature remains above 5^oC for seven consecutive days. Growing season ends on the first day of seven consecutive days where the air temperature is below 5^oC. Webster et al. (2018) defined the growing season as starting on first day where the mean daily air temperature is above 5^oC for five consecutive days beginning on March 1. Growing season

ends on the day when the minimum air temperature is less than − 2°C occurring after August 1st.

Hourly and daily average temperatures collected at the Manitoba Hydro Keeyask Meteorological Station (05UF597) and by the Government of Canada Historical Climate Data at Gillam, Manitoba were used to establish the growing season at Keeyask. The average growing season for the 10-year period from 2014–2023 using the Lund et al. (2010) and Strachan et al. (2016) approach was 134 days. The average growing season for the same period using the Webster et al. (2018) approach was 136 days. The mean/median value of 135 derived from these two approaches was used for modelling pre-flood Keeyask reservoir GHG emissions.

Length of Ice Cover

Determining the number of days when the Keeyask Reservoir and surrounding inland waterbodies are free of ice for the purpose of estimating pre and post flood GHG emissions is challenging. The timing, extent and location of spring melting and winter freeze-up varies within the reservoir and surrounding inland waters within any given year and varies from year to year. The transition between open water and ice cover is best described as a process and not as a precise measurement in time.

The method used for assessing ice thaw and ice formation for this modelling exercise involved examining Sentinel-2 L2A false colour satellite images from April–June and October–December for 2017 to 2024. Based on satellite and field observations, May 15 to November 15 (185 days)

would be a reasonable and conservative estimate to use for the length of the ice-free period Keeyask reservoir GHG modelling.

Table 2-8 illustrates the final CH_4 emission factors used in the Keeyask G-res model. Values are displayed in the G-res Tool emission factor metrics (kg CH_4/ha/yr).

Table 2-7 Calculation of Keeyask Pre-Flood Wetland Composite CH_4 Emission Factor

CALCULATION OF KEEYASK PRE-FLOOD WETLAND COMPOSITE CH_4 EMISSION FACTOR FOR ECOLOGICAL LAND CLASSIFICATION

	% of Total Wetland Area	GROWING SEASON/ OPEN WATER FLUXES mg CH_4 m^2 d	GROWING SEASON/ OPEN WATER FLUXES Weighted Average mg CH_4 m^2 d	GROWING SEASON/ OPEN WATER FLUXES Weighted Average g CH_4 m^2 season Growing Season Days 135 Days	WINTER FLUXES PER SEASON g CH_4 m^2 season 230 Days	Annual Flux kg CH_4 / ha / Year
BOG	77.2%					
Permafrost	8.0%	2.3	0.2	0.02	0.00	0.3
Bog	69.2%	24.6	17.0	2.29	0.44	27.3
FEN	2.6%	54.0	1.4	0.19	0.04	2.2
MARSH	0.7%	106.0	0.7	0.10	0.02	1.1
SWAMP	5.9%	24.6	1.4	0.19	0.04	2.3
RIPARIAN	0.4%	54.0	0.2	0.03	0.00	0.3
Wetland (Sub-Total)	**86.7%**			**2.82**	**0.5**	**33.6**
INLAND AQUATIC						
	% of Total Wetland Area	OPEN WATER FLUXES mg CH_4 m^2 d	OPEN WATER FLUXES Weighted Average mg CH_4 m^2 d	OPEN WATER FLUXES Weighted Average g CH_4 m^2 season 185 Ice Free Days	WINTER SEASONAL FLUXES Weighted Average g CH_4 m^2 / season 180 Ice Cover Days	Annual Flux kg CH_4 / ha / Year
SMALL PEATLAND LAKE	1.7%					
Growing Season Diffusive		16.4	0.3	0.1		0.5
Ebullitive		22.5	0.4	0.1		0.7
Winter Storage					0.02	0.2
Ice Bubble Storage					0.02	0.2
MID-PEATLAND LAKE	11.7%					
Diffusive		18.4	2.1	0.4		4.0
Ebullitive		45.1	5.3	1.0		9.7
Winter Storage					0.10	1.0
Ice Bubble Storage					0.10	1.0
Sub-Total Inland Water Ice Free Days Weighted Average Flux				**1.5**	**0.3**	**17.5**
ANNUAL COMPOSITE WETLAND (WETLAND + INLAND AQUATIC) EMISSION FACTOR						**51.13**

Notes:

Percentage of Wetland based on Keeyask GIS ECO Land Class within 159m Shoreline

Wetland CH_4 Growing Season Fluxes: CH_4 Based on "Warm Season" (~May - October) median values from Kuhn et al 2021 Table 3

Length of Growing Season: Calculated as 135 days for the period 2014-2023. Based on methods of Lund et al (2010), Strachan et al (2016), and Webster et al (2018).

Wetland CH_4 Non-Growing Season Fluxes: Estimated as per Treat et al 2018. Non-growing season CH4 emissions average 16% of annual emissions.

Aquatic (Peatland Lake) CH_4 Ice Free Fluxes (e.g. small and medium sized lakes): from Kuhn et al 2021 Table 4 (Diffusive and Ebullition Emissions)

Aquatic (Peatland Lake) CH_4 Winter Fluxes (e.g. small and medium sized lakes): from Kuhn et al 2021 Table 5 (Storage and Ice Bubble Storage Emissions)

Length of Ice Free Season: Based on Papakyriakou et al (2024), interpretation of satellite imagery (2017 - 2024) and field photography (2017 - 2021).

Table 2-8 Composite CH_4 Emission Factors for Keeyask G-res Model

Land Class	**Annual Emissions kg CH_4/ha/yr (G-res Emission Factor Metrics)**
Boreal Uplands (Forest, and Grassland/Shrubland)	-0.64
Boreal Wetlands	51.13

2.2.3.1.8 Pre-flood Aquatic GHG Emission Factors

The G-res default pre-flood CH_4 emission factor for "Water Bodies" is 4.4 kg CH_4/ha/yr, which is applied to the river/lake to be flooded. This emission factor would not be applied to the peatland pools or other water bodies within the terrestrial landscape (uplands) to be flooded. Alternatively, for Keeyask modelling, the G-res default emission factor was replaced by the pre-flood flux of 5 mg CH_4/m^2/yr which translates into 9.25 kg CH_4/ha/yr. This emission factor was derived by Environnement Illimité inc. from their in-situ measurements of CH4 diffusive emissions from Gull Lake and associated backbays during 2009 – 2013 (Marchand et al., 2015).

G-res does not include pre-flood CO_2 emission factors for water bodies, since G-res does not estimate net CO_2 diffusive emissions by subtracting post-flood CO_2 emissions from pre-flood CO_2 emissions (Prairie et al., 2017). G-res recognizes a portion of CO_2 emissions that occur within the reservoir result from organic material brought into the reservoir from upstream sources. These emissions are "displaced" and would have occurred within the reservoir footprint or downstream regardless of whether the reservoir existed or not. G-res applies a regression model to the gross post-flood CO_2 emissions to estimate net CO_2 reservoir emissions (Prairie et al., 2018). The results of the regression calculation are that over the 100-year life of

the reservoir, an average of 31 (±6) % of CO_2 emissions are allocated to the reservoir (Prairie et al., 2021).

2.2.3.1.9 Pre-Flood Terrestrial and Aquatic GHG Emission Factors

The Keeyask G-res Model pre-flood terrestrial and aquatic GHG emission factors are illustrated in Figure 2-10, below.

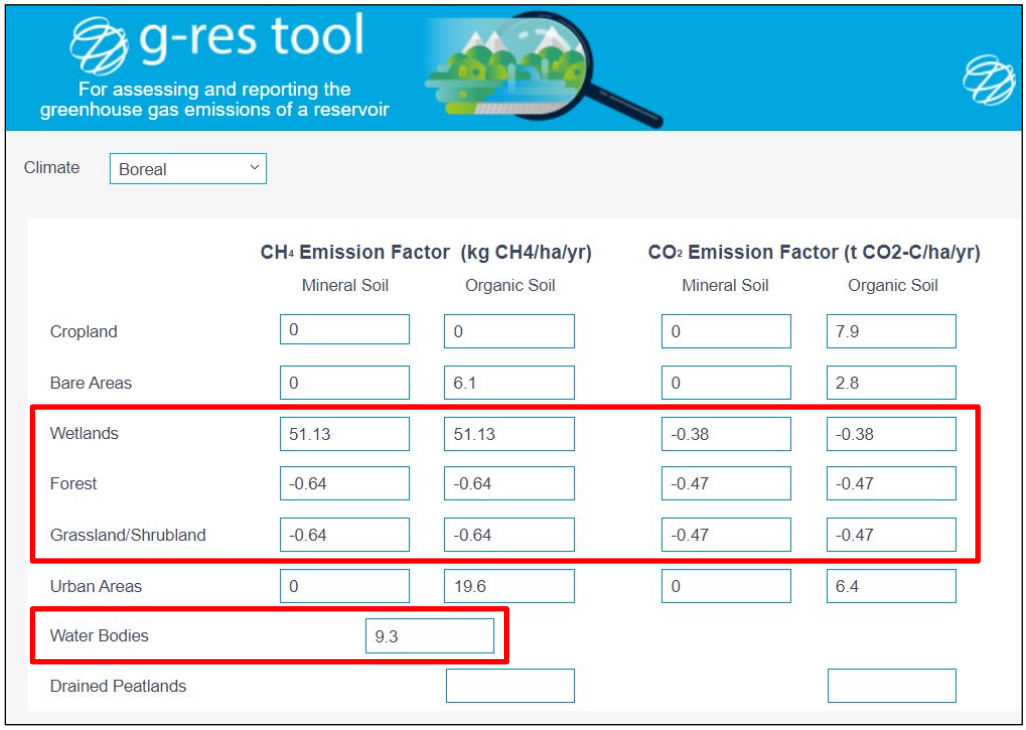


Figure 2-8 Keeyask G-res Model CO_2 and CH_4 Emission Factors

2.2.4 Determine River Area Before Impoundment



Figure 2-9 Keeyask G-res Model River Area Before Impoundment

The River Area before Impoundment was calculated as:

Pre-existing Nelson River to be flooded (48.0 km^2) / Total Reservoir Area (100.4 km^2) = 47.8%

As per the Keeyask Hydropower Limited Partnership (2012a)

plus,

Other pre-existing inland Aquatic Area to be Flooded = 5.4%

5.4% of the pre-flood land was comprised of inland waters (Keeyask EIS Ecological Land Class, Keeyask Hydropower Limited Partnership 2012b). This proportion of inland water (5.4%) was assumed to apply to the reservoir after 30 years of expansion due to shoreline erosion and peatland disintegration.

Total Flooded Aquatic Area used for GHG emissions modelling = (47.8% +5.4%) = 53.2%

3 Reservoir Data

The Reservoir Data input values used are as follows (Figure 3-1):

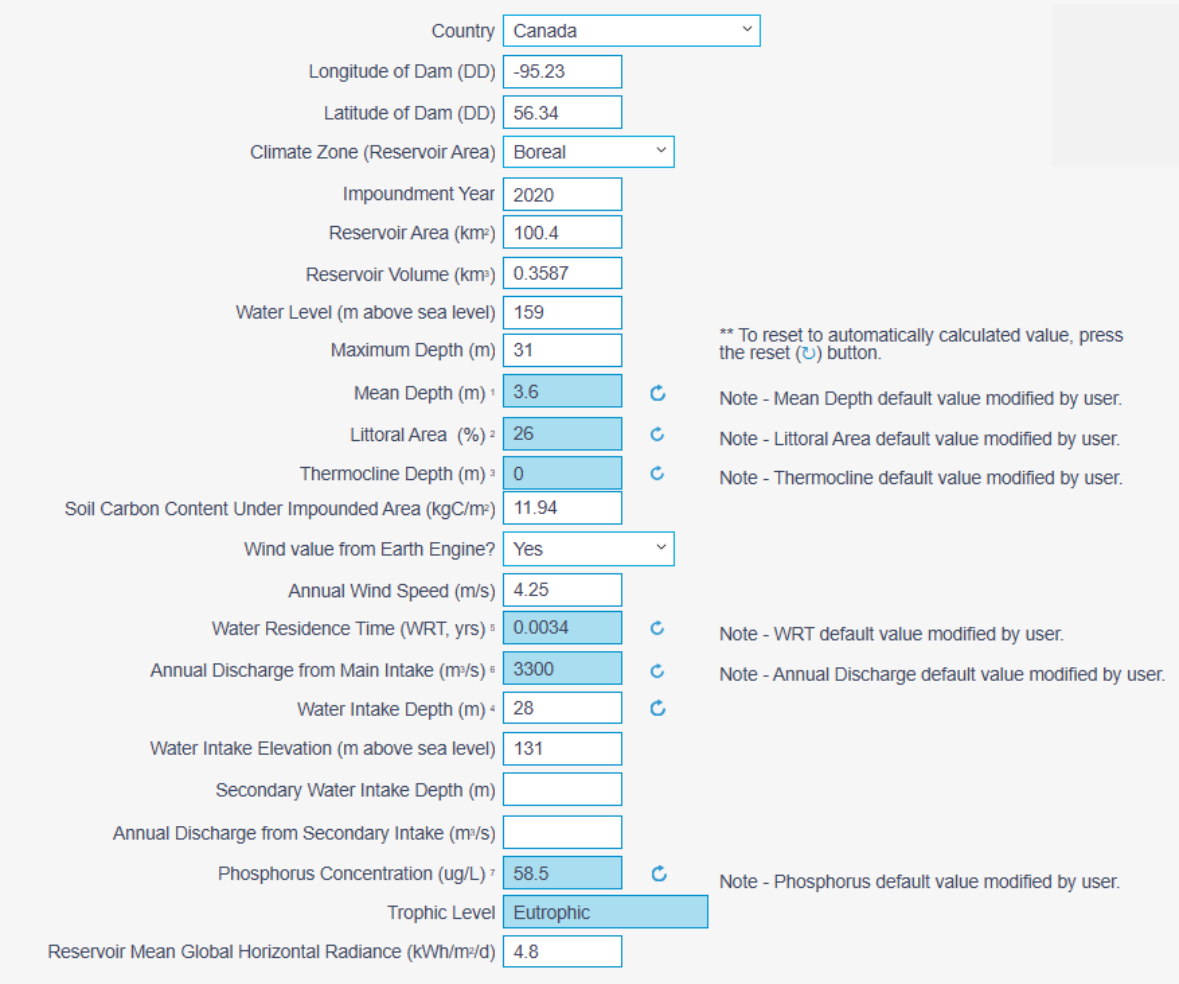


Figure 3-1 Keeyask G-res Model: Reservoir Data

Longitude and Latitude:
The Longitude (-95.23 W) and Latitude (56.34 N) of the Dam refer to the location of the Keeyask Generating Station.

Climate Zone:
The Keeyask Reservoir is located within the **Boreal Shield Ecozone** (Government of Canada, 2013).

Impoundment Year: 2020
Reservoir impoundment (flooding) occurred from August 31 to September 5, 2020 (Manitoba Hydro, 2021).

Reservoir Area (km^2): 100.4 km^2
The Keeyask Reservoir will comprise approximately 52.4 km^2 of flooded land and 48.0 km^2 of existing aquatic systems for a total area of 100.4 km^2 (Keeyask Hydropower Limited Partnership, 2012b).

Reservoir Volume (km^3): 0.3587 km^3
The estimated reservoir volume at the Keeyask Reservoir supply level of 159m ASL is 358.7 million m^3 or 0.3587 km^3 (W. DeWit, Manitoba Hydro, personal communication, May 1, 2020).

Water Level (m above sea level): 159 m above sea level
The normal operating range of the Keeyask Reservoir is 158 to 159 m above sea level (Manitoba Conservation and Water Stewardship, 2014).

Maximum Depth (m): 31 m
The maximum depth will be approximately 31 m, occurring in an excavated channel leading to the powerhouse (Keeyask Hydropower Limited Partnership, 2012b Page 4-83).

Mean Depth (m): 3.6 m
This parameter has not been formally calculated or measured for the Keeyask Reservoir. Dividing the Reservoir Volume above (0.3587 km^3) by the Reservoir Area as described above (100.4 km^2), the Mean Depth is estimated to be 3.6 m. Consideration should be given as to how representative this value is of the Keeyask Reservoir. The Keeyask Reservoir is comprised of a fast flowing and well mixed main channel and shallower backbays on the periphery of the Main Channel. Averaging the depths of these two types of water bodies may not adequately describe GHG production nor emissions within and amongst these water bodies.

Littoral Area (%): 26%
The littoral zone is estimated to comprise approximately 26% of the total Keeyask reservoir area, 30 years after flooding (W. DeWit, Manitoba Hydro, personal communication, July 5, 2023).

Thermocline Depth (m):
The Keeyask Reservoir is not expected to develop a stable thermocline (Keeyask Hydropower Limited Partnership, 2012b) so no value was entered for the G-res Tool model. Water is expected to be well mixed, and expected to be at or near dissolved oxygen saturation in the main channel entering the reservoir and flowing through the reservoir.

Soil Carbon Content Under the Impoundment Area (kg C/m^2): 11.94 kg C/m^2
The value of 11.94 kg C/m^2 was derived from the Earth Engine functionality of the G-res Tool. For comparison, this value aligns well with IPCC 2019 default value of 11.6 ±65% kg C/m^2 for the soil organic carbon stock content for Boreal Moist/Dry wetland soils for 0-30 cm depth (IPCC 2019, Table 2.3).

This value is also similar to the average carbon content of 10.8 kg C/m^2 in peat-forming soils at a depth of 0-30 cm in a boreal forest site located south of James Bay (Magnan et al., 2020). Similarly, Beaulne et al (2021) calculated that between 11.0 – 12.6 kg C/m^2 has been stored in the organic horizons of a boreal peatland site in eastern Canada over the last 200 years.

Annual Wind Speed: 4.25 m/s
The value of 4.25 m/s was derived from the Earth Engine functionality of the G-res Tool.

This value is within the range of average wind speeds of 3.89 m/s to 4.94 m/s recorded in Gillam, Manitoba from 1971 to 2000 (Keeyask Hydropower Limited Partnership, 2012b). The meteorological station in Gillam is located approximately 30 km east of the Keeyask Generating Station/Reservoir (Keeyask Hydropower Limited Partnership, 2012b).

Water Residence Time (WRT, yrs): 0.0034 yrs
The Water Residence Time for the main channel of the Keeyask Reservoir is estimated to vary from 15 to 30 hours; 0.0017 to 0.0034 years (Keeyask Hydropower Limited Partnership, 2012b).

The Water Residence Time for backbays may be up to 30 days; 0.082 years (Keeyask Hydropower Limited Partnership, 2012b) or possibly longer (W. DeWit, Manitoba Hydro, personal communication, May 1, 2020). Water residence time in backbay environments can be very challenging to estimate as it is influenced by water inflows from creeks, wind driven currents and other factors.

The upper boundary of 0.0034 for the main channel was used in the G-res Tool Model for this G-res scenario for the Keeyask Reservoir.

Annual Discharge from Main Intake (m^3/s): 3,300 m^3/s
The average annual discharge is approximately 3,300 m^3s (W. DeWit, Manitoba Hydro, personal communication, May 1, 2020).

Water Intake Depth (m): 28.0 m
The height and depth of the water intake structures are such that the Water Intake Depth is between 5.3 m to 28.0 m below the reservoir water surface. This spans approximately 22.7 m or 73% of the entire water column of the reservoir (Keeyask Hydropower Limited Partnership, 2012b, Figure 2.2).

Water Intake Elevation (m above sea level): 131 m ASL
The elevation of the top of the Water Intake is 131 m ASL (Keeyask Hydropower Limited Partnership, 2012b, Figure 2.2).

Secondary Water Intake Depth (m): Not Applicable

Annual Discharge from Secondary Intake (m^3/s): Not Applicable

Phosphorus Concentration (µg/L): 58.5 µg/L

The Total Phosphorus concentration of 58.5 µg/L was used in the Keeyask G-res Model, as this was the benchmark value established by the Keeyask Generation Project Aquatic Environmental Monitoring Plan (Dowd and Hrenchuck, 2024). Measured post-flood Total Phosphorus concentrations ranged from 28.5 to 158 µg/L during the seasonal sampling events conducted from 2021 to 2023 (Hrenchuk, 2021, 2022; Dowd and Hrenchuck, 2023, 2024). The annual average concentrations measured from 2021-2023, ranged from 51.8 to 56.8 µg/L (Hrenchuk 2021, 2022; Dowd and Hrenchuck, 2023, 2024) which are similar to the Benchmark value of 58.5 µg/L that was used in the G-res model

To be conservative, the value of 58.5 µg/L was used in the G-res Tool modeled estimates.

Trophic Level: Eutrophic

Based on Total Phosphorus concentrations of 58.5 µg/L, the main stem of the Nelson River is classified as Eutrophic for this G-res Tool model.

Reservoir Mean Global Horizontal Radiance (kWh/m^2/d): 4.8

The Reservoir Mean Global Horizontal Radiance value of 4.8 kWh/m^2/d was generated by the G-res Tool Earth Engine.

Mean Temperature per Month (ºC)

Mean Temperature per Month and Mean Annual Air Temperature data were derived by the G-res Tool Earth Engine (Figure 3-4).

Mean Temperature per Month (°C)	
January	-25.6
February	-22.16
March	-15.37
April	-4.37
May	4.58
June	11.13
July	15.23
August	13.61
September	6.8
October	-0.1
November	-11.84
December	-22.62
Mean Annual Air Temperature (°C)	-4.2

Figure 3-2 Mean Average Monthly Temperatures

4 Reservoir Services Data

100% of the Reservoir Services were allocated to the Keeyask Reservoir/hydroelectricity (Figure 4-1).



Figure 4-1 Keeyask G-res Model: Reservoir Services

5 Construction GHG

The G-res Tool was not used to estimate Construction Emissions.

6 Unrelated Anthropogenic Sources Emissions

Since 100% of the purpose of the Keeyask Reservoir is assigned to hydroelectricity, no GHG emissions were allocated to Unrelated Anthropogenic Sources (Figure 6-1).

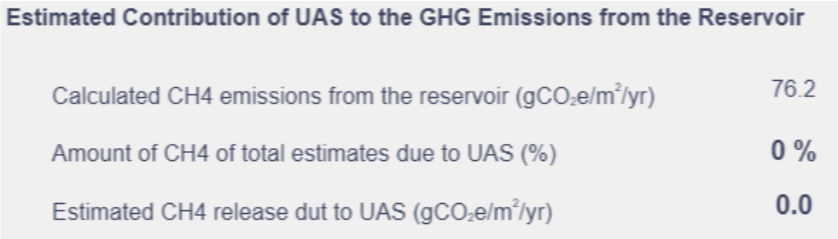


Figure 6-1 Keeyask G-res Model: Contribution of Unrelated Anthropogenic Sources of GHG Emissions

References

Bao, T., Jia, G., & Xu, X. (2021). Wetland Heterogeneity Determines Methane Emissions: A Pan-Arctic Synthesis. *Environmental Science and Technology*, *55*(14), 10152–10163. https://doi.org/10.1021/acs.est.1c01616

Beaulne, J., Garneau, M., Magnan, G., Boucher, É. (2021). Peat deposits store more carbon than trees in forested peatlands of the boreal biome. Sci Rep 11, 2657. https://doi.org/10.1038/s41598-021-82004-x

Boonman, J., Buzacott, A. J. V., van den Berg, M., van Huissteden, C., & van der Velde, Y. (2024). Transparent automated CO2 flux chambers reveal spatial and temporal patterns of net carbon fluxes from managed peatlands. *Ecological Indicators*, *164*. https://doi.org/10.1016/j.ecolind.2024.112121

Delwiche, K. B., Knox, S. H., Malhotra, A., Fluet-Chouinard, E., McNicol, G., Feron, S., Ouyang, Z., Papale, D., Trotta, C., Canfora, E., Cheah, Y. W., Christianson, D., Alberto, M. C. R., Alekseychik, P., Aurela, M., Baldocchi, D., Bansal, S., Billesbach, D. P., Bohrer, G., … Jackson, R. B. (2021). FLUXNET-CH4: A global, multi-ecosystem dataset and analysis of methane seasonality from freshwater wetlands. *Earth System Science Data*, *13*(7), 3607–3689. https://doi.org/10.5194/essd-13-3607-2021

Dowd, M.B and C.L. Hrenchuck. (2023). Results of water quality monitoring in the Nelson River, 2022: Year 1 Operation. Keeyask Generation Project Aquatic Effects Monitoring Plan Report. #AEMP-2023-13. A report prepared for Manitoba Hydro by North/South Consultants Inc,. June 2023. xv +295 pages.

Dowd, M.B and C.L. Hrenchuck. (2024). Results of water quality monitoring in the Nelson River, 2023: Year 2 Operation. Keeyask Generation Project Aquatic Effects Monitoring Plan Report. #AEMP-2024-11. A report prepared for Manitoba Hydro by North/South Consultants Inc,. June 2024. xvi +301 pages.

Government of Canada. (2013). National Ecological Framework for Canada. Ecozones, Ecoregions, and Ecodistricts. https://sis.agr.gc.ca/cansis/publications/maps/eco/all/districts/eco_all_districts_1m_manitoba.jpg

Hrenchuk, C. (2021). Results of water quality monitoring in the Nelson River, 2020: Year 7 Construction. Keeyask Generation Project Aquatic Effects Monitoring Plan Report #AEMP-2021-06. A report prepared for Manitoba Hydro by North/South Consultants Inc., June 2021. xxv + 124 pp.

Hrenchuk, C. (2022). Results of water quality monitoring in the Nelson River, 2021: Year 8 Construction. Keeyask Generation Project Aquatic Effects Monitoring Plan Report #AEMP-2022-14. A report prepared for Manitoba Hydro by North/South Consultants Inc., June 2022. xxviii + 301 pp.

Intergovernmental Panel on Climate Change (IPCC). (2014). 2013 Supplement to the 2006 IPCC Guidelines for National Greenhouse Gas Inventories: Wetlands, Hiraishi, T., Krug, T., Tanabe, K., Srivastava, N., Baasansuren, J., Fukuda, M. and Troxler, T.G. (eds). Published: IPCC,

SwitzerlandJørgensen, S.E., Halling- Sørenen, B., Nielsen, S.N., 1996. Handbook of Environmental and Ecological Modeling. Lewis Publishers, Boca Raton. 672 pp.

Intergovernmental Panel on Climate Change (IPCC). (2019.) Chapter 2: Generic Methodologies Applicable to Multiple Land-Use Categories, Volume 4 Agriculture, Forestry and Other Land Use, 2019 Refinement to the 2006 IPCC Guidelines for National Greenhouse Gas Inventories, 104 pages.

Intergovernmental Panel on Climate Change (IPCC). (2019b). Wetlands. Chapter 7_Volume 4 (Agriculture, Forestry and Other Land Use), 2019 Refinement to the 2006 IPCC Guidelines for National Greenhouse Gas Inventories.

Järveoja, J., Nilsson, M. B., Gažovič, M., Crill, P. M., & Peichl, M. (2018). Partitioning of the net CO2 exchange using an automated chamber system reveals plant phenology as key control of production and respiration fluxes in a boreal peatland. *Global Change Biology*, *24*(8), 3436–3451. https://doi.org/10.1111/gcb.14292

Keeyask Hydropower Limited Partnership. (2012a). Keeyask Generation Project: Environmental Impact Statement; Executive Summary. 60 pages.

Keeyask Hydropower Limited Partnership (2012b). Keeyask Generation Project: Environmental Impact Statement; Physical Environment Response to EIS Guidelines, Supporting Volume. 1018 pages.

Keeyask Hydropower Limited Partnership. (2012c). Keeyask Generation Project: Environmental Impact Statement; Project Description, Supporting Volume. 262 pages.

Keeyask Hydropower Limited Partnership. (2012d). Keeyask Generation Project: Environmental Impact Statement; Terrestrial Environment Supporting Volume. 1346 pages.

Keeyask Hydropower Limited Partnership. (2012e). Keeyask Generation Project: Environmental Impact Statement; Aquatic Environment Supporting Volume. 1745 pages.

Keeyask Hydropower Limited Partnership. (2014). Press Release: Construction Begins on Keeyask Generating Station. https://keeyask.com/wp-content/uploads/2014/07/07-16-KHLP-News-Release01-Revised.pdf

Keeyask Hydropower Limited Partnership. (2020). Post Reservoir Impoundment Information Sheet. https://keeyask.com/wp-content/uploads/2020/09/FINAL-Post-Impoundment_InfoSheet_20200914.pdf

Knox, S. H., Jackson, R. B., Poulter, B., McNicol, G., Fluet-Chouinard, E., Zhang, Z., Hugelius, G., Bousquet, P., Canadell, J. G., Saunois, M., Papale, D., Chu, H., Keenan, T. F., Baldocchi, D., Torn, M. S., Mammarella, I., Trotta, C., Aurela, M., Bohrer, G., … Zona, D. (2019). FluXNET-CH4 synthesis activity objectives, observations, and future directions. Bulletin of the American Meteorological Society, 100(12), 2607–2632. https://doi.org/10.1175/BAMS-D-18-0268.1

Knox, S. H., Bansal, S., McNicol, G., Schafer, K., Sturtevant, C., Ueyama, M., Valach, A. C., Baldocchi, D., Delwiche, K., Desai, A. R., Euskirchen, E., Liu, J., Lohila, A., Malhotra, A., Melling, L., Riley, W., Runkle, B. R. K., Turner, J., Vargas, R., … Jackson, R. B. (2021). Identifying dominant environmental

predictors of freshwater wetland methane fluxes across diurnal to seasonal time scales. *Global Change Biology*, *27*(15), 3582–3604. https://doi.org/10.1111/gcb.15661

Kuhn, M. A., Varner, R. K., Bastviken, D., Crill, P., Macintyre, S., Turetsky, M., Walter Anthony, K., McGuire, A. D., & Olefeldt, D. (2021). BAWLD-CH4: A comprehensive dataset of methane fluxes from boreal and arctic ecosystems. In *Earth System Science Data* (Vol. 13, Issue 11, pp. 5151–5189). Copernicus Publications. https://doi.org/10.5194/essd-13-5151-2021

Lund, M., Lafleur, P. M., Roulet, N. T., Lindroth, A., Christensen, T. R., Aurela, M., Chojnicki, B. H., Flanagan, L. B., Humphreys, E. R., Laurila, T., Oechel, W. C., Olejnik, J., Rinne, J., Schubert, P., & Nilsson, M. B. (2010). Variability in exchange of CO2 across 12 northern peatland and tundra sites. *Global Change Biology*, *16*(9), 2436–2448. https://doi.org/10.1111/j.1365-2486.2009.02104.x

Magnan, G., Garneau, M., Le Stum-Boivin, É., Grondin, P., and Yves Bergeron, Y. (2020). Long-Term Carbon Sequestration in Boreal Forested Peatlands in Eastern Canada. Ecosystems 23, 1481–1493. https://doi.org/10.1007/s10021-020-00483-x

Manitoba Conservation and Water Stewardship. (2014). Interim Licence for the Development of Water Power, Keeyask Site, Nelson River. Issued in accordance with The Water Power Act (C.C.S.M., c.W60), and the Water Power Regulation (MR. 25/88R). Manitoba Conservation and Water Stewardship, The Province of Manitoba.

Manitoba Hydro. (2012). Historical Climate Analysis Technical Memorandum # GN-9.5.1 for the Keeyask Generation Project Stage IV Studies- Physical Environment, Water Resources Engineering Department, 40 pages.

Manitoba Hydro. (2021). 2020-2021 Physical Environment Monitoring Report. Year 7 Construction. Keeyask Generation Project Physical Environment Monitoring Plan Report #PEMP-2021-01. June 2021.

Manitoba Hydro. (2024). 2023-2024 Physical Environment Monitoring Report. Year 3 Operation. Keeyask Generation Project Physical Environment Monitoring Plan Report #PEMP-2024-01. June 2024.

Marchand D., M. Demarty, and R. Gill. (2015). Keeyask Technical Summay – 2014. Summary prepared by Environnement Illimité for Manitoba Hydro, 11 p.

Margolis, H. A., Flanagan, L. B., & Amiro, B. D. (2006). The Fluxnet-Canada Research Network: Influence of climate and disturbance on carbon cycling in forests and peatlands. In *Agricultural and Forest Meteorology* (Vol. 140, Issues 1–4, pp. 1–5). https://doi.org/10.1016/j.agrformet.2006.08.013

Natural Resources Canada. 2020. Photovoltaic Potential and Solar Resource Maps of Canada. © Her Majesty the Queen in Right of Canada, as represented by the Minister of Natural Resources, 2020. https://fgp-pgf.maps.arcgis.com/apps/webappviewer/index.html?id=c91106a7d8c446a19dd1909fd93645d3

Nelson, J. A., Walther, S., Gans, F., Kraft, B., Weber, U., Novick, K., Buchmann, N., Migliavacca, M., Wohlfahrt, G., Šigut, L., Ibrom, A., Papale, D., Göckede, M., Duveiller, G., Knohl, A., Hörtnagl, L., Scott, R. L., Zhang, W., Hamdi, Z. M., … Jung, M. (2024). *X-BASE: the first terrestrial carbon and water flux products from an extended data-driven scaling framework, FLUXCOM-X*. https://doi.org/10.5194/egusphere-2024-165

Olefeldt, D., Hovemyr, M., Kuhn, M. A., Bastviken, D., Bohn, T. J., Connolly, J., Crill, P., Euskirchen, E. S., Finkelstein, S. A., Genet, H., Grosse, G., Harris, L. I., Heffernan, L., Helbig, M., Hugelius, G., Hutchins, R., Juutinen, S., Lara, M. J., Malhotra, A., … Watts, J. D. (2021). The boreal-arctic wetland and lake dataset (BAWLD). *Earth System Science Data*, *13*(11), 5127–5149. https://doi.org/10.5194/essd-13-5127-2021

Pan Y, Birdsey RA, Fang J, et al. (2011). A Large and Persistent Carbon Sink in the World's Forests. Science 333 (6045): 988-993. DOI: 10.1126/science.1201609.

Pastorello, G., Trotta, C., Canfora, E. et al. (2020). The FLUXNET2015 dataset and the ONEFlux processing pipeline for eddy covariance data. Sci Data 7, 225. https://doi.org/10.1038/s41597-020-0534-3

Prairie YT, Alm J, Harby A, Mercier-Blais S, Nahas R. (2017). The GHG Reservoir Tool (Gres) Technical documentation. Updated version 3.31 (03-07-2025). UNESCO/IHA research project on the GHG status of freshwater reservoirs. Joint publication of the UNESCO Chair in Global Environmental Change and the International Hydropower Association. 72 pages.

Prairie, Y. T., Alm, J., Beaulieu, J., Barros, N., Battin, T., Cole, J., del Giorgio, P., DelSontro, T., Guérin, F., Harby, A., Harrison, J., Mercier-Blais, S., Serça, D., Sobek, S., & Vachon, D. (2018). Greenhouse Gas Emissions from Freshwater Reservoirs: What Does the Atmosphere See? *Ecosystems*, *21*(5), 1058–1071. https://doi.org/10.1007/s10021-017-0198-9

Prairie, Y. T., Mercier-Blais, S., Harrison, J. A., Soued, C., Giorgio, P. del, Harby, A., Alm, J., Chanudet, V., & Nahas, R. (2021). A new modelling framework to assess biogenic GHG emissions from reservoirs: The G-res tool. *Environmental Modelling and Software*, *143*. https://doi.org/10.1016/j.envsoft.2021.105117

Rasilo T, Prairie YT and del Giorgio, PA. (2014). Large-scale patterns in summer diffusive CH4 fluxes across boreal lakes, and contribution to diffusive C emissions. Global Change Biology 1: 1–16.

Strachan, I. B., Nugent, K. A., Crombie, S., & Bonneville, M. C. (2015). Carbon dioxide and methane exchange at a cool-temperate freshwater marsh. *Environmental Research Letters*, *10*(6). https://doi.org/10.1088/1748-9326/10/6/065006

Strachan, I. B., Pelletier, L., & Bonneville, M. C. (2016). Inter-annual variability in water table depth controls net ecosystem carbon dioxide exchange in a boreal bog. *Biogeochemistry*, *127*(1), 99–111. https://doi.org/10.1007/s10533-015-0170-8

Strack, M., Mwakanyamale, K., Hassanpour Fard, G., Bird, M., Bérubé, V., & Rochefort, L. (2017). Effect of plant functional type on methane dynamics in a restored minerotrophic peatland. *Plant and Soil*, *410*(1–2), 231–246. https://doi.org/10.1007/s11104-016-2999-6

Thalasso, F., Riquelme, B., Gómez, A., MacKenzie, R., Aguirre, F. J., Hoyos-Santillan, J., Rozzi, R., & Sepulveda-Jauregui, A. (2023). Technical note: Skirt chamber - an open dynamic method for the rapid and minimally intrusive measurement of greenhouse gas emissions from peatlands. *Biogeosciences*, *20*(18), 3737–3749. https://doi.org/10.5194/bg-20-3737-2023

Treat, C. C., Bloom, A. A., & Marushchak, M. E. (2018). Nongrowing season methane emissions–a significant component of annual emissions across northern ecosystems. *Global Change Biology*, *24*(8), 3331–3343. https://doi.org/10.1111/gcb.14137

Treat, C. C., Virkkala, A. M., Burke, E., Bruhwiler, L., Chatterjee, A., Fisher, J. B., Hashemi, J., Parmentier, F. J. W., Rogers, B. M., Westermann, S., Watts, J. D., Blanc-Betes, E., Fuchs, M., Kruse, S., Malhotra, A., Miner, K., Strauss, J., Armstrong, A., Epstein, H. E., … Hugelius, G. (2024). Permafrost Carbon: Progress on Understanding Stocks and Fluxes Across Northern Terrestrial Ecosystems. *Journal of Geophysical Research: Biogeosciences*, *129*(3). https://doi.org/10.1029/2023JG007638

Virkkala, A. M., Aalto, J., Rogers, B. M., Tagesson, T., Treat, C. C., Natali, S. M., Watts, J. D., Potter, S., Lehtonen, A., Mauritz, M., Schuur, E. A. G., Kochendorfer, J., Zona, D., Oechel, W., Kobayashi, H., Humphreys, E., Goeckede, M., Iwata, H., Lafleur, P. M., … Luoto, M. (2021). Statistical upscaling of ecosystem CO2 fluxes across the terrestrial tundra and boreal domain: Regional patterns and uncertainties. *Global Change Biology*, *27*(17), 4040–4059. https://doi.org/10.1111/gcb.15659

Webster, K. L., Bhatti, J. S., Thompson, D. K., Nelson, S. A., Shaw, C. H., Bona, K. A., Hayne, S. L., & Kurz, W. A. (2018). Spatially-integrated estimates of net ecosystem exchange and methane fluxes from Canadian peatlands. *Carbon Balance and Management*, *13*(1). https://doi.org/10.1186/s13021-018-0105-5

Yuan, K., Li, F., McNicol, G., Chen, M., Hoyt, A., Knox, S., Riley, W. J., Jackson, R., & Zhu, Q. (2024). Boreal–Arctic wetland methane emissions modulated by warming and vegetation activity. Nature Climate Change, 14(3), 282–288. https://doi.org/10.1038/s41558-024-01933-3

Zhao, B., & Zhuang, Q. (2023). Peatlands and their carbon dynamics in northern high latitudes from 1990 to 2300: a process-based biogeochemistry model analysis. *Biogeosciences*, *20*(1), 251–270. https://doi.org/10.5194/bg-20-251-2023

Appendix 2

Keeyask Reservoir Lifecycle GHG Model Uncertainty Analysis



Keeyask Forebay, September 21 2023

Contents

1. Data Uncertainty 1
1.1. Pre-Flood Landscape Classification 1
1.1.1. Pre-Flood Landcover Scenarios 2
1.1.2. Pre-flood GHG Emission Factors 2
1.1.3. Pre-Flood Landcover Class Sensitivity Analysis Results 4
1.1.4. Pre-Flood Landcover Class Sensitivity Analysis: Discussion 11
1.2. Pre-Flood CH_4 and CO_2 Emission Factors 14
1.3. Size of Littoral Zone 19
1.4. Concentration of Total Phosphorous 20
1.5. Length of Water Residence Time 24
2. Structural Uncertainty 27
2.1. Pre-Flood Land Cover: Peatlands 27
2.1.1. Description of G-res Database of Boreal Reservoirs 28
2.1.2. G-res Database Reservoirs 20 Years or Less at Time of Sampling 28
2.1.3. Mature Peatland Reservoirs Included in G-res Database 31
2.2. Peat Resurfacing and Floating Peat Mats 36
2.2.4. Eastmain-1 Reservoir 37
2.2.5. Stephens Lake 37
2.3. Littoral Zone 37
2.3.6. Canadian Reservoirs 38
2.3.7. L. Skinnmuddselet, Sweden 39
2.3.8. Mature Reservoirs 41
3. References 48

Figures

Figure 1-1 Landcover and Emission Factor Scenarios 4
Figure 1-2 Modelling Scenarios: Net Annual Average Lifecycle GHG Emissions.....10
Figure 1-3 Modelling Scenarios: Lifecycle Emission Intensity 10
Figure 1-4 Modelling Scenarios: Net Average Annual Keeyask Reservoir Lifecycle GHG Emissions 13
Figure 1-5 Modelling Scenarios: Keeyask Reservoir Net Lifecycle GHG Emissions 13
Figure 1-6 Modelling Scenarios: Keeyask Reservoir Lifecycle GHG Emission Intensity.....14
Figure 1-7 Mean GHG Emission Factors 15
Figure 1-8 Lower Limit GHG Emission Factors.....15
Figure 1-9 Upper Limit GHG Emission Factors 16
Figure 1-10 Total Keeyask Reservoir Net Lifecycle GHG Emissions 18
Figure 1-11 Keeyask Reservoir Lifecycle GHG Emission Intensity 18
Figure 2-1 Pre-Flood Keeyask Reservoir Landcover.....35
Figure 2-2 Floating Peat Islands in Keeyask Reservoir Backbay Near GHG Monitoring Location.....35
Figure 2-3 Floating Peat Islands in Keeyask Reservoir Forebay Near GHG Monitoring Location.....36
Figure 2-4 Stephens Lake Floating Peat Mats Along Northern Shoreline(34 Years After Impoundment) 46
Figure 2-5 Stephens Lake Floating Peat Mats Along Northern Shoreline (34 Years After Impoundment) 46
Figure 2-6 Stephens Lake Semi-Submerged Vegetation Along Northern Shoreline Littoral Zone (34 Years After Impoundment).....47

Tables

Table 1-1 Landcover and Emission Factor Scenarios 4
Table 1-2 Modelling Scenarios: Predicted Net Annual Emissions per m^2 7
Table 1-3 Modelling Scenarios: Predicted Net Annual Emissions 8
Table 1-4 Modelling Scenarios: Predicted Net 100-Year Lifecycle Emissions 9
Table 1-5 Modelling Scenarios: Scenario Class Averages 12
Table 1-6 Results: Pre-Flood GHG Emission Factor Scenarios 17
Table 1-7 Keeyask Reservoir Net Lifecycle GHG Emissions: Littoral Zone Scenarios 20
Table 1-8 Keeyask Reservoir Total Phosphorous Monitoring Results 23
Table 1-9 Keeyask Reservoir Net Lifecycle GHG Emissions: Total Phosphorous Scenarios 24
Table 1-10 Keeyask Reservoir: Water Residence Time Scenario 0.082 Years 26
Table 1-11 Keeyask Reservoir: Water Residence Time Scenario 0.0017 Years 26
Table 2-1 G-res Tool Boreal Reservoir Data Sources: Reservoir Age at Time of Sampling 34
Table 2-2 G-res Tool Boreal Reservoir Data Sources: Reservoir Age at Time of Sampling 20 Years or Younger and Extent of Littoral Zone 40
Table 2-3 G-res Tool Boreal Reservoir Data Sources: Reservoir Age at Time of Sampling Over 20 Years and Extent of Littoral Zone 45

Keeyask Reservoir Lifecycle GHG Model Uncertainty Analysis

The Keeyask Reservoir Lifecycle GHG Model was assessed in terms of Data Uncertainty and Structural Uncertainty. For this study, Data Uncertainty refers to the uncertainty associated with the data inputs that were used to run the Keeyask G-res model. Structural Uncertainty refers to the uncertainty associated with the database of reservoir GHG studies that underpin the G-res Tool equations. The approach to this assessment was generally guided by the uncertainty assessment conducted by Pokorny et al. (2021) on streamflow modelling of the Lower Nelson River as part of the BaySys Project.

1. Data Uncertainty

Data uncertainty will focus on those variables that have the largest impact on the modelled Keeyask reservoir net lifecycle GHG emissions and lifecycle GHG emission intensity values. This includes:

1) Pre-flood Landcover Classification;
2) Pre-flood GHG Emission Factors;
3) Size of Littoral Zone;
4) Concentration of Total Phosphorous; and
5) Length of Water Residence Time.

1.1. Pre-Flood Landscape Classification

The G-res Tool estimates pre-flood GHG emissions by classifying the pre-flood landscape into landcover types and by applying GHG emission factors to each landcover category. This is the largest source of uncertainty related to data entered in the Keeyask G-res model.

Three pre-flood landcover classification schemes were assessed. They involved the Keeyask EIS Vegetation Structure Land Class; the Keeyask EIS Terrestrial Habitat Land Class; and the Keeyask EIS Ecological Land Class. The Keeyask EIS Ecological Land Class was selected to represent the Keeyask pre-flood landcover.

A sensitivity assessment was conducted to compare combinations of these three pre-flood landcover classes, plus a “conservative” scenario, and alternative GHG emission factors against the selected Keeyask G-res Model (Keeyask EIS Ecological Land Classification). This involved

running seventeen scenarios using G-res to create an ensemble of pre-flood and post-flood emissions to compare against the "Keeyask G-res Model" (Table 1-1).

1.1.1. Pre-Flood Landcover Scenarios

The scenarios included the following:

- Scenarios 1-5: (Keeyask EIS Vegetation Structure Land Class) x (alternative GHG emission factors)
- Scenarios 6-10: (Keeyask EIS Terrestrial Habitat Land Class) x (alternative GHG emission factors)
- Scenarios 11-16: (Keeyask EIS Ecological Land Class) x (alternative GHG emission factors)
- Scenario 17: "Conservative" scenario, pre-flood landscape fixed as "Boreal Forest", a net GHG sink

1.1.2. Pre-flood GHG Emission Factors

Below is a description of the 5 Groups of CO_2 and CH_4 emission factors used in Scenarios 1 – 16.

Emission Factors (Group a)
G-res default values.

Emission Factors (Group b)
CO_2 emission factors were adapted from Treat et al (2024); CH_4 emission factors were adapted from the Boreal–Arctic Wetland and Lake Methane Dataset (BAWLD-CH4) (Kuhn et al., 2021) and Treat et al. (2018; 2024). Individual CH_4 and CO_2 emission factors were developed for the G-res input categories Wetlands, and for Forests and Grassland/Shrubland combined. The length of the Growing Season/"Warm Period" was defined by the Kuhn et al. (2021) study as approximately May through October, 188 days.

Emission Factors (Group c)
Developing CO_2 and CH_4 pre-flood emission factors for Wetlands, Forests and Grassland/Shrubland, followed the same approach as that used for Emission Factor Group (b) above. That is, CO_2 emission factors were adapted from Treat et al. (2024); CH_4 emission factors were adapted from the Boreal–Arctic Wetland and Lake Methane Dataset (BAWLD-CH4) (Kuhn et al., 2021; Treat et al., 2018; 2024). Individual CH_4 and CO_2 emission factors were developed for the G-res input categories Wetlands, and Forests and Grassland/Shrubland combined. The difference between Group b and c emission factors is that Group c used a Keeyask-specific growing period of

135 days and an ice-free period of 199 days when calculating annual emissions. The methodology for determining the length of the growing period and ice-free period is described in Appendix 1.

Emission Factors (Group d)
CO_2 and CH4 emission factors were adapted from Treat et al. (2024; 2018). Treat reviewed CH_4 and CO_2 fluxes from nearly 20 synthesis studies, including the Boreal–Arctic Wetland and Lake Methane Dataset (BAWLD-CH4) dataset and the FLUXNET-CH4. The review covered synthesis studies conducted from 2002 – 2024 of the Circum-Arctic Permafrost Region, including Alaska, Canadian tundra, boreal Western Canada, Eastern Canada, and Eurasia. Landscape types included marsh, fen, bog, permafrost wetland, permafrost bog, boreal forest, and upland tundra. Study methods included both eddy covariance and chamber measurement techniques.

Individual CH_4 emission factors were developed for Wetlands, and for Forests and Grassland/Shrubland combined. A composite CO_2 emission factor was developed for the Keeyask uplands, which includes Wetlands, Forests and Grassland/Shrubland combined. The length of the growing season and ice-free season were kept consistent with Scenarios b, and e, at 184 days.

Emission Factors (Group e)
Emission factors were derived from a review of published studies of GHG emissions from northern peatlands, with an emphasis on Canadian research where available. Literature sources included: a synthesis of CO_2 (net ecosystem exchange) and CH_4 emissions from Canadian peatlands (Webster et al., 2018); the Boreal–Arctic Wetland and Lake Methane Dataset (BAWLD-CH4) which is a comprehensive dataset of CH_4 fluxes from circumpolar boreal and arctic ecosystems (Kuhn et al., 2021; Olefeldt et al., 2021); a synthesis of CH_4 emissions from northern high latitude wetlands, including bog, poor fen, rich fen, and swamp (Turetsky et al., 2014); CO_2 and CH_4 emissions at a cool-temperate Canadian freshwater marsh (Strachan et al., 2015), and boreal forest CO_2 emissions (net ecosystem exchange) from the BOReal Ecosystem–Atmosphere Study (BOREAS) Northern Study Area near Thompson, Manitoba (Goulden et al., 2011). The length of the growing season and ice-free season were kept consistent with Scenarios b, and d, at 184 days.

Emission Factors (Scenario 17) (reclassified the pre-flood terrestrial land as boreal forest)
G-res Tool default emission factors were used for modelling.

Table 1-1 Landcover and Emission Factor Scenarios

Net Lifecycle Greenhouse Gas Emissions from the Keeyask Hydroelectric Reservoir Sensitivity Analyses

Landcover and Emission Factor Scenarios Using the G-res Tool

Scenarios
1 Vegetation Structure: G-res Tool Default EF (a)
2 Vegetation Structure: User-Defined EF (b)
3 Vegetation Structure: User-Defined EF (c)
4 Vegetation Structure: User-Defined EF (d)
5 Vegetation Structure: User-Defined EF (e)
6 Terrestrial Habitat (Course and Fine Ecosite Type): G-res Default EF (a)
7 Terrestrial Habitat (Course and Fine Ecosite Type): User-Defined EF (b)
8 Terrestrial Habitat (Course and Fine Ecosite Type): User-Defined EF (c)
9 Terrestrial Habitat (Course and Fine Ecosite Type): User-Defined EF (d)
10 Terrestrial Habitat (Course and Fine Ecosite Type): User-Defined EF (e)
11 Ecological Land Classification: G-res Tool Default EF (a)
12 Ecological Land Classification: User-Defined EF (e)
13 Ecological Land Classification (incl. BOG as Wetland): User-Defined EF (b)
14 Ecological Land Classification (incl. BOG as Wetland): User-Defined EF (c)
15 Ecological Land Classification (incl. BOG as Wetland): User-Defined EF (d)
16 Ecological Land Classification (incl. BOG as Wetland): User-Defined EF (e)
17 Test - Re-Class Pre-Flood Land to Forest

Emission Factor Descriptions

a) G-res Tool Default Preflood CO_2 and CH_4 Emission Factors

b) User-Defined Preflood CO2 and CH4 Emission Factors for Wetlands and Uplands. CO_2 EF adapted from Treat et al (2024); CH_4 adapted from Kuhn et al (2021) and Treat et al (2018; 2024). Growing Season/"Warm Period" as defined by Kuhn et al (2021).

c) User-Defined Preflood CO_2 and CH_4 Emission Factors for Wetlands and Uplands. CO_2 EF adapted from Treat et al (2024); CH_4 adapted from Kuhn et al (2021) and Treat et al (2018; 2024). Growing Season and Ice Free Period user-defined for Keeyask region.

d) User-Defined Preflood CO2 and CH4 Emission Factors for Wetlands and Uplands. CO_2 and CH_4 EF adapted from Treat et al (2018; 2024)

e) User-Defined Preflood CO_2 and CH_4 Emission Factors for Wetlands and Uplands. CO_2 and CH_4 EF adapted from Canadian Studies and International Studies.

Figure 1-1 Landcover and Emission Factor Scenarios

1.1.3. Pre-Flood Landcover Class Sensitivity Analysis Results

Results of the sensitivity analysis are summarized below and illustrated in Figures 1-2 – 1-6, and Tables 1-1 to 1-4).

1.1.3.1. Post-Impoundment Emissions

Minimum Post-Impoundment emissions were 88 $gCO_2e/m^2/yr$; 8,851 tCO_2e/yr; and 885,101 tCO_2e/100-year lifecycle of the reservoir. These emissions were predicted for the Ecological Land Class Scenarios (11-16) and the "All Forest" Scenario (17).

Maximum Post-Impoundment emissions were 93 $gCO_2e/m^2/yr$; 9,363 tCO_2e/yr; and 936,277 tCO_2e/100-year lifecycle of the reservoir. These emissions were predicted for Scenarios 1-5 Vegetation Structure Scenarios (1-5) and Terrestrial Habitat Scenarios (6-10)

Average Post-Impoundment emissions were 90.9 $gCO_2e/m^2/yr$; 9,152 tCO_2e/yr; and 915,205 tCO_2e/100-year lifecycle of the reservoir.

1.1.3.2. Pre-Impoundment Emissions

Minimum Pre-Impoundment emissions were -66 $gCO_2e/m^2/yr$; -6,608 tCO_2e/yr; and -660,758 tCO_2e/100-year lifecycle of the reservoir. These emissions were predicted for Vegetation Structure Class Scenario (5e).

Maximum Pre-Impoundment emissions were 195 $gCO_2e/m^2/yr$; 19,539 tCO_2e/yr; and 1,953,946 tCO_2e/100-year lifecycle of the reservoir. These emissions were predicted for 6 Terrestrial Habitat Class Scenario (6a).

Average Pre-Impoundment emissions were -3.8 $gCO_2e/m^2/yr$; -371 tCO_2e/yr; and -37,031 tCO_2e/100-year lifecycle of the reservoir.

1.1.3.3. Net Emissions

Minimum NET emissions were -101 $gCO_2e/m^2/yr$; -10,177 tCO_2e/yr; and -1,017,669 tCO_2e/100-year lifecycle of the reservoir. These emissions were predicted for Terrestrial Habitat Class Scenario (6a).

Maximum NET emissions were 159 $gCO_2e/m^2/yr$; 15,970 tCO_2e/yr; and 1,597,035 tCO_2e/100-year lifecycle of the reservoir. These emissions were predicted for Vegetation Structure Class Scenario (5e).

Average NET emissions were 95 $gCO_2e/m^2/yr$; 9,522 tCO_2e/yr; and 952,236 tCO_2e/100-year lifecycle of the reservoir.

1.1.3.4. GHG Emission Intensity

GHG Emissions Intensity ranged from a minimum of -2.3 gCO_2e/kWh for Terrestrial Habitat Class Scenario (6a) to a maximum of 3.6 gCO_2e/kWh for Vegetation Structure Class Scenario (5e) and Terrestrial Habitat Class Scenario (8c). The overall average was 2.2 gCO_2e/kWh.

Table 1-2 Modelling Scenarios: Predicted Net Annual Emissions per m^2

Net 100-Year Lifecycle Greenhouse Gas Emissions from the Keeyask Hydroelectric Reservoir
Modelling Scenarios using the G-res Tool

Predicted Net Annual Emissions per m^2

Scenarios	Emissions per m^2 of Reservoir $gCO_2e/m^2/yr$					Emission Intensity gCO_2e/kWh		
	Post-Impoundment	Pre-Impoundment	Net GHG Footprint	95% Confidence Intervals			95% Confidence Intervals	
1 Vegetation Structure: G-res Tool Default EF (a)	93	69	24	13	36	0.5	0	1
2 Vegetation Structure: User-Defined EF (b)	93	5	88	78	100	2.0	2	2
3 Vegetation Structure: User-Defined EF (c)	93	-18	112	101	123	2.5	2	3
4 Vegetation Structure: User-Defined EF (d)	93	47	46	36	58	1.1	1	1
5 Vegetation Structure: User-Defined EF (e)	93	(66)	159	148	171	3.6	3	4
6 Terrestrial Habitat (Course and Fine Ecosite Type): G-res Default EF (a)	93	195	(101)	(112)	(90)	-2.3	-3	-2
7 Terrestrial Habitat (Course and Fine Ecosite Type): User-Defined EF (b)	93	(56)	150	139	161	3.4	3	4
8 Terrestrial Habitat (Course and Fine Ecosite Type): User-Defined EF (c)	93	(63)	156	146	168	3.6	3	4
9 Terrestrial Habitat (Course and Fine Ecosite Type): User-Defined EF (d)	93	(40)	133	123	145	3.0	3	3
10 Terrestrial Habitat (Course and Fine Ecosite Type): User-Defined EF (e)	93	(35)	128	118	140	2.9	3	3
11 Ecological Land Classification: G-res Tool Default EF (a)	88	85	3	(7)	14	0.1	0	0
12 Ecological Land Classification: User-Defined EF (e)	88	(51)	139	129	150	3.2	3	3
13 Ecological Land Classification (incl. BOG as Wetland): User-Defined EF (b)	88	(5)	93	83	104	2.1	2	2
14 Ecological Land Classification (incl. BOG as Wetland): User-Defined EF (c)	88	(18)	106	96	117	2.4	2	3
15 Ecological Land Classification (incl. BOG as Wetland): User-Defined EF (d)	88	2	86	76	97	2.0	2	2
16 Ecological Land Classification (incl. BOG as Wetland): User-Defined EF (e)	88	(54)	142	132	153	3.2	3	3
17 Test - Re-Class Pre-Flood Land to Forest	88	(61)	149	139	160	3.4	3	4
All Scenarios								
Min	88	(66)	(101)	(112)	(90)	(2.3)	-3	-2
Max	93.0	195.0	159.0	148.0	171.0	3.6	3	
Avg	90.9	(3.8)	94.9	84.6	106.3	2.2	2	2
All Scenarios except (All Forest)								
Min	88	(66)	(101)	(112)	(90)	(2.3)	-3	-2
Max	93.0	195.0	159.0	148.0	171.0	3.6	3	4
Avg	91.1	(0.2)	91.5	81.2	102.9	2.1	2	2
Vegetation Structure:								
Min	93	-66	24	13	36	0.5	0	1
Max	93	69	159	148	171	3.6	3	4
Avg	93	7.4	85.8	75.2	97.6	1.9	2	2
Terrestrial Habitat (Course and Fine Ecosite Type):								
Min	93	(63)	(101)	(112)	(90)	(2.3)	-3	-2
Max	93	195	156	146	168	3.6	3	4
Avg	93	0	93	83	105	2.1	2	2
Ecological Land Classification:								
Min	88	(54)	3	(7)	14	0.1	0	0
Max	88	85	142	132	153	3.2	3	3
Avg	88	(7)	95	85	106	2.2	2	2
Test - Re-Class Pre-Flood Land to Forest	88	(61)	149	139	160	3.4	3	4

Explanatory Notes:

a) G-res Tool Default Preflood CO_2 and CH_4 Emission Factors

b) User-Defined Preflood CO_2 and CH_4 Emission Factors for Wetlands and Uplands.
CO_2 EF adapted from Treat et al (2024); CH_4 adapted from Kuhn et al (2021) and Treat et al (2018; 2024). Growing Season/"Warm Period" as defined by Kuhn et al (2021).

c) User-Defined Preflood CO_2 and CH_4 Emission Factors for Wetlands and Uplands.
CO_2 EF adapted from Treat et al (2024); CH_4 adapted from Kuhn et al (2021) and Treat et al (2018; 2024). Growing Season and Ice Free Period user-defined for Keeyask region.

d) User-Defined Preflood CO_2 and CH_4 Emission Factors for Wetlands and Uplands.
CO_2 and CH_4 EF adapted from Treat et al (2018; 2024)

e) User-Defined Preflood CO_2 and CH_4 Emission Factors for Wetlands and Uplands.
CO_2 and CH_4 EF adapted from Canadian Studies and International Studies.

Table 1-3 Modelling Scenarios: Predicted Net Annual Emissions

Net Lifecycle Greenhouse Gas Emissions from the Keeyask Hydroelectric Reservoir
Modelling Scenarios using the G-res Tool

Net Predicted Emissions

Scenarios	Total Reservoir Emissions per Year tCO_2e/yr					Emission Intensity gCO_2e/kWh		
	Post-Impoundment	Pre-Impoundment	Net GHG Footprint	95% Confidence Intervals			95% Confidence Intervals	
1 Vegetation Structure: G-res Tool Default EF (a)	9,363	6,962	2,400	1,335	3,594	0.5	0	1
2 Vegetation Structure: User-Defined EF (b)	9,363	511	8,852	7,791	10,050	2.0	2	2
3 Vegetation Structure: User-Defined EF (c)	9,363	(1,833)	11,195	10,130	12,389	2.5	2	3
4 Vegetation Structure: User-Defined EF (d)	9,363	4,737	4,626	3,574	5,813	1.1	1	1
5 Vegetation Structure: User-Defined EF (e)	9,363	(6,608)	15,970	14,889	17,188	3.6	3	4
6 Terrestrial Habitat (Course and Fine Ecosite Type): G-res Default EF (a)	9,363	19,539	(10,177)	(11,225)	(8,986)	-2.3	-3	-2
7 Terrestrial Habitat (Course and Fine Ecosite Type): User-Defined EF (b)	9,363	(5,653)	15,016	13,976	16,184	3.4	3	4
8 Terrestrial Habitat (Course and Fine Ecosite Type): User-Defined EF (c)	9,363	(6,331)	15,694	14,658	16,857	3.6	3	4
9 Terrestrial Habitat (Course and Fine Ecosite Type): User-Defined EF (d)	9,363	(4,004)	13,367	12,329	14,538	3.0	3	3
10 Terrestrial Habitat (Course and Fine Ecosite Type): User-Defined EF (e)	9,363	(3,528)	12,891	11,857	14,056	2.9	3	3
11 Ecological Land Classification: G-res Tool Default EF (a)	8,851	8,561	290	(663)	1,365	0.1	0	0
12 Ecological Land Classification: User-Defined EF (e)	8,851	(5,081)	13,932	12,932	15,070	3.2	3	3
13 Ecological Land Classification (incl. BOG as Wetland): User-Defined EF (b)	8,851	(488)	9,339	8,343	10,462	2.1	2	2
14 Ecological Land Classification (incl. BOG as Wetland): User-Defined EF (c)	8,851	(1,801)	10,652	9,658	11,777	2.4	2	3
15 Ecological Land Classification (incl. BOG as Wetland): User-Defined EF (d)	8,851	224	8,627	7,630	9,749	2.0	2	2
16 Ecological Land Classification (incl. BOG as Wetland): User-Defined EF (e)	8,851	(5,405)	14,256	13,263	15,381	3.2	3	3
17 Test - Re-Class Pre-Flood Land to Forest	8,851	(6,100)	14,951	13,956	16,074	3.4	3	4
All Scenarios								
Min	8,851	(6,608)	(10,177)	(11,225)	(8,986)	(2.3)	-3	-2
Max	9,363.0	19,539.0	15,970.0	14,889.0	17,188.0	3.6		
Avg	9,152.2	(370.5)	9,522.4	8,496.1	10,680.1	2.2	2	2
All Scenarios except (All Forest)								
Min	8,851	(6,608)	(10,177)	(11,225)	(8,986)	(2.3)	(3.0)	(2.0)
Max	9,363.0	19,539.0	15,970.0	14,889.0	17,188.0	3.6	3.0	4.0
Avg	9,171.0	(12.4)	9,183.1	8,154.8	10,342.9	2.1	1.8	2.3
Vegetation Structure:								
Min	9363	-6608	2400	1335	3594	0.5	0	1
Max	9363	6962	15970	14889	17188	3.6	3	4
Avg	9363	753.8	8608.6	7543.8	9806.8	1.9	2	2
Terrestrial Habitat (Course and Fine Ecosite Type):								
Min	9,363	(6,331)	(10,177)	(11,225)	(8,986)	(2.3)	-3	-2
Max	9,363	19,539	15,694	14,658	16,857	3.6	3	4
Avg	9,363	5	9,358	8,319	10,530	2.1	2	2
Ecological Land Classification:								
Min	8,851	(5,405)	290	(663)	1,365	0.1	0	0
Max	8,851	8,561	14,256	13,263	15,381	3.2	3	3
Avg	8,851	(665)	9,516	8,527	10,634	2.2	2	2
Test - Re-Class Pre-Flood Land to Forest	8,851	(6,100)	14,951	13,956	16,074	3.4	3	4

Explanatory Notes:

a) G-res Tool Default Preflood CO_2 and CH_4 Emission Factors

b) User-Defined Preflood CO_2 and CH_4 Emission Factors for Wetlands and Uplands.
CO_2 EF adapted from Treat et al (2024); CH_4 adapted from Kuhn et al (2021) and Treat et al (2018; 2024). Growing Season/"Warm Period" as defined by Kuhn et al (2021).

c) User-Defined Preflood CO_2 and CH_4 Emission Factors for Wetlands and Uplands.
CO_2 EF adapted from Treat et al (2024); CH_4 adapted from Kuhn et al (2021) and Treat et al (2018; 2024). Growing Season and Ice Free Period user-defined for Keeyask region.

d) User-Defined Preflood CO_2 and CH_4 Emission Factors for Wetlands and Uplands.
CO_2 and CH_4 EF adapted from Treat et al (2018; 2024)

e) User-Defined Preflood CO_2 and CH_4 Emission Factors for Wetlands and Uplands.
CO_2 and CH_4 EF adapted from Canadian Studies and International Studies.

Table 1-4 Modelling Scenarios: Predicted Net 100-Year Lifecycle Emissions

Net 100-Year Lifecycle Greenhouse Gas Emissions from the Keeyask Hydroelectric Reservoir
Modelling Scenarios using the G-res Tool

Predicted Net 100-Year Lifetime Emissions

Scenarios	Total Lifetime Reservoir Emissions tCO_2e					Emission Intensity gCO_2e/kWh		
	Post-Impoundment	Pre-Impoundment	Net GHG Footprint	95% Confidence Intervals			95% Confidence Intervals	
1 Vegetation Structure: G-res Tool Default EF (a)	936,277	696,227	240,049	133,532	359,432	0.5	0	1
2 Vegetation Structure: User-Defined EF (b)	936,277	51,125	885,152	779,104	1,005,004	2.0	2	2
3 Vegetation Structure: User-Defined EF (c)	936,277	(183,272)	1,119,549	1,013,036	1,238,936	2.5	2	3
4 Vegetation Structure: User-Defined EF (d)	936,277	473,690	462,587	357,424	581,316	1.1	1	1
5 Vegetation Structure: User-Defined EF (e)	936,277	(660,758)	1,597,035	1,488,932	1,718,848	3.6	3	4
6 Terrestrial Habitat (Course and Fine Ecosite Type): G-res Default EF (a)	936,277	1,953,946	(1,017,669)	(1,122,472)	(898,580)	-2.3	-3	-2
7 Terrestrial Habitat (Course and Fine Ecosite Type): User-Defined EF (b)	936,277	(565,325)	1,501,602	1,397,568	1,618,448	3.4	3	4
8 Terrestrial Habitat (Course and Fine Ecosite Type): User-Defined EF (c)	936,277	(633,074)	1,569,351	1,465,840	1,685,716	3.6	3	4
9 Terrestrial Habitat (Course and Fine Ecosite Type): User-Defined EF (d)	936,277	(400,389)	1,336,666	1,232,912	1,453,792	3.0	3	3
10 Terrestrial Habitat (Course and Fine Ecosite Type): User-Defined EF (e)	936,277	(352,833)	1,289,110	1,185,724	1,405,600	2.9	3	3
11 Ecological Land Classification: G-res Tool Default EF (a)	885,101	856,087	29,014	(66,264)	136,544	0.1	0	0
12 Ecological Land Classification: User-Defined EF (e)	885,101	(508,131)	1,393,232	1,293,152	1,507,004	3.2	3	3
13 Ecological Land Classification (incl. BOG as Wetland): User-Defined EF (b)	885,101	(48,779)	933,880	834,324	1,046,168	2.1	2	2
14 Ecological Land Classification (incl. BOG as Wetland): User-Defined EF (c)	885,101	(180,058)	1,065,159	965,848	1,177,692	2.4	2	3
15 Ecological Land Classification (incl. BOG as Wetland): User-Defined EF (d)	885,101	22,438	862,663	763,040	974,884	2.0	2	2
16 Ecological Land Classification (incl. BOG as Wetland): User-Defined EF (e)	885,101	(540,457)	1,425,558	1,326,284	1,538,128	3.2	3	3
17 Test - Re-Class Pre-Flood Land to Forest	885,101	(609,966)	1,495,068	1,395,560	1,607,404	3.4	3	4
All Scenarios								
Min	885,101.0	(660,758)	(1,017,669)	(1,122,472)	(898,580)	(2.3)	-3	-2
Max	936,277.0	1,953,946.0	1,597,035.0	1,488,932.0	1,718,848.0	3.6	3	4
Avg	915,204.5	(37,031.1)	952,235.6	849,620.2	1,068,019.8	2.2	2	2
All Scenarios except (All Forest)								
Min	885,101	(660,758)	(1,017,669)	(1,122,472)	(898,580)	(2.3)	(3.0)	(2.0)
Max	936,277.0	1,953,946.0	1,597,035.0	1,488,932.0	1,718,848.0	3.6	3.0	4.0
Avg	917,086.0	(1,222.7)	918,308.6	815,499.0	1,034,308.3	2.1	1.8	2.3
Vegetation Structure:								
Min	936277	-660758	240049	133532	359432	0.5	0	1
Max	936277	696227	1597035	1488932	1718848	3.6	3	4
Avg	936277	75402.4	860874.4	754405.6	980707.2	1.9	2	2
Terrestrial Habitat (Course and Fine Ecosite Type):								
Min	936,277	(633,074)	(1,017,669)	(1,122,472)	(898,580)	(2.3)	-3	-2
Max	936,277	1,953,946	1,569,351	1,465,840	1,685,716	3.6	3	4
Avg	936,277	465	935,812	831,914	1,052,995	2.1	2	2
Ecological Land Classification:								
Min	885,101	(540,457)	29,014	(66,264)	136,544	0.1	0	0
Max	885,101	856,087	1,425,558	1,326,284	1,538,128	3.2	3	3
Avg	885,101	(66,483)	951,584	852,731	1,063,403	2.2	2	2
Test - Re-Class Pre-Flood Land to Forest	885,101	(609,966)	1,495,068	1,395,560	1,607,404	3.4	3	4

Explanatory Notes:

a) G-res Tool Default Preflood CO_2 and CH_4 Emission Factors

b) User-Defined Preflood CO_2 and CH_4 Emission Factors for Wetlands and Uplands.
CO_2 EF adapted from Treat et al (2024); CH_4 adapted from Kuhn et al (2021) and Treat et al (2018; 2024). Growing Season/"Warm Period" as defined by Kuhn et al (2021).

c) User-Defined Preflood CO_2 and CH_4 Emission Factors for Wetlands and Uplands.
CO_2 EF adapted from Treat et al (2024); CH_4 adapted from Kuhn et al (2021) and Treat et al (2018; 2024). Growing Season and Ice Free Period user-defined for Keeyask region.

d) User-Defined Preflood CO2 and CH4 Emission Factors for Wetlands and Uplands.
CO_2 and CH_4 EF adapted from Treat et al (2018; 2024)

e) User-Defined Preflood CO_2 and CH_4 Emission Factors for Wetlands and Uplands.
CO_2 and CH_4 EF adapted from Canadian Studies and International Studies.

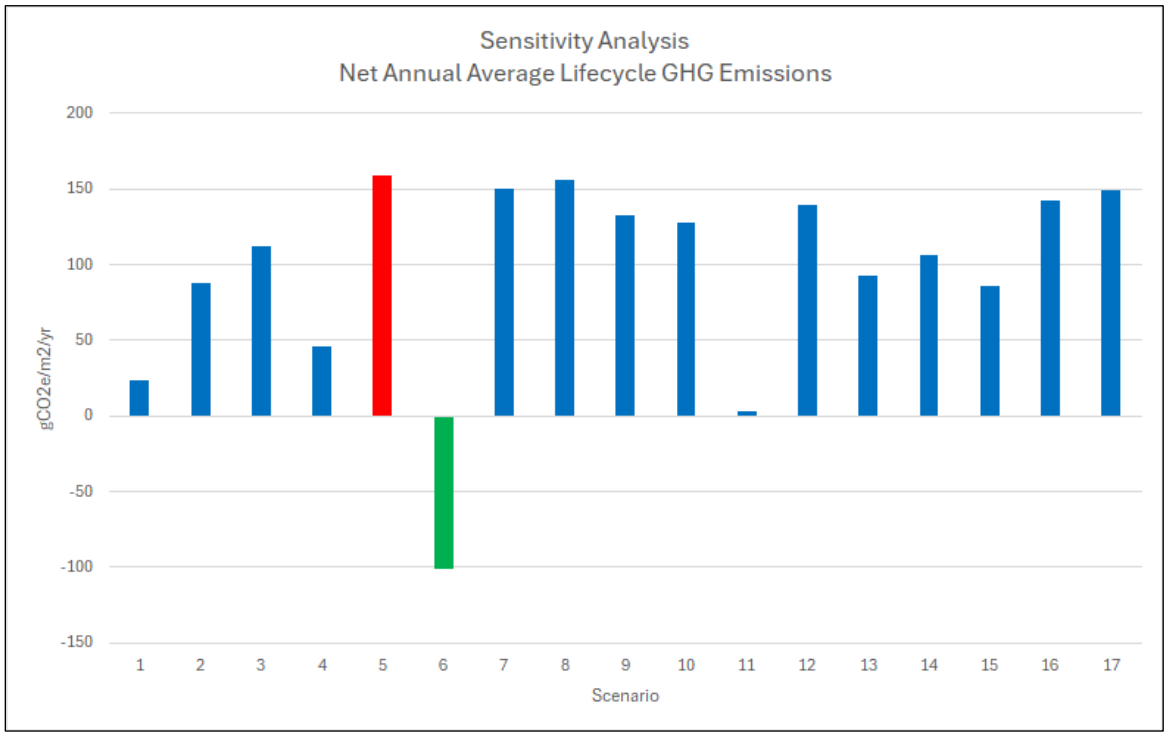


Figure 1-2 Modelling Scenarios: Net Annual Average Lifecycle GHG Emissions

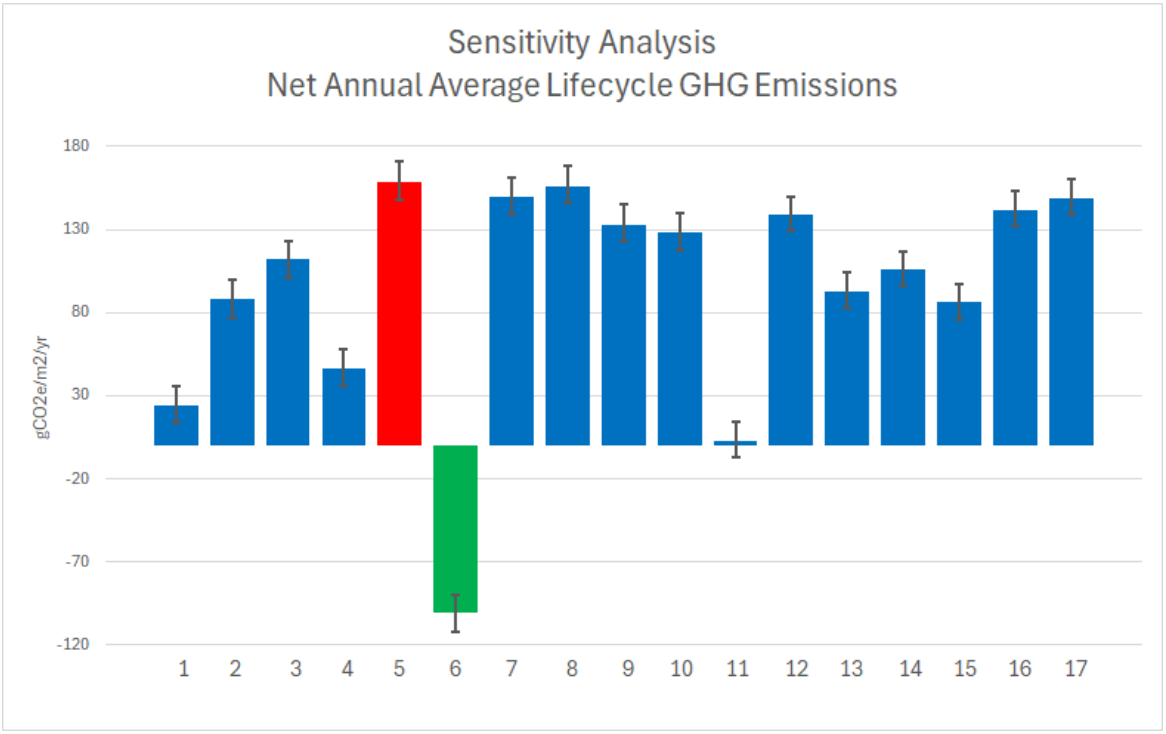


Figure 1-3 Modelling Scenarios: Lifecycle Emission Intensity

1.1.4. Pre-Flood Landcover Class Sensitivity Analysis: Discussion

Scenarios 1-5 are variations of the Vegetation Structure land class and emissions factors; Scenarios 6-10 are variations of the Terrestrial Habitat Ecosite land class; and Scenarios 11-16 are variations of the Ecological Land Classification and emission factors. Scenario 17 is a conservative benchmark, where all pre-flood terrestrial land was set to be as boreal forest (net GHG sink).

Annual Net lifecycle emissions for individual scenarios range from -101 $gCO_2e/m^2/yr$ to 159 $gCO_2e/m^2/yr$, with an average of 95 $gCO_2e/m^2/yr$ (Figure 1-2 and Table 1-2). This represents a decrease of -217% to an increase of 85% as compared to the Keeyask G-res Model. GHG Emission Intensity ranged from -2.3 gCO_2e/kWh to 3.6 gCO_2e/kWh, with an average of 2.2 gCO_2e/kWh for Scenarios 1–16.

Annual Net lifecycle emissions are modelled to be on average 85.8 $gCO_2e/m^2/yr$ for Scenarios 1-5 (Vegetation Structure); 93.2 $gCO_2e/m^2/yr$ for Scenarios 6-10 (Terrestrial Habitat Ecosite); and 94.8 $gCO_2e/m^2/yr$ for Scenarios 11-16 (Ecological Land Classification) (Figure 1-4 and Table 1-4). This compares to 86.0 $gCO_2e/m^2/yr$ for the Keeyask G-res model, represents a decrease of -0.2% to an increase of 10%. Scenario 17 was modelled to be 149.0 $gCO_2e/m^2/yr$.

GHG Emission Intensity is modelled to be on average 1.9 gCO_2e/kWh for Scenarios 1-5 (Vegetation Structure); 2.1 gCO_2e/kWh for Scenarios 6-10 (Terrestrial Habitat Ecosite); and 2.2 gCO_2e/kWh for Scenarios 11-16 (Ecological Land Classification) (Figure 1-6 and Table 1-4). This compares to 2.2 gCO_2e/kWh for the Keeyask G-res model. Scenario 17 was modelled to be 3.4 gCO_2e/kWh.

In conclusion, when comparing individual scenarios, the impact to the G-res model is high, with annual net emission per m^2 ranging from a decrease of -217% to an increase of 85% compared to the Keeyask G-res Model results. When comparing the average for each scenario class (e.g. Vegetation Structure; Terrestrial Habitat; and Ecological Land Class) the results of the Sensitivity Analyses for scenarios 1-16 compared well with the Keeyask G-res model for both annual GHG emissions on a CO_2 equivalency basis per m^2, and for GHG emissions intensity. These scenarios are not a validation of the Keeyask G-res Model. Rather, the Sensitivity Analysis indicates that on average, the scenario results are similar to the Keeyask G-res Model. Scenario 17, which is a

conservative benchmark, results in an estimate of GHG emissions intensity that is also similar to the Keeyask G-res Model.

Table 1-5 Modelling Scenarios: Scenario Class Averages

Net 100-Year Lifecycle Greenhouse Gas Emissions from the Keeyask Hydroelectric Reservoir
Modelling Scenarios using the G-res Tool

Predicted Net Annual Emissions per m^2

Scenarios	Emissions per m^2 of Reservoir $gCO_2e/m^2/yr$					Emission Intensity gCO_2e/kWh		
	Post-Impoundment	Pre-Impoundment	Net GHG Footprint	95% Confidence Intervals			95% Confidence Intervals	
1 Vegetation Structure: Average	93.0	7.4	85.8	75.2	97.6	1.9	2	2
2 Terrestrial Habitat (Course and Fine Ecosite Type): Average	93.0	0.2	93.2	82.8	104.8	2.1	2	2
3 Ecological Land Classification: Average	88.0	-6.8	94.8	84.8	105.8	2.2	2	2

Net 100-Year Lifecycle Greenhouse Gas Emissions from the Keeyask Hydroelectric Reservoir
Modelling Scenarios using the G-res Tool

Predicted Total Reservoir Net Annual Emissions

Scenarios	Total Reservoir Emissions per Year tCO_2e/yr					Emission Intensity gCO_2e/kWh		
	Post-Impoundment	Pre-Impoundment	Net GHG Footprint	95% Confidence Intervals			95% Confidence Intervals	
1 Vegetation Structure: Average	9,363	754	8,609	7,544	9,807	1.9	2	2
2 Terrestrial Habitat (Course and Fine Ecosite Type): Average	9,363	5	9,358	8,319	10,530	2.1	2	2
3 Ecological Land Classification: Average	8,851	(665)	9,516	8,527	10,634	2.2	2	2

Net 100-Year Lifecycle Greenhouse Gas Emissions from the Keeyask Hydroelectric Reservoir
Modelling Scenarios using the G-res Tool

Predicted Net Lifetime Emissions

Scenarios	Total Lifetime Reservoir Emissions tCO_2e					Emission Intensity gCO_2e/kWh		
	Post-Impoundment	Pre-Impoundment	Net GHG Footprint	95% Confidence Intervals			95% Confidence Intervals	
1 Vegetation Structure: Average	936,277	75,402	860,874	754,406	980,707	1.9	2	2
2 Terrestrial Habitat (Course and Fine Ecosite Type): Average	936,277	465	935,812	831,914	1,052,995	2.1	2	2
3 Ecological Land Classification: Average	885,101	(66,483)	951,584	852,731	1,063,403	2.2	2	2

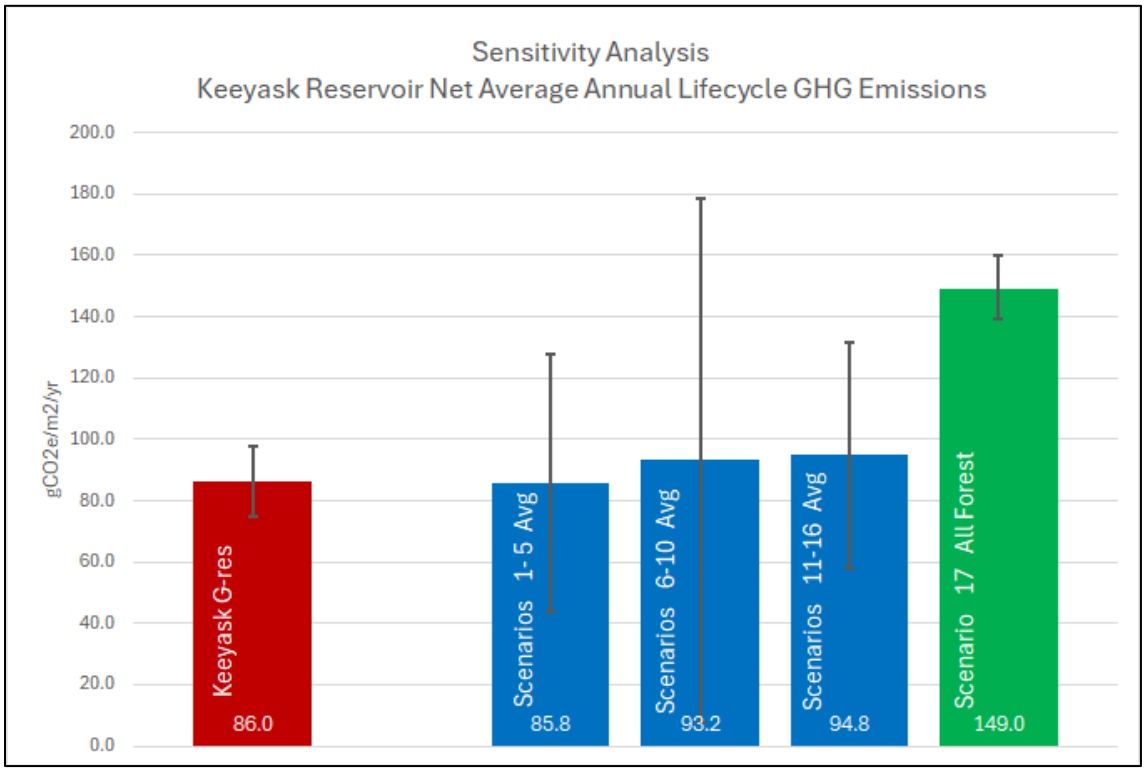


Figure 1-4 Modelling Scenarios: Net Average Annual Keeyask Reservoir Lifecycle GHG Emissions

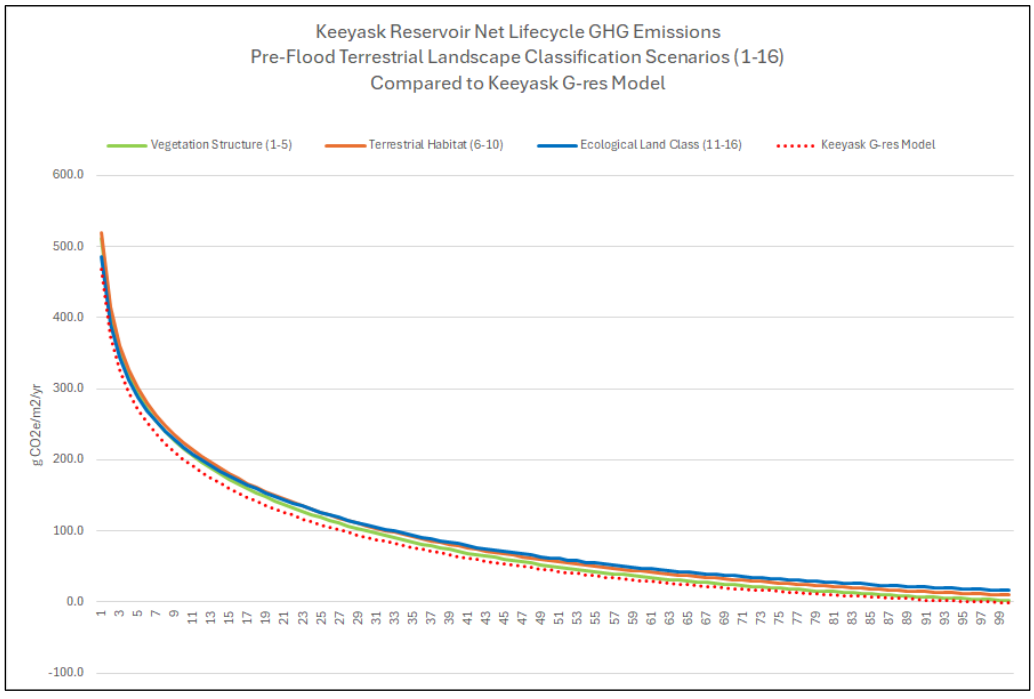


Figure 1-5 Modelling Scenarios: Keeyask Reservoir Net Lifecycle GHG Emissions

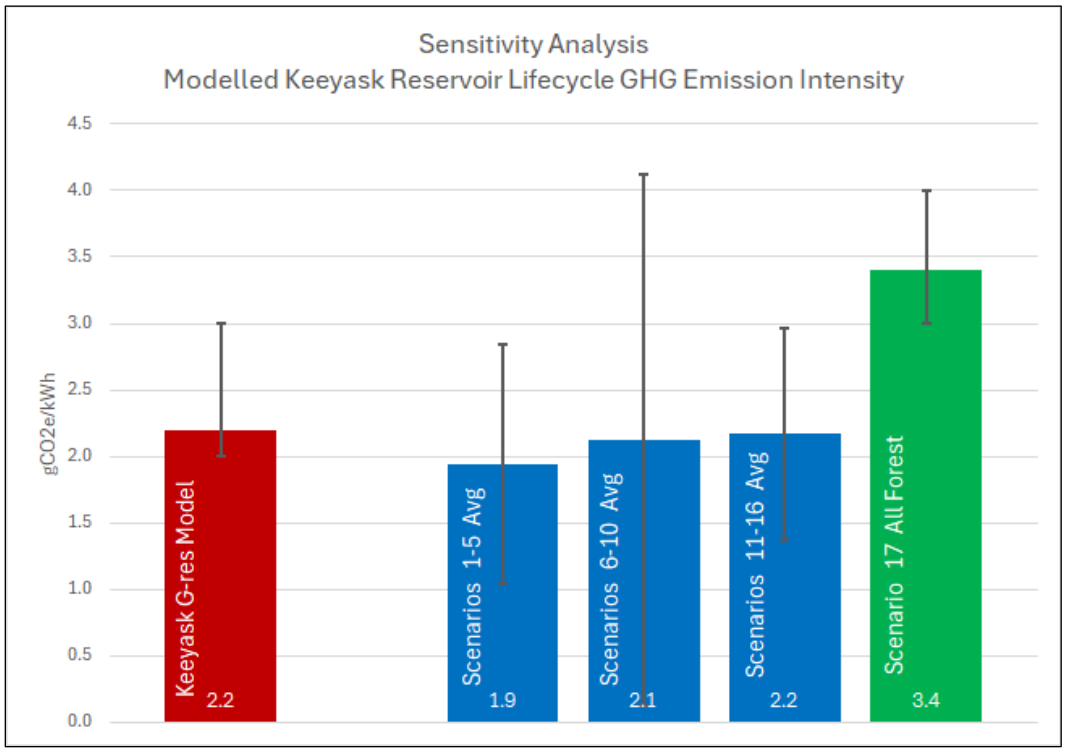


Figure 1-6 Modelling Scenarios: Keeyask Reservoir Lifecycle GHG Emission Intensity

1.2. Pre-Flood CH_4 and CO_2 Emission Factors

The Keeyask Reservoir Lifecycle GHG Model used pre-flood CH_4 emission factors derived from Kuhn et al. (2021a) and CO_2 emission factors derived from Virkkala et al. (2021a). To be conservative, median emission factors were adopted where available, so as not to overstate pre-flood emissions and therefore understate net emissions. Median emission factors were available for CH_4 as published by Kuhn et al. (2021a). Median emission factors were not available for CO_2 from the Virkkala et al. (2021b) dataset, so CO_2 mean were used in the Keeyask G-res model.

To evaluate the uncertainty of GHG pre-flood emission factors, the G-res Keeyask model was also run using the following GHG emission factor scenarios (Figures 1-7 to 1-9):

1) Mean CH_4 and CO_2 emission factors: as published by Kuhn et al. (2021a), and Virkkala et al., (2021a), respectively.
2) Lower Limits: 25th percentile for CH_4, as published by Kuhn et al. (2021a) and the lower limit 90% confidence interval as published by Virkkala et al., (2021a) . (Low pre-flood emission factors that will result in higher **net** emissions).

3) Upper Limits: 75th percentile for CH_4, as published Kuhn et al. (2021a) and the upper 90% confidence interval as published by Virkkala et al., (2021a). (High pre-flood emission factors that will result in lower **net** emissions).

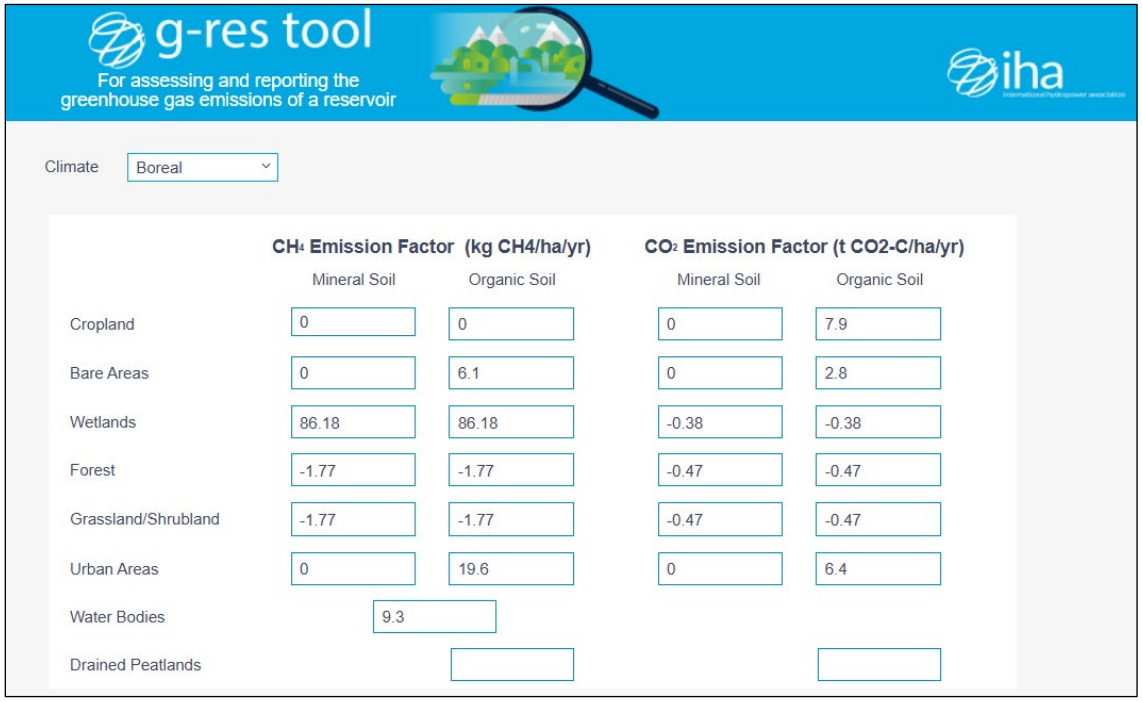


Figure 1-7 Mean GHG Emission Factors

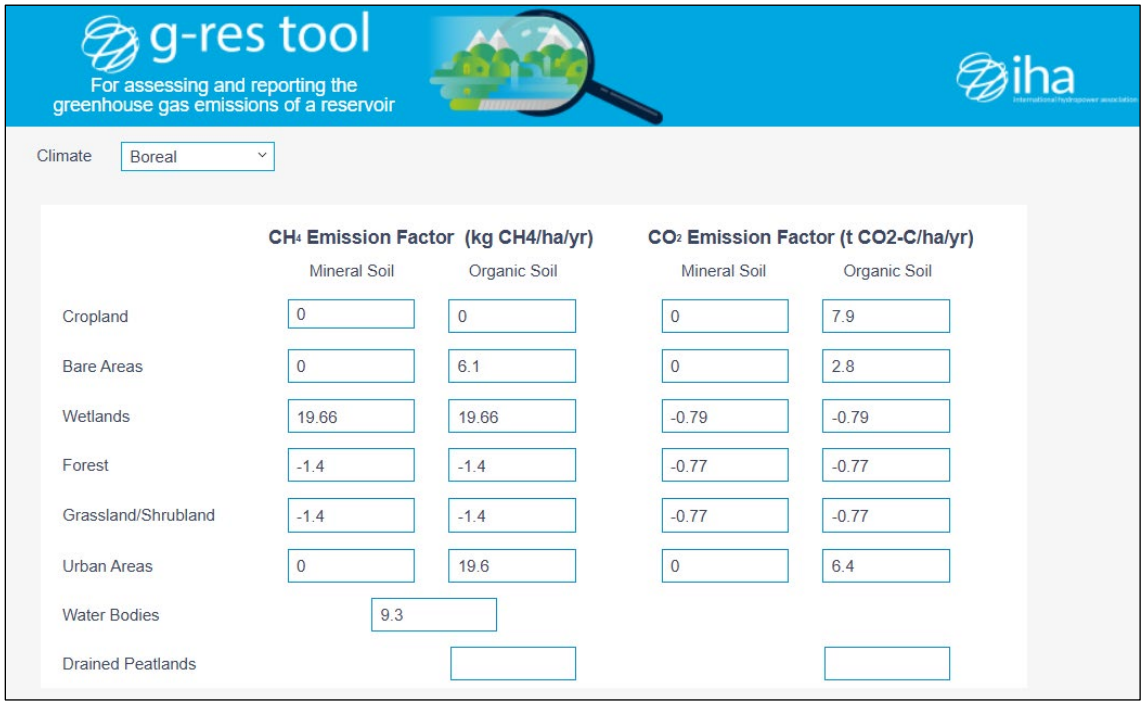


Figure 1-8 Lower Limit GHG Emission Factors

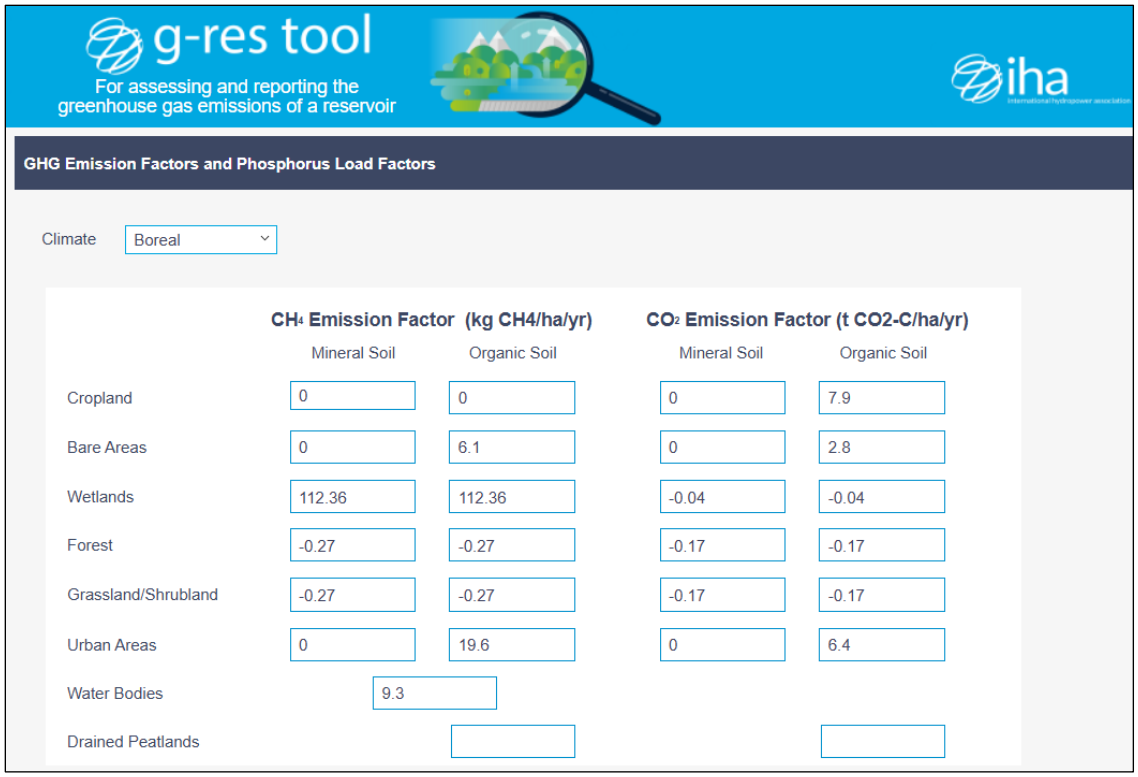


Figure 1-9 Upper Limit GHG Emission Factors

The results are illustrated in Figures 1-10 and 1-11 and Table 1-5 for average annual emissions per m^2 of the reservoir, total 100-year lifetime emissions for the entire reservoir, and 100-year lifecycle GHG emission intensities.

Using **mean** pre-flood emission factors, modelled total net lifetime reservoir emissions declined by 47.3% from 861,990 tCO_2e to 454,301 tCO_2e. Emission intensity drops by 50% from 2.0 to 1.0 gCO_2e/kWh.

Using the **lower and upper limits** of the pre-flood GHG emission factors, modelled total net lifetime reservoir emissions ranged from 1,864,915 tCO_2e to -400,410 tCO_2e, respectively. This represents a percentage change of 116.3% and -146.5%, respectively as compared to the Keeyask model. Emission intensity ranged from 4.2 to -0.9 gCO_2e/kWh, respectively, which are very low values.

Table 1-6 Results: Pre-Flood GHG Emission Factor Scenarios

Estimated Net 100-Year Lifecycle Greenhouse Gas Emissions from the Keeyask Hydroelectric Reservoir
Modelling Using the G-res Tool
and
Keeyask Ecological Land Classification and User-Defined GHG Emission Factors

Keeyask Lifecycle Model

Emissions per m^2 of Reservoir $gCO_2e/m^2/yr$			Total Reservoir Emissions per Year tCO_2e/yr			Total Lifetime Reservoir Emissions tCO_2e			Emission Intensity gCO_2e/kWh		
Net GHG Footprint	95% Confidence Intervals		Net GHG Footprint	95% Confidence Intervals		Net GHG Footprint	95% Confidence Intervals			95% Confidence Intervals	
86	75	98	8,620	7,500	9,879	861,990	749,988	987,936	2	2	2

Scenario: Keeyask Lifecycle Model Using Mean EF Values

Emissions per m^2 of Reservoir $gCO_2e/m^2/yr$			Total Reservoir Emissions per Year tCO_2e/yr			Total Lifetime Reservoir Emissions tCO_2e			Emission Intensity gCO_2e/kWh		
Net GHG Footprint	95% Confidence Intervals		Net GHG Footprint	95% Confidence Intervals		Net GHG Footprint	95% Confidence Intervals			95% Confidence Intervals	
45	34	58	4,543	3,454	5,773	454,301	345,376	577,300	1	1	1

Scenario: Keeyask Lifecycle Model Using Mean EF Values (% Change)

Emissions per m^2 of Reservoir $gCO_2e/m^2/yr$			Total Reservoir Emissions per Year tCO_2e/yr			Total Lifetime Reservoir Emissions tCO_2e			Emission Intensity gCO_2e/kWh		
Net GHG Footprint	95% Confidence Intervals		Net GHG Footprint	95% Confidence Intervals		Net GHG Footprint	95% Confidence Intervals			95% Confidence Intervals	
-47.7%			-47.3%			-47.3%			-50.0%		

Scenario: Keeyask Lifecycle Model Using 25th Percentile CH_4 and 90% CI Lower Limit CO_2 EF Values

Emissions per m^2 of Reservoir $gCO_2e/m^2/yr$			Total Reservoir Emissions per Year tCO_2e/yr			Total Lifetime Reservoir Emissions tCO_2e			Emission Intensity gCO_2e/kWh		
Net GHG Footprint	95% Confidence Intervals		Net GHG Footprint	95% Confidence Intervals		Net GHG Footprint	95% Confidence Intervals			95% Confidence Intervals	
186	175	198	18,649	17,540	19,899	1,864,915	1,753,988	1,989,928	4.2	4	5

Scenario: Keeyask Lifecycle Model Using 25th Percentile CH_4 and 90% CI Lower Limit CO_2 EF Values (% Change)

Emissions per m^2 of Reservoir $gCO_2e/m^2/yr$			Total Reservoir Emissions per Year tCO_2e/yr			Total Lifetime Reservoir Emissions tCO_2e			Emission Intensity gCO_2e/kWh		
Net GHG Footprint	95% Confidence Intervals		Net GHG Footprint	95% Confidence Intervals		Net GHG Footprint	95% Confidence Intervals			95% Confidence Intervals	
116.3%			116.3%			116.3%			110.0%		

Scenario: Keeyask Lifecycle Model Using 75th Percentile CH_4 and 90% CI Upper Limit CO_2 EF Values

Emissions per m^2 of Reservoir $gCO_2e/m^2/yr$			Total Reservoir Emissions per Year tCO_2e/yr			Total Lifetime Reservoir Emissions tCO_2e			Emission Intensity gCO_2e/kWh		
Net GHG Footprint	95% Confidence Intervals		Net GHG Footprint	95% Confidence Intervals		Net GHG Footprint	95% Confidence Intervals			95% Confidence Intervals	
-40	-51	-27	(4,004)	(5,120)	(2,741)	(400,410)	(512,040)	(274,092)	-0.9	-1	-1

Scenario: Keeyask Lifecycle Model Using 75th Percentile CH_4 and 90% CI Upper Limit CO_2 EF Values (% Change)

Emissions per m^2 of Reservoir $gCO_2e/m^2/yr$			Total Reservoir Emissions per Year tCO_2e/yr			Total Lifetime Reservoir Emissions tCO_2e			Emission Intensity gCO_2e/kWh		
Net GHG Footprint	95% Confidence Intervals		Net GHG Footprint	95% Confidence Intervals		Net GHG Footprint	95% Confidence Intervals			95% Confidence Intervals	
-146.5%			-146.5%			-146.5%			-145.0%		

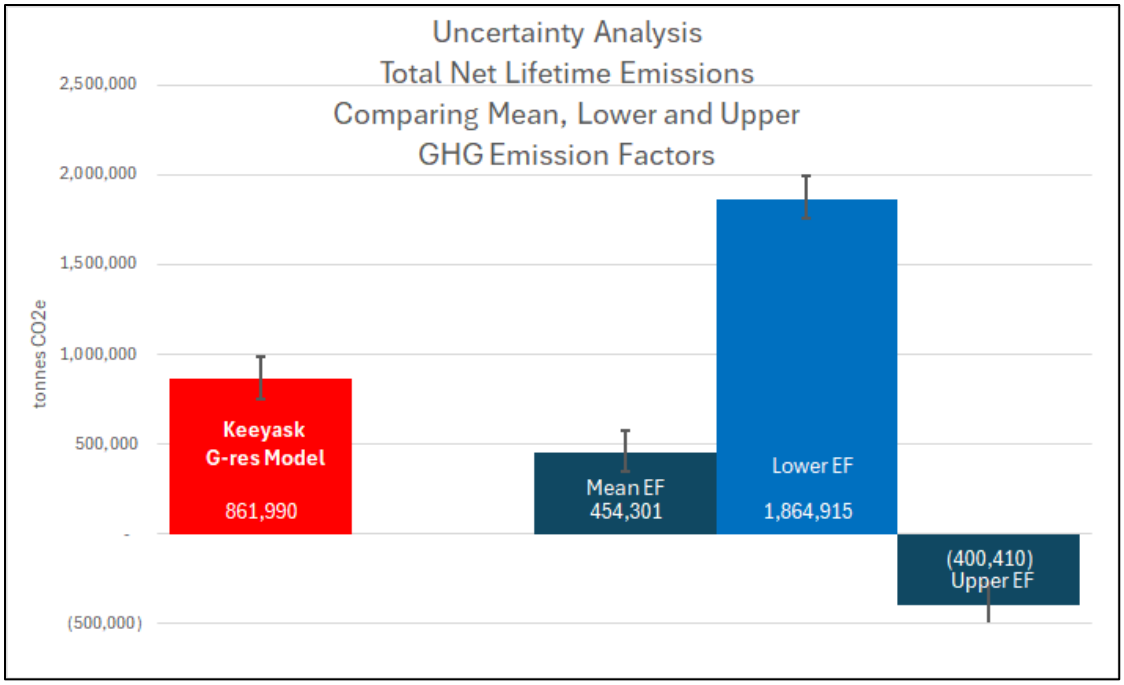


Figure 1-10 Total Keeyask Reservoir Net Lifecycle GHG Emissions

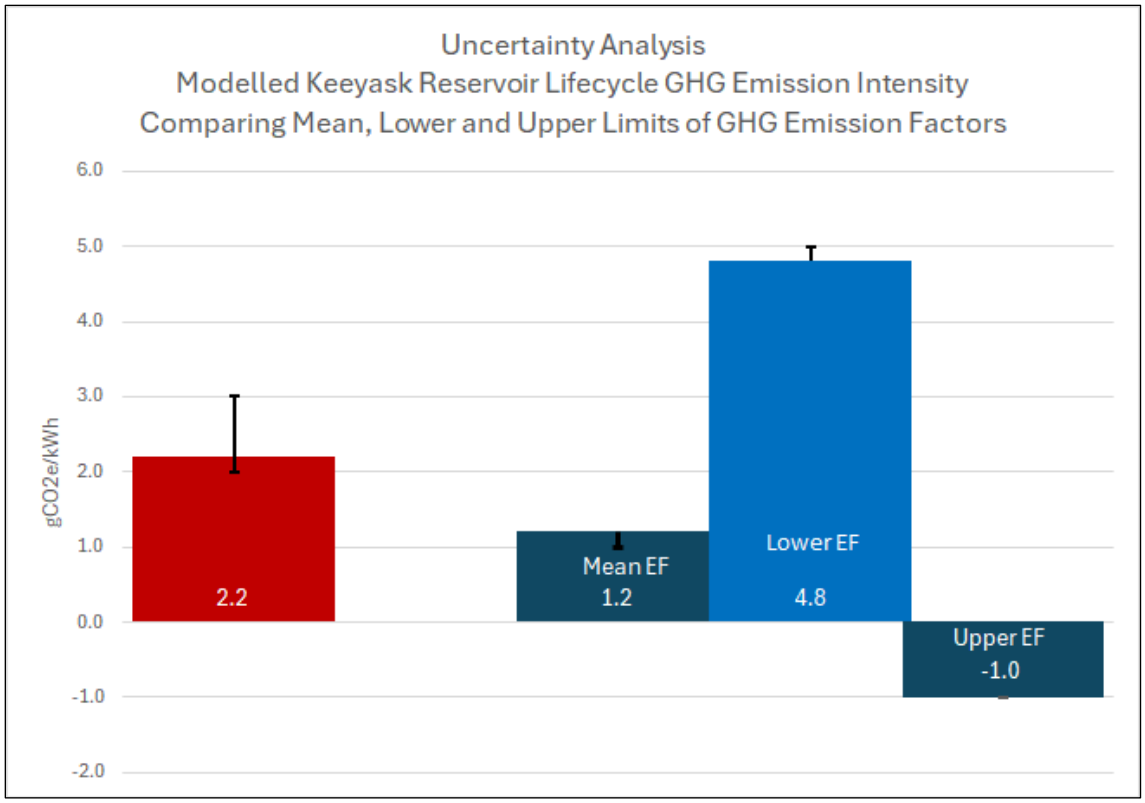


Figure 1-11 Keeyask Reservoir Lifecycle GHG Emission Intensity

1.3. Size of Littoral Zone

The littoral zone of the Keeyask reservoir can be an important source of CO_2 and CH_4 emissions (DelSontro et al., 2017; Prairie et al., 2018).

The littoral zone comprises approximately 20% of the Keeyask reservoir following the impoundment, and is predicted to expand to approximately 26% thirty years after flooding due to shoreline erosion (W. DeWit personal communication, July 5, 2023). To be conservative, the value of 26% was used to model Keeyask lifecycle GHG emissions.

A sensitivity analysis was conducted by running the G-res model for littoral zone values of 20% (initial flooding); 26% (reservoir expansion after 30 years), and 30%. When the extent of the littoral zone was reduced from 26% to 20%, total net lifecycle emissions were reduced by 9.3% (Table 1-6). A 4% increase in the extent of the littoral zone from 26% to 30% resulted in a 6% increase in net lifecycle GHG emissions.

A decrease in the size of the littoral zone from 26% to 20% resulted in Emission Intensity dropping 9.1% from 2.2 to 2.0 gCO_2e/kWh. An increase in the size of the littoral zone from 26% to 30% increased Emission Intensity by 9.1% from 2.2 to 2.4 gCO_2e/kWh.

The size of the littoral zone affects calculations of Post-flood emissions in the G-res model. It does not affect Pre-flood emissions. It impacts CH_4 diffusive and CH_4 bubble emissions, but does not impact CO_2 emissions.

Table 1-7 Keeyask Reservoir Net Lifecycle GHG Emissions: Littoral Zone Scenarios

Estimated Net Lifecycle GHG Emissions from the Keeyask Hydroelectric Reservoir
Modelling Using the G-res Tool
Littoral Zone Scenarios

	Keeyask Model			Littoral Zone Scenarios					
		95%			95%			95%	
	Model	Confidence Interval		Scenario	Confidence Interval		Scenario	Confidence Interval	
Extent of Littoral Zone	**26%**			**20%**			**30%**		
Net Emissions per m^2 of Reservoir									
$gCO_2e/m^2/yr$	86	75	98	78	68	89	91	79	104
Percent Change Compared to Keeyask Model				-9.3%			5.8%		
Total Lifetime Net Reservoir Emissions									
tCO_2e	861,990	749,988	987,936	781,827	680,712	895,568	913,452	7,972	10,452
Percent Change Compared to Keeyask Model				-9.3%			6.0%		
Emission Intensity									
gCO_2e/kWh	2.2	2	3	2.0	2	2	2.4	2	3
Percent Change Compared to Keeyask Model				-9.1%			9.1%		

A 9.1% change in the size of the Keeyask reservoir littoral zone (from 20% littoral zone to 30% littoral zone) impacted lifecycle emission intensity by 0.2 gCO_2e/kWh (range 2.0 to 2.4 gCO_2e/kWh). This is rated as a low impact, given that median GHG life cycle emission factors for what some studies have considered as renewable electricity generation technologies range from 8 to 52 gCO_2e/kWh (National Renewable Energy Laboratory, 2021). The probability of over or underestimating the extent of the Keeyask littoral zone is rated as being low, because the size of the Keeyask littoral zone is based on site-specific measurements and modelling (Hydropower Limited Partnership, 2012a; W. DeWit personal communication, July 5, 2023).

The impact of uncertainty associated with estimating the extent of the littoral zone for the post-flood Keeyask reservoir is rated as Low.

1.4. Concentration of Total Phosphorous

G-res uses the mean concentration of Total Phosphorous as one of the inputs in an elastic regression model to estimate post-flood reservoir CO_2 diffusive emissions (Prairie et al., 2017). This is a user-defined model input.

Total Phosphorus concentration in the main stem of the Nelson River ranged from 30.0 to 40.0 µg/L during pre-flood sampling from 1997 to 2006 (Keeyask Hydropower Limited Partnership, 2012b).

The Keeyask Generation Project Aquatic Environmental Monitoring Plan established a benchmark value of 58.0 µg/L for Total Phosphorus concentrations for the Keeyask reservoir (Dowd and Hrenchuck, 2024). This value is compared against the results of on-going postflood monitoring of phosphorous within, upstream and downstream of the Keeyask reservoir (Hrenchuk 2021, 2022; Dowd and Hrenchuck 2023, 2024).

Monitoring results are summarized in Table 1-8 (summarized from Hrenchuk, 2021, 2022; Dowd and Hrenchuck 2023, 2024).

Total Phosphorus concentrations ranged from 28.5 to 158 µg/L during the seasonal sampling events conducted from 2021 to 2023 (Table 1-8). Average annual concentrations for the entire reservoir were 56.8 µg/L, 51.8 µg/L, and 55.8 µg/L for 2021, 2022, and 2023 respectively (Table 1-8). The concentrations were higher in the backbays than in the main channel, and are most elevated in March under ice cover.

A sensitivity analysis was conducted by running the G-res model for Total Phosphorus concentrations of 28.5 µg/L (minimum monitored value), 58 µg/L (benchmark), and 158 µg/L (maximum monitored value). A reduction of 29.5 µg/L in the concentration of Total Phosphorous from 58 µg/L (benchmark) to 28.5 µg/L (minimum) resulted in a 7.7% decrease in total net reservoir lifecycle emissions (t/CO_2e) (Table 1-9). A 100 µg/L increase in phosphorous concentrations from 58 µg/L (benchmark) to 158 µg/L (maximum) resulted in a 13.0% increase in total net lifecycle GHG emissions (Table 1-8).

A decrease in phosphorous concentrations from 58 to 28.5 µg/L resulted in Emission Intensity dropping 9.1% from 2.2 to 2.0 gCO_2e/kWh. An increase in phosphorous concentrations from 58 to 158 µg/L resulted in Emission Intensity increasing 13.6% from 2.2 to 2.5 gCO_2e/kWh.

The uncertainty associated with Total Phosphorous concentrations is rated as being **Low**. This is due to two factors. One, the annual average concentrations measured from 2021-2023 (ranging

from 51.8 to 56.8 µg/L) are similar to the Benchmark value of 58 µg/L that was used in the G-res model. Second, the impact of substituting the minimum measured Total Phosphorous concentration of 28.5 µg/L or the maximum measured concentration of 158 µg/L impacted the modelled Keeyask GHG Emission Intensity by only 0.5 gCO_2e/kWh (i.e. range of 2.0 to 2.5 gCO_2e/kWh).

Table 1-8 Keeyask Reservoir Total Phosphorous Monitoring Results

Keeyask Reservoir Total Phosphorous Monitoring Results

mg/L

	Monitoring Zones									
	Main Channel	Backbays							Reservoir Annual Average	Backbay Annual Average
	1b	4	8	11	12	Min	Max	Mean		
2023										
March	0.05850	0.05220	**0.11700**	**0.09120**	**0.09330**	0.05220	0.11700	0.08244		
June	0.03820	0.04180	**0.05990**	**0.05970**	0.04860	0.03820	0.05990	0.04964		
July	0.04460	0.05320	0.04980	0.05020	0.05030	0.04460	0.05320	0.04962		
August	0.04850	0.05780	0.04630	0.05160	0.05410	0.04630	0.05780	0.05166		
September	0.04990	0.05170	0.04810	0.04970	0.05380	0.04810	0.05380	0.05064	0.05680	0.05902
2022										
March	0.04070	0.04210	0.10000	**0.07750**	**0.12400**	0.04070	0.12400	0.07686		
June	0.03340	0.03440	0.04360	0.04090	0.04550	0.03340	0.04550	0.03956		
July	0.03880	0.04300	**0.06650**	**0.06950**	0.05480	0.03880	0.06950	0.05452		
August	0.03220	**0.06440**	0.05280	**0.06310**	0.05000	0.03220	0.06440	0.05250		
October	0.03480	0.03500	0.03650	0.03340	0.03680	0.03340	0.03680	0.03530	0.05175	0.05569
2021										
March	0.04240	0.04300	**0.15600**	0.04070	0.04560	0.04070	0.15600	0.06554		
	0.04460	0.03980	**0.14900**	0.04100	0.04330	0.03980	0.14900	0.06354		
	0.04170	0.04270	**0.15700**	**0.13400**	0.04690	0.04170	0.15700	0.08446		
	0.04300	0.04050	0.15800	**0.13200**	0.04680	0.04050	0.15800	0.08406		
		0.04020	0.04300	0.04150	0.04170	0.04020	0.04300	0.04160		
		0.04430	0.04190	0.03860	0.04180	0.03860	0.04430	0.04165		
		0.04350	0.04270	0.04140	0.04090	0.04090	0.04350	0.04213		
		0.04410	0.04170	0.03890	0.04190	0.03890	0.04410	0.04165		
				0.09830	0.04200	0.04200	0.09830	0.07015		
				0.06510	0.04060	0.04060	0.06510	0.05285		
				0.06580	0.04280	0.04280	0.06580	0.05430		
				0.07350	0.04520	0.04520	0.07350	0.05935		
June	0.03640	0.03170	0.04510	0.03980	0.04060	0.03170	0.04510	0.03872		
	0.03410	0.03180	0.04690	0.04260	0.04150	0.03180	0.04690	0.03938		
	0.03600	0.03100	0.03510	0.04510	0.05280	0.03100	0.05280	0.04000		
	0.03550	0.03270	0.04610	0.03990	0.04290	0.03270	0.04610	0.03942		
	0.03700		0.04000	0.02850	0.04250	0.02850	0.04250	0.03700		
				0.03030	0.04440	0.03030	0.04440	0.03735		
July	0.03820	0.03470	**0.07780**	**0.09090**	0.04230	0.03470	0.09090	0.05678		
	0.04090	0.03670	**0.11300**	**0.07880**	**0.14100**	0.03670	0.14100	0.08208		
	0.03780	0.03940	0.04060	**0.07400**	**0.14100**	0.03780	0.14100	0.06656		
	0.03850	0.03580	0.05320	0.04930	**0.07390**	0.03580	0.07390	0.05014		
	0.03750	0.03700	0.04670	**0.07190**	**0.10200**	0.03700	0.10200	0.05902		
				0.09440	0.03990	0.03990	0.09440	0.06715		
					0.05640	0.05640	0.05640	0.05640		
					0.07320	0.07320	0.07320	0.07320		
					0.10500	0.10500	0.10500	0.10500		
August	0.03890	0.03770	**0.07860**	**0.08050**	0.03960	0.03770	0.08050	0.05506		
	0.04050	0.05760	0.04000	**0.07610**	**0.11800**	0.04000	0.11800	0.06644		
	0.03900	0.04760	0.05600	**0.06500**	**0.06240**	0.03900	0.06500	0.05400		
	0.03880	**0.05860**	0.04520	0.04520	0.04620	0.03880	0.05860	0.04680		
	0.03970			**0.05950**	0.05220	0.03970	0.05950	0.05047		
				0.07470	**0.06400**	0.06400	0.07470	0.06935		
					0.08070	0.08070	0.08070	0.08070		
September	0.04060	0.04460	0.04800	**0.07370**	0.05040	0.04060	0.07370	0.05146		
	0.04570	0.05630	0.04410	**0.06760**	0.10100	0.04410	0.10100	0.06294		
	0.04170	0.04570	0.05230	0.05600	**0.05970**	0.04170	0.05970	0.05108		
	0.04650	0.05790	0.04620	0.05410	0.05000	0.04620	0.05790	0.05094		
	0.04160			0.05640	0.05390	0.04160	0.05640	0.05063		
				0.06800	**0.06260**	0.06260	0.06800	0.06530	0.05582	0.05883
Min	0.03220	0.03100	0.03510	0.02850	0.03680					
Max	0.05850	0.06440	0.15800	0.13400	0.14100					
Average	0.04048	0.04373	0.06569	0.06217	0.06022					

Benchmark 0.058 mg/L

Red Font = exceedance of Benchmark 0.058 mg/L

= Maximum Value

= Minimum Value

Summarized from Hrenchuk 2021, 2022; Dowd and Hrenchuck 2024, 2023

Table 1-9 Keeyask Reservoir Net Lifecycle GHG Emissions: Total Phosphorous Scenarios

Estimated Net Lifecycle GHG Emissions from the Keeyask Hydroelectric Reservoir
Modelling Using the G-res Tool
Total Phosphorous Scenarios

	Keeyask Model			Total Phosphorous					
		95%			95%			95%	
	Model	**Confidence Interval**		**Scenario**	**Confidence Interval**		**Scenario**	**Confidence Interval**	
Concentration of Total Phosphorous (µg/L)	**58**			**28.5**			**158**		
Net Emissions per m^2 of Reservoir									
$gCO_2e/m^2/yr$	86	75	98	79	69	90	97	85	110
Percent Change Compared to Keeyask Model				-8.1%			12.8%		
Total Lifetime Net Reservoir Emissions									
tCO_2e	861,990	749,988	987,936	795,369	695,772	907,616	973,833	854,404	1,108,416
Percent Change Compared to Keeyask Model				-7.7%			13.0%		
Emission Intensity									
gCO_2e/kWh	2.2	2	3	2.0	2	2	2.5	2	3
Percent Change Compared to Keeyask Model				-9.1%			13.6%		

1.5. Length of Water Residence Time

The Water Residence Time refers to the amount of time a molecule of water spends in the reservoir. Longer water residence times allows more time for dissolved organic material to decompose within the reservoir (Vachon et al., 2017).

G-res uses Water Residence Time to calculate degassing emissions, and displaced emissions (those emissions that occur in the reservoir but would have occurred downstream anyways if the reservoir was not in place) (Prairie et al., 2017).

Water Residence Time is a user-defined input. The Water Residence Time for the main channel of the Keeyask Reservoir is estimated to vary from 15 to 30 hours; 0.0017 to 0.0034 years (Keeyask Hydropower Limited Partnership, 2012b). The Water Residence Time for backbays may be up to 30 days; 0.082 years (Keeyask Hydropower Limited Partnership, 2012b) or possibly longer (personal communication W. DeWit, P.Eng. Manitoba Hydro May 1, 2020). Water residence time in backbay environments can be very challenging to estimate as it is influenced by water inflows from creeks, wind driven currents and other factors.

The upper boundary of 0.0034 for the main channel was used for the Keeyask reservoir G-res Model.

For comparison, the G-res Tool was also run using the Water Residence Time value of 0.082 years (the estimated water residence time for backbays).

Total Net Lifecycle GHG emissions were estimated to increase by 58.5% from 861,990 to 1,366,083 tCO_2e (Table 1-10).

The driving force for this was a 212.3% increase in CH_4 emissions, resulting from a modelled rise in Degassing Emissions.

Lifecycle Emission Intensity rose from 2.2 to 3.5 gCO_2e/kWh.

This scenario has demonstrated that Water Residence Time has a significant impact on G-res results. Water Residence Time is used by G-res to model degassing emissions only. It is not used to model diffusive or bubble emissions. As discussed above, the Keeyask reservoir comprises a main channel whose Water Residence Time is approximately 15 – 30 hours, and shallow backbays whose Water Residence Time can be up to 30 days. It is appropriate to use Water Residence Times that represents the main channel for the G-res model since this is the flow that will pass through the generating station and spillway and release degassing emissions. The longer Water Residence Times of the backbays may contribute to the elevated emissions observed in-situ at these locations. Longer water residence times can extend the period for microbial decomposition of organic material and elevate GHG emissions in the reservoir (Prairie et al 2018; Wang et al., 2018). The characteristics that generate backbay emissions may not be representative of the forebay and main channel waters. G-res may benefit from exploring empirical models and reservoir processes separately for backbay and the main channel portions of the reservoir.

For comparison, the G-res Tool was also run using the Water Residence Time value of 0.0017 years (the lower boundary of estimated water residence time for the main channel). Total Net Lifecycle GHG Emission estimates declined by 3.5% and Lifecycle GHG Emission Intensity declined from 2.2 to 2.1 gCO_2e/kWh (Table 1-11). These changes are assessed as being small and therefore, the uncertainty associated with Water Residence Time is rated as being **Low**.

Table 1-10 Keeyask Reservoir: Water Residence Time Scenario 0.082 Years

Estimated Net Lifecycle GHG Emissions from the Keeyask Hydroelectric Reservoir
Modelling Using the G-res Tool
Water Residence Time

	Keeyask Model			Water Residence Time		
		95%			95%	
	Model	Confidence Intervals		Scenario	Confidence Intervals	
Water Residence Time (Years)	**0.0034**			**0.082**		
Net Emissions per m^2 of Reservoir						
$gCO_2e/m^2/yr$	86	75	98	136	119	155
Percent Change Compared to Keeyask Model				58.1%		
Total Lifetime Net Reservoir Emissions						
tCO_2e	861,990	749,988	987,936	1,366,083	1,197,772	1,556,200
Percent Change Compared to Keeyask Model				58.5%		
Emission Intensity						
gCO_2e/kWh	2.2	2.0	3.0	3.5	3	4
Percent Change Compared to Keeyask Model				59.1%		

Table 1-11 Keeyask Reservoir: Water Residence Time Scenario 0.0017 Years

Estimated Net Lifecycle GHG Emissions from the Keeyask Hydroelectric Reservoir
Modelling Using the G-res Tool
Water Residence Time

	Keeyask Model			Water Residence Time		
		95%			95%	
	Model	Confidence Intervals		Scenario	Confidence Intervals	
Water Residence Time (Years)	**0.0034**			**0.0017**		
Net Emissions per m^2 of Reservoir						
$gCO_2e/m^2/yr$	86	75	98	83	73	95
Percent Change Compared to Keeyask Model				-3.5%		
Total Lifetime Net Reservoir Emissions						
tCO_2e	861,990	749,988	987,936	832,289	727,900	949,784
Percent Change Compared to Keeyask Model				-3.4%		
Emission Intensity						
gCO_2e/kWh	2.2	2.0	3.0	2.1	2	2
Percent Change Compared to Keeyask Model				-4.5%		

2. Structural Uncertainty

Structural uncertainty is defined in this assessment as the uncertainty associated with the data that was used to develop the semi-empirical models that are the foundation of the G-res Tool.

The semi-empirical models that underpin the logic of the G-res Tool were developed from GHG measurements collected from reservoirs worldwide prior to 2016 (Prairie et al., 2021a). These reservoirs varied in age, size, geographic location, configuration, pre-flooded land cover type, etc. (Prairie et al., 2021b) which are variables that affect the rate and composition of reservoir GHG emissions (Goldenfum, 2010; DelSontro et al., 2016; Scherer & Pfister, 2016; Harrison et al., 2021; (Soued et al., 2022).

There is a degree of uncertainty in applying G-res, or applying any model, to the Keeyask reservoir that was built from data derived from other reservoirs. The uncertainty lies in how well the measurements from other reservoirs represent the Keeyask reservoir? In other words, how well is G-res able to model Keeyask reservoir GHG lifecycle emissions if G-res has been calibrated with GHG measurements from reservoirs that may not be similar to Keeyask?

The following sections examine reservoir preflood land cover, floating peatlands, and reservoir configuration (shallow shorelines) as potential sources of structural uncertainty when applying G-res to the Keeyask reservoir.

2.1. Pre-Flood Land Cover: Peatlands

A distinguishing characteristic of the Keeyask reservoir is that approximately 90% of the pre-flooded landscape was comprised of heterogeneous peatlands (Keeyask Hydropower Limited Partnership, 2012a). This is an important attribute that should be considered when modelling Keeyask lifecycle emissions. Peatlands are complex wetland systems (Baird et al., 2009) and northern peatlands store a large amount of carbon (Amesbury et al., 2019; Gong et al., 2020; Hugelius et al., 2020). Peatland GHG emissions vary in time (i.e. diurnally, seasonally, and annually) and in space (i.e. from within the same peatland, amongst peatlands in the same physiographic region, and amongst peatlands in different physiographic regions (Strack 2008; Pelletier et al., 2007; 2011, 2014, 2015; Trudeau et al., 2013; Turetsky et al., 2014; Treat et al., 2021).

A potential source of uncertainty is that G-res may not have been calibrated with GHG emissions data that represents a similar pre-flood land cover as the Keeyask reservoir. The uncertainty with applying data from other reservoirs involves: 1) the areal extent of peatlands flooded; 2) the age of flooded peatland reservoirs when GHG measurements were conducted; 3) and presence of floating peat mats.

2.1.1. Description of G-res Database of Boreal Reservoirs

Data from 61 boreal reservoirs were used to calibrate G-res for modelling lifecycle GHG emissions from boreal reservoirs (Prairie et al., 2021b).

Of these, 13 reservoirs were sampled within 20 years after impoundment (Table 2-1). The 20-year timeframe is of interest for this peatland assessment as 20 years is the timeframe the IPCC (2019) considers the bulk of CO_2 emissions to occur from reservoir flooding.

The following analysis of the G-res boreal reservoir database will be discussed in two parts. It will segregate those reservoirs that were 20 years or less of age at the time of collecting GHG measurements, and those that were over 20 years at the time of measurement.

2.1.2. G-res Database Reservoirs 20 Years or Less at Time of Sampling

Twelve of the thirteen reservoirs in the G-res database that were less than 20 years of age at the time of sampling are located in Canada (Table 2-1) (Prairie et al., 2021b). These include10 in Quebec, 1 in Newfoundland, and 1 in British Columbia. One reservoir is in Sweden (Table 2-1).

None of these 13 reservoirs flooded peatlands to the extent of the Keeyask reservoir. That is, none of these reservoirs had a pre-flood land cover of 90% peatlands.

2.1.2.1. Quebec Reservoirs Included in Calibration of G-res

La Grande 3 and 4: The distribution of peatland ranges from approximately 50% in the western portion of La Grande Rivière watershed close to the James Bay coastline to approximately 25% in the eastern region that is about 200 km inland (Garneau et al., 2014). La Grande 3 and 4 are located

approximately 200 km and 375 km east of James Bay, respectively, within the La Grande Rivière watershed being closer to the peatland distribution of 25%.

La Grande 3 and 4 were sampled at 19 and 20 years after the impoundment (Prairie et al., 2021). These GHG data missed the initial release of GHG emissions after flooding La Grande 3 and 4 and may not represent the early stages of the newly flooded Keeyask reservoir and its extensive peatlands.

Laforge 1 and 2: Peatlands comprise approximately 15% of the Laforge region, which is located in the northeastern portion of La Grande Rivière watershed (Trudeau et al., 2013; Garneau et al., 2014; 2018). Peatlands in this region are dominated by poor fens and hollows (Van Bellen et al., 2013). This compares to the Keeyask region where bogs encompass the majority of the flooded land (approximately 70%) and fens cover roughly 11% (Keeyask EIS Ecological Land Classification - Keeyask Hydropower Limited Partnership, 2012b). This difference could be significant for modelling Keeyask reservoir lifecycle GHGs. Synthesis studies have shown that CH_4 emissions from northern fens have been higher than those of northern bogs (Kuhn et al., 2021), and CH_4 emissions tend to be slightly higher in poor fens than bogs in the Canadian Boreal Shield (Webster et al., 2018). Furthermore, bogs in Canada's Boreal Shield can be net sinks of CO_2 whereas poor fens can be a slight source of CO_2 (Webster et al., 2018).

The Laforge 2 reservoir was sampled 19 years after impoundment (Prairie et al., 2021a) and may not be representative of a newly flooded peatland reservoir. Laforge 1 was sampled during the first year of impoundment, and during years 4, 5, and 9 after impoundment. These data may provide insight into flooding a newly created and young northern reservoir with some underlying peatlands, which could be applicable to the Keeyask reservoir.

Eastmain-1: Peatlands cover approximately 18% of the Eastmain region in general (Pelletier et al., 2009) and about 14% of the Eastmain-1 reservoir footprint (Teodoru et al., 2012a). Bogs (open and treed) comprise about 98% of these peatlands (Grenier et al., 2008).

The Eastmain-1 reservoir is one of the most extensively studied northern reservoirs in the world. Peatland GHG studies were conducted before and after flooding Eastmain-1 (Pelletier et al., 2009)

and pre-flood and post-flood watershed and reservoir GHG studies were conducted over multiple years (Teodoru et al., 2012; Demarty & Tremblay, 2019). Although this extensive dataset provides valuable information for modelling boreal reservoir GHG emissions, the proportion of flooded peatlands at Eastmain (~14%) is considerably less than that of Keeyask (~90%) and may not be the most suitable reservoir to predict the effect of flooding the peatlands of the Keeyask reservoir.

Romaine-2: The Romaine Complex will flood approximately 6.5 km^2 of peatlands or 2.3% of the reservoir footprint (Hydro-Québec 2008).

Romaine-2 was sampled during the first year after flooding. Although there are ongoing extensive GHG studies of the Romaine Complex, which include peatland measurements (Rust et al., 2022; Barbosa et al., 2023; del Giorgio et al 2023), the pre-flood landscape was not dominated by peatlands.

Peribonka and Sainte-Marguerite 3: The Peribonka and Sainte-Marguerite 3 reservoirs are located in zones where peatlands cover less than 1% of the landscape.

2.1.2.2. Newfoundland Reservoirs Included in Calibration of G-res

Cat Arm Dam West: The Cat Arm Dam West reservoir of Newfoundland is located in a region where peatlands in general cover less than 1% of the landscape.

2.1.2.3. British Columbia Reservoirs Included in Calibration of G-res

Revelstoke Reservoir: The Revelstoke reservoir of British Columbia is in a region where peatlands in general cover less than 1% of the landscape. Wetlands comprised approximately 5% of the flooded land (Utzig et al., 2008; G. Utzig & Schmidt, 2011).

2.1.2.4. Sweden Reservoirs Included in Calibration of G-res

L. Skinnmuddselet: Approximately 29% of the landscape in the vicinity of the L. Skinnmuddselet reservoir in Sweden are peatlands and the reservoir was sampled 12 years after flooding (Åberg et al., 2004).

Although nearly one third (29%) of the preflood reservoir footprint was comprised of peatlands, there was little post-flood microbiological activity in the littoral zone due to fluctuations in reservoir water levels and ice erosion (Åberg et al., 2004). For this reason, the L. Skinnmuddselet reservoir may not be fully representative of the young, peatland Keeyask reservoir.

2.1.3. Mature Peatland Reservoirs Included in G-res Database

The second stage of the peatland assessment was to review mature reservoirs within the G-res database that flooded large areas of peatlands. These mature reservoirs were more than 20 years of age at the time of sampling.

2.1.3.1. Stephens Lake, Manitoba

A close surrogate to the Keeyask reservoir for assessing flooded and re-surfaced peat is Stephens Lake, which is immediately downstream of the Keeyask reservoir on the Nelson River. Stephens Lake is the reservoir for Manitoba Hydro's Kettle Generating station and it is a mature reservoir. It was impounded in 1971 (Keeyask Hydropower Limited Partnership, 2012c), flooding approximately 221 km^2 of land and approximately 98 km^2 of water, for a total reservoir size of 319 km^2 (Manitoba Hydro, 2015). The landcover is similar to that of Keeyask where approximately 90% is classified as wetlands (Keeyask Hydropower Limited Partnership, 2012b). The wetland area comprises bogs (91%), fens (8%), and swamps (1%) (Keeyask Hydropower Limited Partnership, 2012b). Stephens Lake was used as a proxy during the Keeyask environmental impact assessment to estimate peatland disintegration for the Keeyask reservoir (Keeyask Hydropower Limited Partnership, 2012b). Figure 2-1 illustrates the Keeyask environmental impact assessment wetland study area, which includes Stephens Lake.

G-res includes GHG monitoring data from Stephens Lake for 2004 to 2007 (Demarty et al., 2009; Prairie et al., 2021a). The Stephens Lake data was derived from a continuous GHG monitor system installed within the Kettle Generating Station by Manitoba Hydro, in collaboration with Fisheries and Oceans Canada and Environnement Illimité Inc. (Demarty et al., 2009). These data pertain to dissolved concentrations of CO_2 and CH_4 in the forebay waters passing through the station and flowing downstream. The data is relevant for calculating diffusive fluxes at the reservoir forebay surface and degassing emissions as reservoir water passes through the generating station turbines

and spillway. These data may not be representative of emissions occurring in Stephens Lake backbays. Furthermore, the data represents GHG concentrations associated with a mature reservoir, and not necessarily a newly flooded reservoir such as Keeyask.

Additional data has been collected from Stephens Lake and downstream of the Kettle Generating station that could help with future calibration of G-res for northern reservoirs that have flooded extensive peatland areas. Continuous CO_2 and CH_4 partial pressure data were collected from 2004 – 2012 from sensors installed within the Kettle Powerhouse; and spatial, point-in-time partial pressure measurements and direct diffusive flux measurements of CO_2 and CH_4 were collected within Stephens Lake (which included the main channel and shallow backbays), from 2009 to 2014 (Bastien et al., 2011; Marchand et al., 2015a). In addition, CO_2 and CH_4 measurements (continuous partial pressure measurements, spatial point-in-time partial pressure measurements, and spatial point-in-time direct diffusive flux measurements) were collected within the Nelson River downstream of Stephens Lake/Kettle Generating Station from 2009 to 2014 (Marchand et al., 2015b). Point-in-time partial pressure measurements were also to be collected in Stephens Lake as part of the Keeyask Physical Environment Monitoring Plan (Keeyask Hydropower Limited Partnership, 2015). These additional datasets could be used to refine the G-res calibration.

2.1.3.2. Lokka and Porttipahta Reservoirs, Finland

The G-res database includes measurements from two mature northern reservoirs, Lokka and Porttipahta located in Finland (Prairie et al 2021), which are amongst the two largest reservoirs in Western Europe (Huttunen et al., 2002).

The Lokka reservoir is approximately 417 km^2, and about 76% of the flooded land was comprised of peatlands (Huttunen et al., 2002; Maljanen et al., 2009). The reservoir is similar to Keeyask in that it is shallow with a mean depth of 2.3 to 5.0 meters, the water column is well mixed and eutrophic (Huttunen et al., 2002; Maljanen et al., 2009). There are also significant differences, such as the reservoir is lake-like (as opposed to river-like) with long water residence times ranging from 218 to 901 days (Huttunen et al 2002). In comparison, Keeyask water residence times are estimated to vary from 15 to 30 hours for the main channel (Keeyask Hydropower Limited Partnership, 2012b) and up to 30 days (Keeyask Hydropower Limited Partnership, 2012b) or possibly longer (personal communication W. DeWit, Manitoba Hydro, May 1, 2020). Longer water residence times can extend

the period for microbial decomposition of organic material and elevate GHG emissions in the reservoir (Prairie et al., 2018; Wang et al., 2018).

Sampling was conducted in the Lokka reservoir 26 and 27 years after impoundment (Huttunen et al., 2002). Although the post-flood reservoir CH_4 emissions were high compared to other northern aquatic ecosystems, they were lower than the pre-flood CH_4 emissions from the peatland footprint (Maljanen et al., 2009). This is because the pre-flooded peatland fens were high CH_4 emitters (Maljanen et al., 2009). Although this finding is insightful for modelling future Keeyask emissions from the flooded peatlands, it may not be directly comparable to Keeyask. The majority of flooded peatlands at Keeyask were bogs (91%) (Keeyask Hydropower Limited Partnership, 2012b), and bogs tend to have lower CH_4 emissions than fens (Webster et al., 2018; Kuhn et al., 2021). Post-flood Lokka reservoir CO_2 emissions were similar to boreal ponds and lakes (Huttunen et al., 2002).

The Porttipahta reservoir is approximately 214 km^2 and about 45% of the footprint comprises peatlands (Huttunen et al., 2002; Maljanen et al., 2009). The Porttipahta reservoir is similar to the Keeyask reservoir, as it is shallow with a mean depth ranging from 4.4 – 6.3 meters and it is river-like (Huttunen et al 2002). It is different from Keeyask in terms of its trophic state (mesotrophic as opposed to Keeyask being eutrophic), and it has longer water residence times ranging from 62 to 559 days (Huttunen et al., 2002). Sampling occurred 25 years after the impoundment (Huttunen et al., 2002). Similar to the Lokka reservoir, post-flood CH_4 emissions were lower than the pre-flood CH_4 emissions from the peatland footprint, as the pre-flooded fens were high CH_4 emitters (Maljanan et al., 2009). As with the Lokka reservoir, post-flood CO_2 emissions were similar to boreal ponds and lakes (Huttunen et al., 2002).

Huttunen et al. (2002) concluded that flooded biomass and fresh organic carbon from primary production, as opposed to old peat deposits, were the main contributors to CO_2 and CH_4 emissions in the Lokka and Porttipahta reservoirs. Flooded biomass was not defined in terms of how much comprised flooded peat. The study does raise the question of how much of a contribution does flooded peat make to CH_4 and CO_2 emissions. An important source of primary production for both the Lokka and Porttipahta reservoirs was plankton and not vegetation in the littoral zones (Huttunen et al., 2002). Erosion by ice scouring and wave action prevented the growth of littoral zone vegetation (Huttunen et al., 2002). This appears to be different from what is observed in the young

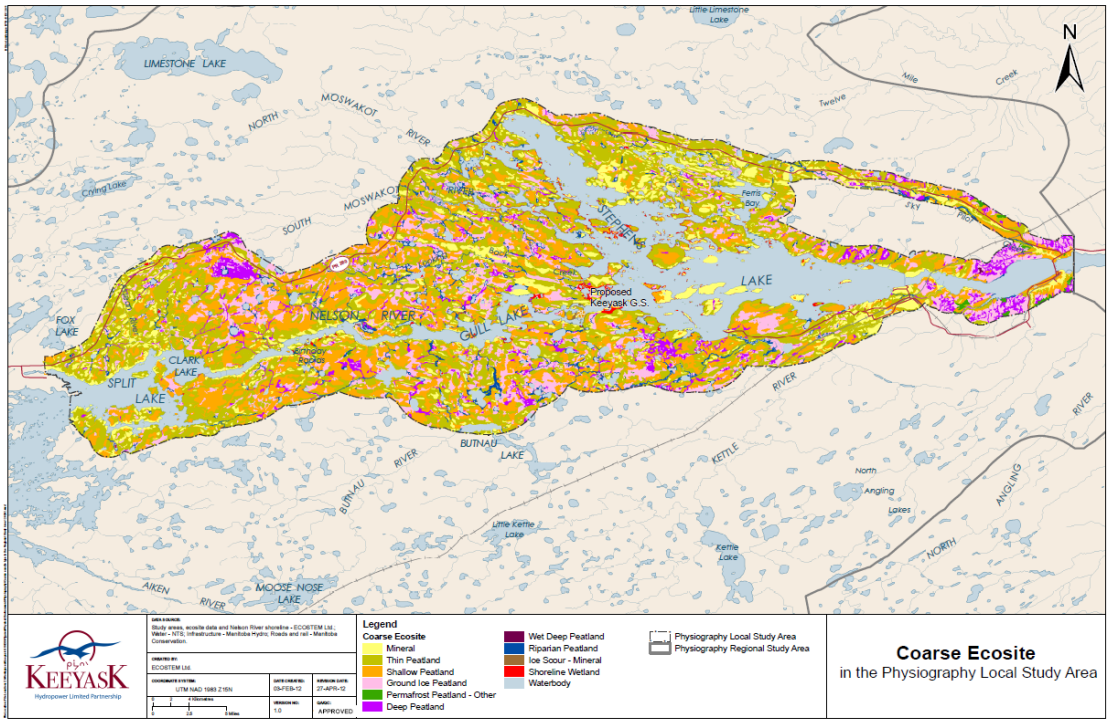
Keeyask reservoir, where floating and semi-submerged vegetation is observed along the shallow forebay and backbays (Figures 2-2 and 2-3). Primary production appeared to be limited by phosphorous and nitrogen in the Lokka reservoir and by nitrogen in the Porttipahta reservoir (Huttunen et al., 2002). The Keeyask reservoir on the other hand appears to be light limited due to high turbidity (Gedig et al., 2025).

The Lokka and Porttipahta reservoirs are not direct surrogates for the Keeyask reservoir because of their predominant type of peatland that was flooded (fen versus bog), longer water residence time, and because their post-flood CH_4 emissions were higher than their pre-flood CH_4 emissions.

Table 2-1 G-res Tool Boreal Reservoir Data Sources: Reservoir Age at Time of Sampling 20 Years or Younger

Reservoir Name	Impoundment year	Year of samping	Age at Sampling	Approximate Peatland Coverage	
Newfoundland and Labrador					
Cat Arm Dam West	1985	2003	18	0% - <1%	Tarnocai et al 2011 (1)
Quebec					
Caniapiscau Barrage	1984	2003	19	15%	Garneau et al 2014; Trudeau et al 2013
Eastmain-1	2005	2006	1	14%	Teodoru et al 2012
Eastmain-1	2005	2007	2	14%	Teodoru et al 2012
Eastmain-1	2005	2008	3	14%	Teodoru et al 2012
Eastmain-1	2005	2009	4	14%	Teodoru et al 2012
La Grande 4	1983	2003	20	50%	Garneau et al 2014
La Grande 3	1984	2003	19	50%	Garneau et al 2014
Laforge 1	1993	1993	0	15%	Garneau et al 2014; Trudeau et al 2013
Laforge 1	1993	1997	4	15%	Garneau et al 2014; Trudeau et al 2013
Laforge 1	1993	1998	5	15%	Garneau et al 2014; Trudeau et al 2013
Laforge 1	1993	2002	9	15%	Garneau et al 2014; Trudeau et al 2013
Laforge 2	1984	2003	19	15%	Garneau et al 2014; Trudeau et al 2013
Peribonka	2008	2008	0	0% - <1%	Tarnocai et al 2011 (1)
Robertson	1994	2002	8	0% - <1%	Tarnocai et al 2011 (1)
Romaine-2	2014	2015	1	<3%	Hydro-Québec 2008
Sainte-Marguerite 3	1998	2002	4	0% - <1%	Tarnocai et al 2011 (1)
British Columbia					
Revelstoke	1984	1992	8	5% (wetlands)	Utzig and Holt 2008; Utig and Schmidt 2011
Sweeden					
Skinnmuddselet	1989	2001	12	30%	Åberg et al 2004

Source: Adapted from Prairie et al 2021
(1) Tarnocai et al 2011 Peatland Distribution of Canadian Petland Map



Keeaysk Hydropower Limited Partnership, 2012a
Figure 2-1 Pre-Flood Keeyask Reservoir Landcover


Figure 2-2 Floating Peat Islands in Keeyask Reservoir Backbay Near GHG Monitoring Location



Figure 2-3 Floating Peat Islands in Keeyask Reservoir Forebay Near GHG Monitoring Location

2.2. Peat Resurfacing and Floating Peat Mats

The Keeyask Environmental Impact Statement predicted approximately 15-16 km^2 of flooded peat would resurface, which is about 35%-36% of the total area of flooded peatlands (Keeyask Hydropower Limited Partnership, 2012a). Peat resurfacing was forecasted to occur within the first 10 years after the impoundment, with about two thirds of the reemergence happening in the first year after flooding (Keeyask Hydropower Limited Partnership, 2012a). More than 80% of the resurfacing was anticipated to occur in water less than two meters deep (Keeyask Hydropower Limited Partnership, 2012a).

After impounding the Keeyask reservoir in 2020, floating peat mats have been observed within the forebay along the shallow shorelines and drifting adjacent to the Keeyask generating station, and within the shallow, flooded backbays (Manitoba Hydro, 2023).

Research has shown that floating peat can lead to elevated CO_2 and CH_4 emissions (Saque, 2003). This was demonstrated during an experimentally flooded reservoir where CH_4 emissions were initially elevated from floating peat (Scott et al., 1999). CH_4 emissions were generated in the anoxic zone that lay below the water table. The oxic zone above the water table was restricted, resulting in

less oxidation of CH_4 as CH_4 travels through the peat strata to the atmosphere (St.Louis et al., 2003). The experiment indicated that CH_4 fluxes could diminish as the peat islands age (Scott et al., 1999).

A source of uncertainty is, has G-res been calibrated with reservoir GHG data that represents a similar degree of peatland flooding and floating peat as the Keeyask reservoir.

2.2.4. Eastmain-1 Reservoir

Floating peat mats have been observed at the Eastmain-1 reservoir. During the first year of impoundment, 72 floating peat islands were recorded for a total of 21.7 hectares (Hydro-Québec, 2014). This amount of floating peat represents approximately 0.05% of the flooded terrestrial area (0.217 km^2 / 452.8 km^2) at Eastmain-1. Although these data pertain to the first year of flooding only, the areal extent of floating peat is quite small compared to the total flooded Eastmain-1 area, and it is small compared to the amount of resurfaced peat observed and modelled within the Keeyask reservoir.

2.2.5. Stephens Lake

As discussed above, Stephens Lake can be used as a surrogate to model the Keeyask reservoir for peatland disintegration and floating peat (Keeyask Hydropower Limited Partnership, 2012b). Although G-res includes GHG monitoring data from Stephens Lake for 2004 to 2007 (Demarty et al., 2009; Prairie et al., 2021) and floating peat was observed in Stephens Lake during that time period, (Figures 2-4 to 2-6) these data would not be able to estimate emissions being released from floating peat surfaces. The Stephens Lake GHG measurement data included in the G-res database pertains to CO_2 and CH_4 partial pressure which relates to estimate GHG diffusion emissions from the reservoir surface and degassing emissions. These data cannot be used to estimate emissions from the floating peat surface.

2.3. Littoral Zone

G-res defines the littoral zone as the area along the reservoir shoreline where water is less than 3 m deep (Prairie et al., 2017). The size of the littoral zone is used by G-res to estimate Post-flood CH_4 diffusive emissions, and Post-flood CH_4 bubble emissions (Prairie et al., 2017).

The littoral zone can be an important area of a reservoir for generating GHGs. Water flow can be slower through the shallow shorelines and backbays, providing more time for photosynthesis (carbon fixation/carbon production); microbial and photo degradation of carbon resulting in GHG production; accumulation of nutrients, which can facilitate microbial degradation and primary production; and carbon burial within reservoir sediments (Wang et al., 2018; Prairie et al., 2018).

There are two aspects to how the uncertainty related to the littoral zone may affect the Keeyask G-res modelling results. One, is the uncertainty associated with estimating the extent of the littoral zone for the post-flood Keeyask reservoir. The second is related to how well the reservoirs in the G-res database represent the Keeyask littoral zone. The G-res database was used to develop formulas that calculate GHG emissions in the littoral zones. This aspect is discussed below:

The following section reviews the G-res database of reservoir emissions to assess how well these data represent the Keeyask littoral zone. These data were used to develop formulas that estimate lifecycle GHG emissions. If the reservoirs that underpin the G-res formulas are significantly different from Keeyask, the G-res lifecycle estimates may not be suitable predictors of Keeyask emissions.

The first stage of the review focuses on the 13 reservoirs within the G-res database that were 20 years of age or less at the time of sampling (Table 2-2). The 20-year timeframe is of interest for this uncertainty assessment as this is the period the IPCC (2019) considers the bulk of CO_2 emissions to occur from reservoir flooding. As discussed earlier, 12 of the reservoirs are located in Canada and one is located in Sweden.

2.3.6. Canadian Reservoirs

Laforge 1 and 2, Québec

The littoral zones of Laforge 1 and 2 comprise approximately 26% and 27% respectively (Prairie et al., 2021b). This is similar to the Keeyask reservoir whose littoral zone is predicted to expand from approximately 20% at impoundment to about 26% 30 years after flooding due to shoreline erosion (Keeyask Hydropower Limited Partnership, 2012a; W. DeWit personal communication July 5, 2023). Since peatlands cover a relatively smaller portion of the Laforge region (15%) than Keeyask (90%),

GHG emissions occurring in the littoral zones of the Laforge and Keeyask reservoirs may not be directly comparable.

Eastmain-1, Québec

The littoral zone of the Eastmain-1 reservoir is estimated to be 16% of the total reservoir (Prairie et al., 2021). This is close to the extent of the Keeyask reservoir littoral zone at the time of initial flooding (20%), but less than the predicted 26% after 30 years of shoreline erosion. Brothers et al., (2012) studied respiration (CO_2 emissions) within the Eastmain-1 water column and sediments. Although they suspected respiration rates may be higher in the littoral zone, this was not quantified. Since the extent of peatlands underlying the Eastmain reservoir is less than that of Keeyask, and since the percentage of the reservoir that is littoral zone is smaller than that of Keeyask, it is uncertain as to how well the Eastmain-1 data represents the Keeyask reservoir.

2.3.6.1. Other Canadian Reservoirs

The Caniapiscau Barrage Reservoir, Québec, was not researched further because of the small extent of littoral zone (11%) and because it is situated in an area with low peatland coverage (15%). The remaining young Canadian reservoirs were not assessed further because of their small littoral zones (10% or less).

2.3.7. L. Skinnmuddselet, Sweden

Although nearly one third (29%) of the preflood reservoir footprint was comprised of peatlands, there was little post-flood microbiological activity in the littoral zone due to fluctuations in reservoir water levels and ice erosion (Åberg et al., 2004). This is quite different than Keeyask reservoir where reservoir levels are kept within one meter (Manitoba Conservation and Water Stewardship, 2014). GHG measurements from the L. Skinnmuddselet reservoir, which were collected 12 years after the reservoir was impounded, do not appear to be an ideal surrogate for modelling GHG emissions from the Keeyask littoral zone.

Table 2-2 G-res Tool Boreal Reservoir Data Sources: Reservoir Age at Time of Sampling 20 Years or Younger and Extent of Littoral Zone

G-res Tool Boreal Reservoir Data Sources
Littoral Area at Time of Sampling: Reservoirs 20 Years or Younger

Reservoir Name	Impoundment year	Year of samping	Age at Sampling	Littoral Area (%)
Newfoundland and Labrador				
Cat Arm Dam West	1985	2003	18	2.9
Quebec				
Caniapiscau Barrage	1984	2003	19	11.5
Eastmain-1	2005	2006	1	16.1
Eastmain-1	2005	2007	2	16.1
Eastmain-1	2005	2008	3	16.1
Eastmain-1	2005	2009	4	16.1
La Grande 4	1983	2003	20	7.8
La Grande 3	1984	2003	19	10.4
Laforge 1	1993	1993	0	15.3
Laforge 1	1993	1997	4	26.2
Laforge 1	1993	1998	5	26.2
Laforge 1	1993	2002	9	14.4
Laforge 2	1984	2003	19	27.2
Peribonka	2008	2008	0	6.0
Robertson	1994	2002	8	-
Romaine-2	2014	2015	1	4.1
Sainte-Marguerite 3	1998	2002	4	4.3
British Columbia				
Mica	1973	1992	19	7.1
Revelstoke	1984	1992	8	5.0
Sweeden				
Skinnmuddselet	1989	2001	12	28.6

Source: Adapted from Prairie et al 2021b Supplementary Information

(1) Tarnocai et al 2011 Peatland Distribution of Canadian Petland Map

2.3.8. Mature Reservoirs

2.3.8.1. Canadian Reservoirs

2.3.8.1.1. Stephens Lake, Manitoba

The closest surrogate to the Keeyask reservoir for assessing the littoral zone is Stephens Lake, which is immediately downstream of the Keeyask reservoir. Stephens Lake is the reservoir for the Kettle Generating Station and is a mature reservoir. The littoral zone is estimated to be 27% (Prairie et al., 2021b) and the pre-flood landscape is similar to that of Keeyask (Keeyask Hydropower Limited Partnership, 2012b).

As discussed earlier, G-res includes GHG monitoring data from Stephens Lake for 2004 to 2007 that was derived from continuous GHG monitors installed within the Kettle Generating Station (Demarty et al., 2009; Prairie et al., 2021). These data may not be representative of emissions from the shallow reservoir backbays (Marchand et al., 2015a). From 2009 to 2014 spatial, point-in-time partial pressure measurements and direct diffusive flux measurements of CO_2 and CH_4 were collected within the Stephens Lake main channel and shallow backbays (Bastien et al., 2010; Marchand et al., 2015a) which could help to calibrate G-res for modelling the Keeyask reservoir.

2.3.8.1.2. Cedar Lake, Manitoba

Cedar Lake is the reservoir for the Manitoba Hydro Grand Rapids Generating Station, located on the Saskatchewan River as the river flows into Lake Winnipeg. Cedar lake is a mature reservoir that was impounded in 1968 and is approximately 3500 km^2 (Manitoba Environment and Climate Change, 2026). As calculated by Prairie et al. (2021b) using G-res, the littoral zone comprises approximately 33% of the reservoir (Table 2-3).

G-res includes GHG monitoring data from Cedar Lake for 2006 to 2007 (Demarty et al., 2009; Prairie et al., 2021). The Cedar Lake data was derived from a continuous GHG monitor installed within the Grand Rapid Generating Station as part of Manitoba Hydro's reservoir GHG program (Demarty et al., 2009). These data pertain to dissolved concentrations of CO_2 and CH_4 in the forebay waters passing through the station and flowing downstream. The data can be used to calculate diffusive fluxes at the reservoir surface and degassing emissions as reservoir water passes through the

generating station turbines and spillway. These data are representative of a mature reservoir and not necessarily of the emissions from the littoral zones when the reservoir was initially flooded.

Continuous CO_2 and CH_4 partial pressure data was collected from 2006 – 2012 using a continuous monitor installed within the Grand Rapids Powerhouse (Marchand et al., 2012). These data could help calibrate G-res for northern Manitoba reservoirs.

2.3.8.1.3. Churchill Falls Reservoir, Labrador

The Churchill Falls reservoir is approximately 6,988 km^2 and the littoral zone is estimated to be 25% of the reservoir (Prairie et al., 2021b). The reservoir is mature, being impounded in 1974, and was 32 years of age when the data used in G-res were collected (Prairie et al., 2021b). Approximately 634 km^2, or 26%, of the flooded land (2,449 km^2) was comprised of bogs, fens, and marshes (Bajzak & Roberts, 2011). The percentage of littoral zone is similar to that of Keeyask (25% Churchill Falls; 26% Keeyask), the extent of flooded peatlands is less for the Churchill Falls reservoir than Keeyask reservoir (26% Churchill Falls; 90% Keeyask). Given the large size, mature age, and smaller extent of flooded peatlands of the Churchill Falls reservoir, it may not represent GHG emissions from the littoral zones of the young Keeyask reservoir. The Churchill Falls data provides insight into GHG emissions from a mature northern reservoir, but not necessarily for the recently flooded Keeyask reservoir.

2.3.8.1.4. Québec Reservoirs

The Bersimis, Gouin, Manicouagan 2, and Opinaca reservoirs have large littorals zones at 77%, 43%, 25%, and 22% respectively (Table 2-3) (Prairie et al., 2021b). All of these reservoirs were mature when the data used in G-res were collected (Prairie et al., 2021b). As discussed for the Churchill Falls data, these reservoirs provide insight into GHG emissions from a mature northern reservoir, and may provide helpful insight for modelling Keeyask emissions as the reservoir ages.

The La Grande 1 reservoir and the Robert-Bourassa reservoir were estimated to have relatively small littoral zones, 11% and 14% respectively (Prairie et al., 2021b). These reservoirs are located in the western portion of the La Grande Rivière watershed where peatlands cover approximately 50% of the landscape (Garneau et al., 2014). They were relatively mature when the samples used in

the G-res database were collected (14 to 28 years old) and may provide helpful insight for modelling Keeyask emissions as the reservoir ages.

2.3.8.1.5. Whatshan Reservoir, British Columbia

The Whatshan reservoir is located in the Monashee mountains of British Columbia. The reservoir is approximately 15 km^2 and the littoral zone is estimated to be 18% of the reservoir (Prairie et al., 2021b). The reservoir is mature, being impounded in 1951, and was 51 years of age when the data used in G-res were collected (Prairie et al., 2021b). The pre-flood landcover included marsh, marsh to fen transitional, and fen; and the post-flood reservoir includes submerged and emergent vegetation (G3 Consulting, 2012; 2016). Although this is a small reservoir, the GHG measurement data could provide helpful information on emissions from riparian fens which were present in the Keeyask pre-flooded landscape.

2.3.8.2. Lokka and Porttipahta Reservoirs, Finland

The G-res database includes measurements from two mature northern reservoirs, Lokka and Porttipahta located in Finland (Prairie et al., 2021). The Lokka reservoir is approximately 417 km^2 (Huttunen et al., 2002) and the littoral zone was estimated to be 31% (Prairie et al., 2021b). Sampling was conducted in the Lokka reservoir 26 and 27 years after impoundment (Huttunen et al., 2002). The Porttipahta reservoir is approximately 214 km^2 (Huttunen et al., 2002) and the littoral zone was estimated to be 31% (Prairie et al., 2021b). Erosion by ice scouring and wave action prevented the development of littoral zone vegetation (Huttunen et al., 2002). This appears to be different from what is observed in the young Keeyask reservoir, where floating and semi-submerged vegetation is observed along the shallow forebay and backbays.

2.3.8.3. Bianco Reservoir, Switzerland

The Bianco Reservoir is a small (1.5 km^2), mature (92 years at time of sampling), deep (maximum 53 meters; average 14 meters), alpine reservoir with relatively long water retention times (100 – 200 days) and negligible CH_4 emissions (Diem et al., 2012). Although the littoral zone is estimated as being 15% (Prairie et al., 2021b), it is not representative of the Keeyask reservoir for the reasons described above.

2.3.8.4. Other Mature Northern Reservoirs

The remaining mature northern reservoirs in the G-res database were not assessed further because of their small littoral zones (less than 10%).

Table 2-3 G-res Tool Boreal Reservoir Data Sources: Reservoir Age at Time of Sampling Over 20 Years and Extent of Littoral Zone

Table:
G-res Tool Boreal Reservoir Data Sources
Littoral Area : Mature Reservoirs (Over 20 Years)

Reservoir Name	Littoral Area (%)	Age at Sampling
Bersimis	77.41	46
Gouin	42.59	35
Porttipahta	33.45	25
Grand Rapids (Cedar Lake)	33.33	39
Lokka	31.01	27 - 28
Kettle Rapids (Stephens Lake)	27.06	31
Churchill Falls	25.04	32
Manicouagan 2	24.49	34
Opinaca	22.44	23
Whatshan	18.01	40 - 51
Bianco	14.98	92
La Grande 2	13.53	14 - 28
La Grande 1	10.78	24
Outardes 3	8.58	30
Seven Mile	8.44	23
Outardes 4	8.02	31
Dillon	7.36	26
W.A.C. Bennett	5.83	23 - 41
Grand Coulee	5.37	59
Lungern	5.24	85
Spitallamm	5.03	73
Follsjo	4.85	37
Manicouagan 3	4.00	28
Oberaar	3.83	52
Daniel Johnson	3.49	35 - 38
Bersimis 2	3.33	43
Luzzone	3.23	42
Lac Ste. Anne Principal	3.22	45 - 53
Zeuzier	2.85	46
Duncan	2.17	37
Hugh Keenleyside	2.04	22 - 23
Grande Dixence	1.89	42
Santa Maria	1.76	37
Sayano-Shushenskaya	1.34	36
Corra-Linn	1.19	70
Skellefte		100
Indal		64
Sainte-Marguerite 2		51
EOL		24
Mainskaya		30

Source: Adapted from Prairie et al 2021b Supplementary Information



Photo: B. Gill October 29, 2007
Figure 2-4 Stephens Lake Floating Peat Mats Along Northern Shoreline(34 Years After Impoundment)



Photo: B. Gill October 29, 2007
Figure 2-5 Stephens Lake Floating Peat Mats Along Northern Shoreline
(34 Years After Impoundment)



Photo: B. Gill October 29, 2007

Figure 2-6 Stephens Lake Semi-Submerged Vegetation Along Northern Shoreline Littoral Zone
(34 Years After Impoundment)

3. References

Åberg, J., Bergström, A. K., Algesten, G., Söderback, K., & Jansson, M. (2004). A comparison of the carbon balances of a natural lake (L. Örträsket) and a hydroelectric reservoir (L. Skinnmuddselet) in northern Sweden. *Water Research*, *38*(3), 531–538. https://doi.org/10.1016/j.watres.2003.10.035

Amesbury, M. J., Gallego-Sala, A., & Loisel, J. (2019). Peatlands as prolific carbon sinks. In *Nature Geoscience* (Vol. 12, Issue 11, pp. 880–881). Nature Publishing Group. https://doi.org/10.1038/s41561-019-0455-y

Atlantica Centre for Energy (2024). Newfoundland and Labrador Energy Map. https://www.atlanticaenergy.org/energy-knowledge-centre/energy-maps/newfoundland-and-labradors-energy-resources/

Baird, Andrew & Belyea, Lisa & Comas, Xavier & Reeve, A.S. & Slater, Lee. (2009). Understanding Carbon Cycling in Northern Peatlands: Recent Developments and Future Prospects. DOI 10.1029/2008GM000875. In book: Carbon Cycling in Northern Peatlands. Geophysical Monograph Series 184 (pp.1-3)Chapter: Understanding Carbon Cycling in Northern Peatlands: Recent Developments and Future ProspectsPublisher: American Geophysical UnionEditors: Andrew J. Baird, Lisa R. Belyea, Xavier Comas, A.S. Reeve, Lee D. Slater

Bajzak, D., & Roberts, B. A. (2011). Environmental Impact of Flooding in the Main (Smallwood) Reservoir of the Churchill Falls Power Plant, Labrador, Canada. I. Background and Descriptions of Flooded Conditions Related to Vegetation and Land Cover Types. *Journal of Water Resource and Protection*, *03*(03), 147–152. https://doi.org/10.4236/jwarp.2011.33018

Barbosa, P. M., Bodmer, P., Stadler, M., Rust, F., Tremblay, A., & del Giorgio, P. A. (2023). Ecosystem Metabolism Is the Dominant Source of Carbon Dioxide in Three Young Boreal Cascade-Reservoirs (La Romaine Complex, Québec). *Journal of Geophysical Research: Biogeosciences*, *128*(4). https://doi.org/10.1029/2022JG007253

Bastien, J., Gravel, R., Demarty, M., Smith, M., and Gill, R. (2010). Reservoir Greenhouse Gas Monitoring Report – 2008-2009. Report prepared by Environnement Illimité inc. for Manitoba Hydro, 111 p. and 1 appendix.

Bastien, J., M. Demarty, M. Smith and R. Gill. (2011). Reservoir Greenhouse Gas Monitoring Report – 2010. Report prepared by Environnement Illimité inc. for Manitoba Hydro, Tier 1: 40 p. and 2 appendices; Tier 2: 55 p

Bergström, A. K., Algesten, G., Sobek, S., Tranvik, L., & Jansson, M. (2004). Emission of CO2 from hydroelectric reservoirs in northern Sweden. *Archiv Fur Hydrobiologie*, *159*(1), 25–42. https://doi.org/10.1127/0003-9136/2004/0159-0025

Bilodeau, F., Tremblay, A., Chavaillaz, Y., Demarty, M., Deblois, C. (2023). Greenhouse Gas Emissions: Monitoring at the La Grande Complex, West Sectors Spatial Variation in Lakes and Reservoirs. Mini-Symposium, 8-9 November, Montréal.

Brothers, S. M., Prairie, Y. T., & Del Giorgio, P. A. (2012). Benthic and pelagic sources of carbon dioxide in boreal lakes and a young reservoir (Eastmain-1) in eastern Canada. *Global Biogeochemical Cycles*, *26*(1). https://doi.org/10.1029/2011GB004074

delGiorgio, P. (2023). La Romaine Project: looking ahead the CarBBAS Team. L'Université du Québec à Montréal. Mini-Symposium, 8-9 November, Montréal.

DelSontro, T., Perez, K. K., Sollberger, S., & Wehrli, B. (2016). Methane dynamics downstream of a temperate run-of-the-river reservoir. *Limnology and Oceanography*, *61*, S188–S203. https://doi.org/10.1002/lno.10387

DelSontro, T., del Giorgio, P. A., & Prairie, Y. T. (2017). No Longer a Paradox: The Interaction Between Physical Transport and Biological Processes Explains the Spatial Distribution of Surface Water Methane Within and Across Lakes. Ecosystems, 21(6), 1073–1087. https://doi.org/10.1007/s10021-017-0205-1

Demarty, M., Bastien, J., Tremblay, A., Hesslein, R. H., & Gill, R. (2009). Greenhouse gas emissions from boreal reservoirs in Manitoba and Québec, Canada, measured with automated systems. *Environmental Science and Technology*, *43*(23), 8908–8915. https://doi.org/10.1021/es8035658

Demarty, M., & Tremblay, A. (2019). Long term follow-up of pCO2, pCH4 and emissions from Eastmain 1 boreal reservoir, and the Rupert diversion bays, Canada. *Ecohydrology and Hydrobiology*, *19*(4), 529–540. https://doi.org/10.1016/j.ecohyd.2017.09.001

Diem, T., Koch, S., Schwarzenbach, S., Wehrli, B., & Schubert, C. J. (2012). Greenhouse gas emissions (CO2, CH4, and N2O) from several perialpine and alpine hydropower reservoirs by diffusion and loss in turbines. *Aquatic Sciences*, *74*(3), 619–635. https://doi.org/10.1007/s00027-012-0256-5

Dowd, M.B and C.L. Hrenchuck. (2023). Results of water quality monitoring in the Nelson River, 2022: Year 1 Operation. Keeyask Generation Project Aquatic Effects Monitoring Plan Report. #AEMP-2023-13. A report prepared for Manitoba Hydro by North/South Consultants Inc,. June 2023. xv +295 pages.

Dowd, M.B and C.L. Hrenchuck. (2024). Results of water quality monitoring in the Nelson River, 2023: Year 2 Operation. Keeyask Generation Project Aquatic Effects Monitoring Plan Report. #AEMP-2024-11. A report prepared for Manitoba Hydro by North/South Consultants Inc,. June 2024. xvi +301 pages.

G3 Consulting Ltd. (2012). WGSMON-2: Whatshan Reservoir Vegetation Monitoring Program, Phase 2 (2011). Prepared for BC Hydro and Power Authority, Burnaby, BC by G3 Consulting Ltd., Surrey, BC. 41pages + Appendices.

G3 Consulting Ltd. (2016). WGSMON-2: Whatshan Reservoir Vegetation Monitoring Program, Phase 3 (2015). Prepared for BC Hydro and Power Authority, Burnaby, BC by G3 Consulting Ltd., Surrey, BC. 37 pages + Appendices.

Garneau, M., van Bellen, S., Magnan, G., Beaulieu-Audy, V., Lamarre, A., & Asnong, H. (2014). Holocene carbon dynamics of boreal and subarctic peatlands from Québec, Canada. Holocene, 24(9), 1043–1053. https://doi.org/10.1177/0959683614538076

Garneau, M., Tremblay, L., & Magnan, G. (2018). Holocene pool formation in oligotrophic fens from boreal Québec in northeastern Canada. *Holocene*, *28*(3), 396–407. https://doi.org/10.1177/0959683617729439

Gedig, D. P., Soloway, A. D., Gill, R., & Papakyriakou, T. N. (2025). Aquatic metabolism after impoundment of a low productivity boreal reservoir using free water oxygen. Inland Waters, 15(1). https://doi.org/10.1080/20442041.2025.2489254

Goldenfum, J. A. . (2010). *GHG measurement guidelines for freshwater reservoirs : derived from: The UNESCO/IHA Greenhouse Gas Emissions from Freshwater Reservoirs Research Project*. International Hydropower Association (IHA).

Gong, Y., Wu, J., Vogt, J., & Ma, W. (2020). Greenhouse gas emissions from peatlands under manipulated warming, nitrogen addition, and vegetation composition change: A review and data synthesis. In *Environmental Reviews* (Vol. 28, Issue 4, pp. 428–437). Canadian Science Publishing. https://doi.org/10.1139/er-2019-0064

Goulden, M. L., Mcmillan, A. M. S., Winston, G. C., Rocha, A. V., Manies, K. L., Harden, J. W., & Bond-Lamberty, B. P. (2011). Patterns of NPP, GPP, respiration, and NEP during boreal forest succession. *Global Change Biology*, *17*(2), 855–871. https://doi.org/10.1111/j.1365-2486.2010.02274.x

Grenier, M., Labrecque, S., Garneau, M., & Tremblay, A. (2008). Object-based classification of a SPOT-4 image for mapping wetlands in the context of greenhouse gases emissions: The case of the Eastmain region, Québec, Canada. *Canadian Journal of Remote Sensing*, *34*, S398–S413. https://doi.org/10.5589/m08-049

Harrison, J. A., Prairie, Y. T., Mercier-Blais, S., & Soued, C. (2021). Year-2020 Global Distribution and Pathways of Reservoir Methane and Carbon Dioxide Emissions According to the Greenhouse Gas From Reservoirs (G-res) Model. *Global Biogeochemical Cycles*, *35*(6). https://doi.org/10.1029/2020GB006888

Hrenchuk, C. (2021). Results of water quality monitoring in the Nelson River, 2020: Year 7 Construction. Keeyask Generation Project Aquatic Effects Monitoring Plan Report #AEMP-2021-06. A report prepared for Manitoba Hydro by North/South Consultants Inc., June 2021. xxv + 124 pp.

Hrenchuk, C. (2022). Results of water quality monitoring in the Nelson River, 2021: Year 8 Construction. Keeyask Generation Project Aquatic Effects Monitoring Plan Report #AEMP-2022-14. A report prepared for Manitoba Hydro by North/South Consultants Inc., June 2022. xxviii + 301 pp.

Hugelius, G., Loisel, J., Chadburn, S., Jackson, R. B., Jones, M., MacDonald, G., Marushchak, M., Olefeldt, D., Packalen, M., Siewert, M. B., Treat, C., Turetsky, M., Voigt, C., & Yu, Z. (2020). Large stocks of peatland carbon and nitrogen are vulnerable to permafrost thaw. *Proceedings of the National Academy of Sciences of the United States of America*, *117*(34), 20438–20446. https://doi.org/10.1073/pnas.1916387117

Huttunen, J. T., Väisänen, T. S., Hellsten, S. K., Heikkinen, M., Nykänen, H., Jungner, H., Niskanen, A., Virtanen, M. O., Lindqvist, O. V., Nenonen, O. S., & Martikainen, P. J. (2002). Fluxes of CH4, CO2, and N2O in hydroelectric reservoirs Lokka and Porttipahta in the northern boreal zone in Finland. *Global Biogeochemical Cycles*, *16*(1). https://doi.org/10.1029/2000gb001316

Hydro-Québec (2008). Romaine Complex: Environmental Impact Statement Summary. Hydro-Québec Production.

Hydro-Québec (2014). Eastmain-1 Hydroelectric Development: Environmental Activities, 2002–2013 – Highlights October 2014, Legal deposit – 4th quarter 2014, Library and Archives Canada, Bibliothèque et Archives nationales du Québec. ISBN: 978-2-550-71782-9, 32 pages.

IPCC. (2019). Wetlands. Chapter 7_Volume 4 (Agriculture, Forestry and Other Land Use), 2019 Refinement to the 2006 IPCC Guidelines for National Greenhouse Gas Inventories.

Keeyask Hydropower Limited Partnership (2012a). Keeyask Generation Project: Environmental Impact Statement; Physical Environment Response to EIS Guidelines, Supporting Volume. 1018 pages.

Keeyask Hydropower Limited Partnership (2012b). Keeyask Generation Project: Environmental Impact Statement; Terrestrial Environment Response to EIS Guidelines, Supporting Volume. 1346 pages.

Keeyask Hydropower Limited Partnership (2012c). Keeyask Generation Project: Environmental Impact Statement; Aquatic Environment Response to EIS Guidelines, Supporting Volume. 1745 pages.

Keeyask Hydropower Limited Partnership. (2015). Keeyask Generation Project: Physical Environment Monitoring Plan. Prepared by Keeyask Hydropower Limited Partnership. Winnipeg, Manitoba. 97 pages. https://keeyask.com/wp-content/uploads/2014/08/KGP-Physical-Environment-Monitoring-Plan-Final.pdf

Kuhn, M. A., Varner, R. K., Bastviken, D., Crill, P., Macintyre, S., Turetsky, M., Walter Anthony, K., McGuire, A. D., & Olefeldt, D. (2021). BAWLD-CH4: A comprehensive dataset of methane fluxes from boreal and arctic ecosystems. In *Earth System Science Data* (Vol. 13, Issue 11, pp. 5151–5189). Copernicus Publications. https://doi.org/10.5194/essd-13-5151-2021

Levasseur, A., Mercier-Blais, S., Prairie, Y.T., Tremblay, A., Turpin, C. (2021). Improving the accuracy of electricity carbon footprint: Estimation of hydroelectric reservoir greenhouse gas emissions. *Renewable and Sustainable Energy Reviews*, 136, 110433, 1364-0321. https://doi.org/10.1016/j.rser.2020.110433.

Li, M. & He, N. (2022). Carbon intensity of global existing and future hydropower reservoirs. *Renewable and Sustainable Energy Reviews*, 162, 112433, 1364-0321. https://doi.org/10.1016/j.rser.2022.112433.

Louis, V. L. S., Partridge, A. D., Kelly, C. A., & Rudd, J. W. M. (2003). *Mineralization rates of peat from eroding peat islands in reservoirs*.

Maljanen, M., Sigurdsson, B. D., Guðmundsson, J., Oskarsson, H. ´, Huttunen, J. T., & Martikainen, P. J. (2009). Land-use and greenhouse gas balances of peatlands Land-use and greenhouse gas balances of peatlands in the Nordic countries-present knowledge and gaps Land-use and greenhouse gas balances of peatlands. In *Biogeosciences Discuss* (Vol. 6). www.biogeosciences-discuss.net/6/6271/2009/

Manitoba Conservation and Water Stewardship. (2014). Interim Licence for the Development of Water Power, Keeyask Site, Nelson River. Issued in accordance with The Water Power Act (C.C.S.M., c.W60), and the Water Power Regulation (MR. 25/88R). Manitoba Conservation and Water Stewardship, The Province of Manitoba.

Manitoba Hydro. (2015). Flooded Areas for Manitoba Hydro System. [Unpublished manuscript]. Manitoba Hydro, Winnipeg, Manitoba.

Manitoba Hydro. (2023). The "Isle of Pete" puts problem solving skills to test at Keeyask. Manitoba Hydro Hydrogram 8/10/2023 https://mhcloud.sharepoint.com/sites/Hydrogram/SitePages/TIsland-Called-Pete--peat-island-puts-problem-solving-skills-to-test.aspx

Marchand D., M. Demarty and R. Gill. (2012). Reservoir Greenhouse Gas Monitoring Report –2012. Report prepared by Environnement Illimité inc. for Manitoba Hydro, Tier 1: 34 p. and 1 appendix and Tier 2: 51 p.

Marchand D., M. Demarty and R. Gill. (2015a). Keeyask Technical Summay – 2014. Summary prepared by Environnement Illimité for Manitoba Hydro, 11 p.

Marchand D., M. Demarty and R. Gill. (2015b). Conawapa Technical Summay – 2014. Summary prepared by Environnement Illimité for Manitoba Hydro, 6 p.

National Renewable Energy Laboratory (2021). Life Cycle Greenhouse Gas Emissions from Electricity Generation. NREL/FS-6A50-80580

Nicholson, S., & Heath, G. (2012). *Life Cycle Greenhouse Gas Emissions from Electricity Generation: Update Life Cycle Assessment of Energy Systems*. https://data.nrel.gov/submissions/171

Olefeldt, D., Hovemyr, M., Kuhn, M. A., Bastviken, D., Bohn, T. J., Connolly, J., Crill, P., Euskirchen, E. S., Finkelstein, S. A., Genet, H., Grosse, G., Harris, L. I., Heffernan, L., Helbig, M., Hugelius, G., Hutchins, R., Juutinen, S., Lara, M. J., Malhotra, A., … Watts, J. D. (2021). The boreal-arctic wetland and lake dataset (BAWLD). Earth System Science Data, 13(11), 5127–5149. https://doi.org/10.5194/essd-13-5127-2021

Pelletier, Luc. (2007). Carbon dioxide and methane fluxes of three peatlands in the La Grande Rivière watershed, James Bay lowland, Canada. Library and Archives Canada = Bibliothèque et Archives Canada.

Pelletier, L., Garneau, M., & Tremblay, A. (2009). CO 2 and CH 4 ecosystem exchange from peatlands: Eastmain-1 hydroelectric project, Quebec, Canada. In Verh. Internat. Verein. Limnol (Vol. 30).

Pelletier, L., Garneau, M., & Moore, T. R. (2011). Variation in CO2 exchange over three summers at microform scale in a boreal bog, Eastmain region, Québec, Canada. *Journal of Geophysical Research: Biogeosciences*, *116*(3). https://doi.org/10.1029/2011JG001657

Pelletier, L., Strachan, I. B., Garneau, M., & Roulet, N. T. (2014). Carbon release from boreal peatland open water pools: Implication for the contemporary C exchange. *Journal of Geophysical Research: Biogeosciences*, *119*(3), 207–222. https://doi.org/10.1002/2013JG002423

Pelletier, L., Strachan, I. B., Roulet, N. T., Garneau, M., & Wischnewski, K. (2015). Effect of open water pools on ecosystem scale surface-atmosphere carbon dioxide exchange in a boreal peatland. *Biogeochemistry*, *124*(1–3), 291–304. https://doi.org/10.1007/s10533-015-0098-z

Pelletier, Luc. (2007). *Carbon dioxide and methane fluxes of three peatlands in the La Grande Rivière watershed, James Bay lowland, Canada*. Library and Archives Canada = Bibliothèque et Archives Canada.

Pokorny, S., Stadnyk, T. A., Ali, G., Lilhare, R., Déry, S. J., & Koenig, K. (2021). Cumulative effects of uncertainty on simulated streamflow in a hydrologic modeling environment. *Elementa*, *9*(1). https://doi.org/10.1525/elementa.431

Prairie YT, Alm J, Harby A, Mercier-Blais S, Nahas R. (2017). The GHG Reservoir Tool (Gres) Technical documentation. Updated version 3.31 (03-07-2025). UNESCO/IHA research project on the GHG status of freshwater reservoirs. Joint publication of the UNESCO Chair in Global Environmental Change and the International Hydropower Association. 72 pages.

Prairie, Y. T., Alm, J., Beaulieu, J., Barros, N., Battin, T., Cole, J., del Giorgio, P., DelSontro, T., Guérin, F., Harby, A., Harrison, J., Mercier-Blais, S., Serça, D., Sobek, S., & Vachon, D. (2018). Greenhouse Gas Emissions from Freshwater Reservoirs: What Does the Atmosphere See? *Ecosystems*, *21*(5), 1058–1071. https://doi.org/10.1007/s10021-017-0198-9

Prairie, Y. T., Mercier-Blais, S., Harrison, J. A., Soued, C., Giorgio, P. del, Harby, A., Alm, J., Chanudet, V., & Nahas, R. (2021a). A new modelling framework to assess biogenic GHG emissions from reservoirs: The G-res tool. *Environmental Modelling and Software*, *143*. https://doi.org/10.1016/j.envsoft.2021.105117

Prairie, Y. T., Mercier-Blais, S., Harrison, J. A., Soued, C., Giorgio, P. del, Harby, A., Alm, J., Chanudet, V., & Nahas, R. (2021b). A new modelling framework to assess biogenic GHG emissions from reservoirs: The G-res tool. *Environmental Modelling and Software*, *143*. https://doi.org/10.1016/j.envsoft.2021.105117

Rust, F., Bodmer, P., & del Giorgio, P. (2022). Modeling the spatial and temporal variability in surface water CO2 and CH4 concentrations in a newly created complex of boreal hydroelectric reservoirs. *Science of the Total Environment*, *815*. https://doi.org/10.1016/j.scitotenv.2021.152459

Saque, M.A.M. 2003. Greenhouse gas flux and budget from an experimentally flooded wetland using stable isotopes and geochemistry, Master of Science thesis, University of Waterloo, Waterloo, Ontario, Canada, 2003.

St. Louis, V.L., Kelly, C.A., Duchemin, É, Rudd, J.W.M., Rosenberg, D.M. 2000. Reservoir Surfaces as Sources of Greenhouse Gases to the Atmosphere: A Global Estimate: Reservoirs are sources of greenhouse gases to the atmosphere, and their surface areas have increased to the point where they should be included in global inventories of anthropogenic emissions of greenhouse gases, BioScience, Volume 50, Issue 9, September 2000, Pages 766–775, https://doi.org/10.1641/0006-3568(2000)050[0766:RSASOG]2.0.CO;2

St. Louis, V.L., Partridge, A.D., Kelly, C.A., Rudd, J. (2003). Mineralization rates of peat from eroding peat islands in reservoirs. Biogeochemistry 64, 97–110. https://doi.org/10.1023/A:1024982915493

Scherer, L., & Pfister, S. (2016). Hydropower's biogenic carbon footprint. *PLoS ONE*, *11*(9). https://doi.org/10.1371/journal.pone.0161947

Scott, K. J., Kelly, C. A., & Rudd, J. W. M. (1999). The importance of floating peat to methane fluxes from flooded peatlands. In *Biogeochemistry* (Vol. 47, Issue 9). KluwerAcademic Publishers.

Soued, C., Harrison, J. A., Mercier-Blais, S., & Prairie, Y. T. (2022). Reservoir CO2 and CH4 emissions and their climate impact over the period 1900–2060. *Nature Geoscience*, *15*(9), 700–705. https://doi.org/10.1038/s41561-022-01004-2

Strachan, I. B., Nugent, K. A., Crombie, S., & Bonneville, M. C. (2015). Carbon dioxide and methane exchange at a cool-temperate freshwater marsh. *Environmental Research Letters*, *10*(6). https://doi.org/10.1088/1748-9326/10/6/065006

Strack, M (ed). (2008). Peatlands and Climate Change. International Peat Society, ISBN 9529940114, 9789529940110, 223 pages

Tarnocai, C., & Bockheim, J. G. (2011). Cryosolic soils of Canada: Genesis, distribution, and classification. *Canadian Journal of Soil Science*, *91*(5), 749–762. https://doi.org/10.4141/cjss10020

Teodoru, C. R., Bastien, J., Bonneville, M. C., Del Giorgio, P. A., Demarty, M., Garneau, M., Hélie, J. F., Pelletier, L., Prairie, Y. T., Roulet, N. T., Strachan, I. B., & Tremblay, A. (2012b). The net carbon footprint of a newly created boreal hydroelectric reservoir. *Global Biogeochemical Cycles*, *26*(2). https://doi.org/10.1029/2011GB004187

Treat, C. C., Bloom, A. A., & Marushchak, M. E. (2018). Nongrowing season methane emissions–a significant component of annual emissions across northern ecosystems. *Global Change Biology*, *24*(8), 3331–3343. https://doi.org/10.1111/gcb.14137

Treat, C. C., Jones, M. C., Brosius, L., Grosse, G., Walter Anthony, K., & Frolking, S. (2021). The role of wetland expansion and successional processes in methane emissions from northern wetlands during the Holocene. *Quaternary Science Reviews*, *257*. https://doi.org/10.1016/j.quascirev.2021.106864

Treat, C. C., Virkkala, A. M., Burke, E., Bruhwiler, L., Chatterjee, A., Fisher, J. B., Hashemi, J., Parmentier, F. J. W., Rogers, B. M., Westermann, S., Watts, J. D., Blanc-Betes, E., Fuchs, M., Kruse, S., Malhotra, A., Miner, K., Strauss, J., Armstrong, A., Epstein, H. E., … Hugelius, G. (2024). Permafrost Carbon: Progress on Understanding Stocks and Fluxes Across Northern Terrestrial Ecosystems. *Journal of Geophysical Research: Biogeosciences*, *129*(3). https://doi.org/10.1029/2023JG007638

Trudeau, N. C., Garneau, M., & Pelletier, L. (2013). Methane fluxes from a patterned fen of the northeastern part of the La Grande river watershed, James Bay, Canada. *Biogeochemistry*, *113*(1–3), 409–422. https://doi.org/10.1007/s10533-012-9767-3

Turetsky, M. R., Kotowska, A., Bubier, J., Dise, N. B., Crill, P., Hornibrook, E. R. C., Minkkinen, K., Moore, T. R., Myers-Smith, I. H., Nykänen, H., Olefeldt, D., Rinne, J., Saarnio, S., Shurpali, N., Tuittila, E. S., Waddington, J. M., White, J. R., Wickland, K. P., & Wilmking, M. (2014). A synthesis of methane emissions from 71 northern, temperate, and subtropical wetlands. *Global Change Biology*, *20*(7), 2183–2197. https://doi.org/10.1111/gcb.12580

Utzig, G. F., Holt, P. A. R. F., & Bio, R. P. (2008). *Terrestrial Productivity in the Flooded Terrestrial Ecosystems of the Columbia Basin: Impacts, Mitigation and Monitoring*.

Utzig, G., & Schmidt, D. (2011). *Dam Footprint Impact Summary BC Hydro Dams in the Columbia Basin*.

Vachon, D., Prairie, Y. T., Guillemette, F., & del Giorgio, P. A. (2017). Modeling Allochthonous Dissolved Organic Carbon Mineralization Under Variable Hydrologic Regimes in Boreal Lakes. *Ecosystems*, *20*(4), 781–795. https://doi.org/10.1007/s10021-016-0057-0

Van Bellen, S., Garneau, M., Ali, A. A., Lamarre, A., Robert, É. C., Magnan, G., Asnong, H., & Pratte, S. (2013). Poor fen succession over ombrotrophic peat related to late Holocene increased surface wetness in subarctic Quebec, Canada. *Journal of Quaternary Science*, *28*(8), 748–760. https://doi.org/10.1002/jqs.2670

Virkkala, A. M., Aalto, J., Rogers, B. M., Tagesson, T., Treat, C. C., Natali, S. M., Watts, J. D., Potter, S., Lehtonen, A., Mauritz, M., Schuur, E. A. G., Kochendorfer, J., Zona, D., Oechel, W., Kobayashi, H., Humphreys, E., Goeckede, M., Iwata, H., Lafleur, P. M., … Luoto, M. (2021a). Statistical upscaling of ecosystem CO2 fluxes across the terrestrial tundra and boreal domain: Regional patterns and uncertainties. *Global Change Biology*, *27*(17), 4040–4059. https://doi.org/10.1111/gcb.15659

Virkkala, A. M., Aalto, J., Rogers, B. M., Tagesson, T., Treat, C. C., Natali, S. M., Watts, J. D., Potter, S., Lehtonen, A., Mauritz, M., Schuur, E. A. G., Kochendorfer, J., Zona, D., Oechel, W., Kobayashi, H., Humphreys, E., Goeckede, M., Iwata, H., Lafleur, P. M., … Luoto, M. (2021b). Statistical upscaling of ecosystem CO2 fluxes across the terrestrial tundra and boreal domain: Regional

patterns and uncertainties. *Global Change Biology*, *27*(17), 4040–4059. https://doi.org/10.1111/gcb.15659

Wang, F., Maberly, S. C., Wang, B., & Liang, X. (2018). Effects of dams on riverine biogeochemical cycling and ecology. *Inland Waters*, *8*(2), 130–140. https://doi.org/10.1080/20442041.2018.1469335

Webster, K. L., Bhatti, J. S., Thompson, D. K., Nelson, S. A., Shaw, C. H., Bona, K. A., Hayne, S. L., & Kurz, W. A. (2018). Spatially-integrated estimates of net ecosystem exchange and methane fluxes from Canadian peatlands. *Carbon Balance and Management*, *13*(1). https://doi.org/10.1186/s13021-018-0105-5

Yu, Z., Joos, F., Bauska, T.K. et al. No support for carbon storage of >1,000 GtC in northern peatlands. Nat. Geosci. 14, 465–467 (2021). https://doi.org/10.1038/s41561-021-00769-2

Appendix 3

Application of the G-res Tool to the Kettle Generating Station Reservoir (Stephens Lake)

Report on Data Inputs

This document describes the inputs used to apply the G-res Tool to the Kettle Reservoir (Stephens Lake) located in northern Manitoba.

1 Kettle Generating Station / Stephens Lake:



Figure 1-1 Kettle Generating Station Reservoir Forebay and Downstream Flow
Photo: B. Gill October 29, 2007

The Kettle Generating Station is a 1220 MW hydroelectric facility located at the former Kettle Rapids on the lower Nelson River (Figures 1-1 and 1-2), approximately 3 kilometers upstream of the Canadian National Railway crossing near the Town of Gillam (Manitoba Hydro, 2013). Construction of the generating station began in 1966 and was completed in 1974. The Kettle

Generating Station is Manitoba Hydro's second largest hydroelectric generating station, next to the Limestone Generating Station whose electricity generating capacity is 1350 MW.

The operating head, or waterfall created by the station, is approximately 30m. The discharge capacities of the generating station and spillway are 4,333 m^3/s and 8,349 m^3/s of water, respectively (Manitoba Hydro, 2013).

The reservoir, Stephens Lake, was created in 1971 by flooding the Nelson River and Moose Lake to the north. Flooding involved approximately 221 km^2 of land and 98 km^2 of water, for a total reservoir size of approximately 319 km^2 (Manitoba Hydro, 2015). The reservoir is located almost immediately downstream of the Keeyask Generating Station/reservoir. The water level on Stephens Lake is controlled by the Kettle Generating Station and operates between 139.2 m ASL and 141.1 m ASL at the 5^{th} and 95^{th} percentile, respectively (Keeyask Hydropower Limited Partnership, 2012a).

Stephens Lake can be roughly described as having a lotic environment in the south and a lentic environment in the north (Figure 1-3) (Keeyask Hydropower Limited Partnership, 2012b). The Nelson River thalweg is located in the south where the water quality is similar to that of the upstream and downstream portions of the Nelson River, prior to the creating the Keeyask reservoir (Keeyask Hydropower Limited Partnership, 2012b). The southern portion of Stephens Lake has higher concentrations of nutrients and oxygen (over winter) than the northern portion, and it does not stratify (Keeyask Hydropower Limited Partnership, 2012b). The northern portion can have low oxygen levels, become anoxic and may stratify near some shorelines and in some backbays over winter (Keeyask Hydropower Limited Partnership, 2012b). Some backbays may also stratify during the open water season during hot and very low wind conditions (Keeyask Hydropower Limited Partnership, 2012b). The western and northern portions of the reservoir comprise a large amount of flooded land.

Approximately 85% of the landcover is comprised of heterogeneous peatlands and approximately 78% of the landscape is underlain by extensive discontinuous and sporadic discontinuous permafrost (Keeyask Hydropower Limited Partnership, 2012a).

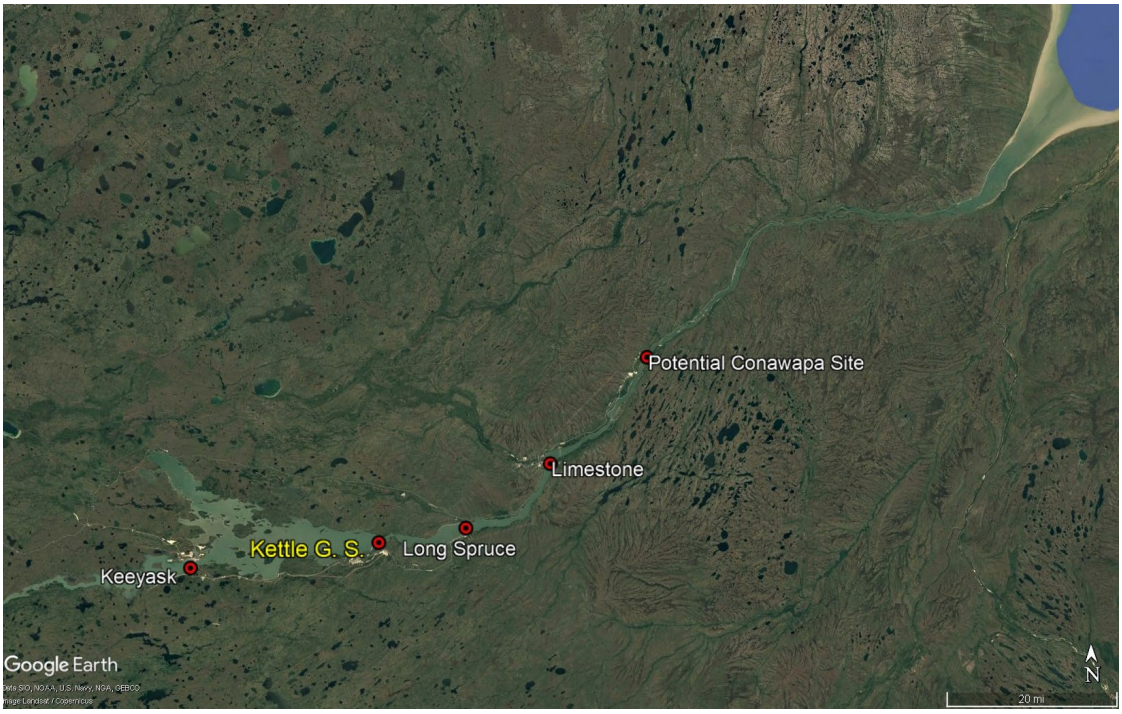
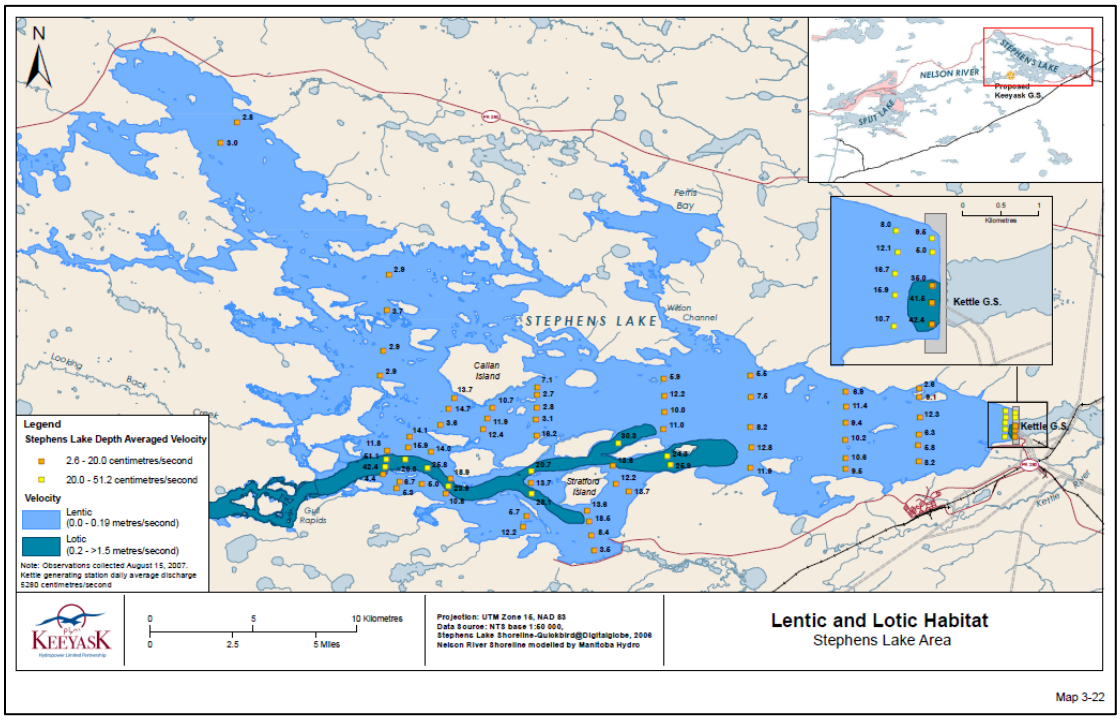


Figure 1-2 Kettle Generating Station

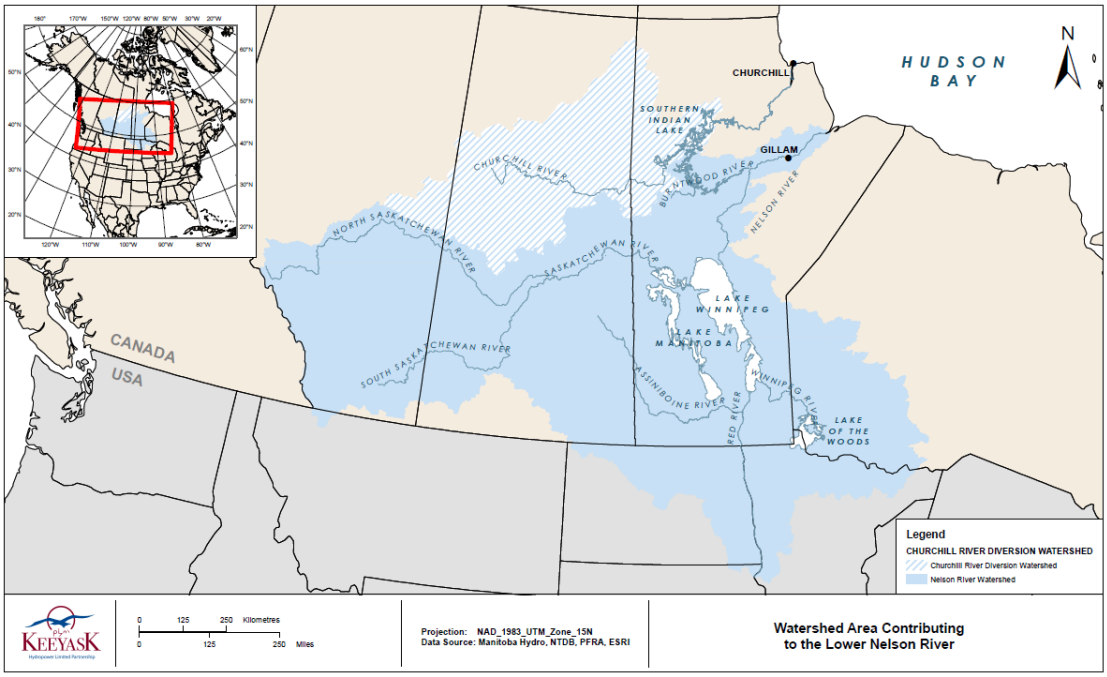


Source: Keeyask Hydropower Limited Partnership, 2012b

Figure 1-3 Stephens Lake: Lentic and Lotic Environments

2 G-res Tool "Catchment Data"

The Kettle Reservoir watershed area is illustrated below in Figure 2-1.



Source: Keeyask Hydropower Limited Partnership 2012a (Map 4.3-1)
Figure 2-1 Lower Nelson River Watershed

Model inputs pertaining to: Catchment Area, Population in the Catchment, and Catchment Annual Runoff were derived from the G-res Tool Earth Engine.

Community Wastewater Treatment was selected as being biological upstream of the Keeyask generating station. To be conservative, the release of phosphorus from community sewage and the release of phosphorus from industrial sewage were set to zero. Therefore, no portion of the reservoir GHG emissions will be assigned to another anthropogenic source other than the Kettle Generating Station/Stephens Lake Reservoir.

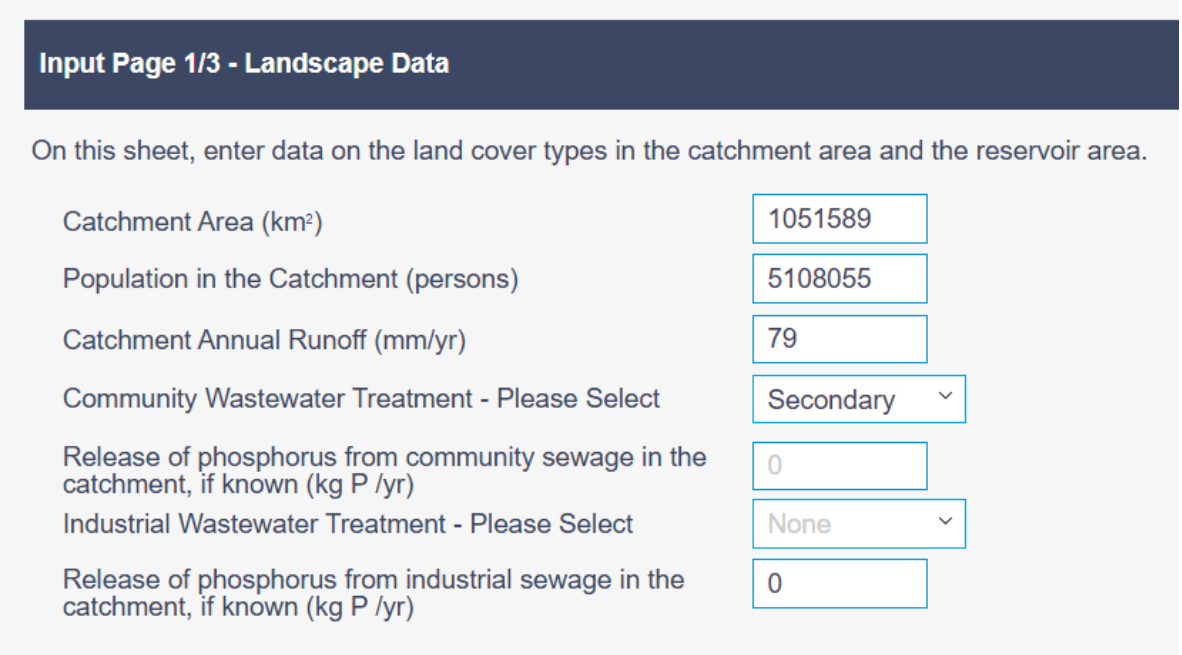


Figure 2-2 G-res Landscape Data Generated G-res Earth Engine

2.1 Land Cover in the Catchment Area

Land Cover in the Catchment Area inputs were derived from the G-res Tool Earth Engine. It is understood that these inputs will not be used in the G-res Tool calculations of pre-flood GHG emissions. Pre-flood GHG remissions will be calculated using the G-res Pre-Impoundment Land Cover in the Reservoir Area input sheet, which were derived from Kettle reservoir/Stephens Lake site-specific information, as described in Section 2.2 below.

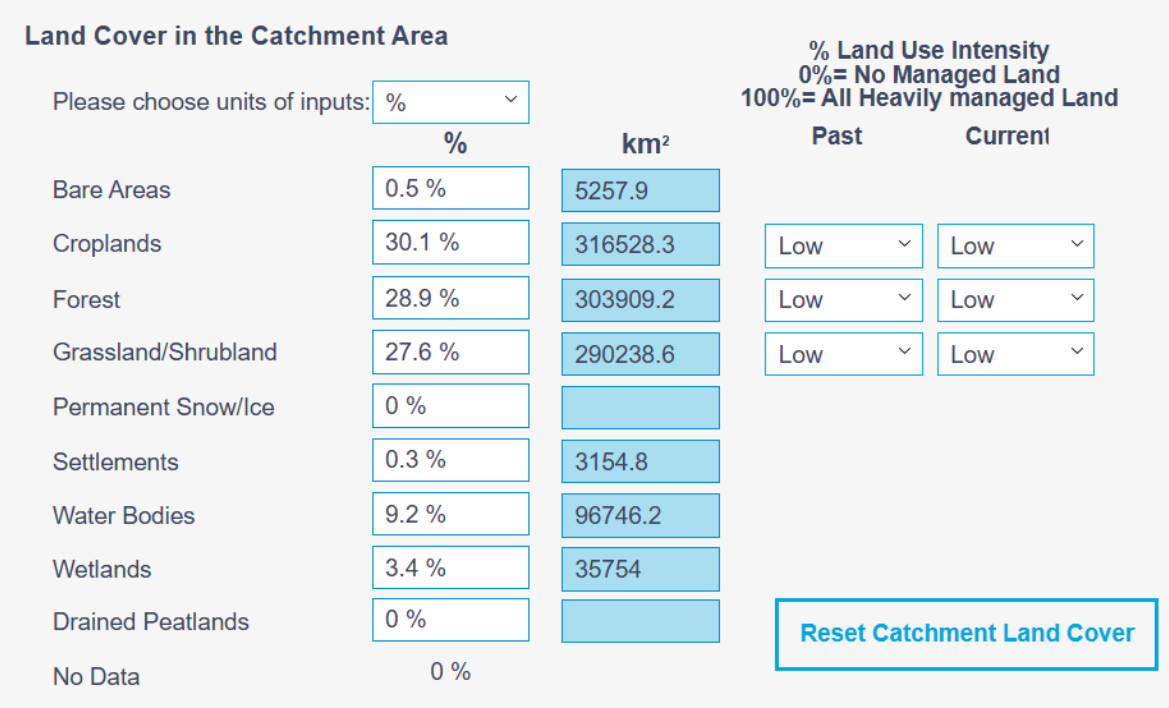


Figure 2-3 Landcover Data Generated by the Keeyask G-res Earth Engine

2.2 Pre-Impoundment Land Cover in the Reservoir Area

Pre-Impoundment Land Cover in the Reservoir Area inputs were derived from the following sources:

2.2.1 Reservoir Area (km2)

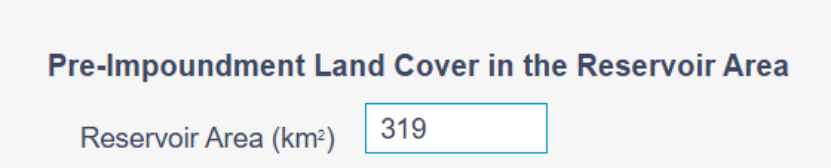


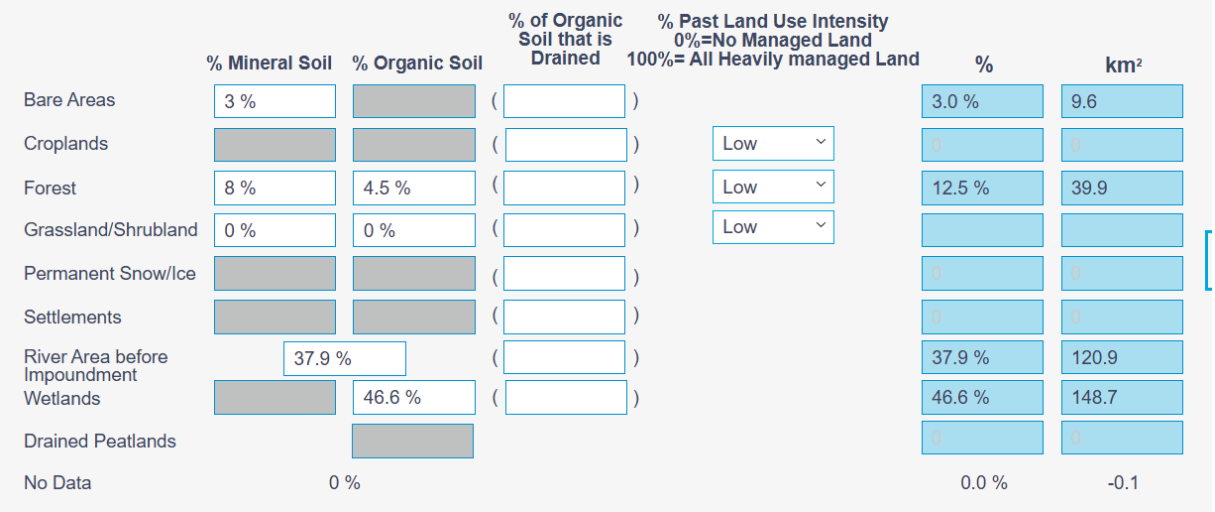
Figure 2-4 Total Kettle Reservoir Area (km^2)

The Kettle reservoir comprises approximately 221 km^2 of flooded land and 98.0 km^2 of existing aquatic systems for a total area of 319 km^2 (Manitoba Hydro, 2015).

2.2.2 Pre-Impoundment Land Cover in the Reservoir Area

2.2.2.1 Input Values

The input values used are as follows:



	% Mineral Soil	% Organic Soil	% of Organic Soil that is Drained	% Past Land Use Intensity 0%=No Managed Land 100%= All Heavily managed Land	%	km²
Bare Areas	3 %				3.0 %	9.6
Croplands				Low	0	0
Forest	8 %	4.5 %		Low	12.5 %	39.9
Grassland/Shrubland	0 %	0 %		Low		
Permanent Snow/Ice					0	0
Settlements					0	0
River Area before Impoundment	37.9 %				37.9 %	120.9
Wetlands		46.6 %			46.6 %	148.7
Drained Peatlands					0	0
No Data	0 %				0.0 %	-0.1

Figure 2-5 Kettle Reservoir Pre-Impoundment Landcover Data

2.2.2.2 Overview of Pre-Impoundment Land Cover in the Reservoir Area

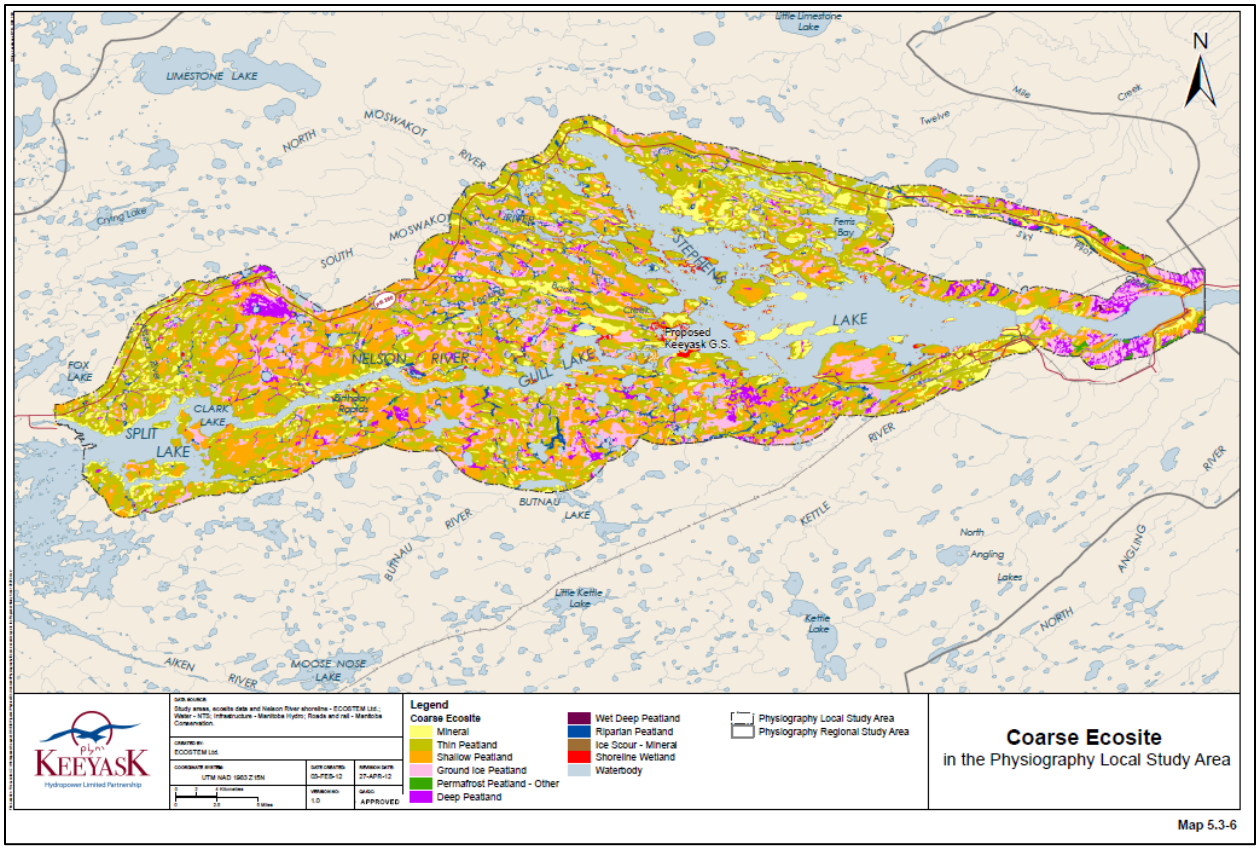
The pre-flood landcover classification that was used for the Keeyask G-res Model, “Keeyask Ecological Land Classification” was applied to the pre-flood Kettle landcover. The Keeyask Ecological Land Classification is described in thesis Chapter 3 and Appendix 1. The Keeyask Environmental Impact Assessment provided a detailed description of the Keeyask Local Study Area (Figure 2-6) which included the landcover of the pre-flood Keeyask reservoir footprint and the area surrounding Stephens Lake (Keeyask Hydropower Limited Partnership, 2012a). This information was used in the absence of detailed pre-flood land cover data for the Kettle reservoir. The Keeyask pre-flood land cover categories were apportioned to the pre-flood Kettle reservoir (Table 2-1).

Table 2-1 Kettle Pre-Flood Land Cover Derived from Keeyask Pre-Flood Land Cover "Ecological Land Classification"

Keeyask Pre-Flood ECO LandClass Applied to Pre-Flood Kettle Reservoir Terrestrial Land

Landcover	Soil Type	Pre-Flood Terrestrial Area m^2	% of Keeyask Pre-Flood Land	Apply to Pre-Flood Kettle Reservoir Land [(1)] 69.3%
Forest	Mineral	5,297,344.18	11.5%	8.0%
Forest	Organic	3,018,704.20	6.5%	4.5%
Wetlands	Organic			46.6%
	Bog	27,596,341.24	59.9%	41.5%
	Fen	926,959.14	2.0%	1.4%
	Marsh	239,536.09	0.5%	0.4%
	Swamp	2,097,416.86	4.6%	3.2%
	Riparian	126,928.33	0.3%	0.2%
Aquatic (allocate to pre-flood aquatic = River area Before Impoundment)				7.2%
	Lake	4,567,784.98	9.9%	6.9%
	Aquatic Veg	200,326.79	0.4%	0.3%
None		1,837,796.26	4.0%	2.8%
None		186,504.34	0.4%	0.3%
		46,095,642.41	**100.0%**	**69.3%**

(1) Pre-Flood Land = 69.3% of Total Kettle Reservoir
[98 km^2 (pre-flood land) / 331 km^2 (total reservoir) = 69.3%]



Source: Keeyask Hydropower Limited Partnership, 2012a

Figure 2-6 Keeyask Environmental Impact Assessment Local Study Area Land Cover Classification

The Kettle reservoir pre-flood terrestrial land cover and aquatic area were derived as follows for the G-res Kettle Reservoir Model (Table 2-2).

Table 2-2 Kettle Reservoir G-res Model Landcover Classification

Pre-Impoundment Land Cover in the Kettle Reservoir Area
Adaptation of Keeyask Ecological Land Classification

	% Mineral Soil	% Organic Soil	% Total
Croplands			
Bare Areas	3.0%		3.0%
Wetlands		46.6%	46.6%
Forest	8.0%	4.5%	12.5%
Grassland/Shrubland			
Permanent Snow/Ice			
Settlements			
Total Terrestrial			**62.1%**
Water Bodies on Land			7.2%
Total			**69.3%**

2.2.1 Replacement of G-res Tool Generic Emission Factors

Default G-res Tool pre-flood CO_2 and CH_4 emission factors for "Forest", "Grassland/Shrubland", and "Wetlands" were replaced by CO_2 emission factors developed by Virkkala et al. (2021) and by CH4 emission factors adopted from Kuhn et al. (2021) and Treat et al. (2018). The default G-res Tool pre-flood emission factors for "Water Bodies" were replaced by in-situ measurements of CH_4 diffusive emissions of Gull Lake and associated backbays conducted by Environnement Illimité inc. during 2009 – 2013 (Marchand et al., 2015). The development of these emission factors is summarized below. Details are described in thesis Chapter 3 and in Appendix 1.

2.2.1.1 CO_2 Terrestrial Emission Factors

Annual CO_2 emission factors (Net Ecosystem Exchange) for the Boreal Upland and Boreal Wetland were selected from Virkkala et al., (2021). They were based on a study period of 1990-

2015 (Table 2-3). Virkkala et al. (2021) did not develop separate emission factors for mineral and organic soils. These emission factors were used as composite emission factors for both mineral and organic soils in the Keeyask G-res model. The Virkkala et al. (2021) Boreal Upland CO_2 emission factors were used for the G-res categories of Forest and Grassland/Shrubland, and the Boreal Wetland CO_2 emission factors were used for the G-res Wetland category.

Table 2-3 CO_2 Emission Factors Used for the Kettle Reservoir G-res Model

CO_2 Emission Factors for Ecological Land Classification		
Land Class	**Annual NEE g CO_2-C/m^{-2}/yr**	**Annual NEE t CO_2-C/ha/yr (Converted for G-res)**
Boreal Uplands (Forest, and Grassland/Shrubland)	-47	-0.47
Boreal Wetlands	-38	-0.38
Source: Virkakkala et al., 2021 (Table 1)		

2.2.1.2 CH_4 Terrestrial Emission Factors

CH_4 emission factors were adapted from the Boreal–Arctic Wetland and Lake Methane Dataset (BAWLD-CH4) (Kuhn et al., 2021).

Growing season CH_4 terrestrial emission factors were adopted from Kuhn et al. (2021) Table 3 median values for Boreal Forest, Permafrost Bog, Bog, Fen, and Marsh land classes. Non-growing season emission factors were not included in the BAWLD-CH4 database/Kuhn et al. (2021) study. They were therefore estimated as being 16% of total annual emissions according to Treat et al. (2018). The Keeyask Ecological Land Classifications of “Swamps” and “Riparian” were assigned the same emissions factors as the BAWLD-CH4 emission factors for bogs and fens, respectively, following descriptions by Kuhn et al. (2021).

A composite wetland emission factor was developed by developing a weighted average for the land classifications of Permafrost Bog, Bog, Fen, Marsh, and Peatland Lakes (small and

medium). This involved multiplying each [wetland class] by their [CH_4 emission factor], by their [areal extent (km^2) as defined by the Keeyask Ecological Land Classification, and by summing these calculations. The results are displayed in Table 2-4.

Table 2-4 Composite CH4 Emission Factors Used for the Kettle Reservoir G-res Model

Land Class	**Annual Emissions kg CH_4/ha/yr (G-res Emission Factor Metrics)**
Boreal Uplands (Forest, and Grassland/Shrubland)	-0.64
Boreal Wetlands	51.13

2.2.1.3 Pre-flood Aquatic GHG Emission Factors

The G-res default pre-flood CH_4 emission factor for "Water Bodies" is 4.4 kg CH_4/ha/yr, which is applied to the river/lake to be flooded. This emission factor would not be applied to the peatland pools or other water bodies within the terrestrial landscape (uplands) to be flooded. Alternatively, for Keeyask modelling, the G-res default emission factor was replaced by the pre-flood flux of 5 mg CH_4/m^2/yr which translates into 9.25 kg CH_4/ha/yr. This emission factor was derived by Environnement Illimité inc. from their in-situ measurements of CH_4 diffusive emissions from Gull Lake and associated backbays during 2009 – 2013 (Marchand et al., 2015).

G-res does not include pre-flood CO_2 emission factors for water bodies.

Pre-Flood Emission Factors used in the Kettle Reservoir G-res Model

Table 2-5 illustrates the pre-flood emission factors used in the Kettle Reservoir G-res Model. The site-specific emission factors developed for "Forest", "Grassland/Shrubland", "Wetlands" and "Water Bodies" are highlighted.

Table 2-5 Kettle Reservoir G-res Model Pre-Flood Emission Factors

Climate: Boreal

	CH_4 Emission Factor (kg CH4/ha/yr)		CO_2 Emission Factor (t CO2-C/ha/yr)	
	Mineral Soil	Organic Soil	Mineral Soil	Organic Soil
Cropland	0	0	0	7.9
Bare Areas	0	6.1	0	2.8
Wetlands	51.13	51.13	-0.38	-0.38
Forest	-0.64	-0.64	-0.47	-0.47
Grassland/Shrubland	-0.64	-0.64	-0.47	-0.47
Urban Areas	0	19.6	0	6.4
Water Bodies	9.3			
Drained Peatlands				

2.2.3 Determine River Area Before Impoundment

River Area before Impoundment	37.9 %

Figure 2-7 Kettle G-res Model River Area Before Impoundment

The River Area before Impoundment was calculated as:

Pre-existing river area to be Flooded (98 km^2) / Total Reservoir Area (319 km^2) = 30.7%.

Plus, pre-existing water bodies on land to be flooded = 7.2%

Total "River Area before Impoundment" = 37.9%

3 Reservoir Data

3.1 Input Values

The input values used are as follows:

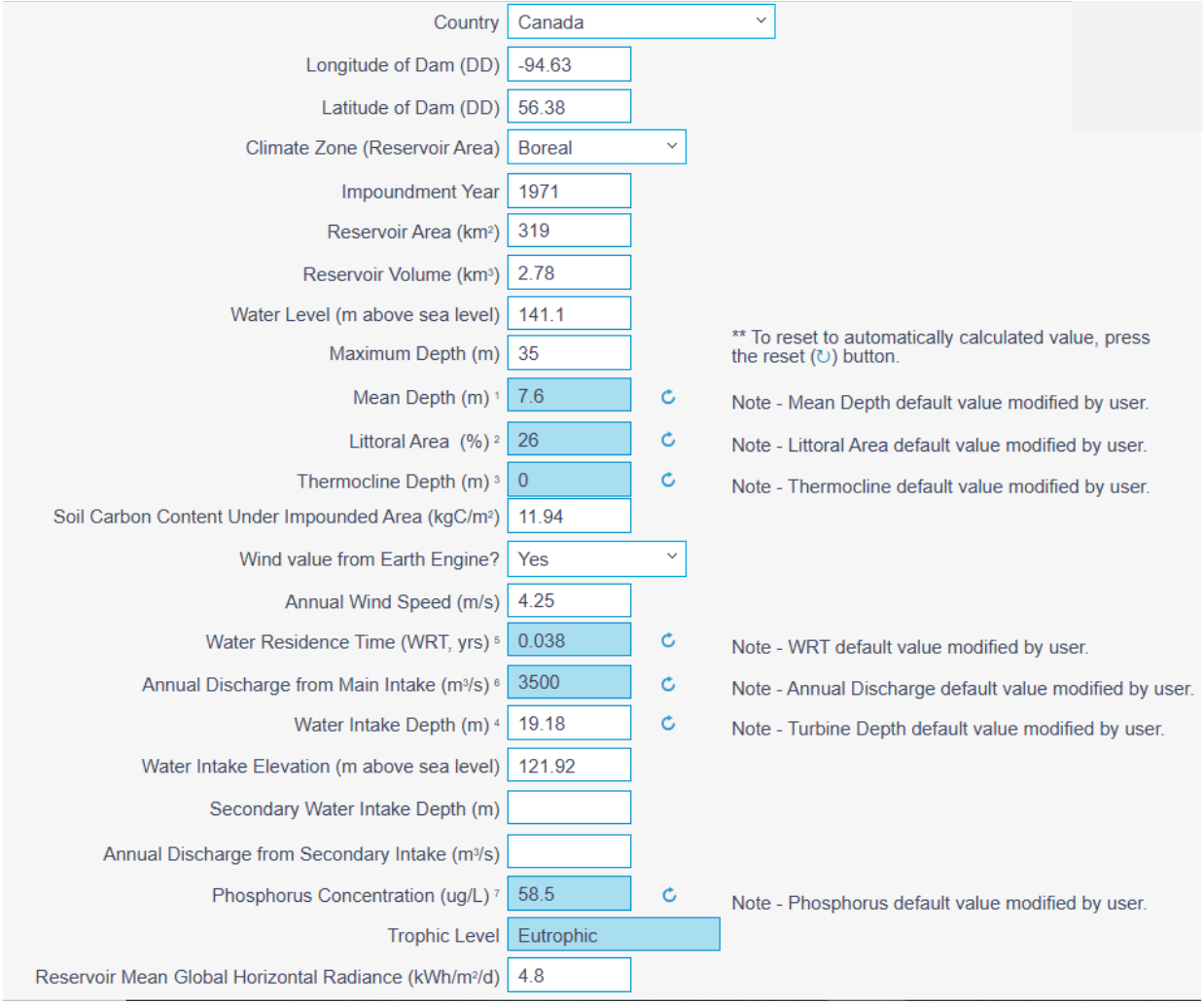


Figure 3-1 Kettle G-res Model: Reservoir Data

Longitude and Latitude:
The Longitude (-94.63 W) and Latitude (56.38 N) of the Dam refer to the location of the Kettle Generating Station.

Climate Zone:
The Keeyask Reservoir is located within the **Boreal Shield Ecozone** (Government of Canada, 2013).

Impoundment Year: 1971
Reservoir impoundment (flooding) occurred during 1971 (Manitoba Hydro, 2015).

Reservoir Area (km^2): 319 km^2
The Kettle Reservoir comprises approximately 221 km^2 of flooded land and 98 km^2 of existing aquatic systems for a total area of 319 km^2 (Manitoba Hydro, 2015).

Reservoir Volume (km^3): 2.78 km^3
The estimated reservoir volume of the Kettle Reservoir is 2.78 km^2 (Keeyask Hydropower Limited Partnership, 2012b Table 2E-1).

Water Level (m above sea level): 141.1 m above sea level

The water level on Stephens Lake is controlled by the Kettle Generating Station and operates between 139.2 m ASL and 141.1 m ASL at the 5^{th} and 95^{th} percentile, respectively (Keeyask Hydropower Limited Partnership, 2012a).

The Maximum Licence Forebay Elevation is 141.12 m ASL (Manitoba Hydro, 2022).

Maximum Depth (m): 35 m
The maximum depth of the reservoir is 35 m at 139.13 m above sea level (Keeyask Hydropower Limited Partnership, 2012b Table 2E-1).

Mean Depth (m): 3.6 m
The mean depth of the reservoir is 3.6 m at 139.13 m above sea level (Keeyask Hydropower Limited Partnership, 2012b Table 2E-1).

Littoral Area (%): 26%
In lieu of site-specific data on the extent of the littoral zone for Stephens Lake, the Keeyask reservoir was used as a surrogate for the Kettle reservoir since the terrain of the two reservoirs are similar, as are the maximum and average depths of the reservoirs.

Thermocline Depth (m): 0
The thermocline depth was set as 0 m. The southern portion of Stephens Lake does not stratify (Keeyask Hydropower Limited Partnership, 2012b). The northern portion may stratify near some shorelines and in some backbays over winter (Keeyask Hydropower Limited Partnership, 2012b). Some backbays may also stratify temporarily during the open water season during unusually hot and very low wind conditions (Keeyask Hydropower Limited Partnership, 2012b).

Soil Carbon Content Under the Impoundment Area (kg C/m^2): 11.94 kg C/m^2
The value of 11.94 kg C/m^2 was derived from the Earth Engine functionality of the G-res Tool. For comparison, this value aligns well with IPCC 2019 default value of 11.6 ±65% kg C/m^2 for the soil organic carbon stock content for Boreal Moist/Dry wetland soils for 0-30 cm depth (IPCC 2019, Table 2.3).

This value is also similar to the average carbon content of 10.8 kg C/m^2 in peat-forming soils at a depth of 0-30 cm in a boreal forest site located south of James Bay (Magnan et al., 2020). Similarly, Beaulne et al. (2021) calculated that between 11.0 – 12.6 kg C/m^2 has been stored in the organic horizons of a boreal peatland site in eastern Canada over the last 200 years.

Annual Wind Speed: 4.25 m/s

The value of 4.25 m/s was derived from the Earth Engine functionality of the G-res Tool.

This value is within the range of average wind speeds of 3.89 m/s to 4.94 m/s recorded in Gillam, Manitoba from 1971 to 2000 (Keeyask Hydropower Limited Partnership, 2012a). The meteorological station in Gillam is located approximately 30 km east of the Keeyask Generating Station/Reservoir (Keeyask Hydropower Limited Partnership, 2012a).

Water Residence Time (WRT, yrs): 0.038 yrs

The Water Residence Time for Stephens Lake was estimated to range from 5.61 days to 35.08 days, with a mean of 14.03 days (Hesslein and Cooley, 2016). The mean of 14.03 days (0.038 years) was used for the model.

Annual Discharge from Main Intake (m^3/s): 3,500 m^3/s

The average annual discharge is approximately 3,500 m^3/s. This value is based on the annual average water discharge rate at the Manitoba Hydro water gauge (05UF006) located on the Nelson River at the Kettle Generating Station for the years 1987 to 2023. This is the time period where data is available for this station at the Environment Canada Water Office website: https://wateroffice.ec.gc.ca/search/historical_e.html

Water Intake Depth (m): 19.18 m

The height and depth of the water intake structures are such that the Water Intake Depth is between 19.2 m to 37.2 m below the reservoir water surface. This spans approximately 18 m or 48% of the entire water column of the reservoir (Manitoba Hydro, 2022).

Water Intake Elevation (m above sea level):

The elevation of the top and bottom of the Water Intake are 121.92 m ASL and 103.94 m ASL, respectively (Manitoba Hydro, 2022). 121.92 m ASL was entered for the G-res Kettle model.

Phosphorus Concentration (µg/L): 58.5 µg/L

Total Phosphorus concentration in the main stem of the Nelson River ranged from 30.0 to 40.0 µg/L during pre-flood sampling from 1997 to 2006 (Keeyask Hydropower Limited Partnership 2012c). Based on Total Phosphorus concentrations, the main stem of the Nelson River is classified as meso-eutrophic to eutrophic (Keeyask Hydropower Limited Partnership, 2012b). Based on Keeyask environmental impact assessment measurements, small tributaries were classified as oligotrophic and large tributaries were classified as mesotrophic (Keeyask Hydropower Limited Partnership, 2012b).

Based on chlorophyll *a* concentrations, the mainstem is classified as mesotrophic (Keeyask Hydropower Limited Partnership, 2012b).

To be conservative, the Keeyask Aquatic Effects Monitoring Plan benchmark of 58.5 µg/L was used in the G-res Kettle model.

Total Phosphorus concentrations are measured monthly from June – September and in March, in the upstream (Near Field) and downstream (Far Field) portions of Stephens Lake as part of the Keeyask Aquatic Effects Monitoring Plan. Concentrations are typically highest in March, under ice cover, and typically do not exceed the Benchmark (Hnatiuk Stewart and Hrenchuck 2025; Dowd and Hrenchuck, 2023, 2024)

Trophic Level: Eutrophic

Total phosphorus concentrations measured in the Stephens Lake main stem from 2001 to 2004 were 37 µg/L, 34 µg/L and 36 µg/L at locations STL1, STL2 and GT1, respectively (Keeyask Hydropower Limited Partnership, 2012b). Total phosphorus concentrations measured 16 µg/L at location ScL3 in the north arm during 2004 (Keeyask Hydropower Limited Partnership, 2012b). The main stem and the north channel are classified as mesotrophic using chlorophyll *a* concentrations as the means for categorizing Trophic Level (Keeyask Hydropower Limited Partnership, 2012b).

Based on Total Phosphorus concentrations, the main stem of the Nelson River is classified as meso-eutrophic to eutrophic (Keeyask Hydropower Limited Partnership, 2012b).

So as not to underestimate GHG emissions, Stephens Lake was classified as eutrophic for the G-res Kettle Model.

Reservoir Mean Global Horizontal Radiance (kWh/m^2/d): 4.8

The Reservoir Mean Global Horizontal Radiance value of 4.8 kWh/m^2/d was generated by the G-res Tool Earth Engine.

For comparison, the on-line, interactive Photovoltaic Potential and Solar Resource Maps of Canada estimates mean annual global insolation values of 3.19 kWh/m^2/d and 3.18 kWh/m^2/d for the Community of Split Lake and the Town of Gillam, Manitoba respectively (Natural Resources Canada, 2020). The estimates are based on horizontal 0-degree orientation on a 60 arc seconds (approximately 2 km grid). Split Lake is located approximately 20 km upstream of the Keeyask Reservoir, and Gillam is located approximately 30 km downstream of the Keeyask Reservoir.

To be conservative, the elevated value of 4.8 kWh/m^2/d was used in the G-res Tool modeled estimates.

Mean Temperature per Month (°C)

Mean Temperature per Month and Mean Annual Air Temperature data were derived by the G-res Tool Earth Engine.

Mean Temperature per Month (°C)	
January	-25.6
February	-22.16
March	-15.37
April	-4.37
May	4.58
June	11.13
July	15.23
August	13.61
September	6.8
October	-0.1
November	-11.84
December	-22.62
Mean Annual Air Temperature (°C)	-4.2

Figure 3-2 Mean Average Monthly Temperatures

4 Reservoir Services Data

100% of the Reservoir Services were allocated to the Keeyask Reservoir/hydroelectricity.

Allocation of Reservoir Purposes		Percentage Allocation
Flood Control		0
Fisheries		0
Irrigation		0
Navigation		0
Environmental Flow		0
Recreation		0
Water Supply		0
Hydroelectricity	Primary	100

Please provide, if available, the following information on your Hydropower system:

Installed Capacity (MW)	1220
Total Annual Generation (GWh/yr)	7430

Figure 4-1 Kettle G-res Model: Reservoir Services

5 Construction GHG

The G-res Tool was not used to estimate Construction Emissions.

6 Unrelated Anthropogenic Sources Emissions

Since 100% of the purpose of the Keeyask Reservoir is assigned to hydroelectricity, no GHG emissions were allocated to Unrelated Anthropogenic Sources.

Estimated Contribution of UAS to the GHG Emissions from the Reservoir

Calculated CH4 emissions from the reservoir ($gCO_2e/m^2/yr$)	56.4
Amount of CH4 of total estimates due to UAS (%)	**0 %**
Estimated CH4 release dut to UAS ($gCO_2e/m^2/yr$)	

Figure 6-1 Kettle G-res Model: Contribution of Unrelated Anthropogenic Sources of GHG Emissions

References

Beaulne, J., Garneau, M., Magnan, G., Boucher, É. (2021). Peat deposits store more carbon than trees in forested peatlands of the boreal biome. Sci Rep 11, 2657. https://doi.org/10.1038/s41598-021-82004-x

Dowd, M.B and C.L. Hrenchuck. (2023). Results of water quality monitoring in the Nelson River, 2022: Year 1 Operation. Keeyask Generation Project Aquatic Effects Monitoring Plan Report. #AEMP-2023-13. A report prepared for Manitoba Hydro by North/South Consultants Inc,. June 2023. xv +295 pages.

Dowd, M.B and C.L. Hrenchuck. (2024). Results of water quality monitoring in the Nelson River, 2023: Year 2 Operation. Keeyask Generation Project Aquatic Effects Monitoring Plan Report. #AEMP-2024-11. A report prepared for Manitoba Hydro by North/South Consultants Inc,. June 2024. xvi +301 pages.

Government of Canada. (2013). National Ecological Framework for Canada. Ecozones, Ecoregions, and Ecodistricts.
https://sis.agr.gc.ca/cansis/publications/maps/eco/all/districts/eco_all_districts_1m_manitoba.jpg

Government of Canada. (2025). Monthly Discharge Data for Nelson River at Kettle Generating Station (05UF006) [MB].
https://wateroffice.ec.gc.ca/report/historical_e.html?stn=05UF006&dataType=Monthly&parameterType=Flow&year=2023&mode=Table&mean1=1&scal…

Hesslein, R., and Cooley, M. (2016). Status of Greenhouse Gas Emissions at Manitoba Hydro's Mature Reservoirs. Prepared for Manitoba Hydro by North/South Consultants Inc. Winnipeg, Manitoba. 68 pages.

Hnatiuk Stewart, S. and C.L. Hrenchuck. (2025). Results of water quality monitoring in the Nelson River, 2024: Year 3 Operation. Keeyask Generation Project Aquatic Effects Monitoring Plan Report. #AEMP-2025-09. A report prepared for Manitoba Hydro by North/South Consultants Inc,. June 2025. xvi +319 pages.

IPCC (2019). Chapter 2: Generic Methodologies Applicable to Multiple Land-Use Categories, Volume 4 Agriculture, Forestry and Other Land Use, 2019 Refinement to the 2006 IPCC Guidelines for National Greenhouse Gas Inventories, 104 pages.

Keeyask Hydropower Limited Partnership (2012a). Keeyask Generation Project: Environmental Impact Statement; Physical Environment Response to EIS Guidelines, Supporting Volume. 1018 pages.

Keeyask Hydropower Limited Partnership (2012b). Keeyask Generation Project: Environmental Impact Statement; Aquatic Environment Supporting Volume. 1745 pages.

Kuhn, M. A., Varner, R. K., Bastviken, D., Crill, P., Macintyre, S., Turetsky, M., Walter Anthony, K., McGuire, A. D., & Olefeldt, D. (2021). BAWLD-CH4: A comprehensive dataset of methane fluxes from boreal and arctic ecosystems. In *Earth System Science Data* (Vol. 13, Issue 11, pp. 5151–5189). Copernicus Publications. https://doi.org/10.5194/essd-13-5151-2021

Magnan, G., Garneau, M., Le Stum-Boivin, É., Grondin, P., and Yves Bergeron, Y. (2020). Long-Term Carbon Sequestration in Boreal Forested Peatlands in Eastern Canada. Ecosystems 23, 1481–1493. https://doi.org/10.1007/s10021-020-00483-x

Manitoba Hydro (2012). Historical Climate Analysis Technical Memorandum # GN-9.5.1 for the Keeyask Generation Project Stage IV Studies- Physical Environment, Water Resources Engineering Department, 40 pages.

Manitoba Hydro (2013). Kettle Generating Station. Public Affairs. Manitoba Hydro, Winnipeg, Manitoba.

Manitoba Hydro. (2015). Flooded Areas for Manitoba Hydro System. [Unpublished manuscript]. Manitoba Hydro, Winnipeg, Manitoba.

Manitoba Hydro (2022). Water Power Act Licences Kettle Generating Station Short Term Licence Extension Application Supporting Documentation. Prepared for: Manitoba Environment, Climate and Parks, 18 pages.

Marchand D., M. Demarty, and R. Gill. (2015). Keeyask Technical Summay – 2014. Summary prepared by Environnement Illimité for Manitoba Hydro, 11 p.

Natural Resources Canada (2020). Photovoltaic Potential and Solar Resource Maps of Canada. © Her Majesty the Queen in Right of Canada, as represented by the Minister of Natural Resources, 2020. https://fgp-pgf.maps.arcgis.com/apps/webappviewer/index.html?id=c91106a7d8c446a19dd1909fd93645d3

Treat, C. C., Bloom, A. A., & Marushchak, M. E. (2018). Nongrowing season methane emissions–a significant component of annual emissions across northern ecosystems. *Global Change Biology*, *24*(8), 3331–3343. https://doi.org/10.1111/gcb.14137

Virkkala, A. M., Aalto, J., Rogers, B. M., Tagesson, T., Treat, C. C., Natali, S. M., Watts, J. D., Potter, S., Lehtonen, A., Mauritz, M., Schuur, E. A. G., Kochendorfer, J., Zona, D., Oechel, W., Kobayashi, H., Humphreys, E., Goeckede, M., Iwata, H., Lafleur, P. M., … Luoto, M. (2021). Statistical upscaling of ecosystem CO2 fluxes across the terrestrial tundra and boreal domain: Regional patterns and uncertainties. *Global Change Biology*, *27*(17), 4040–4059. https://doi.org/10.1111/gcb.15659

Appendix 4

Application of the G-res Tool to the Long Spruce Generating Station Reservoir

Report on Data Inputs

This document describes the inputs used to apply the G-res Tool to the Long Spruce Reservoir located in northern Manitoba.

1 Long Spruce Generating Station:



Source: B. Gill October 29, 2007
Figure 1-1 Long Spruce Generating Station

The Long Spruce Generating Station is a 980 MW hydroelectric facility located at the former Long Spruce Rapids on the lower Nelson River (Figures 1-1 and 1-2) (Manitoba and Manitoba Hydro, 2015). The station is located approximately 16 km downstream of the Kettle Generating

Station and 23 km upstream of the Limestone Generating Station (Manitoba and Manitoba Hydro, 2015). Provincial Road 280 crosses the Nelson River at the generation station. Construction of the generating station began in 1971 and was completed in 1979.

The operating head, or waterfall created by the station, is approximately 24.4 m (Manitoba and Manitoba Hydro, 2015). The discharge capacities of the generating station and spillway are 4,528 m^3/s and 9,700 m^3/s of water, respectively (Manitoba and Manitoba Hydro, 2015).

The Long Spruce reservoir flooded approximately 14.5 km^2 of land and 15.9 km^2 of water, for a total reservoir size of approximately 30.4 km^2 (Manitoba Hydro, 2015b). The reservoir is located downstream of the Kettle Generating Station and is contained almost entirely within the natural banks of the Nelson River (Manitoba Hydro, 2014) with the assistance of approximately 13 km of dykes (Manitoba and Manitoba Hydro, 2015). The reservoir is operated as a run of the river reservoir where the water levels are controlled by the discharges of the Kettle Generating Station (Manitoba and Manitoba Hydro, 2014). The water level on the reservoir generally operates just below 110.0 m ASL in the open water period and just below 110.3 m ASL during the winter, and is positioned above 109.4 ASL in the forebay approximately 95% of the time (Manitoba and Manitoba Hydro, 2014).

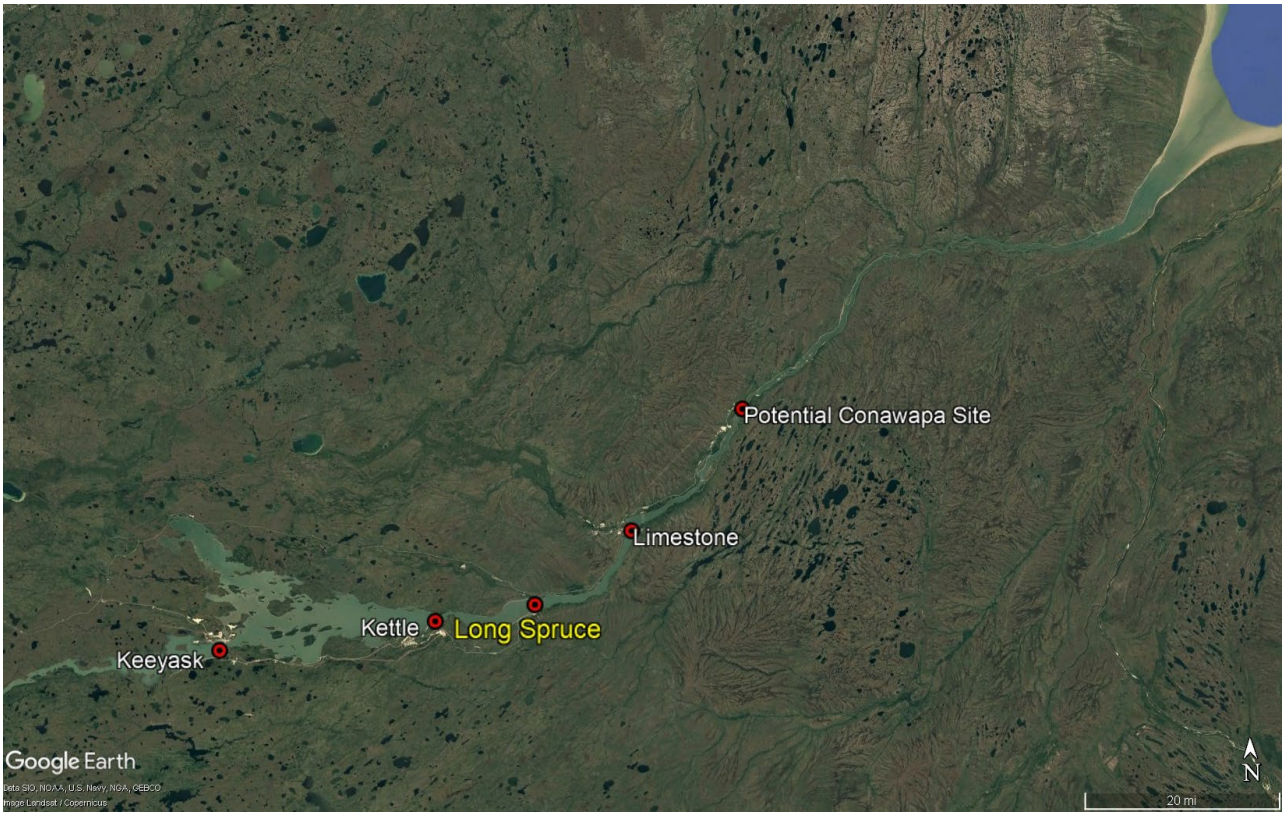
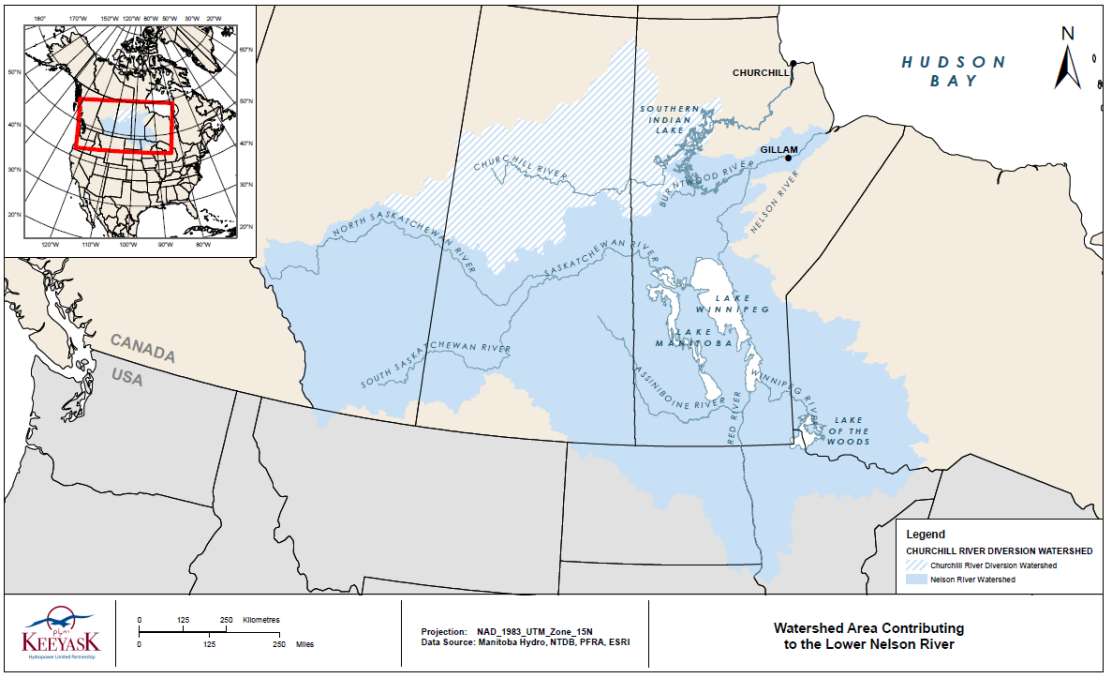


Figure 1-2 Long Spruce Generating Station

2 G-res Tool "Catchment Data"

The Long Spruce Reservoir watershed area is illustrated below in Figure 2-1.



Source: Keeyask Hydropower Limited Partnership 2012a (Map 4.3-1)
Figure 2-1 Lower Nelson River Watershed

Model inputs pertaining to: Catchment Area, Population in the Catchment, and Catchment Annual Runoff were derived from the G-res Tool Earth Engine.

So as not to underestimate reservoir GHG emissions by assigning a portion to wastewater and sewage treatment, the release of phosphorus from community sewage and the release of phosphorus from industrial sewage were set to zero. Therefore, no portion of the reservoir GHG emissions were assigned to another anthropogenic source other than the Long Spruce Reservoir.

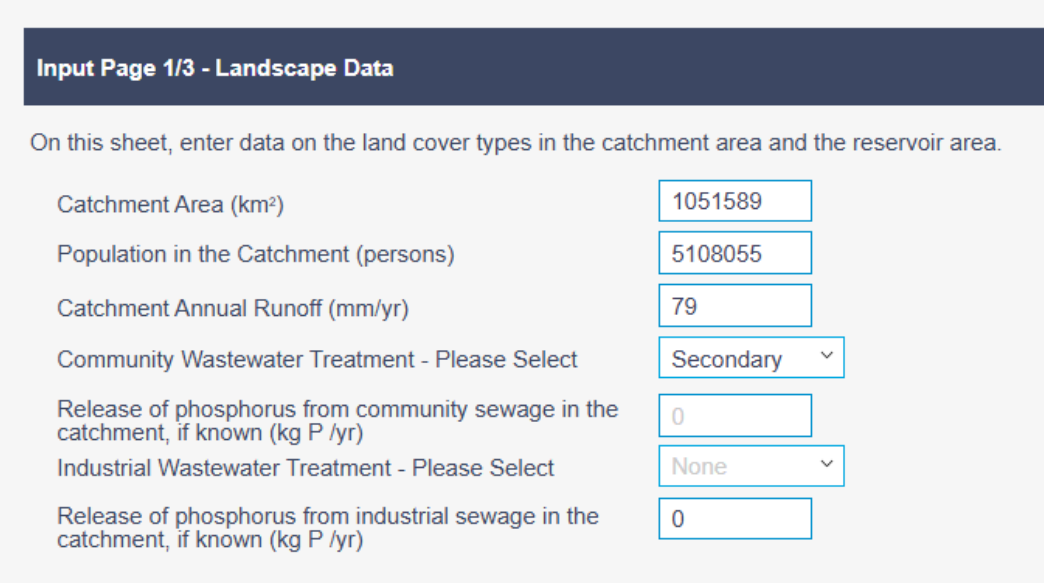


Figure 2-2 G-res Landscape Data Generated by G-res Earth Engine

2.1 Land Cover in the Catchment Area

Land Cover in the Catchment Area inputs were derived from the G-res Tool Earth Engine. It is understood that these inputs will not be used in the G-res Tool calculations of pre-flood GHG emissions. Pre-flood GHG remissions will be calculated using the G-res Pre-Impoundment Land Cover in the Reservoir Area input sheet, which were derived from Long Spruce reservoir site-specific information, as described in Section 2.2 below.

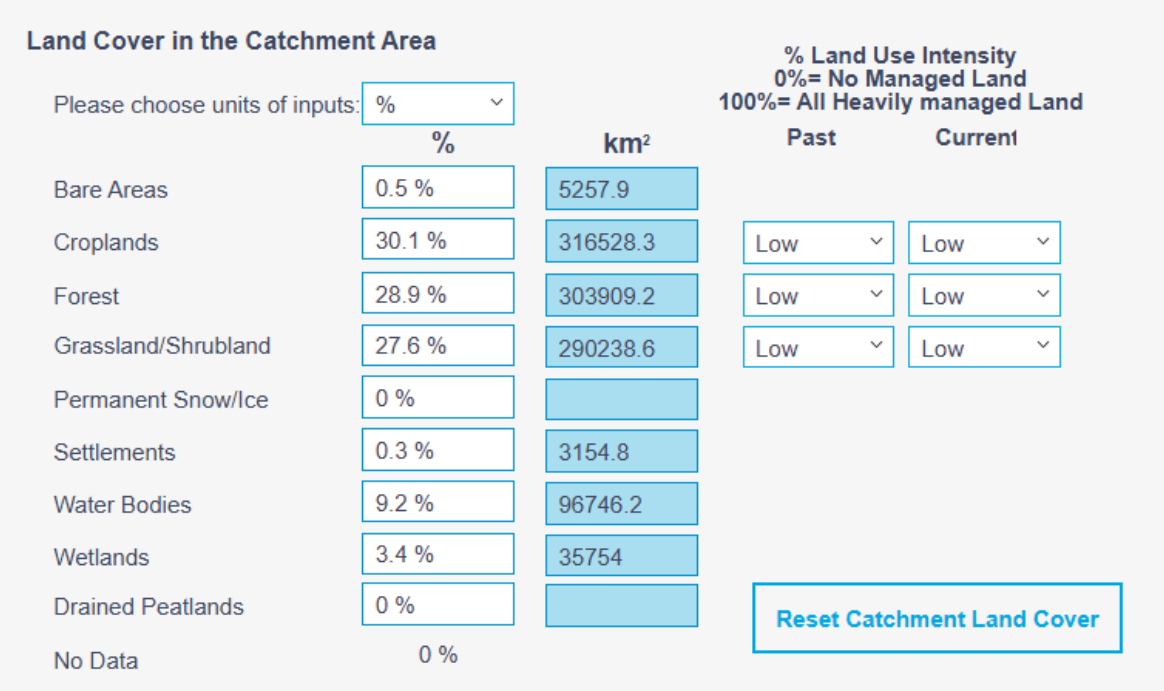


Figure 2-3 Landcover Data Generated by the Long Spruce G-res Earth Engine

2.2 Pre-Impoundment Land Cover in the Reservoir Area

Pre-Impoundment Land Cover in the Reservoir Area inputs were derived from the following sources:

2.2.1 Reservoir Area (km2)



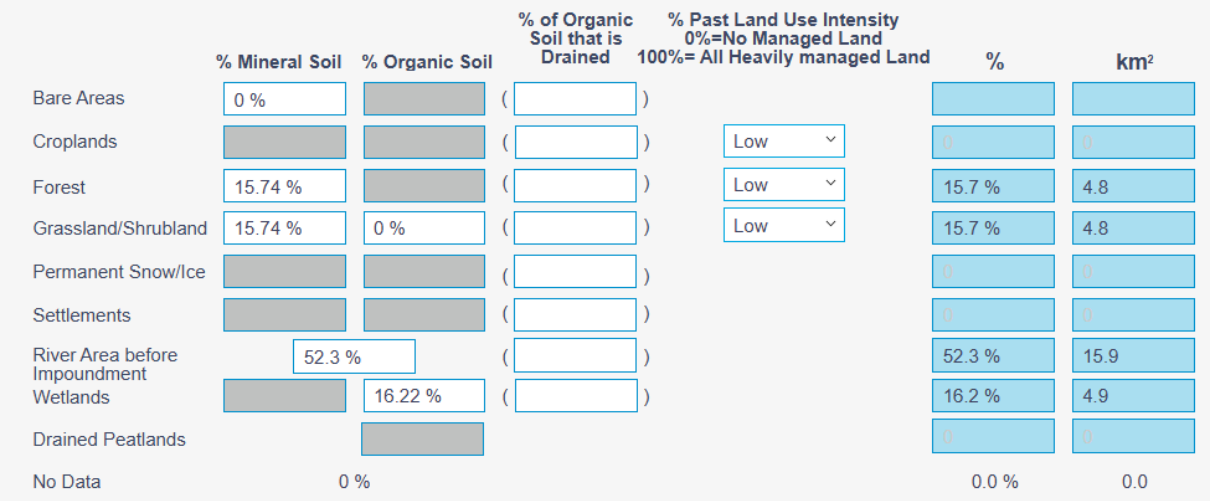
Figure 2-4 Total Long Spruce Reservoir Area (km^2)

The Long Spruce reservoir comprises approximately 14.5 km^2 of flooded land and 15.9 km^2 of existing aquatic systems for a total area of 30.4 km^2 (Manitoba Hydro, 2015b).

2.2.2 Pre-Impoundment Land Cover in the Reservoir Area

2.2.2.1 Input Values

The input values used are as follows:



	% Mineral Soil	% Organic Soil	% of Organic Soil that is Drained	% Past Land Use Intensity 0%=No Managed Land 100%= All Heavily managed Land	%	km²
Bare Areas	0 %					
Croplands				Low	0	0
Forest	15.74 %			Low	15.7 %	4.8
Grassland/Shrubland	15.74 %	0 %		Low	15.7 %	4.8
Permanent Snow/Ice					0	0
Settlements					0	0
River Area before Impoundment	52.3 %				52.3 %	15.9
Wetlands		16.22 %			16.2 %	4.9
Drained Peatlands					0	0
No Data	0 %				0.0 %	0.0

Figure 2-5 Long Spruce Reservoir Pre-Impoundment Landcover Data

2.2.2.2 Overview of Pre-Impoundment Land Cover in the Reservoir Area

The Long Spruce reservoir is located almost entirely within the natural banks of the Nelson River (Manitoba and Manitoba Hydro, 2014). The Regional Cumulative Effects Study (Manitoba and Manitoba Hydro, 2014) describes the Nelson River reach between the Kettle and Limestone Generating Stations as:

- Having the highest banks of the Nelson River
- Approximately 80% of this river reach is comprised of ice-scoured till banks
    - Vegetation below the winter trim line is comprised of grasses and stunted willows
    - Vegetation above the winter trim line includes closed forest of white and black spruce
    - Bedrock is often observed at the open water shoreline
- The remaining 20% is composed of slumping overburden.
    - The bottom half is often steep and bare

Below are illustrations of the current Long Spruce reservoir shoreline (Figures 2-6 & 2-7), a stretch of grass and shrub shoreline within the Limestone reservoir (Figure 2-8), and

illustrations of the steep banks of the Nelson River and bare shorelines upstream of the potential Conawapa site (Figures 2-9 to 2-11). Figures 2-7 to 2-11 may provide an indication of the pre-flood landcover of the Long Spruce reservoir, which was contained mostly within the natural banks of the Nelson River.

In the absence of detailed pre-flood landcover data for the Long Spruce reservoir, the above information was used to estimate the pre-flood land cover categories for the Long Spruce G-res model. Approximately 1/3 of the pre-flood landscape was allocated to each of the following: Forest, Grasslands/Shrublands, and Wetlands (to address the riparian edges of the Nelson River and tributaries). The Long Spruce reservoir pre-flood terrestrial and aquatic landcover types were allocated as illustrated in Table 2-1.



Figure 2-6 Long Spruce Reservoir Downstream of Kettle G.S. October 29, 2007
Photo by B. Gill



Figure 2-7 Long Spruce Reservoir Approaching Limestone G.S. (in background) October 29, 2007
Photo by B. Gill



Figure 2-8 Limestone Reservoir – Segment of Grass and Shrub Shoreline October 29, 2007
Photo by B. Gill



Figure 2-9 Nelson River Upstream of Potential Conawapa Site.
Photo by B. Gill
Illustration of Steep Riverbanks and Bare Shorelines October 29, 2007



Figure 2-10 Nelson River Upstream of Potential Conawapa Site.
Illustration of Steep Riverbanks and Bare Shorelines Photo by B. Gill



Figure 2-11 Looking Upstream at the Potential Conawapa Site. Illustrating Steep Riverbanks
Photo by B. Gill

Table 2-1 Long Spruce Reservoir G-res Model Landcover Classification

Long Spruce Reservoir Pre-Impoundment Landcover

	% Mineral Soil	% Organic Soil	% Total
Croplands			
Bare Areas	0.0%		0.0%
Wetlands		16.2%	16.2%
Forest	15.7%	0.0%	15.7%
Grassland/Shrubland	15.7%	0.0%	15.7%
Permanent Snow/Ice			
Settlements			
Total Terrestrial			**47.7%**
River Area Before Impoundment			52.3%
Total			**100.0%**

2.2.1 Replacement of G-res Tool Generic Emission Factors

Default G-res Tool pre-flood CO_2 and CH_4 emission factors for "Forest", "Grassland/Shrubland", and "Wetlands" were replaced by CO_2 emission factors developed by Virkkala et al. (2021) and by CH_4 emission factors adopted from Kuhn et al. (2021) and Treat et al. (2018). The default G-res Tool pre-flood emission factors for "Water Bodies" were replaced by in-situ measurements of CH_4 diffusive emissions of Gull Lake and associated backbays conducted by Environnement Illimité inc. during 2009 – 2013 (Marchand et al., 2015). The development of these emission factors is summarized below. Details are described in thesis Chapter 3 and in Appendix 1.

2.2.1.1 CO_2 Terrestrial Emission Factors

Annual CO_2 emission factors (Net Ecosystem Exchange) for the Boreal Upland and Boreal Wetland were selected from Virkkala et al. (2021). They were based on a study period of 1990-2015 (Table 2-2). Virkkala et al. (2021) did not develop separate emission factors for mineral and organic soils. These emission factors were used as composite emission factors for both mineral and organic soils in the Keeyask G-res model. The Virkkala et al. (2021) Boreal Upland CO_2 emission factors were used for the G-res categories of Forest and Grassland/Shrubland, and the Boreal Wetland CO_2 emission factors were used for the G-res Wetland category.

Table 2-2 CO_2 Emission Factors Used for the Long Spruce Reservoir G-res Model

CO_2 Emission Factors for Ecological Land Classification		
Land Class	**Annual NEE g CO_2-C/m^{-2}/yr**	**Annual NEE t CO_2-C/ha/yr (Converted for G-res)**
Boreal Uplands (Forest, and Grassland/Shrubland)	-47	-0.47
Boreal Wetlands	-38	-0.38
Source: Virkakkala et al., 2021 (Table 1)		

2.2.1.2 CH_4 Terrestrial Emission Factors

CH_4 emission factors were adapted from the Boreal–Arctic Wetland and Lake Methane Dataset (BAWLD-CH4) (Kuhn et al., 2021).

Growing season CH_4 terrestrial emission factors were adopted from Kuhn et al. (2021) Table 3 median values for Boreal Forest, Permafrost Bog, Bog, Fen, and Marsh land classes. Non-growing season emission factors were not included in the BAWLD-CH4 database/Kuhn et al. (2021) study. They were therefore estimated as being 16% of total annual emissions according to Treat et al. (2018). The Keeyask Ecological Land Classifications of "Swamps" and "Riparian" were assigned the same emissions factors as the BAWLD-CH4 emission factors for bogs and fens, respectively, following descriptions by Kuhn et al. (2021).

A composite wetland emission factor was developed by developing a weighted average for the land classifications of Permafrost Bog, Bog, Fen, Marsh, and Peatland Lakes (small and medium). This involved multiplying each [wetland class] by their [CH_4 emission factor], by their [areal extent (km^2) as defined by the Keeyask Ecological Land Classification, and by summing these calculations. The results are displayed in Table 2-3.

Table 2-3 Composite CH4 Emission Factors Used for the Long Spruce Reservoir G-res Model

Land Class	**Annual Emissions kg CH_4/ha/yr (G-res Emission Factor Metrics)**
Boreal Uplands (Forest, and Grassland/Shrubland)	-0.64
Boreal Wetlands	51.13

2.2.1.3 Pre-flood Aquatic GHG Emission Factors

The G-res default emission factor was replaced by the pre-flood flux of 5 mg $CH_4/m^2/yr$ which translates into 9.25 kg CH_4/ha/yr. This emission factor was derived by Environnement Illimité inc. from their in-situ measurements of CH_4 diffusive emissions from Gull Lake and associated backbays during 2009 – 2013 (Marchand et al., 2015).

G-res does not include pre-flood CO_2 emission factors for water bodies.

Table 2-4 illustrates the pre-flood emission factors used in the Long Spruce Reservoir G-res Model. The site-specific emission factors developed for "Forest", "Grassland/Shrubland", "Wetlands" and "Water Bodies" are highlighted.

Table 2-4 Long Spruce Reservoir G-res Model Pre-Flood Emission Factors

Climate: Boreal

	CH_4 Emission Factor (kg CH4/ha/yr)		CO_2 Emission Factor (t CO2-C/ha/yr)	
	Mineral Soil	Organic Soil	Mineral Soil	Organic Soil
Cropland	0	0	0	7.9
Bare Areas	0	6.1	0	2.8
Wetlands	51.13	51.13	-0.38	-0.38
Forest	-0.64	-0.64	-0.47	-0.47
Grassland/Shrubland	-0.64	-0.64	-0.47	-0.47
Urban Areas	0	19.6	0	6.4
Water Bodies	9.3			
Drained Peatlands				

2.2.3 Determine River Area Before Impoundment

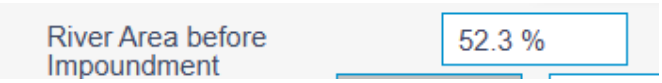


Figure 2-12 Long Spruce G-res Model River Area Before Impoundment

The River Area before Impoundment was calculated as:

Pre-existing river area to be Flooded (15.9 km^2) / Total Reservoir Area (30.4 km^2) = 52.3%.

3 Reservoir Data

3.1 Input Values

The input values used are as follows:

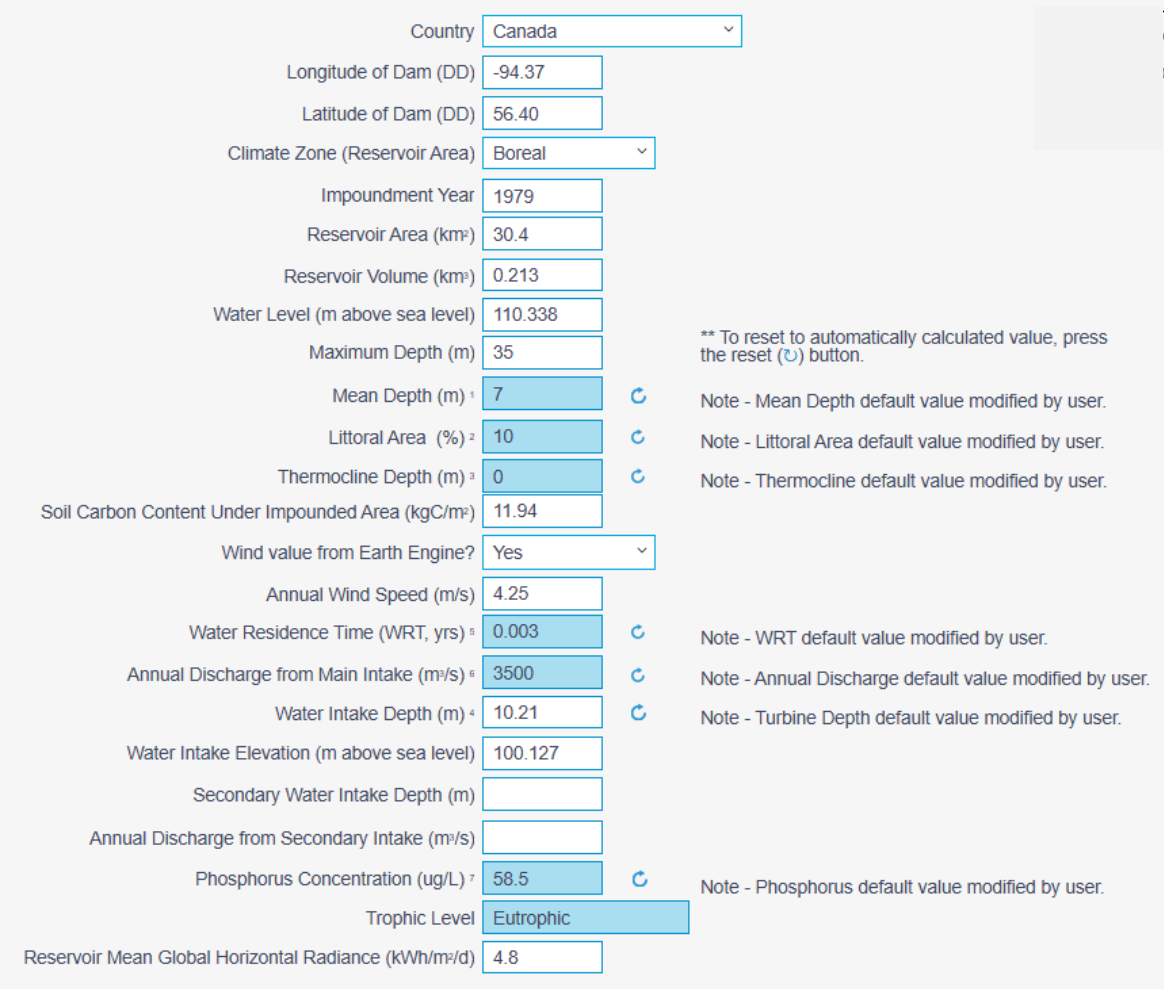


Figure 3-1 Long Spruce G-res Model: Reservoir Data

Longitude and Latitude:
The Longitude (-94.37 W) and Latitude (56.40 N) of the Dam refer to the location of the Long Spruce Generating Station.

Climate Zone:
The upstream portion of the Long Spruce Reservoir is located within the Boreal Shield Ecozone and the downstream portion is located in the Hudson Plains Ecozone (Government of Canada, 2013). The climate is classified as Cool Continental/Sub Arctic (Dfc) based on the Köppen–Geiger Climate Classification (Kottek et al., 2006, Amani et al., 2019). The "Boreal" climate zone was selected from the G-res Tool.

Impoundment Year: 1979
Reservoir impoundment (flooding) recorded as 1979, the year the generating station became fully operational (Manitoba and Manitoba Hydro, 2014).

Reservoir Area (km^2): 30.4 km^2
The Long Spruce Reservoir comprises approximately 14.5 km^2 of flooded land and 15.9 km^2 of existing aquatic systems for a total area of 30.4 km^2 (Manitoba Hydro, 2015b).

Reservoir Volume (km^3): 0.213 km^3
The estimated reservoir volume of the Long Spruce Reservoir is 0.213 km^2 (Hesslein and Cooley, 2016).

Water Level (m above sea level): 110.3 m above sea level
The water level on the Long Spruce reservoir is controlled by the Kettle Generating Station. The water level on the reservoir generally operates just below 110.0 m ASL in the open water period and just below 110.3 m ASL during the winter, and is positioned above 109.4 ASL in the forebay approximately 95% of the time (Manitoba and Manitoba Hydro, 2014).

The Maximum Licence Forebay Elevation is 110.3 m ASL (Manitoba Hydro, 2018).

Maximum Depth (m): 35 m
The maximum depth of the reservoir was estimated to be 35 m, the same as the Kettle reservoir. The model was also run for a maximum depth of 30 m, which did not change the results.

Mean Depth (m): 7 m
The mean depth of the reservoir was estimated as 7 m, following Hesslein and Cooley (2016).

Littoral Area (%): 10%
In lieu of site-specific data on the extent of the littoral zone for the Long Spruce Reservoir, a value of 10% was used for this scenario.

Thermocline Depth (m): 0
The thermocline depth was set as 0 m.

Soil Carbon Content Under the Impoundment Area (kg C/m^2): 11.94 kg C/m^2
The value of 11.94 kg C/m^2 was derived from the Earth Engine functionality of the G-res Tool. For comparison, this value aligns well with IPCC 2019 default value of 11.6 ±65% kg C/m^2 for the soil organic carbon stock content for Boreal Moist/Dry wetland soils for 0-30 cm depth (IPCC 2019, Table 2.3).

This value is also similar to the average carbon content of 10.8 kg C/m^2 in peat-forming soils at a depth of 0-30 cm in a boreal forest site located south of James Bay (Magnan et al., 2020). Similarly, Beaulne et al. (2021) calculated that between 11.0 – 12.6 kg C/m^2 has been stored in the organic horizons of a boreal peatland site in eastern Canada over the last 200 years.

Annual Wind Speed: 4.25 m/s
The value of 4.25 m/s was derived from the Earth Engine functionality of the G-res Tool.

This value is within the range of average wind speeds of 3.89 m/s to 4.94 m/s recorded in Gillam, Manitoba from 1971 to 2000 (Keeyask Hydropower Limited Partnership, 2012a). The meteorological station in Gillam is located approximately 30 km east of the Keeyask Generating Station/Reservoir (Keeyask Hydropower Limited Partnership, 2012a).

Water Residence Time (WRT, yrs): 0.003 yrs
The Water Residence Time for Stephens Lake was estimated to range from 0.49 days to 3.08 days, with a mean of 1.23 days (Hesslein and Cooley, 2016). The mean of 1.23 days (0.003 years) was used for the model.

Annual Discharge from Main Intake (m^3/s): 3,500 m^3/s
The average annual discharge is approximately 3,500 m^3/s. This value is based on the annual average water discharge rate at the Manitoba Hydro water gauge (05UF007) located on the Nelson River at the Long Spruce Generating Station for the years 1987 to 2023. This is the time period where data is available for this station at the Environment Canada Water Office website: https://wateroffice.ec.gc.ca/search/historical_e.html

Water Intake Depth (m): 10.2 m
The Water Intake Depth is estimated to be between 10 m to 30 m below the reservoir water surface, roughly adapted from the intake levels of the Keeyask and Lettle Generating Stations. This spans approximately 20 m or 67% of the entire water column of the reservoir

Water Intake Elevation (100.3 m above sea level):
The elevation of the top and bottom of the Water Intake was estimated at 100 m ASL and 80 m ASL, respectively. 100 m ASL was entered for the G-res Kettle model.

Phosphorus Concentration (µg/L): 58.5 µg/L

The Keeyask Aquatic Effects Monitoring Plan benchmark of 58.5 µg/L was used in the G-res Long Spruce model.

Trophic Level: Eutrophic
Based on Total Phosphorus concentrations, the main stem of the Nelson River is classified as meso-eutrophic to eutrophic (Keeyask Hydropower Limited Partnership, 2012b).

So as not to underestimate GHG emissions, the Long Spruce reservoir was classified as eutrophic for the G-res Model.

Reservoir Mean Global Horizontal Radiance ($kWh/m^2/d$): 4.8
The Reservoir Mean Global Horizontal Radiance value of 4.8 $kWh/m^2/d$ was generated by the G-res Tool Earth Engine.

For comparison, the on-line, interactive Photovoltaic Potential and Solar Resource Maps of Canada estimates mean annual global insolation values of 3.18 kWh/m^2/d for the Town of Gillam, Manitoba (Natural Resources Canada, 2020). The estimates are based on horizontal 0-degree orientation on a 60 arc seconds (approximately 2 km grid). Gillam is located approximately 27 km west (upstream) of the Long Spruce Generating Station.

To be conservative, the elevated value of 4.8 kWh/m^2/d was used in the G-res Tool modeled estimates.

Mean Temperature per Month (ºC)

Mean Temperature per Month and Mean Annual Air Temperature data were derived by the G-res Tool Earth Engine.

Mean Temperature per Month (°C)	
January	-25.6
February	-22.16
March	-15.37
April	-4.37
May	4.58
June	11.13
July	15.23
August	13.61
September	6.8
October	-0.1
November	-11.84
December	-22.62
Mean Annual Air Temperature (°C)	-4.2

Figure 3-2 Mean Average Monthly Temperatures

4 Reservoir Services Data

100% of the Reservoir Services were allocated to the Long Spruce Reservoir/hydroelectricity.

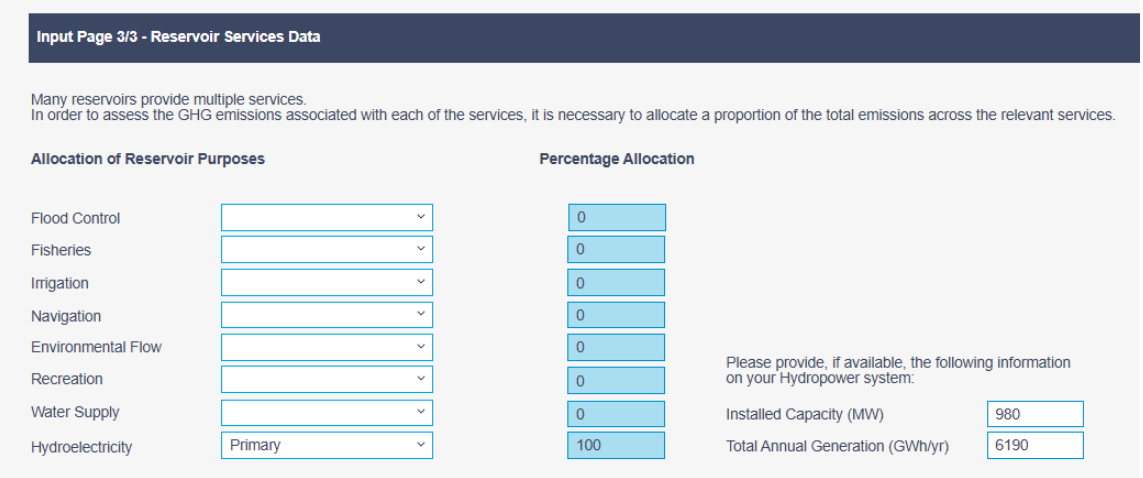


Figure 4-1 Long Spruce G-res Model: Reservoir Services

5 Construction GHG

The G-res Tool was not used to estimate Construction Emissions.

6 Unrelated Anthropogenic Sources Emissions

Since 100% of the purpose of the Long Spruce Reservoir is assigned to hydroelectricity, no GHG emissions were allocated to Unrelated Anthropogenic Sources.

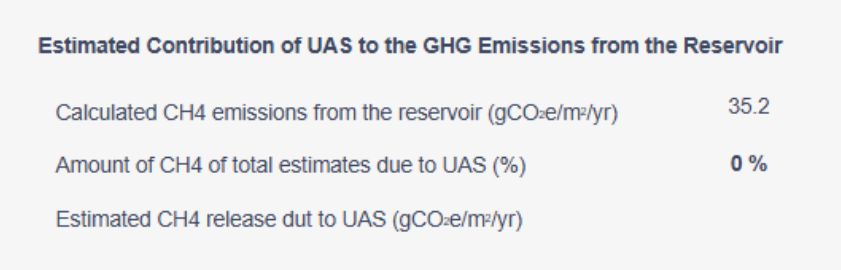


Figure 6-1 Long Spruce G-res Model: Contribution of Unrelated Anthropogenic Sources of GHG Emissions

References

Amani, M., Mahdavi, S., Afshar, M., Brisco, B., Huang, W., Mirzadeh, S.M.J., White, L., Banks, S.N., Montgomery, J., Hopkinson, Cs. (2019). Canadian Wetland Inventory using Google Earth Engine: The First Map and Preliminary Results. Remote Sensing. 11. 842. 10.3390/rs11070842.

Beaulne, J., Garneau, M., Magnan, G., Boucher, É. (2021). Peat deposits store more carbon than trees in forested peatlands of the boreal biome. Sci Rep 11, 2657. https://doi.org/10.1038/s41598-021-82004-x

Government of Canada. (2013). National Ecological Framework for Canada. Ecozones, Ecoregions, and Ecodistricts.
https://sis.agr.gc.ca/cansis/publications/maps/eco/all/districts/eco_all_districts_1m_manitoba.jpg

Government of Canada. (2025). Monthly Discharge Data for Nelson River at Kettle Generating Station (05UF006) [MB].
https://wateroffice.ec.gc.ca/report/historical_e.html?stn=05UF006&dataType=Monthly&parameterType=Flow&year=2023&mode=Table&mean1=1&scal…

Hesslein, R., and Cooley, M. (2016). Status of Greenhouse Gas Emissions at Manitoba Hydro's Mature Reservoirs. Prepared for Manitoba Hydro by North/South Consultants Inc. Winnipeg, Manitoba. 68 pages.

IPCC (2019). Chapter 2: Generic Methodologies Applicable to Multiple Land-Use Categories, Volume 4 Agriculture, Forestry and Other Land Use, 2019 Refinement to the 2006 IPCC Guidelines for National Greenhouse Gas Inventories, 104 pages.

Keeyask Hydropower Limited Partnership (2012a). Keeyask Generation Project: Environmental Impact Statement; Physical Environment Response to EIS Guidelines, Supporting Volume. 1018 pages.

Keeyask Hydropower Limited Partnership (2012b). Keeyask Generation Project: Environmental Impact Statement; Aquatic Environment Supporting Volume. 1745 pages.

Kottek, M., Grieser, J., Beck, C., Rudolf, B., Rubel, F. (2006). World map of the Köppen-Geiger climate classification updated. Meteorol. Z., 15, 259–263.

Kuhn, M. A., Varner, R. K., Bastviken, D., Crill, P., Macintyre, S., Turetsky, M., Walter Anthony, K., McGuire, A. D., & Olefeldt, D. (2021). BAWLD-CH4: A comprehensive dataset of methane fluxes from boreal and arctic ecosystems. In *Earth System Science Data* (Vol. 13, Issue 11, pp. 5151–5189). Copernicus Publications. https://doi.org/10.5194/essd-13-5151-2021

Magnan, G., Garneau, M., Le Stum-Boivin, É., Grondin, P., and Yves Bergeron, Y. (2020). Long-Term Carbon Sequestration in Boreal Forested Peatlands in Eastern Canada. Ecosystems 23, 1481–1493. https://doi.org/10.1007/s10021-020-00483-x

Manitoba and Manitoba Hydro. (2014). Regional Cumulative Effects Assessment for Hydroelectric Developments on the Churchill, Burntwood and Nelson River Systems. Phase I Report. May 2014. https://www.hydro.mb.ca/docs/regulatory_affairs/pdf/rcea/part123_rcea_phase1.pdf

Manitoba and Manitoba Hydro. (2015). Regional Cumulative Effects Assessment for Hydroelectric Developments on the Churchill, Burntwood and Nelson River Systems. Phase II Report: Hydroelectric Development Project Description in the Region of Interest. Part II. December 2015. https://www.hydro.mb.ca/docs/regulatory_affairs/pdf/rcea/rcea_phase2_part_ii_hydroelectric_development_project_description.pdf

Manitoba Hydro. (2015). Flooded Areas for Manitoba Hydro System. [Unpublished manuscript]. Manitoba Hydro, Winnipeg, Manitoba.

Manitoba Hydro. (2018). Manitoba Hydro Long Spruce Generating Station Licence Implementation Guide for Water Levels. Report No. PS&O 18/07. https://www.gov.mb.ca/sd/pubs/water/licensing/long_spruce/long_spruce_lig.pdf

Marchand D., M. Demarty, and R. Gill. (2015). Keeyask Technical Summay – 2014. Summary prepared by Environnement Illimité for Manitoba Hydro, 11 p.

Natural Resources Canada (2020). Photovoltaic Potential and Solar Resource Maps of Canada. © Her Majesty the Queen in Right of Canada, as represented by the Minister of Natural Resources, 2020. https://fgp-pgf.maps.arcgis.com/apps/webappviewer/index.html?id=c91106a7d8c446a19dd1909fd93645d3

Treat, C. C., Bloom, A. A., & Marushchak, M. E. (2018). Nongrowing season methane emissions–a significant component of annual emissions across northern ecosystems. *Global Change Biology*, *24*(8), 3331–3343. https://doi.org/10.1111/gcb.14137

Virkkala, A. M., Aalto, J., Rogers, B. M., Tagesson, T., Treat, C. C., Natali, S. M., Watts, J. D., Potter, S., Lehtonen, A., Mauritz, M., Schuur, E. A. G., Kochendorfer, J., Zona, D., Oechel, W., Kobayashi, H., Humphreys, E., Goeckede, M., Iwata, H., Lafleur, P. M., … Luoto, M. (2021). Statistical upscaling of ecosystem CO2 fluxes across the terrestrial tundra and boreal domain: Regional patterns and uncertainties. *Global Change Biology*, *27*(17), 4040–4059. https://doi.org/10.1111/gcb.15659

Appendix 5

Application of the G-res Tool to the Limestone Generating Station Reservoir

Report on Data Inputs

This document describes the inputs used to apply the G-res Tool to the Limestone Reservoir located in northern Manitoba.

1 Limestone Generating Station:



Source: B. Gill October 29, 2007
Figure 1-1 Limestone Generating Station

The Limestone Generating Station is a 1350 MW hydroelectric facility located at the former Limestone Rapids on the lower Nelson River (Figures 1-1 and 1-2) and it is Manitoba Hydro's largest hydroelectric generating station (Manitoba and Manitoba Hydro, 2015; Manitoba Hydro, 2026). The station is located approximately 23 km downstream of the Long Spruce Generating Station and approximately 55 km from the Town of Gillam, Manitoba (Manitoba and Manitoba Hydro, 2015).

The operating head, or waterfall created by the station, is approximately 27.6 m (Manitoba Hydro, 2021). The discharge capacities of the generating station and spillway are 5,000 m^3/s and 9,600 m^3/s of water, respectively (Manitoba and Manitoba Hydro, 2015).

The Limestone reservoir flooded approximately 2.2 km^2 of land and 25.0 km^2 of water, for a total reservoir size of approximately 27.2 km^2 (Manitoba and Manitoba Hydro, 2015). The reservoir is contained almost entirely within the natural banks of the Nelson River (Maclaren Plansearch Inc. & InterGroup Consultants Ltd., 1986). The banks of the pre-flood Limestone reservoir footprint are ice-scoured and typically, seasonal vegetation does not occur below the well-defined high-ice trim line, and little organic material is present in the overburden (Maclaren Plansearch Inc. & InterGroup Consultants Ltd., 1986). The reservoir water level is maintained below the winter trimline except near the Limestone Generating Station (Maclaren Plansearch Inc. & InterGroup Consultants Ltd., 1986). Flooding was predicted at the mouths of Brook Creek and Clements Creek (Maclaren Plansearch Inc. & InterGroup Consultants Ltd., 1986).

The reservoir is operated as a run of the river reservoir where the water levels are controlled by the discharges of the Kettle Generating Station (Manitoba and Manitoba Hydro, 2014). The water level on the reservoir generally operates at 85.3 m ASL (Manitoba Hydro, 2021). The maximum operating forebay elevation during open water is 85.313 m ASL and the normal minimum operating forebay elevation is 82.296 m ASL (Manitoba and Manitoba Hydro, 2014).

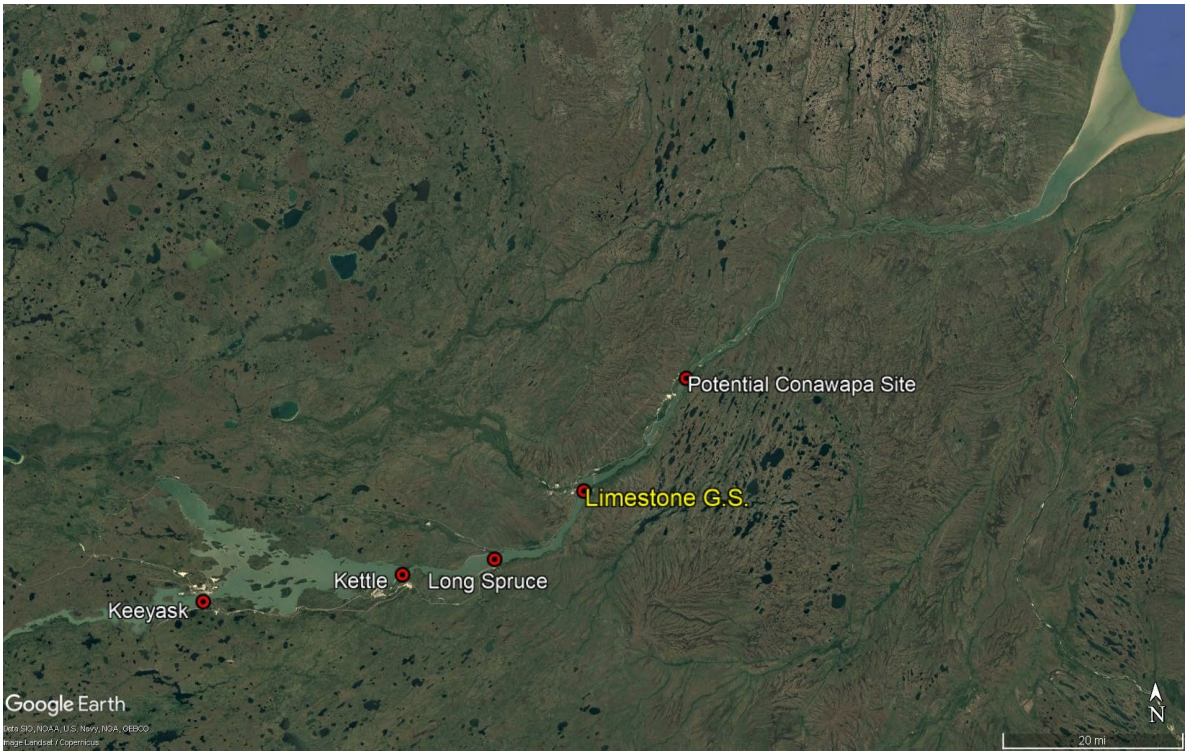
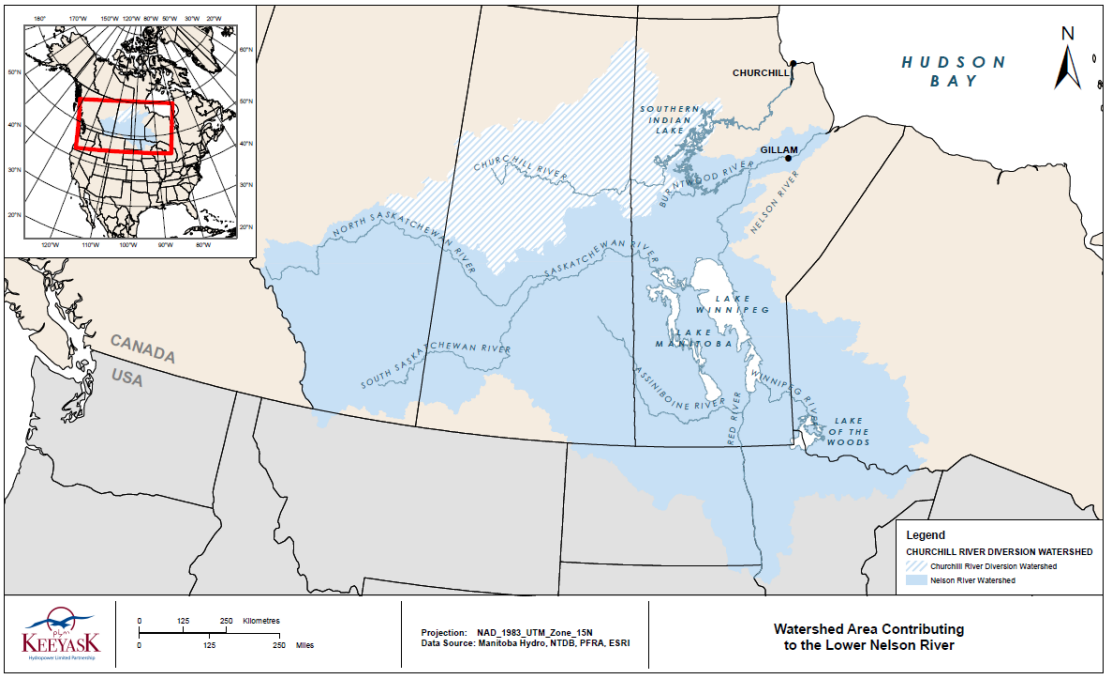


Figure 1-2 Limestone Generating Station

2 G-res Tool "Catchment Data"

The Limestone Reservoir watershed area is illustrated below in Figure 2-1.



Source: Keeyask Hydropower Limited Partnership 2012a (Map 4.3-1)
Figure 2-1 Lower Nelson River Watershed

Model inputs pertaining to: Catchment Area, Population in the Catchment, and Catchment Annual Runoff were derived from the G-res Tool Earth Engine.

So as not to underestimate reservoir GHG emissions by assigning a portion to wastewater and sewage treatment, the release of phosphorus from community sewage and the release of phosphorus from industrial sewage were set to zero. Therefore, no portion of the reservoir GHG emissions were assigned to another anthropogenic source other than the Limestone Reservoir.

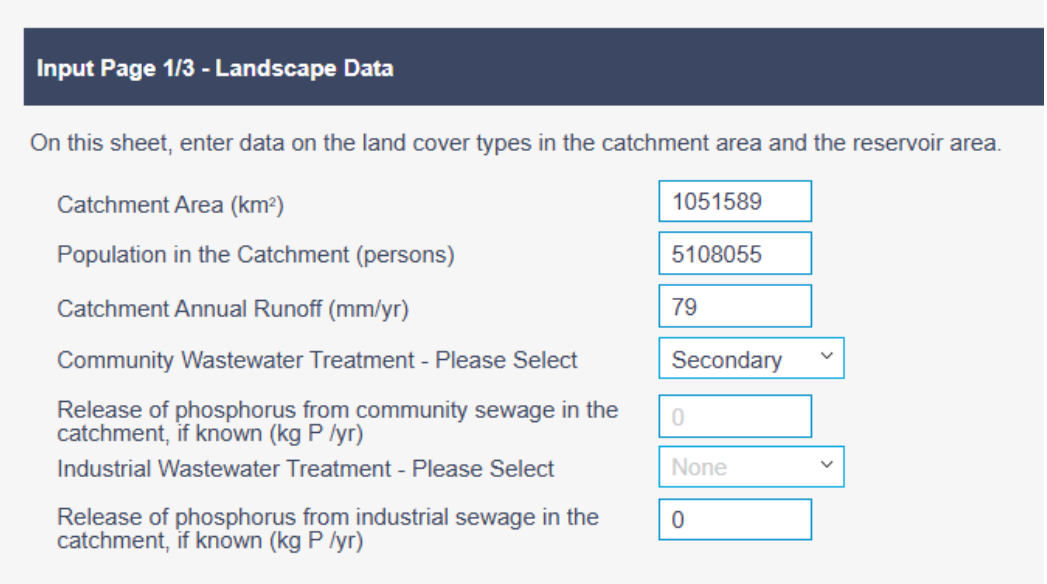


Figure 2-2 G-res Landscape Data Generated by G-res Earth Engine

2.1 Land Cover in the Catchment Area

Land Cover in the Catchment Area inputs were derived from the G-res Tool Earth Engine. It is understood that these inputs will not be used in the G-res Tool calculations of pre-flood GHG emissions. Pre-flood GHG remissions will be calculated using the G-res Pre-Impoundment Land Cover in the Reservoir Area input sheet, which were derived from Limestone reservoir site-specific information, as described in Section 2.2 below.

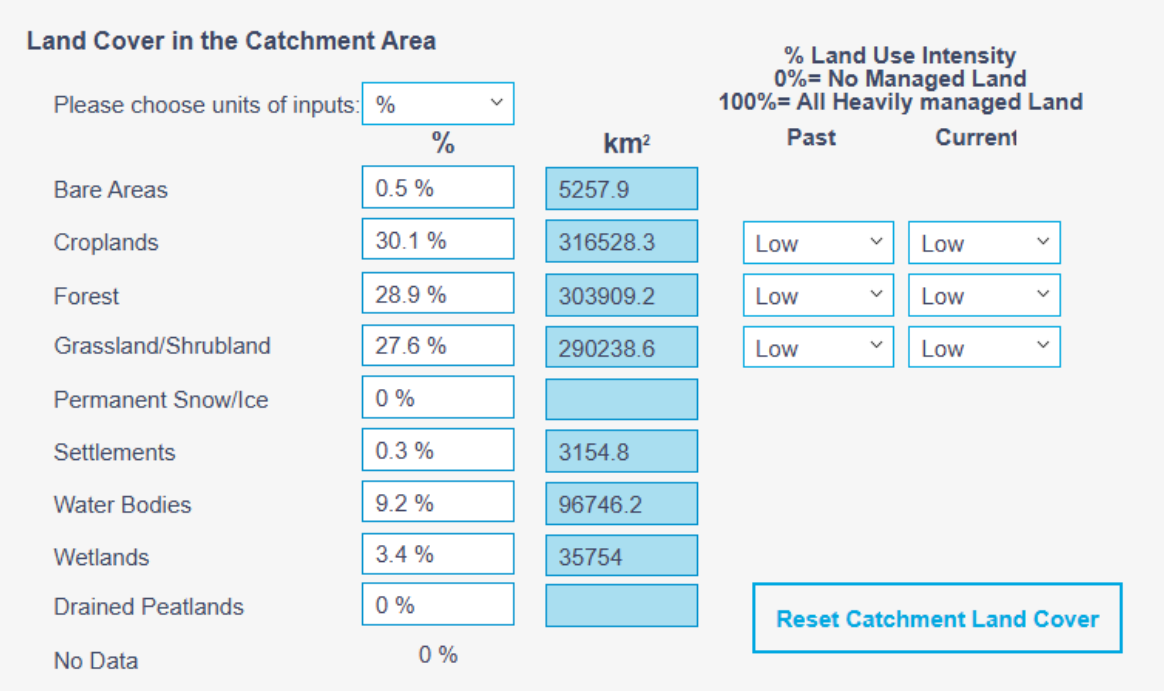


Figure 2-3 Landcover Data Generated by the Limestone G-res Earth Engine

2.2 Pre-Impoundment Land Cover in the Reservoir Area

Pre-Impoundment Land Cover in the Reservoir Area inputs were derived from the following sources:

2.2.1 Reservoir Area (km2)



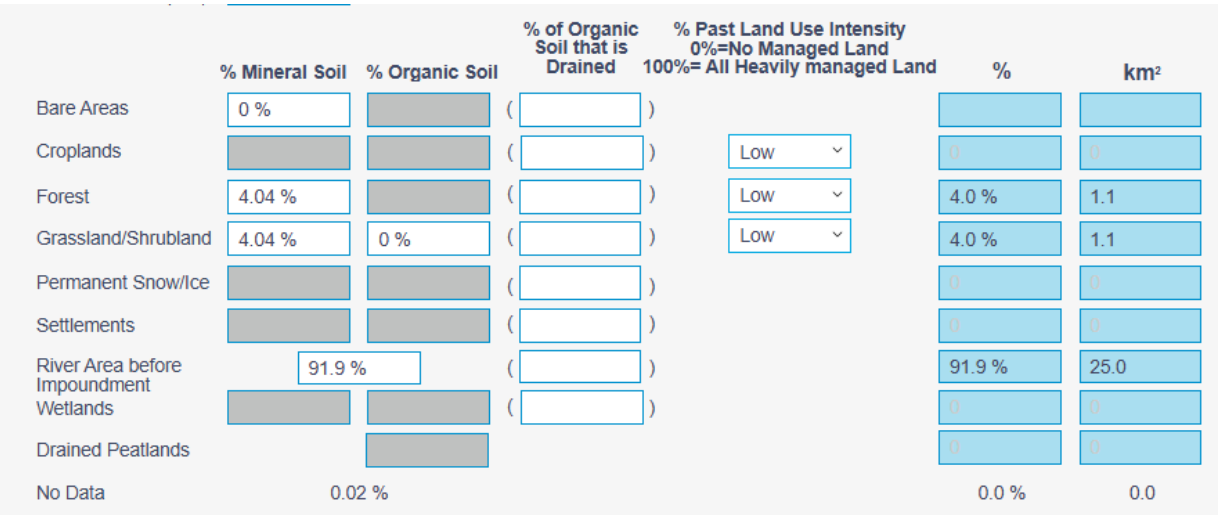
Figure 2-4 Total Limestone Reservoir Area (km^2)

The Limestone reservoir comprises approximately 2.2 km^2 of flooded land and 25.0 km^2 of existing aquatic systems for a total area of 27.2 km^2 (Manitoba Hydro, 2015).

2.2.2 Pre-Impoundment Land Cover in the Reservoir Area

2.2.2.1 Input Values

The input values used are as follows:



	% Mineral Soil	% Organic Soil	% of Organic Soil that is Drained	% Past Land Use Intensity 0%=No Managed Land 100%= All Heavily managed Land	%	km²
Bare Areas	0 %		( )			
Croplands			( )	Low	0	0
Forest	4.04 %		( )	Low	4.0 %	1.1
Grassland/Shrubland	4.04 %	0 %	( )	Low	4.0 %	1.1
Permanent Snow/Ice			( )		0	0
Settlements			( )		0	0
River Area before Impoundment	91.9 %		( )		91.9 %	25.0
Wetlands			( )		0	0
Drained Peatlands					0	0
No Data	0.02 %				0.0 %	0.0

Figure 2-5 Limestone Reservoir Pre-Impoundment Landcover Data

2.2.2.2 Overview of Pre-Impoundment Land Cover in the Reservoir Area

The banks in the pre-flood Limestone reservoir footprint are ice-scoured and typically, seasonal vegetation does not occur below the well-defined high-ice trim line, and little organic material is present in the overburden (Maclaren Plansearch Inc. & InterGroup Consultants Ltd., 1986). The reservoir water level is maintained below the winter trimline except near the Limestone Generating Station (Maclaren Plansearch Inc. & InterGroup Consultants Ltd., 1986). Flooding was predicted at the mouths of Brook Creek and Clements Creek (Maclaren Plansearch Inc. & InterGroup Consultants Ltd., 1986).

Below are illustrations of the current Limestone reservoir (Figure 2-6), and illustrations of the steep banks of the Nelson River and bare shorelines upstream of the potential Conawapa site (Figures 2-7 to 2-9). Figures 2-7 to 2-9 may provide an indication of the pre-flood landcover of the Limestone reservoir, which was contained mostly within the natural banks of the Nelson River.

In the absence of detailed pre-flood landcover data for the Limestone reservoir, the above information was used to estimate the pre-flood land cover categories for the Limestone G-res model. Approximately 92% (25 km^2 / 27.2 km^2) of the reservoir is comprised of flooded water.

The remaining 8% was flooded land. For the G-res Model, one half of the flooded land was allocated to “Forest” and one half to “Grassland/Shrubland” on mineral soils.

The Limestone reservoir pre-flood terrestrial and aquatic landcover types were allocated as illustrated in Table 2-1.



Figure 2-6 Limestone Reservoir – Segment of Grass and Shrub Shoreline October 29, 2007



Figure 2-7 Nelson River Upstream of Potential Conawapa Site.
Illustration of Steep Riverbanks and Bare Shorelines October 29, 2007



Figure 2-8 Nelson River Upstream of Potential Conawapa Site.
Illustration of Steep Riverbanks and Bare Shorelines



Figure 2-9 Looking Upstream at the Potential Conawapa Site. Illustrating Steep Riverbanks

Table 2-1 Limestone Reservoir G-res Model Landcover Classification

Limestone Reservoir Pre-Impoundment Land Cover

	% Mineral Soil	% Organic Soil	% Total
Croplands			
Bare Areas	0.00%		0.00%
Wetlands		0.00%	0.00%
Forest	4.04%	0.00%	4.04%
Grassland/Shrubland	4.04%	0.00%	4.04%
Permanent Snow/Ice			
Settlements			
Total Terrestrial			**8.1%**
River Area Before Impoundment			91.9%
Total			**100.0%**

2.2.1 Replacement of G-res Tool Generic Emission Factors

Default G-res Tool pre-flood CO_2 and CH_4 emission factors for "Forest", "Grassland/Shrubland", and "Wetlands" were replaced by CO_2 emission factors developed by Virkkala et al. (2021) and by CH4 emission factors adopted from Kuhn et al. (2021) and Treat et al. (2018). The default G-res Tool pre-flood emission factors for "Water Bodies" were replaced by in-situ measurements of CH_4 diffusive emissions of Gull Lake and associated backbays conducted by Environnement Illimité inc. during 2009 – 2013 (Marchand et al., 2015). The development of these emission factors is summarized below. Details are described in thesis Chapter 3 and in Appendix 1.

2.2.1.1 CO_2 Terrestrial Emission Factors

Annual CO_2 emission factors (Net Ecosystem Exchange) for the Boreal Upland and Boreal Wetland were selected from Virkkala et al. (2021). They were based on a study period of 1990-2015 (Table 2-3). Virkkala et al. (2021) did not develop separate emission factors for mineral and organic soils. These emission factors were used as composite emission factors for both mineral and organic soils in the Keeyask G-res model. The Virkkala et al. (2021) Boreal Upland CO_2 emission factors were used for the G-res categories of Forest and Grassland/Shrubland, and the Boreal Wetland CO_2 emission factors were used for the G-res Wetland category.

Table 2-2 CO_2 Emission Factors Used for the Limestone Reservoir G-res Model

CO_2 Emission Factors for Ecological Land Classification		
Land Class	**Annual NEE g CO_2-C/m^{-2}/yr**	**Annual NEE t CO_2-C/ha/yr (Converted for G-res)**
Boreal Uplands (Forest, and Grassland/Shrubland)	-47	-0.47
Boreal Wetlands	-38	-0.38
Source: Virkakkala et al., 2021 (Table 1)		

2.2.1.2 CH_4 Terrestrial Emission Factors

CH_4 emission factors were adapted from the Boreal–Arctic Wetland and Lake Methane Dataset (BAWLD-CH4) (Kuhn et al., 2021).

Growing season CH_4 terrestrial emission factors were adopted from Kuhn et al. (2021) Table 3 median values for Boreal Forest, Permafrost Bog, Bog, Fen, and Marsh land classes. Non-growing season emission factors were not included in the BAWLD-CH4 database/Kuhn et al. (2021) study. They were therefore estimated as being 16% of total annual emissions according to Treat et al. (2018). The Keeyask Ecological Land Classifications of "Swamps" and "Riparian" were assigned the same emissions factors as the BAWLD-CH4 emission factors for bogs and fens, respectively, following descriptions by Kuhn et al. (2021).

A composite wetland emission factor was developed by developing a weighted average for the land classifications of Permafrost Bog, Bog, Fen, Marsh, and Peatland Lakes (small and medium). This involved multiplying each [wetland class] by their [CH_4 emission factor], by their [areal extent (km^2) as defined by the Keeyask Ecological Land Classification, and by summing these calculations. The results are displayed in Table 2-3.

Table 2-3 Composite CH4 Emission Factors Used for the Limestone Reservoir G-res Model

Land Class	**Annual Emissions kg CH_4/ha/yr (G-res Emission Factor Metrics)**
Boreal Uplands (Forest, and Grassland/Shrubland)	-0.64
Boreal Wetlands	51.13

2.2.1.3 Pre-flood Aquatic GHG Emission Factors

The G-res default emission factor was replaced by the pre-flood flux of 5 mg $CH_4/m^2/yr$ which translates into 9.25 kg CH_4/ha/yr. This emission factor was derived by Environnement Illimité inc. from their in-situ measurements of CH_4 diffusive emissions from Gull Lake and associated backbays during 2009 – 2013 (Marchand et al., 2015).

G-res does not include pre-flood CO_2 emission factors for water bodies.

Table 2-4 illustrates the pre-flood emission factors used in the Limestone Reservoir G-res Model. The site-specific emission factors developed for "Forest", "Grassland/Shrubland", "Wetlands" and "Water Bodies" are highlighted.

Table 2-4 Limestone Reservoir G-res Model Pre-Flood Emission Factors

Climate: Boreal

	CH_4 Emission Factor (kg CH4/ha/yr)		CO_2 Emission Factor (t CO2-C/ha/yr)	
	Mineral Soil	Organic Soil	Mineral Soil	Organic Soil
Cropland	0	0	0	7.9
Bare Areas	0	6.1	0	2.8
Wetlands	51.13	51.13	-0.38	-0.38
Forest	-0.64	-0.64	-0.47	-0.47
Grassland/Shrubland	-0.64	-0.64	-0.47	-0.47
Urban Areas	0	19.6	0	6.4
Water Bodies	9.3			
Drained Peatlands				

2.2.3 Determine River Area Before Impoundment

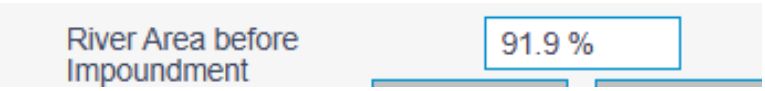


Figure 2-10 Limestone G-res Model River Area Before Impoundment

The River Area before Impoundment was calculated as:

Pre-existing river area to be flooded (25.0 km^2) / Total Reservoir Area (27.2 km^2) = 91.9%.

3 Reservoir Data

3.1 Input Values

The input values used are as follows:

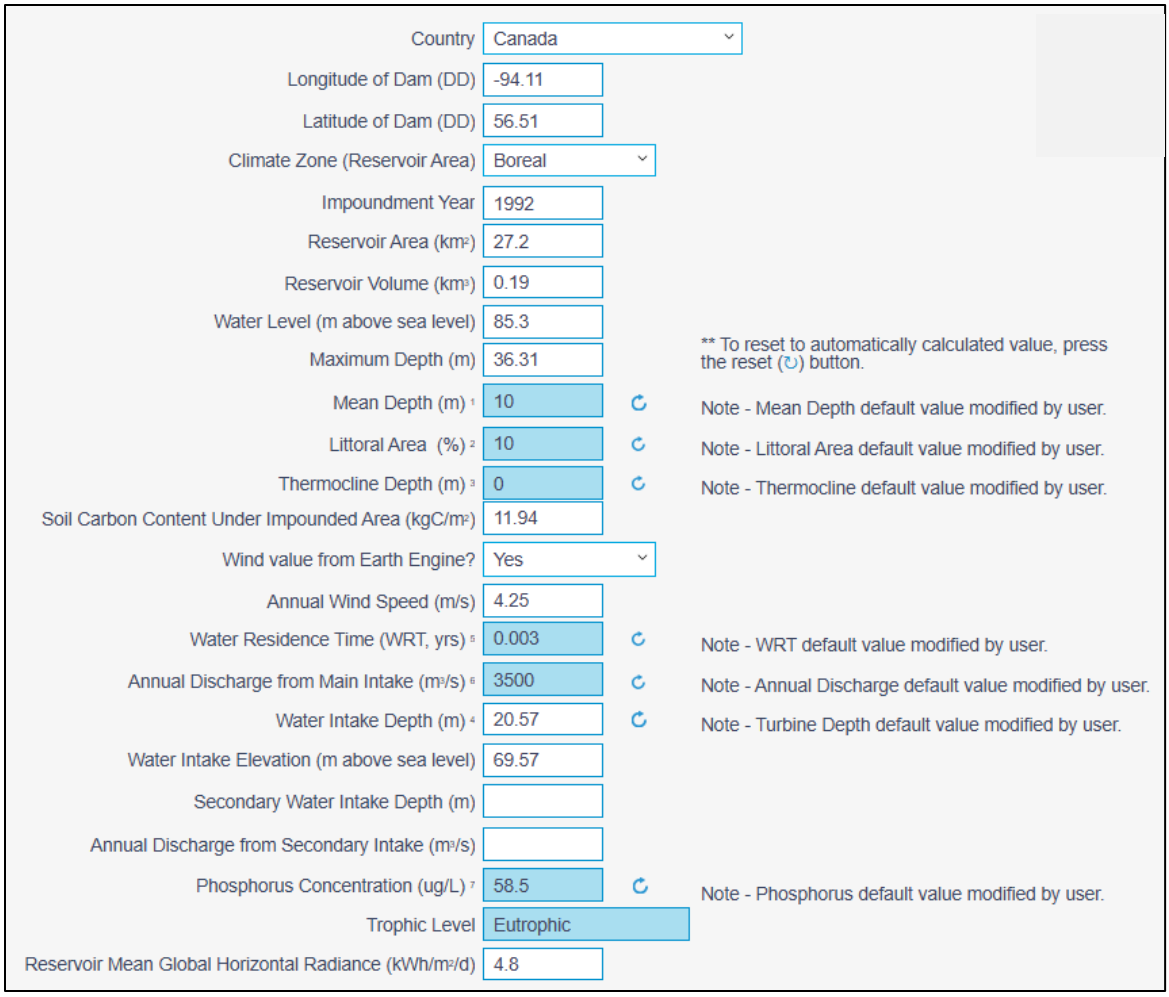


Figure 3-1 Limestone G-res Model: Reservoir Data

Longitude and Latitude:
The Longitude (-94.11 W) and Latitude (56.51 N) of the Dam refer to the location of the Limestone Generating Station.

Climate Zone:
The Limestone Reservoir is located within the Hudson Plains Ecozone (Government of Canada, 2013). The climate is classified as Cool Continental/Sub Arctic (Dfc) based on the Köppen–Geiger Climate Classification (Kottek et al., 2006, Amani et al., 2019). The "Boreal" climate zone was selected from the G-res Tool.

Impoundment Year: 1992
Reservoir impoundment (flooding) recorded as 1992, the year the generating station became fully operational (Manitoba and Manitoba Hydro, 2014).

Reservoir Area (km^2): 27.2 km^2
The Limestone Reservoir comprises approximately 2.2 km^2 of flooded land and 25.0 km^2 of existing aquatic systems for a total area of 27.2 km^2 (Manitoba Hydro, 2015b).

Reservoir Volume (km^3): 0.019 km^3
The estimated reservoir volume of the Limestone Reservoir is 0.19 km^2 (Hesslein and Cooley, 2016).

Water Level (m above sea level): 85.3 m above sea level
The water level on the Limestone reservoir is controlled by the Kettle Generating Station. The water level on the reservoir generally operates at 85.3 m ASL (Manitoba Hydro, 2021). The maximum operating forebay elevation during open water is 85.313 m ASL and the normal minimum operating forebay elevation is 82.296 m ASL (Manitoba Hydro, 2014).

The Maximum Licence Forebay Elevation is 85.3 m ASL (Manitoba Hydro, 2018).

Maximum Depth (m): 36.31 m
The maximum depth of the reservoir was estimated to be 36.31 m. The model was also run for a maximum depth of 30 m, which did not change the results.

Mean Depth (m): 7 m
The mean depth of the reservoir was estimated as 7 m, following Hesslein and Cooley, (2016).

Littoral Area (%): 10%
In lieu of site-specific data on the extent of the littoral zone for the Limestone Reservoir, a value of 10% was used for this scenario.

Thermocline Depth (m): 0
The thermocline depth was set as 0 m.

Soil Carbon Content Under the Impoundment Area (kg C/m^2): 11.94 kg C/m^2
The value of 11.94 kg C/m^2 was derived from the Earth Engine functionality of the G-res Tool. For comparison, this value aligns well with IPCC 2019 default value of 11.6 ±65% kg C/m^2 for the soil organic carbon stock content for Boreal Moist/Dry wetland soils for 0-30 cm depth (IPCC 2019, Table 2.3).

This value is also similar to the average carbon content of 10.8 kg C/m^2 in peat-forming soils at a depth of 0-30 cm in a boreal forest site located south of James Bay (Magnan et al., 2020). Similarly, Beaulne et al. (2021) calculated that between 11.0 – 12.6 kg C/m^2 has been stored in the organic horizons of a boreal peatland site in eastern Canada over the last 200 years.

Annual Wind Speed: 4.25 m/s
The value of 4.25 m/s was derived from the Earth Engine functionality of the G-res Tool.

This value is within the range of average wind speeds of 3.89 m/s to 4.94 m/s recorded in Gillam, Manitoba from 1971 to 2000 (Keeyask Hydropower Limited Partnership, 2012a). The meteorological station in Gillam is located approximately 30 km east of the Keeyask Generating Station/Reservoir (Keeyask Hydropower Limited Partnership, 2012a).

Water Residence Time (WRT, yrs): 0.003 yrs
The Water Residence Time for the Limestone reservoir was estimated to range from 0.44 days to 2.75 days, with a mean of 1.1 days (Hesslein and Cooley, 2016). The mean of 1.1 days (0.003 years) was used for the model.

Annual Discharge from Main Intake (m^3/s): 3,500 m^3/s
The average annual discharge is approximately 3,500 m^3/s. This value is based on the annual average water discharge rate at the Manitoba Hydro water gauge (05UF007) located on the Nelson River at the Long Spruce Generating Station for the years 1987 to 2023. This is the time period where data is available for this station at the Environment Canada Water Office website: https://wateroffice.ec.gc.ca/search/historical_e.html

Water Intake Depth (m): 15.7 m
The Water Intake Depth is estimated to be between 15 m to 30 m below the reservoir water surface, adapted from the Kettle Generating Station. This spans approximately 20 m or 42% of the entire water column of the reservoir.

Water Intake Elevation (69.57 m above sea level):
The elevation of the top and bottom of the Water Intake are roughly 70 m ASL and 49 m ASL, respectively. 70 m ASL was entered for the G-res Limestone model.

Phosphorus Concentration (µg/L): 58.5 µg/L
The Keeyask Aquatic Effects Monitoring Plan benchmark of 58.5 µg/L was used in the G-res Limestone model.

Trophic Level: Eutrophic
Based on Total Phosphorus concentrations, the main stem of the Nelson River is classified as meso-eutrophic to eutrophic (Keeyask Hydropower Limited Partnership, 2012b).

So as not to underestimate GHG emissions, the Limestone reservoir was classified as eutrophic for the G-res Model.

Reservoir Mean Global Horizontal Radiance ($kWh/m^2/d$): 4.8
The Reservoir Mean Global Horizontal Radiance value of 4.8 $kWh/m^2/d$ was generated by the G-res Tool Earth Engine.

For comparison, the on-line, interactive Photovoltaic Potential and Solar Resource Maps of Canada estimates mean annual global insolation values of 3.18 $kWh/m^2/d$ for the Town of Gillam, Manitoba (Natural Resources Canada, 2020). The estimates are based on horizontal 0-degree orientation on a 60 arc seconds (approximately 2 km grid). Gillam is located approximately 55 km west (upstream) of the Limestone Generating Station (Figure 1-2).

To be conservative, the elevated value of 4.8 kWh/m^2/d was used in the G-res Tool modeled estimates.

Mean Temperature per Month (ºC)

Mean Temperature per Month and Mean Annual Air Temperature data were derived by the G-res Tool Earth Engine.

Mean Temperature per Month (°C)	
January	-25.6
February	-22.16
March	-15.37
April	-4.37
May	4.58
June	11.13
July	15.23
August	13.61
September	6.8
October	-0.1
November	-11.84
December	-22.62
Mean Annual Air Temperature (°C)	-4.2

Figure 3-2 Mean Average Monthly Temperatures

4 Reservoir Services Data

100% of the Reservoir Services were allocated to the Limestone Reservoir/hydroelectricity.

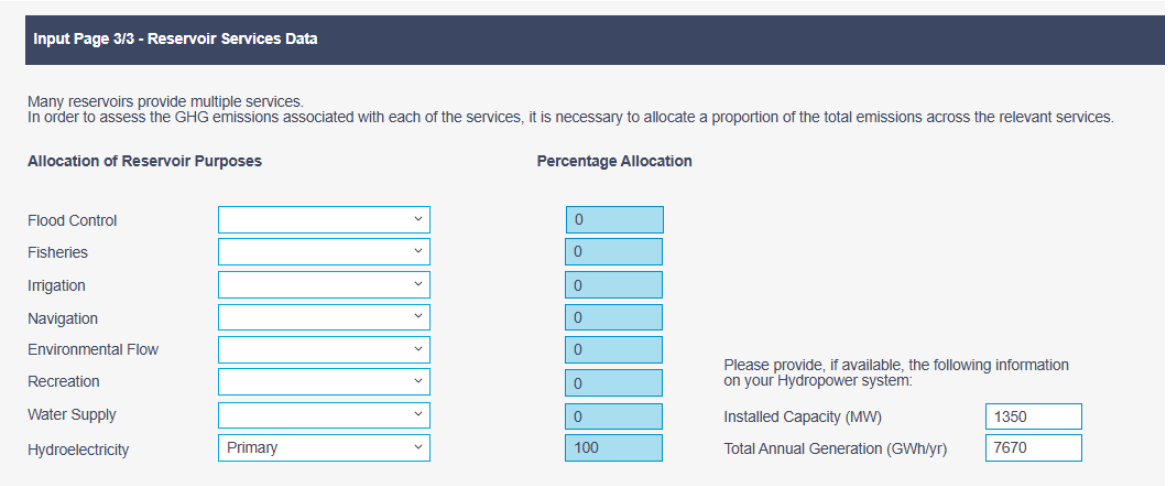


Figure 4-1 Limestone G-res Model: Reservoir Services

5 Construction GHG

The G-res Tool was not used to estimate Construction Emissions.

6 Unrelated Anthropogenic Sources Emissions

Since 100% of the purpose of the Limestone Reservoir is assigned to hydroelectricity, no GHG emissions were allocated to Unrelated Anthropogenic Sources.

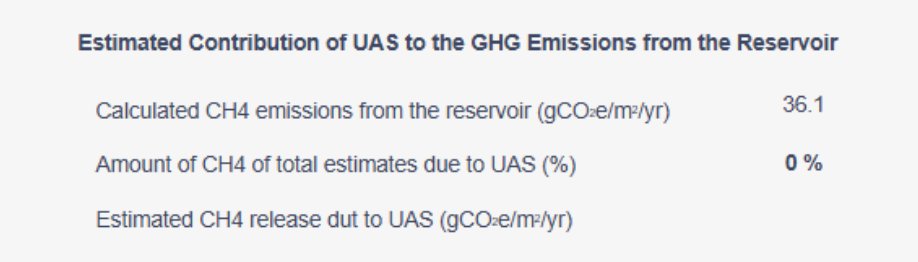


Figure 6-1 Limestone G-res Model: Contribution of Unrelated Anthropogenic Sources of GHG Emissions

References

Amani, M., Mahdavi, S., Afshar, M., Brisco, B., Huang, W., Mirzadeh, S.M.J., White, L., Banks, S.N., Montgomery, J., Hopkinson, Cs. (2019). Canadian Wetland Inventory using Google Earth Engine: The First Map and Preliminary Results. Remote Sensing. 11. 842. 10.3390/rs11070842.

Beaulne, J., Garneau, M., Magnan, G., Boucher, É. (2021). Peat deposits store more carbon than trees in forested peatlands of the boreal biome. Sci Rep 11, 2657. https://doi.org/10.1038/s41598-021-82004-x

Government of Canada. (2013). National Ecological Framework for Canada. Ecozones, Ecoregions, and Ecodistricts.
https://sis.agr.gc.ca/cansis/publications/maps/eco/all/districts/eco_all_districts_1m_manitoba.jpg

Government of Canada. (2025). Monthly Discharge Data for Nelson River at Kettle Generating Station (05UF006) [MB].
https://wateroffice.ec.gc.ca/report/historical_e.html?stn=05UF006&dataType=Monthly&parameterType=Flow&year=2023&mode=Table&mean1=1&scal…

Hesslein, R., and Cooley, M. (2016). Status of Greenhouse Gas Emissions at Manitoba Hydro's Mature Reservoirs. Prepared for Manitoba Hydro by North/South Consultants Inc. Winnipeg, Manitoba. 68 pages.

IPCC (2019). Chapter 2: Generic Methodologies Applicable to Multiple Land-Use Categories, Volume 4 Agriculture, Forestry and Other Land Use, 2019 Refinement to the 2006 IPCC Guidelines for National Greenhouse Gas Inventories, 104 pages.

Keeyask Hydropower Limited Partnership (2012a). Keeyask Generation Project: Environmental Impact Statement; Physical Environment Response to EIS Guidelines, Supporting Volume. 1018 pages.

Keeyask Hydropower Limited Partnership (2012b). Keeyask Generation Project: Environmental Impact Statement; Aquatic Environment Supporting Volume. 1745 pages.

Kottek, M., Grieser, J., Beck, C., Rudolf, B., Rubel, F. (2006). World map of the Köppen-Geiger climate classification updated. Meteorol. Z., 15, 259–263.

Kuhn, M. A., Varner, R. K., Bastviken, D., Crill, P., Macintyre, S., Turetsky, M., Walter Anthony, K., McGuire, A. D., & Olefeldt, D. (2021a). BAWLD-CH4: A comprehensive dataset of methane fluxes from boreal and arctic ecosystems. In *Earth System Science Data* (Vol. 13, Issue 11, pp. 5151–5189). Copernicus Publications. https://doi.org/10.5194/essd-13-5151-2021

MacLaren Plansearch Inc. & InterGroup Consultants Ltd. (1986). Limestone Generating Station Environmental Impact Study : Final Report. 167 pages.

Magnan, G., Garneau, M., Le Stum-Boivin, É., Grondin, P., and Yves Bergeron, Y. (2020). Long-Term Carbon Sequestration in Boreal Forested Peatlands in Eastern Canada. Ecosystems 23, 1481–1493. https://doi.org/10.1007/s10021-020-00483-x

Manitoba and Manitoba Hydro. (2014). Regional Cumulative Effects Assessment for Hydroelectric Developments on the Churchill, Burntwood and Nelson River Systems. Phase I Report. May 2014. https://www.hydro.mb.ca/docs/regulatory_affairs/pdf/rcea/part123_rcea_phase1.pdf

Manitoba and Manitoba Hydro. (2015). Regional Cumulative Effects Assessment for Hydroelectric Developments on the Churchill, Burntwood and Nelson River Systems. Phase II Report: Hydroelectric Development Project Description in the Region of Interest. Part II. December 2015. https://www.hydro.mb.ca/docs/regulatory_affairs/pdf/rcea/rcea_phase2_part_ii_hydroelectric_development_project_description.pdf

Manitoba Hydro. (2015). Flooded Areas for Manitoba Hydro System. [Unpublished manuscript]. Manitoba Hydro, Winnipeg, Manitoba.

Manitoba Hydro. (2018). Manitoba Hydro Limestone Generating Station Licence Implementation Guide for Water Levels. Manitoba Hydro. July 2018 Report No. PS&O 18/08 https://www.gov.mb.ca/sd/pubs/water/licensing/limestone/limestone_lig.pdf

Manitoba Hydro. (2021). Water Power Act Licences 2021 Annual Water Levels and Flows Compliance Report. Manitoba Hydro. 346 pages. https://www.gov.mb.ca/sd/pubs/water/licensing/2021_awl_hydro.pdf

Manitoba Hydro. (2026). Manitoba Hydro Generation. https://www.hydro.mb.ca/corporate/operations/generation

Marchand D., M. Demarty, and R. Gill. (2015). Keeyask Technical Summay – 2014. Summary prepared by Environnement Illimité for Manitoba Hydro, 11 p.

Natural Resources Canada (2020). Photovoltaic Potential and Solar Resource Maps of Canada. © Her Majesty the Queen in Right of Canada, as represented by the Minister of Natural Resources, 2020. https://fgp-pgf.maps.arcgis.com/apps/webappviewer/index.html?id=c91106a7d8c446a19dd1909fd93645d3

Treat, C. C., Bloom, A. A., & Marushchak, M. E. (2018). Nongrowing season methane emissions–a significant component of annual emissions across northern ecosystems. *Global Change Biology*, *24*(8), 3331–3343. https://doi.org/10.1111/gcb.14137

Virkkala, A. M., Aalto, J., Rogers, B. M., Tagesson, T., Treat, C. C., Natali, S. M., Watts, J. D., Potter, S., Lehtonen, A., Mauritz, M., Schuur, E. A. G., Kochendorfer, J., Zona, D., Oechel, W., Kobayashi, H., Humphreys, E., Goeckede, M., Iwata, H., Lafleur, P. M., … Luoto, M. (2021). Statistical upscaling of ecosystem CO2 fluxes across the terrestrial tundra and boreal domain: Regional patterns and uncertainties. *Global Change Biology*, *27*(17), 4040–4059. https://doi.org/10.1111/gcb.15659

Appendix 6

Application of the G-res Tool to a Possible Scenario for the Potential Conawapa Generating Station Reservoir

Report on Data Inputs

This document describes the inputs used to apply the G-res Tool to the model potential future development of the Potential Conawapa Reservoir.

Developing a hydroelectric generating station at the Conawapa site on the lower Nelson River was an option conceived in the early 1970s, and Manitoba Hydro commissioned studies for a potential Conawapa Generation Project in the 2000s (Manitoba and Manitoba Hydro, 2015). This author is not aware of plans to build the Conawapa Generating Station. Such a development is not included as a potential option in Manitoba Hydro's 2025 Integrated Resource Plan for meeting future energy needs to 2025 (Manitoba Hydro, 2025).

The inputs used in the Conawapa G-res Model represent a possible scenario for modelling reservoir GHG emissions from future hydroelectric development. They do not represent a development plan being proposed by Manitoba Hydro.

1 Possible Site of Potential Conawapa Generating Station:



Source: B. Gill October 29, 2007
Figure 1-1 Looking Downstream at the Site "Axis B" of the Potential Conawapa Generating Station

The Potential Conawapa Generating Station modelling scenario is a 1,485 MW hydroelectric facility located on the lower Nelson River (Figures 1-1 and 1-2) and it would become Manitoba Hydro's largest hydroelectric generating station if built (Manitoba and Manitoba Hydro, 2015). The station would be located approximately 28.5 km downstream of the Limestone Generating Station and approximately 90 km northeast of the Town of Gillam (Manitoba and Manitoba Hydro, 2015).

Under this modelling scenario the Conawapa reservoir could flood approximately 11 km^2 of land and 27.8 km^2 of water, for a total reservoir size of approximately 38.8 km^2. To be conservative and not underestimate potential reservoir GHG emissions, the amount of flooded land used in this modelling scenario is double that which has been cited as a possible planning

concept (Manitoba Hydro, 2013). The reservoir would be contained almost entirely within the natural banks of the Nelson River.

The reservoir would be operated as a run of the river reservoir where the water levels are controlled by the discharges of the Kettle Generating Station. The Full Supply Level of the reservoir could be 57.2 m ASL (Manitoba Hydro, 2013).

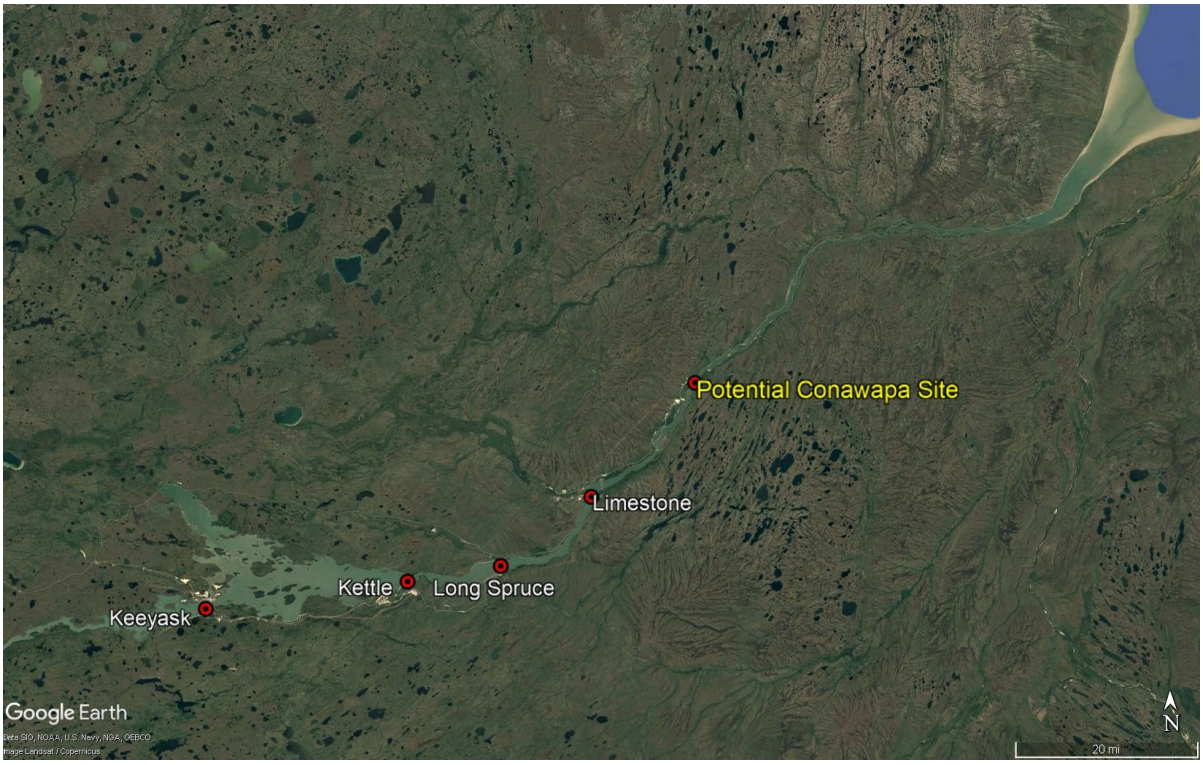
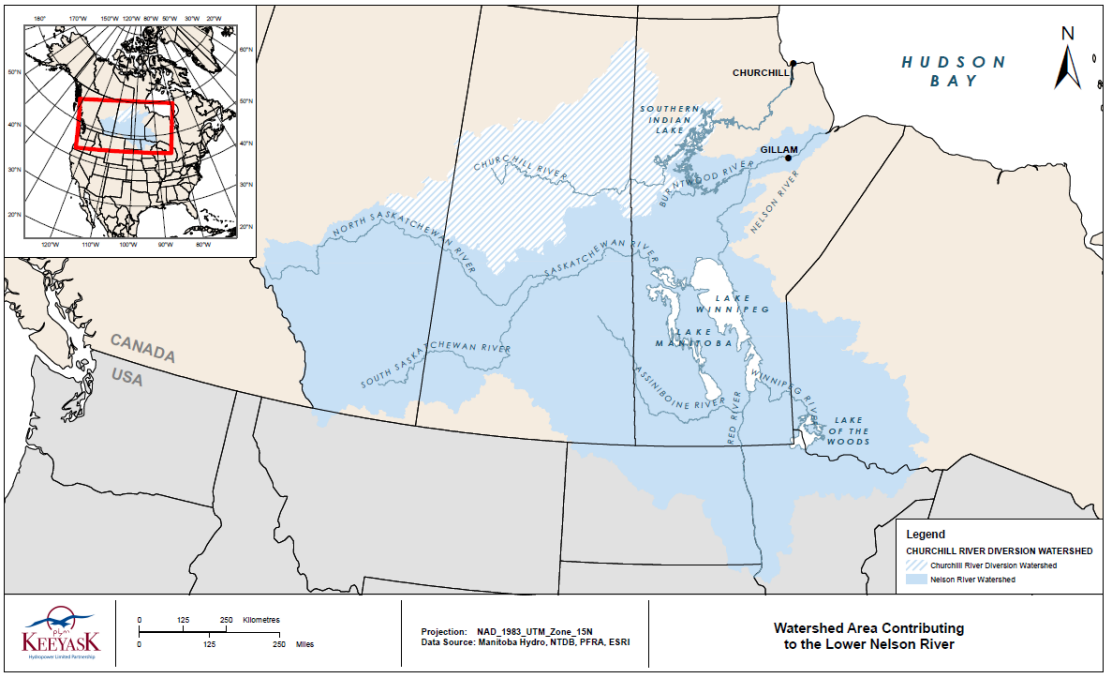


Figure 1-2 Location of a Possible Future Conawapa Generating Station

2 G-res Tool "Catchment Data"

The Potential Conawapa Reservoir watershed area is illustrated below in Figure 2-1.



Source: Keeyask Hydropower Limited Partnership, 2012a (Map 4.3-1)
Figure 2-1 Lower Nelson River Watershed

Model inputs pertaining to: Catchment Area, Population in the Catchment, and Catchment Annual Runoff were derived from the G-res Tool Earth Engine.

So as not to underestimate reservoir GHG emissions by assigning a portion to wastewater and sewage treatment, the release of phosphorus from community sewage and the release of phosphorus from industrial sewage were set to zero. Therefore, no portion of the reservoir GHG emissions were assigned to another anthropogenic source other than the Potential Conawapa Reservoir.

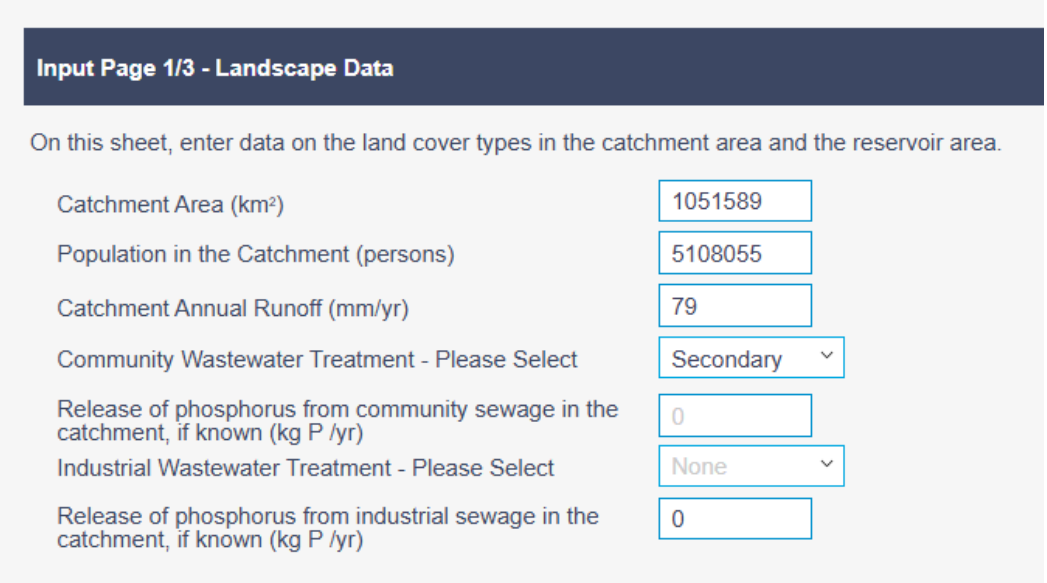


Figure 2-2 G-res Landscape Data Generated by G-res Earth Engine

2.1 Land Cover in the Catchment Area

Land Cover in the Catchment Area inputs were derived from the G-res Tool Earth Engine. It is understood that these inputs will not be used in the G-res Tool calculations of pre-flood GHG emissions. Pre-flood GHG remissions will be calculated using the G-res Pre-Impoundment Land Cover in the Reservoir Area input sheet, which were derived from Potential Conawapa reservoir site-specific information, as described in Section 2.2 below.

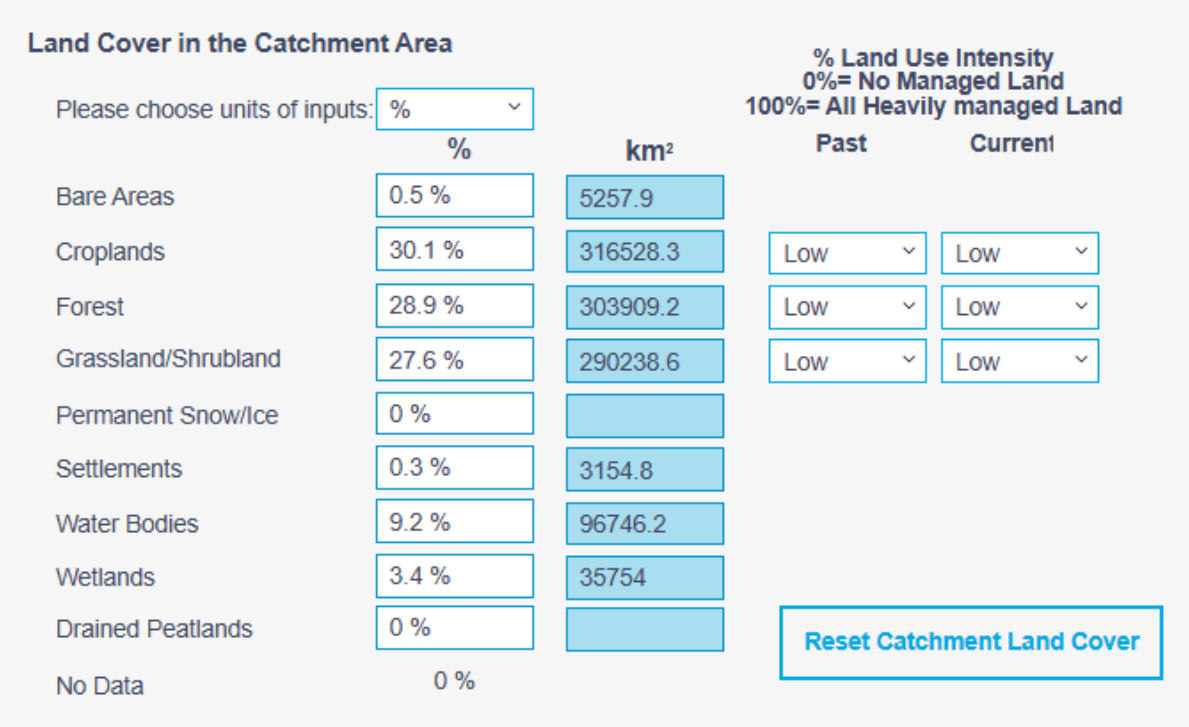


Figure 2-3 Landcover Data Generated by the Conawapa G-res Earth Engine

2.2 Pre-Impoundment Land Cover in the Reservoir Area

Pre-Impoundment Land Cover in the Reservoir Area inputs were derived from the following sources:

2.2.1 Reservoir Area (km2)



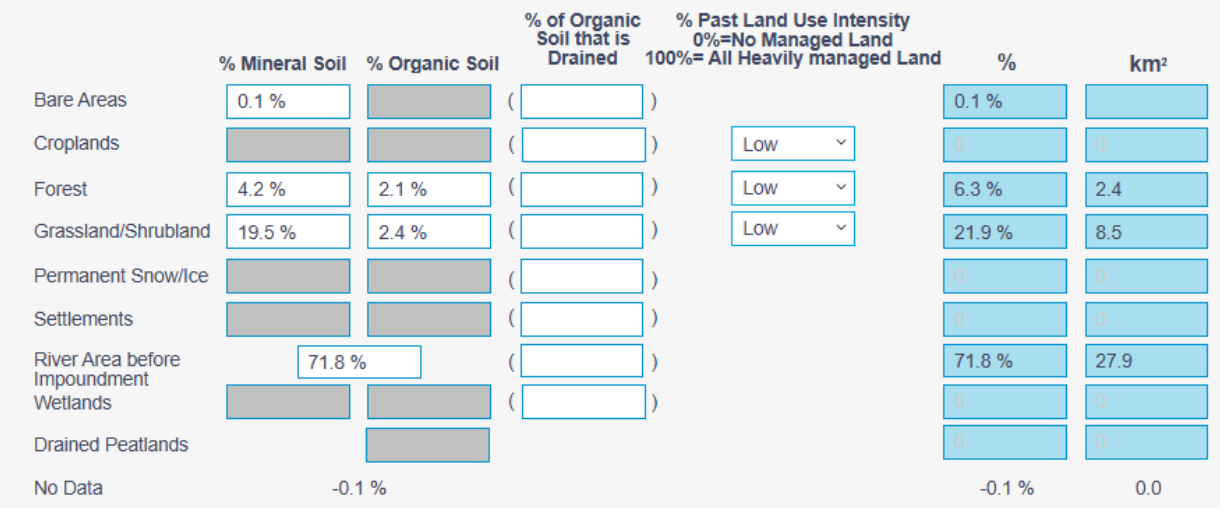
Figure 2-4 Total Potential Conawapa Reservoir Area (km^2)

Under this modelling scenario, the Potential Conawapa reservoir could flood approximately 11.0 km^2 of land and 27.8 km^2 of existing aquatic systems for a total area of 38.8 km^2.

2.2.2 Pre-Impoundment Land Cover in the Reservoir Area

2.2.2.1 Input Values

The input values used are as follows:



	% Mineral Soil	% Organic Soil	% of Organic Soil that is Drained	% Past Land Use Intensity 0%=No Managed Land 100%= All Heavily managed Land	%	km²
Bare Areas	0.1 %		( )		0.1 %	
Croplands			( )	Low	0	0
Forest	4.2 %	2.1 %	( )	Low	6.3 %	2.4
Grassland/Shrubland	19.5 %	2.4 %	( )	Low	21.9 %	8.5
Permanent Snow/Ice			( )		0	0
Settlements			( )		0	0
River Area before Impoundment	71.8 %		( )		71.8 %	27.9
Wetlands			( )		0	0
Drained Peatlands					0	0
No Data	-0.1 %				-0.1 %	0.0

Figure 2-5 Conawapa Reservoir Pre-Impoundment Landcover Data

2.2.2.2 Overview of Pre-Impoundment Land Cover in the Reservoir Area

The reservoir would be contained almost entirely within the natural banks of the Nelson River, Figures 2-6 to 2-8.

The pre-flood landcover types for the Conawapa G-res model are illustrated in Table 2-1.



Figure 2-6 Nelson River Upstream of Potential Conawapa Site.
Illustration of Steep Riverbanks and Bare Shorelines October 29, 2007



Figure 2-7 Nelson River Upstream of Potential Conawapa Site.
Illustration of Steep Riverbanks and Bare Shorelines



Figure 2-8 Looking Upstream at the Potential Conawapa Site. Illustrating Steep Riverbanks

Table 2-1 Conawapa Reservoir G-res Model Landcover Classification

Pre-Impoundment Land Cover in the Potential Conawapa Reservoir Area

	% Mineral Soil	% Organic Soil	% Total
Croplands			
Bare Areas	0.1%	0.0%	0.1%
Wetlands	0.0%	0.0%	0.0%
Forest	4.2%	2.1%	6.2%
Grassland/Shrubland	19.5%	2.4%	21.9%
Permanent Snow/Ice			
Settlements			
Total Terrestrial			**28.2%**
Water Bodies			71.8%
Total			**100.0%**

2.2.1 Replacement of G-res Tool Generic Emission Factors

Default G-res Tool pre-flood CO_2 and CH_4 emission factors for "Forest", "Grassland/Shrubland", and "Wetlands" were replaced by CO_2 emission factors developed by Virkkala et al. (2021) and by CH_4 emission factors adopted from Kuhn et al. (2021) and Treat et al. (2018). The default G-res Tool pre-flood emission factors for "Water Bodies" were replaced by in-situ measurements of CH_4 diffusive emissions of Gull Lake and associated backbays conducted by Environnement Illimité inc. during 2009 – 2013 (Marchand et al., 2015). The development of these emission factors is summarized below. Details are described in thesis Chapter 3 and in Appendix 1.

2.2.1.1 CO_2 Terrestrial Emission Factors

Annual CO_2 emission factors (Net Ecosystem Exchange) for the Boreal Upland and Boreal Wetland were selected from Virkkala et al. (2021). They were based on a study period of 1990-2015 (Table 2-3). Virkkala et al. (2021) did not develop separate emission factors for mineral and organic soils. These emission factors were used as composite emission factors for both mineral and organic soils in the Keeyask G-res model. The Virkkala et al. (2021) Boreal Upland CO_2 emission factors were used for the G-res categories of Forest and Grassland/Shrubland, and the Boreal Wetland CO_2 emission factors were used for the G-res Wetland category.

Table 2-2 CO_2 Emission Factors Used for the Potential Conawapa Reservoir G-res Model

CO_2 Emission Factors for Ecological Land Classification		
Land Class	**Annual NEE g CO_2-C/m^{-2}/yr**	**Annual NEE t CO_2-C/ha/yr (Converted for G-res)**
Boreal Uplands (Forest, and Grassland/Shrubland)	-47	-0.47
Boreal Wetlands	-38	-0.38
Source: Virkakkala et al., 2021 (Table 1)		

2.2.1.2 CH_4 Terrestrial Emission Factors

CH_4 emission factors were adapted from the Boreal–Arctic Wetland and Lake Methane Dataset (BAWLD-CH4) (Kuhn et al., 2021).

Growing season CH_4 terrestrial emission factors were adopted from Kuhn et al. (2021) Table 3 median values for Boreal Forest, Permafrost Bog, Bog, Fen, and Marsh land classes. Non-growing season emission factors were not included in the BAWLD-CH4 database/Kuhn et al. (2021) study. They were therefore estimated as being 16% of total annual emissions according to Treat et al. (2018). The Keeyask Ecological Land Classifications of "Swamps" and "Riparian" were assigned the same emissions factors as the BAWLD-CH4 emission factors for bogs and fens, respectively, following descriptions by Kuhn et al. (2021).

A composite wetland emission factor was developed by developing a weighted average for the land classifications of Permafrost Bog, Bog, Fen, Marsh, and Peatland Lakes (small and medium). This involved multiplying each [wetland class] by their [CH_4 emission factor], by their [areal extent (km^2) as defined by the Keeyask Ecological Land Classification, and by summing these calculations. The results are displayed in Table 2-3.

Table 2-3 Composite CH_4 Emission Factors Used for the Potential Conawapa Reservoir G-res Model

Land Class	**Annual Emissions kg CH_4/ha/yr (G-res Emission Factor Metrics)**
Boreal Uplands (Forest, and Grassland/Shrubland)	-0.64
Boreal Wetlands	51.13

2.2.1.3 Pre-flood Aquatic GHG Emission Factors

The G-res default emission factor was replaced by the pre-flood flux of 5 mg $CH_4/m^2/yr$ which translates into 9.25 kg CH_4/ha/yr. This emission factor was derived by Environnement Illimité inc. from their in-situ measurements of CH_4 diffusive emissions from Gull Lake and associated backbays during 2009 – 2013 (Marchand et al., 2015).

G-res does not include pre-flood CO_2 emission factors for water bodies.

Table 2-4 illustrates the pre-flood emission factors used in the Potential Conawapa Reservoir G-res Model scenario. The site-specific emission factors developed for "Forest", "Grassland/Shrubland", "Wetlands" and "Water Bodies" are highlighted.

Table 2-4 Potential Conawapa Reservoir G-res Model Pre-Flood Emission Factors

Climate: Boreal

	CH_4 Emission Factor (kg CH4/ha/yr)		CO_2 Emission Factor (t CO2-C/ha/yr)	
	Mineral Soil	Organic Soil	Mineral Soil	Organic Soil
Cropland	0	0	0	7.9
Bare Areas	0	6.1	0	2.8
Wetlands	51.13	51.13	-0.38	-0.38
Forest	-0.64	-0.64	-0.47	-0.47
Grassland/Shrubland	-0.64	-0.64	-0.47	-0.47
Urban Areas	0	19.6	0	6.4
Water Bodies	9.3			
Drained Peatlands				

2.2.3 Determine River Area Before Impoundment

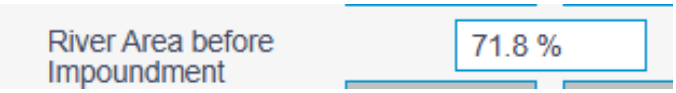


Figure 2-9 Conawapa G-res Model River Area Before Impoundment

The River Area before Impoundment was calculated as:

Pre-existing river area to be flooded (27.8 km^2) / Total Reservoir Area (38.8 km^2) = 71.8%.

3 Reservoir Data

3.1 Input Values

The input values used are as follows:

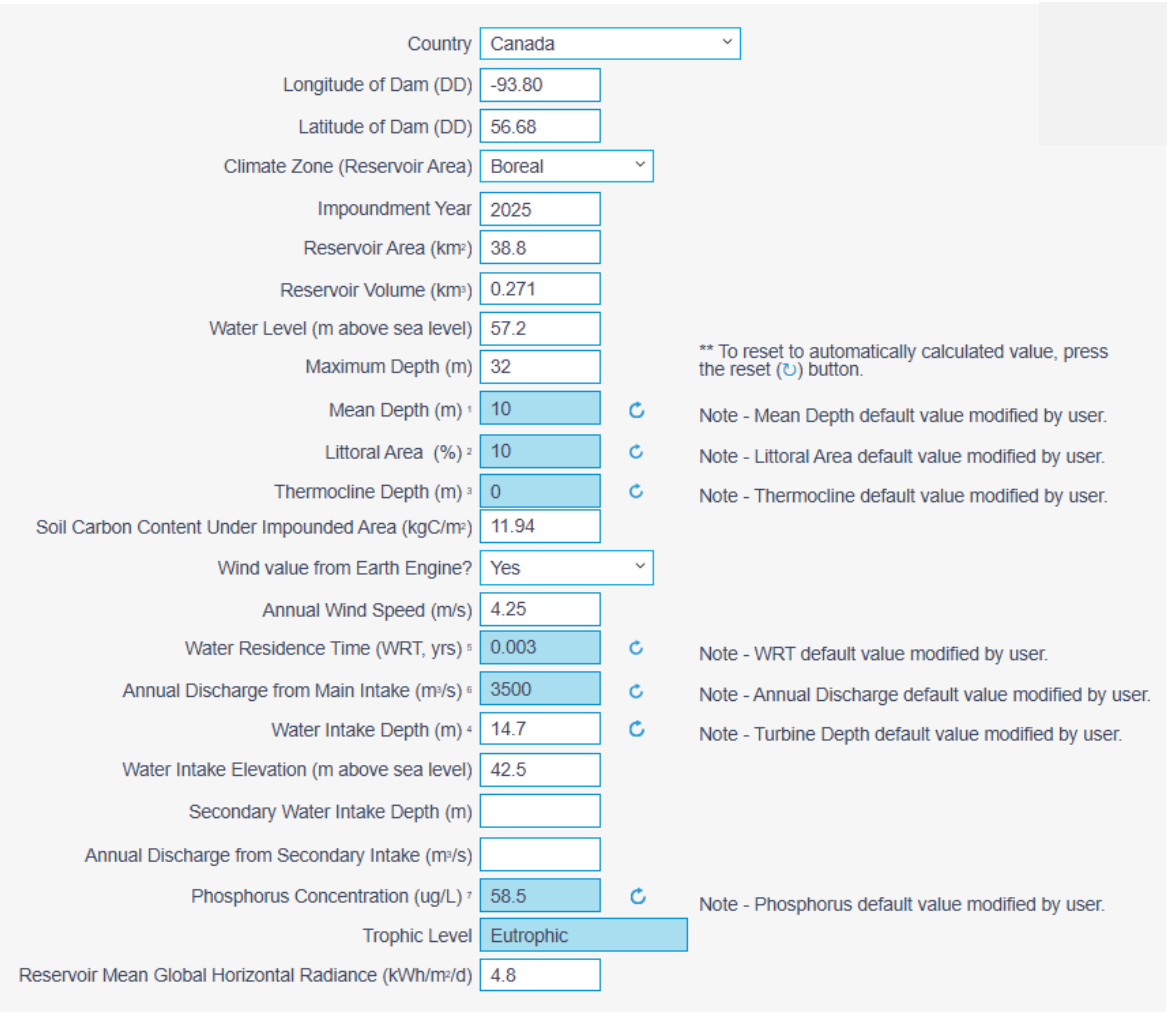


Figure 3-1 Potential Conawapa G-res Model: Reservoir Data

Longitude and Latitude:
The Longitude (-93.80 W) and Latitude (56.68 N) of the Dam refer to the location of the Potential Conawapa Generating Station.

Climate Zone:
The Potential Conawapa Reservoir is located within the Hudson Plains Ecozone (Government of Canada 2013). The climate is classified as Cool Continental/Sub Arctic (Dfc) based on the Köppen–Geiger Climate Classification (Kottek et al., 2006, Amani et al., 2019). The "Boreal" climate zone was selected from the G-res Tool.

Impoundment Year: 2050
For modelling purposes, the year 2050 was selected. This is to coincide with Manitoba's and Canada's 2050 carbon neutral economy goals. There is no proposal, timeline, nor decision to build Conawapa.

Reservoir Area (km^2): 38.8 km^2
Under the modelling scenario, the Potential Conawapa reservoir could flood approximately 11.0 km^2 of land and 27.8 km^2 of existing aquatic systems for a total area of 38.8 km^2.

Reservoir Volume (km^3): 0.271 km^3
The volume of the Potential Conawapa Reservoir for this modelling scenario is 0.271 km^2. The surface area (km^2) of the Potential Conawapa reservoir is 1.426 x larger than the Limestone reservoir. The estimated volume of the Limestone reservoir (0.19 km^3) was multiplied by 1.426 to estimate the volume of the Conawapa reservoir. This is a source of uncertainty in the Conawapa G-res Model.

Water Level (m above sea level): 57.2 m above sea level
Under this scenario, the water level of the Potential Conawapa reservoir would be controlled by the Kettle Generating Station. The Full Supply Level of the reservoir is estimated to be 57.2 m ASL.

Maximum Depth (m): 32 m
The maximum depth of the reservoir was estimated to be 32 m. The model was also run for a maximum depth of 30 m, which did not change the results.

Mean Depth (m): 10 m
The mean depth of the reservoir was estimated as 10 m. This is based on the minimum and maximum depth of the reservoir being estimated as 5 and 32 m respectively. The G-res Model was also run with a mean depth of 7 m as estimated for the Limestone reservoir. The results remained the same.

Littoral Area (%): 10%
A value of 10% was used for the Conawapa Model.

Thermocline Depth (m): 0
The thermocline depth was set as 0 m. It was assumed that this run-of-river reservoir would not stratify, and would be similar as the upstream Limestone and Long Spruce reservoirs which are also run-of-river reservoir and of similar size.

Soil Carbon Content Under the Impoundment Area (kg C/m^2): 11.94 kg C/m^2
The value of 11.94 kg C/m^2 was derived from the Earth Engine functionality of the G-res Tool. For comparison, this value aligns well with IPCC 2019 default value of 11.6 ±65% kg C/m^2 for the soil organic carbon stock content for Boreal Moist/Dry wetland soils for 0-30 cm depth (IPCC 2019, Table 2.3).

This value is also similar to the average carbon content of 10.8 kg C/m^2 in peat-forming soils at a depth of 0-30 cm in a boreal forest site located south of James Bay (Magnan et al., 2020). Similarly, Beaulne et al (2021) calculated that between 11.0 – 12.6 kg C/m^2 has been stored in the organic horizons of a boreal peatland site in eastern Canada over the last 200 years.

Annual Wind Speed: 4.25 m/s

The value of 4.25 m/s was derived from the Earth Engine functionality of the G-res Tool.

This value is within the range of average wind speeds of 3.89 m/s to 4.94 m/s recorded in Gillam, Manitoba from 1971 to 2000 (Keeyask Hydropower Limited Partnership, 2012b). The meteorological station in Gillam is located approximately 90 km southwest of the Potential Conawapa Generating Station (Manitoba Hydro, 2015).

Water Residence Time (WRT, yrs): 0.003 yrs

The Water Residence Time for the potential Conawapa reservoir was estimated as being 0.003 years. In lieu of available data, the Limestone reservoir was used as a poxy since it is similar in surface area and length (Table 3-1).

Table 3-1 Comparison of Limestone and Conawapa Reservoirs

Limestone and Potential Conawapa Reservoirs

	Surface Area (km^2)	Length (km)
Limestone	27.2 [1]	23 [2]
Potential Conawapa	38.8 [3]	30 [3]

Source:
1) Manitoba Hydro 2015
2) Google Earth measurement by author

Annual Discharge from Main Intake (m^3/s): 3,500 m^3/s

The average annual discharge was estimated to be 3,500 m^3/s. This value is based on the annual average water discharge rate at the Manitoba Hydro water gauge (05UF007) located on the Nelson River at the Long Spruce Generating Station for the years 1987 to 2023. This is the time period where data is available for this station at the Environment Canada Water Office website: https://wateroffice.ec.gc.ca/search/historical_e.html.

This could be an overestimate, as the estimated average flow has been reported in the Needs For and Alternatives To Appendix 7.2 – Range of Resource Options as 3,200 m^3/s (Manitoba Hydro, 2013). The difference from using an annual discharge of 3,200 m^3/s as compared to

3,500 m^3/s amounted to a 0.6% change in annual and 100-year lifecycle Net emissions. There was no change to Emission Intensity.

Water Intake Depth (m): 14.7 m
The height of the water intake structures were estimated to be between 15 m below the reservoir water surface. This is roughly adapted from the Keeyask Generating Station.

Water Intake Elevation (42.5 m above sea level):
The elevation of the top and bottom of the Water Intake was estimated to be 42 m ASL.

Phosphorus Concentration (µg/L): 58.5 µg/L
The Keeyask Aquatic Effects Monitoring Plan benchmark of 58.5 µg/L was used in the G-res Potential Conawapa model.

Trophic Level: Eutrophic
Based on Total Phosphorus concentrations, the main stem of the Nelson River is classified as meso-eutrophic to eutrophic (Keeyask Hydropower Limited Partnership, 2012b).

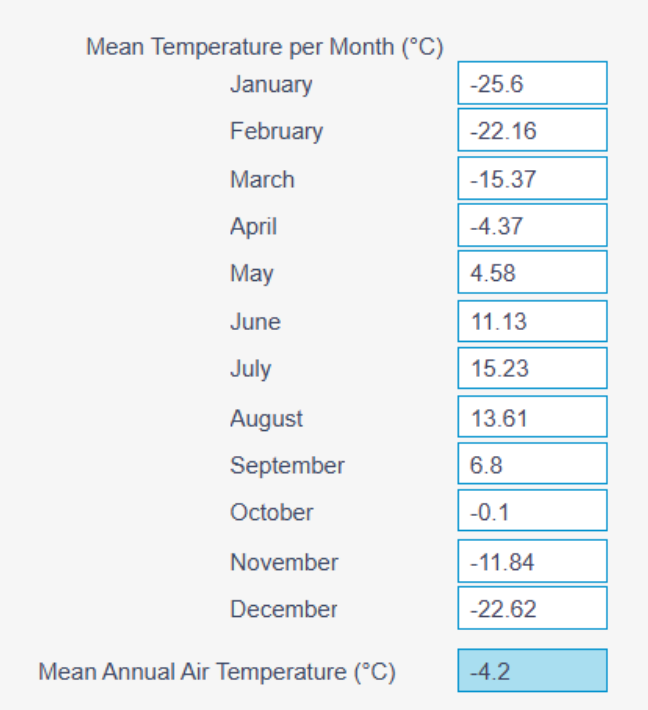
So as not to underestimate GHG emissions, the Potential Conawapa reservoir was classified as eutrophic for the G-res Model.

Reservoir Mean Global Horizontal Radiance (kWh/m^2/d): 4.8
The Reservoir Mean Global Horizontal Radiance value of 4.8 kWh/m^2/d was generated by the G-res Tool Earth Engine.

For comparison, the on-line, interactive Photovoltaic Potential and Solar Resource Maps of Canada estimates mean annual global insolation values of 3.18 kWh/m^2/d for the Town of Gillam, Manitoba (Natural Resources Canada, 2020). The estimates are based on horizontal 0-degree orientation on a 60 arc seconds (approximately 2 km grid). Gillam is located approximately 90 km southwest (upstream) of the Potential Conawapa Generating Station (Figure 1-2).

To be conservative, the elevated value of 4.8 kWh/m^2/d was used in the G-res Tool modeled estimates.

Mean Temperature per Month (°C)
Mean Temperature per Month and Mean Annual Air Temperature data were derived by the G-res Tool Earth Engine.



Mean Temperature per Month (°C)	
January	-25.6
February	-22.16
March	-15.37
April	-4.37
May	4.58
June	11.13
July	15.23
August	13.61
September	6.8
October	-0.1
November	-11.84
December	-22.62
Mean Annual Air Temperature (°C)	-4.2

Figure 3-2 Mean Average Monthly Temperatures

4 Reservoir Services Data

100% of the Reservoir Services were allocated to the Potential Conawapa Reservoir/hydroelectricity.

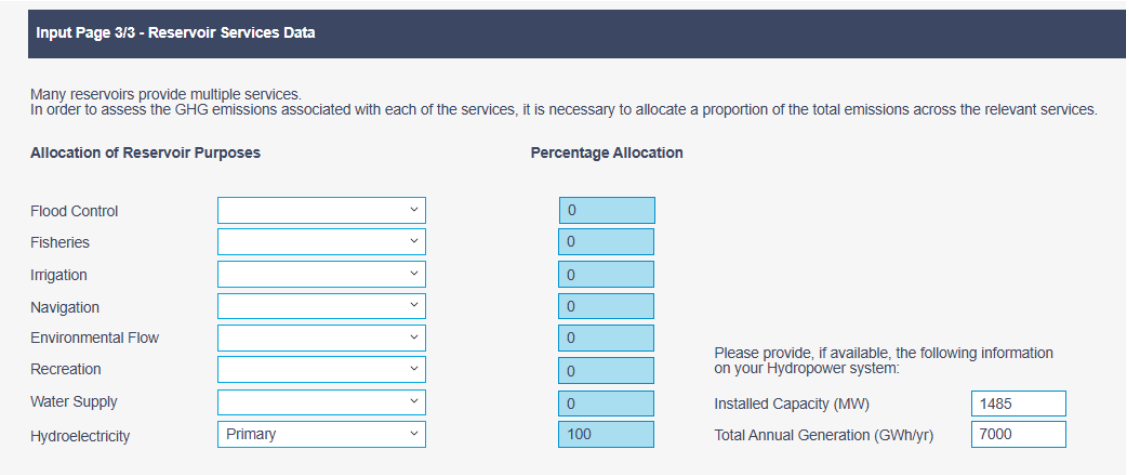


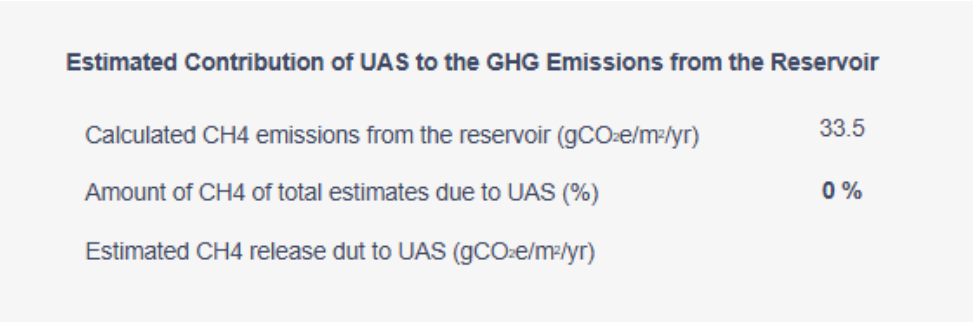
Figure 4-1 Conawapa G-res Model: Reservoir Services

5 Construction GHG

The G-res Tool was not used to estimate Construction Emissions.

6 Unrelated Anthropogenic Sources Emissions

Since 100% of the purpose of the Potential Conawapa Reservoir is assigned to hydroelectricity, no GHG emissions were allocated to Unrelated Anthropogenic Sources.



Estimated Contribution of UAS to the GHG Emissions from the Reservoir	
Calculated CH4 emissions from the reservoir ($gCO_2e/m^2/yr$)	33.5
Amount of CH4 of total estimates due to UAS (%)	**0 %**
Estimated CH4 release dut to UAS ($gCO_2e/m^2/yr$)	

Figure 6-1 Conawapa G-res Model: Contribution of Unrelated Anthropogenic Sources of GHG Emissions

References

Amani, M., Mahdavi, S., Afshar, M., Brisco, B., Huang, W., Mirzadeh, S.M.J., White, L., Banks, S.N., Montgomery, J., Hopkinson, Cs. (2019). Canadian Wetland Inventory using Google Earth Engine: The First Map and Preliminary Results. Remote Sensing. 11. 842. 10.3390/rs11070842.

Beaulne, J., Garneau, M., Magnan, G., Boucher, É. (2021). Peat deposits store more carbon than trees in forested peatlands of the boreal biome. Sci Rep 11, 2657. https://doi.org/10.1038/s41598-021-82004-x

Government of Canada. (2013). National Ecological Framework for Canada. Ecozones, Ecoregions, and Ecodistricts.
https://sis.agr.gc.ca/cansis/publications/maps/eco/all/districts/eco_all_districts_1m_manitoba.jpg

Government of Canada. (2025). Monthly Discharge Data for Nelson River at Kettle Generating Station (05UF006) [MB].
https://wateroffice.ec.gc.ca/report/historical_e.html?stn=05UF006&dataType=Monthly&parameterType=Flow&year=2023&mode=Table&mean1=1&scal…

IPCC (2019). Chapter 2: Generic Methodologies Applicable to Multiple Land-Use Categories, Volume 4 Agriculture, Forestry and Other Land Use, 2019 Refinement to the 2006 IPCC Guidelines for National Greenhouse Gas Inventories, 104 pages.

Keeyask Hydropower Limited Partnership (2012a). Keeyask Generation Project: Environmental Impact Statement; Physical Environment Response to EIS Guidelines, Supporting Volume. 1018 pages.

Keeyask Hydropower Limited Partnership (2012b). Keeyask Generation Project: Environmental Impact Statement; Aquatic Environment Supporting Volume. 1745 pages.

Kottek, M., Grieser, J., Beck, C., Rudolf, B., Rubel, F. (2006). World map of the Köppen-Geiger climate classification updated. Meteorol. Z., 15, 259–263.

Kuhn, M. A., Varner, R. K., Bastviken, D., Crill, P., Macintyre, S., Turetsky, M., Walter Anthony, K., McGuire, A. D., & Olefeldt, D. (2021a). BAWLD-CH4: A comprehensive dataset of methane fluxes from boreal and arctic ecosystems. In *Earth System Science Data* (Vol. 13, Issue 11, pp. 5151–5189). Copernicus Publications. https://doi.org/10.5194/essd-13-5151-2021

Magnan, G., Garneau, M., Le Stum-Boivin, É., Grondin, P., and Yves Bergeron, Y. (2020). Long-Term Carbon Sequestration in Boreal Forested Peatlands in Eastern Canada. Ecosystems 23, 1481–1493. https://doi.org/10.1007/s10021-020-00483-x

Manitoba and Manitoba Hydro. (2013). Needs For and Alternatives To Appendix 7.2 – Range of Resource Options. 367 pages.
https://www.pubmanitoba.ca/nfat/pdf/hydro_application/appendix_07_2_range_of_resource_options.pdf

Manitoba and Manitoba Hydro. (2015). Regional Cumulative Effects Assessment for Hydroelectric Developments on the Churchill, Burntwood and Nelson River Systems. Phase II Report. https://www.hydro.mb.ca/docs/regulatory_affairs/pdf/rcea/rcea_phase2_part_ii_hydroelectric_development_project_description.pdf

Manitoba Hydro. (2025). 2025 Integrated Resource Plan: Road Map. https://www.hydro.mb.ca/docs/corporate/irp/2025-irp-roadmap.pdf

Marchand D., M. Demarty, and R. Gill. (2015). Keeyask Technical Summay – 2014. Summary prepared by Environnement Illimité for Manitoba Hydro, 11 p.

Natural Resources Canada (2020). Photovoltaic Potential and Solar Resource Maps of Canada. © Her Majesty the Queen in Right of Canada, as represented by the Minister of Natural Resources, 2020. https://fgp-pgf.maps.arcgis.com/apps/webappviewer/index.html?id=c91106a7d8c446a19dd1909fd93645d3

Treat, C. C., Bloom, A. A., & Marushchak, M. E. (2018). Nongrowing season methane emissions–a significant component of annual emissions across northern ecosystems. *Global Change Biology*, *24*(8), 3331–3343. https://doi.org/10.1111/gcb.14137

Virkkala, A. M., Aalto, J., Rogers, B. M., Tagesson, T., Treat, C. C., Natali, S. M., Watts, J. D., Potter, S., Lehtonen, A., Mauritz, M., Schuur, E. A. G., Kochendorfer, J., Zona, D., Oechel, W., Kobayashi, H., Humphreys, E., Goeckede, M., Iwata, H., Lafleur, P. M., … Luoto, M. (2021). Statistical upscaling of ecosystem CO2 fluxes across the terrestrial tundra and boreal domain: Regional patterns and uncertainties. *Global Change Biology*, *27*(17), 4040–4059. https://doi.org/10.1111/gcb.15659

Appendix 7

Application of the G-res Tool to the Churchill River Diversion

Report on Data Inputs

This document describes the inputs used to apply the G-res Tool to the Churchill River Diversion located in northern Manitoba.

1 Churchill River Diversion:

The Churchill River Diversion (CRD) has the potential to redirect approximately 80% of the water flowing through the Churchill River into the Nelson River basin (Manitoba and Manitoba Hydro, 2015b). The CRD was developed to augment flows for hydropower generating stations on the Burtwood-Nelson River system. Studies conducted during the 1960s concluded it would be more economical to develop hydropower on the Burntwood-Nelson River system with enhanced flows from the Churchill River as opposed to developing hydropower on both the Burntwood-Nelson system and the Churchill River (Know History Inc., 2016). Construction of the CRD commenced in 1973 and was operational in 1976 (Manitoba and Manitoba Hydro, 2014).

The CRD comprises three main components: 1) Missi Falls Control Structure; 2) South Bay Diversion Channel; and 3) Notigi Control Structure (Figures 1-1 & 1-2).

1.1 Missi Falls Control Structure

The Missi Falls Control Structure is a dam that was built at Missi Falls, which is the natural outlet of Southern Indian Lake (Manitoba and Manitoba Hydro, 2014, 2015b) (Figures 1-3 & 1-4). Southern Indian Lake is a natural swelling or enlargement of the Churchill River. The control structure regulates the amount of water that discharges downstream through the Churchill

River and amount of water impounded in Southern Indian Lake, and subsequently diverted into the Nelson River basin. In accordance with the final Manitoba Water Power Act Licence for the CRD, minimum releases from the control structure shall not be less than 14 m^3/s during the open water period and 42 m^3/s during the ice cover period (Manitoba Conservation and Climate, 2021).

1.2 South Bay Channel Diversion

The South Bay Diversion Channel is a passage way that was excavated to connect the South Bay of Southern Indian Lake to Issett Lake of the Rat River-Burntwood River-Nelson River system (Manitoba and Manitoba Hydro, 2015b) (Figure 1-5). The channel is approximately 61 m wide at its base and approximately 9.3 km long (Manitoba and Manitoba Hydro, 2015b). It became operational in 1976.

1.3 Notigi Control Structure

The Notigi Control Structure is located on the Rat River at the outlet of Notigi Lake. The structure controls the flow of the diverted Churchill River/Southern Indian Lake and the Rat River into the Burntwood River-Nelson River system (Manitoba and Manitoba Hydro, 2015b) (Figures 1-6 and 1-7). In accordance with the final Manitoba Water Power Act Licence for the CRD, average weekly flows released from the Notigi Control Structure shall not exceed 991 m^3/s from May 16th and October 31st, and shall not exceed 963 m^3/s from November 1st and May 15th (Manitoba Conservation and Climate, 2021). Mean monthly water levels in the Notigi forebay range from approximately 254.4 m to 258.3 m ASL (Manitoba and Manitoba Hydro, 2014).

1.4 CRD Flooding

The Missi Falls and Notigi Control Structures are operated so the mean daily water level (without the effect of wind and waves) on Southern Indian Lake is not greater than 258.32 m above sea level (Manitoba Conservation and Climate, 2021; Manitoba Hydro, 2022). Water levels on Southern Indian Lake are approximately 2.7 m higher than pre-CRD levels and

approximately 15.2 m higher upstream of the Notigi Control Structure (Manitoba and Manitoba Hydro, 2014).

The surface area of the flooded aquatic system in the Regional Cumulative Effects Assessment (RCEA) Zone 4 (e.g. Southern Indian Lake) and RCEA Zone 6 (e.g. Rat River, Issett Lake, Karsakawigimak Lake, Pemichigamau Lake, Central and West Mynarski Lakes, Rat Lake, and Notigi Lake) (Figure 1-3 & 1-6) are estimated to be 2,914 km^2 (Newbury et al., 1984; Manitoba and Manitoba Hydro, 2014). This includes approximately 759 km^2 of flooded land (Manitoba and Manitoba Hydro, 2014).

As discussed by McCullough (1981) the impact of flooding on water retention times varied amongst the flooded area. The retention times of water bodies that were on the path of the diverted Churchill River did not change markedly, whereas retention times for those basins that were isolated from the main flow doubled. The largest impact was in the area near the South Bay Diversion Channel where water retention times decreased by two orders of magnitude. Overall, estimated water retention times increased from 0.51 year pre-flood to 0.72 years after flooding (McCullough, 1981).

1.5 Preflood Landcover and Relevance for GHG Modelling

The CRD is located within the Precambrian Shield Physiographic Region (Natural Resources Canada, 2019). The northern portion of the CRD, which includes the portion of Southern Indian Lake north of Long Point, is located in the Taiga Shield Ecozone, Selwyn Lake Upland, Northern Indian Lake Ecodistrict (Smith et al., 1998). The southern portion of the CRD is located within the Boreal Shield Ecozone, Churchill River Upland Ecoregion, Southern Indian Lake Ecodistrict (Smith et al., 1998). Similarly, the northern portion of the CRD, which includes the northern

part of Southern Indian Lake, is in the Low Subarctic Wetland Region and the southern portion of the CRD is located within the High Boreal Wetland Region (Tarnocai, 2006).

1.5.1 Geology

The surficial geology is primarily comprised of Quaternary glaciolacustrine sediments that were deposited in glacial Lake Agassiz (Matile and Keller, 2006). The northern boundary of glacial Lake Agassiz migrated across RCEA Zones 4 and 6 of the present-day Churchill River Diversion approximately 10,300 to 9,000 years ago, based on the reconstruction of ice margins of the retreating Laurentide Ice Sheet (Gauthier et al., 2022). Most of Lake Agassiz had drained from Manitoba by approximately 7,700 years ago, except for Manitoba's contemporary "Great Lakes" (e.g. Lake Winnipeg, Lake Winnipegosis, Lake Manitoba) (Buchner, 1990). The layered Quaternary deposits are composed of clay, silt, and to a lesser amount sand, that range approximately 1 to 20 m thick (Matile and Keller, 2006). Theses clayey glaciolacustrine deposits extensively cover the area and have smoothed the underlying bedrock into a landscape that ranges from undulating to hummocky, with episodes of steeps slopes, irregular bedrock ridges and outcrops (Smith et al., 1998). Below these deposits are Paleozoic carbonates, and beneath these are Precambian granitoid and greenstone (Gauthier et al., 2022).

1.5.2 Peatlands

Peatlands cover much of the poorly drained clayey deposits, with deeper accumulations occuring in the topographic depressions (Smith et al., 1998; Tarnocai et al., 2011). Peat types include shallow peat, peat veneer, peat plateau bogs, and less frequently, fens and palsa bogs

(Smith et al., 1998). Discontinuous permafrost is occurs widely throughout the area and is associated with peat deposits (Smith et al., 1998).

1.5.3 Significance of Landcover and Geology

The significance of the landcover and underlying geology involves two characteristics that are related to modelling CRD GHG emissions. They are associated with flooding peatlands and flooding carbonate watersheds.

1.5.3.1 Modelling Peatlands

Peatlands are complex wetlands that store and cycle large amounts of carbon through intricate and interrelated systems (Baird et al., 2009; Amesbury et al., 2019; Nichols and Petreet, 2019; Hugelius et al., 2020; Yu et al., 2021). Northern peatlands have been considered as a "worst-case" scenario for flooding to create reservoirs (St. Louis et al., 2000) as they store thousands of years of net carbon accumulation (Nichols and Petreet, 2019). Once impounded, the flooded carbon can potentially become available for decomposition and the release of CO_2 and CH_4, plus, flooding will eliminate an important, pre-flood carbon sink (St. Louis et al., 2000; St. Louis et al., 2003).

The pre-flood CRD reservoir footprint is comprised of a variety of peatland types (Smith et al., 1998). Each of these peatland types have the potential to store, generate, and release GHGs at varying rates (Pelletier 2007, 2011, 2015; Turetsky et al., 2014; Treat et al., 2021;). Peatland GHG emissions vary in space and in time and are impacted by variables such as peat landform type, hydrological controls, regional climate, vegetation type, soil respiration, trophic level, and composition and abundance of microbial populations (Strack, 2008; Trudeau et al., 2013; Webster et al., 2018; Kuhn et al., 2021; Graham et al., 2022).

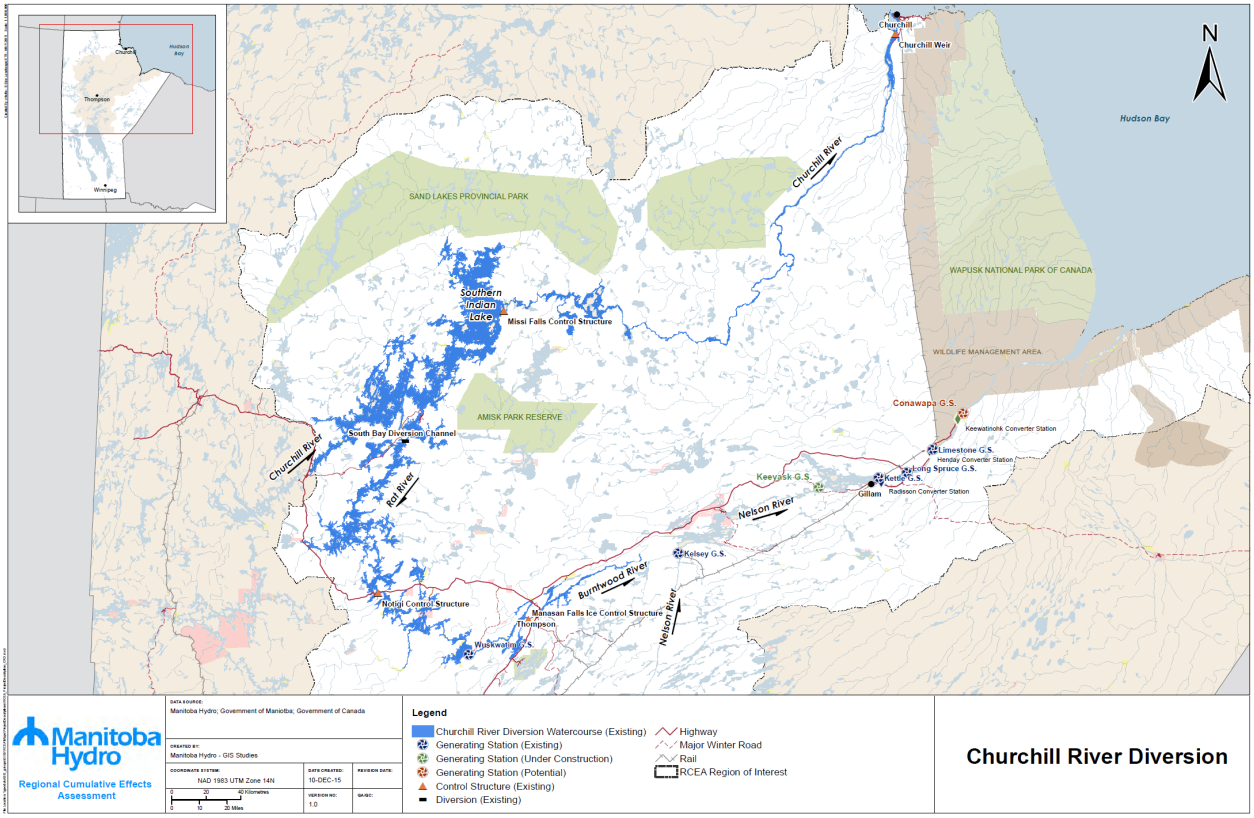
A challenge for modelling net CRD GHG emissions involves assigning or developing appropriate GHG emission factors to adequately represent GHG emissions from the pre-flood diverse peat landscape. This challenge is further complicated when trying to model post-flood GHG emissions as peatlands respond to environmental change in a non-linear manner (Baird et al.,

2009; Mahdiyasa et al., 2023). That is, a small change to the peatland environment can lead to a disproportionate change in GHG emissions (Belyea, 2009; Mozafari et al., 2023).

1.5.3.2 Modelling Carbonate Watersheds

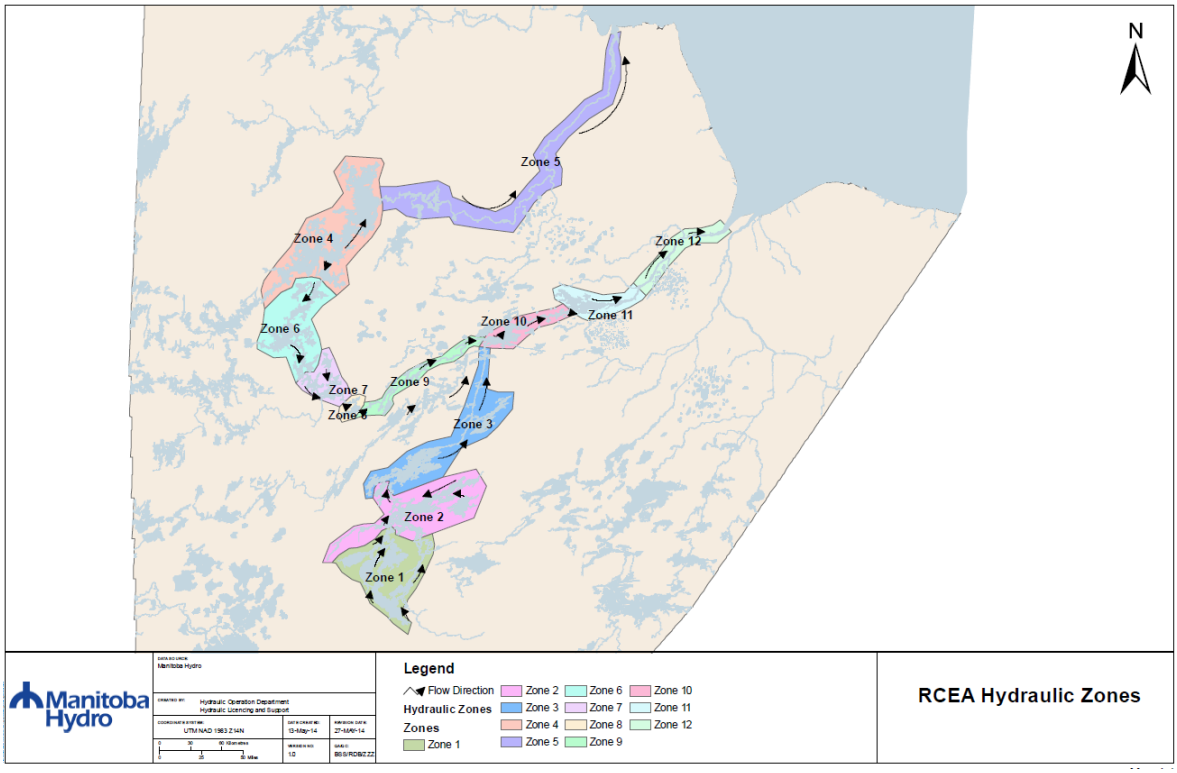
It is necessary to understand how carbon is cycled amongst terrestrial and aquatic systems before and after flooding in order to determine the impact that hydroeletric reservoirs have on GHG emissions. An aspect of carbon cycling that is challenging and not well studied is the lateral transfer of all organic and inorganic species of carbon from land to surface waters (Tank et al., 2018; Wang et al., 2019), including the transport of dissolved inorganic carbon (DIC) (Jarvie et al., 2017). In areas with carbonate strata (such as the Paleozoic carbonates that are beneath the CRD), chemical weathering of carbonate rock can produce significant quantities of DIC in the form of bicarbonate HCO_3^- (Jarvie et al., 2017; Tank et al., 2018). The contribution of DIC from chemical weathering can be the dominant form of carbon in some river systems, such as those that flow in karst terrain, as the Wujiang River, SW China (Han et al., 2018). After impounding this river for hydroelectric development, it appeared that biological processes became the key influence of carbon cycling over chemical weathering within the reservoir (Han et al., 2018).

A challenge for modelling CRD GHG emissions is applying a model such as G-res, whose formulas were developed from reservoir datasets that may not represent the carbonate deposits that lay beneath the CRD. For example, data collected from Quebec reservoirs (and which underpin in part, G-res formulas) may be more representative of Precambian bedrock (Vincent, 1985) than the carbonate strata underlying the CRD. It is challenging to model GHG emissions from flooding and land use change if the modells have not been calibrated with data that is site-specific to the area of interest.



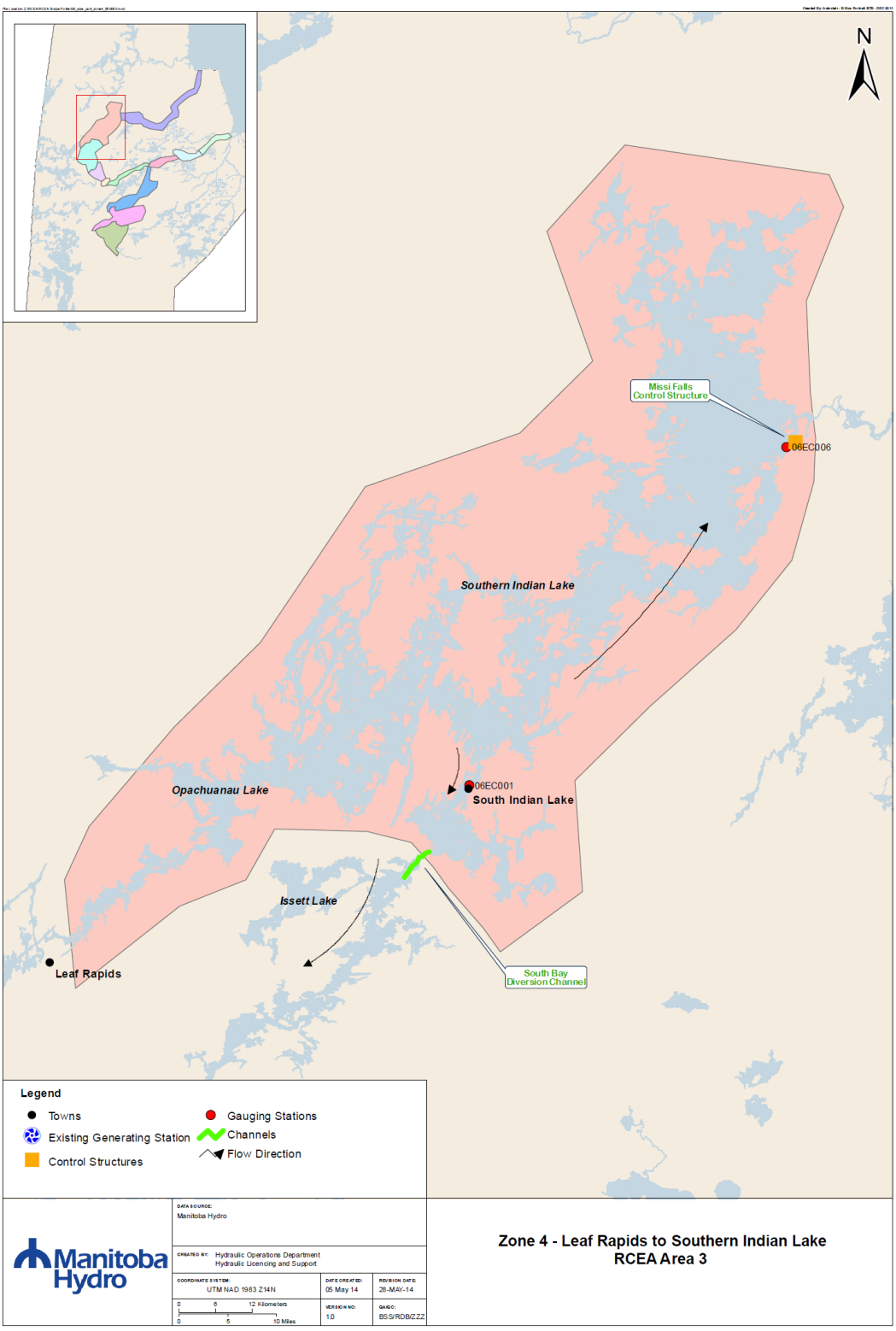
Source: Manitoba and Manitoba Hydro, 2014

Figure 1-1 Churchill River Diversion



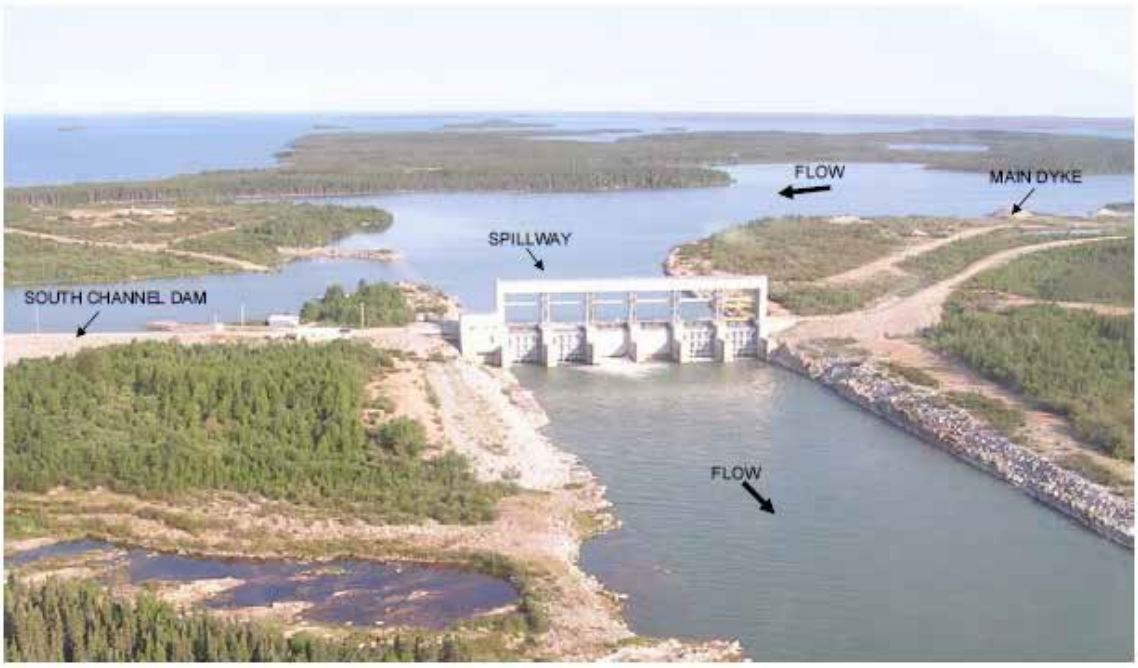
Source: Manitoba and Manitoba Hydro, 2014

Figure 1-2 Regional Cumulative Effects Assessment, Hydraulic Study Zones



Source: Manitoba and Manitoba Hydro, 2014

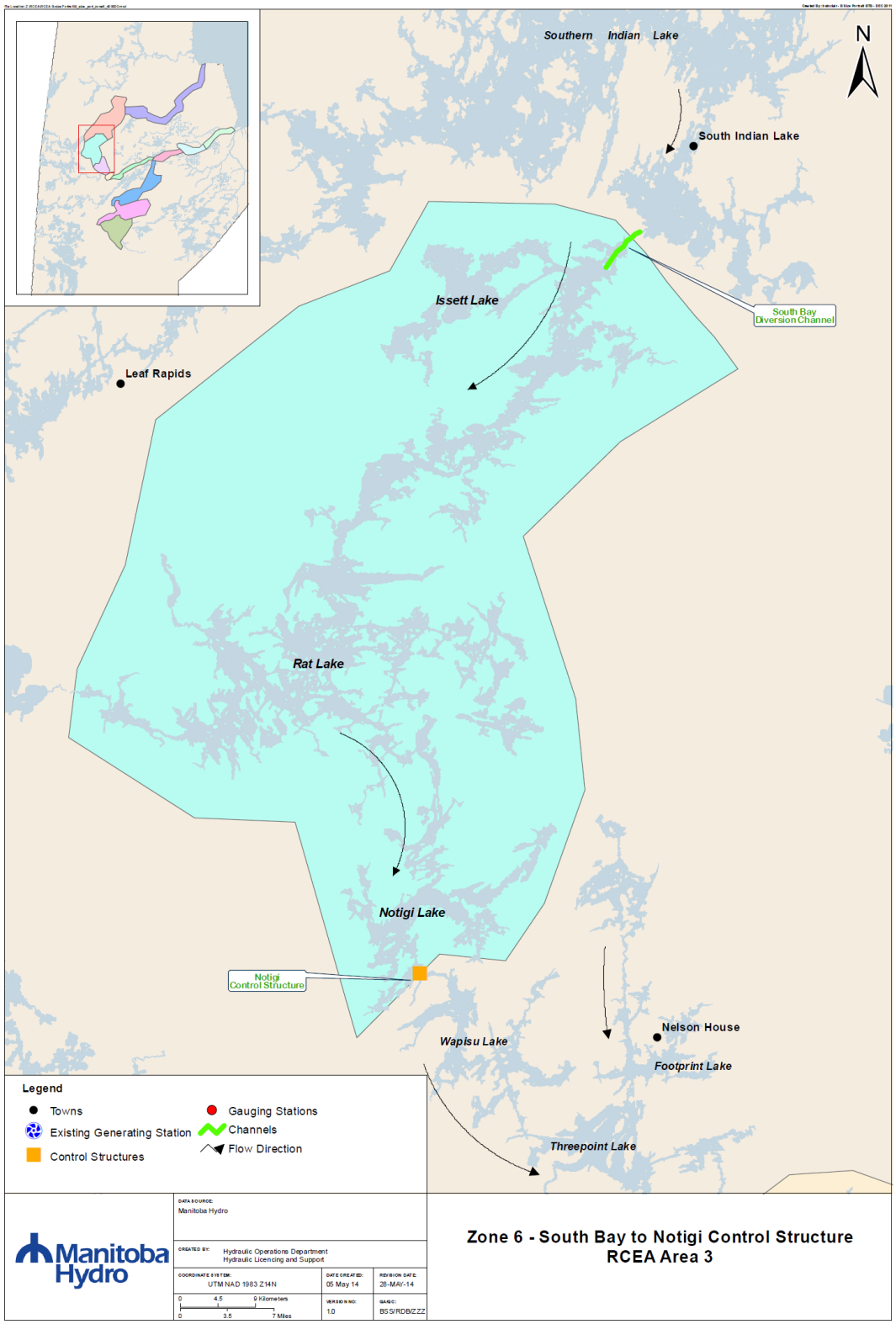
Figure 1-3 Regional Cumulative Effects Assessment, Hydraulic Zone 4



Source: Manitoba and Manitoba Hydro, 2015
Figure 1-4 Missi Falls Control Structure



Source: Manitoba and Manitoba Hydro, 2015
Figure 1-5 South Bay Diversion Channel



Source: Manitoba and Manitoba Hydro, 2014

Figure 1-6 Regional Cumulative Effects Assessment, Hydraulic Zone 6



Source: Manitoba and Manitoba Hydro, 2015
Figure 1-7 Notigi Control Structure

2 Pre-Impoundment Land Cover in the Reservoir Area

Pre-Impoundment Land Cover in the Reservoir Area inputs were derived from the following sources:

2.1 Reservoir Area (km2)

Pre-Impoundment Land Cover in the Reservoir Area

Reservoir Area (km²)	2914

Figure 2-1 Total Churchill River Diversion Area (km^2)

The total size of the flooded area was calculated to be 2914 km^2.

This includes:

- approximately 2,330 km^2 of flooded land in RCEA Zone 4 (Regional Cumulative Effects Assessment Phase 1 Report, Manitoba and Manitoba Hydro, 2014) plus
- approximately 584 km^2 flooded land in RCEA Zone 6 (Newbury et al., 1984)

2.2 Pre-Impoundment Land Cover in the Reservoir Area

2.2.1 Input Values

The input values used are as follows:

	% Mineral Soil	% Organic Soil	% of Organic Soil that is Drained	% Past Land Use Intensity 0%=No Managed Land 100%= All Heavily managed Land	%	km²
Bare Areas	1.1 %		( )		1.1 %	32.1
Croplands			( )	Low	0	0
Forest	3 %	1.7 %	( )	Low	4.7 %	137.0
Grassland/Shrubland	0 %	0 %	( )	Low		
Permanent Snow/Ice			( )		0	0
Settlements			( )		0	0
River Area before Impoundment	76.7 %		( )		76.7 %	2235.0
Wetlands		17.5 %	( )		17.5 %	510.0
Drained Peatlands					0	0
No Data	0 %				0.0 %	-0.1

Figure 2-2 CRD Pre-Impoundment Landcover Data

2.2.2 Overview of Pre-Impoundment Land Cover in the Reservoir Area

The pre-flood landcover classification that was used for the Keeyask G-res Model, "Keeyask Ecological Land Classification" was applied to the pre-flood CRD landcover. The Keeyask Ecological Land Classification is described in Chapter 3 and Appendix 1. As described above in Section 1.5 Pre-flood Landcover and Relevance for GHG Modelling, the pre-flood landscape includes peatlands, similar to the pre-flood Keeyask area. The Keeyask Ecological Land Classification was used in the absence of detailed pre-flood land cover data for the CRD flooded area. The Keeyask pre-flood land cover categories were apportioned to the pre-flood CRD area (Table 2-1).

Table 2-1 CRD Pre-Flood Land Cover Derived from Keeyask Pre-Flood Land Cover "Ecological Land Classification"

Keeyask Pre-Flood ECO LandClass Applied to Pre-Flood CRD Terrestrial Land

Landcover	Soil Type	Pre-Flood Terrestrial Area m^2	% of Keeyask Pre-Flood Land	Apply to Pre-Flood CRD [(1)] 26.0%
Forest	Mineral	5,297,344.18	11.5%	3.0%
Forest	Organic	3,018,704.20	6.5%	1.7%
Wetlands	Organic			17.5%
	Bog	27,596,341.24	59.9%	15.6%
	Fen	926,959.14	2.0%	0.5%
	Marsh	239,536.09	0.5%	0.1%
	Swamp	2,097,416.86	4.6%	1.2%
	Riparian	126,928.33	0.3%	0.1%
Aquatic (allocate to pre-flood aquatic = River area Before Impoundment)				2.7%
	Lake	4,567,784.98	9.9%	2.6%
	Aquatic Veg	200,326.79	0.4%	0.1%
None		1,837,796.26	4.0%	1.0%
None		186,504.34	0.4%	0.1%
		46,095,642.41	**100.0%**	**26.0%**

(1) Pre-Flood Land = 26.0% of Total CRD
[759 km^2 (pre-flood land) / 2914 km^2 (total CRD) = 26.0%]

The CRD pre-flood terrestrial land cover and aquatic area were derived as follows the G-res CRD Model (Table 2-2).

Table 2-2 CRD G-res Model Landcover Classification

Pre-Impoundment Land Cover in the CRD Area
Adaptation of Keeyask Ecological Land Classification

	% Mineral Soil	% Organic Soil	% Total
Croplands			
Bare Areas	1.1%		1.1%
Wetlands		17.5%	17.5%
Forest	3.0%	1.7%	4.7%
Grassland/Shrubland			
Permanent Snow/Ice			
Settlements			
Total Terrestrial			**23.4%**
Water Bodies on Land			2.7%
Total			**26.0%**

2.2.3 Replacement of G-res Tool Generic Emission Factors

Default G-res Tool pre-flood CO_2 and CH_4 emission factors for "Forest", "Grassland/Shrubland", and "Wetlands" were replaced by CO_2 emission factors developed by Virkkala et al., (2021) and by CH_4 emission factors adopted from Kuhn et al., (2021) and Treat et al., (2018). The G-res Tool default pre-flood emission factor of 2 kg/CH_4/ha/yr for "Water Bodies" was used in the absence of in-situ measurements.

2.2.3.1 CO_2 Terrestrial Emission Factors

Annual CO_2 emission factors (Net Ecosystem Exchange) for the Boreal Upland and Boreal Wetland were selected from Virkkala et al., (2021). They were based on a study period of 1990-2015 (Table 2-3). Virkkala et al. (2021) did not develop separate emission factors for mineral and organic soils. These emission factors were used as composite emission factors for both mineral and organic soils in the Keeyask G-res model. The Virkkala et al., (2021) Boreal Upland

CO_2 emission factors were used for the G-res categories of Forest and Grassland/Shrubland, and the Boreal Wetland CO_2 emission factors were used for the G-res Wetland category.

Table 2-3 CO_2 Emission Factors Used for the CRD G-res Model

CO_2 Emission Factors for Ecological Land Classification		
Land Class	**Annual NEE g CO_2-C/m^{-2}/yr**	**Annual NEE t CO_2-C/ha/yr (Converted for G-res)**
Boreal Uplands (Forest, and Grassland/Shrubland)	-47	-0.47
Boreal Wetlands	-38	-0.38
Source: Virkakkala et al., 2021 (Table 1)		

2.2.3.2 CH_4 Terrestrial Emission Factors

CH_4 emission factors were adapted from the Boreal–Arctic Wetland and Lake Methane Dataset (BAWLD-CH4) (Kuhn et al., 2021).

Growing season CH_4 terrestrial emission factors were adopted from Kuhn et al. (2021) Table 3 median values for Boreal Forest, Permafrost Bog, Bog, Fen, and Marsh land classes. Non-growing season emission factors were not included in the BAWLD-CH4 database/Kuhn et al. (2021) study. They were therefore estimated as being 16% of total annual emissions according to Treat et al. (2018). The Keeyask Ecological Land Classifications of "Swamps" and "Riparian" were assigned the same emissions factors as the BAWLD-CH4 emission factors for bogs and fens, respectively, following descriptions by Kuhn et al. (2021).

A composite wetland emission factor was developed by developing a weighted average for the land classifications of Permafrost Bog, Bog, Fen, Marsh, and Peatland Lakes (small and medium). This involved multiplying each [wetland class] by their [CH_4 emission factor], by their [areal extent (km^2) as defined by the Keeyask Ecological Land Classification, and by summing these calculations. The results are displayed in Table 2-4.

Table 2-4 Composite CH4 Emission Factors Used for the CRD G-res Model

Land Class	**Annual Emissions kg CH_4/ha/yr (G-res Emission Factor Metrics)**
Boreal Uplands (Forest, and Grassland/Shrubland)	-0.64
Boreal Wetlands	51.13

2.2.3.3 Pre-flood Aquatic GHG Emission Factors

The G-res default pre-flood CH_4 emission factor for "Water Bodies" is 4.4 kg CH_4/ha/yr, which is applied to the river/lake to be flooded.

G-res does not include pre-flood CO_2 emission factors for water bodies.

Table 2-5 illustrates the pre-flood emission factors used in the CRD G-res Model. The site-specific emission factors developed for "Forest", "Grassland/Shrubland", "Wetlands" and "Water Bodies" are highlighted.

Table 2-5 CRD G-res Model Pre-Flood Emission Factors

Climate: Boreal

	CH_4 Emission Factor (kg CH4/ha/yr)		CO_2 Emission Factor (t CO2-C/ha/yr)	
	Mineral Soil	Organic Soil	Mineral Soil	Organic Soil
Cropland	0	0	0	7.9
Bare Areas	0	6.1	0	2.8
Wetlands	51.13	51.13	-0.38	-0.38
Forest	-0.64	-0.64	-0.47	-0.47
Grassland/Shrubland	-0.64	-0.64	-0.47	-0.47
Urban Areas	0	19.6	0	6.4
Water Bodies	2.0			
Drained Peatlands				

2.2.1 Determine River Area Before Impoundment



Figure 2-3 CRD G-res Model River Area Before Impoundment

The River Area before Impoundment was calculated as:

Pre-existing river area to be Flooded (2155 km^2) / Total Reservoir Area (2914 km^2) = 74%.

Plus, pre-existing water bodies on land to be flooded = 2.7%

Total "River Area before Impoundment" = 76.7%

3 Reservoir Data

3.1 Input Values

The input values used are as follows:

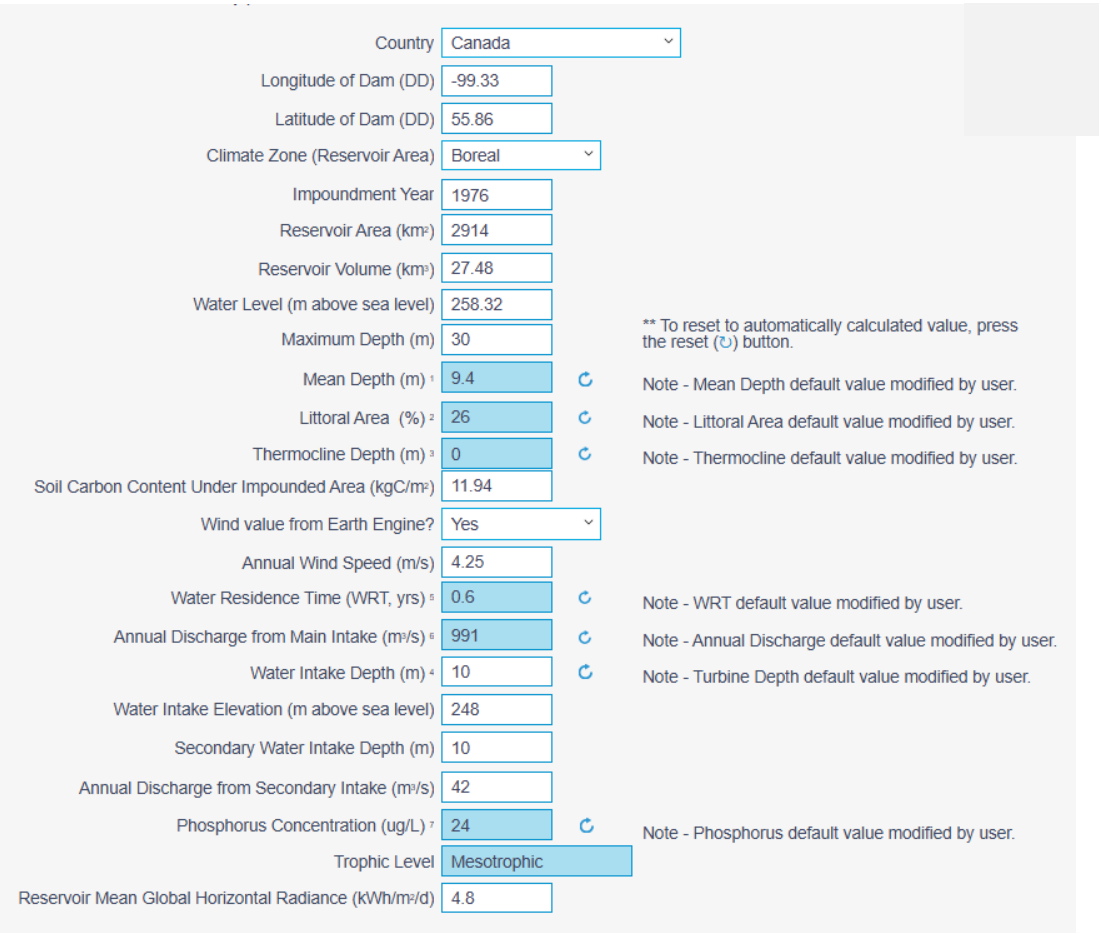


Figure 3-1 CRD G-res Model: Reservoir Data Inputs

Longitude and Latitude:
The Longitude (-99.33 W) and Latitude (55.86 N) of the Dam refer to the location of the CRD.

Climate Zone:
The CRD G-res model was set to **Boreal** climate zone.

The G-res choices are: Boreal, Temperate, Sub-Tropical, and Tropical.

The CRD is located within the Precambrian Shield Physiographic Region (Natural Resources Canada, 2019). The northern portion of the CRD, which includes the portion of Southern Indian Lake north of Long Point, is located in the Taiga Shield Ecozone, Selwyn Lake Upland, Northern Indian Lake Ecodistrict (Smith et al., 1998). The southern portion of the CRD is located within the Boreal Shield Ecozone, Churchill River Upland Ecoregion, Southern Indian Lake Ecodistrict (Smith et al., 1998).

Impoundment Year: 1976
Reservoir impoundment (flooding) occurred during 1976 (Manitoba and Manitoba Hydro, 2014).

Reservoir Area (km^2): 2914 km^2
The surface area of the flooded aquatic system in the Regional Cumulative Effects Assessment (RCEA) Zone 4 (e.g. Southern Indian Lake) and RCEA Zone 6 (e.g. Rat River, Issett Lake, Karsakawigimak Lake, Pemichigamau Lake, Central and West Mynarski Lakes, Rat Lake, and Notigi Lake) (Figure 1-3 & 1-6) are estimated to be 2,914 km^2 (Newbury et al., 1984; Manitoba and Manitoba Hydro, 2014). This includes approximately 759 km^2 of flooded land (Manitoba and Manitoba Hydro, 2014).

Reservoir Volume (km^3): 27.48 km^3
The estimated reservoir volume of the CRD flooded area 27.48 km^2.

This comprises 23.38 km^2 for RCEA Zone 4 (Southern Indian Lake) as derived by McCullough (1981) and 4.1 km^2 for RCEA Zone 6 (Rat River, Issett Lake, Karsakawigimak Lake, Pemichigamau Lake, Central and West Mynarski Lakes, Rat Lake, and Notigi Lake) as derived by Newbury et al. (1984).

Water Level (m above sea level): 258.32 m above sea level

As per the final Manitoba Water Power Act Licence for the CRD, the Missi Falls and Notigi Control Structures are to be operated so the maximum water level on Southern Indian Lake is to be 258.32 m above sea level (Manitoba Conservation and Climate, 2021).

Maximum Depth (m): 30 m
The maximum depth of Southern Indian Lake according to the World Lake Database (2025) is 30 m.

Mean Depth (m): 9.4 m
The mean depth was calculated to be 9.4 m. This was derived as a weighted average as follows:

Southern Indian Lake:
[Mean depth (as per Newbury et al., 1984) 9.8 m] X [Area (as per McCullough, 1981) 23.8 km^2]

+

Notigi Reservoir (Rat River, Issett Lake, Karsakawigimak Lake, Pemichigamau Lake, Central and West Mynarski Lakes, Rat Lake, and Notigi Lake)

[Mean depth (as per Newbury et al., 1984) 7.8 m] X [Area (as per Newbury et al., 1984) 4.1 km^2]

= 9.4 m

Littoral Area (%): 26%
In lieu of site-specific data on the extent of the littoral zone for CRD, the Keeyask reservoir was used as a surrogate for the CRD flooded area since the terrain of the two regions are similar.

Thermocline Depth (m): 0
The thermocline depth was set as 0 m.

As noted by Planas and Hecky (1984) thermal stratification in Southern Indian Lake is weak to non-existent during the ice-free period.

Soil Carbon Content Under the Impoundment Area (kg C/m^2): 11.94 kg C/m^2
The value of 11.94 kg C/m^2 was derived from the Earth Engine functionality of the G-res Tool. For comparison, this value aligns well with IPCC 2019 default value of 11.6 ±65% kg C/m^2 for the soil organic carbon stock content for Boreal Moist/Dry wetland soils for 0-30 cm depth (IPCC 2019, Table 2.3).

This value is also similar to the average carbon content of 10.8 kg C/m^2 in peat-forming soils at a depth of 0-30 cm in a boreal forest site located south of James Bay (Magnan et al 2020). Similarly, Beaulne et al (2021) calculated that between 11.0 – 12.6 kg C/m^2 has been stored in the organic horizons of a boreal peatland site in eastern Canada over the last 200 years.

Annual Wind Speed: 4.25 m/s
The value of 4.25 m/s was derived from the Earth Engine functionality of the G-res Tool.

This value is within the range of average wind speeds of 3.89 m/s to 4.94 m/s recorded in Gillam, Manitoba from 1971 to 2000 (Keeyask Hydropower Limited Partnership, 2012).

Water Residence Time (WRT, yrs): 0.6 yrs
The Water Residence Time was calculated to be 0.6 years. This was derived as a weighted average as follows:

Southern Indian Lake:
[WRT (as per McCullough, 1981) 0.72 yrs] X [Area (as per McCullough, 1981) 23.8 km^2]

+

Notigi Reservoir (Rat River, Issett Lake, Karsakawigimak Lake, Pemichigamau Lake, Central and West Mynarski Lakes, Rat Lake, and Notigi Lake)

[WRT (as per Newbury et al., 1984) 0.17 yrs] X [Area (as per Newbury et al., 1984) 4.1 km^2]

= 0.6 yrs

Annual Discharge from Main Intake (m^3/s): 991 m^3/s
As per the final Manitoba Water Power Act Licence for the CRD, the maximum average weekly flows permitted at the Notigi Control Structure are as follows (Manitoba Conservation and Climate, 2021).

May 16 – October 31: 991 m^3/s
November 1 – May 15: 963 m^3/s

The maximum discharge of 991 m^3/s during May 16 – October 31 was selected for modelling so as not to underestimate lifecycle emissions.

Water Intake Depth (m): 10 m
There are two control structures releasing water from the CRD. They are the Notigi Control Structure that releases water into the Rat-Burntwood-Nelson River System and the Missi Falls Control Structure that releases water into the Churchill River System. The Notigi Control Structure was selected as the primary station as the discharge rates are larger than those of the Missi Falls Control Structure.

For modelling purposes, the depth of the water intake for the Notigi Control Structure was estimated as being of 10 m below reservoir surface.

Water Intake Elevation (m above sea level):
The water intake elevation was estimated as 248 m ASL, which is 10 m below the maximum water level allowed on Southern Indian Lake (258.32 m ASL) as per the terms of the final Manitoba Water Power Act Licence for the CRD (Manitoba Conservation and Climate, 2021).

Secondary Water Intake Depth (m): 10 m
The Missi Falls Control Structure was selected as the secondary station as the discharge rates are smaller than those of the Notigi Control Structure.

For modelling purposes, the depth of the water intake for the Missi Falls Control Structure was estimated as being of 10 m below reservoir surface.

Annual Discharge from Secondary Intake (m^3/s): 42 m^3/s

As per the final Manitoba Water Power Act Licence for the CRD, the maximum average weekly flows permitted at the Missi Falls Control Structure are as follows (Manitoba Conservation and Climate, 2021).

Ice Cover Period: 42 m^3/s
Open Water Period: 14 m^3/s

The maximum discharge of 42 m^3/s during the ice cover period was selected for modelling so as not to underestimate lifecycle emissions.

Phosphorus Concentration (µg/L): 24.0 µg/L

The median concentrations of Total Phosphorous for regions of the CRD as measured by the Coordinated Aquatic Monitoring Program (CAMP) from 2008 to 2019 were reported as follows (Coordinated Aquatic Monitoring Program, 2024: pages 3-68 to 3-72):

Opachuanau Lake	0.022 mg/l
Southern Indian Lake – Area 1	0.020 mg/l
Southern Indian Lake – Area 4	0.014 mg/l
Southern Indian Lake – Area 6	0.024 mg/l
Rat Lake	0.022 mg/l
Central Mynarski Lake	0.017 mg/l
Notigi Lake – East	0.018 mg/l
Notigi Lake – West	0.016 mg/l

The median value of 24.0 µg/L for Southern Indian Lake – Area 6 was selected as a conservative representation of Total Phosphorous for the CRD so as not to underestimate lifecycle GHG emissions.

Trophic Level: Mesotrophic

G-res assigned the Trophic Value as Mesotrophic. This aligns with the Coordinated Aquatic Monitoring Program (2024) assessment where the measured areas of the CRD, as described above, are within the mesotrophic to meso-eutrophic range.

Reservoir Mean Global Horizontal Radiance ($kWh/m^2/d$): 4.8

The Reservoir Mean Global Horizontal Radiance value of 4.8 $kWh/m^2/d$ was generated by the G-res Tool Earth Engine.

For comparison, the on-line, interactive Photovoltaic Potential and Solar Resource Maps of Canada estimates mean annual global insolation values of 3.15 kWh/m^2/d the Community of South Indian Lake, Manitoba (Natural Resources Canada, 2020). The estimates are based on horizontal 0-degree orientation on a 60 arc seconds (approximately 2 km grid).

To be conservative, the elevated value of 4.8 kWh/m^2/d was used in the G-res Tool modeled estimates.

Mean Temperature per Month (°C)

Mean Temperature per Month and Mean Annual Air Temperature data were derived by the G-res Tool Earth Engine.

Mean Temperature per Month (°C)	
January	-25.6
February	-22.16
March	-15.37
April	-4.37
May	4.58
June	11.13
July	15.23
August	13.61
September	6.8
October	-0.1
November	-11.84
December	-22.62
Mean Annual Air Temperature (°C)	-4.2

Figure 3-2 Mean Average Monthly Temperatures

4 Reservoir Services Data

100% of the Reservoir Services were allocated to the CRD.

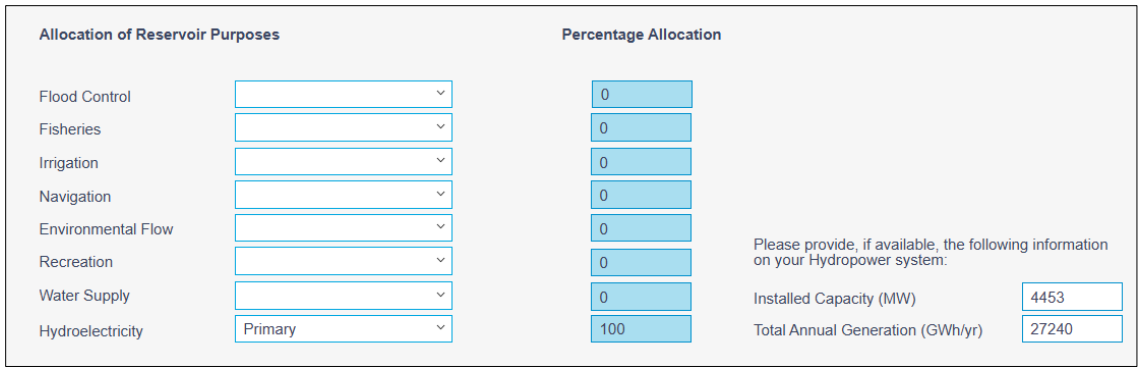


Figure 4-1 CRD G-res Model: Reservoir Services

5 Construction GHG

The G-res Tool was not used to estimate Construction Emissions.

6 Unrelated Anthropogenic Sources Emissions

Since 100% of the purpose of the CRD flooded area is assigned to hydroelectricity, no GHG emissions were allocated to Unrelated Anthropogenic Sources.

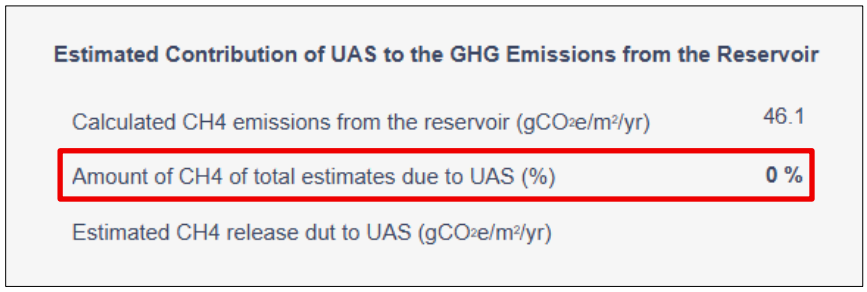


Figure 6-1 CRD G-res Model: Contribution of Unrelated Anthropogenic Sources of GHG Emissions

References

Amesbury, M. J., Gallego-Sala, A., & Loisel, J. (2019). Peatlands as prolific carbon sinks. In *Nature Geoscience* (Vol. 12, Issue 11, pp. 880–881). Nature Publishing Group. https://doi.org/10.1038/s41561-019-0455-y

Baird, A., Belyea, L., Comas, X., Reeve, A.S., Slater, L. (2009). Understanding Carbon Cycling in Northern Peatlands: Recent Developments and Future Prospects. DOI 10.1029/2008GM000875. In book: Carbon Cycling in Northern Peatlands. Geophysical Monograph Series 184 (pp.1-3) Chapter: Understanding Carbon Cycling in Northern Peatlands: Recent Developments and Future Prospects. Publisher: American Geophysical Union Editors: Andrew J. Baird, Lisa R. Belyea, Xavier Comas, A.S. Reeve, Lee D. Slater

Beaulne, J., Garneau, M., Magnan, G., Boucher, É. (2021). Peat deposits store more carbon than trees in forested peatlands of the boreal biome. Sci Rep 11, 2657. https://doi.org/10.1038/s41598-021-82004-x

Belyea, L.R., 2009. Nonlinear dynamics of peatlands and potential feedbacks on the climate system. Carbon Cycling in Northern Peatlands, pp. 5–18.

Buchner, A.P. (1990). Manitoba History: Glacial Lake Agassiz. Manitoba History, Number 19, Spring 1990. https://www.mhs.mb.ca/docs/mb_history/19/lakeagassiz.shtml

Coordinated Aquatic Monitoring Program (CAMP). 2024. CAMP Twelve Year Data Report (2008-2019). Report prepared for Manitoba/Manitoba Hydro CAMP Steering Committee by Manitoba Hydro and North/South Consultants Inc., Winnipeg, MB. 435 pages.

Gauthier, M. S., Breckenridge, A.&Hodder,T. J. (2022). Patterns of ice recession and ice stream activity for the MIS 2 Laurentide Ice Sheet in Manitoba, Canada. Boreas, Vol. 51, pp. 274–298. https://doi.org/10.1111/bor.12571, ISSN 0300-9483.

Graham, J. D., Ricciuto, D. M., Glenn, N. F., & Hanson, P. J. (2022). Incorporating Microtopography in a Land Surface Model and Quantifying the Effect on the Carbon Cycle. *Journal of Advances in Modeling Earth Systems*, *14*(2). https://doi.org/10.1029/2021MS002721

Government of Canada. (2013). National Ecological Framework for Canada. Ecozones, Ecoregions, and Ecodistricts.
https://sis.agr.gc.ca/cansis/publications/maps/eco/all/districts/eco_all_districts_1m_manitoba.jpg

Han, Q., Wang, B., Liu, C-Q., Wang, F., Peng, X., Liu, X-L. (2018). Carbon biogeochemical cycle is enhanced by damming in a karst river, Science of The Total Environment, Volumes 616–617, 2018, Pages 1181-1189, ISSN 0048-9697, https://doi.org/10.1016/j.scitotenv.2017.10.202.

Hugelius, G., Loisel, J., Chadburn, S., Jackson, R. B., Jones, M., MacDonald, G., Marushchak, M., Olefeldt, D., Packalen, M., Siewert, M. B., Treat, C., Turetsky, M., Voigt, C., & Yu, Z. (2020). Large stocks of peatland carbon and nitrogen are vulnerable to permafrost thaw. *Proceedings of the National Academy of Sciences of the United States of America*, *117*(34), 20438–20446.
https://doi.org/10.1073/pnas.1916387117

IPCC (2019). Chapter 2: Generic Methodologies Applicable to Multiple Land-Use Categories, Volume 4 Agriculture, Forestry and Other Land Use, 2019 Refinement to the 2006 IPCC Guidelines for National Greenhouse Gas Inventories, 104 pages.

Jarvie, H.P., King, S.M., Neal, C. (2017). Inorganic carbon dominates total dissolved carbon concentrations in British rivers: application of the THINCARB model – Thermodynamic modelling of inorganic carbon in freshwaters. Sci. Total Environ., 575 (2017), pp. 496-512

Keeyask Hydropower Limited Partnership (2012). Keeyask Generation Project: Environmental Impact Statement; Physical Environment Response to EIS Guidelines, Supporting Volume. 1018 pages.

Know History Inc. (2016). Hydroelectric Development in Northern Manitoba: A History of the Development of the Churchill, Burntwood and Nelson Rivers, 1960–2015. A report to the Manitoba Clean Environment Commission, 305-155 Carlton St., Winnipeg, MB, R3C 3H8, Canada.

Kuhn, M. A., Varner, R. K., Bastviken, D., Crill, P., Macintyre, S., Turetsky, M., Walter Anthony, K., McGuire, A. D., & Olefeldt, D. (2021). BAWLD-CH4: A comprehensive dataset of methane fluxes from boreal and arctic ecosystems. In *Earth System Science Data* (Vol. 13, Issue 11, pp. 5151–5189). Copernicus Publications. https://doi.org/10.5194/essd-13-5151-2021

Magnan, G., Garneau, M., Le Stum-Boivin, É., Grondin, P., and Yves Bergeron, Y. (2020). Long-Term Carbon Sequestration in Boreal Forested Peatlands in Eastern Canada. Ecosystems 23, 1481–1493. https://doi.org/10.1007/s10021-020-00483-x

Mahdiyasa, A. W., Large, D. J., Muljadi, B. P., & Icardi, M. (2023). Modelling the influence of mechanical-ecohydrological feedback on the nonlinear dynamics of peatlands. *Ecological Modelling*, *478*. https://doi.org/10.1016/j.ecolmodel.2023.110299

Manitoba Conservation and Climate. (2021). Final Licence for the Diversion of Water From the Churchill River to the Nelson River, and the Impoundment of Water on the Rat River and Southern Indian Lake. Province of Manitoba. https://www.gov.mb.ca/sd/water/water-power/churchill/cover_letter_licence_churchill_river_diversion.pdf

Manitoba and Manitoba Hydro. (2014). Regional Cumulative Effects Assessment for the Hydroelectric Developments on the Churchill, Nelson and Burntwood River Systems: Phase I Report. 966 pages.

Manitoba and Manitoba Hydro. (2015a). Appendix 4.3c: An Assessment of the Hydraulic Impacts of the Churchill River Diversion on the Rat and Burntwood Rivers. Regional Cumulative Effects Assessment – Phase II. Physical Environment –Water Regime– Appendix 4.3C. 52 pages.

Manitoba and Manitoba Hydro. (2015b). Regional Cumulative Effects Assessment for the Hydroelectric Developments on the Churchill, Nelson and Burntwood River Systems: Phase II Report: Hydroelectric Development
Project Description in the Region of Interest. 152 pages.

Manitoba Hydro. (2022). Manitoba Hydro Churchill River Diversion Licence Implementation Guide. Prepared for: Manitoba Environment, Climate and Parks, 56 pages. https://www.gov.mb.ca/sd/pubs/water/licensing/crd_lig.pdf

Matile, G.L.D. and Keller, G.R. (2006). Surficial geology of the Uhlman Lake map sheet (NTS 64B), Manitoba; Manitoba Science, Technology, Energy and Mines, Manitoba Geological Survey, Surficial Geology Compilation Map Series, SG-64B, scale 1:250 000.

McCullough, G.K. (1981). Water budgets for Southern Indian Lake, before and after impoundment and Churchill River diversion, 1972-79. Can. MS Rep. Fish. Aquat. Sci. 1620: iv + 22 p.

Mozafari, B., Bruen, M., Donohue, S., Renou-Wilson, F., & O'Loughlin, F. (2023). Peatland dynamics: A review of process-based models and approaches. In *Science of the Total Environment* (Vol. 877). Elsevier B.V. https://doi.org/10.1016/j.scitotenv.2023.162890

Natural Resources Canada. (2019). The Atlas of Canada - Physiographic Regions. https://atlas.gc.ca/phys/en/index.html

Natural Resources Canada. (2020). Photovoltaic Potential and Solar Resource Maps of Canada. © Her Majesty the Queen in Right of Canada, as represented by the Minister of Natural Resources, 2020. https://fgp-pgf.maps.arcgis.com/apps/webappviewer/index.html?id=c91106a7d8c446a19dd1909fd93645d3

Newbury, R. W., G. K. McCullough, and R. E. Hecky. (1984). The Southern lndian Lake impoundment and Churchill River diversion. Can. J. Fish. Aquat. Sci. 41: 548-557.

Nichols, J. E., & Peteet, D. M. (2019). Rapid expansion of northern peatlands and doubled estimate of carbon storage. *Nature Geoscience*, *12*(11), 917–921. https://doi.org/10.1038/s41561-019-0454-z

Pelletier, Luc. (2007). *Carbon dioxide and methane fluxes of three peatlands in the La Grande Rivière watershed, James Bay lowland, Canada*. Library and Archives Canada = Bibliothèque et Archives Canada.

Pelletier, L., Garneau, M., & Moore, T. R. (2011). Variation in CO2 exchange over three summers at microform scale in a boreal bog, Eastmain region, Québec, Canada. *Journal of Geophysical Research: Biogeosciences*, *116*(3). https://doi.org/10.1029/2011JG001657

Pelletier, L., Strachan, I. B., Roulet, N. T., Garneau, M., & Wischnewski, K. (2015). Effect of open water pools on ecosystem scale surface-atmosphere carbon dioxide exchange in a boreal peatland. *Biogeochemistry*, *124*(1–3), 291–304. https://doi.org/10.1007/s10533-015-0098-z

Planas, D., and R. E. Hecky. (1984). Comparison of phosphorus turnover times in northern Manitoba reservoirs with lakes of the Experimental Lakes Area. Can. 8. Fish. Aquat. Sci. 41: 605-612.

Smith, R.E., H. Veldhuis, G.F. Mills, R.G. Eilers, W.R. Fraser, and G.W. Lelyk. (1998). Terrestrial Ecozones, Ecoregions, and Ecodistricts of Manitoba, An Ecological Stratification of Manitoba's Natural Landscapes. Technical Bulletin 1998-9E. Land Resource Unit, Brandon Research Centre, Research Branch, Agriculture and Agri-Food Canada, Winnipeg, Manitoba. Report and map at 1:1 500 000 scale. https://sis.agr.gc.ca/cansis/publications/ecostrat/provDescriptions/mbteee/mbteee_report.pdf

St. Louis, V. L., Kelly, C. A., Duchemin, É., Rudd, J. W. M., & Rosenberg, D. M. (2000). Reservoir surfaces as sources of greenhouse gases to the atmosphere: A global estimate. In *BioScience* (Vol. 50, Issue 9, pp. 766–775). Oxford University Press. https://doi.org/10.1641/0006-3568(2000)050[0766:RSASOG]2.0.CO;2

St. Louis, V.L., Partridge, A.D., Kelly, C.A., Rudd, J. (2003). Mineralization rates of peat from eroding peat islands in reservoirs. Biogeochemistry 64, 97–110. https://doi.org/10.1023/A:1024982915493

Strack, M (ed). (2008). Peatlands and Climate Change. International Peat Society, ISBN 9529940114, 9789529940110, 223 pages

Tank, S., J. Fellman, J., Hood, E., & Kritzberg, E. (2018). Beyond respiration: Controls on lateral carbon fluxes across the terrestrial-aquatic interface. Limnology and Oceanography Letters. 3. 10.1002/lol2.10065.

Tarnocai, C. (2006). The effect of climate change on carbon in Canadian peatlands. Global Planet. Change, 53 (2006), pp. 222-232, 10.1016/j.gloplacha.2006.03.012

Tarnocai, C., I.M. Kettles and B. Lacelle. (2011). Peatlands of Canada; Geological Survey of Canada, Open File 6561 (digital database); CD-ROM. https://geoscan.nrcan.gc.ca/text/geoscan/metadata/of6561-e.pdf

Treat, C. C., Bloom, A. A., & Marushchak, M. E. (2018). Nongrowing season methane emissions–a significant component of annual emissions across northern ecosystems. *Global Change Biology*, *24*(8), 3331–3343. https://doi.org/10.1111/gcb.14137

Treat, C. C., Jones, M. C., Brosius, L., Grosse, G., Walter Anthony, K., & Frolking, S. (2021). The role of wetland expansion and successional processes in methane emissions from northern wetlands during the Holocene. *Quaternary Science Reviews*, *257*. https://doi.org/10.1016/j.quascirev.2021.106864

Trudeau, N. C., Garneau, M., & Pelletier, L. (2013). Methane fluxes from a patterned fen of the northeastern part of the La Grande river watershed, James Bay, Canada. *Biogeochemistry*, *113*(1–3), 409–422. https://doi.org/10.1007/s10533-012-9767-3

Turetsky, M. R., Kotowska, A., Bubier, J., Dise, N. B., Crill, P., Hornibrook, E. R. C., Minkkinen, K., Moore, T. R., Myers-Smith, I. H., Nykänen, H., Olefeldt, D., Rinne, J., Saarnio, S., Shurpali, N., Tuittila, E. S., Waddington, J. M., White, J. R., Wickland, K. P., & Wilmking, M. (2014). A synthesis of methane emissions from 71 northern, temperate, and subtropical wetlands. *Global Change Biology*, *20*(7), 2183–2197. https://doi.org/10.1111/gcb.12580

Vincent, J.-S. (1985) Surficial geology, Réservoir LaGrande 2, Québec, Geological Survey of Canada, Map 1590A, scale 1:100 000. https://ostrnrcan-dostrncan.canada.ca/entities/publication/43e721e4-5e64-4a1a-943c-d15520397394

Virkkala, A. M., Aalto, J., Rogers, B. M., Tagesson, T., Treat, C. C., Natali, S. M., Watts, J. D., Potter, S., Lehtonen, A., Mauritz, M., Schuur, E. A. G., Kochendorfer, J., Zona, D., Oechel, W., Kobayashi, H., Humphreys, E., Goeckede, M., Iwata, H., Lafleur, P. M., … Luoto, M. (2021). Statistical upscaling of ecosystem CO2 fluxes across the terrestrial tundra and boreal domain: Regional patterns and uncertainties. *Global Change Biology*, *27*(17), 4040–4059. https://doi.org/10.1111/gcb.15659

Wang, W., Li, S-L., Zhong, J., Li, C., Yi, Y., Chen, S., Ren, Y. (2019). Understanding transport and transformation of dissolved inorganic carbon (DIC) in the reservoir system using δ13CDIC and water chemistry, Journal of Hydrology, Volume 574, Pages 193-201, ISSN 0022-1694, https://doi.org/10.1016/j.jhydrol.2019.04.036.

Webster, K. L., Bhatti, J. S., Thompson, D. K., Nelson, S. A., Shaw, C. H., Bona, K. A., Hayne, S. L., & Kurz, W. A. (2018). Spatially-integrated estimates of net ecosystem exchange and methane fluxes from Canadian peatlands. *Carbon Balance and Management*, *13*(1). https://doi.org/10.1186/s13021-018-0105-5

World Lake Database (2025). Southern Indian Lake. International Lake Environment Committee Foundation. https://wldb.ilec.or.jp/Display/html/3434

Yu, Z., Joos, F., Bauska, T. K., Stocker, B. D., Fischer, H., Loisel, J., Brovkin, V., Hugelius, G., Nehrbass-Ahles, C., Kleinen, T., & Schmitt, J. (2021). No support for carbon storage of >1,000 GtC in northern peatlands. *Nature Geoscience*, *14*(7), 465–467. https://doi.org/10.1038/s41561-021-00769-2